Abbreviations and Acronyms

Å	angstrom
δ	chemical shift in ppm, downfield from tetramethylsilane
°C	degree celsius
μ	micro
μL	microlitre
μM	micromole per litre
ν	wavenumber
A	adenine
Ac	acetyl
ACV	acyclovir
AdSS	adenylosuccinate synthetase
AIBN	azobisisobutyronitrile
AIDS	acquired immunodeficiency syndrome
ALG	alginate
AMP	adenosine monophosphate
aq.	aqueous
Ar	aryl
Asn	asparagines
Asp	aspartic acid
ax	axial
AZT	zidovudine or azidodideothymidine
BBN	9-borabicyclo[3.3.1]nonane
[bmim][BF_4]	1-butyl-3-methylimidazolium tetrafluoroborate
Bn	benzyl
Boc	*t*-butyloxycarbonyl
b.p.	boiling point
br	broad
BSA	*N*,*O*-bis(trimethylsilyl)acetimide
Bu	*n*-butyl
^{t}Bu	*tert*-butyl
Bz	benzoyl
C	cytosine
ca.	approximately
cal	calories
cat.	Catalytic
Cbz	carbobenzyloxy
CC_{50}	50% cytotoxic concentration
CDC	Centres for Disease Control and Prevention, U.S.
CE	2-cyanoethyl
Chx	cyclohexyl
CI	Chemical Ionisation
cm	centimeter(s)
CMV	cytomegalovirus
COSY	correlation spectroscopy
CoV	coronavirus
6-CP	6-chloropurine
Cp*	pentamethylcyclopentadienyl
m-CPBA	*meta*-chloroperoxybenzoic acid
CSA	(+)-10-camphorsulfonic acid
CuACC	copper catalysed azide-alkyne cycloaddition
Cy	cyclohexyl
d	doublet or day(s)
Da	Dalton
DABCO	1,4-diazabicyclo[2.2.2]octane
dba	dibenzylideneacetone
DBU	1,8-diazabicyclo[5.4.0]undec-7-ene
DCC	*N,N'*-dicyclohexylcarboiimide
DCE	1,2-dichloroethane
DCU	*N,N* -dicyclohexylurea
dd	doublet of doublet
ddd	doublet of doublets of doublets
DDQ	2,3-dichloro-5,6-dicyano-1,4-benzoquinone
de	diastereomeric excess
DEAD	diethyl azodicarboxylate
DEI	Desorption electron impact
DEPT	distortionless enhancement by polarisation transfer

DFT	density functional theory
DIAD	diisopropyl azodicarboxylate
DIBAL-H	diisobutylaluminium hydride
DIC	N,N′-diisopropylcarbodiimide
dil.	dilute
DIPA	diisopropylamine
DIPEA	diisopropylethylamine
DMA	dimethylacetamide
DMAD	dimethylacetylene dicarboxylate
DMAP	4-(dimethylamino)pyridine
DMBz	2,4-di-methoxybenzoyl
DMDO	dimethyldioxirane
DME	dimethoxyethane
DMF	*N*,*N*-dimethylformamide
DMP	Dess-Martin periodinane
3,5-DMP	3,5-dimethylpyrazole
DMSO	dimethylsulfoxide
DMT	di-(*p*-methoxyphenyl)phenylmethyl or 4,4′-dimethoxytrityl
DNA	deoxyribonucleic acid
DOS	diversity oriented synthesis
DPMS	diphenylmethylsilyl
dppf	1,1′-bis(diphenylphosphino)ferrocene
dr	diastereomeric ratio
ds	double-stranded
dt	doublet of triplets
DTBS	di-*t*-butylsilylene
EBV	Epstein-Barr virus
EC_{50}	50% effective concentration
EDG	electron donating group
ee	enantiomeric excess
EI	electron impact
eq	equatorial
equiv.	equivalent(s)
er	enantiomeric ratio
Et	ethyl
eV	electron volt(s)
EWG	electron withdrawing group
FAB	fast atom bombardment
^{5F}C	5-fluorocytosine
FDA	Food and Drug Administration, U.S.
Fmoc	9-fluorenylmethoxycarbonyl
fod	6,6,7,7,8,8,8-heptafluoro-2,2-dimethyl-3,5-octanedianato
^{5F}U	5-fluorouracil
Fuc-T	fucosyl transferase
g	gram(s)
G	guanine
G*	2-*N*-acetyl-6-*O*-(diphenylcarbamoyl)guanine
Gal	galactose
GABA	gamma-aminobutyric acid
gly	glycine or glycinyl
GTP	guanosine triphosphate
hν	ultraviolet radiation
h	hour(s)
HAdV	human adenovirus
HBV	hepatitis B virus
HCoV	human coronavirus
HCV	human hepatitis C virus
HDA	hetero Diels-Alder
HIV	human immunodeficiency virus
HMBC	heteronuclear multiple bond correlation
HMDS	hexamethyldisilazane
HMPA	hexamethylphosphoramide
HOBt	1-hydroxybenzotriazole
HPLC	high performance liquid chromatography
HPV	human papillomavirus
HRMS	high resolution mass spectroscopy
HSQC	heteronuclear single quantum correlation
HSV	herpes simplex virus
HTLV	human T-lymphotropic virus
Hz	hertz
IC_{50}	50% inhibitory concentrations
^{d}Icr	isocaranyl
IHA	intramolecular hydrogen abstraction or radical oxidative cyclisation

IHMA	intramolecular hetero-Michael addition
IMP	inosine monophosphate
INC	intramolecular nitrone cycloaddition
Ipc	isopinocampheyl
IR	infra-red
J	NMR coupling constant
k	kilo
KHMDS	potassium hexamethyldisilazide or potassium *bis*(trimethylsilyl)amide
LDA	lithium diisopropylamine
Leu	leucine
LiDBB	lithium 4,4'-di-*tert*-butylbiphenylide
LG	leaving group
LiHMDS	lithium hexamethyldisilazide or lithium *bis*(trimethylsilyl)amide
lit.	literature
m	multiplet or milli
m	*meta*
M	mole per litre or mega
Me	methyl
Mes	mesityl or 2,4,6-trimethylphenyl
mg	milligram(s)
MGMT	O^6-methylguanine-DNA methyltransferase
MHz	megahertz
min	minute(s)
mL	milliliter
mmol	millimole(s)
mol	mole(s)
MOM	methyoxymethyl
m.p.	melting point
mRNA	messenger ribonucleic acid
MS	molecular sieves or mass spectroscopy
Ms	methanesulfonyl or mesyl
m/z	mass to charge ratio
NBS	*N*-bromosuccinimide
NIAID	National Institute of Allergy and Infectious Diseases, U.S.
NIH	National Institute of Health, U.S.
NIS	*N*-iodosuccinimide
NMO	*N*-methylmorpholine *N*-oxide
NMR	nuclear magnetic resonance
NNRTI	non-nucleoside reverse transcriptase inhibitor
NOE	nuclear overhauser effect
NOESY	nuclear overhauser effect spectroscopy
NRTI	nucleoside reverse transcriptase inhibitor
o	*ortho*
p	*para*
PCC	pyridinium chlorochromate
PEG	polyethylene glycol
pep	peptide or peptidyl
Ph	phenyl
Phe	phenylalanine
PHIL	Public Health Image Library, U.S.
PLC	preparative thin layer chromatography
PMA	phosphomolybdic acid
PMB	*para*-methoxybenzyl
PNBz	*p*-nitrobenzoate
PP	Protein Phosphatase
ppm	parts per million
PPTS	pyridinium *para*-toluenesulphate
Pr	propyl
^{i}Pr	isopropyl
PTP	Protein Tyrosine Phosphatase
py	pyridine
PyBOP	(Benzotriazol-1-yloxy)tripyrrolidinophosphonium hexafluorophosphate
q	quartet
quat.	quaternary
RCM	ring closing metathesis
Refs.	references
RNA	ribonucleic acid
RSV	human respiratory syncytial virus

RT	reverse transcription or reverse transcriptase
rt	room temperature
s	singlet
SAR	structure-activity relationship
SARS	severe acute respiratory syndrome
sat.	saturated
Ser	serine
sLe^x	sialyl Lewis X
SI	selectivity index, the ratio of CC_{50} to EC_{50}
SIMes	*N*,*N*′-bis(2,4,6-trimethylphenyl)-4,5-dihydro-imidazol-2-ylidene
ss	single-stranded
Su	succinimide
t	triplet
T	thymine
TBAF	tetra-*N*-butylammonium fluoride
TBDPS	*tert*-butyldiphenylsilyl
TBS	*tert*-butyldimethylsilyl
TBTA	*tris*-[(1-benzyl-1*H*-1,2,3-triazol-4-yl)methyl]amine
TCEP	*tris*(carboxyethyl)phosphine
TEMPO	2,2,6,6,-tetramethyl-1-piperidinyloxyl
tert	tertiary
TES	triethylmethyl
Tf	trifluoromethanesulfonyl or triflic
TFA	trifluoroacetic acid
THF	tetrahydrofuran
Thr	threonine
TIPDS	1,3-(1,1,3,3-tetraisopropyldisiloxanylidene)
TIPS	triisopropylsilyl
TLC	thin layer chromatography
TMDSO	tetramethyldisiloxane
TMEDA	*N*,*N*,*N*′-trimethylethylenediamine
TMS	trimethylsilyl
Tol	4-toluoyl
TosMIC	tosylmethyl isocyanide
TPAP	tetrapropylammonium perruthenate
Tr	trityl or triphenylmethyl
Ts	toluenesulfonyl or tosyl
TSAO	[2′,5′-Bis-*O*-(*tert*-butyldimethylsilyl)-β-D-ribofuranose]-3′-spiro-5″-[4″-amino-1″,2″-oxathiole-2″2″-dioxide]
U	uracil
UNAIDS	United Nations Programme on HIV/AIDS
UV	ultraviolet
VZV	varicella zoster virus
WHO	World Health Organisation
w/v	weight by volume
w/w	weight by weight

Table of Contents

Chapter One:

Introduction: Chemistry of Spiroacetals

1.1 Why do we Modify Natural Products?

There is a continual need to develop new drug candidates, not only to combat the increasingly common and widespread multi-drug resistant infectious diseases, but also to find potential treatments for diseases that have no cure, and most importantly, to find potent "wonder drugs" with significant beneficial activities and minimal side effects.

The number of possible "drug-like" candidates is unimaginably large. Gilda *et al.*[1] estimated that more than 10^{60} compounds fit into criteria that are commonly found in other drugs (no more than 30 non-hydrogen atoms; consist of H, C, N, O, P, S, F, Cl; a molecular weight of less than 500 Da, possibly stable in water and oxygen at ambient temperature and pressure). However, only a fraction of these possible "drug-like" candidates (~10^7) have ever been synthesised and an even smaller number have reached preclinical development.[2,3]

Nature has traditionally been the most important source of lead compounds for drug discovery. Evolutionary selection pressures have resulted in chemical biodiversity that was exploited not only by the pharmaceutical industry, but also by many ancient civilisations in the pre-historical era. With the structural diversity of those compounds, it is not surprising that about 53% of the clinically used drugs are derived either directly, indirectly or from knowledge gained from natural products.[4,5]

Unfortunately, the use of natural products as drug candidates has its limitations. Most pharmacologically active natural compounds are only available sparingly from their original source and painstaking isolation procedures are required.[6] Even if the compound were reproduced synthetically in the laboratory, some candidates are so structurally complex that their scale-up syntheses necessitate a slow and costly, multi-step synthesis procedure.[7]

As a result, modification of biologically active natural products is an attractive option. The structurally similar, but non-natural, synthetic analogues are designed such that the molecular complexity is kept to a minimum, but the beneficial pharmacologically activities are retained or improved and the unwanted side-effects reduced. This structural "fine-tuning" also leads to syntheses that require fewer steps, cheaper and faster development and are able to be translated to a larger scale synthesis.[7] It has been shown that it is more likely for compounds based on established targets to enter preclinical development (17%) than those that based on new targets (3%).[3] Approximately 26% of new drugs approved by regulatory agencies, such as the Food and Drug Administration of the United States, between 1981 and 2006 were derived from such modifications.[5]

The number of biological targets available for screening has increased substantially in recent years through better understanding of biological pathways and the successful sequencing of the human genome.[8] Hence, it has become increasingly common to subject natural product analogues to

broad phenotypic discovery screens to identify any biological activity that is not found in the original natural product. Despite the genetic diversities, protein domains are structurally conserved through evolution due to the importance of their role.[9]

Combining biologically active motifs within a natural product-inspired scaffold system can easily generate a library of compounds for screening of potential bioactivity.[6,10] The choice of molecular scaffold system is crucial as it inevitably induces structural changes to the geometry of the compound, thus affecting its biological activity.[11] In most cases, the scaffold is chosen to be relatively rigid based on a structure that is widely observed in many natural products. Rigidity preserves the molecular shape and reduces the entropic cost of binding, thus leading to improved bioavailability, an important factor for both natural products and their modified analogues.[6]

1.2 6,6-Spiroacetals

Spiroacetals are polycyclic ether ring systems in which the rings are fused together at the alpha (anomeric) carbon to the oxygen of the cyclic ether. In most cases, the term "spiroacetal" applies to a bicyclic ether ring system, whereas the term "*bis*-spiroacetal" applies to a tricyclic ether ring system.

Spiroacetals, in particular 1,7-dioxaspiro[5.5]undecanes **(1)**, 1,6-dioxaspiro[4.5]decanes **(2)** and 1,6-dioxaspiro[4.4]nonanes **(3)** (Figure 1.1), are widespread substructures of naturally occurring biologically active compounds. Spiroacetals of other ring sizes are also found but less frequently. The occurrence of spiroacetals in natural products has been reviewed extensively.[12-14] As a result, the present work will only focus on the investigation of 1,7-dioxaspiro[5.5]undecane motifs or 6,6-spiroacetals **1** ("spiroacetal") using selected recent examples.

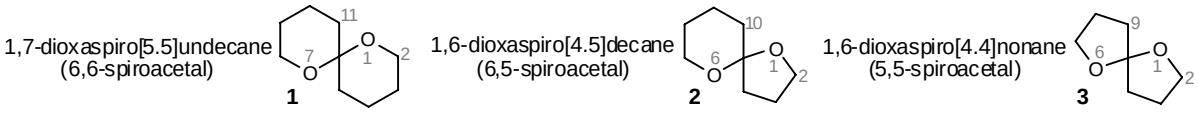

Figure 1.1: Commonly found dioxaspiroacetals **1**–**3** in nature.

1.2.1 Naturally Occurring 6,6-Spiroacetals ("Spiroacetals")

Spiroacetals are a common structural element in many natural products and possess a wide range of biological activities e.g. marine and plant toxins, insect pheromones, insecticides, antibiotics and antitumour agents.[12-14] Many insect secretions or pheromones contain volatile spiroacetals with simple substituents and may play an important role in intraspecific or interspecific chemical communications.[12,14] Other spiroacetals are isolated from a variety of sources with diverse structures.

Representative examples of naturally occurring compounds containing spiroacetals are listed below (Table 1.1).

Insect Secretions or Pheromones[12,14] **4–6**	**4**: Fruit flies: *Bactrocera oleae, B. cacuminata;* Bees: *Partamona cupira*. **5**: Bees: *Andrena ocreata, A. ovatula, A. wikella;* Rove Beetles: *Ontholestes murinus, O. tesselatus;* Wasps: *Polistes dominulusi, P. gallicus*. **6**: Fruit flys: *B. dorsalis, B latifrons;* Bees: *A. ovatula, A. ocreata, A. haemorrhoa*; Wasps: *Ichneumon extensorius, I. submarginatus* 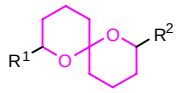 |	R^1	R^2 | **4** H H **5** Me Me **6** Me Pr
Talaromycin B[15] **(7)**	• Toxic metabolite produced by fungus *Talaromyces stipitatus* isolated from wood-shavings-based chicken litter. 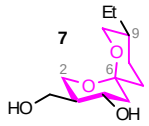 **7**
Routiennocin (CP-61,405)[16] **(8)**	• Pyrrolylcarbonyl spiroacetal ionophore antibiotics isolated from *Streptomyces routiennii*. • Active against a range of Gram positive and anaerobic bacteria *in vitro* and against poultry *Coccidia*. • Forms lipophilic complexes with various cations. 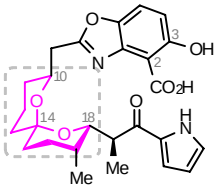 **8**
Okadaic Acid[17,18] **(9)**	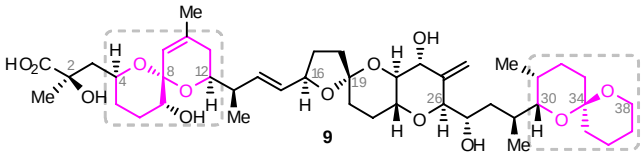 **9** • Isolated from marine sponges, *Halichondria okadai* and *H. melanodocia*. • Metabolite of apiphytic dinoflagellates, *Prorocentrum lima* and *Dinophysis sp*. • Causative agent of diarrhetic shellfish poisoning. • Inhibitor of protein serine/threonine phosphatase (PP), important regulators of many cellular processes [IC_{50}(PP1) = 20–50 nM, IC_{50}(PP2A) = 0.1–0.3 nM].
Tautomycin[18,19] **(10)**	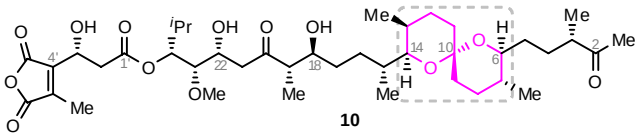 **10** • Antifungal antibiotic isolated from *Streptomyces spiroverticillatus*. • Inhibitor of serine/threonine phosphatase (PP), important regulators of many cellular processes [IC_{50}(PP1) = 22–32 nM, IC_{50}(PP2A) = 75 nM).
Integramycin[20] **(11)**	• Isolated from bacteria *Actinoplanes* sp. extracts. • Inhibit HIV-1 integrase functions: coupled reaction (IC_{50} = 3 μM) and strand transfer reaction (IC_{50} = 4 μM). • HIV integrase inserts the HIV genome into the host genome—the critical step in HIV replications. 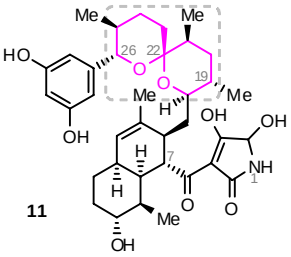 **11**

Auripyrone A[21] **(12)**	• Isolated from the sea hare, *Dolabella auricularia* (Aplysiidae) from Japan. • Cytotoxic against Human cervix carcinoma HeLa S_3 cells (IC_{50} = 0.26 μg mL^{-1}).	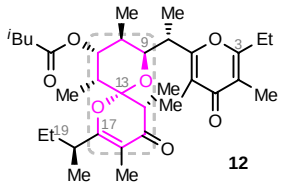 **12**
Milbemycin *β*3[22] **(13)** **and** **Avermectin B_{1a}**[23] **(14)**	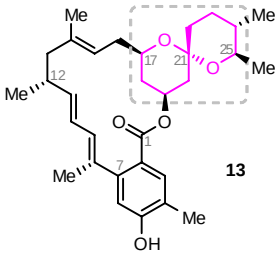 **13** 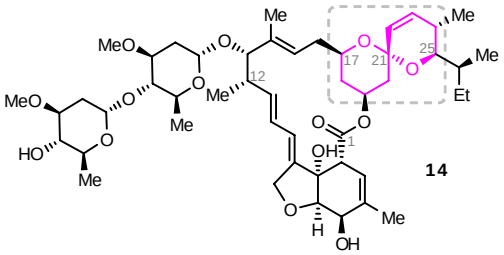 **14** • Structurally related macrolides isolated from *Streptomyces* bacteria found in soils. • Potent anthelmintic, insecticidal and acaricidal agents with low mammalian toxicity.[24] • Avermectin B_{1a} **(14)** is the most potent anthelmintic agent of the family.	
Spongistatin 1[25] **(altohyrtin A)** **(15)**	• Anticancer macrolides isolated from marine sponges *Spongia sp*. and *Spirastrella spinispirulifera*. • Potent antimitotic agents that bind to tubulins and inhibit their assembly. • Inhibit growth of a range of human tumour cells including several highly chemoresistant cell lines at subnanomolar IC_{50} levels.	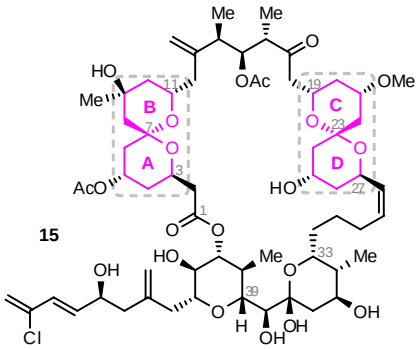 **15**

Table 1.1: Examples of naturally occurring spiroacetals.

1.2.2 Biologically Active Synthetic 6,6-Spiroacetals

The syntheses of spiroacetals based on natural products have yielded a range of biologically active products. Some of these syntheses have used the simplified spiroacetal cores present in the natural products themselves as biological leads while some syntheses resulted in modifications of the spiroacetal moiety. Spiroacetals can also be used as scaffolds to replace part of the natural products.

Uckun *et al*.[26] rationally designed SPIKET-P **(16)** as the basic pharmacophore of spongistatin 1 **(15)** based on the construction of two spiroacetal units, which in computational model studies, served as the critical binding components to tubulins. SPIKET-P **(16)** has been shown to inhibit tubulin polymerisation, which in turn, inhibited mitosis and induced apoptosis in human breast cancer cells in a manner similar to spongistatin 1 **(15)**.

Simple spiroacetal **17**, derived from the enantiomeric spiroacetal units found in okadaic acid **(9)** and tautomycin **(10)**, has been shown to be a potent apoptosis inducer towards human T cell leukaemia Jurkat cells under serum-deprived conditions (LC_{50} = 14 μM).[27]

Ley *et al*.[28] synthesised a sialyl Lewis X (sLe^x) mimetic **18** in which the *N*-acetylglucosamine-galactose disaccharide core was replaced with a spiroacetal scaffold to rigidly hold the sialyl carboxylic acid and the fucose residue in a particular orientation. It was subsequently shown that mimetic **18** inhibited the sLe^x–E-selectin binding. The binding of sLe^x expressed on neutrophils with E-selectins expressed on stimulated endothelial cells causes transient adhesion and rolling of neutrophils along the endothelial cells—the key process in the migration of neutrophils during inflammation.

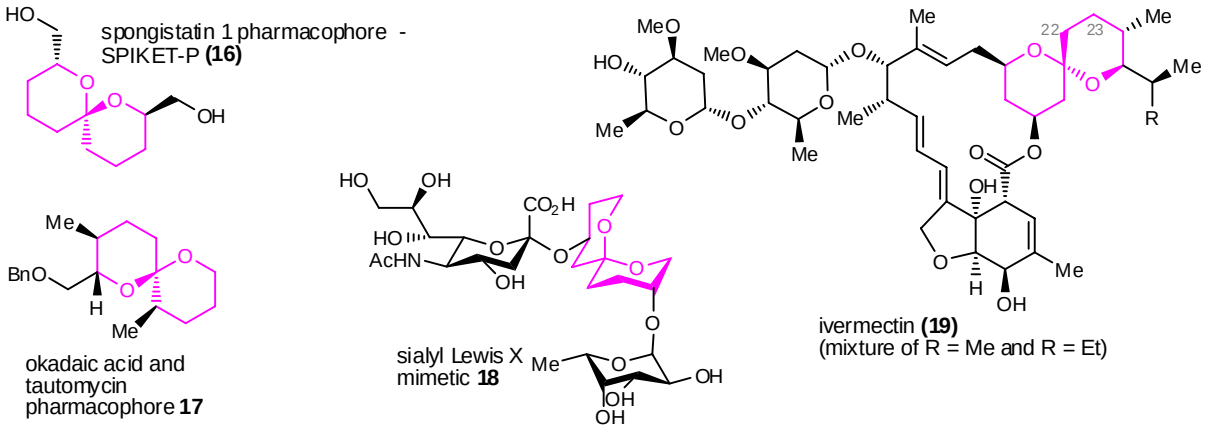

Figure 1.2: Examples of naturally inspired and biologically active synthetic spiroacetal analogues **16**–**19**.

The commercially available ivermectin **(19)** is one of the "top pharmaceuticals that changed the world".[29] It is a semi-synthetic lactone macrolide derived from biotechnically harvested avermectin B_{1a} **(14)** and B_{1b} by selective hydrogenation (C22–C23) using Wilkinson catalyst.[30,31] The resulting saturated spiroacetal moiety was also the core structure found in the related milbemycins[22,31]. Ivermectin **(19)** is a potent anthelmintic, ectoparasitic, insecticidal and acaricidal agent. Initially used in animals, it was later used in humans to treat onchocerciasis (river blindness) commonly found in developing countries caused by the parasitic *Onchocerca volvulus* transmitted through infected black flies.[29-31] Through Merck's donation program, invermectin has tremendously improved the quality of life and the social economy of people living in developing countries.[29]

1.3 Stereochemistry of 6,6-Spiroacetals

As a frequently occurring motif in natural products, the spiroacetal ring system provides a rigid scaffold and conformational framework that holds the molecule in a particular shape.[6] Spiroacetals exist as two diastereomers **20** and **22**, which can be interconverted under acidic conditions *via* an oxonium ion intermediate **21** (Scheme 1.1). Many factors, such as steric interactions, anomeric and

other stereoelectronic effects, intramolecular hydrogen bondings and chelation effects, additively play important roles in governing the thermodynamic stability and configuration preference of the spiroacetals.[10]

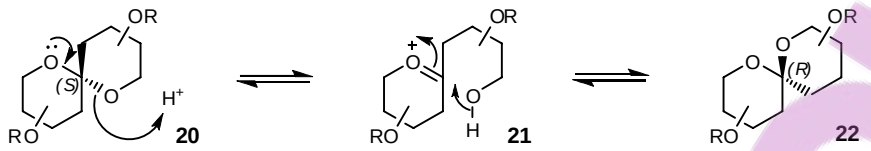

Scheme 1.1: (*S*)- and (*R*)-6,6-Spiroacetal and their interconvertions.

1.3.1 Stereoelectronic Effects

In carbocycles, the most stable conformer has the majority of its substituents residing in equatorial positions if possible, to minimise the unfavourable steric repulsions. However, in tetrahydropyrans, there is a thermodynamic preference for the polar groups bonded to the anomeric position of the heterocycle to take up an axial position—the anomeric effect.[32]

Deslongchamps *et al*.[33] have conducted thorough studies based on experimental results and suggested that the minimum value for such anomeric stabilisation to be 1.4–1.5 kcal mol^{-1}. In some cases, the additive anomeric stabilisation was so significant that it overrides the steric factors in controlling the conformation of the tetrahydropyran.[34]

For unsymmetrical 2,8-disubstituted 1,7-dioxaspiro[5.5]undecane, there are four possible chair-chair conformer, interconvertable to each other by inversion of each ring (Scheme 1.2).[34] Based on Deslongchamps *et al*.[33], **23** is the most stable conformer due to the presence of double anomeric stabilisation and minimum steric repulsions.

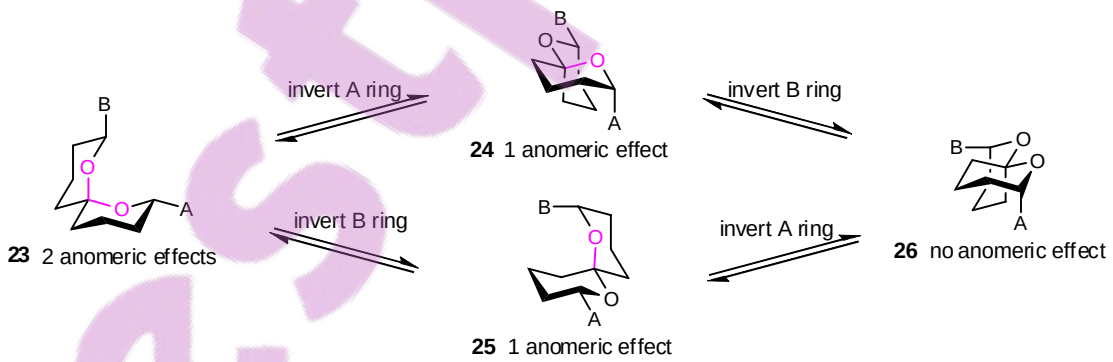

Scheme 1.2: Four conformers **23**–**26** of 2,8-disubstituted spiroacetal.

Many theories have been raised in attempts to explain the anomeric effect. The most widely accepted theory suggests that there is a stabilising interaction between the non-bonding electrons on the oxygen (HOMO) and the vacant σ* non-bonding orbital of the adjacent carbon-heteroatom bond (LUMO) (Scheme 1.3a). This stabilising interaction is maximized when the involving donor and

acceptor orbitals are antiperiplanar to each other resulting in a maximum overlap (Scheme 1.3c).[34] Depending on the origin of the non-bonding electron pair donor, the stabilisation can be sub-divided into two classes. In the dominating *endo* anomeric effect, the donor electron pair originates from the *endo* cyclic heteroatom and is only observed in the axial anomer. In the *exo* anomeric effect, the donor electron pair originates from the *exo* cyclic heteroatom and is observed in both the axial and equatorial anomer (Scheme 1.3b).[34]

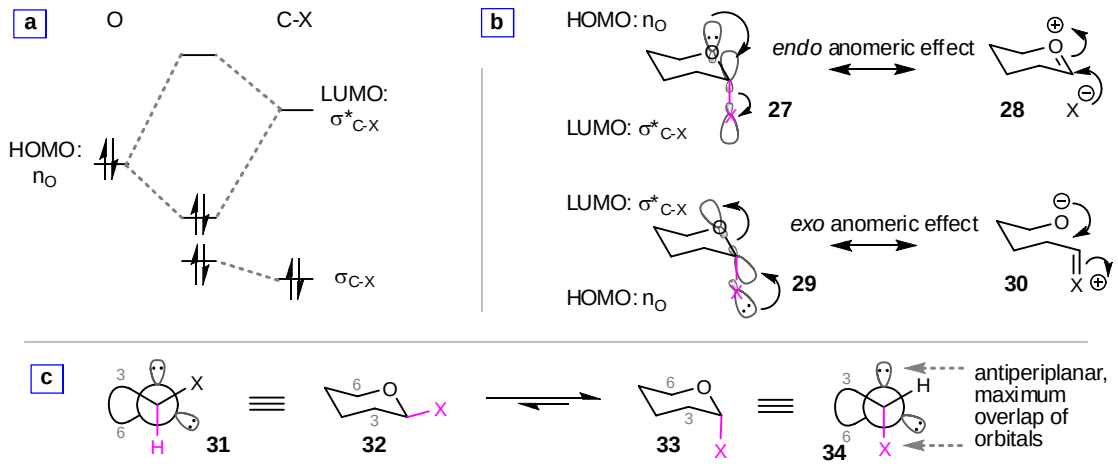

Scheme 1.3: [a] HOMO-LUMO diagram. [b] *Endo* and *exo* anomeric effects. [c] Newman projection of equatorial anomer **31** and axial anomer **34**.

However, it is likely that other stereoelectronic factors, such as dipole moments (Scheme 1.4a) and electrostatic repulsion between the lone pair electrons (Scheme 1.4b), exert a small but significant contribution to the overall configuration of the tetrahydropyran. Depending on the molecule, these effects can reinforce or oppose the anomeric effect and is possibly the reason behind some of the reverse anomeric effects observed.[34]

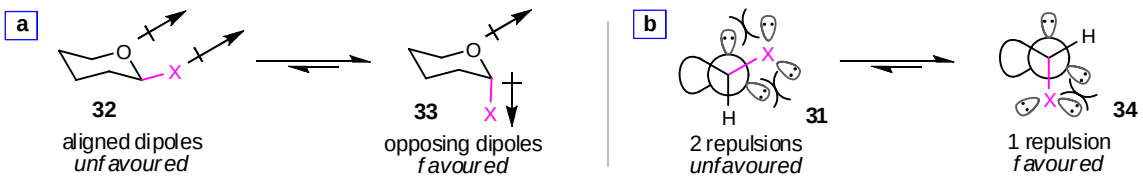

Scheme 1.4: [a] Dipole stabilisation. [b] Electrostatic repulsion between the lone pair electrons.

1.4 Synthesis of 6,6-Spiroacetals

There are a number of strategies to synthesise 6,6-spiroacetals which differ depending on the configuration, disconnection, functionality and structure of the spiroacetal concerned. Several reviews have covered this topic extensively.[12-14,35,36] Hence, the following section will only focus on the general overview of the synthetic strategies and selected recent examples will be discussed (Scheme 1.5).[36]

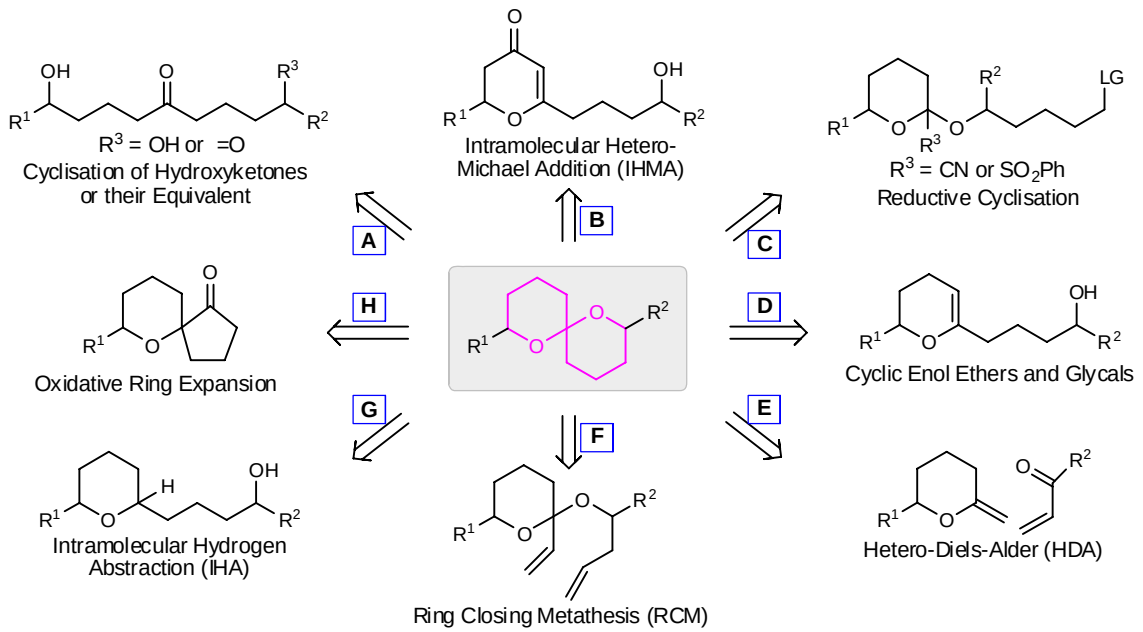

Scheme 1.5: General methods for the synthesis of spiroacetals.[12-14,35,36]

Cyclisations of hydroxyketones or equivalents [**A**] and intramolecular hetero-Michael addition (IHMA) [**B**] are mostly used methods to prepare thermodynamically stable spiroacetals and when the energy difference between the possible isomers is large. Other strategies [**C**]–[**H**], though capable of producing the same isomer, are mainly developed for the enantioselective synthesis of the less stable spiroacetals (Scheme 1.5).

1.4.1 Cyclisation of Hydroxyketones or their Equivalent [A]

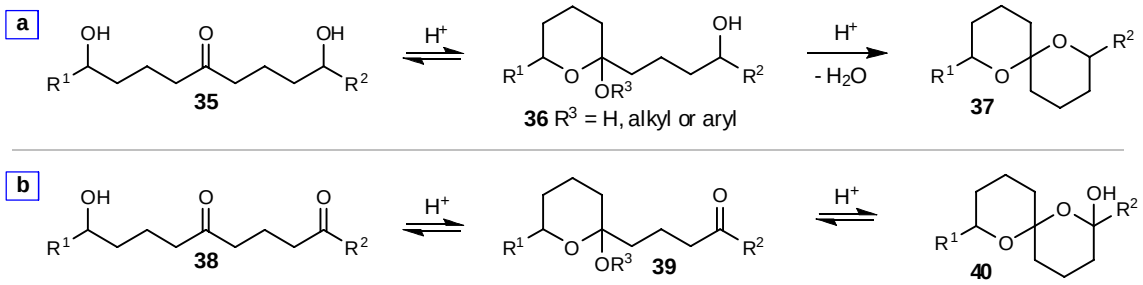

Scheme 1.6: [a] Cyclisation of dihydroxyketones **35** to hemiacetals and acetals **36**, which then dehydrate under acidic conditions to give spiroacetals **37**. [b] Hydroxy diketones **38** equilibrate into spiro-hemiacetals **40** *via* carbonyl cascade cyclisation under acidic conditions.

Cyclisations of hydroxyketones, hemiacetals and acetals are the most commonly used strategy for the synthesis of spiroacetals because the deprotection and cyclisation steps can be done in one step with an appropriate choice of protecting groups and deprotection conditions. The carbonyl group of the acyclic precursors also provides a useful handle for their synthesis. The acyclic hydroxyketones, are usually assembled by the union of functionality bearing units through the $C_{C=O}$–C_{α}

or C_{α}–C_{β} bond followed by acid-catalysed dehydrative cyclisation, *via* the hemiacetal and acetal intermediates, to form the spiroacetals.[12,35,36] Such cyclisations are usually driven by thermodynamic preference and lead to the *bis*-anomerically stabilised spiroacetals (Scheme 1.6).

In the synthesis of spongistatin 1 **(15)**, Paterson *et al.*[37] used aldol condensations extensively to assemble the C1–C15 carbon backbone **45** of the AB rings. The synthesis began with the preparation of chiral ketone **42** from achiral aldehyde **41** and aldehyde **44** from chiral ester **43**. The syntheses of both intermediates involved a crucial boron-mediated aldol condensation to establish the required chirality. The union of ketone **42** and aldehyde **44** was carried by yet another boron-mediated aldol condensation. Triple asymmetric induction, in which the stereo-directing factors from all three chiral components (aldehyde, ketone and boron reagent), acted in a synergistic fashion resulting in a superb yield with high stereoselectivity (97:3 *dr*). Selective desilylation and acid cyclisation of the ketone **45** by catalytic PPTS afforded the thermodynamically favoured spiroacetal **46** (Scheme 1.7).

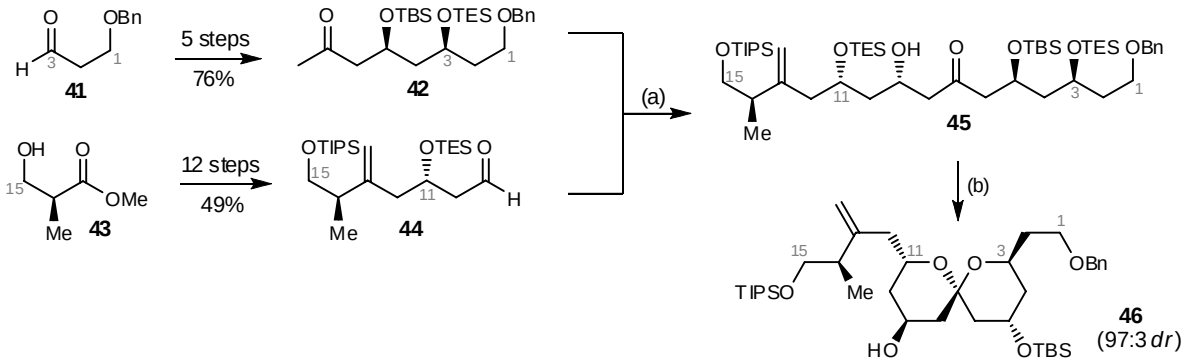

Reagents and conditions: (a) i. **42**, (–)-Ipc_2BCl, NEt_3, Et_2O, 0 °C, 40 min; ii. **44**, Et_2O, -78→-20 °C, 19 h; iii. aq. H_2O_2, MeOH, pH 7 buffer, 0 °C→rt, 2.5 h, 100%; (b) i. cat. PPTS, CH_2Cl_2–MeOH, rt, 40 min; ii. separation and resubjection, 88% (97:3 *dr*).

Scheme 1.7: Synthesis of the C1–C15 spiroacetal **46** present in spongistatin 1 **(15)** by Paterson *et al.*[37]

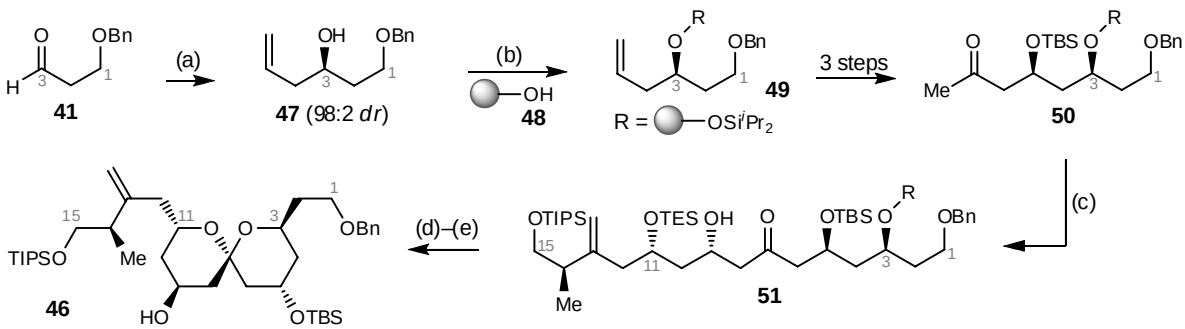

Reagents and conditions: (a) i. 2-^{d}Icr_2BOMe, allylmagnesium bromide, Et_2O, -78 °C, 4 h; ii. aq. H_2O_2, NaOH, H_2O, reflux, 16 h, 93% (98:2 *dr*); (b) i. ^{i}Pr_2SiCl_2, imidazole, DMF, rt, 2 h; ii. hydroxymethylpolystyrene resin **48**, DMF, rt, 24 h; (c) i. NEt_3, (–)-Ipc_2BCl, Et_2O, -78→0 °C, 3 h; ii. **44**, Et_2O, -78→-20 °C, 20 h; iii. aq. H_2O_2, MeOH–DMF, pH 7 buffer, 0 °C→rt, 2.5 h; (d) HF•pyridine, pyridine, THF, rt, 30 min; (e) cat. PPTS, CH_2Cl_2–MeOH, rt, 1 h, 5% over 7 steps on solid support.

Scheme 1.8: Solid phase synthesis of the C1–C15 spiroacetal **46** present in spongistatin 1 **(15)** by Paterson *et al.*[38]

Solid phase syntheses have received enormous attention due to their simple purification procedures, allowing automation and rapid generation of library for biological screening. Paterson *et al*.[38] demonstrated the use of solid phase synthesis for the preparation of the same C1–C15 spiroacetal **46** of spongistatin 1 **(15)** under the equivalent reaction conditions developed for the solution phase synthesis. Ketone **50** was attached to the solid support *via* a silyl bridge which doubled as a protecting group of O3. The union of aldehyde **44** and solid-bound ketone **50** was carried out by boron-mediated aldol condensation under equivalent conditions. Selective desilylation using HF•pyridine cleaved TES ether and the silyl linker of ketone **51** allowing *in situ* cyclisation and subsequent equilibration under acidic conditions to afford the thermodynamically favoured spiroacetal **46** (Scheme 1.8).

Lister and Perkins[39] used the carbonyl cascade cyclisation to form the C7–C20 spiroacetal dihydropyrone core **59** during the total synthesis of auripyrone A **(12)**. An aldol condensation was used to exclusively construct the carbon backbone carrying the hydroxy diketone and other functionalities. The synthesis started with the preparation of C14–C20 ketone **54** from chiral aldehyde **52** and pentan-3-one **(53)** and C7–C13 aldehyde **57** from dipropionate equivalent **55** and chiral aldehyde **56**. Addition of the lithium enolate of ketone **54** to aldehyde **57**, followed by desilylation and oxidation, yielded the linear trione **58**. Hydrogenation of trione **58** unmasked the C9 hydroxyl and triggered acid-catalysed cyclisation to give a spiro-hemiacetal. Subsequent dehydration yielded the thermodynamically favoured C7–C20 spiroacetal dihydropyrone **59** with high diastereoselectivity (94:6 *dr*) (Scheme 1.9).

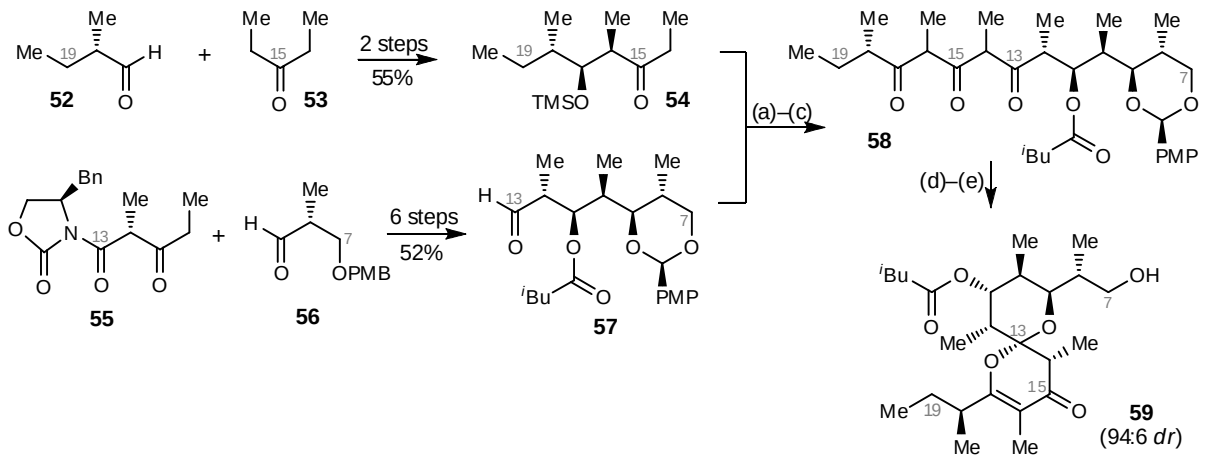

Reagents and conditions: (a) i. **54**. LiHMDS, THF, -78 °C, 30 min; ii. **57**, THF, -78 °C, 2 h, 92% (85% *de*); (b) HF•pyridine, pyridine, THF, rt, 45 min, 96%; (c) Dess-Martin periodinane, H_2O, CH_2Cl_2, rt, 1 h, 100%; (d) H_2, cat. Pd/C, EtOH, rt, 30 min, 87%; (e) cat. Amberlyst-15, CH_2Cl_2, -50 °C→rt, 5 h, 63% (94:6 *dr*).

Scheme 1.9: Synthesis of the C7–C20 spiroacetal dihydropyrone **59** core of auripyrone A **(12)** by Lister and Perkins.[39]

Dias *et al*.[40] used this strategy to synthesise the C9–C20 spiroacetal cores **64** and **65** of antibiotic spirofungins A and B[41], which are epimeric at the C15 spiroacetal centre. Hydrazone **61** was lithiated and added to alkyl iodide **62** which was subsequently hydrolysed to give ketone **63**. One-pot

desilylation and acidolysis of ketone **63** by HF•pyridine afforded a 3:7 diastereomeric mixture of *bis*-anomerically stabilised spiroacetal **64** (core of spirofungin A) and *mono*-anomerically stabilised spiroacetal **65** (core of spirofungin B) in 84% combined yield (Scheme 1.10).

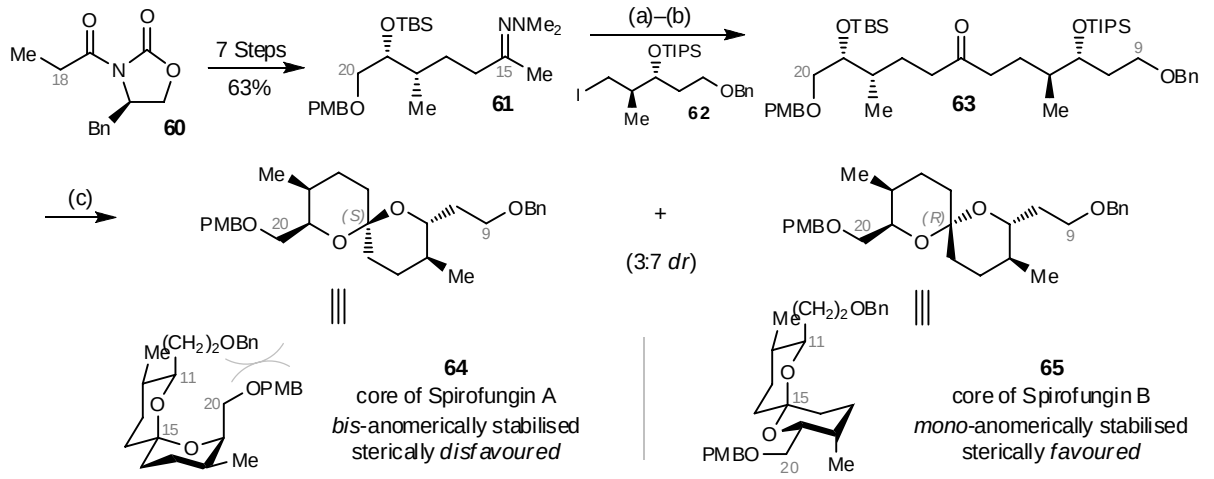

Reagents and conditions: (a) i. BuLi, THF, -78 °C; ii. **62**, THF, -78 °C, 24 h; (b) SiO_2, CH_2Cl_2, rt, 48 h, 87%; (c) HF•pyridine, THF, 25 °C, 84% (**64**:**65**, 3:7 *dr*)

Scheme 1.10: Synthesis of the C9–C20 spiroacetal cores **64** and **65** present in spirofungins A and B by Dias *et al*.[40]

In spirofungin, it was postulated that steric congestion within its spiroacetal core between the C11 and C19 substituents overwrote the anomeric effect to disfavour the *bis*-anomerically stabilised core of spirofungin A **64** and favoured the *mono*-anomerically stabilised core of spirofungin B **65**. As a result, cyclisations performed under thermodynamic conditions would yield a mixture of the two spiroacetals.[40-42] The similar problem was also encountered during the synthesis of closely related reveromycins (Scheme 1.23).

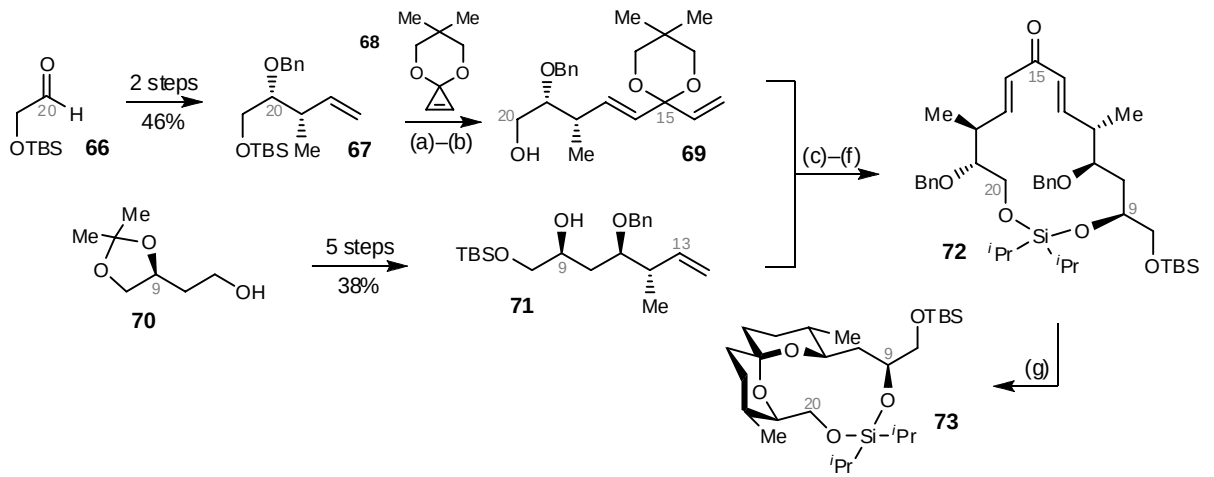

Reagents and conditions: (a) **68**, Grubbs' II catalyst **123**, benzene, 90 °C, 3.5 h, 72%; (b) TBAF, THF, 0 °C→rt, 7 h, 84%; (c) **71**, $^{i}Pr_2SiCl_2$, imidazole, CH_2Cl_2, 0 °C→rt, 17 h; (d) **69**, imidazole, CH_2Cl_2, 0 °C→rt, 4 h; (e) aq. oxalic acid, SiO_2, CH_2Cl_2, rt, 65% over 3 steps; (f) Grubbs' II catalyst **123**, benzene, 90 °C, 8 h, 85%; (g) H_2, cat. Pd/C, EtOAc, rt, 1 h, 98%.

Scheme 1.11: Synthesis of the C9–C20 spiroacetal cores **73** present in spirofungins A by Marjanovic and Kozmin.[42]

Marjanovic and Kozmin[42] solved this problem by exploiting the "nearby" spatial arrangement between the C11 and C19 substituents of the spirofungin A core. By installing a temporary connection between the sterically clashing substituent to form a macrocycle, the cyclisation would be forced to give the desired *bis*-anomerically stabilised spiroacetal. The synthesis began with an intermolecular ring-opening metathesis between alkene **67** and propenone acetal **68** which gave diene **69** after desilylation. Sequential two-step silylation established the required dialkoxysilane connector between alkenes **69** and **71**. Selective removal of 1,3-dioxane and subsequent ring-closing metathesis (RCM) set up the desired 15-membered dienone macrocycle **72**. Hydrogenation unmasked the keto-diol functionality followed by the spontaneous cyclisation, to exclusively gave tricyclic adduct **73** which bore the *bis*-anomerically stabilised spiroacetal required for the spirofungin A core with a silane bridge connecting the C11 and C19 substituents (Scheme 1.11).

Yadav *et al*.[43] utilised a three-component double alkylation of tosylmethyl isocyanide (TosMIC, **76**) to prepare the C19–C36 spiroacetal containing subunit **80** of bistramide A.[44] TosMIC **76** is a synthetically versatile synthon equivalent to a carbonyl dianion[45], similar to that of 1,3-dithiane. The synthesis started with the preparation of iodide **75** and **79** from allyl alcohol **74** and dithiane **78** respectively. TosMIC **76** was sequentially alkylated, first by iodide **75** to yield tosyl isocyanide **77** followed by iodide **79** to afford the crude linear precursor. Subsequent one-pot acid-catalysed desilylation and hydrolysis unmasked the keto-diol functionality of the linear precursor followed by the *in situ* cyclisation to give spiroacetal **80** (Scheme 1.12).

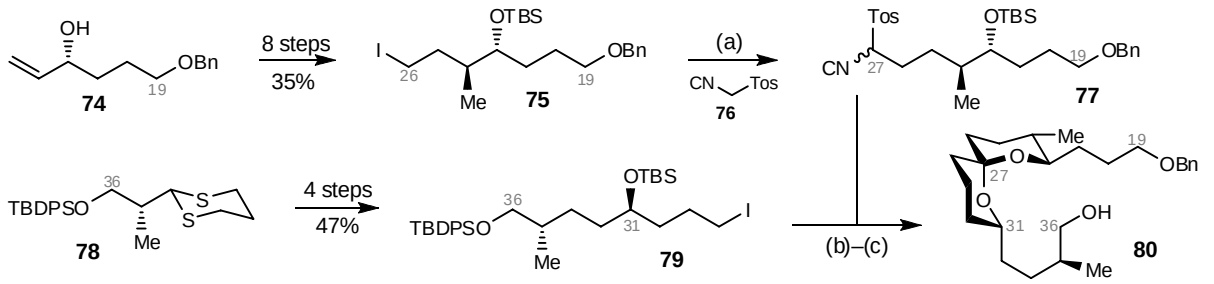

Reagents and conditions: (a) i. **76**, BuLi, HMPA, THF, -78 °C, 45 min; ii. **75**, THF, -78 °C→rt, 1 h, 90%; (b) i. **77**, BuLi, HMPA, THF, -78 °C, 45 min; ii. **79**, THF, -78 °C→rt, 1 h, 83%; (c) aq. HF, MeOH–THF, rt, 1 d, 85%.

Scheme 1.12: Synthesis of the C19–C36 spiroacetal **80** present in bistramide A by Yadav *et al*.[43]

1.4.2 Intramolecular Hetero-Michael Addition (IHMA) [B]

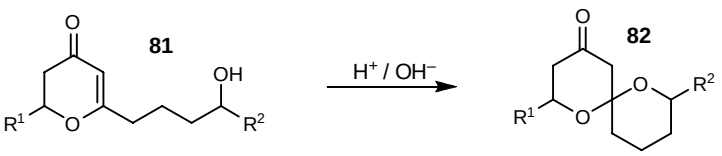

Scheme 1.13: Acid- or base-catalysed intramolecular hetero-Michael addition (IHMA).

In contrast to the cyclisation of dihydroxyketones, intramolecular hetero-Michael addition (IHMA) can be catalysed by base as well as acid (Scheme 1.13). This enables a one-pot deprotection

and cyclisation with an appropriate choice of base labile protecting groups. The carbonyl group in the spiroacetal also provides a versatile handle for prior assembly of the cyclisation precursor as well as functionalisation of the final spiroacetal.[46]

Paterson *et al.*[47] used this strategy to synthesise the C16–C28 CD-rings **89** of spongistatin 1 **(15)**. Boron-mediated aldol coupling between aldehyde **84** and ketone **86** followed by oxidation yielded the dione **87**. Subsequent deprotection and dehydrative cyclisation under acidic conditions gave dihydropyranone **88**. Desilylation unmasked the intermediate alcohol which underwent intramolecular hetero-Michael reaction under basic conditions to give a mixture of spiroacetals **89** and **90**, with only a small preference for the formation of the desired, less stable spiroacetal **89** (Scheme 1.14).

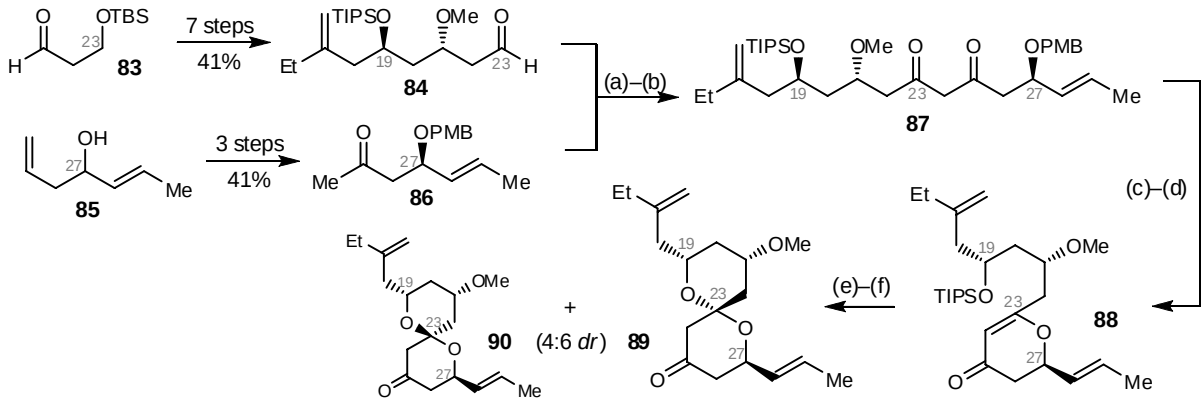

Reagents and conditions: (a) i. **86**, Chx_2BCl, NEt_3, Et_2O, 0 °C, 30 min; ii. **84**, Et_2O, -78→-20 °C, 21 h, iii. aq. H_2O_2, pH 7 buffer, MeOH, 0 °C→rt, 2 h, 72% (84:16 *dr*); (b) Dess-Martin periodinane, CH_2Cl_2, rt, 30 min, 85%; (c) DDQ, CH_2Cl_2–pH 7 buffer, rt, 1 h; (d) PPTS, CD_2Cl_2, rt, 7 d, 72% over 2 steps; (e) TMSOTf, CH_2Cl_2, -78 °C, 15 min; (f) DBU, CH_2Cl_2, rt, 16 h, 67% over 2 steps (6:4 **89**:**90** *dr*).

Scheme 1.14: Synthesis of the C16–C28 spiroacetal **89** present in spongistatin 1 **(15)** by Paterson *et al.*[47]

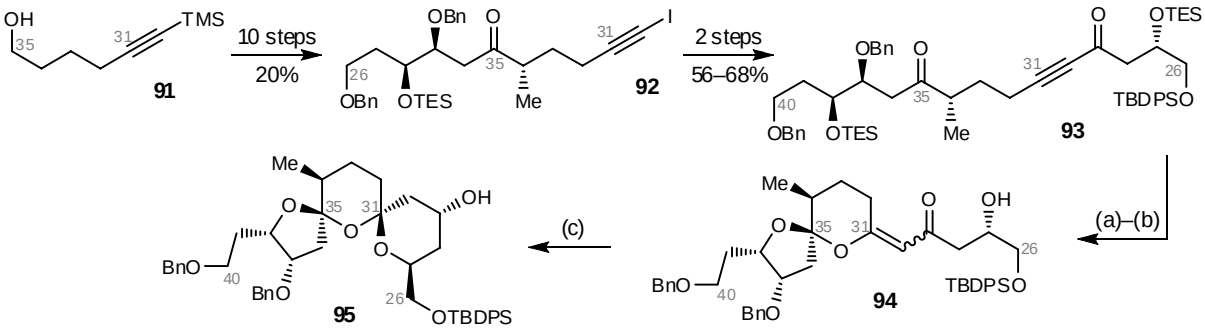

Reagents and conditions: (a) TMSOTf, CH_2Cl_2–MeOH, -78 °C, 5 min; (b) KO^{t}Bu, THF–^{t}BuOH, -20 °C, 20 min; (c) i. cat. CSA, benzene, rt; ii. $NaBH_4$, MeOH, rt, 20 min, 50% over 3 steps.

Scheme 1.15: Synthesis of the C26–C40 *bis*-spiroacetal core **95** present in spirastrellolide B by Wang and Forsyth.[48]

Wang and Forsyth[48] applied a double IHMA for the synthesis of C26–C40 *bis*-spiroacetal core **95** of spirastrellolide B as an extension of this synthetic methodology. The linear ynone **93** was

prepared from iodoacetylene **92** using the Nozaki-Hiyama-Kishi coupling which was, in turn, synthesised from TMS-acetylene **91** using the Mukaiyama aldol coupling. The initial attempts failed to trigger the spontaneous cyclisations of ynone **93** under a variety of acidic conditions or activation of alkyne. On the other hand, the use of a hindered base at low temperature induced the first IHMA of ynone **93** yielding enone **94**. The second IHMA was triggered under acidic conditions and subsequent *in situ* reduction of unstable pyranone gave the desired bis-spiroacetal **95** (Scheme 1.15).

1.4.3 Reductive Cyclisation [C]

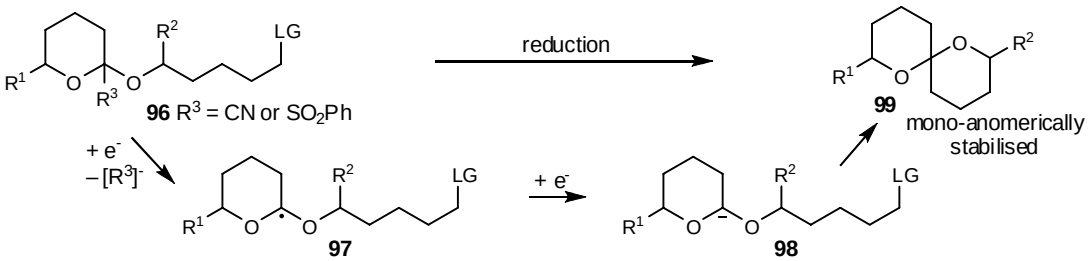

Scheme 1.16: Reductive cyclisation of nitriles or sulfones **96**.

Reductive cyclisation was "the first rational and general synthetic approach" to mono-anomerically stabilised spiroacetals.[49] The excellent stereoselectivity observed arises from the conformational preference of the axial anomeric radical in the transition state which leads to the axial anomeric anion with subsequent intramolecular nucleophilic substitution giving the desired mono-anomerically stabilised spiroacetal (Scheme 1.16).[50]

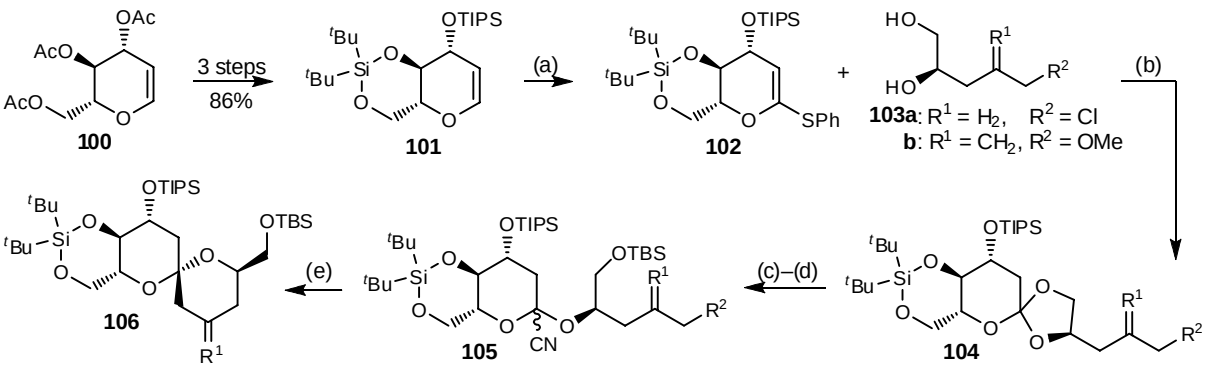

Reagents and conditions: (a) i. ^{t}BuLi, THF, -78→0 °C, 2.5 h; ii. PhSSPh. THF, -78→0 °C, 2 h, 93%; (b) CSA, CH_2Cl_2, 40 °C, 1–3 h, 24–84%; (c) TMSCN, BF_3•OEt_2, CH_2Cl_2, rt, 1 h, 84–88%; (d) TBSCl, imidazole, cat. DMAP, DMF, rt, 19–20 h, 96–97%; (e) LiDBB, THF, -78–-40 °C, 1 h, 71–91%.

Scheme 1.17: Synthesis of mono-anomerically stabilised spiroacetals **106** by Rychnovsky *et al*.[49]

Rychnovsky *et al*.[49] first reported the use of reductive cyclisation for the synthesis of spiroacetals starting with glycals. Glycal **101** was transformed into hemi-thioketene acetals **102**, which then reacted with diols **103** under acid conditions to produce spiro-orthoesters **104**. Cleavage of orthoesters **104** with BF_3•OEt_2 and TMSCN and subsequent silylation gave the diastereomeric

nitriles **105**. Reductive lithiation of anomeric nitriles **105** then generated the desired axial radical. Further reduction yielded the organolithium species which underwent intramolecular alkylation to afford the mono-anomerically stabilised spiroacetals **106** as a single diastereomer (Scheme 1.17).

La Cruz and Rychnovsky[51] applied this strategy to the synthesis of the mono-anomerically stabilised C9–C20 spirofungin B core **114**. Using a similar approach, hemi-thioketene acetal **109** reacted with diol **111** under acid conditions to produce spiro-orthoester **112** which was subsequently cleaved and silylated to give the diastereomeric nitriles **113**. Reductive cyclisation of anomeric nitriles **113** produced the desired spirofungin B spiroacetal core **114** stereospecifically (Scheme 1.18).

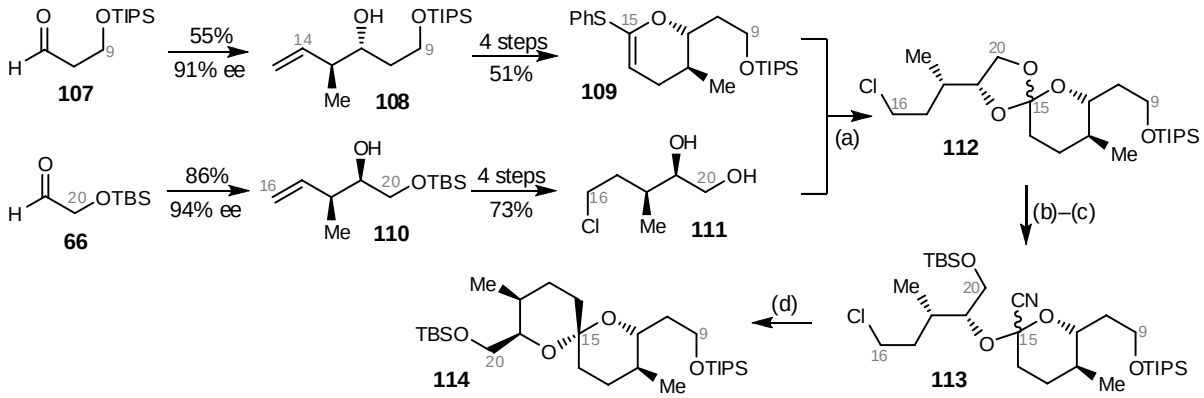

Reagents and conditions: (a) CSA, CH_2Cl_2, rt→40 °C, 1 h, 77%; (b) TMSCN, BF_3•OEt_2, CH_2Cl_2, -78 °C, 16 h, 72%; (c) TBSCl, imidazole, cat. DMAP, DMF, rt, 18 h, 91%; (d) LiDBB, THF, -78 °C, 37 min, 92%.

Scheme 1.18: Synthesis of the C9–C20 spiroacetal **114** present in spirofungin B by La Cruz and Rychnovsky.[51]

1.4.4 Cyclisation of Enol Ethers and Glycals [D]

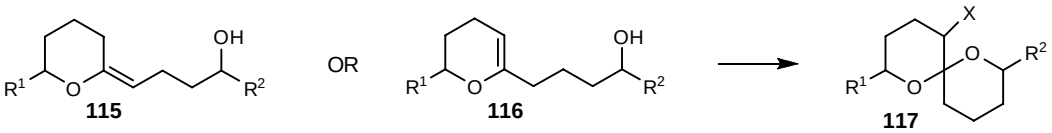

Scheme 1.19: Cyclisation of enol ethers **115** and glycals **116** into spiroacetals **117**.

The acid cyclisation of enol ethers **115** and glycals **116** to afford the thermodynamically stable spiroacetals **117** has been the subject of several reviews.[12,35,36] However, these systems also offer the opportunity to introduce a stereo-directing group which guides the intramolecular electrophilic cyclisation, enabling the synthesis of the less thermodynamically stable isomers of spiroacetals (Scheme 1.19).

Holson and Roush[52] used kinetically controlled iodo-spiroacetalisation to synthesise the mono-anomerically stabilised C17–C28 spiroacetal **126** present in the CD rings of spongistatin 1 **(15)**. The synthesis started with the preparation of carboxylic acid **119** from ester **118**, and alcohol **121** from ester **120**. Union of carboxylic acid **119** and alcohol **121** *via* the Yamaguchi coupling followed by

olefination, ring closing metathesis (RCM) and desilylation yielded glycal **124**. Activation of glycal **124** by *N*-iodosuccinimide (NIS) under kinetic control gave iodonium ion **125** which directed the *trans*-diaxial addition of δ-hydroxyl group to afford the mono-anomerically stabilised spiroacetal **126** (Scheme 1.20).

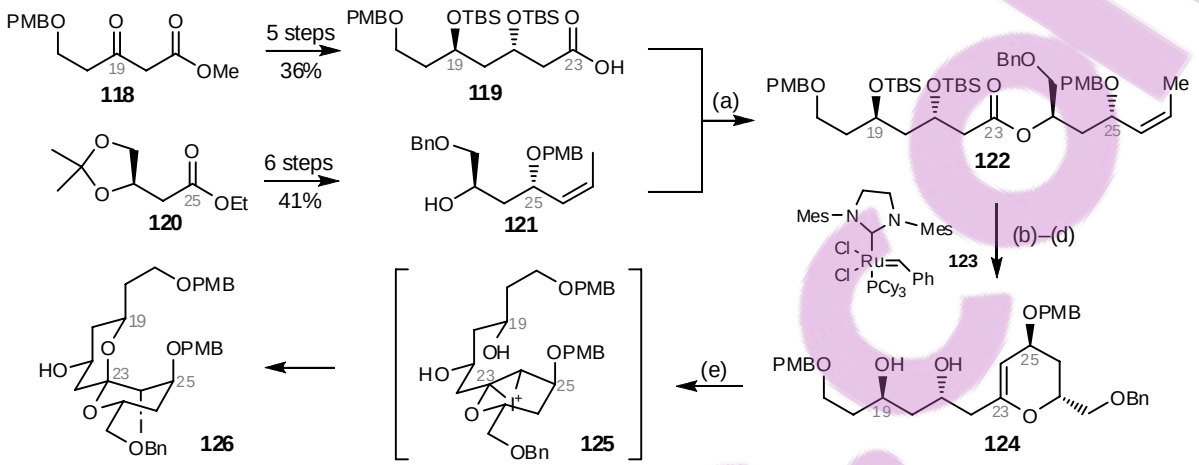

Reagents and conditions: (a) i. **119**, $Cl_3C_6H_2COCl$, NEt_3, CH_2Cl_2, 0 °C→rt, 3 h; ii. **121**, cat. DMAP, CH_2Cl_2, 0 °C→rt, 4 h, 98%; (b) Tebbe reagent, pyridine, THF, 0 °C→rt, 2 h, 75%; (c) Grubbs' II catalyst **123**, benzene, 45 °C, 4 h, 81%; (d) TBAF, THF, 0 °C→rt, 12 h, 90%; (e) NIS, CH_2Cl_2, -90 °C, 1 h, 63%.

Scheme 1.20: Synthesis of the C17–C28 spiroacetal **126** present in spongistatin 1 **(15)** by Holson and Roush.[52]

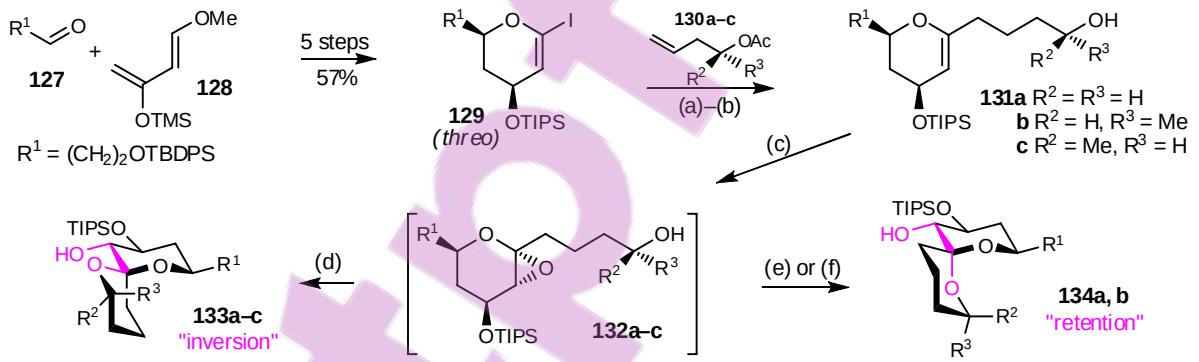

Reagents and conditions: (a) i. **130**, 9-BBN, THF, rt, 3 h; ii. aq. NaOH, rt, 30 min; iii, **129**, cat. $Pd(dppf)Cl_2$, THF–H_2O, rt, 1 h, 85–90%; (b) K_2CO_3, THF–MeOH, rt, 3 h, 98–100%; (c) DMDO, CH_2Cl_2–acetone, -63 °C, 20 min; (d) MeOH, -63 °C, 1 h, 85–93%; (e) *p*-TsOH, CH_2Cl_2, rt, 1 h, 99–100%; (f) $Ti(O^iPr)_4$, CH_2Cl_2–acetone, -78→0 °C, 1 h, 74%.

Scheme 1.21: Stereocontrolled synthesis of spiroacetals **133** and **134** by Tan *et al.*[53] Only spiroacetals from the *threo* series are depicted here. Spiroacetals from the *erythro* series are listed in Scheme 1.32.

Tan *et al.*[53] investigated the spirocyclisation of glycals **131**, *via* reactive epoxides **132** generated *in situ*, to access the mono-anomerically stabilised spiroacetals **133**. Glycals **131** were obtained from *B*-alkyl Suzuki-Miyaura cross-coupling between vinyl iodide **129** and the reactive alkylborate reagents *in situ*, produced by one-pot generation (alkenes **130** + 9-BBN) and base activation of the resulting alkylborane reagents. Vinyl iodide **129**, in turn, was synthesised *via* hetero-Diels-Alder reaction between aldehyde **127** and diene **128**. *Anti*-epoxidation of glycals **131** by dimethyldioxirane (DMDO) at -63 °C formed epoxide **132** *in situ* and subsequent fast addition of

excess MeOH at -63 °C facilitated the *trans*-diequatorial opening of the epoxide ring ("inversion") to give the mono-anomerically stabilised spiroacetals **133** with 100% stereoselectivity. On the other hand, addition of $Ti(O^iPr)_4$ to the epoxides **132** formed a tether between the epoxide ring oxygen and the side chain hydroxyl group. The Lewis acid then activated the epoxide electrophile to form an oxonium intermediate which was trapped by the tethered nucleophilic hydroxyl group ("retention") yielding the *bis*-anomerically stabilised spiroacetals **134**. Exposure of the diastereomeric mixtures to *p*-TsOH also gave the thermodynamically stable spiroacetals **134** in excellent yields (Scheme 1.21).

1.4.5 Cyclisation by Hetero-Diels-Alder Reaction (HDA) [E]

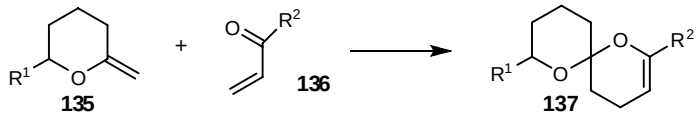

Scheme 1.22: Hetero Diels-Alder reaction (HDA) between methylene pyrans **135** and α,β-unsaturated carbonyls **136**.

The hetero-Diels-Alder (HDA, Scheme 1.22) reaction provides a high level of stereoselectivity with the use of an appropriate catalyst.[36] When executed under kinetic conditions in order to avoid equilibration, this method is particularly useful for the synthesis of spiroacetals that are not the most thermodynamically stable isomer.

In the spiroacetal core of reveromycin A[54], a steric clash between the substitutents at the anomeric positions caused an undesired isomerisation between the *bis*- and mono-anomerically stabilised spiroacetals. The same problem was also encountered during the synthesis of closely related spirofungins (Scheme 1.10 and 1.11).

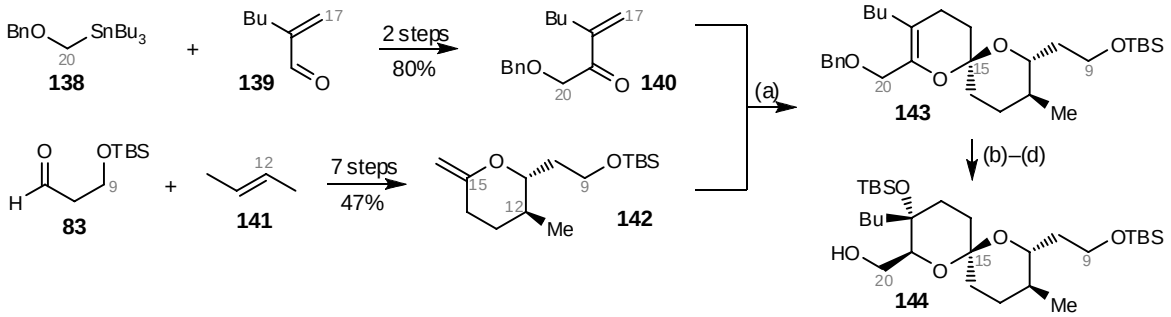

Reagents and conditions: (a) cat. $Eu(fod)_3$, neat, 0 °C, 72 h, 40%; (b) i. BH_3•THF, THF, 0 °C, 2.5 h; ii. aq. H_2O_2, NaOH, rt, 2 h, 72%; (c) TBSOTf, 2,6-lutidine, CH_2Cl_2, -78 °C; (d) H_2, cat. $Pd(OH)_2$, MeOH, rt, 2 h, 90% over 2 steps.

Scheme 1.23: Synthesis of the C9–C20 spiroacetal **144** present in reveromycin A by Rizzacasa *et al.*[55]

Rizzacasa *et al.*[55] circumvented this problem of reveromycin A by using an inverse electron demand HDA reaction in their synthesis of the C9–C20 spiroacetal core **144**. The synthesis started with the preparation of *α,β*-unsaturated ketone **140** from stannane **138** and aldehyde **139**, and chiral

methylene pyran **142** from aldehyde **83** and *trans*-2-butene **(141)**. The key cycloaddition between the neat mixture of enone **140** and dienophile **142** was catalysed by Lewis acid $Eu(fod)_3$ to afford the desired glycal **143** as one diastereoisomer. Subsequent hydroboration, silylation and debenzylation yielded spiroacetal **144** (Scheme 1.23).

1.4.6 Cyclisation by Ring Closing Metathesis (RCM) [F]

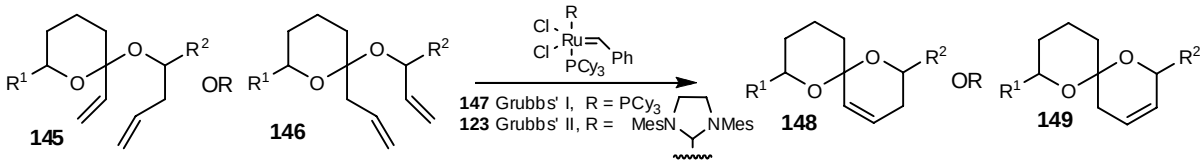

Scheme 1.24: Cyclisation of dienes **145** or **146** by ring closing metathesis (RCM) mediated by Grubbs' first generation **147** or second generation **123** catalysts.

Ring-closing metathesis (RCM, Scheme 1.24) is an important strategy for natural product synthesis.[56] However, there are only few examples in which RCM has been used for the synthesis of spiroacetals.[57]

Hsung *et al*.[58,59] applied this "conceptually different but general" strategy for the synthesis of the alkene containing C11–*epi*–C22–C23 spiroacetal **156** * , an epimer of the BC rings of spirastrellolide A[60]. The synthesis started with the transformation of glucose **(150)** into vinyl alcohol **151** which was then converted to lactone **152**. Addition of vinylmagnesium bromide to lactone **152** gave lactol **153** which was then condensed with chiral alcohol **154** using Brønsted acid (*bis*-trifluoromethanesulfonyl)amine (Tf_2NH), to yield the desired acetal **155**. RCM of diene **155** using Grubbs' first generation catalyst **147** yielded spiroacetal **156** with no loss of stereochemical integrity at the spiro centre (Scheme 1.25).

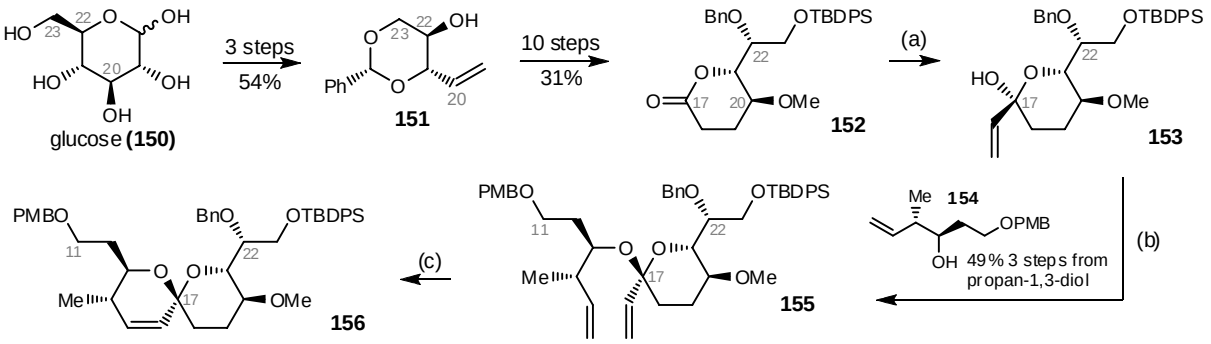

Reagents and conditions: (a) vinylmagnesium bromide, Et_2O, -78 °C, 1 h, 73%; (b) **154**, Tf_2NH, 4 Å MS, CH_2Cl_2, -78 °C, 30 min; (c) Grubbs' I catalyst **147**, benzene, rt, 30 min, 50% over 2 steps.

Scheme 1.25: Synthesis of the C11-*epi*-C22-C23 spiroacetal **156** present in spirastrellolide A by Hsung *et al*.[58,59]

* The stereochemistry at C22 was not assigned at the time when the study began. Since then, the authors had steered their focus to the feasibility of the acetal-tethered RCM approach to the synthesis of spiroacetals.

1.4.7 Intramolecular Hydrogen Abstraction (IHA) [G]

Alkoxy radicals **159**, generated photolytically from alcohol **157** and hypoiodite oxidant (IOAc), undergo an intramolecular abstraction of hydrogen atom at the anomeric position followed by oxidation and cyclisation to give the spiroacetal **37**.[36] This mild radical oxidative cyclisation proceeds under kinetic control to construct a spiroacetal unit in which the energy difference between isomers is small.[61]

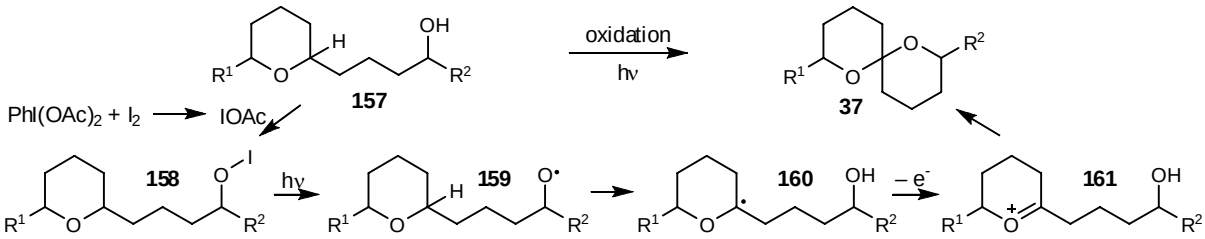

Scheme 1.26: Synthesis of spiroacetals **37** from alcohols **157** by intramolecular hydrogen abstraction (IHA).

Suárez *et al*.[62] used this strategy to construct a 6,6,5-*bis*-spiroacetal model system and the first IHA leading to the preparation of 6,6-spiroacetal segment is discussed here. The study began with the synthesis of pyran **163** from acetonide **162**. Benzyl pyran **163** was then transformed into hydroxybutyl pyran **164** which was subsequently cyclised by photolysis in the presence of iodobenzene diacetate and iodine to give isomeric spiroacetals **165** and **166**. The mono-anomerically stablised spiroacetal **166** was converted into the more stable spiroacetal **165** quantitatively under acidic conditions (Scheme 1.27).

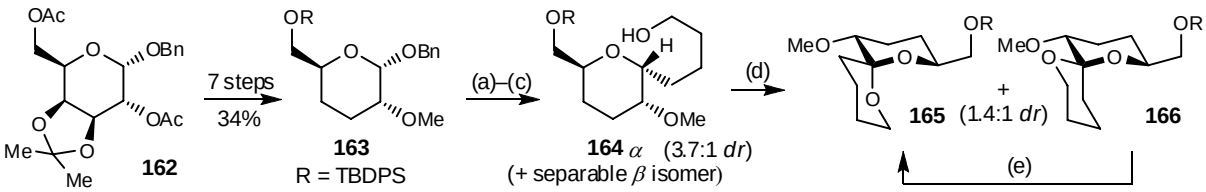

Reagents and conditions: (a) BCl_3•SMe_2, CH_2Cl_2, rt, 14 h, 74%; (b) i. Ph_3P, CCl_4, THF, reflux, 3 h; ii. CH_2=$CH(CH_2)_3MgBr$, Et_2O, 0 °C, 1 h, 74%, (α:β 3.7:1 *dr*); (c) i. O_3, CH_2Cl_2–MeOH, -78 °C; ii. $NaBH_4$, rt, 4 h, 95%; (d) $PhI(OAc)_2$, I_2, hν, cyclohexane, 40 °C, 70 min, 87% (**165**:**166**, 1.4:1 *dr*); (e) HCl, AcOH, rt, 2 h, 100%.

Scheme 1.27: Synthesis of spiroacetals **165** and **166** by Suárez *et al*.[62]

1.4.8 Oxidative Ring Expansion [H]

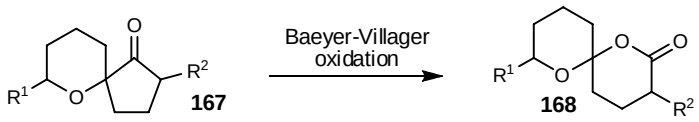

Scheme 1.28: Oxidative ring expansion of cyclopentanones **167** by Baeyer-Villager oxidation.

In contrast to other strategies, the bicyclic structure is formed prior to the spiroacetal-forming ring expansion step in the Baeyer-Villager oxidation of cyclopentanones **167** (Scheme 1.28). This

strategy is rarely used due to the intolerance of the functionality and the development of better alternative approaches.

Haddad *et al*.[63] investigated the use of this strategy for the diastereoselective synthesis of model spiroacetal systems. Cyclobutane **171** was synthesised diastereoselectively by the coupling of malonate **169** and bromide **170** followed by an intramolecular photocycloaddition of the resulting adduct. Cyclobutane **171** was subsequently cleaved under acidic conditions to give cyclopentanone **172a**. Alternatively, reduction and oxidation of cyclobutane **171** yielded cyclopentanone **172b**. Baeyer-Villager oxidation of cyclopentanones **172** by *m*-CPBA yielded spirolactones **173** with no epimerisation at the spiro-centre (Scheme 1.29).

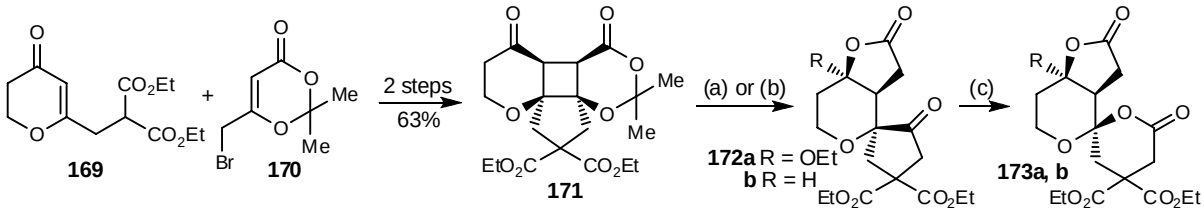

Reagents and conditions: (a) cat. *p*-TsOH, EtOH, rt, 18 h, **172a**: 57%; (b) i. $NaBH_4$, EtOH–THF, -70 °C, 25 min; ii. Jones' reagent, EtOAc–Et_2O, rt, 6 h, **172b**: 54%; (c) *m*-CPBA, cat. Li_2CO_3, CH_2Cl_2, rt, 5 h, 70–75%.

Scheme 1.29: Synthesis of oxaspirolactones **173** by Haddad *et al*.[63]

1.5 Diversity-Oriented Synthesis of 6,6-Spiroacetals

Diversity-oriented synthesis (DOS) involves the deliberate, simultaneous and efficient synthesis of more than one target compound with the intention of answering complex problems such as binding, catalysis, phenotypic effects etc.[64] It requires a forward-synthetic analysis: a problem-solving technique for transforming a collection of simple and similar starting materials into a collection of structurally more complex and diverse products.[65] Prevalidated by nature, the spiroacetal framework makes an ideal candidate for the development of natural product derived compounds and the incorporation of this rigid scaffold into DOS.[66]

1.5.1 An Early Example

Mead and Zemribo[67] stated that "the majority of spiroacetals found in nature, the ring system is functionalised alpha (C2) to at least one ring oxygen", thus conducting a study of nucleophilic substitution at the C2 position of spiroacetals. Their early work involved the preparation of hydroxy dicarbonyl equivalent **178** from cyclopentanone **(174)** and alkene **175**. Subsequent Lewis acid-catalysed carbonyl cascade cyclisation of hydroxy dicarbonyl equivalent **178** yielded methoxy spiroacetal **179**. Addition of TMSOTf generated a C2-centered oxonium ion from methoxy

spiroacetal **179** which was trapped by silylated nucleophiles to give spiroacetals **180**. It was later found that β-lactone **177**, the precursor of hydroxy dicarbonyl equivalent **178**, can be directly cyclised and substituted diastereospecifically in one-pot under the influence of a Lewis acid to give spiroacetals **181** (Scheme 1.30).[67]

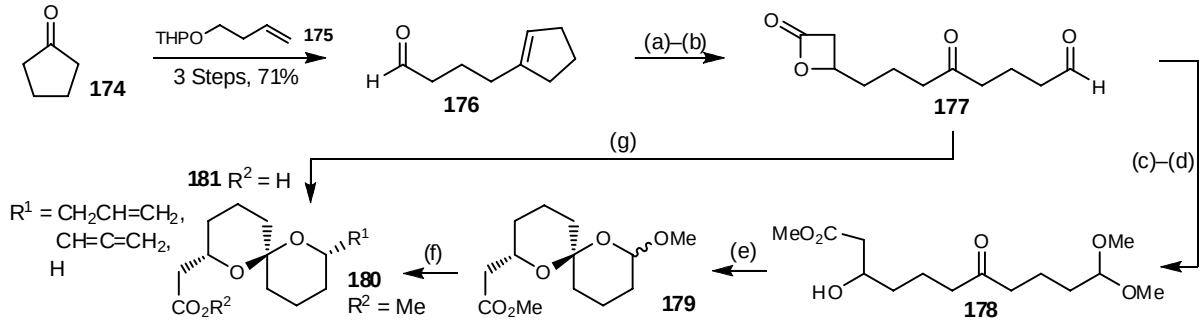

Reagents and conditions: (a) i. TMS-ketene, cat. BF_3•OEt_2, CH_2Cl_2, 0 °C; ii. KF•$2H_2O$, MeCN, rt, 73%; (b) i. O_3, MeOH, -78 °C; ii. Me_2S, 77%; (c) *p*-TsOH, MeOH, rt; (d) K_2CO_3, MeOH, rt, 5 min, 92% over 2 steps; (e) cat. BF_3•OEt_2, CH_2Cl_2, -5 °C, 78%; (f) allyltrimethylsilane or propargyltrimethylsilane or diphenylmethylsilane, TMSOTf, CH_2Cl_2, -50 °C, 1.0–1.5 h, **180**: 65–68%; (g) allyltrimethylsilane or propargyltrimethylsilane or diphenylmethylsilane, TMSOTf, CH_2Cl_2, -50 °C, 30–45 min, **181**: 65–75%.

Scheme 1.30: Early studies on the synthesis of spiroacetals **179**–**181** by Mead and Zemribo.[67]

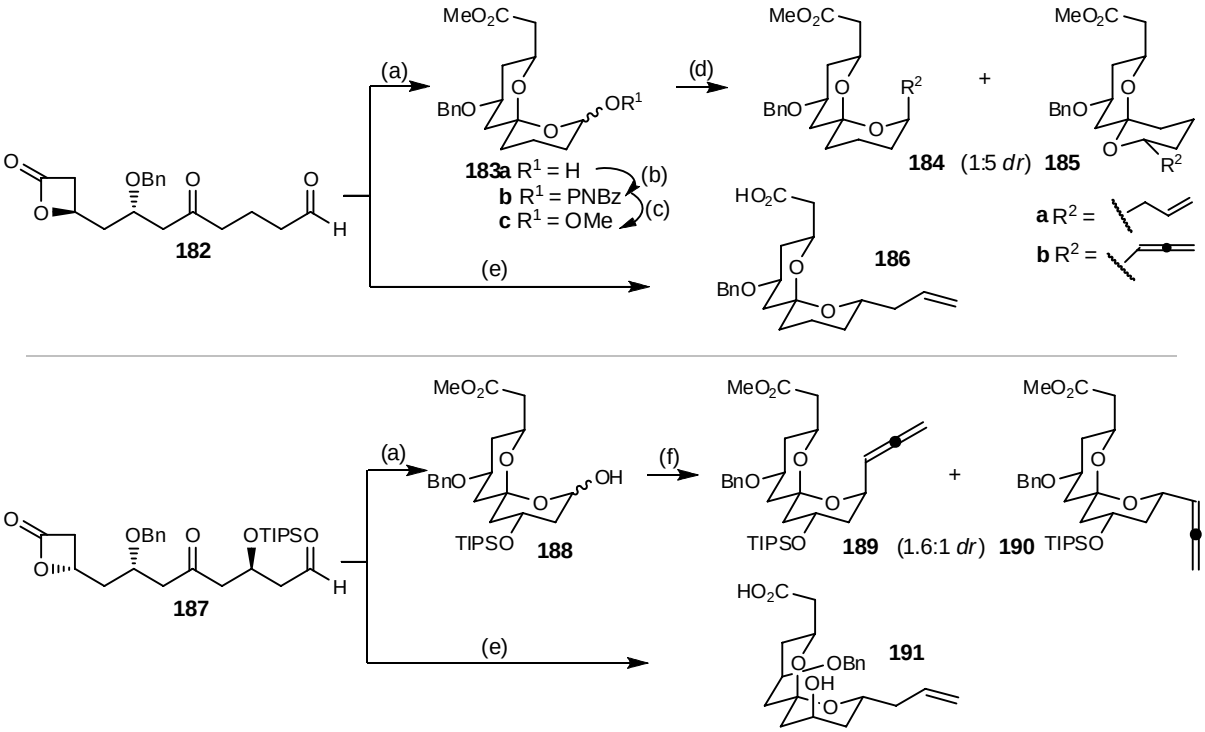

Reagents and conditions: (a) K_2CO_3, MeOH, rt, 93–94% (eq:ax 3:1 *dr*); (b) PNBzCl, NEt_3, Et_2O, rt, 87% (eq:ax 3:1 *dr*); (c) MeOH, TMSOTf, MeCN, -37 °C, 88% (eq only); (d) one of the following: **183a**, allyltrimethylsilane, BF_3•OEt_2, CH_2Cl_2, -42 °C, 75% (**184a**:**185a** 1:5 *dr*); or **183a**, propargyltrimethylsilane, BF_3•OEt_2, CH_2Cl_2, -42→-20 °C, 76% (**184b**:**185b** 1:5 *dr*); or **183b**, allyltrimethylsilane, TMSOTf, MeCN, -38 °C, 86% (**184a**:**185a** 1:5 *dr*); or **183c**, allyltrimethylsilane, TMSOTf, CH_2Cl_2, -42→-20 °C, 51% (**184a**:**185a** 1:5 *dr*); (e) allyltrimethylsilane, TMSOTf, CH_3CN, -37 °C, 69–75%; (f) propargyltrimethylsilane, BF_3•OEt_2, CH_2Cl_2, -42→15 °C, 82% (**189**:**190** 1.6:1 *dr*).

Scheme 1.31: Studies on the synthesis of spiroacetals **183**–**186** and **188**–**191** by Mead *et al.*[68]

These findings prompted further investigation into the stereospecific β-lactone-initiated spiroacetal synthesis with other substitution patterns. When spiroacetals such as **183** or **188**, which contained a methyl ester on the adjacent ring, were used, the C2 substitution reaction gave a mixture of equatorial and axial spiroacetals **184**/**185** or **189**/**190** in a particular ratio (**184**:**185** 1:5 *dr* or **189**:**190** 1.6:1 *dr*) regardless of the reaction conditions, the nature and stereochemistry of the leaving group or the Lewis acid used. This indicated the involvement of an oxonium transition state and a small energy difference between the isomers. Hence, it was difficult to predict the equilibrium position between the isomers. However, during the one-pot β-lactone-initiated spiroacetal synthesis using β-lactone such as **182** or **187**, the neighbouring carboxylic acid participated in the oxonium ion transition state which effectively shielded the axial face from nucleophilic attack. This resulted in the diastereospecific formation of a single spiroacetal **186** or **191** with equatorial substitution (Scheme 1.31).[68]

1.5.2 Process-driven Generation of Spiroacetal Libraries during the Development of Synthetic Methods

Tan *et al*.[53] developed a method for the stereocontrolled spirocyclisation of epoxides **132** or **192** to access a range of spiroacetals with both "inversion" and "retention" of configuration. Additions of MeOH to epoxides **132** or **192** at -63 °C resulted in cyclisation with "inversion" of configuration in which the epoxide oxygen was *anti* to the oxygen of the newly cyclised ring. This method afforded mono-anomerically stabilised spiroacetal **133** from *threo* epoxide **132** or *bis*-anomerically stabilised spiroacetal **193** from *erythro* epoxide **192** (Scheme 1.32).

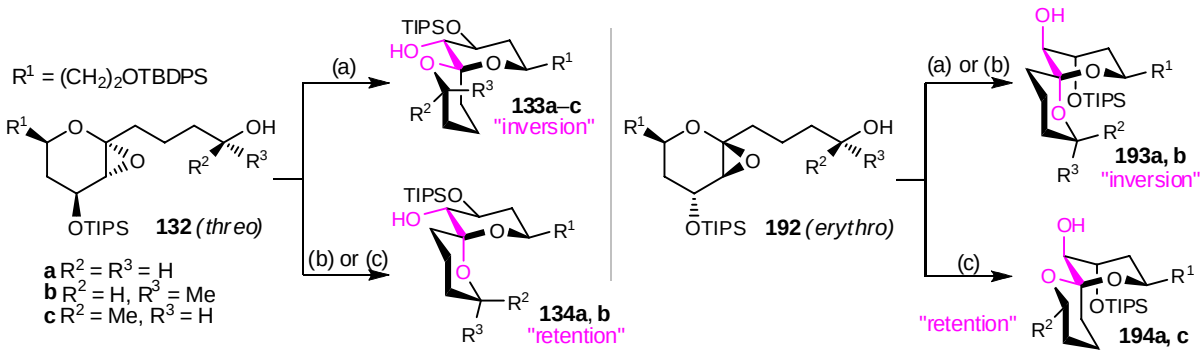

Reagents and conditions: (a) MeOH, -63 °C, 1 h, 73–93%; (b) *p*-TsOH, CH_2Cl_2, rt, 1 h, 82–100%; (c) $Ti(O^iPr)_4$, CH_2Cl_2–acetone, -78→0 °C, 1 h, 74–82%.

Scheme 1.32: Stereocontrolled synthesis of spiroacetals by Tan *et al*.[53] The synthesis of *threo* epoxide **132** was depicted in Scheme 1.21. Only the 6,6-spiroacetals are shown here.

On the other hand, additions of $Ti(O^iPr)_4$ to epoxides **132** or **192** resulted in the coordination of the participating oxygens leading to the cyclisation with "retention" of configuration such that the epoxide oxygen was *syn* to the oxygen of the newly cyclised ring (Scheme 1.21). This method afforded *bis*-anomerically stabilised spiroacetal **134** from *threo* epoxide **132** or mono-anomerically

stabilised spiroacetal **194** from *erythro* epoxide **192**. Addition of *p*-TsOH effected the equilibration of the diastereomeric mixtures into the most thermodynamically stable isomer, usually the *bis*-anomerically stabilised spiroacetal such as **134** or **193** (Scheme 1.32). These stereocontrolled cyclisations were then applied to other epoxides generating a library of spiroacetals of different ring sizes and substitution patterns.[53]

Hsung *et al*.[59,69] used RCM for the construction of a library consisting of 20+ simple spiroacetals. Using glycal **195** as the starting material, RCM was demonstrated to be applicable for the synthesis of spiroacetals of different ring sizes up to a eight-membered ring with no loss of stereochemical integrity at the spirocentre. The presence of the resulting alkene in the resulting spiroacetal ring also allowed further functionalisation such as dihydroxylation or hydrogenation as shown below (Scheme 1.33).

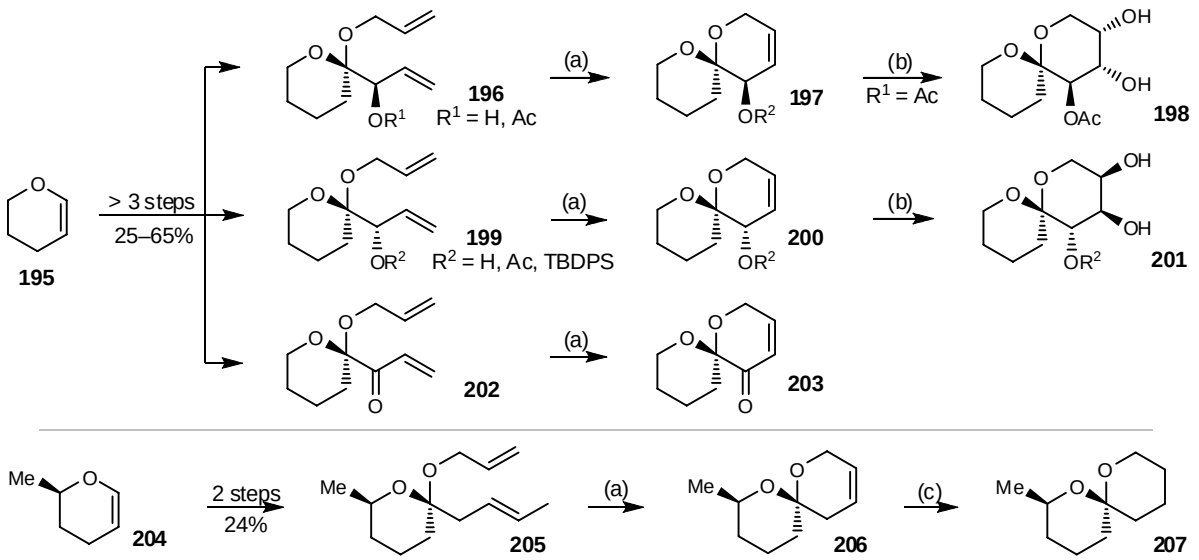

Reagents and conditions: (a) Grubbs' I catalyst **147**, CH_2Cl_2, rt, 30 min, 70–90%; (b) cat. K_2OsO_4•$2H_2O$, NMO, acetone–H_2O, rt, 12 h, 82–90%; (c) H_2, cat. Pd/C, EtOAc, rt, 3 h, 75%.

Scheme 1.33: Synthesis of simple spiroacetals framework using RCM by Hsung *et al*.[59,69] Only the 6,6-spiroacetals are shown here.

1.5.3 Product-driven Systematic Generation of Spiroacetal Libraries

Porco *et al*.[70] conducted the first product-driven systematic combinatorial synthesis of a library based on a spiroacetal scaffold **214** with three sites of elaboration. The synthesis of spiroacetal core **213** started with aldol coupling between silyl enol ether of ketone **209** and aldehyde **211** to give diastereomeric β-hydroxy ketones **212**. Oxidation and one-pot acidic desilylation and cyclisation constructed the basic spiroacetal framework which was then transformed into the spiroacetal core **213**. Elaboration of spiroacetal **213** using solution phase parallel synthesis techniques led to the preparation of a library of 21 spiroacetal analogues **214**.

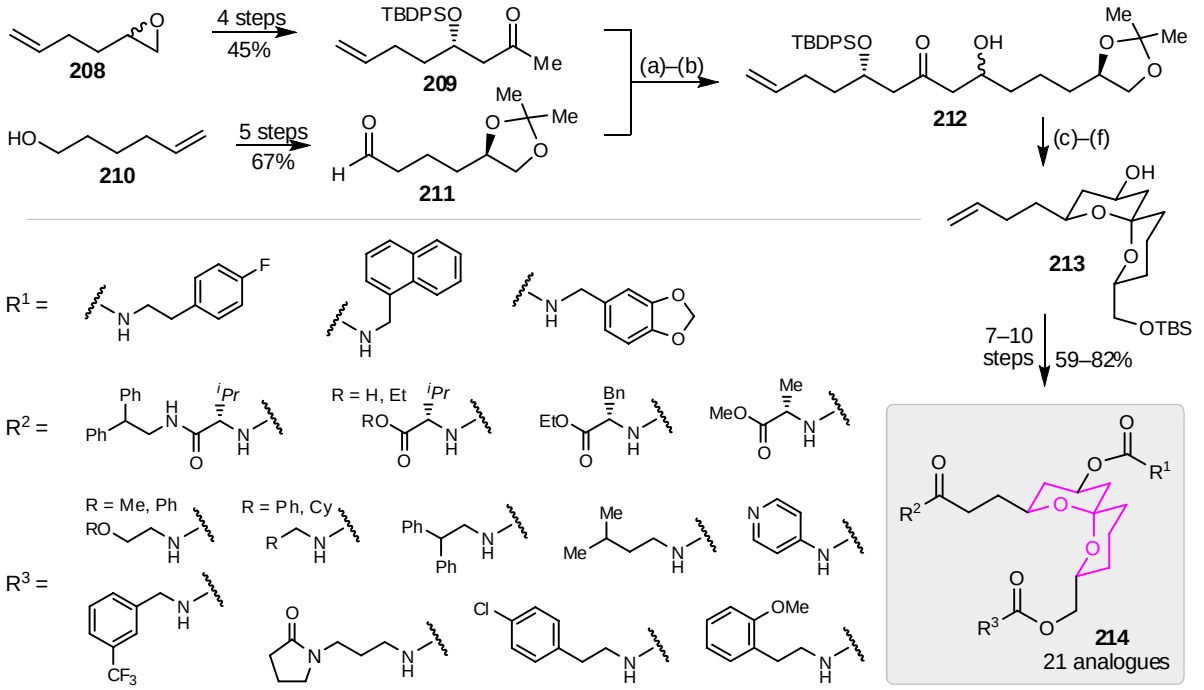

Reagents and conditions: (a) i. **209**, KHMDS, THF, -78 °C, 1.5 h; ii. TMSCl, -78 °C, 2 h, 98%; (b) **211**, BF_3•OEt_2, -78 °C, 1.5 h, 65%; (c) CrO_3, Celite®, pyridine, CH_2Cl_2, rt, 3.5 h, 64%; (d) aq. HF, CH_3CN–CH_2Cl_2, rt, 24 h, 80%; (e) TBSCl, imidazole, DMF, rt, 12 h, 90%; (f) $CeCl_3$•$7H_2O$, $NaBH_4$, MeOH, 0 °C, 30 min, 70%.

Scheme 1.34: Combinatorial synthesis of molecules based on spiroacetal scaffold **214** by Porco *et al.*[70]

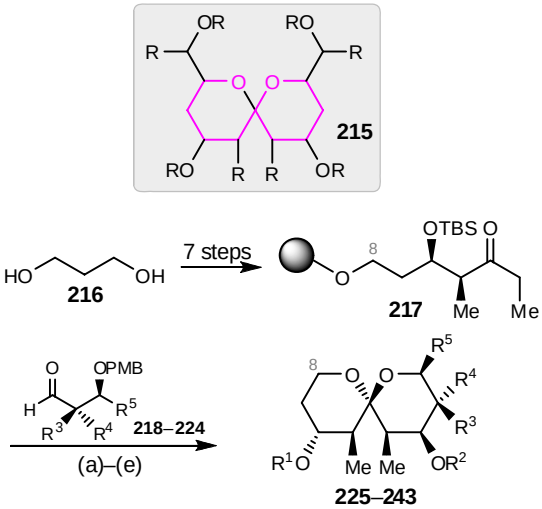

	R^1	R^2	R^3	R^4	R^5	Overall Yields
225	TBS	TBS	H	H	H	16%
f → **226**	H	H	H	H	H	13%
227	TBS	Ac	H	H	H	14%
228	TBS	TBS	H	Me	H	13%
229	TBS	Ac	H	Me	H	10%
f → **230**	H	Ac	H	Me	H	8%
231	TBS	TBS	Me	H	H	10%
232	TBS	Ac	Me	H	H	11%
233	TBS	TBS	H	H	CH_2Bn	6%
234	TBS	Ac	H	H	CH_2Bn	9%
f → **235**	H	Ac	H	H	CH_2Bn	5%
236	TBS	TBS	H	H	CH_2OTBS	7%
237	TBS	Ac	H	H	CH_2OTBS	5%
238	TBS	Ac	H	H	CH_2OBn	4%
239	TBS	TBS	H	H	$(CH_2)_2OH$	7%
240	TBS	Ac	H	H	$(CH_2)_2OBn$	14%
f → **241**	H	Ac	H	H	$(CH_2)_2OBn$	10%
242	TBS	TBS	H	H	Me	6%
243	TBS	Ac	H	H	Me	7%

Reagents and conditions: (a) $(Cy)_2BCl$, NEt_3, Et_2O, 0 °C, 24 h; (b) **218–224**, Et_2O, -78→20 °C, 26 h; (c) aq. H_2O_2, pH 7 buffer, MeOH–DMF, 0 °C, 4 h; (d) TBSCl, cat. DMAP, imidazole, CH_2Cl_2–DMF, rt, 24 h or Ac_2O, pyridine, cat. DMAP, THF, rt, 20 h; (e) DDQ, pH 7 buffer, CH_2Cl_2, 0 °C→rt, 6 h; (f) TBAF, THF, rt, 1–2 d.

Scheme 1.35: Natural product inspired synthesis of spiroacetals **225–243** by Waldmann *et al.*[66] A second series of 16 spiroacetals bearing a C8-substituent (Me or CH_2OBn) was generated similarly using modified solid-bound ketones (not shown).

Waldmann *et al.*[66] chose the general structure **215** with up to 8 possible sites of diversification, as their target aiming to construct a structurally diverse spiroacetal-based library. The library synthesis began with the transformation of propanediol **(216)** into solid-bound ketone **217**. Boron-mediated aldol coupling between ketone **217** and a range of aldehydes **218**–**224** yielded the first series of 19 spiroacetals **225**–**243** (Scheme 1.35). The second series of 16 spiroacetals bearing a C8-substituent (Me or CH_2OBn) was also generated similarly using modified solid-bound ketones (not shown). Subsequent bio-assays suggested that **229** was a moderate inhibitor of protein tyrosine phosphatase 1b [IC_{50} = 39 μM] and a good inhibitor of phosphatase VHR (IC_{50} = 6 μM) whereas **232** was a moderate inhibitor of phosphatase VHR (IC_{50} = 31 μM). Both **229** and **232** showed no activity against phosphatase Cdc25a and serine-threonine phosphatase 1 (PP1) but affected the organisation of the microtubule cytoskeleton in cells without direct targeting of microtubules.

Ley *et al.*[10] synthesised a collection of structurally diverse spiroacetal-based molecules for broad phenotypic screening evaluations. The spiroacetal precursor alkene **245** was prepared from *(R)*-glycidol **(244)**. Subsequent Sharpless asymmetric dihydroxylation and double conjugate addition of dithiol yielded the desired *β*-keto-1,3-dithiane. Acid-catalysed cyclisation of this precursor followed by dithiane removal afforded a separable diastereomeric mixture of spiroacetal scaffolds **246**–**248** (Scheme 1.36). All three spiroacetals **246**–**248** were elaborated into a diverse range of analogues and those derived from spiroacetal **246** are listed below (Figure 1.3).

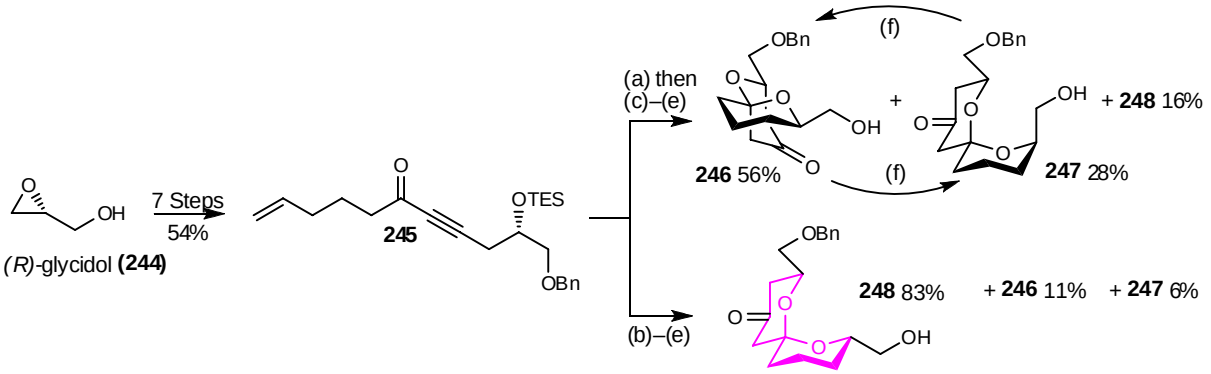

Reagents and conditions: (a) AD-mix-*β*, ^{t}BuOH–H_2O, 0 °C, 18 h, 94% (86:14 *dr*); (b) AD-mix-*α*, ^{t}BuOH–H_2O, 0 °C, 18 h, 96% (87:14 *dr*); (c) $HS(CH_2)_3SH$, NaOMe, MeOH–CH_2Cl_2. -10 °C, 18 h, 90%; (d) aq. $HClO_4$, MeCN–CH_2Cl_2, 0 °C, 30 min, yields are quoted in the scheme; (e) $NaClO_2$, NaH_2PO_4, 2-methyl-2-butene, MeOH–H_2O, rt, 45 min, 100%; (f) aq. $HClO_4$, MeCN–CH_2Cl_2, 0 °C, 1 h, 100% (**246**:**247** 2:1 *dr*).

Scheme 1.36: Synthesis of spiroacetal scaffolds **246**–**248** by Ley *et al.*[10]

Ley *et al.*[10] first functionalised spiroacetal **248** at C4 with epoxide **249** and dioxirane **250**. The study then focused on elaboration at C8. Silylation and debenzylation of **248** gave alcohol **251** allowing differentiation of the hydroxy groups whereas oxidation of **248** afforded aldehyde **252** and carboxylic acid **253** intermediates. Triazole **254**, amide **255** and carbamates **256** and **257** were prepared from the corresponding azide intermediate, carboxylic acid **253** and alcohol **248** respectively, and represented viable procedures for elaborations. A range of protected-amino acids **258**–**263**, was

prepared from alcohol **248** and were used as building blocks for the synthesis of a series of ureas **264**–**268** and sulfonamides **269**–**272**. Derivatisation of scaffold **246** and **247** were also carried out similarly to generate a series of 13 analogues (not shown). These syntheses were specifically designed to afford spiroacetal analogues suitable for biological screening, and more importantly, to obey the Lipinski rule of five[71] which is an evaluation of estimated solubility and permeability—important characteristics for drug candidates (Figure 1.3).

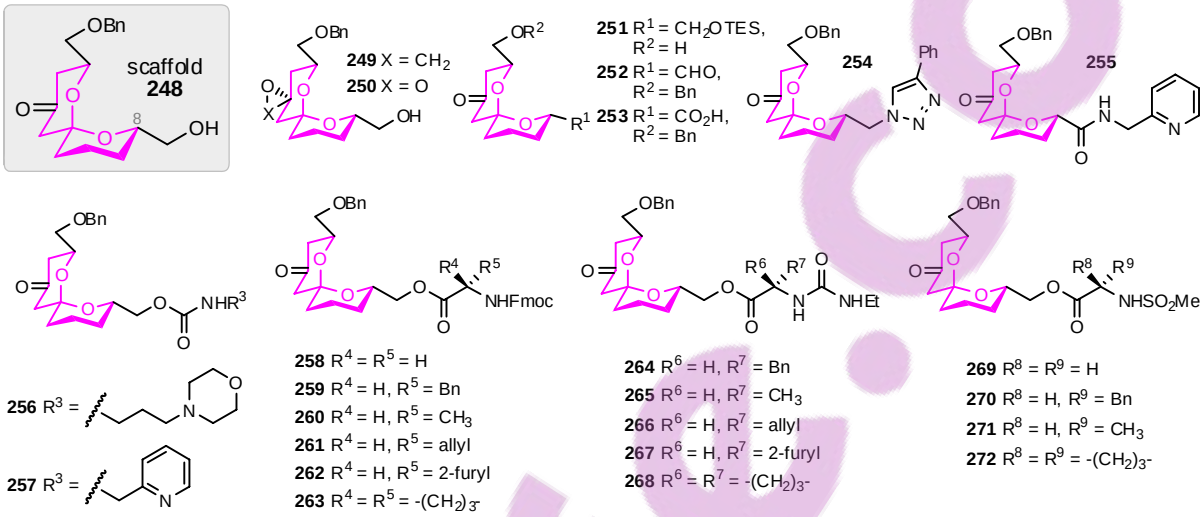

Figure 1.3: A collection of spiroacetal derivatives **249**–**272** elaborated from scaffold **248** by Ley *et al.*[10] Derivatisation of scaffold **246** and **247** were also carried out similarly to generate another series of 13 analogues (not shown).

1.6 Research Opportunities Based on the Use of 6,6-Spiroacetal Analogues

Our research group has had a long interest in the synthesis of spiroacetals with different ring sizes found in a wide range of biologically significant compounds (Figure 1.4).[72] This synthetic effort has prompted the investigation of an opportunity to elaborate 6,6-spiroacetals to provide novel functionality. In particular, we were interested in the chemical attachment of the spiroacetal scaffold to biologically useful units such as nucleobases, triazoles or amino acids, thus generating hybrids that have, to date, never been previously synthesised or biologically tested. The combination of these important bioactive motifs would lead to a collection of novel small hybrid molecules that can be used as biological probes for broad phenotypic assays to screen for potential bioactivity.

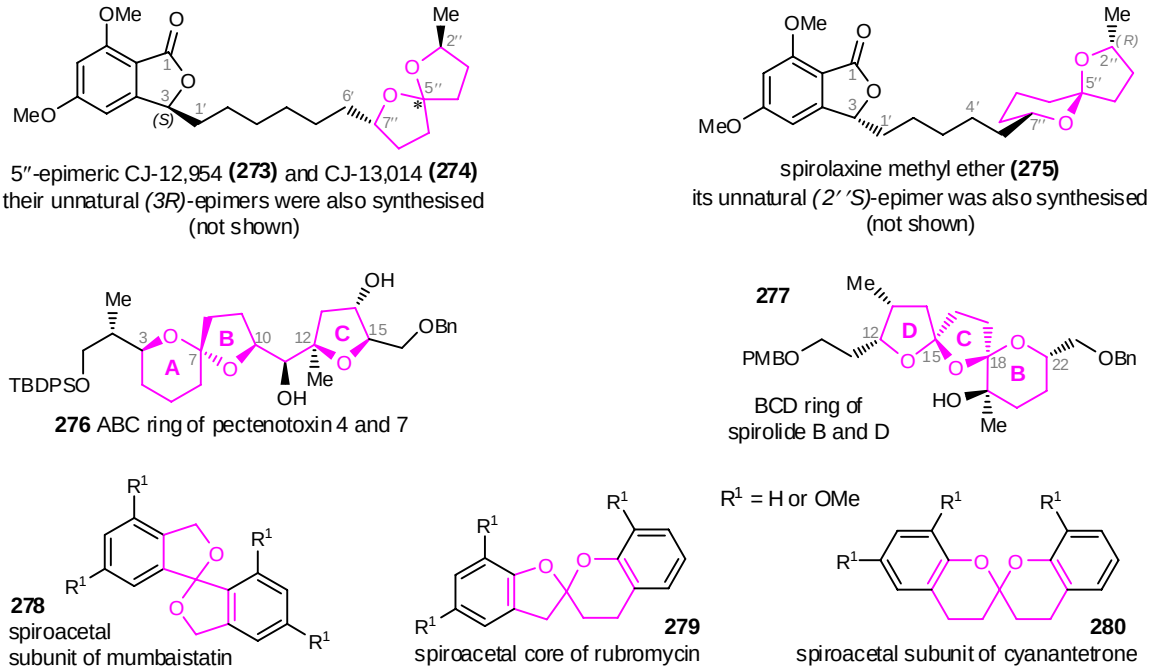

Figure 1.4: Examples of spiroacetals **273**–**280** published by Brimble *et al.*[72] between 2005 and 2007.

The following chapters will examine, in detail, the rationale behind the chosen nucleobase, triazole and amino acid motifs. The syntheses of these hybrid molecules, in particular those spiroacetal based hybrids, will be discussed and relevant examples will be illustrated.

1.7 References

1. R. S. Bohacek, C. McMartin and W. C. Guida, *Med. Res. Rev.*, 1996, **16**, 3-50.
2. H. C. Kolb and K. B. Sharpless, *Drug Discov. Today*, 2003, **8**, 1128-1137.
3. Accenture and CMR International, *Pharmaceutical Companies Must Re-think Innovation Strategies to Address Pipeline Challenges*, Accenture and CMR International, London, 2005.
4. M. S. Butler, *Nat. Prod. Rep.*, 2005, **22**, 162-195; D. J. Newman, G. M. Cragg and K. M. Snader, *J. Nat. Prod.*, 2003, **66**, 1022-1037.
5. D. J. Newman and G. M. Cragg, *J. Nat. Prod.*, 2007, **70**, 461-477.
6. D. S. Tan, *Comb. Chem. High Throughput Screening*, 2004, **7**, 631-643.
7. I. Paterson and E. A. Anderson, *Science*, 2005, **310**, 451-453.
8. J. C. Venter, *et al.*, *Science*, 2001, **291**, 1304-1351.
9. R. Breinbauer, I. R. Vetter and H. Waldmann, *Angew. Chem. Int. Ed.*, 2002, **41**, 2879-2890.
10. G. Zinzalla, L.-G. Milroy and S. V. Ley, *Org. Biomol. Chem.*, 2006, **4**, 1977-2002.
11. H. Zhao, *Drug Discov. Today*, 2007, **12**, 149-155.
12. F. Perron and K. F. Albizati, *Chem. Rev.*, 1989, **89**, 1617-1661.
13. M. F. Jacobs and W. Kitching, *Curr. Org. Chem.*, 1998, **2**, 395-436.
14. W. Francke and W. Kitching, *Curr. Org. Chem.*, 2001, **5**, 233-251.

15. D. G. Lynn, N. J. Phillips, W. C. Hutton, J. Shabanowitz, D. I. Fennell and R. J. Cole, *J. Am. Chem. Soc.*, 1982, **104**, 7319-7322.
16. *U.S. Pat.*, US 4547523, 1985; W. P. Cullen*, et al.*, *J. Ind. Microbiol.*, 1988, **2**, 349-357; N. R. Kotecha, S. V. Ley and S. Mantegani, *Synlett*, 1992, 395-399.
17. K. Tachibana, P. J. Scheuer, Y. Tsukitani, H. Kikuchi, D. Van Engen, J. Clardy, Y. Gopichand and F. J. Schmitz, *J. Am. Chem. Soc.*, 1981, **103**, 2469-2471; A. B. Dounay and C. J. Forsyth, *Curr. Med. Chem.*, 2002, **9**, 1939-1980.
18. R. E. Honkanen and T. Golden, *Curr. Med. Chem.*, 2002, **9**, 2055-2075.
19. X. C. Cheng*, et al.*, *J. Antibiot.*, 1987, **40**, 907-909; M. Ubukata, X.-C. Cheng, M. Isobe and K. Isono, *J. Chem. Soc., Perkin Trans. 1*, 1993, 617-624; H. Oikawa, *Curr. Med. Chem.*, 2002, **9**, 2033-2054.
20. S. B. Singh, D. L. Zink, B. Heimbach, O. Genilloud, A. Teran, K. C. Silverman, R. B. Lingham, P. Felock and D. J. Hazuda, *Org. Lett.*, 2002, **4**, 1123-1126.
21. K. Suenaga, H. Kigoshi and K. Yamada, *Tetrahedron Lett.*, 1996, **37**, 5151-5154.
22. H. Mishima, M. Kurabayashi, C. Tamura, S. Sato, H. Kuwano and A. Saito, *Tetrahedron Lett.*, 1975, 711-714.
23. G. Albers-Schönberg, B. H. Arison, J. C. Chabala, A. W. Douglas, P. Eskola, M. H. Fisher, A. Lusi, H. Mrozik, J. L. Smith and R. L. Tolman, *J. Am. Chem. Soc.*, 1981, **103**, 4216-4221; R. W. Burg*, et al.*, *Antimicrob. Agents Chemother.*, 1979, **15**, 361-367.
24. M. H. Fisher, *Pure Appl. Chem.*, 1990, **62**, 1231-1240.
25. G. R. Pettit, Z. A. Cichacz, F. Gao, C. L. Herald, M. R. Boyd, J. M. Schmidt and J. N. A. Hooper, *J. Org. Chem.*, 1993, **58**, 1302-1304; J. S. Guo, K. J. Duffy, K. L. Stevens, P. I. Dalko, R. M. Roth, M. M. Hayward and Y. Kishi, *Angew. Chem. Int. Ed.*, 1998, **37**, 187-192; M. M. Hayward, R. M. Roth, K. J. Duffy, P. I. Dalko, K. L. Stevens, J. S. Guo and Y. Kishi, *Angew. Chem. Int. Ed.*, 1998, **37**, 192-196.
26. H. Huang, C. Mao, S.-T. Jan and F. M. Uckun, *Tetrahedron Lett.*, 2000, **41**, 1699-1702; F. M. Uckun, C. Mao, A. O. Vassilev, H. Huang and S.-T. Jan, *Bioorg. Med. Chem. Lett.*, 2000, **10**, 541-545; F. M. Uckun, *Curr. Pharm. Design*, 2001, **7**, 1627-1639.
27. S. Mitsuhashi, H. Shima, T. Kawamura, K. Kikuchi, M. Oikawa, A. Ichihara and H. Oikawa, *Bioorg. Med. Chem. Lett.*, 1999, **9**, 2007-2012.
28. A. A. Birkbeck, S. V. Ley and J. C. Prodger, *Bioorg. Med. Chem. Lett.*, 1995, **5**, 2637-2642.
29. T. G. Geary, *Trends in Parasit.*, 2005, **21**, 530-532; L. Raber, *Chem. Eng. News*, 2005, **83**.
30. *US Pat.*, 5,656,748, 1997.
31. H. G. Davies and R. H. Green, *Nat. Prod. Rep.*, 1986, **3**, 87-121.
32. A. D. McNaught and A. Wilkinson, *Compendium of Chemical Terminology—IUPAC Recommendations*, 2nd edn., Blackwell Science, Inc., UK, 1997.
33. P. Deslongchamps, D. D. Rowan, N. Pothier, T. Sauvé and J. K. Saunders, *Can. J. Chem.*, 1981, **59**, 1105-1121.
34. E. Juaristi and G. Cuevas, *The Anomeric Effect*, 1st edn., CRC Press, Inc., Boca Raton, 1995; A. J. Kirby, *Stereoelectronic Effects*, 1st edn., Oxford University Press, Oxford, 1996.
35. T. L. B. Boivin, *Tetrahedron*, 1987, **43**, 3309-3362.
36. K. T. Mead and B. N. Brewer, *Curr. Org. Chem.*, 2003, **7**, 227-256.
37. I. Paterson, M. J. Coster, D. Y.-K. Chen, R. M. Oballa, D. J. Wallace and R. D. Norcross, *Org. Biomol. Chem.*, 2005, **3**, 2399-2409.
38. I. Paterson, D. Gottschling and D. Menche, *Chem. Comm.*, 2005, 3568-3570.
39. T. Lister and M. V. Perkins, *Angew. Chem. Int. Ed.*, 2006, **45**, 2560-2564.
40. L. C. Dias and L. G. de Oliveira, *Org. Lett.*, 2004, **6**, 2587-2590; L. G. de Oliveira, L. C. Dias, H. Sakauchi and H. Kiyota, *Tetrahedron Lett.*, 2006, **47**, 2413-2418.
41. A. Höltzel, C. Kempter, J. W. Metzger, G. Jung, I. Groth, T. Fritz and H. P. Fiedler, *J. Antibiot.*, 1998, **51**, 699-707; S. D. Zanatta, J. M. White and M. A. Rizzacasa, *Org. Lett.*, 2004, **6**, 1041-1044.
42. J. Marjanovic and S. A. Kozmin, *Angew. Chem. Int. Ed.*, 2007, **46**, 8854-8857.
43. J. S. Yadav and L. Chetia, *Org. Lett.*, 2007, **9**, 4587-4589; J. S. Yadav and V. R. Gadgil, *Tetrahedron Lett.*, 1990, **31**, 6217-6218.
44. J.-F. Biard, C. Roussakis, J.-M. Kornprobst, D. Gouiffes-Barbin, J.-F. Verbist, P. Cotelle, M. P. Foster, C. M. Ireland and C. Debitus, *J. Nat. Prod.*, 1994, **57**, 1336-1345 and references cited therein.

45. D. van Leusen and A. M. van Leusen, *Org. React.*, 2001, **57**, 417-666.
46. J. Hao and C. J. Forsyth, *Tetrahedron Lett.*, 2002, **43**, 1-2.
47. I. Paterson, M. J. Coster, D. Y. K. Chen, K. R. Gibson and D. J. Wallace, *Org. Biomol. Chem.*, 2005, **3**, 2410-2419.
48. C. Wang and C. J. Forsyth, *Heterocycles*, 2007, **72**, 621-632.
49. L. R. Takaoka, A. J. Buckmelter, T. E. LaCruz and S. D. Rychnovsky, *J. Am. Chem. Soc.*, 2005, **127**, 528-529.
50. S. D. Rychnovsky, J. P. Powers and T. J. Lepage, *J. Am. Chem. Soc.*, 1992, **114**, 8375-8384.
51. T. E. La Cruz and S. D. Rychnovsky, *Org. Lett.*, 2005, **7**, 1873-1875.
52. E. B. Holson and W. R. Roush, *Org. Lett.*, 2002, **4**, 3719-3722.
53. J. S. Potuzak, S. B. Moilanen and D. S. Tan, *J. Am. Chem. Soc.*, 2005, **127**, 13796-13797; S. B. Moilanen, J. S. Potuzak and D. S. Tan, *J. Am. Chem. Soc.*, 2006, **128**, 1792-1793.
54. H. Osada, H. Koshino, K. Isono, H. Takahashi and G. Kawanishi, *J. Antibiot.*, 1991, **44**, 259-261.
55. M. El Sous, D. Ganame, P. A. Tregloan and M. A. Rizzacasa, *Org. Lett.*, 2004, **6**, 3001-3004; M. El Sous, D. Ganame, S. Zanatta and M. A. Rizzacasa, *ARKIVOC*, 2006, 105-119; A. N. Cuzzupe, C. A. Hutton, M. J. Lilly, R. K. Mann, K. J. McRae, S. C. Zammit and M. A. Rizzacasa, *J. Org. Chem.*, 2001, **66**, 2382-2393.
56. A. Deiters and S. F. Martin, *Chem. Rev.*, 2004, **104**, 2199-2238.
57. P. A. V. van Hooft, M. A. Leeuwenburgh, H. S. Overkleeft, G. A. van der Marel, C. A. A. van Boeckel and J. H. van Boom, *Tetrahedron Lett.*, 1998, **39**, 6061-6064; M. A. Leeuwenburgh, C. C. M. Appeldoorn, P. A. V. van Hooft, H. S. Overkleeft, G. A. van der Marel and J. H. van Boom, *Eur. J. Org. Chem.*, 2000, 873-877.
58. J. Liu and R. P. Hsung, *Org. Lett.*, 2005, **7**, 2273-2276.
59. S. K. Ghosh, C. Ko, J. Liu, J. Wang and R. P. Hsung, *Tetrahedron*, 2006, **62**, 10485-10496.
60. D. E. Williams, M. Roberge, R. Van Soest and R. J. Andersen, *J. Am. Chem. Soc.*, 2003, **125**, 5296-5297; D. E. Williams, M. Lapawa, X. Feng, T. Tarling, M. Roberge and R. J. Andersen, *Org. Lett.*, 2004, **6**, 2607-2610.
61. M. A. Brimble, *Molecules*, 2004, **9**, 394-404.
62. R. L. Dorta, A. Martin, J. A. Salazar, E. Suárez and T. Prangé, *J. Org. Chem.*, 1998, **63**, 2251-2261.
63. N. Haddad, Z. Abramovich and I. Ruhman, *Tetrahedron Lett.*, 1996, **37**, 3521-3524; N. Haddad, I. Rukhman and Z. Abramovich, *J. Org. Chem.*, 1997, **62**, 7629-7636.
64. D. R. Spring, *Org. Biomol. Chem.*, 2003, **1**, 3867-3870; S. L. Schreiber, *Science*, 2000, **287**, 1964-1969.
65. M. D. Burke and S. L. Schreiber, *Angew. Chem. Int. Ed.*, 2004, **43**, 46-58.
66. O. Barun, K. Kumar, S. Sommer, A. Langerak, T. U. Mayer, O. Müller and H. Waldmann, *Eur. J. Org. Chem.*, 2005, 4773-4788.
67. K. T. Mead and R. Zemribo, *Synlett*, 1996, 1063-1064; K. T. Mead and R. Zemribo, *Synlett*, 1996, 1065-1066.
68. R. Zemribo and K. T. Mead, *Tetrahedron Lett.*, 1998, **39**, 3891-3894; R. Zemribo and K. T. Mead, *Tetrahedron Lett.*, 1998, **39**, 3895-3898; R. Zemribo and K. T. Mead, *Synlett*, 2000, 1569-1572.
69. S. K. Ghosh, R. P. Hsung and J. S. Wang, *Tetrahedron Lett.*, 2004, **45**, 5505-5510.
70. B. A. Kulkarni, G. P. Roth, E. Lobkovsky and J. A. Porco, Jr., *J. Comb. Chem.*, 2002, **4**, 56-72.
71. C. A. Lipinski, F. Lombardo, B. W. Dominy and P. J. Feeney, *Adv. Drug Delivery Rev.*, 1997, **23**, 3-25.
72. J. E. Robinson and M. A. Brimble, *Chem. Comm.*, 2005, 1560-1562; K. Meilert and M. A. Brimble, *Org. Lett.*, 2005, **7**, 3497-3500; K. Meilert and M. A. Brimble, *Org. Biomol. Chem.*, 2006, **4**, 2184-2192; R. Halim, M. A. Brimble and J. Merten, *Org. Biomol. Chem.*, 2006, **4**, 1387-1399; M. A. Brimble, C. L. Flowers, M. Trzoss and K. Y. Tsang, *Tetrahedron*, 2006, **62**, 5883-5896; M. A. Brimble and C. J. Bryant, *Chem. Comm.*, 2006, 4506-4508; M. A. Brimble and C. V. Burgess, *Synthesis*, 2007, 754-760; M. A. Brimble and C. J. Bryant, *Org. Biomol. Chem.*, 2007, **5**, 2858-2866; J. E. Robinson and M. A. Brimble, *Org. Biomol. Chem.*, 2007, **5**, 2572-2582; K. Y. Tsang and M. A. Brimble, *Tetrahedron*, 2007, **63**, 6015-6034.

Chapter Two:

Introduction: Nucleosides

As previously mentioned, the aim of this research is to synthesise spiroacetal-nucleoside hybrids as potential antiviral agents or biological probes for broad phenotypic assays. In order to understand the rationale behind the choice of nucleoside as the motif, we must first examine the basics of virus.

2.1 Viruses and Diseases

Viruses were first identified in the late 19th century as ultra-small disease causing agents that could only replicate within specific host cells. It was not until 1935 that the generalised picture of viruses began to emerge due to scientific advances.[1]

2.1.1 The Structure of a Virus

Viruses are small (10–300 nm), diverse in size, shape and genome. In general, viruses consist of a nucleic acid core encapsulated within a protein shell called capsid. The capsid may be rod-shaped helical, polyhedral, round, or more complex in shape (as in the case of bacterial viruses or bacteriophages) and is assembled from repeating subunit of identical protein(s) called capsomeres. Viral genomes can be a combination of positive or negative, single or double stranded, linear or circular, DNA or RNA. Some viruses carry unique enzyme(s) to aid their replication once inside the host cells. In enveloped viruses, the capsid shell is further enclosed by a lipoprotein membrane envelope containing antigenic viral glycoproteins for specific host recognition (Figure 2.1).[1-3]

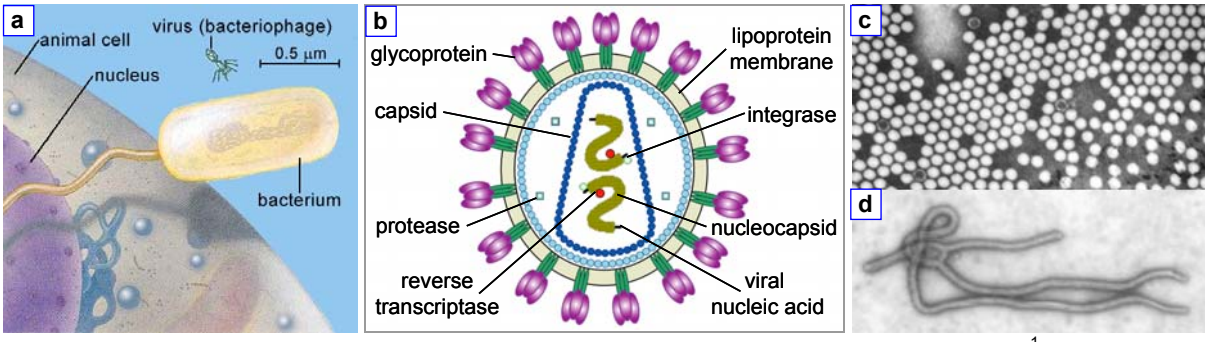

Figure 2.1: [a] Comparison of the sizes of an animal cell, a bacterium and a bacteriophage virus.[1] [b] Generalised structure of an enveloped virus.[4] [c] Electron micrography of polioviruses.[5] [d] Electron micrography of Ebola viruses.[6]

The information a virus carries differs greatly. The smallest viruses have only four genes whilst the largest have several hundred, reflecting each unique pathway of replication. Nevertheless, the genome encodes crucial viral specific coat proteins and enzymes to ensure its selective and successful replication within a host cell.[1]

2.1.2 The Replication Cycle of a Virus

Regarded as the simplest form of life, an isolated virus is incapable of replication due to the lack of enzymes for metabolism and ribosomes for protein synthesis. Once it invades a viable host cell, it hijacks and exploits the host's biochemical pathways (energy generation, DNA and RNA replication and protein synthesis) and is often referred to as an obligate intracellular parasite. Although the exact details may differ between viruses, the replication cycle can be generalised into the steps described below.[1,2]

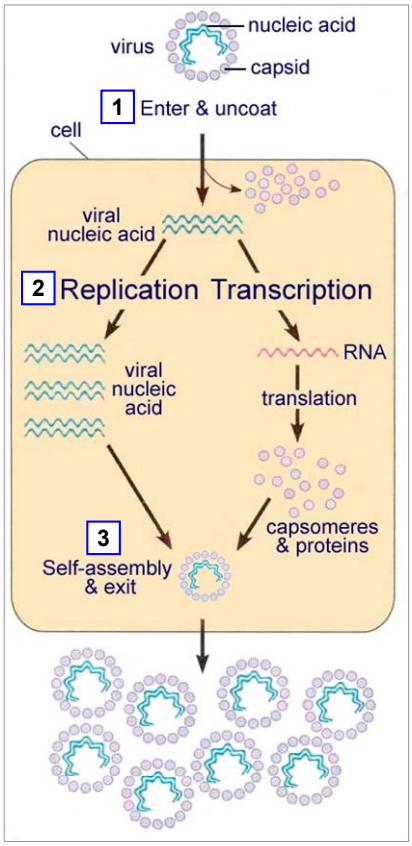

Figure 2.2: Simplified replication cycle of virus.[1]

[1] Entry into the Host Cell and Uncoating of the Viral Genome

The viral life cycle begins with the entry of the viral genome into the host cell *via* various mechanisms. For an enveloped virus, the viral lipid envelope fuses with the cell's plasma membrane and the viral capsid and genome enters the cytoplasm. A non-enveloped virus enters the host by encapsulation within a vacuole (endocytosis/vacuolar ingestion). Subsequent fusion of the vacuolar membrane with an internal membrane system such as the Golgi bodies or endoplasmic reticulum releases the viral capsid and its genome.[1,3]

[2] Replication and Transcription of Viral DNA, Translation of Viral Capsomeres and Proteins

After the removal of the viral capsid by cellular enzymes, the viral chromosome commands and re-programs the host cell to transcribe and translate the viral coating and surface recognition proteins, as well as to replicate the viral genome.[1]

[3] Self-assembly and Release of Progeny Viruses from Infected cell

The viral capsomeres and chromosomes self-assemble within the cytoplasm and the progeny viruses exit, either by lysing open the host cell or by budding from the cell surface. Budding, like exocytosis of a normal cell, involves wrapping the viral particle with part of the host's plasma membrane embedded with viral recognition proteins. Unlike cell lysis, budding does not kill the host cell.[1]

Apart from cell lysis, the host cell may also die as a result of viral interference with host macromolecular synthesis (DNA, RNA and protein), changes in cellular activities (transcriptions and protein-protein interactions), morphologies, plasma membrane physiologies (movement of ions and

formation of secondary messengers to modulate cellular processes) and irreversible damages to the host's genome.[7] Viral infection also triggers the host's immune system to eliminate the infected host cells in order to halt the replication and spread of viruses.[3]

2.1.3 Prevalence of Diseases Caused by Viruses

Virus Group	*Virus Family*	*Diseases (Causative Virus)*
I. dsDNA	Adenovirus	respiratory disease, gastroenteritis and conjunctivitis/pink eye (HAdV).
	Herpesvirus	cold sores and genital sores (HSV), shingles and chicken pox (VZV), retinitis and glandular fever/infectious mononucleosis (EBV, CMV).
	Papillomavirus	warts, cervical cancer (HPV).
	Poxvirus	small pox, cow pox (Orthopoxvirus).
II. ssDNA	Parvovirus	erythema infectiosum/rash (Parvovirus B19).
III. dsRNA	Reovirus	diarrhoea (Rotavirus).
IV. (+)-ssRNA: serves as mRNA	Coronavirus	respiratory and gastrointestinal tract infections/common colds (HCoV), SARS (SARS-CoV).
	Flavivirus	hepatitis C, cirrhosis, liver cancer (HCV), encephalitis (West Nile virus), haemorrhagic fevers (Dengue fever virus, Yellow fever virus).
	Picornavirus	polio (Enterovirus), hepatitis A (Hepatovirus), respiratory tract infections/common colds (Rhinovirus).
	Togavirus	rubella (Rubivirus).
V. (-)-ssRNA: template for mRNA synthesis	Filovirus	haemorrhagic fevers (Ebolavirus, Marburgvirus).
	Orthomyxovirus	influenza A–C (Influenzavirus).
	Paramyxovirus	measles (Morbillivirus), mumps (Rubulavirus), respiratory tract infections (RSV).
	Rhabdovirus	rabies (Lyssavirus).
VI. ssRNA-RT	Retrovirus	T-cell leukaemia and lymphoma (HTLV), AIDS (HIV).
VII. dsDNA-RT	Hepadnavirus	hepatitis B, cirrhosis, liver cancer (HBV).

Table 2.1: Clinically important viral groups, families and the associated diseases.[1-3]

Despite their small sizes, viruses cause a wide range of diseases and an enormous health problem worldwide (Table 2.1).

- > 2 billion people worldwide infected with HBV (Hepatitis B) including 350 million chronically infected and at risk of developing liver cirrhosis and cancer.[8]
- 3% of world population infected with HCV (Hepatitis C) including 170 million chronically infected and at risk of developing liver cirrhosis and cancer.[9]
- 40 million people infected with HIV (AIDS) and 3 million infected died in 2006 worldwide.[10]
- influenza caused 3–5 million cases of severe illness per year in the world.[11]
- emerging and re-emerging viral diseases such as Ebola, SARS and avian influenza continuously threaten public health systems in the world.[12]

2.2 Antiviral Therapy

The small sizes of viruses and their intracellular parasitic life cycle make viral diseases particularly difficult to treat. Their massive rate of proliferation means a rapid, overwhelming and deeply penetrating treatment is required to provoke a therapeutic response. However, the number of viral-specific targets is limited as a result of the similarities between host-directed and virus-directed processes. Hence, antiviral agents can potentially cause collateral damage to the uninfected cells, thus limiting the agent's usefulness.[3,13,14] Without the mechanism for proof-reading and repair of nucleic acid employed by eukaryotic cells to ensure the accuracy in replication, viruses (especially RNA viruses) have a high rate of mutation which may give rise to a resistant strain that render the antiviral agent ineffective.[14] *In vivo* activity of the antiviral agent is often difficult to predict because viral biochemistry is not yet fully understood.[3]

As a result of these drawbacks, the development of selective antiviral drugs has been relatively slow. Only 7.7% of new drugs approved by regulatory agencies such as the FDA between 1981 and 2006 were antiviral. Of these 78 agents, only 41 agents are small antiviral molecules and the rest were either vaccines or biogenic peptides isolated from an organism or cell line.[15]

2.2.1 Targets for Selective Toxicity

Selective toxicity towards the virus without harming the host is an important property for all chemotherapeutic agents including antiviral agents. To achieve this, the agent must exploit the biochemical difference between the infected and uninfected hosts and selectively target viral unique molecules. Regardless how small the viral genome is, it encodes specific enzymes such as polymerases, kinases and proteases which are critical to its replication cycle and maturation. Inhibition of these enzymes selectively blocks the production of the viral nucleic acids and terminates the viral replication. This is why all antiviral agents are only effective towards replicating viruses but not against those at their latent stage. The following lists various stages of the viral replication cycle that have been targeted by chemotherapeutic antiviral agents.[2,3,14,16,17]

- Adsorption, penetration and uncoating (e.g. amantadine and rimantadine).
- Various stages of nucleic acid replication involving viral specific enzymes such as kinases, polymerases, integrases. Most antiviral agents target this step (e.g. nucleoside analogues).
- Translation of viral mRNA (e.g. interferon, fomivirsen).
- Post-translation modifications and maturation. In HIV, viral proteases cleave larger protein precursors into smaller functional units after self-assembly (e.g. saquinavir, ritonavir).
- Release of virus progeny (e.g. zanamivir and oseltamivir inhibit the spread of influenza by inhibiting neuraminidase which segregate and disperse viral particles for further infection).[18]

2.3 Nucleoside Analogues

Viral replication is the most vulnerable point for inhibition and provides the required differentiation due to the slow replication of mammalian cells. Nucleoside analogues are an important class of antiviral agents which imitate their naturally occurring counterparts as substrates for viral nucleic acid processing enzymes such as polymerases and kinases. With their structure manipulated appropriately, nucleoside analogues inhibit viral replication by terminating the elongation of the nucleic acid chain. Many clinically significant antiviral agents belong to this class.[16,17]

2.3.1 Nucleosides, Nucleotides and Nucleic Acids

The basic structure of naturally occurring nucleosides **282** consists of two parts (Figure 2.3):[1,17]

- A furanose sugar—either deoxyribose (2-deoxy-β-D-ribofuranose) in DNA or ribose (β-D-ribofuranose) in RNA. The furanose supports the important 4′-hydroxymethyl and 3′-hydroxy group for elongation.
- A heterocyclic base at the 1′ position—either a purine (adenine and guanine) or a pyrimidine (cytosine, thymine and uracil). The base is linked to the furanose through a β-*N*-glycosidic bond (N9 of purine and N1 of pyrimidine). Adenine, guanine, cytosine and thymine are found in natural DNA nucleosides, whereas uracil is found instead of thymine in RNA nucleosides.

The furanose acts as a scaffold to present the 4′-hydroxymethyl group and 1′-heterobase in a 1,3-*syn* conformation for the recognition of nucleic acid processing enzymes. The glycoside also supports the 3′-hydroxyl group as an attachment to the phosphate group of the next nucleoside unit during nucleic acid polymerisation.[1,17]

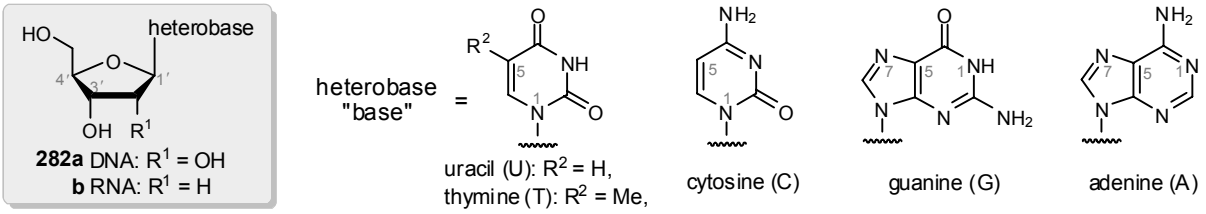

Figure 2.3: Structures of natural nucleosides **282**: uridine, thymidine, cytidine, guanosine and adenosine.

Nucleotides **283** are 5′-phosphate esters of nucleosides **282** and are obtained by intracellular sequential phosphorylations of nucleosides **282** under the control of kinases (Scheme 2.1a). The resulting triphosphate chelates metal ions in kinases and polymerases, and anchors the nucleotide correctly to the enzyme. The high energy stored within the triphosphate also drives the nucleic acid polymerisation, a highly favourable hydrolysis controlled by polymerases. They mediate the formation

of phosphodiester linkages between the 3′-hydroxyl of the growing nucleic acid chain and the next free nucleotide that has lined up due to the complementary base-pairing (Scheme 2.1b).[1,17]

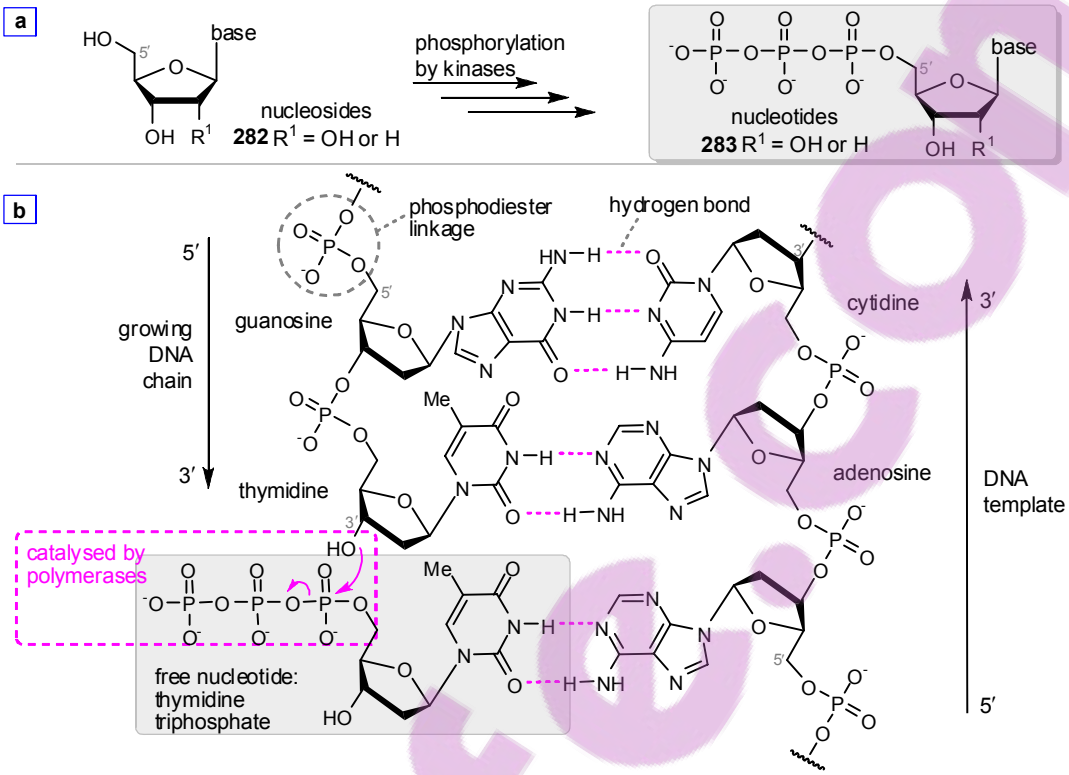

Scheme 2.1: [a] Sequential phosphorylation of nucleoside **282** by kinases gives nucleotide **283** (nucleoside triphosphate).[17] [b] Nucleic acid is formed from polymerisation of nucleotides **282** joined together by phosphodiester bridges between 5′ and 3′ of neighbouring furanoses. The formation of these linkages between the free 3′-hydroxyl of the nucleic acid and the 5′-phosphate of the next nucleoside triphosphate is catalysed by polymerases and pyrophosphate ($P_2O_7^{4-}$) is released as a by-product. Nucleotides recognise their complementary base partner (C–G, A–T/U) by hydrogen bondings (complementary base pairing).[1,17]

2.3.2 Basic Structure of Nucleoside Analogues

As substrates for polymerases and nucleic acid replication, nucleotide analogues are rarely used as therapeutic agents because they are too polar to cross the cell membrane to the site of viral replication. On the other hand, nucleoside analogues are useful prodrugs that are actively taken up by the cells and activated by kinases. Selectivity towards the infected cells occurs when this phosphorylation is preferential i.e. the antiviral agent has higher affinity for viral kinases leading to the accumulation of the activated agent within the infected cells.[2,3,16,17]

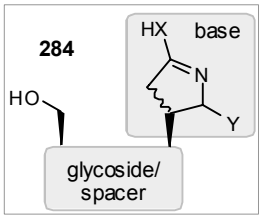

Figure 2.4: Generalised structure of nucleoside analogues **284**.

The generalised structure of nucleoside analogues **284** consists of a hydroxymethyl group, a spacer and a heterocyclic base (Figure 2.4). The hydroxymethyl group is crucial for the intracellular phosphorylation whereas

the furanose is not strongly recognised by enzymes and merely acts as a spatial scaffold (spacer) to present the hydroxymethyl substituent and the heterocyclic base in the required orientation. Interplay between the spacers and bases provides an enormous opportunity for potential antiviral agents.[17]

2.3.3 Examples of Clinically Used Antiviral Nucleoside Analogues

Most activated/phosphorylated nucleoside analogues are inhibitors of polymerases and nucleic acid chain terminators. Selectivity towards viral infected cells is achieved by higher affinity of the agent towards viral kinases and/or viral polymerases as observed in the following examples.[2,3,16,17]

(a) Acyclovir or 9-(2-Hydroxyethoxymethyl)guanine (ACV, 288)

Acyclovir[19] **(288)** is an acyclic guanosine analogue that is highly selective towards HSV (cold sores and genital sores) and VZV (shingles and chicken pox). **288** is preferentially phosphorylated and accumulated within the viral infected cells due to its high affinity towards viral thymidine kinase. The resulting acyclovir triphosphate is a highly potent inhibitor of viral DNA polymerase. Once incorporated, it terminates the elongation of the DNA chain and halts viral replication due to the lack of the 3′-hydroxyl group for the attachment of the next nucleotide. Several other acyclic guanosine based analogues (e.g. ganciclovir[20], valaciclovir[21] and famiciclovir[22]) have been approved clinically with similar efficacy but improved oral availability and pharmacokinetics for lower dosage.[2,3,16,17,23]

Acyclovir **(288)** has been involved in an on-going patent-war since its discovery. Many syntheses had been described with variable yields and drawbacks particularly at industrial level.[24] In Cabri's (Secifarma) process,[25] guanine **(285)** was silylated by TMSI (HMDS + I^-) *in situ* which also acted as a catalyst for the subsequent *N*-alkylation/nucleosidation under Vorbrüggen conditions to give N9-guanosine **287** regioselectively under thermodynamic control. Subsequent deacetylation of **287** yielded acyclovir **(288)** in excellent yield.

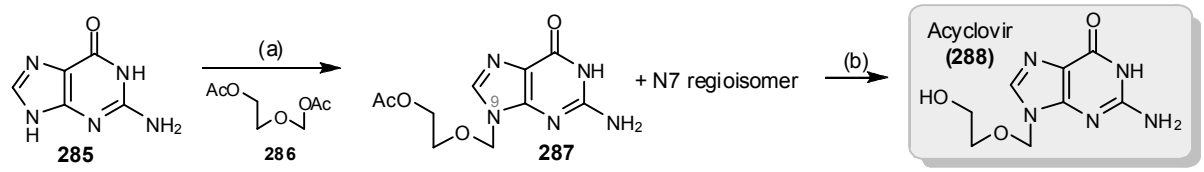

Reagents and conditions: (a) i. HMDS, cat. Bu_4NI, xylene, reflux, 8–12 h; ii.**286**; iii. MeOH, 95% (N9:N7 99:1); (b) NaOH, H_2O, 80%.

Scheme 2.2: Total synthesis of acyclovir **(288)** by Cabri's (Secifarma) process.[25]

(b) Zidovudine or 3′-Azido-2′,3′-dideoxythymidine (AZT, 292)

AZT[26] **(292)** is an anti-HIV thymidine analogue. After phosphorylation by cellular kinases, AZT triphosphate is a highly specific inhibitor towards viral reverse transcriptase (RNA-dependent DNA

polymerase) which converts viral RNA into proviral DNA before its integration into the host's genome. AZT triphosphate terminates the replicating viral nucleic acid chain due to the lack of 3′-hydroxyl group—a structural feature commonly found in anti-HIV nucleoside reverse transcriptase inhibitors (NRTI). Mammalian DNA polymerase is relatively unaffected by AZT **(292)** but the sensitivity of mitochondria DNA polymerase caused many of the observed side effects.[2,3,16,17,23]

Czernecki and Valery[27] described an efficient synthesis of AZT **(292)** starting from thymidine **289**. Double Mitsunobu reaction transformed thymidine **289** to protected 2,3′-anhydro derivative **290** under one-pot/two-step conditions. Subsequent ring opening of **290** by LiN_3 and deprotection under basic conditions gave AZT **(292)**. This process efficiently substituted 3′-OH with 3′-N_3 with overall retention of configuration proceeding *via* activated intermediate **290**.

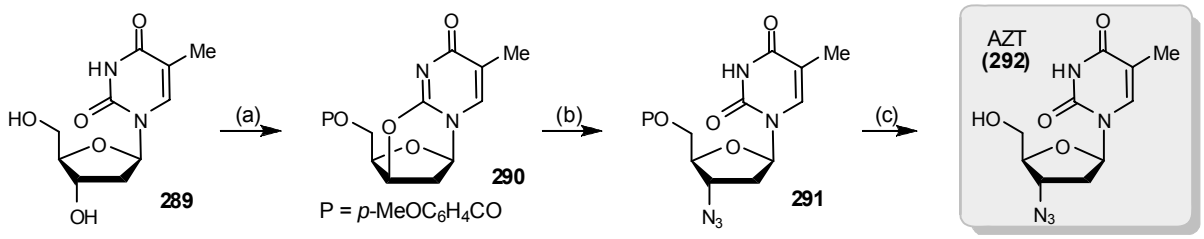

Reagents and conditions: (a) i. *p*-$MeOC_6H_4CO_2H$, DIAD, PPh_3, DMF, rt, 15 min; ii. DIAD, PPh_3, DMF, rt, 30 min, 86%; (b) LiN_3, DMF, 125 °C, 5 h, 90%; (c) NaOMe, MeOH, rt, 12 h, 94%.

Scheme 2.3: Total synthesis of AZT **(292)** by Czernecki and Valery.[27]

2.4 Synthesis of Nucleoside Analogues

There are four principle methods to synthesise nucleoside analogues (Scheme 2.5). All are based on the disconnection of the *N*-glycosidic bond between the heterobase and glycoside. The following section will discuss these strategies and selected recent examples will be summarised.[23,28,29]

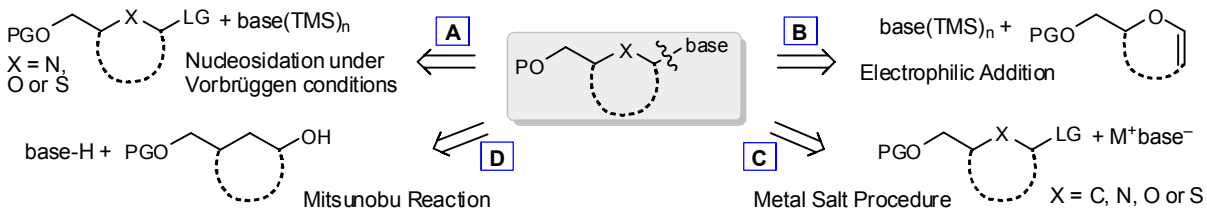

Scheme 2.4: General methods for the synthesis of nucleoside analogues.[28]

2.4.1 Nucleosidation under Vorbrüggen Conditions [A]

Nucleosidation under Vorbrüggen conditions is frequently applied to the synthesis of nucleoside analogues and has been extensively reviewed.[23,28,29] Under the influence of a Lewis acid

such as TMSOTf or $SnCl_4$, oxonium ion **294** is generated from glycoside **293** that bears a leaving group (usually acyl) at the anomeric position and is subsequently trapped *in situ* by a persilylated base to yield nucleoside **295**. This coupling is usually not stereoselective unless the neighbouring 2′-acyl functionality participates in the formation of the oxonium ion and/or facial discrimination taken place by steric hindrance. This strategy is not applicable to molecules such as carbacycles that do not possess a β-heteroatom, which was required for the generation of oxonium ion.[23,28]

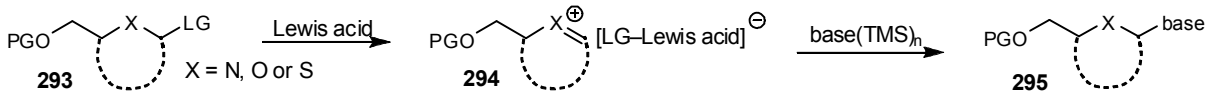

Scheme 2.5: Coupling of glycoside **293** and a persilylated base in the presence of a Lewis acid.[23,28]

Entry	Glycosides/Spacers	Heterobases	Conditions	Products and Yields
[1] Lescop and Huet[30]	**296** 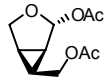	$T(TMS)_2$, $^{Bz}A(TMS)_2$, $G^*(TMS)_2$	TMSOTf, MeCN, 0 °C→rt, 2 h.	**297** 61–90% 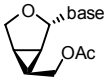
[2] Parsch and Engels[31]	**298** 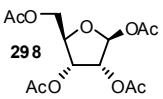	R = H, allyl 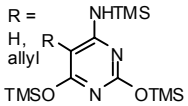	TMSOTf, DCE, rt, 1 d.	**299** 46–83% 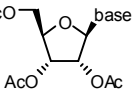
[3] Ewing *et al.*[32]	**300** 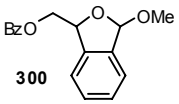	$T(TMS)_2$, $U(TMS)_2$	TMSOTf, MeCN, -15→0 °C, 2 h.	**301** 65–70% 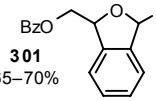 (*trans*>*cis*)
[4] Mirand *et al.*[33]	**302** R^1 = H, OBz 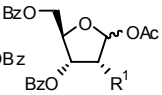	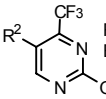 R^2 = Bn, Et, ^{i}Pr	$SnCl_4$, MeCN, -25 °C, 3 h.	4 examples **303** R^1 = OBz, 76–90% (β only) 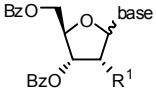 R^1 = H, R^2 = ^{i}Pr, 67% (β:α 2.5:1)
[5] Yokomatsu *et al.*[34]	**304** R = Et or Ac 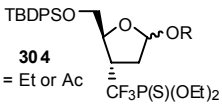	$T(TMS)_2$, $U(TMS)_2$, $^{Bz}C(TMS)_2$, $^{5F}U(TMS)_2$	$TiCl_4$, CH_2Cl_2, 0 °C, 3 h.	**305** 52–93% (β>α) 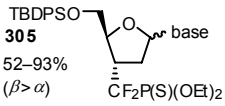
	306 R = Bn, TBDPS 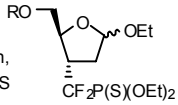	$^{Bz}A(TMS)_2$	$SnCl_4$, MeCN, rt, 15–24 h.	**307** R = Bn, 42% (β:α 1.6:1) R = TBDPS, 77% (β:α 1:1.4) 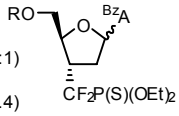
[6] Chiacchio *et al.*[35]	**308** 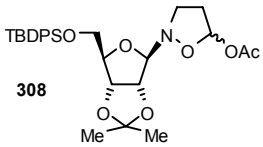	$T(TMS)_2$, $U(TMS)_2$, $C(TMS)_2$, $^{5F}U(TMS)_2$, $^{5F}C(TMS)_2$, $A(TMS)_2$	TMSOTf, MeCN, reflux, 1 h. (A: TMSOTf, MeCN, rt, 6 h)	**309** 29–46% 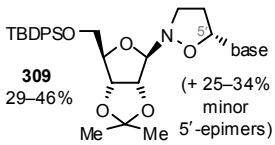 (+ 25–34% minor 5′-epimers)
[7] Wengel *et al.*[36]	**310** 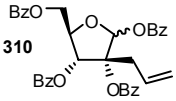	$T(TMS)_2$	$SnCl_4$, MeCN, reflux, 3 h.	**311** 54% after debenzoylation 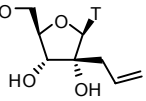
[8] Chun *et al.*[37]	**312** 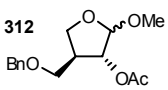	$^{Bz}C(TMS)_2$	TMSOTf, MeCN, rt, 18 h.	**313** 83% (β:α 6:1) 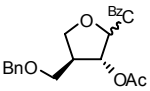
	314 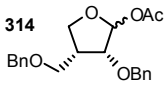	$^{Bz}C(TMS)_2$	TMSOTf, DCE, -35 °C, 1 h.	**315** 65% (β:α 2:1) 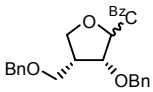
[9] Nielsen *et al.*[38]	**316** R = Ac, Bz 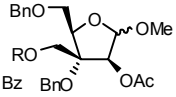	$T(TMS)_2$	TMSOTf, MeCN, 70 °C, 1 d.	**317** 40–68% 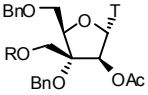

[10] Rozner and Liu[39]	**318** 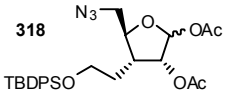	U(TMS)$_2$, C(TMS)$_2$, ^{Bz}A(TMS)$_2$, G*(TMS)$_2$	TMSOTf, DCE, reflux, 1 h. (U: TMSOTf, CH_2Cl_2, rt, 3 h,) (A: $SnCl_4$, rt, MeCN, 30 min)	**319** 56–99% 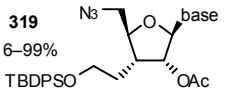
[11] You *et al.*[40]	**320** 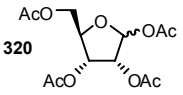	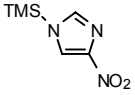	$SnCl_4$, DCE, rt, 8–14 h.	**321** 90% (β:α 3:1) 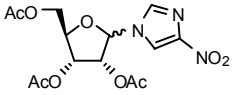
[12] Chattopad-hyaya *et al.*[41]	**322** 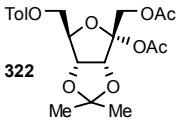	U(TMS)$_2$, ^{Bz}C(TMS)$_2$, ^{Bz}A(TMS)$_2$, G*(TMS)$_2$	TMSOTf, MeCN, 4.5 h, 0 °C–rt. (A & G*: TMSOTf, MeCN, 90 °C, 30 min)	**323** 39–77% (β>>α) 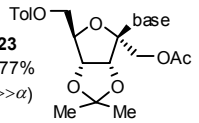
	324 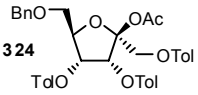	U(TMS)$_2$, ^{Bz}C(TMS)$_2$, ^{Bz}A(TMS)$_2$, G*(TMS)$_2$	TMSOTf, MeCN, 40 °C, 2.5 h, (A & G*: TMSOTf, MeCN, 80 °C, 1.5 h)	**325** 60–78% (β>α) 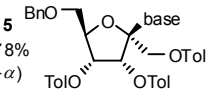
[13] Enders *et al.*[42]	**326** 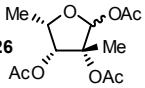	persilylated hypoxanthine, 2,6-dichloropurine	TMSOTf, DBU, 1.5 h, MeCN, -30 °C→reflux. (purine: -15 °C→rt)	**327** 70–84% 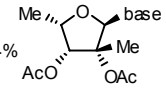
[14] Piccirilli *et al.*[43,44]	**328** 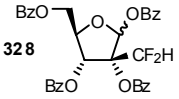	U(TMS)$_2$	$SnCl_4$, MeCN, reflux, 2 d.	**329** 78% 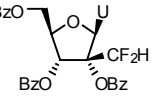
	330 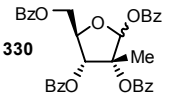	^{Ac}G(TMS)$_3$	TMSOTf, *p*-xylene, reflux, 6 h.	**331** 80% 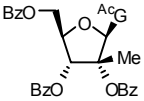
[15] Camplo *et al.*[45]	**332** X = CH_2 or S 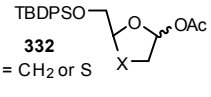	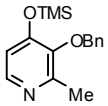	TMSOTf, DCE, rt, 20–24 h.	**333** 63–82% (*cis*>*trans*) 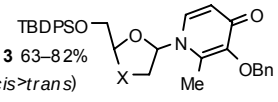
[16] Mandal *et al.*[46]	**334a** R^1 = OAc, R^2 = Me; **334b** R^1 = OH, R^2 = CH_2N_3; **334c** R^1 = OAc, R^2 = CH_2N_3 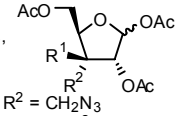	U(TMS)$_2$	TMSOTf, MeCN, reflux, 4 h.	**335a** R^1 = OAc, R^2 = Me; **335b** R^1 = OTMS, R^2 = CH_2N_3; **335c** R^1 = OAc, R^2 = CH_2N_3 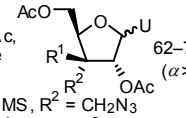 62–70% (α>β)
	336a R^1 = OAc, R^2 = H; **336b** R^1 = Me, R^2 = OAc 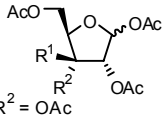	U(TMS)$_2$	TMSOTf, MeCN, reflux, 4 h.	**337a, b** 62–70% 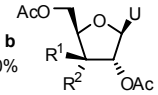
[17] Ravn *et al.*[47]	**338** 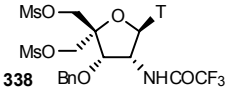	^{Bz}A(TMS)$_2$, G*(TMS)$_2$	TMSOTf, DCE.	**339** 57–58% 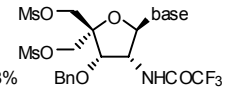
[18] Alibés *et al.*[48]	**340** 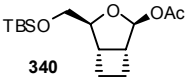	T(TMS)$_2$, 6-CP(TMS)$_2$	TMSOTf, MeCN, rt, 2 h.	**341** 67–85% 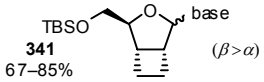 (β>α)
[19] Shashikanth *et al.*[49]	**342** 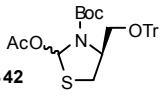	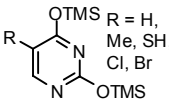 R = H, Me, SH, Cl, Br	TMSOTf or $SnCl_4$, MeCN, 0 °C, 16 h.	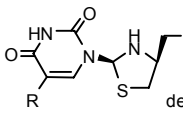 **343** 52–58% after deprotections
[20] Kim and Hong[50]	**344** 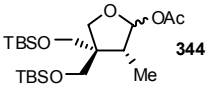	T(TMS)$_2$, U(TMS)$_2$, C(TMS)$_2$, 6-CP(TMS)$_2$	TMSOTf, DCE, rt, 2 h.	**345** 34–64% (β:α 1:1) 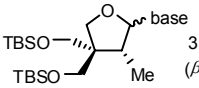

Table 2.2: Selected examples of nucleosidations under Vorbrüggen conditions. Silylations of bases are omitted for simplicity. Examples from pyran and spironucleosides are discussed separately in Session 2.5 and 2.6.

2.4.2 Electrophilic Addition [B]

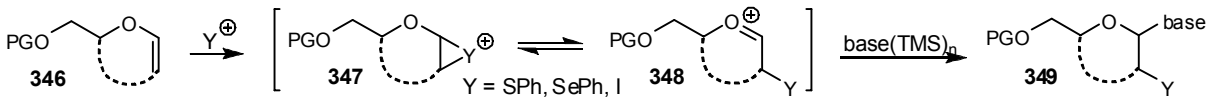

Scheme 2.6: Synthesis of nucleoside **349** from glycal **346** and persilylated base in the presence of an electrophile.[23,28]

Activation of glycal **346** by a electrophilie such as NIS, I_2, PhSCl or PhSeCl generates the bicyclic cation **347**, which is subsequently trapped *in situ* by a persilylated base to afford β-substituted nucleoside **349**. Stereoselectivity can only be achieved when the electrophilic addition is facially selective and equilibrium to oxonium ion **348** is insignificant. This strategy is less commonly used than other approaches.[23,28]

Entry	Glycals/Spacers	Heterobases	Conditions	Products and Yields
[1] Kasson and Castillón[51]	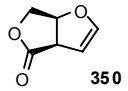 **350**	$U(TMS)_2$	PhSeCl, AgOTf, benzene, rt, 40 min	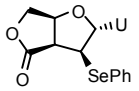 **351** 51%
	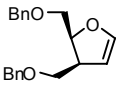 **352**	$U(TMS)_2$	PhSeCl, AgOTf, benzene, rt, 20 min	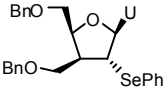 **353** 65%
[2] Dong and Paquette[52]	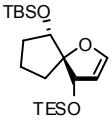 **354**	$T(TMS)_2$	NIS, CH_2Cl_2, rt, 1 h	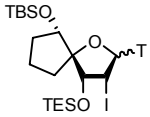 **355** 76% (α:β 3:1)
[3] Dong and Paquette[53]	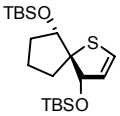 **356**	$T(TMS)_2$	PhSeCl or NIS, MeCN, 0 °C, 1 h	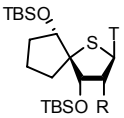 **357** 52–53% R = SePh, I (+ 13% β-phenylseleno/iodo α-isomer)
	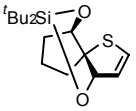 **358**	$T(TMS)_2$, $U(TMS)_2$	PhSeCl, MeCN, 0 °C, 1 h	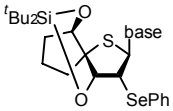 **359** 63–71%

Table 2.3: Selected examples of the nucleosides synthesised by the electrophilic addition.

2.4.3 Metal Salt Procedure [C]

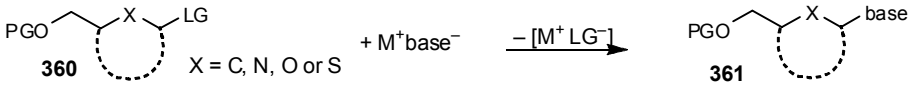

Scheme 2.7: Synthesis of nucleosides **361** from glycoside **360** and the metal salt of a heterobase.[23,28]

In most cases, the nucleophilic metal salt of a heterobase reacts with glycoside **360** bearing a good leaving group such as Cl or Br *via* S_N2 type displacement. The stereochemistry of the nucleoside product **361** is determined by the nature of the glycoside precursor which can be a carbo-

or hetero-, cyclic or acyclic molecule. Although operating through a different mechanism, this category also includes palladium-catalysed allylic substitutions and nucleosidations mediated by mercury. Inorganic mercuric salts (such as $HgBr_2$, $HgCl_2$ and $Hg[CN]_2$) generate both the mercuric-heterobase complex and the oxonium ion from the glycosyl halide, which was required for the coupling reaction.[23,28]

Entry	*Glycosides/Spacers*	*Heterobases*	*Conditions*	*Products and Yields*
[1] Tyler *et al.*[54]	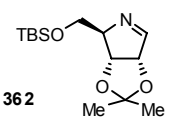 **362**	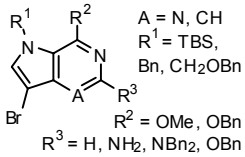 A = N, CH; R^1 = TBS, Bn, CH_2OBn; R^2 = OMe, OBn; R^3 = H, NH_2, NBn_2, OBn	BuLi, anisole, Et_2O, -70 →0 °C	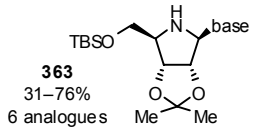 **363** 31–76% 6 analogues
[2] Mirand *et al.*[33]	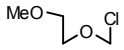 **364**	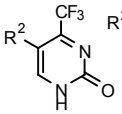 R^2 = Bn, Et, ^iPr	NaI, CH_2Cl_2, reflux, 4 h	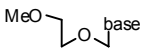 **365** 63–80%
[3] Kim and Jacobson[55]	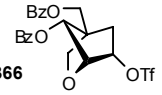 **366**	adenine	K_2CO_3, 18-crown-6, DMF, 40–45 °C, 6 h	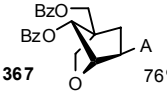 **367** 76%
[4] Ludek and Meier[56]	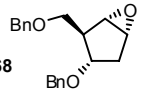 **368**	thymine	LiH or NaH, DMF, 140 °C, 3 d; or Et_3Al, THF, ultrasound, rt, 12 h,	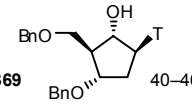 **369** 40–46%
[5] Kim and Hong[57]	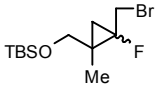 **370**	thymine, uracil, cytosine, adenine	Cs_2CO_3, DMF, rt	8 analogues 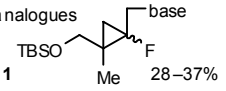 **371** 28–37%
[6] Liotta *et al.*[58]	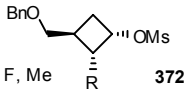 R = F, Me **372**	3-*N*-(4-methoxybenzyl)-5-fluorouracil	K_2CO_3, 18-crown-6, DMF, 120 °C	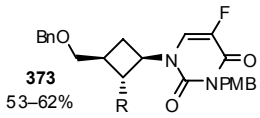 **373** 53–62%
[7] Zhou and Zemlicka[59]	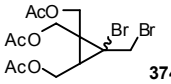 **374**	adenine, 2-amino-6-chloropurine	K_2CO_3, DMF, 100–105 °C, 2.5–3.5 h	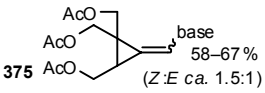 **375** 58–67% (*Z*:*E ca.* 1.5:1)
[8] Zhou *et al.*[60]	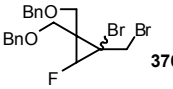 **376**	adenine, 2-amino-6-chloropurine	K_2CO_3, DMF, rt, 6–7 h, then 100–105 °C, 3–4 h	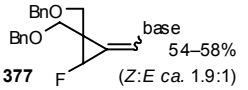 **377** 54–58% (*Z*:*E ca.* 1.9:1)
Pd-catalysed allylic substitution				
[9] Miller *et al.*[61]	 **378**	2-amino-6-chloropurine	cat. $Pd(OAc)_2$, PPh_3, THF, DMSO, 0 °C→rt, 18 h	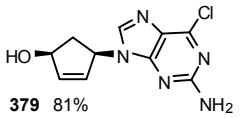 **379** 81%
[10] Schmalz *et al.*[62]	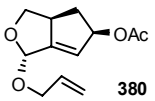 **380**	thymine, uracil, 5-bromouracil, 4-*N*-benzoylcytosine, Adenine	i. NaH (A: Cs_2CO_3), DMSO, 30 min, 80 °C→rt; ii. cat. $Pd(PPh_3)_4$, PPh_3, THF, 50–80 °C, 16 h	**381** 46–74% 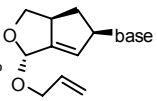
Mercuric salt-mediated nucleosidation				
[11] Piccirilli *et al.*[43]	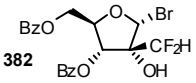 **382**	$^{Bz}C(TMS)_2$, $^{Bz}A(TMS)_2$, $G^*(TMS)_2$	HgO, $HgBr_2$, toluene, 80–90 °C, 2–5 h	**383** 31–65% 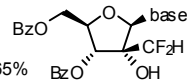
	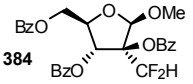 **384**	$^{Bz}C(TMS)_2$, $U(TMS)_2$	i. HBr (30% in AcOH), 75 °C, 4 h ii. persilylated base, HgO, $HgBr_2$, benzene, rt, 3 d	**385** 48–55% 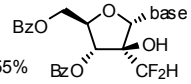

Table 2.4: Selected examples of nucleosidation using metal salt procedures.

2.4.4 Mitsunobu Reaction [D]

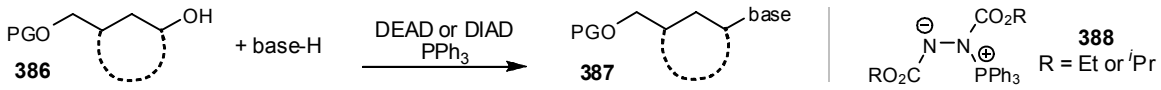

Scheme 2.8: Synthesis of nucleoside **387** from glycoside **386** and heterobase by Mitsunobu reaction.[23,28]

The Mitsunobu reaction[63] directly couples a heterobase with glycoside **386** bearing a hydroxyl group. Betaine **388**, generated *in situ* from a dialkyl azocarboxylate and a phosphine, deprotonates the heterobase while the hydroxyl group of the glycoside forms a triphenylphosphonium adduct. This adduct triggers the S_N2 substitution of the hydroxy group by deprotonated heterobase forming nucleoside **387** with inversion of configuration. This reaction is commonly used for the carbo-glycosides and has become increasingly popular in recent years.[23,28]

Entry	Glycosides/Spacers	Heterobases	Conditions	Products and Yields
[1] Huet *et al.*[64]	**389** 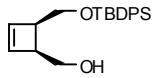	adenine, 3-*N*-benzoylthymine	PPh_3, DEAD, THF, rt, 20 h (A: 7 d)	**390** 60–94% 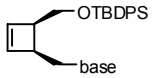
[1] Huet *et al.*[65]	**391** 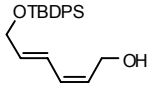	adenine, 3-*N*-benzoylthymine	PPh_3, DEAD, THF, rt, 2 d	**392** 48–67% 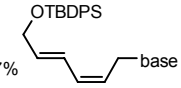
[2] Marquez *et al.*[66]	**393** R^1 = OBz, R^2 = N_3; **394** R^1 = OBn, R^2 = OTBDPS 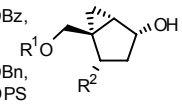	6-chloropurine	PPh_3, DEAD, THF, 0 °C→rt, 18 h	**395** 55–94% 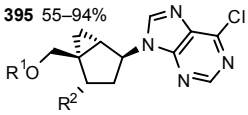
[3] Meier *et al.*[56]	**396** 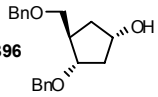	R = Me, F, (*E*)-bromovinyl 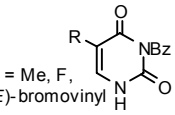	PPh_3, DIAD, MeCN, -40 °C→rt, 16 h	**397** 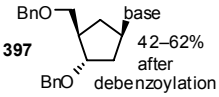 42–62% after debenzoylation
[4] Dahl *et al.*[67]	**398** 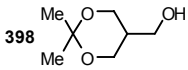	3-*N*-benzoylthymine	PPh_3, DIAD, THF, rt, 18 h	**399** 61% 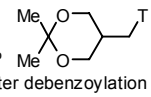 after debenzoylation
[5] Audran *et al.*[68]	**400** 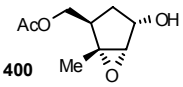	adenine, 6-chloropurine, 2-amino-6-chloropurine	PPh_3, DIAD, THF, 0→40 °C, 16 h	**401** 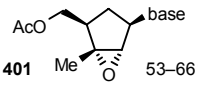 53–66%
[6] Yoshimura *et al.*[69]	**402** 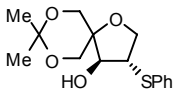	6-chloropurine, 3-*N*-benzoylthymine	PPh_3, DEAD, THF, rt, 1–3 h	**403** 52–83% 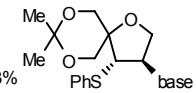
[7] Liotta *et al.*[58]	**404** 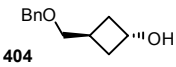	3-*N*-benzoyl-5-fluorouracil	PPh_3, DEAD, THF, rt	**405** 30% 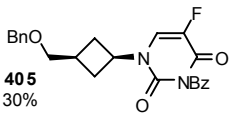
[8] Hostetler *et al.*[70]	**406** 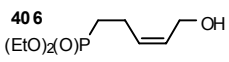	3-*N*-benzoylthymine, 3-*N*-benzoyluracil, adenine, 2-amino-6-chloropurine	PPh_3, DIAD, DMF, 0 °C, 2 h (purines: 0 °C→rt, 18 h)	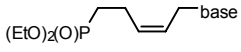 **407** 42–81% after debenzoylation
[9] Moon *et al.*[71]	**408** 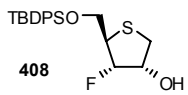	3-*N*-benzoylthymine, 3-*N*-benzoyluracil, 6-chloropurine	PPh_3, DEAD, THF, rt, 18 h	**409** 62–88% 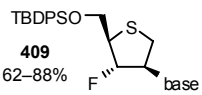
[10] Li and Zemlicka[72]	**410** 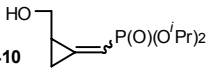	adenine, 2-amino-6-chloropurine	PPh_3, DEAD, THF, 0 °C→rt, 18 h	**411** 47–87% 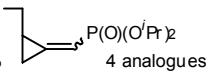 4 analogues

Table 2.5: Selected examples of nucleosidation using the Mitsunobu reaction.

2.5 Pyran-based Nucleoside Analogues

All natural nucleosides contain a five-membered furanose to hold the 1′-heterocyclic base, 3′- and 5′-hydroxy group in a defined spatial orientation. However, furanose merely acts as a scaffold structure and is not strictly recognised by enzymes (see acyclovir and its analogues). As a result, modifications to this glycoside unit generate a large range of nucleoside analogues. Small modification to the heterocyclic base is possible, but due to the neatly tailored base recognition processes, there is limited scope for such variation without damaging the hydrogen-bonding elements and the electronic effects within the nucleobases.[17,23,29,73]

Compared to the number of furan-based analogues, pyran-based nucleosides are less common due to the diminished conformational flexibility which is important for enzyme recognitions. Nevertheless, steric and electronic fits can be achieved between the six-membered ring substrate and enzyme. As a result, a number of the pyran-based nucleosides have been synthesised and evaluated for their potential antiviral (or anticancer) activity and as building blocks in nucleic acid synthesis.[23,73,74]

Herdewijn *et al.*[75] synthesised mannitol nucleosides **415** as potential anti-herpes agents and to increase the understanding of the structure-activity relationship (SAR) of hexitol nucleosides. The synthesis started with the transformation of protected glycoside **412** into epoxide **413** and the ring opening of **413** by metal salt displacement yielded uridine **414**. Subsequent functional group manipulations of **414** gave nucleosides **415a–d** (Scheme 2.9). Antiherpes activity was observed for uridine **415b** [IC_{50}(HSV-1) = 150 μg mL^{-1}], 5-iodouridine **415c** [IC_{50}(HSV-1) = 7 μg mL^{-1}, IC_{50}(HSV-2) = 70 μg mL^{-1}] and cytidine **415d** [IC_{50}(HSV-1 and HSV-2) = 70 μg mL^{-1}, IC_{50}(VZV and CMV) = 10 μg mL^{-1}].

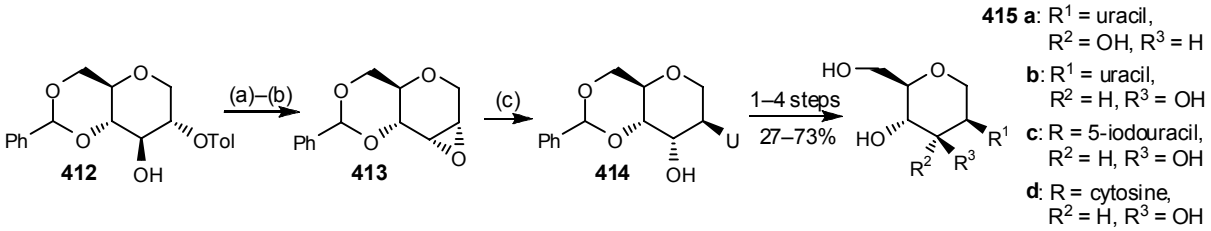

Reagents and conditions: (a) TsCl, cat. DMAP, NEt_3, CH_2Cl_2, rt, 83%; (b) NaOMe, MeOH, dioxane, 50 °C, 81%; (c) uracil, NaH, DMF, 120 °C, 69%.

Scheme 2.9: Synthesis of mannitol derived nucleoside **415a–d** by Herdewijn *et al.*[75]

Wiessler *et al.*[76] synthesised monosaccharide-linked nucleoside analogues **421** as potential inhibitors of the suicidal human DNA repair protein, O^6-methylguanine-DNA methyltransferase (MGMT) which desensitised the tumour cells against alkylating therapeutics. The analogues were prepared in three steps: glycosylation (attachment of the glycoside–heterobase linker), nucleophilic substitution (attachment of the heterobase to the linker), and deprotection (Scheme 2.10). Variation of the linker

and heterobase resulted in the preparation of nine nucleosides with anti-MGMT activity (IC_{50} = 0.03–25 μM).

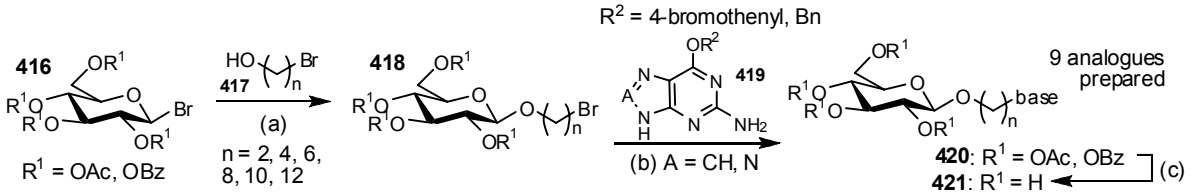

Reagents and conditions: (a) **417**, TMSOTf, 4 Å MS, CH_2Cl_2, rt or Ag_3PO_4, 3 Å MS, $MeNO_2$, rt, 10–62%; (b) **419**, LiH, 4 Å MS, DMF, 80 °C, 15–37%; (c) NaOMe, MeOH, rt, 63–99%.

Scheme 2.10: Synthesis of pyran-nucleosides **421** as potential anti-MGMT agents by Wiessler *et al.*[76]

Banwell *et al.*[77] prepared glucose- and cyclitol-base nucleosides **426** and **430** as novel analogues of the anti-viral agent showdomycin.[78] Nucleosides **426** and **430** were synthesised with the following key steps: epoxidation, indium-catalysed ring opening by pyrrole **424**, deprotections and finally, oxidation of pyrrole to maleimides **426** and **430** (Scheme 2.11). Unfortunately, both nucleosides **426** and **430** failed to show any anti-viral activity and their nephrotoxicity (IC_{50} = 5 μM) hampered their exploitation as therapeutic agents.

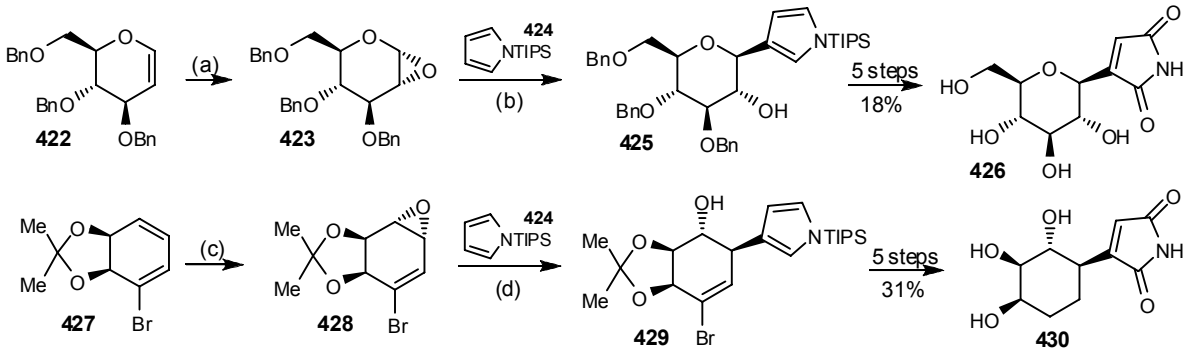

Reagents and conditions: (a) DMDO, CH_2Cl_2, 0 °C, 1 h; (b) **424**, cat. $InCl_3$, CH_2Cl_2, 0 °C→rt, 19 h, 37% over 2 steps; (c) *m*-CPBA, CH_2Cl_2, 0 °C→rt, 15 h, 90%; (d) **424**, cat. $InCl_3$, CH_2Cl_2, rt, 5 d, 54%.

Scheme 2.11: Synthesis of glucose- and cyclitol-based nucleosides **426** and **430** by Banwell *et al.*[77]

Peseke *et al.*[79] synthesised novel iso-*C*-nucleoside analogues **441**–**446** as potential antiviral agents. The synthesis began with the transformation of epoxide **431** to aldehyde **432** which, in turn, served as a precursor for ynone **433** and vinyl nitrile **438**. Addition-cyclisation of hydrazines, amidinium salts or 2-aminobenzimidazole to ynone **433** yielded pyrazoles **434**, pyrimidines **435** or fused heterocycles **436**, respectively. Alternatively, vinyl nitriles **438** reacted with elemental sulphur in the presence of triethylamine to give aminothiophenes **439**. **439** were then treated with triethyl orthoformate (and ethanolic ammonia for R^4 = CN) to afford thieno[2.3-*d*]pyrimidine and thieno[2.3-*d*]pyrimidinones **440**. Subsequent deprotections of selected analogues in **434**–**436**, **439** and **440** yielded iso-*C*-nucleoside analogues **441**–**446** (Scheme 2.12).

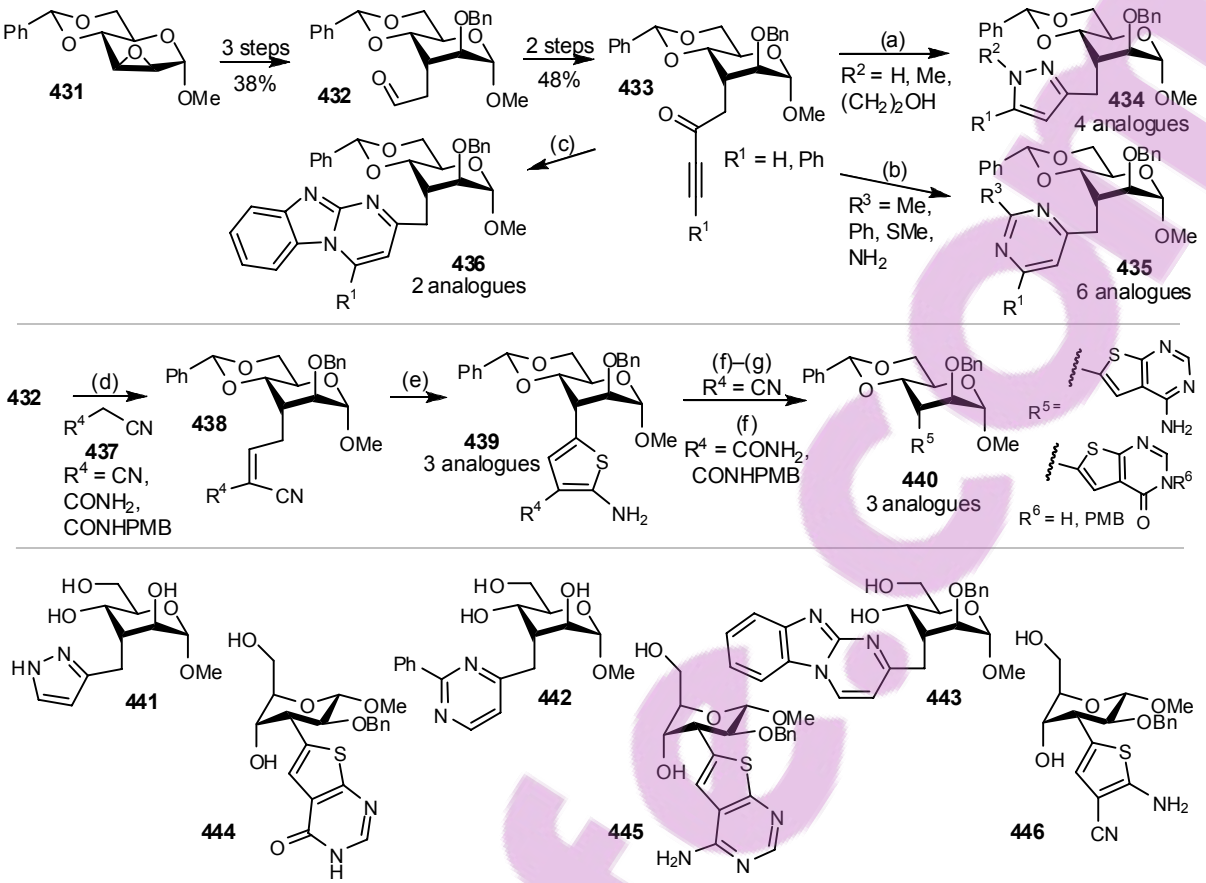

Reagents and conditions: (a) R^2NHNH_2, MeOH, rt, 1 h, 73–90%; (b) $R^3C(NH_2)=NH_2^+X^-$, Na_2CO_3, EtOAc–H_2O, reflux, 24 h, 40–95%; (c) 2-aminobenzimidazole, MeOH, reflux, 2 h, 33–40%; (d) **437**, Al_2O_3, toluene, rt–reflux, 1 h–1 d, 70–90%; (e) S_8, NEt_3, DMF, rt, 15 min–12 h, 45–85%; (f) $(EtO)_3CH$, reflux, 1–7 h, 56–65%; (g) NH_3, EtOH, reflux, 2 h, 50% over 2 steps.

Scheme 2.12: Synthesis of pyran-based iso-*C*-nucleosides **441**–**446** by Peseke *et al*.[79]

Van Aerschot *et al*.[80] developed potential hexitol universal nucleosides that "paired equally with all four natural bases" after their incorporation into oligodeoxynucleotides, to solve problems caused by the degeneracy of genetic code or incomplete peptide sequence data. The synthesis started with the S_N2 displacement of tosylate **447** by the sodium salt of the heterobase to afford nucleosides **448**. Subsequent removal of benzylidene, tritylation and phosphitylation afforded phosphoramidites **449**, ready for the standard oligonucleotide assembly procedures (Scheme 2.13).

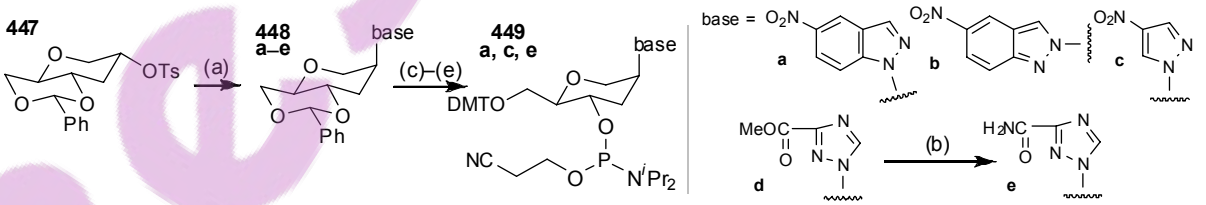

Reagents and conditions: (a) i. base-H, NaH, DMF, 60 °C, 1 h; ii. **447**, DMF; 70–110 °C, 6–60 h, 52–82%; (b) NH_3, MeOH, rt, 3 h, 86%; (c) AcOH, H_2O, 70 °C, 1 h, 83–87%; (d) DMTCl, pyridine, rt, 2 h, 77–97%; (e) $PCl(OCH_2CH_2CN)[N(^iPr)_2]$, DIPEA, CH_2Cl_2, rt, 15–45 min, 40–89%.

Scheme 2.13: Synthesis of potential hexitol universal nucleosides **449** by Van Aerschot *et al*.[80]

Komiotis *et al.*[74] synthesised fluoro-ketopyranosyl nucleosides **453** and **454** as potential antiviral agents. The synthesis began with the transformation of furanose derivative **450** into pyranose **451** followed by the nucleosidation under Vorbrüggen conditions to afford protected cytidine **452**. Further functional group manipulations gave fluoro-ketopyranosyl nucleosides **453** and **454** (Scheme 2.14). *In vitro* testings showed that **453** and **454** inhibited rotavirus infection and **454b** also partially inhibited VSV infection.

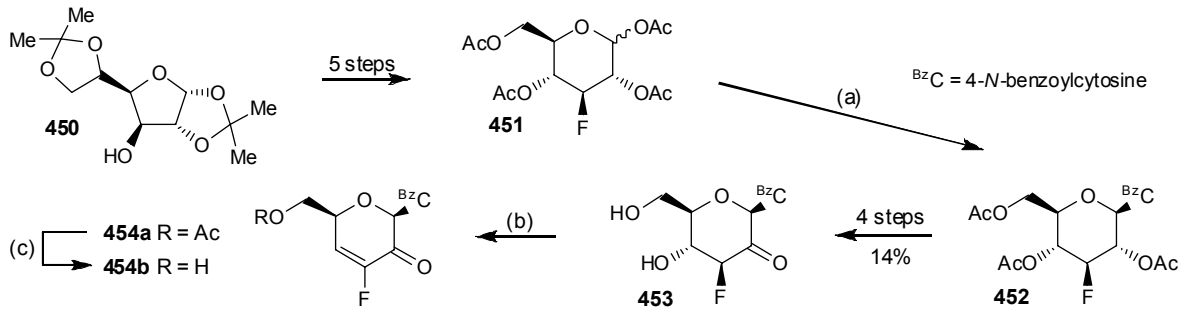

Reagents and conditions: (a) i. 4-*N*-benzoylcytosine, HMDS, saccharine, MeCN, reflux, 30 min; ii. **451**, TMSOTf, reflux, 5 h, 68%; (b) Ac_2O, pyridine, 0 °C, 1 h, 66%; (c) AcCl, MeOH, CH_2Cl_2, rt, 24 h, 50%.

Scheme 2.14: Synthesis of fluoro-ketopyranosyl nucleosides **453** and **454** by Komiotis *et al.*[74]

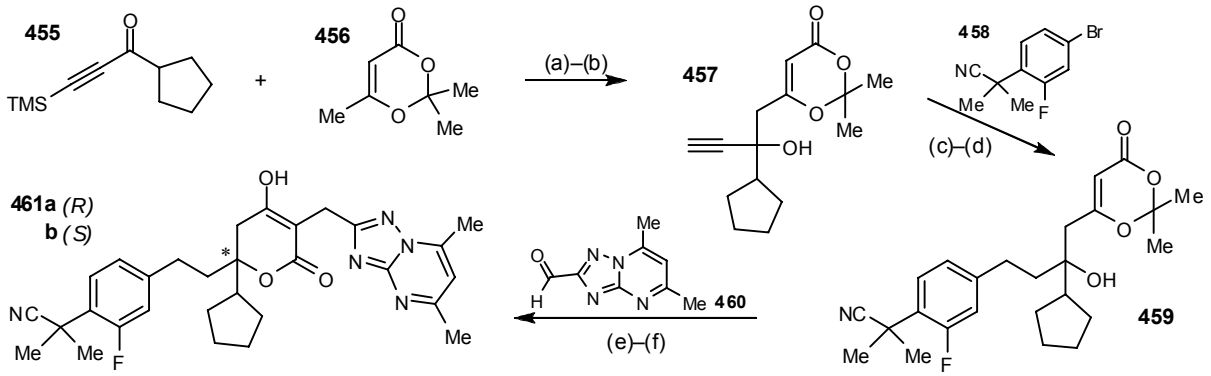

Reagents and conditions: (a) i. **456**, LDA, THF, -78 °C, 30 min; ii. **455**, -78→-30 °C, 1 h; (b) CsF, MeOH, rt, 18 h, 61% over 2 steps; (c) **458**, cat. $Pd(PPh_3)_2Cl_2$, cat. CuI, DIPA, DMF, 90 °C, 20 min, 74%; (d) cat. $Pd(OH)_2$, H_2, EtOH, rt, 6 h, 99%; (e) NaOH, MeOH, rt, 3 h, 56%; (f) **460**, BH_3•SMe_2, MeOH, rt, 3 h, 80%.

Scheme 2.15: Synthesis of enantiomeric dihydropyrone antiviral (anti-HCV) agents **461** by Li *et al.*[81] Dihydropyrone **461a** was subsequently selected for scale-up operations (not shown).[82]

Li *et al.*[81] developed a novel class of dihydropyrone antiviral agent which inhibited HCV NS5B polymerase by binding at an allosteric site. A series of SAR studies had led to the discovery of racemic **461** with potent antiviral activity (IC_{50} = 3 nM and EC_{50} = 30 nM) and low cytotoxicity (CC_{50} = 320 μM). The synthesis started with an aldol coupling between ynone **455** and dioxinone **456** and followed by desilylation to yield ynol **457**. Palladium-catalysed Sonogashira coupling between alkyne **457** and bromide **458** and subsequent hydrogenation gave adduct **459**. One-pot deprotection and cyclisation furnished a dihydropyrone which was then coupled with aldehyde **460** in the presence of BH_3•SMe_2 to afford a racemic mixture of **461**. The individual enantiomers **461a** and **461b** were

separated using chiral HPLC and *(R)*-dihydropyrone **461a** had shown slightly superior potencies and pharmacokinetic profiles (Scheme 2.15).[81,82]

2.6 Spirocyclic Nucleoside Analogues

Spirocyclic nucleoside analogue is a novel class of structurally unique and conformationally restricted nucleosides. The discovery of bioactive spirocyclic nucleosides such as naturally occurring herbicidal (+)-hydantocidin **(465)**[83] and synthetic anti-HIV TSAO-T **511a**[84] has triggered considerable interest in the synthesis and biological activity of this novel class.[23,29,85]

2.6.1 1'-Spironucleosides—Hydantocidin Analogues and other Novel Examples

(a) Hydantocidin Analogues

(+)-Hydantocidin **(465)** is a naturally occurring spironucleoside isolated from the culture broth of *Streptomyces hygroscopicus*. It exhibits potent growth inhibition and herbicidal activity against annual, perennial, monocotyledonous and dicotyledonous weeds with a similar efficacy to that of glyphosate while showing low toxicity against fish and mice.[83] Once phosphorylated, it competitively inhibits adenylosuccinate synthetase (AdSS) which catalyses the GTP-dependent conversion of inosine monophosphate (IMP) and aspartic acid to adenosine monophosphate (AMP)—the *de novo* purine synthesis of the target plant.[86] AdSS is also the target for therapeutic agents such as L-alanosine[87] (antitumour, antiviral, antibiotic and immunosuppressive agent) and hadacidin[88] (antitumour agent, antibiotic and plant growth inhibitor).

(+)-Hydantocidin **(465)** is structurally distinct from other nucleosides due to the presence of a spiro-annulated heterobase (hydantoin) at the anomeric centre of the ribofuranose. As a result of this unusual structure and the biological implication of its target AdSS, considerable investigations were carried out on the total synthesis and biological properties of hydantocidin **(465)** as well as the development of its derivatives as potential therapeutic agents (Figure 2.5).[29]

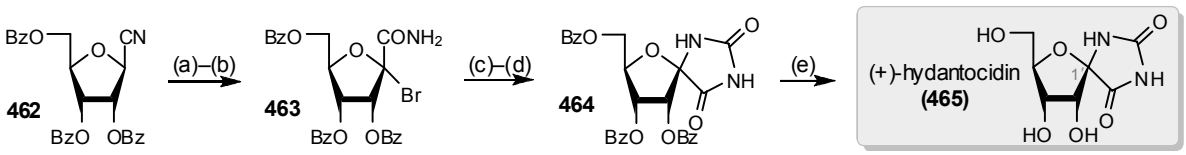

Reagents and conditions: (a) MnO_2, CH_2Cl_2, 95%; (b) NBS, $(PhCOO)_2$, CCl_4, reflux, 51%; (c) AgOCN, $MeNO_2$, 80 °C; (d) CSA, $MeNO_2$, 70 °C, 44% over 2 steps; (e) LiOOH, THF–H_2O, 0 °C, 90%.

Scheme 2.16: Total synthesis of (+)-hydantocidin **(465)** by Harrington and Jung.[89]

The total synthesis of (+)-hydantocidin **(465)** by Harrington and Jung[89] started with a mild hydration of nitrile **462** followed by radical bromination to give α-bromo-β-amide **463**. Spirocyclisation was then triggered by silver cyanate and the mixture was equilibrated under acid conditions to afford benzoyl-protected hydantocidin **464**. Subsequent debenzoylation yielded the desired (+)-hydantocidin **(465)** (Scheme 2.16).

Pyne *et al*.[90] synthesised carbacyclic hydantocidin derivatives **470** and **471** starting with a phosphine-catalysed [3 + 2]-cycloaddition between *bis*-protected 5-methylenehydantoin **466** and an ylide generated from the addition of phosphine to a 2-butynoic acid derivative such as ester **467**. This strategy differed from most other syntheses of nucleosides in which the hydantoin moiety was formed prior to the construction of the ribofuranose surrogates. Subsequent acid-catalysed isomerisation, reduction, dihydroxylation and deprotection yielded carbocyclic hydantocidin **470** and 6,7-diepi-carbocyclic hydantocidin **471** (Scheme 2.17).

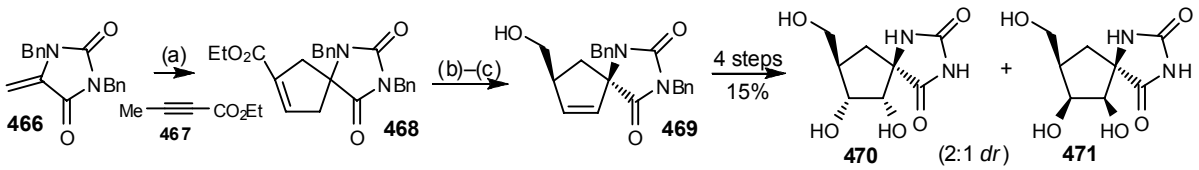

Reagents and conditions: (a) ethyl 2-butynoate **(467)**, benzene, PBu_3, rt, 15 h, 79%; (b) aq. HCl, MeCN–H_2O, 90 °C, 15 h, 99%; (c) BH_3•SMe_2, THF, 0 °C, 6 h, 95%.

Scheme 2.17: Synthesis of carbacyclic hydantocidin analogues **470** and **471** by Pyne *et al*.[90]

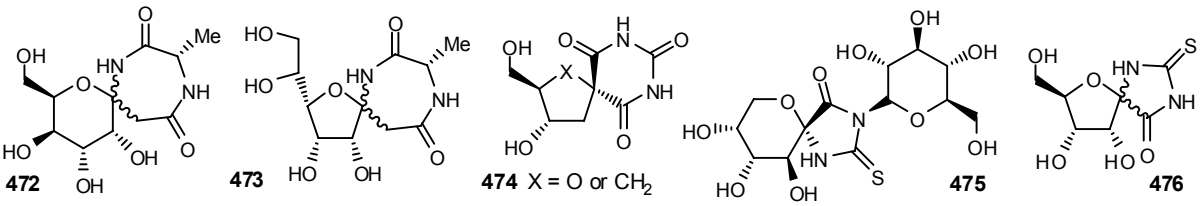

Figure 2.5: Selected recent example of hydantocidin derivatives **472**–**476** synthesised.[91]

(b) Further Examples of Novel 1′-Spironucleosides

Chatgilialoglu *et al*.[92] synthesised 1′-anomeric spironucleoside analogues **479**, **480**, **483** and **484** incorporating a tether to restrain the rotation of the base around the *N*-glycosidic bond. The synthesis began with the homologation of protected uridine **477** to give 6-hydroxymethyl-ribouridine **478**. Cyclisation by radical intramolecular hydrogen abstraction of uridine **478** installed the required tether (see Chapter 1.4.7) and yielded tricyclic ribonucleoside **479** after desilylation. Subsequent removal of the 2′-hydroxy group afforded deoxyribonucleoside **480**. Analogues with a carbacyclic tether were synthesised from aldehyde **481**. Homologation under modified Corey–Fuchs protocols, radical cyclisation and desilylation gave spironucleoside **483** whereas hydrogenation of **482** gave spironucleoside **484** (Scheme 2.18).

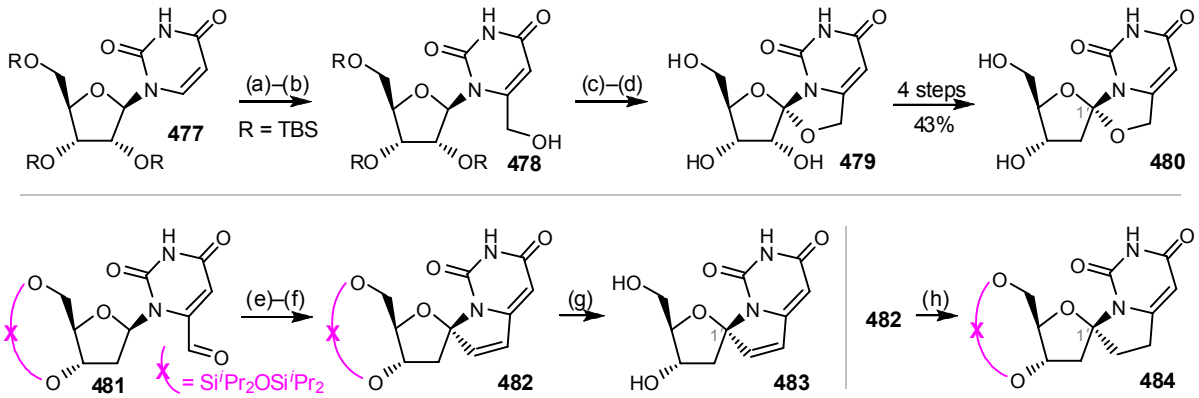

Reagents and conditions: (a) i. LDA, THF, -70 °C, 3 h; ii. HCO_2Et, -60 °C, 2 h; (b) $NaBH_4$, MeOH, rt, 30 min, 68% over 2 steps; (c) $PhI(OAc)_2$, I_2, cyclohexane, hν, 28 °C, 6 h, 36%; (d) TBAF, SiO_2, THF, rt, 2 h, 90%; (e) $Ph_3P{=}CBr_2$, CH_2Cl_2–DMF, rt, 2 h, 42%; (f) $(Bu_3Sn)_2$, benzene, hν, 80 °C, 12 h, 52%; (g) TBAF, AcOH, THF, rt, 1 d, 90%; (h) cat. Rh/Al, H_2, NEt_3, MeOH, rt, 5 h, 68%.

Scheme 2.18: Synthesis of 1′-anomeric spironucleoside analogues by Chatgilialoglu *et al.*[92]

Gimisis *et al.*[93] synthesised structurally similar 1′-branched spironucleoside analogues **487**–**490** starting from radical debromination of protected uridine **485**. Base-promoted addition-cyclisation of the resulting uridine **486** in the presence of HMPA under thermodynamic conditions gave nucleoside **487**. On the other hand, the same base-promoted addition-cyclisation of uridine **486** in the absence of HMPA under kinetic conditions gave nucleoside **489**. Subsequent desilylation of **487** and **489** afforded nucleosides **488** and **490** (Scheme 2.19). The best cytostatic activity was observed for nucleoside **489** bearing 3′- and 5′-OTBS groups [IC_{50} = 5.95–9.46 μM]. Interesting, bis-silylation (2′- and 5′-OTBS) was also required for the observed biological activities for TSAO analogues (see Chapter 2.6.3).

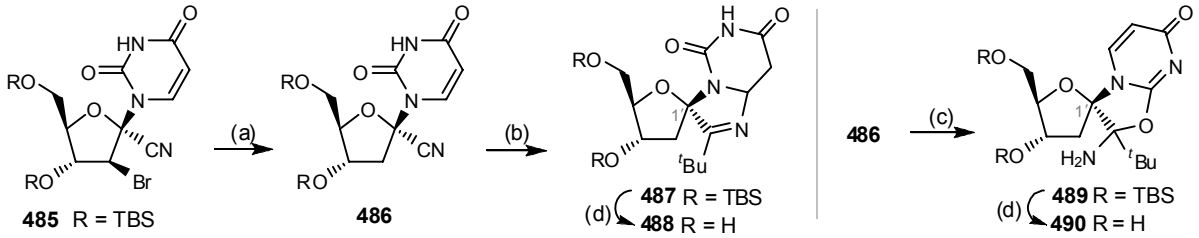

Reagents and conditions: (a) $(TMS)_3SiH$, AIBN, toluene, 80 °C, 2 h, 94%; (b) i. ^{t}BuLi, HMPA, THF, reflux, 12 h; ii. aq. Li_2CO_3, H_2O, rt, 71%; (c) i. ^{t}BuLi, THF, rt, 5 min; ii. aq. Li_2CO_3, H_2O, rt, 3 h, 77%; (d) NH_4F, MeOH, reflux, 18 h, 92–98%.

Scheme 2.19: Synthesis of 1′-branched spironucleoside analogues **487**–**490** by Gimisis *et al.*[93]

Mandal *et al.*[94] applied intramolecular nitrone cycloaddition (INC) for the synthesis of carbacyclic spironucleosides **497**–**499**. The synthesis began with the deprotection of acetonide **491** to yield aldehyde **492** which underwent INC with *N*-benzyl hydroxylamine to give a mixture of bis-isoxazolidines **494** and **495** bearing a 5,6-spiro framework. On the other hand, oxidative cleavage of α-hydroxyaldehyde **492** afforded aldehyde **493** which reacted with *N*-benzyl hydroxylamine to give bis-isoxazolidine **496** bearing a 5,5-spiro framework. Cleavage of the bis-isoxazolidine rings in

494–496 by hydrogenolysis afforded hydroxyamino spirocyclic intermediates which were then converted into spiroadenosines **497–499** in two steps (Scheme 2.20).

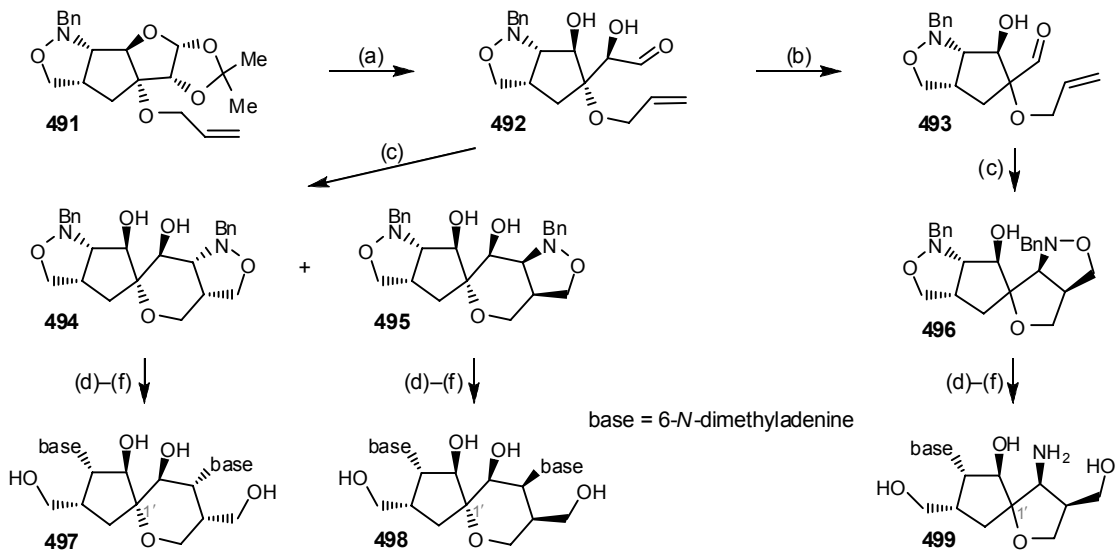

Reagents and conditions: (a) aq. H_2SO_4, MeCN–H_2O, rt, 1 d, 90%; (b) aq. $NaIO_4$, EtOH, 0 °C, 40 min, 82%; (c) BnNHOH, EtOH, rt–60 °C, 25 h, **494**: 43%, **495**: 27%, **496**: 67%; (d) cat. Pd/C, cyclohexene, EtOH, reflux, 4 h; (e) 5-amino-4,6-dichloropyrimidine, NEt_3, BuOH, reflux, 18 h; (e) $HC(OEt)_3$, *p*-TsOH, DMF, rt, 24–30 h, 19–22% over 3 steps.

Scheme 2.20: Synthesis of 1′-spiroadenosine **497–499** by Mandal *et al.*[94]

2.6.2 2′-Spironucleosides

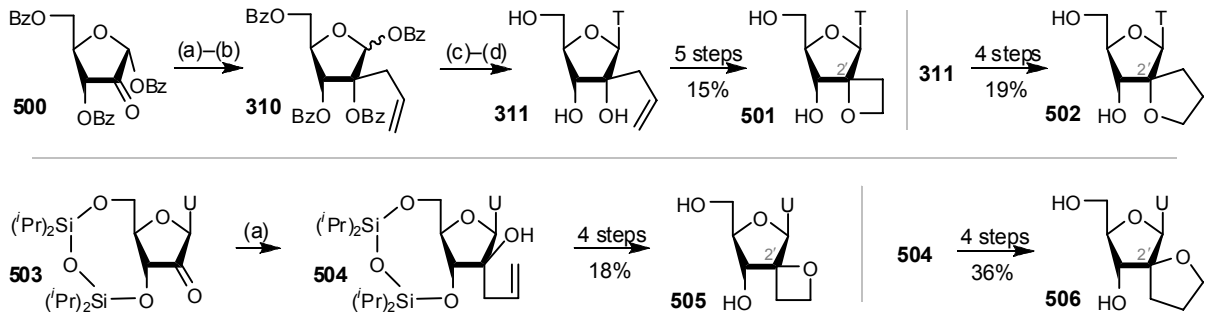

Reagents and conditions: (a) allylmagnesium bromide, $CeCl_3$, THF, -78 °C, 2 h, **504**: 75%; (b) BzCl, cat. DMAP, NEt_3, CH_2Cl_2, rt, 12 h, **310**: 53% over 2 steps; (c) i. thymine, BSA, MeCN, reflux, 1 h; ii. $SnCl_4$, reflux, 3 h; (d) NH_3, MeOH, rt, 2 d, 54% over 2 steps.

Scheme 2.21: Synthesis of 2′-spiroribo and 2′-spiroarabinonucleosides by Wengel *et al.*[36] Corresponding phosphoramidate derivatives of **501**, **502**, **505** and **506** were also synthesised and subsequently incorporated into oligonucleotides for hybridisation studies.

Wengel *et al.*[36] synthesised 2′-spiroribo and 2′-spiroarabinonucleosides as conformationally restricted probes for DNA processing enzymes. The synthesis of the 2′-spiroribothymidines began with cerium-mediated chemoselective allylation of furanone derivative **500** and benzoylation of the newly formed hydroxyl group. Nucleosidation under Vorbrüggen conditions and debenzoylation gave

thymidine **311**. The resulting alkene **311** was either oxidatively cleaved or hydroborated affording an alcohol which was subsequently cyclised to yield 5,4- and 5,5-spiro-ribothymidines **501** and **502**. The synthesis of the 2′-spiroarabinouridines started with cerium-mediated allylation of furanone derivative **503** to give uridine **504**. The resulting alkene **504** was then exposed to reaction sequences similar to those used for thymidines and afforded 5,4- and 5,5-spiroarabino-uridines **505** and **506** (Scheme 2.21).

2.6.3 3′-Spironucleosides—TSAO Nucleoside Analogues

[2′,5′-Bis-*O*-(*tert*-butyldimethylsilyl)-β-D-ribofuranose]-3′-spiro-5″-[4″-amino-1″,2″-oxathiole-2″,2″-dioxide] (TSAO) nucleosides are synthetic 3′-spironucleosides with a potent anti-HIV-1 activity. They target the hydrophobic allosteric non-substrate binding site located near the polymerase active site. Intracellular phosphorylation was not required and they possess similar properties to those of the HIV-1 specific non-nucleoside reverse transcriptase inhibitors (NNRTIs).[23,85]

Initial synthesis started with the transformation of *bis*-TBS-protected nucleoside **507** into cyano mesylate. However, a mixture of 3′-epimer was obtained with the desired (3′*S*)-ribo epimer isolated as the minor product.[95] In the revised strategy, treatment of cyclopentanone **508** with cyanide and mesylation gave the desired (3′*S*)-cyano mesylate **509** as the only stereoisomer. Acetonide removal, acetylation and nucleosidation under Vorbrüggen conditions gave nucleosides **510**. Spiro-derivatives were then formed by *in situ* trapping of the carbanion, generated by the abstraction of the acidic H_α from mesylate, by the nearby 3′-nitrile group. Subsequent deprotection and silylation afforded TSAO pyrimidines **511a–c** (Scheme 2.22).[96] Among these prototypes, thymidine analogue (TSAO-T) **511a** offered the best selectivity index (SI = 226) with a good cytopathicity inhibition (EC_{50} = 58 ng L^{-1}) and low cytotoxicity (CC_{50} = 13 μg mL^{-1}).[84,97]

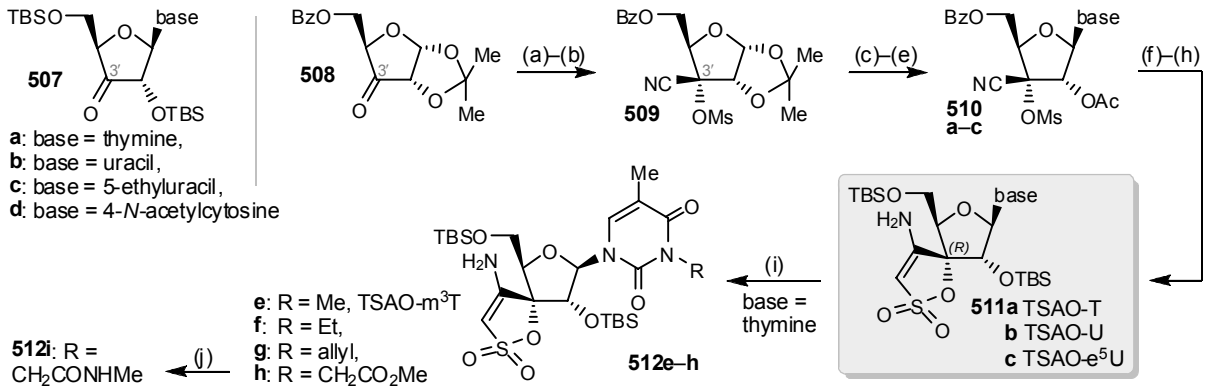

Reagents and conditions: (a) NaCN, $NaHCO_3$, Et_2O–H_2O, rt, 4 h; (b) MsCl, pyridine, 8–10 °C, 16 h, 78% over 2 steps; (c) TFA–H_2O, rt, 4 h; (d) Ac_2O, pyridine, rt, 18 h, 95% over 2 steps; (e) i. base, HMDS, cat. $(NH_4)_2SO_4$, reflux; ii. TMSOTf, MeCN, reflux, 5 h, 77–93%; (f) Cs_2CO_3, MeCN, rt, 3–6 h; (g) NH_3, MeOH, rt, 18 h; (h) TBSCl, cat. DMAP, MeCN, rt, 1–2 d, 24–32% over 3 steps; (i) RX, K_2CO_3, acetone, reflux, 3–8 h, 55–89%; (j) $MeNH_2$, EtOH, rt, 2 h, 70%.

Scheme 2.22: Synthesis of TSAO pyrimidine prototype **511a–d** including the pharmacophore TSAO-T **511a**. Alkylation of TSAO-T gave **512e–i** with reduced cytotoxicity and improved selectivity.[95-98]

Alkylation at N3 of TSAO-T prototype **511a** gave a small number of analogues **512e–g** with an improved selectivity index over that of TSAO-T (Scheme 2.22). In particular, N3-methyl derivative of TSAO-T (TSAO-m^3T) **512e** had shown excellent selectivity (SI = 4088) with an inhibitory level (EC_{50} = 56 ng L^{-1}) similar to that of TSAO-T but with much less cytotoxicity (CC_{50} = 230 μg mL^{-1}).[84,96,97]

Extensive research has been conducted to generate a large number (600+) of TSAO derivatives in order to improve the activity/toxicity profile (Figure 2.6).[99] These SAR studies had revealed that the (3′*R*)-spiro unit, amino and bis-silyl groups were crucial for RT inhibition.[23,85] Based on the result of TSAO-m^3T, San-Félix *et al*.[98] proposed that derivatisation at N3 of TSAO-T provided a unique opportunity to explore the HIV-RT dimer interface.

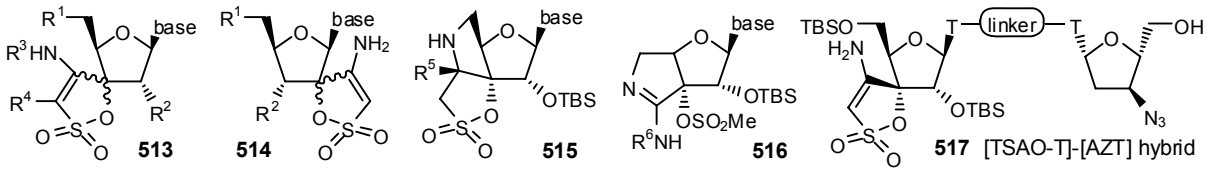

Figure 2.6: Selected recent example of TSAO analogues synthesised.[23,84,85,95,96,99,100]

Based on the SAR studies, a variety of N3 substituted TSAO-T analogues were then synthesised using a similar alkylation procedure and functional group manipulations (Scheme 2.22, only ester **512h** and carboxamide **512i** were shown). Among the 31 analogues synthesised, carboxamide derivative **512i** was found to be the most active with the highest selectivity index ever reported for TSAO nucleosides (SI ≥ 12500, EC_{50} = 30 ng L^{-1} and CC_{50} ≥ 250 μg mL^{-1}).[98]

A range of TSAO-triazole analogues was also synthesised during the SAR studies to determine the role of heterobase in the interaction between TSAO derivatives and the target enzymes. Their synthesis and inhibition activities are discussed in Chapter 6.2.

2.6.4 4′-Spironucleosides—Paquette's Spirocyclic Nucleosides

Paquette's research group conducted extensive diversity oriented synthesis (DOS) studies on a range of 4′-spirocyclic nucleosides including oxacycles, thiacycles and carbacycles (Figure 2.7). These molecules feature conformational restrictions in order to achieve better ring puckering and mimicking the optimal C4′–C5′ torsion angle of the furanose (equivalent to C5′–C6′ of the spirocyclic system). Both of these properties have an important role in the sugar-phosphate nucleic acid backbone and may control the secondary structure of nucleic acid and base recognition. Alkylation at C4′ of the furanose (equivalent to C5′ of the spirocyclic system) also inhibits radical-induced hydrogen atom abstraction/degradation of the nucleic acid. Carba and thiacyclic nucleosides also offer additional stability against metabolic degradation due to the absence or strengthening of glycosidic lineage. Each series was further subdivided into two types of analogues. In *syn* analogues, the 6′-OH

of the spirocycle (equivalent to 5′-OH of the furanose) was *syn* to the endocyclic heteroatom with a (6′*S*)-configuration whereas in *anti* analogues, the 6′-OH of the spirocycle was *anti* to the endocyclic heteroatom with a (6′*R*)-configuration.[52,53,101-114]

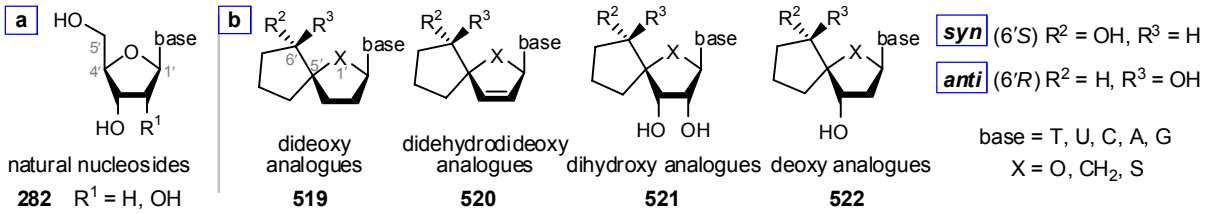

Figure 2.7: [a] General structure of natural deoxyribose and ribose nucleosides **282**. [b] The collection of 4′-spironucleoside analogues synthesised in DOS studies conducted by the Paquette group.[52,53,101-114]

(a) The 4′-Spiraoxacyclic Nucleosides

The initial synthesis for the 4′-spirocyclic framework of the oxa-series started with the addition of lithiated dihydrofuran **524** to cyclobutanone **(523)**. The resulting carbinol **525** rearranged under electrophile-promoted (H^+ or Br^+) conditions and subsequent optical resolution using (*R*)-(–)-mandelic acid or Johnson's (*S*)-(+)-sulfoximine gave (+)-**526** or (–)-**529**, respectively. Stereoselective reduction of ketone **526** under Meerwein-Pondorf-Verley conditions yielded carbinol **527** (*anti*) whereas reduction by L-selectride yielded carbinol **528** (*syn*). Alternatively, dehydrobromination of **529** under basic conditions furnished alkene **530**, which after stereoselective reduction, hydroxyl protection and allylic oxidation yielded lactone **531** (*anti*) or **532** (*syn*) (Scheme 2.23).[106,107]

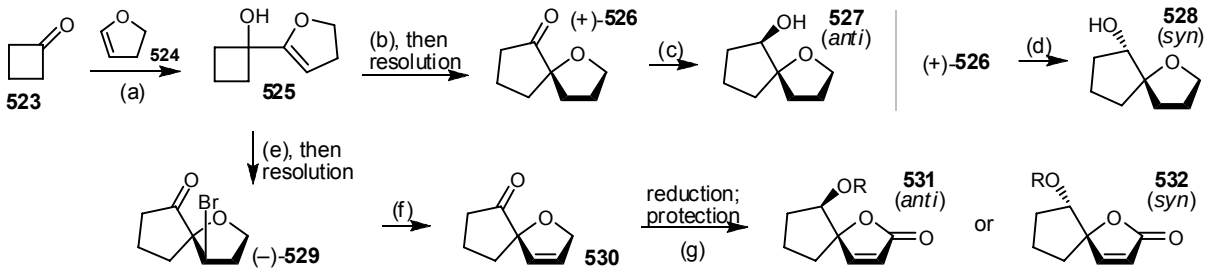

Reagents and conditions: (a) i. **524**, ^{t}BuLi, THF, -78→0 °C, 1.5 h; ii. **523**, -78 °C→rt, 1 d; (b) Amberlyst-15, CH_2Cl_2, rt, 2 h, 87% over 2 steps; (c) Al(O^{i}Pr)$_3$, ^{i}PrOH, reflux, 1 h, 70%; (d) L-selectride, THF, -78 °C, 1 h, 96%; (e) NBS, propylene oxide, ^{i}PrOH, -78 °C→rt, 18 h, 96%; (f) DBU, toluene, reflux, 18 h, 82%; (g) PCC, CrO_3, 3,5-DMP, 3 Å MS, CH_2Cl_2, -20 °C, 1 h, 65–92%.

Scheme 2.23: Initial synthesis for 4′-spirocyclic framework of oxa-series by Paquette *et al.*[106,107]

In the pilot studies conducted towards *syn*-spironucleoside, lactone **533** was first transformed into acetate **534**. However, subsequent palladium-catalysed coupling between acetate **534** and 6-chloropurine or *O*-methylthymine gave a mixture of nucleosides **535** with the undesired α-anomer as the major isomer. Alternatively, lactone **533** was converted to triacetate **536** and subsequent nucleosidation under Vorbrüggen conditions yielded the desired β-thymidine **537** due to the

neighbouring group participation by the 3′-acetate. Deacetylation of **537** gave dihydroxythymidine **538** (Scheme 2.24).[103]

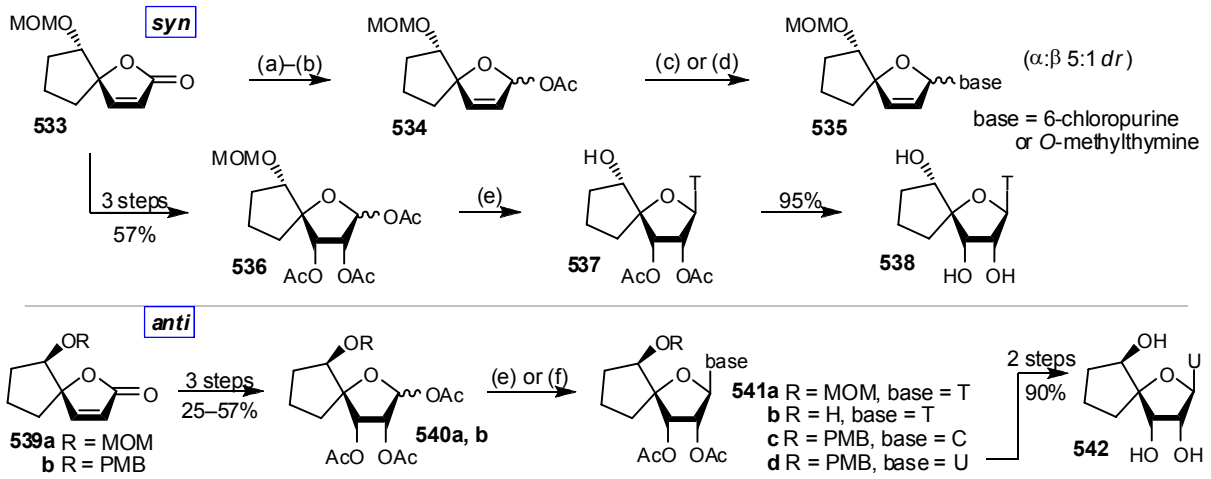

Reagents and conditions: (a) DIBAL-H, CH_2Cl_2, -78 °C, 1.5 h; (b) Ac_2O, NEt_3, CH_2Cl_2, rt, 20 min, 91% over 2 steps; (c) 6-chloropurine, cat. $Pd_2(dba)_3$•$CHCl_3$, NEt_3, PPh_3, THF, rt→50 °C, 2 d, 50% (*α*:*β* 5:1 *dr*); (d) *O*-methylthymine, cat. (π-allylPdCl)$_{2}$., Cs_2CO_3, PPh_3, THF, rt→50 °C, 2 d, 50% (*α*:*β* 5:1 *dr*); (e) **536** or **540a**, $T(TMS)_2$, TMSOTf, THF, 0 °C→rt, 18 h, **537**: 76%, **541a**: 28%, **541b**: 15%; (f) **540b**, $C(TMS)_2$ or $U(TMS)_2$, TMSOTf, DCE or CH_2Cl_2, rt, 18 h, **541c**: 60% or **541d**: 54%.

Scheme 2.24: Pilot studies of *syn* and *anti* spironucleoside analogues by Paquette *et al.*[103,104]

Similarly, the synthesis of *anti*-spironucleoside started from the transformation of MOM-protected lactone **539a** to acetate **540a**. However, the MOM group sterically hindered the crucial nucleosidation of acetate **540a** resulting in a low yield of thymidines **541a** and **b**. Alternatively, PMB-protected acetate **540b** was used and the nucleosidations of acetate **540b** proceeded in moderate yields to give cytidine **541c** and uridine **541d**. Deprotection of **541d** gave dihydroxyuridine **542** (Scheme 2.24).[104]

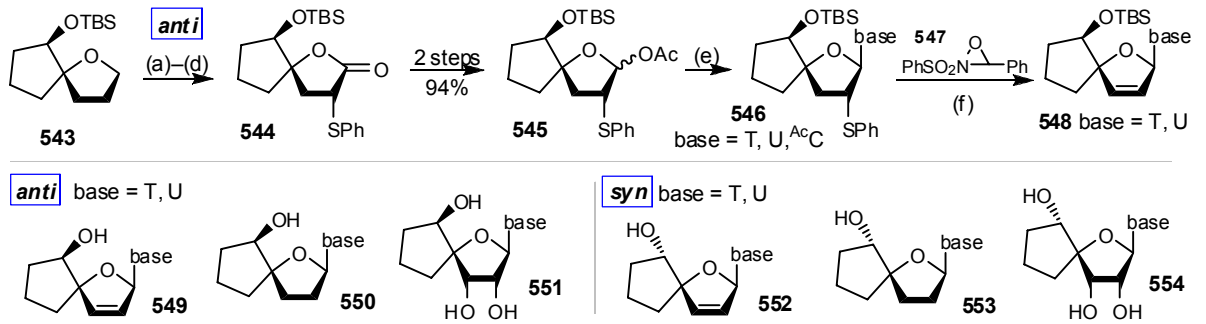

Reagents and conditions: (a) cat. $RuCl_3$, $NaIO_4$, CCl_4–MeCN–H_2O, rt, 30 min, 93%; (b) i. LiHMDS, THF, -78 °C, 1.5 h; ii. $PhSSO_2Ph$, THF, -78→-25 °C, 5 h, 75%; (c) EtMgBr, THF, -10 °C, 1 h, 95%; (d) DBU, THF, rt, 18 h, 83%; (e) persilylated base, $SnCl_4$, CH_2Cl_2, -78 °C→rt, 1 h, 55–65%; (f) i. Davis oxaziridine **547**, $CHCl_3$, rt, 16–24 h; ii. pyridine, xylene, reflux, 4 h, 88–94%.

Scheme 2.25: Synthesis of *syn*- and *anti*-spiropyrimidine analogues **549**–**554** by Paquette *et al.*[101]

An improved synthetic route was used to synthesise additional *anti*-spiropyrimidine analogues starting with the transformation of spirocycle **543** to acetate **545**.[101,107] Subsequent nucleosidation of

545 and oxidative-elimination of the stereo-directing 2-phenylthio substituent using Davis oxaziridine **547** gave nucleosides **548**. Functionalisation of **548** then afforded didehydrodideoxy, dideoxy and dihydroxyspironucleoside analogues **549**–**551**. The *syn*-analogues were synthesised similarly to afford didehydrodideoxy, dideoxy and dihydroxyspironucleoside analogues **552**–**554** (Scheme 2.25).[101]

Anti-spiroadenosine analogues **558** were synthesised *via* S_N2 displacement of anomeric chlorides **559** generated *in situ*, by the 6-chloropurine anion. The nucleosidation was not stereocontrolled, but anomeric purines **557** were easily separated by chromatography and isomerised under acidic conditions. Subsequent amination and desilylation afforded spiroadenosines **558**. *Anti*-TBS-protected guanosine analogues **559** and *syn*-spiroadenosine were also generated in a similiar fashion. However, the desilylations of guanosine derivatives **559** were attempted under a variety of conditions but all failed to give the desired unmasked carbinols (Scheme 2.26).[102]

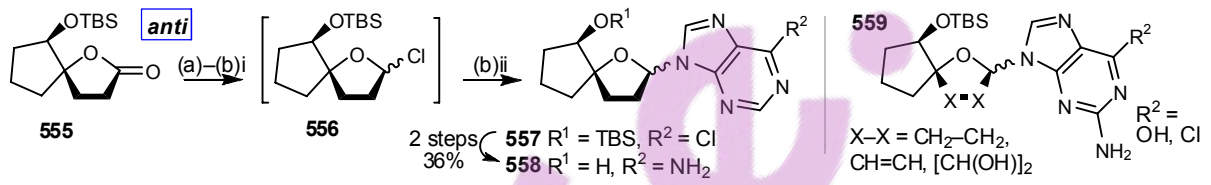

Reagents and conditions: (a) DIBAL-H, CH_2Cl_2, -78 °C, 30 min; (b) i. PPh_3, CCl_4, THF, 60 °C, 3 h; ii. 6-chloropurine, NaH, DMF, 0 °C, 5 h, 49% over 2 steps (β:α 1.8:1 *dr*).

Scheme 2.26: Synthesis of *anti*-spiroadenosine **558** by Paquette *et al.*[102] *Anti*-TBS-protected guanosine analogues **559** and *syn*-spiroadenosine (not shown) were also synthesised accordingly.

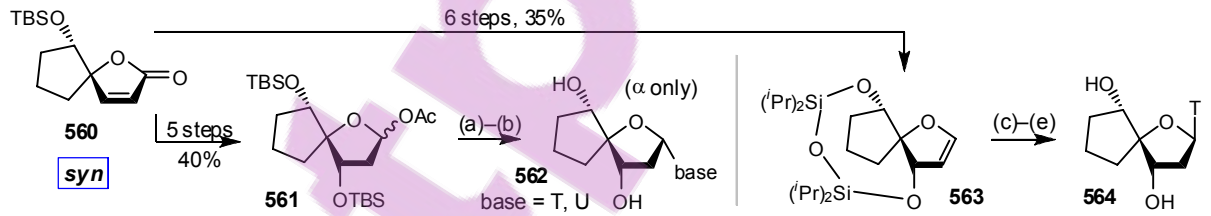

Reagents and conditions: (a) $T(TMS)_2$ or $U(TMS)_2$, $SnCl_4$, CH_2Cl_2, -78 °C→rt, 15 min, 45–59%; (b) TBAF, THF, rt, 12 h, 48–52%; (c) $T(TMS)_2$, CH_2Cl_2, NIS, rt, 1 h, 70%; (d) AIBN, Bu_3SnH, toluene, 70 C, 4 h; (e) TBAF, THF, rt, 100% over 2 steps.

Scheme 2.27: Synthesis of 3′-deoxyspironucleosides. Nucleosidation of acetate **561** under Vorbrüggen conditions and desilylation gave the undesired α-anomer of nucleosides **562** exclusively for the *syn* analogues or a 1:1 mixture of anomers for *anti* analogues (base = T, C, A, not shown).[105] Alternatively, electrophilic addition of persilylated thymine to TIPDS-protected glycal **563** produced β-thymidine **564** exclusively after deprotection.[52]

The synthesis of the 3′-deoxyspironucleoside analogues started with the transformation of lactone **560** to acetate **561** which involved a samarium-induced α-deoxygenation of a dihydroxy intermediate. Subsequent nucleosidation under Vorbrüggen conditions was problematic due to the lack of a stereo-directing neighbouring group and produced either the undesired α-anomer of nucleosides **562** exclusively or a 1:1 mixture of anomers.[105] Replacement of the TBS ether with a TES

ether did not improve the yield nor the selectivity (see Wendeborn *et al.*[115] and Table 2.3). After intensive research, β-selectivity was achieved *via* electrophilic addition of a persilylated heterobase to TIPDS-protected glycal **563**. Computational studies had shown that the TIPDS tether effectively shielded the β-face while reducing the steric hindrance for the initial α-face electrophilic attack, thus affording high selectivity for β-nucleosides. Subsequent radical dehalogenation and desilylation furnished 3′-deoxyspiro-thymidine **564** successfully (Scheme 2.27).[52]

(b) The 4′-Spiracarbacyclic Nucleosides

Interest in carbacyclic nucleosides has been increasing dramatically due to the emergence of promising anti-viral agents from this class. Furthermore, carbacyclic nucleosides possessed enhanced stability against metabolic degradation due to the lack of a labile glycosidic linkage.[106]

The first study of 4′-spirocarbacyclic nucleosides by Paquette *et al.*[108] involved the transformation of spirocyclic alcohol (+) or (–)-**565** to **566** or **571** which converted the hydroxyl group to the required stereochemistry for the subsequent displacement. Mitsunobu coupling between a benzoyl-protected pyrimidine and spirocyclic alcohol **566** or **571** followed by debenzoylation and desilylation gave dideoxynucleosides **568** and **573**. However, Mitsunobu coupling between a purine and alcohol **566** or **571** led to a poor yield with no recoverable starting material. These drawbacks prompted the use of direct S_N2 displacement of mesylate **567** or **572** by an anion of the heterobase. After desilylation, this alternative synthesis gave the target dideoxynucleosides **568** and **573** successfully[110] (Scheme 2.28).

3′-Deoxycarbaspironucleoside derivatives were also synthesised from spirocyclic alcohol (+) or (–)-**565**, which was converted to mesylate **569** or **574** respectively. Direct S_N2 displacement of mesylate **569** or **574** with an anion of heterobase followed by desilylation gave the desired 3′-deoxycarbaspironucleoside **570** or **575** (Scheme 2.28).[109]

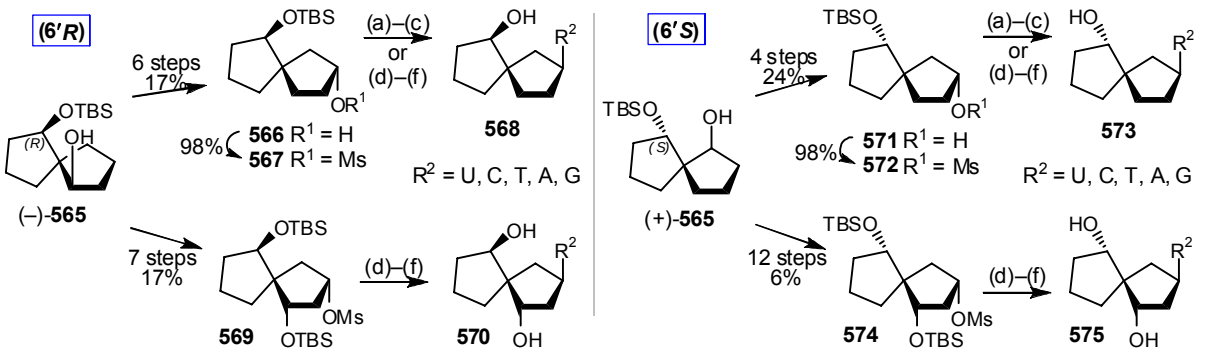

Reagents and conditions: (a) **566** or **571**, 3-*N*-benzoylthymine or 4-*N*-benzoylcytosine or 6-chloropurine, DIAD, PPh_3, THF or dioxane, 30–52%; (b) NH_3, MeOH, 80 °C, 74–91%; (c) TBAF, THF, rt, 74–95%; (d) **567** or **569** or **572** or **574**, base-H (U, C, T, A, 2-amino-6-chloropurine), NaH, DMF, 80 °C, 12 h, 12–80%; (e) for guanosine only: 2-mercaptoethanol, NaOMe, MeOH, 40–60 °C, 63–87%; (f) TBAF, THF, rt, 62–96%.

Scheme 2.28: Synthesis of dideoxy and 2′-deoxyspirocarbacyclic nucleosides by Paquette *et al.*[108-110]

Dihydroxycarbaspironucleoside analogues were prepared from α,β-unsaturated lactone **576**, which was then dihydroxylated and protected as acetonide **577**. Ketone **577** was then reduced stereospecifically and protected as triflate **578**. S_N2 displacement of **578** by an anion of the heterobase followed by desilylation produced the desired dihydroxycarbaspironucleosides **579**. The epimeric (6′*S*)-nucleosides **580** were synthesised similarly (Scheme 2.29).[111]

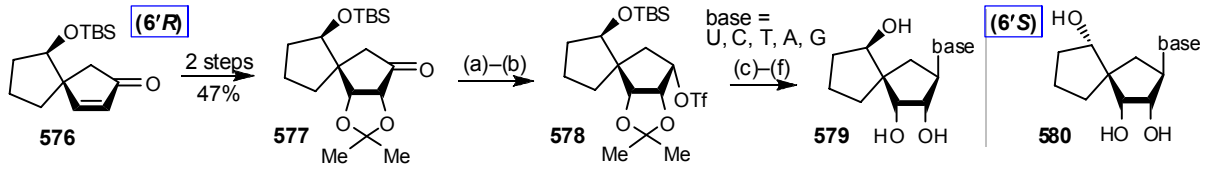

Reagents and conditions: (a) L-selectride, THF, -78 °C, 20 min, 95%; (b) Tf_2O, pyridine, CH_2Cl_2, 0 °C, 40 min, 100%; (c) base-H (U, C, T, A, 2-amino-6-chloropurine), KH, DMF, rt, 2 d, 76–97%; (d) TBAF, THF, rt, 1 d, 60–100%; (e) for guanosine only: 2-mercaptoethanol, NaOMe, MeOH, 80 °C, 4 h, 100%; (f) *p*-TsOH, MeOH, rt, 1 d, 62–99%.

Scheme 2.29: Synthesis of dihydroxycarbaspironucleosides **579** and **580** by Hartung and Paquette.[111]

(c) The 4′-Spirathiacyclic Nucleosides

Substitution of the furanose ring oxygen with a sulphur atom can have an interesting effect on the biological activity as well as improvement in the metabolic stability due to the presence of a stronger thioglycoside bond. Some of these derivatives are promising antiviral and anticancer agents.[53,106,113]

The first study of thiacyclic spironucleosides by Paquette *et al*.[112,113] started from the synthesis of ketone (+)-**583** from cyclobutanone **(523)** and lithiated 2,3-dihydrothiophene **(581)** similar to the synthesis of ketone **526** from the oxa-series (Scheme 2.23). Functional group manipulations of ketone **583** furnished separable *anti*- and *syn*-sulfoxides **584** and **585**. Subsequent zinc-catalysed Pummerer reaction followed by desilylation gave dideoxythiaspironucleosides **586** and **587** (Scheme 2.30).

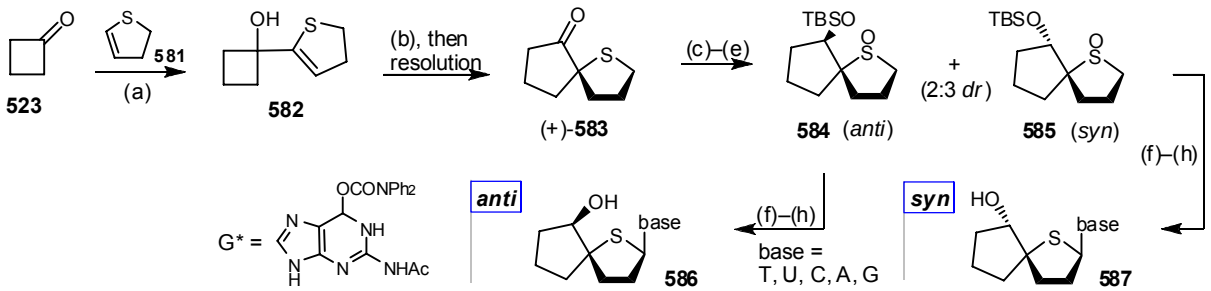

Reagents and conditions: (a) i. **581**, ^{t}BuLi, THF, -78→0 °C, 1.5 h; ii. **523**, -78 °C→rt, 1 d; (b) Dowex-50x, CH_2Cl_2, rt, 2 d, 89% over 2 steps; (c) $LiAlH_4$, Et_2O, rt, 4 h, 85% (*anti*:*syn* 2:3 *dr*); (d) TBSOTf, 2,6-lutidine, CH_2Cl_2, 0 °C→rt, 18 h, 90–95%; (e) $NaIO_4$, SiO_2, CH_2Cl_2–hexane, rt, 12 h, 90–95%. (f) i. base (T, U, C, A or G*), NEt_3, TMSOTf, toluene, rt, 15 min; ii. **584** or **585**, ZnI_2, rt, 2 d; (g) TBAF, THF, 0 °C→rt, 1 d, 12–18% over 2 steps; (h) for guanosine only: NH_3, MeOH, 0 °C, 18 h, 90%.

Scheme 2.30: Synthesis of dideoxythiaspironucleosides **586** and **587** by Paquette *et al*.[112,113]

Synthesis of 3′-deoxythiaspironucleoside analogues began with a selenium-promoted ring expansion of carbinol **582** to give selenide **588**,[113] which was then converted to TIPDS-protected thiaglycals **592** and **594**. Subsequent selenium-promoted electrophilic addition of a persilylated base to thiaglycal **592** or **594** followed by reductive deselenylation, desilylation and amination afforded deoxy-thiaspironucleosides **593** and **595** (Scheme 2.31). The excellent β-selectivity observed was due to the preferential shielding of the β-face by the TIPDS tether while reducing the steric hindrance for the initial α-face electrophilic attack similar to that of glycal **563** (Scheme 2.27). Attempts to optimise the electrophilic addition by using NIS as an electrophilic activator, TBS-protected or DTBS-protected thiaglycal failed to improve the current yield of the reactions (Table 2.3).[53]

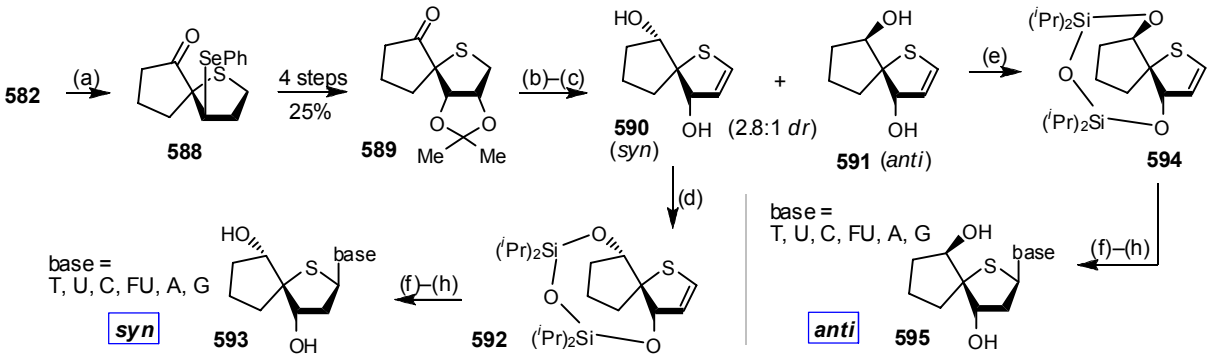

Reagents and conditions: (a) propylene oxide, PhSeCl, ^{i}PrOH, -78 °C→rt, 5 h, 70%; (b) Al(O^{i}Pr)$_3$, ^{i}PrOH, reflux, 17 h, 83% (*syn*:*anti* 2.8:1 *dr*); (c) ^{t}BuLi, HMPA, THF, -78 °C→rt, 7 h, 49–70%; (d) TIPDSCl$_2$, AgNO$_3$, pyridine, THF, rt, 18 h, 90%; (e) TIPDSCl$_2$, AgNO$_3$, 2,4,6-collidine, DMF, rt, 3 h, 91%; (f) persilylated base (T, U, ^{Ac}C, FU, ^{Bz}A, ^{Ac}G), PhSeCl, MeCN, 0 °C, 1 h, 42–89%; (g) Bu$_3$SnH, BEt$_3$, O$_2$, toluene, -78 °C, 1 h; (h) TBAF, THF, 0 °C, 2 h, 90–100% over 2 steps; (i) for ^{Ac}C, ^{Bz}A, ^{Ac}G only: NH$_3$, MeOH, rt, 5–18 h, 91–98% over 3 steps.

Scheme 2.31: Synthesis of deoxythiaspironucleosides **593** and **595** by Dong and Paquette.[53]

Synthesis of dihydroxy analogues started with the transformation of acetonide **596** to TIPDS-protected sulfoxide **597**. Subsequent TMSOTf-promoted Pummerer reaction followed by deprotections afforded dihydroxythiaspironucleosides **598**. The β-selectivity was induced by the facial discrimination of the TIPDS tether as seen in other TIPDS-protected glycals. The *anti* analogues were synthesised using similar approach to yield dihydroxythiaspironucleosides **600** (Scheme 2.32).[114]

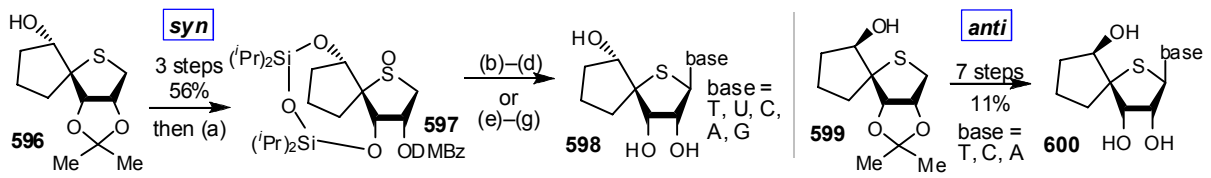

Reagents and conditions: (a) Davis oxaziridine **547**, CHCl$_3$, 0 °C, 4 h, 75%; (b) i. pyrimidine (T, U, ^{Ac}C), NEt$_3$, TMSOTf, toluene, rt, 1 h; ii. **597**, NEt$_3$, CH$_2$Cl$_2$–toluene, rt, 5 min, 30–35%; (c) TBAF, THF, 0 °C, 30 min; (d) NH$_3$, MeOH, rt, 1 d, 94–100% over 2 steps; (e) i. purine (6-chloropurine, 2-amino-6-chloropurine), NEt$_3$, TMSOTf, DCE–MeCN, rt, 1 h; ii. **597**, NEt$_3$, DCE, rt→reflux, 1 d, 22–29%; (f) TBAF, AcOH, THF, rt, 10 min; (g) for adenine: NH$_3$, EtOH, seal tube, 100 °C, 1 d, 85% over 2 steps; for guanosine: 2-mercaptoethanol, NaOMe, MeOH, reflux, 1 d, 62% over 2 steps.

Scheme 2.32: Synthesis of dihydroxythiaspironucleosides **598** and **600** by Paquette and Dong.[114]

2.7 Research Opportunities Based on 6,6-Spiroacetal Nucleoside Analogues

This chapter has provided an overview regarding the biology and chemistry of nucleoside analogues supported with selected examples. As previously indicated, we were interested in the chemical scaffold bearing biologically active structural motifs. With the structural features offered by 6,6-spiroacetals and the benefit of heterobases, the hybrid of these motifs might lead to potentially interesting bioactivity.

The synthesis of these spiroacetal-nucleobase hybrids will be discussed in detail in Chapter 4. Herein, the next chapter will examine the rationale behind other motifs chosen for hybridisation—the triazoles and amino acids.

2.8 References

1. N. A. Campbell and J. B. Reece, *Biology*, 7th edn., Benjamin Cummings, San Francisco, 2005; B. Alberts, D. Bray, J. Lewis, M. Raff, K. Roberts and J. D. Watson, *Molecular Biology of the Cell*, 3rd edn., Garland, New York, 1994; B. Alberts, A. Johnson, J. Lewis, M. Raff, K. Roberts and P. Walter, *Molecular Biology of the Cell*, 4th edn., Garland Science, New York, 2002.
2. H. P. Rang, M. M. Dale and J. M. Ritter, *Pharmacology*, 4th edn., Churchill Livingstone, Edinburgh, 1999.
3. T. M. Brody, J. Larner and K. P. Minneman, *Human Pharmacology: Molecular to Clinical*, 3rd edn., Mosby, St. Louis, 1998.
4. Office of Communications and Public Liaison, *How HIV Causes AIDS*, Fact Sheet howhiv, NIAID, NIH, U.S. Department of Health and Human Service, Bethesda, 2004.
5. F. Murphy and S. Whitfield, *Electron micrograph of the poliovirus*, Photograph ID: 1875, PHIL, CDC, U.S. Department of Health and Human Service, Atlanta, 1975.
6. C. Goldsmith, *Transmission Electron Micrograph of the Ebola Virus*, Photograph ID: 1832, PHIL, CDC, U.S. Department of Health and Human Service, Atlanta.
7. T. Albrecht, M. Fons, I. Boldogh and A. S. Rabson, in *Medical Microbiology*, ed. S. Baron, The University of of Texes Medical Branch, Galveston, 4th edn., 1996.
8. N. Previsani and D. Lavanchy, *Hepatitis B*, Guide WHO/CDS/CSR/LYO/2002.2:Hepatitis B, Department of Communicable Disease Surveillance and Response, WHO, Geneva, 2002.
9. N. Previsani and D. Lavanchy, *Hepatitis C*, Guide WHO/CDS/CSR/LYO/2002.? Hepatitis C, Department of Communicable Disease Surveillance and Response, WHO, Geneva, 2003.
10. *AIDS Epidemic Update*, Special Report UNAIDS/06.29E, UNAIDS and WHO, Geneva, 2006.
11. Media Centre, *Influenza*, Fact Sheet No. 211, WHO, Geneva, 2003.
12. Media Centre, *Global infectious disease surveillance*, Fact Sheet No. 200, WHO, Geneva, 1998.
13. M. Urban, *Infections—Viral Infections*, The Merck Manual: Online Medical Library Home edn., Merck Research Laboratories, Merch and Co., Inc., Whitehouse Station, 2007.
14. F. Dianzani, *Scand. J. Infect. Dis.*, 2003, **35**, 6-7.
15. D. J. Newman and G. M. Cragg, *J. Nat. Prod.*, 2007, **70**, 461-477.

16. R. G. Finch, D. Greenwood, S. R. Norrby and R. J. Whitney, *Antibiotics and Chemotherapy: Anti-Infective Agents and their Use in Therapy*, 8th edn., Churchill Livingstone, 2003.
17. R. Challand and R. J. Young, *Antiviral Chemotherapy*, Oxford University Press, Oxford, 1997.
18. A. Moscona, *N. Engl. J. Med*, 2005, **353**, 1363-1373; I. R. McNicholl and J. J. McNicholl, *Ann. Pharmacother.*, 2001, **35**, 57-70.
19. G. B. Elion, P. A. Furman, J. A. Fyfe, P. De Miranda, L. Beauchamp and H. J. Schaeffer, *Proc. Natl. Acad. Sci. USA*, 1977, **74**, 5716-5720; H. J. Schaeffer, L. Beauchamp, P. de Miranda, G. B. Elion, D. J. Bauer and P. Collins, *Nature*, 1978, **272**, 583-585.
20. K. K. Ogilvie, U. O. Cheriyan, B. K. Radatus, K. O. Smith, K. S. Galloway and W. L. Kennell, *Can. J. Chem.*, 1982, **60**, 3005-3010; K. O. Smith, K. S. Galloway, W. L. Kennell, K. K. Ogilvie and B. K. Radatus, *Antimicrob. Agents Chemother.*, 1982, **22**, 55-61; A. Markham and D. Faulds, *Drugs*, 1994, **48**, 455-484.
21. L. M. Beauchamp, G. F. Orr, P. de Miranda, T. Burnette and T. A. Krenitsky, *Antiviral Chem. Chemother.*, 1992, **3**, 157-164; C. M. Perry and D. Faulds, *Drugs*, 1996, **52**, 754-772.
22. G. R. Geen, T. J. Grinter, P. M. Kincey and R. L. Jarvest, *Tetrahedron*, 1990, **46**, 6903-6914; G. R. Geen, P. M. Kincey and B. M. Choudary, *Tetrahedron Lett.*, 1992, **33**, 4609-4612; C. M. Perry and A. J. Wagstaff, *Drugs*, 1995, **50**, 396-415.
23. C. Simons, *Nucleoside Mimetics: Their Chemistry and Biological Properties*, Gordon and Breach Science, Amsterdam, 2001.
24. W. Cabri and R. Di Fabio, *From Bench to Market: the Evolution of Chemical Synthesis*, Oxford Univerisity Press, Oxford, 2000 and references cited therein.
25. *Italy Pat.*, IT MI97A 000931, 1997.
26. H. Mitsuya, K. J. Weinhold, P. A. Furman, M. H. St. Clair, S. N. Lehrman, R. C. Gallo, D. Bolognesi, D. W. Barry and S. Broder, *Proc. Natl. Acad. Sci. USA*, 1985, **82**, 7096-7100.
27. S. Czernecki and J.-M. Valery, *Synthesis*, 1991, 239-240.
28. H. Vorbrüggen and C. Ruh-Pohlenz, *Org. React.*, 2000, **55**, 1-630; H. Vorbrüggen and C. Ruh-Pohlenz, *Handbook of Nucleoside Synthesis*, John Wiley & Sons, Inc., Chichester, UK, 2001.
29. J.-L. Girardet and S. A. Lang, in *Progress in Heterocyclic Chemistry*, eds. G. W. Gribble and J. A. Joule, Elsevier, Oxford, 2007, vol. 18.
30. C. Lescop and F. Huet, *Tetrahedron*, 2000, **56**, 2995-3003.
31. U. Parsch and J. W. Engels, *Chem. Eur. J*, 2000, **6**, 2409-2424.
32. D. F. Ewing, N.-E. Fahmi, C. Len, G. Mackenzie and A. Pranzo, *J. Chem. Soc., Perkin Trans. 1*, 2000, 3561-3565.
33. H. Berber, M. Soufyane, C. Mirand, S. Schmidt and A.-M. Aubertin, *Tetrahedron*, 2001, **57**, 7369-7375.
34. T. Murano, S. Muroyama, T. Yokomatsu and S. Shibuya, *Synlett*, 2002, 1657-1660; T. Murano, Y. Yuasa, S. Muroyama, T. Yokomatsu and S. Shibuya, *Tetrahedron*, 2003, **59**, 9059-9073.
35. U. Chiacchio, A. Corsaro, D. Iannazzo, A. Piperno, V. Pistara, A. Rescifina, R. Romeo, V. Valveri, A. Mastino and G. Romeo, *J. Med. Chem.*, 2003, **46**, 3696-3702.
36. B. R. Babu, L. Keinicke, M. Petersen, C. Nielsen and J. Wengel, *Org. Biomol. Chem.*, 2003, **1**, 3514-3526.
37. D. Z. Jin, S. H. Kwon, H. R. Moon, P. Gunaga, H. O. Kim, D.-K. Kim, M. W. Chun and L. S. Jeong, *Bioorg. Med. Chem.*, 2004, **12**, 1101-1109.
38. P. K. Sharma, M. Petersen and P. Nielsen, *J. Org. Chem.*, 2005, **70**, 4918-4928.
39. E. Rozners and Y. Liu, *J. Org. Chem.*, 2005, **70**, 9841-9848.
40. D.-L. Li, H.-L. Bao, Q.-T. Tan, Y.-P. Ke and T.-P. You, *Chin. J. Chem.*, 2005, **23**, 1659-1664.
41. M. Bogucka, P. Nauš, W. Pathmasiri, J. Barman and J. Chattopadhyaya, *Org. Biomol. Chem.*, 2005, **3**, 4362-4372.
42. D. Enders, I. Breuer and E. Drosdow, *Synthesis*, 2005, 3239-3244.
43. J.-D. Ye, X. Liao and J. A. Piccirilli, *J. Org. Chem.*, 2005, **70**, 7902-7910.
44. N.-S. Li and J. A. Piccirilli, *J. Org. Chem.*, 2006, **71**, 4018-4020.
45. K. Barral, J. Balzarini, J. Neyts, E. De Clercq, R. C. Hider and M. Camplo, *J. Med. Chem.*, 2006, **49**, 43-50.
46. S. Sahabuddin, R. Ghosh, B. Achari and S. B. Mandal, *Org. Biomol. Chem.*, 2006, **4**, 551-557.
47. J. Ravn, C. Rosenbohm, S. M. Christensen and T. Koch, *Nucleosides Nucleotides & Nucleic Acids*, 2006, **25**, 843-847.
48. R. Alibés, A. Alvárez-Larena, P. de March, M. Figueredo, J. Font, T. Parella and A. Rustullet, *Org. Lett.*, 2006, **8**, 491-494.

49. S. N. Sriharsha, S. Satish, S. Shashikanth and K. A. Raveesha, *Bioorg. Med. Chem.*, 2006, **14**, 7476-7481.
50. A. Kim and J. H. Hong, *Nucleosides Nucleotides & Nucleic Acids*, 2007, **26**, 291-302.
51. M. Kassou and S. Castillón, *J. Org. Chem.*, 1997, **62**, 3696-3701.
52. S. Dong and L. A. Paquette, *J. Org. Chem.*, 2006, **71**, 1647-1652.
53. S. Dong and L. A. Paquette, *J. Org. Chem.*, 2005, **70**, 1580-1596 and references cited therein.
54. G. B. Evans, R. H. Furneaux, T. L. Hutchison, H. S. Kezar, P. E. Morris, V. L. Schramm and P. C. Tyler, *J. Org. Chem.*, 2001, **66**, 5723-5730.
55. H. S. Kim and K. A. Jacobson, *Org. Lett.*, 2003, **5**, 1665-1668.
56. O. R. Ludek and C. Meier, *Synthesis*, 2003, 2101-2109.
57. A. Kim and J. H. Hong, *Eur. J. Med. Chem.*, 2007, **42**, 487-493.
58. Y. Li, S. Mao, M. W. Hager, K. D. Becnel, R. F. Schinazi and D. C. Liotta, *Bioorg. Med. Chem. Lett.*, 2007, **17**, 3398-3401.
59. S. Zhou and J. Zemlicka, *Nucleosides Nucleotides & Nucleic Acids*, 2007, **26**, 391-402.
60. S. Zhou, J. Zemlicka, E. R. Kern and J. C. Drach, *Nucleosides Nucleotides & Nucleic Acids*, 2007, **26**, 231-243.
61. W. Huang, M. J. Miller, E. De Clercq and J. Balzarini, *Org. Biomol. Chem.*, 2007, **5**, 1164-1166.
62. J. Velcicky, J. Lex and H.-G. Schmalz, *Org. Lett.*, 2002, **4**, 565-568.
63. L. Kürti and B. Czakó, *Strategic Applications of Named Reactions in Organic Synthesis*, 1st edn., Elsevier Academic Press, San Diego, 2005 and references cited therein; D. L. Hughes, *Org. React.*, 1992, **42**, 335-656.
64. C. Hubert, C. Alexandre, A.-M. Aubertin and F. Huet, *Tetrahedron*, 2002, **58**, 3775-3778.
65. C. Hubert, C. Alexandre, A.-M. Aubertin and F. Huet, *Tetrahedron*, 2003, **59**, 3127-3130.
66. Y. Choi, C. George, P. Strazewski and V. E. Marquez, *Org. Lett.*, 2002, **4**, 589-592.
67. A. B. Petersen, M. Å. Petersen, U. Henriksen, S. Hammerum and O. Dahl, *Org. Biomol. Chem.*, 2003, **1**, 3293-3296.
68. Y. Aubin, G. Audran and H. Monti, *Synlett*, 2006, 2215-2218.
69. Y. Yoshimura, K. Asami, H. Matsui, H. Tanaka and H. Takahata, *Org. Lett.*, 2006, **8**, 6015-6018.
70. H. Choo, J. R. Beadle, Y. Chong, J. Trahan and K. Y. Hostetler, *Bioorg. Med. Chem.*, 2007, **15**, 1771-1779.
71. K. R. Kim, H. R. Moon, A.-Y. Park, M. W. Chun and L. S. Jeong, *Bioorg. Med. Chem.*, 2007, **15**, 227-234.
72. C. Li and J. Zemlicka, *Nucleosides Nucleotides & Nucleic Acids*, 2007, **26**, 111-120.
73. P. Herdewijn, in *Anti-infectives: Recent Advances in Chemistry and Structure-Activity Relationships*, eds. P. H. Bentley and P. J. O'Hanlon, The Royal Society of Chemistry, Cambridge, 1997, pp. 316-327.
74. S. Manta, G. Agelis, T. Botić, A. Cencić and D. Komiotis, *Bioorg. Med. Chem.*, 2007, **15**, 980-987.
75. M.-J. Pérez-Pérez, E. De Clercq and P. Herdewijn, *Bioorg. Med. Chem. Lett.*, 1996, **6**, 1457-1460.
76. J. Reinhard, W. E. Hull, C.-W. von der Lieth, U. Eichhorn, H.-C. Kliem, B. Kaina and M. Wiessler, *J. Med. Chem.*, 2001, **44**, 4050-4061.
77. J. Renner, I. Kruszelnicki, B. Adamiak, A. C. Willis, E. Hammond, S. Su, C. Burns, E. Trybala, V. Ferro and M. G. Banwell, *Aust. J. Chem.*, 2005, **58**, 86-93.
78. H. Nishimura, N. Shimaoka, Y. Tanaka, Y. Komatsu, H. Kato and M. Mayama, *J. Antibiot.*, 1964, **17**, 148-155.
79. I. Otero, H. Feist, L. Herrera, M. Michalik, J. Quincoces and K. Peseke, *Aust. J. Chem.*, 2005, **58**, 104-111; I. Otero, H. Feist, L. Herrera, M. Michalik, J. Quincoces and K. Peseke, *Carbohydr. Res.*, 2005, **340**, 547-555.
80. C. Lambertucci, G. Schepers, G. Cristalli, P. Herdewijn and A. Van Aerschot, *Tetrahedron Lett.*, 2007, **48**, 2143-2145.
81. H. Li*, et al.*, *J. Med. Chem.*, 2007, **50**, 3969-3972.
82. D. Camp, C. F. Matthews, S. T. Neville, M. Rouns, R. W. Scott and Y. Truong, *Org. Process Res. Dev.*, 2006, **10**, 814-821.
83. M. Nakajima, K. Itoi, Y. Takamatsu, T. Kinoshita, T. Okazaki, K. Kawakubo, M. Shindo, T. Honma, M. Tohjigamori and T. Haneishi, *J. Antibiot.*, 1991, **44**, 293-300; *Germany Pat.*, DE 4129616 A1, 1992; *Japan Pat.*, JP 04222589 A, 1992.
84. J. Balzarini, M.-J. Pérez-Pérez, A. San-Félix, D. Schols, C.-F. Perno, A.-M. Vandamme, M.-J. Camarasa and E. De Clercq, *Proc. Natl. Acad. Sci. USA*, 1992, **89**, 4392-4396.
85. M.-J. Camarasa, M.-J. Pérez, S. Veláquez, A. San-Félix, R. Alvarez, S. Ingate, M.-L. Jimeno, E. De Clercq and J. Balzarini, in *Anti-infectives: Recent Advances in Chemistry and Structure-Activity Relationships*, eds. P. H. Bentley and P. J. O'Hanlon, The Royal Society of Chemistry, Cambridge, 1997, pp. 259-268.

86. D. L. Siehl, M. V. Subramanian, E. W. Walters, S.-F. Lee, R. J. Anderson and A. G. Toschi, *Plant Physiology*, 1996, **110**, 753-758.
87. M. A. F. Jalal, M. B. Hossain and D. Van Der Helm, *Acta Crystallogr., Sect. C: Cryst. Struct. Commun.*, 1986, **42**, 733-738 and references cited therein.
88. E. G. E. Jahngen, Jr. and E. F. Rossomando, *Synth. Commun.*, 1982, **12**, 601-606 and references cited therein.
89. P. M. Harrington and M. E. Jung, *Tetrahedron Lett.*, 1994, **35**, 5145-5148.
90. T. Q. Pham, S. G. Pyne, B. W. Skelton and A. H. Whitet, *J. Org. Chem.*, 2005, **70**, 6369-6377.
91. A. Renard, J. Lhomme and M. Kotera, *J. Org. Chem.*, 2002, **67**, 1302-1307; C. Taillefumier, S. Thielges and Y. Chapleur, *Tetrahedron*, 2004, **60**, 2213-2224; J. Fuentes, B. A. B. Salameh, M. A. Pradera, F. J. F. de Córdoba and C. Gasch, *Tetrahedron*, 2006, **62**, 97-111.
92. C. Chatgilialoglu, T. Gimisis and G. P. Spada, *Chem. Eur. J*, 1999, **5**, 2866-2876.
93. C. Chatgilialoglu, C. Ferreri, T. Gimisis, M. Roberti, J. Balzarini and E. De Clercq, *Nucleosides Nucleotides & Nucleic Acids*, 2004, **23**, 1565-1581.
94. K. Singha, A. Roy, P. K. Dutta, S. Tripathi, S. Sahabuddin, B. Achari and S. B. Mandal, *J. Org. Chem.*, 2004, **69**, 6507-6510.
95. M.-J. Camarasa, M.-J. Pérez-Pérez, A. San-Félix, J. Balzarini and E. De Clercq, *J. Med. Chem.*, 1992, **35**, 2721-2727; M.-J. Pérez-Pérez, A. San-Félix, M.-J. Camarasa, J. Balzarini and E. De Clercq, *Tetrahedron Lett.*, 1992, **33**, 3029-3032.
96. M.-J. Pérez-Pérez, A. San-Félix, J. Balzarini, E. De Clercq and M.-J. Camarasa, *J. Med. Chem.*, 1992, **35**, 2988-2995.
97. J. Balzarini, M.-J. Pérez-Pérez, A. San-Félix, S. Velazquez, M.-J. Camarasa and E. De Clercq, *Antimicrob. Agents Chemother.*, 1992, **36**, 1073-1080; J. Balzarini, M.-J. Pérez-Pérez, A. San-Félix, M.-J. Camarasa, I. C. Bathurst, P. J. Barr and E. De Clercq, *J. Biol. Chem.*, 1992, **267**, 11831-11838.
98. M.-C. Bonache, C. Chamorro, S. Velazquez, E. De Clercq, J. Balzarini, F. R. Barrios, F. Gago, M.-J. Camarasa and A. San-Félix, *J. Med. Chem.*, 2005, **48**, 6653-6660.
99. M.-J. Camarasa, S. Velázquez, A. San-Félix, M.-J. Pérez-Pérez, M.-C. Bonache and S. De Castro, *Curr. Pharm. Design*, 2006, **12**, 1895-1907.
100. S. Velázquez, M.-L. Jimeno, M.-J. Camarasa and J. Balzarini, *Tetrahedron*, 1994, **50**, 11013-11022; E. Lobatón, M.-L. Camarasa and S. Velázquez, *Synlett*, 2000, 1312-1314; S. de Castro*, et al.*, *J. Med. Chem.*, 2005, **48**, 1158-1168; S. Velázquez, V. Tuňón, M.-L. Jimeno, C. Chamorro, E. De Clercq, J. Balzarini and M.-J. Camarasa, *J. Med. Chem.*, 1999, **42**, 5188-5196; M.-C. Bonache, C. Chamorro, A. Cordeiro, M.-J. Camarasa, M.-L. Jimeno and A. San-Félix, *J. Org. Chem.*, 2004, **69**, 8758-8766.
101. L. A. Paquette, C. K. Seekamp and A. L. Kahane, *J. Org. Chem.*, 2003, **68**, 8614-8624.
102. L. A. Paquette, A. L. Kahane and C. K. Seekamp, *J. Org. Chem.*, 2004, **69**, 5555-5562.
103. L. A. Paquette, R. T. Bibart, C. K. Seekamp and A. L. Kahane, *Org. Lett.*, 2001, **3**, 4039-4041.
104. L. A. Paquette, D. R. Owen, R. T. Bibart and C. K. Seekamp, *Org. Lett.*, 2001, **3**, 4043-4045.
105. L. A. Paquette, C. K. Seekamp, A. L. Kahane, D. G. Hilmey and J. Gallucci, *J. Org. Chem.*, 2004, **69**, 7442-7447.
106. L. A. Paquette, *Aust. J. Chem.*, 2004, **57**, 7-17 and references cited therein.
107. L. A. Paquette, D. R. Owen, R. T. Bibart, C. K. Seekamp, A. L. Kahane, J. C. Lanter and M. A. Corral, *J. Org. Chem.*, 2001, **66**, 2828-2834.
108. L. A. Paquette, R. E. Hartung and D. J. France, *Org. Lett.*, 2003, **5**, 869-871.
109. R. Hartung and L. A. Paquette, *J. Org. Chem.*, 2005, **70**, 1597-1604.
110. R. E. Hartung and L. A. Paquette, *Heterocycles*, 2006, **67**, 75-78.
111. R. E. Hartung and L. A. Paquette, *Synthesis*, 2005, 3209-3218.
112. L. A. Paquette, U. Dullweber and B. M. Branan, *Heterocycles*, 1994, **37**, 187-191.
113. L. A. Paquette, F. Fabris, F. Gallou and S. Dong, *J. Org. Chem.*, 2003, **68**, 8625-8634 and references cited therein.
114. L. A. Paquette and S. Dong, *J. Org. Chem.*, 2005, **70**, 5655-5664.
115. S. Wendeborn, G. Binot, M. Nina and T. Winkler, *Synlett*, 2002, 1683-1687.

Chapter Three:

Introduction: Triazoles and Amino Acids

As previously mentioned, the aim of this research is to synthesise spiroacetal-triazole and amino acid hybrids as biological probes for broad phenotypic assays. In order to understand the rationale behind the choice of motifs, we must first briefly examine the basics of amino acids.

3.1 Amino Acids in Brief

Amino acids are building blocks of proteins which are involved in almost every process within an organism. They are essential for survival and are found in enzymes (such as polymerases), structural elements (such as collagens, actins, tubulins), hormones (such as insulin, erythropoietin), small molecule carriers (such as haemoglobins) and antibodies (such as immunoglobins) etc. Some amino acids are also important neurotransmitters (such as glycine, γ-aminobutyric acid [GABA], glutamate) in the central nervous system.[1,2]

3.1.1 Structures of Amino Acids

Amino acids are bifunctional molecules which contain both amino and carboxylic acid groups. There are 20 common amino acids found in proteins and all of them are L-α-amino acids in which the stereocentre is of the *(S)*-configuration except cysteine.[1,2]

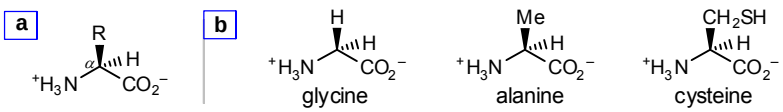

Figure 3.1: [a] General structure of an α-amino acid. [b] Examples of common amino acids.[1,2]

3.1.2 Peptide Bonds

A peptide is a chain of amino acids joined together by amide/peptide bonds formed through enzymatic condensation. The lone pair of electrons on nitrogen is delocalised by the conjugation with the adjacent carbonyl group resulting a partial double bond character along the C–N bond and the planarity of the amide group. Due to this delocalisation, the amide nitrogens are non-basic and a large dipole moment is observed. The peptide bonds are reasonably stable at physiological conditions but are susceptible towards enzymatic cleavage or degradation (Scheme 3.1).[1,2]

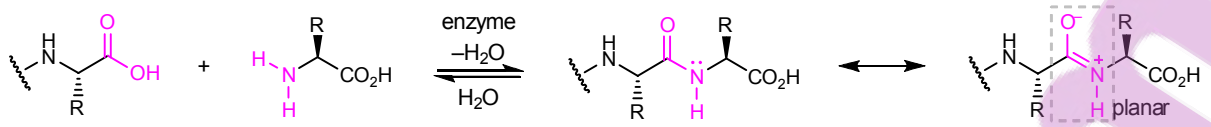

Scheme 3.1: The formation of a peptide bond between the adjacent amino acids is under the strict control of enzymes within an organism. Delocalisation of the lone pair of electrons on nitrogen results in a partial double bond character along the C–N bond.[1,2]

3.2 1,2,3-Triazoles

Isosteres are structures or moieties that share similar electronic and topological features. Therefore, they are able to mimic or even enhance the target structure's biological activity while potentially minimising certain disadvantages of the biological target structure.[3-5]

The 1,4-disubstituted 1,2,3-triazoles ("triazoles") are used as the isosteres of amide/peptide bonds. Being a rigid linker, a triazole holds the substitutents in a similar geometry and distance to those of an amide as well as providing a comparable dipole moment (Table 3.1). However, unlike the amide counterpart, triazoles are stable towards hydrolytic cleavage (especially under enzymatic conditions), oxidation and reduction.[3,5,6]

Properties	***trans-Amide/Peptide Bonds*** 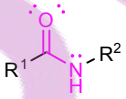	***1,4-Disubstituted 1,2,3-Triazoles ("Triazoles")*** 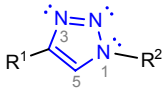
Geometry	planar	planar
R^1 to R^2 Distance	3.9 Å	5.0 Å
Dipole Moment	~ 3.7–4.0 Debye	~ 5.0 Debye
Hydrogen Bond Acceptor(s)	C=O	N2 and N3
Hydrogen Bond Donor	NH	H5
Stability	reasonably stable at most physiological conditions.	stable against hydrolytic cleavage, oxidation and reduction.

Table 3.1: Comparisons of properties between *trans*-amide/peptide bonds and their triazole isosteres.[3,5,6]

Triazoles are formed *via* chemoselective cycloaddition of an azide to an acetylene which will be discussed in detail in Section 3.4.

3.2.1 Applications of Triazole Containing Derivatives

Both triazole and amide functional groups serve as efficient and versatile linkers bringing two subunits together in a well-defined and predictable geometry. In particular, amide functionalities have

been used profoundly by nature. Given the close similarity with the amide bond, it is not surprising that molecules bearing triazole subunits can be found in many areas such as biological, pharmaceutical and materials science. Triazoles have sparked an enormous interest in the past few decades. Representative examples of various applications are listed in Table 3.2.[3,5,7-9]

Tazobactam (610)[10]	• A potent irreversible β-lactamase inhibitor (IC_{50} = 0.06–5.4 μM). • Forms a stable complex with the target enzyme ("suicidal inhibitors"). • Clinically used in combination with piperacilin (Zosyn®), a broad spectrum antibacterial *β*-lactam to treat polymicrobial infection.	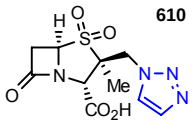 **610**
Inhibitors of Fucosyl Transferase (Fuc-T)[11]	• Fuc-T catalysed the fucosylation of glycolipids, glycoproteins and oligosaccharides responsible for cell-cell interactions and cell migrations. • **611**: IC_{50} = 0.15–1.0 μM.	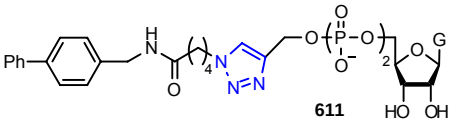 **611**
Inhibitors of Platelet Aggregation[12]	• **612** inhibits arachidonic acid or collagen-induced platelet aggregation (IC_{50} = 2.2 and 21.6 μM). • Exhibited anti-inflammatory and analgesic activity. • No gastric ulcerogenic effect was observed.	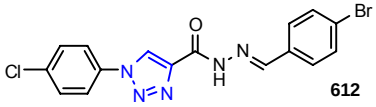 **612**
Inhibitors of HIV-1 Protease[13]	• **613** inhibits HIV-1 protease, both wild type (IC_{50} = 6 nM) and mutant (IC_{50} = 19–46 nM). • Triazole acts as a mimic of amide bond and retains all hydrogen bonds in the active site.	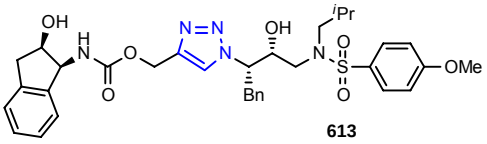 **613**
Peptidomimetic: Inhibitors of Tyrosinase[14]	• Tyrosinase involved in the browning of plant-derived food products and human dermatological disorders. • **614** and **615**: IC_{50} = 0.5–0.6 mM.	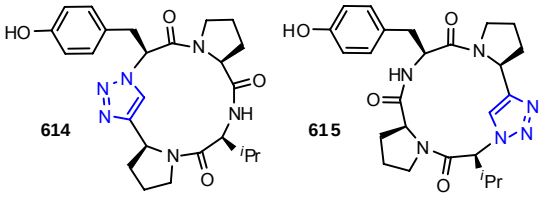 **614** **615**
Glycopeptide Mimics[15]	• Glycopeptides mediate many cellular functions. • Replacement of the glycosidic linkage by a triazole improves chemical and enzymatic stability.	R^1 = H, Ac, Bn 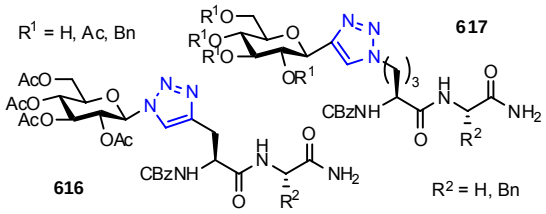 **617** **616** R^2 = H, Bn
Oligosaccharide Mimics: *Pseudo*-starch Fragments[16]	• To model starch in biochemical and physicochemical studies. • **618** is used as a surrogate for branch points in amylopectin structure.	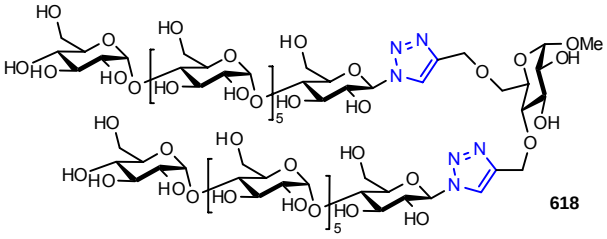 **618**

Oligodeoxyribo-nucleotide Mimics[17]	• The native phosphodiester groups are replaced by triazole internucleosidic linkages. • Potential antisense agents and inhibitors of gene expression (gene silencing).	**619** 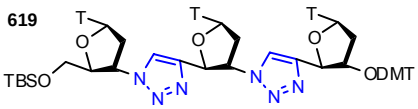
Dendrimers[18]	• A dendrimer's properties can be tailored by using the appropriate subunits to suit applications such as vectors, sensors, catalysts. • **620** is a redox sensor for oxo anions and transition metal cations.	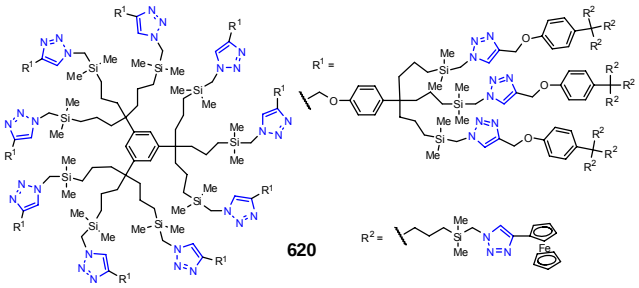

Table 3.2: Selected examples of triazole containing analogues and their applications.

The advances in this field have been further fuelled by the ease of installation of triazoles due to the development of the efficient synthetic procedure, particularly the copper-catalysed azide-alkyne cycloaddition (CuAAC, Section 3.4).[3,5,7-9]

3.3 Click Chemistry

It has been observed that in nature, small molecules such as nucleotides, amino acids and monosaccharides are condensed typically through the formation of carbon-heteroatom (C–X) bonds rather than carbon-carbon (C–C) bonds into large macromolecular polymers such as nucleic acids, peptides, polysaccharides.[3,19]

In 2001, Sharpless *et al.*[19] proposed the concept of click chemistry after following nature's lead and assembled a set of powerful, highly reliable, and selective reactions for the rapid synthesis of new compounds through these carbon-heteroatom linkages.

The criteria for these click reactions are:

- Modular, wide in scope, high yielding and stereospecific.
- Readily available starting materials, simple reaction conditions and product isolation.
- By-products, if generated, can be removed easily by non-chromatographic method.
- Product must be stable and can be purified by non-chromatographic methods.

These near-perfect criteria are driven by a large thermodynamic driving force (> 20 kcal mol^{-1}) due to the use of highly energetic and "spring-loaded" reactants and/or generation of very stable products.[19]

The set of reliable reactions that obey the criteria of click chemistry are:

- Cycloadditions e.g. 1,3-dipolar cycloadditions and Diels-Alder reactions.
- Nucleophilic ring-opening of strained heterocycles e.g. epoxides and aziridines.
- Non-aldol carbonyl chemistry e.g. formation of ureas, aromatic heterocycles and amides.
- Addition to carbon-carbon multiple bonds e.g. epoxidations and dihydroxylation.

Since the introduction of this concept, the 1,3-dipolar cycloaddition of azides to alkynes is the most extensively studied and applied click chemistry to date, particularly due to the versatility of triazoles and the introduction of copper-catalysed azide-alkyne cycloaddition (CuAAC).[3,8,19,20]

3.4 Synthesis of Triazoles

3.4.1 Huisgen's 1,3-Dipolar Cycloadditions

Traditionally, triazoles are synthesised by Huisgen's 1,3-dipolar cycloadditions of a 1,3-dipolar azide to a dipolarophile alkyne *via* a concerted mechanism (Scheme 3.2). Both substrates are highly energetic thermodynamically which provided the driving force for the cycloaddition. However, the formation of the triazole is not spontaneous due to the kinetic stability of the substrates.[3,8,19-21]

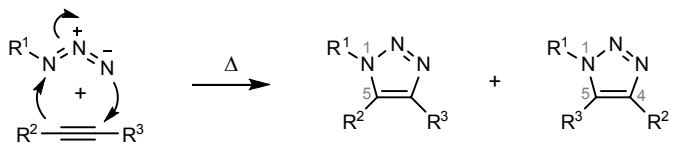

Scheme 3.2: Huisgen's 1,3-dipolar cycloaddition of azide to alkyne *via* a concerted one-step mechanism.

The kinetic stabilities of azides* and alkynes can be advantageous in biological and chemical settings. Both functional groups are relatively safe to handle, resistant towards dimerisation and hydrolysis, inert towards most aqueous and potentially oxidising biological conditions as well as many

* Metallic azides and small organic azides are explosive. However, the general "rule of six" can be applied for larger organic azides. That is, six or more carbons (or other atoms of similar size) per azide or other energetic functional group would provide sufficient dilution to render the compound relatively safe. The presence of certain transition metal species, such as Fe and Co triads, catalyse the exothermic decomposition of azides with the loss of N_2 and should be avoided.

reaction conditions used in organic synthesis. They are also easy to install and remain inert until needed.[3,5,19,21]

However, this kinetic stability means that the cycloaddition of azides to alkynes is relatively slow. The cycloadditions usually required longer reaction times, elevated reaction temperatures and/or the use of electron deficient alkynes to accelerate the reaction.[5,19,21-24]

Due to the similarity in activation energies when an asymmetrical alkyne is reacted with an azide, a mixture of 1,4- and 1,5-disubstituted triazoles is usually formed.[25] Regiospecific cycloaddition can be achieved under mild conditions and/or by using highly electron-deficient terminal alkynes to give the 1,4-regioisomer exclusively (Table 3.3).[3,5,8,19-21,24,26]

Entry	*Azides*	*Alkynes*	*Conditions*	*Products and Yields*
[1] Häbich *et al.*[27]	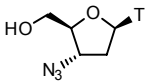 AZT **(292)**	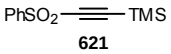 **621**	DME, reflux, 20 h	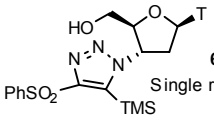 **622** 63% Single regioisomer only; 22 examples were carried out using various alkynes. But most of these cycloadditions produced a mixture of regioisomers.
[2] Yamashita *et al.*[28]	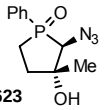 **623**	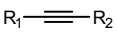 **624** 8 alkynes	DME, reflux, 12 h–5 d	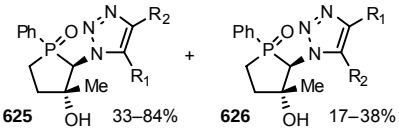 **625** 33–84% + **626** 17–38%; R_1 = H, CH_2OH, CO_2H, CO_2Me, CO_2Et; R_2 = Ph, ^{t}Bu, CH_2OH, CMe_2OH, CO_2H, CO_2Me, CO_2Et, TMS
[3] Katritzky and Singh[29]	 **627** 3 azides	**628** 2 alkynes	neat, microwave, 55–85 °C, 30 min	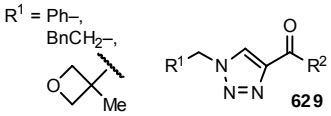 **629** R^1 = Ph–, $BnCH_2$–; R^2 = NHBn, piperidinyl; 65–84% 6 examples 1,4- regioisomer only
[4] Dondoni *et al.*[30] (See Table 3.4 for the Cu-catalysed version)	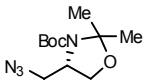 **630**	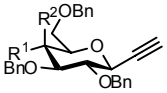 **632a** R^1 = H, R^2 = OBn; **632b** R^1 = OBn, R^2 = H	neat, 120 °C, 12 h	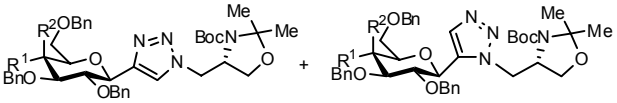 **633a** 13% **633b** 32% + **634a** 67% **634b** 48%
	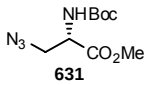 **631**		neat, 120 °C, 2 h	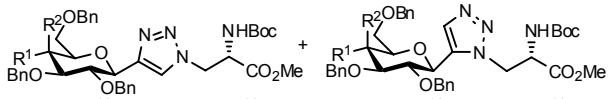 **635a** 13% **635b** 31% + **636a** 68% **636b** 47%
[5] Li and Wang[31] (1 pot)	R^1—X + NaN_3 **637** X = Cl, Br; R^1 = benzyl, alkyl; 14 azides	 **638** R^2 = aryl, alkyl; 6 alkynes	H_2O, 100 °C, 1 d	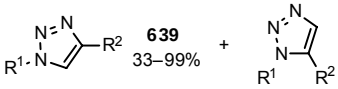 **639** 33–99% + **640** 0–39%; 19 examples

Table 3.3: Selected examples of uncatalysed Huisgen's 1,3-dipolar cycloaddition of azides to alkynes.

3.4.2 Copper-Catalysed Azide-Alkyne 1,3-Dipolar Cycloaddition (CuAAC)

Prior to 2002, the use of triazoles as synthetic biological sub-structures was hindered by the lack of regioselective syntheses. Attempts to control the regiochemistry under various conditions, including the use of metal acetylide (such as sodium and lithium), have been reported with limited success.[20,26]

In 2002, Meldal *et al.*[22] and Sharpless *et al.*[24] independently published the discoveries of copper-catalysed azide-alkyne cycloaddition (CuAAC), which gave 1,4-disubstituted triazoles exclusively (Scheme 3.4 and Table 3.4). Together with the concept of click chemistry, the triazole substructure has become one of the most widely used moieties in all areas of chemistry during the past decade and these have been reflected in the sheer number of reviews published recently.[3,5,7-9,19-21,23,26,32]

3.4.3 Aspects of CuAAC reaction

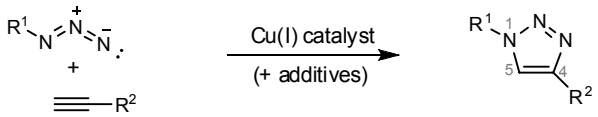

Scheme 3.3: Copper-catalysed azide-alkyne cycloaddition (CuAAC).

The use of the CuACC is a robust catalytic procedure† with the following features:[7,22,24,25]

- The reaction is usually performed at neutral pH (pH 7–9) but also reported to be carried out over a range of pH 4 to pH 12.
- The reaction is usually carried out at room temperature but also reported to proceed over a temperature range from 0 °C to 160 °C.
- The reaction is usually carried out in a variety of solvents including organic solvents (such as toluene, CH_2Cl_2), water, alcohols, ionic liquids and even biological fluids (such as serum and whole blood).
- Dramatic rate enhancement upon catalysis (*ca.* 10^7) is observed.
- The reaction is usually completed within minutes or hours compared to hours or days in the uncatalysed cycloadditions.
- Excellent yields are observed in most cases.
- Only the 1,4-disubstituted triazole is formed as the only regioisomer.
- The reaction is insensitive to steric and electronic properties of the substituents on the azide and the alkyne.
- Internal alkynes have no reactivity under CuAAC.
- The reaction tolerates a large range of functional group such as hydroxyl and amine groups, thereby minimising the need for the functional group protection and subsequent deprotection steps.

† CuAAC adheres to the principle of click chemistry so well that some literature procedures simply inferred that a "click reaction" to mean the use of CuAAC and *vice versa*.

(a) Copper Catalysts

Copper(I) is the active form of the catalyst and is used in the form of a salt (such as CuI, CuBr). Coordination complexes (such as $CuOTf•C_6H_6$, $Cu[MeCN]_4PF_6$, $CuI•P[OEt]_3$ and $CuBr•PPh_3$) and carbene complex (Cu[SIMes]Cl[33]) are also used due to their superior stability and solubility in the organic solvents. Recyclable heterogeneous catalysts (such as impregnated charcoal with copper [Cu/C][34], Amberlyst A-21•CuI[35] and cellulose based copper(II) alginate [Cu(II)-ALG][36]) have also been reported (Table 3.4). Direct addition of unstable Cu(I) catalyst to the reaction mixtures may require the exclusion of oxygen to improve product purity and yield.[7,22-24]

The unstable Cu(I) catalyst can be generated *in situ* by reduction of Cu(II). The popular "aqueous ascorbate" procedure involves the *in situ* reduction of a stable Cu(II) salt [such as $CuSO_4$ or $Cu(OAc)_2$] by sodium ascorbate in a mixture of water and *tert*-butanol at room temperature.[7,24] Another air-stable and water-soluble mild reducing agent, *tris*(2-carboxyethyl)phosphine (TCEP) was also used to generate Cu(I) *in situ* (Table 3.4).[37]

Alternatively, the addition of copper wires/turnings (with or without $CuSO_4$ accelerant) generates the Cu(I) catalyst required through the disproportionation of Cu(0) and Cu(II). This method can be slow but is experimentally simple and produces very pure triazole with low metal contamination. Exclusion of oxygen is not necessary for both the ascorbate and copper wires/turnings procedures.[7,23]

The direct use of Cu(II) salt, namely $Cu(OAc)_2$, as the catalyst for cycloaddition was also reported (Table 3.4).[38]

(b) Ligand Additives

CuAAC often requires the addition of a nitrogen base, such as NEt_3, DIPEA or 2,6-lutidine for deprotonation as well as Cu(I) stabilisation, thereby increasing the rate of reaction.[7,22-24,34]

Addition of other Cu(I) stabilising ligands can further enhance the reaction rate of CuAAC. Fokin *et al*.[39] discovered *tris*-[(1-benzyl-1*H*-1,2,3-triazol-4-yl)methyl]amine (TBTA, **641**, Figure 3.2) after observing unusually fast cycloadditions of certain polyvalent substances. This tetradentate ligand binds tightly to the Cu(I) ion, thus stabilising the catalyst which leads to a higher yield and faster reaction (Table 3.4).[7]

Fluorescence quenching assays conducted by Finn *et al*.[40] identified bathophenanthroline-sulfonic acid **(642)** as a potent ligand for Cu(I) in CuAAC. Phenanthroline **642** has a better solubility in water, but the reaction conducted is more air-sensitive than that of TBTA **641**. Exclusion of oxygen and/or addition of excess reducing agent might be required as a result (Figure 3.2).[7]

Fukase *et al*.[41] discovered the addition of non-basic N^{im}-benzylhistidine **643** or its *N*-Boc derivative **644** accelerated the CuAAC involving peptide substituents and were suitable for base-sensitive reaction systems (Figure 3.2). Both imidazole and amino acid moieties of the histidine catalyst are required for the acceleration and "self-activating" solid phase CuAAC was observed when N^{im}-benzylhistidine residue was incorporated as part of the peptide structure (Table 3.4).

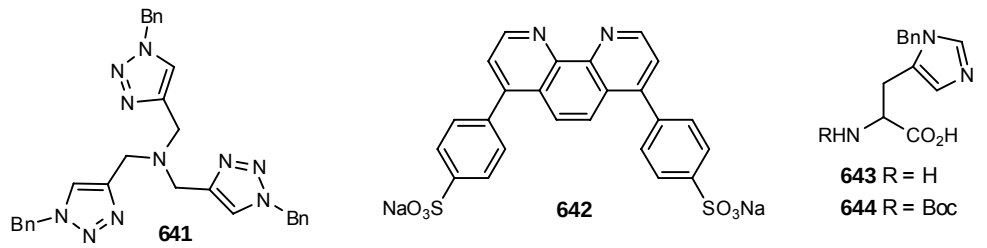

Figure 3.2: TBTA **(641)**, bathophenanthroline sulfonic acid **(642)**, N^{im}-benzylhistidine **643** and its *N*-Boc derivative **644**.

(c) Limitations

The regiochemistry of triazole formation resulting from the case of CuAAC is limited to 1,4-disubstitution. The corresponding 1,5-regioisomers are not formed under these conditions.

Only terminal alkynes would participate in the CuAAC due to its involvement in the formation of a copper acetylide intermediate. Homo-coupling between terminal alkynes (Glaser coupling) was also observed producing dialkynes as the major impurity in the solution-phase reaction. This side reaction can be minimised by the exclusion of oxygen and an excess of the alkynes was usually used in order to compensate for the losses.[22,24] The cross-coupling was not observed in the solid-phase CuAAC.[22]

Other side-products, such as bis-triazoles[24,42] and 5-hydroxytriazoles[24], were also observed, thus further reducing the product yield and purity. The CuAAC of sulfonyl azide to alkyne also gave rearrangement products, such as *N*-sulfonylamidines[43] and *N*-acylsulfonamides[44], depending on the reaction conditions and substituents involved.[7,45] The formation of these side products are base-dependent and can be minimised by the appropriate choice of base such as 2,6-lutidine.[24,42,45]

3.4.4 Mechanisms of CuACC

In contrast to the concerted mechanism of the thermal cycloaddition, Sharpless *et al*.[24] proposed a stepwise mechanism (Scheme 3.4) to account for observations such as regioselectivity, rate acceleration and lack of reactivity towards internal alkynes. This proposal was further supported by a series of computational studies which ruled out the concerted mechanism due to its high potential

energy barrier. The calculations also revealed a lower activation barrier (*ca*. 10 kcal mol^{-1}) for the stepwise copper-catalysed cycloaddition relative to the concerted thermal cycloaddition, leading to the observed enormous rate acceleration.[5,25] The catalytic cycle is summarised as follows:[7,25]

- Step 1: formation of copper acetylide **647**. This is facilitated by the initial π-coordination of alkyne **646** to copper catalyst **645**.
- Step 2: activation of azide **648** by its coordination to copper complex **647**.
- Step 3: formation of a six-membered copper(III) metallacycle **650** by intramolecular attack of alkyne to azide.
- Step 4: ring contraction of metallacycle **650** to from the triazoyl-copper intermediate **651**.
- Step 5: protonation of **651**. This releases triazole product **652** and regenerates copper(I) catalyst **645** for the next cycle.

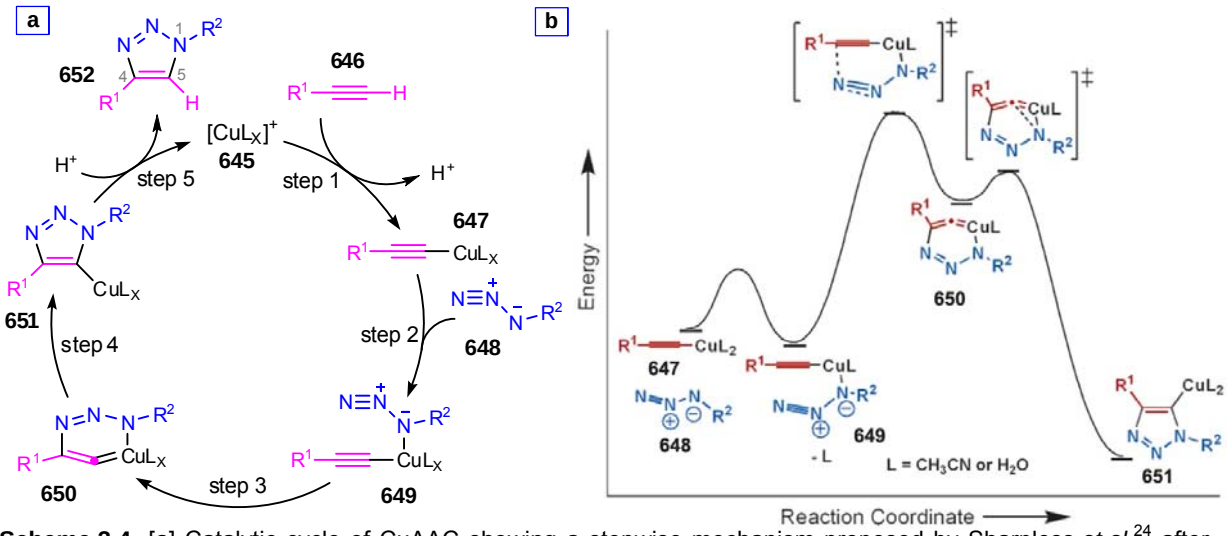

Scheme 3.4: [a] Catalytic cycle of CuAAC showing a stepwise mechanism proposed by Sharpless *et al*.[24] after extensive computational studies.[25] [b] Calculated energy profile of the CuAAC reaction from DFT study conducted by Sharpless *et al*.[25]

Further in-depth investigation revealed the possible involvement of a second copper atom due to the ability of copper acetylide to form highly aggregated but stabilised species.[7,46]

3.4.5 Selected Examples of CuAAC

Since the discovery of CuAAC, the application of this transformation has been increasing rapidly. Some representative examples are listed below.

Entry	Conditions	Products	Yields
[1] Meldal *et al.*[22]	cat. CuI, DIPEA, THF, rt, 16 h	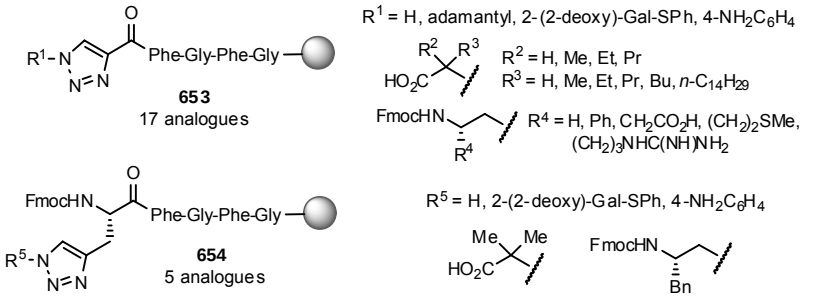	>95% (>75% purity)
[2] Sharpless *et al.*[24]	cat. $CuSO_4$, Na ascorbate, $^tBuOH–H_2O$, rt, 8 h	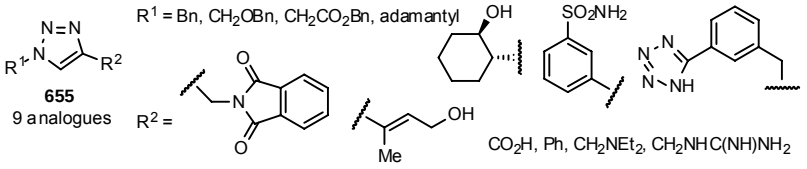	82–93%
[3] Fokin *et al.*[39]	cat. $[Cu(MeCN)_4]PF_6$, TBTA, rt, $^tBuOH–H_2O$, 1 d	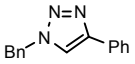 656	84% (without TBTA: 1%)
[4] Chang *et al.*[45]	cat. CuI, 2,6-lutidine, $CHCl_3$, 0 °C, 12 h	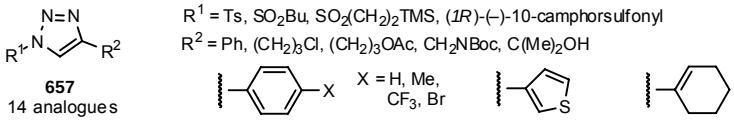	56–95% (without 2,6-lutidine: 3%)
[5] Lipshutz and Taft[34]	cat. Cu/C, NEt_3, dioxane, 10–120 min, 60 °C	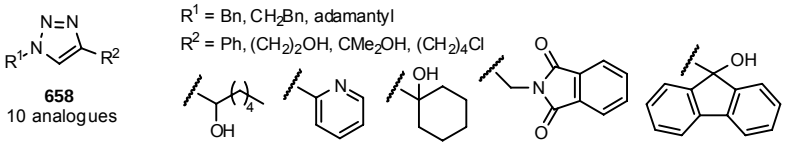	92–99% (uncatalysed: 0%; without NEt_3: 4 h)
[6] Kantam *et al.*[38]	cat. $Cu(OAc)_2$, H_2O, rt, 20 h	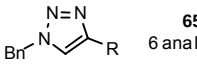 659 6 analogues R = Ph–, Tol–, 3-MeOC6H4– –CH2OH, –CMe2OH, –CMe(Ph)OH	71–100% (uncatalysed: 0–20%)
[7] Nolan *et al.*[33]	cat. Cu(SIMes)Br, neat, rt, 10 min–5 h	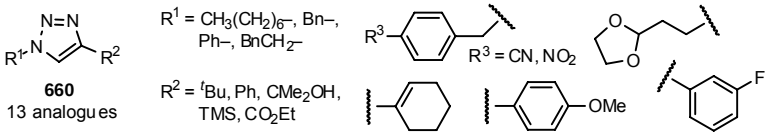	86–98%
[8] Dondoni *et al.*[30]	cat. CuI, DIPEA, toluene, rt, 15 h	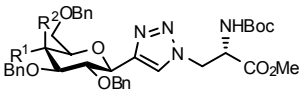 635a R^1 = H, R^2 = OBn 635b R^1 = OBn, R^2 = H See also Table 3.3 for the uncatalysed cycloaddition	80–82% (uncatalysed: 13–31%)
[9] Vargas-Berenguel *et al.*[47]	cat. CuI•$P(OEt)_3$, toluene, reflux, 45 min	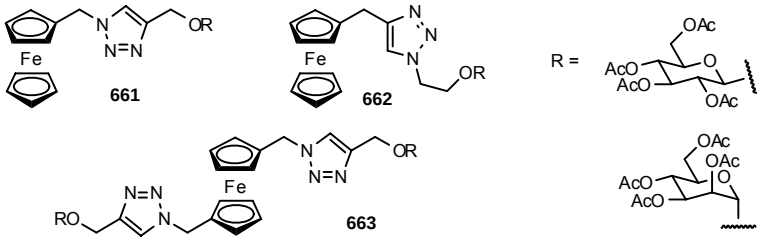	88–98%
[10] IJsselstijn and Cintrat[48]	cat. $Cu(OAc)_2$, Na ascorbate, $^tBuOH–H_2O$, rt, 18 h	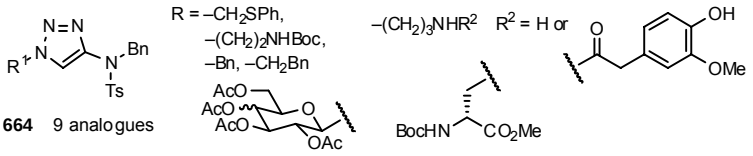	38–96%

[11] Fokin *et al.*[13]	cat. $CuSO_4$, Cu turnings, rt, $^tBuOH–H_2O$, 2 d	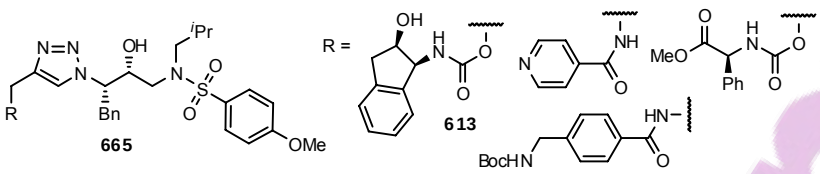	Yields were not stated but disappearance of the limiting azide was observed.
[12] Fukase *et al.*[41]	CuI, DMF, rt, **643** or **644**, 10 min	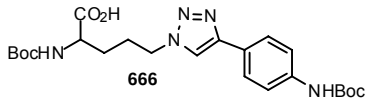	100% (without **643** or **644**: 20% over 3 d)
	CuI, **644**, DMF, rt	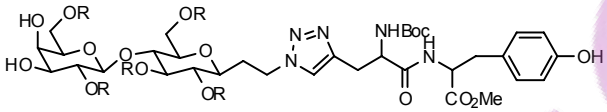	For R = H: 78% For R = Bz: 51%
	CuI, DMF, rt, 12 h	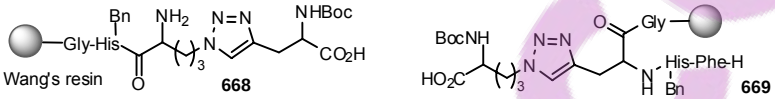	57–100% after cleavage of Boc and resin
	Various amounts of 5-iodotriazole by-products were also isolated due to the excuss use of CuI. See Section 3.4.7 and Scheme 3.18 for discussions.		
[13] Seela and Sirivolu[37]	Method A: cat. $CuSO_4$, Na ascorbate, THF–H_2O, rt Method B: cat. $CuSO_4$, TBTA, TCEP, $^tBuOH–H_2O$, rt	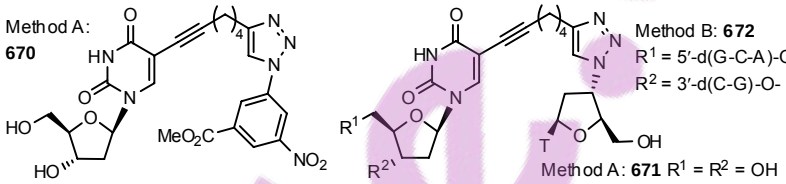	Method A: 69–80% Method B: yield was not stated
[14] Astruc *et al.*[18]	$CuSO_4$, Na ascorbate, THF–H_2O, rt, 30 min	triazole linked ferrocenyl dendrimers 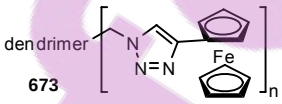 Generation G_0: n = 9 Generation G_1: n = 27 Generation G_2: n = 81, **620**	G_0: 94%, G_1: 71%, G_2: 56%
[15] Massi *et al.*[17]	CuI, DIPEA, toluene–DMF, rt, 18 h	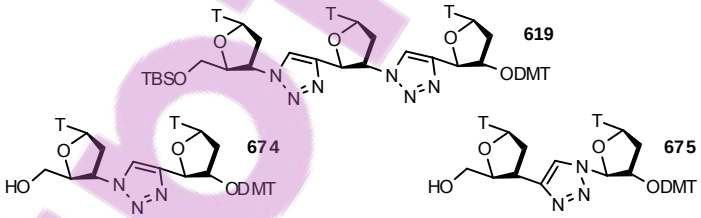	55–73%

Table 3.4: Selected examples of CuAAC.

3.4.6 One-pot Synthesis of Triazoles

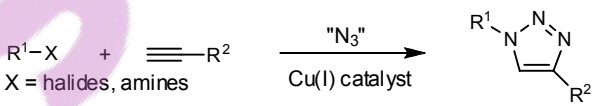

Scheme 3.5: One-pot synthesis of triazoles from the corresponding halide or amine. Azide is formed *in situ* and then trapped by alkyne under CuAAC.

One-pot syntheses of triazoles by *in situ* generated azide provide a synthetically convenient alternative route to further enhance the comprehensiveness and versatility of CuAAC. These one-pot procedures avoid the isolation of potentially unstable organic azides. Therefore, this synthesis provides access to a wider range of azides that are not readily available from commercial or synthetic

sources, especially those with low molecular weights or bearing multiple azide functionalities (Scheme 3.5).[7,21] Under these conditions, azide was usually generated *in situ* from the S_N2 reaction between the corresponding halide or amine and an azide source such as NaN_3, TfN_3 or $TMSN_3$. The following table briefly summaries the various reaction conditions involved:

Entry	*Halide/Amine*	*Conditions*	*Yields*
[1] Fokin *et al.*[49]	alkyl, allyl or benzyl halides	NaN_3, cat. $CuSO_4$, Na ascorbate, DMF–H_2O, rt–65 °C	72–93%
[2] Fokin *et al.*[49] and Hsung *et al.*[50]	aryl or vinyl iodides	NaN_3, cat. $CuSO_4$, Na ascorbate, L-proline, Na_2CO_3 (or K_2CO_3), DMSO–H_2O, 60–70 °C, 14–18 h	31–98%
[3] Fokin *et al.*[51]	alkyl or benzyl halides	NaN_3, Cu turnings, cat. $CuSO_4$, microwave, ^{t}BuOH–H_2O, 125 °C, 10–15 min	81–93%
[4] Wang *et al.*[52]	glycosyl bromides	NaN_3, $BuNHSO_4$, $NaHCO_3$, cat. $CuSO_4$, Na ascorbate, $CHCl_3$–EtOH, rt, 18 h (with or without H_2O) (80 °C for mannose)	53–98%
[5] Liang *et al.*[53]	aryl iodides	NaN_3, cat. CuI, **676**, Na ascorbate, DMSO–H_2O, rt, 1–18 h 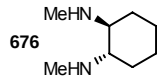	38–99%
	aryl bromides	NaN_3, cat. CuI, **676**, Na ascorbate, DMSO–H_2O, 70 °C, 1–18 h	74–98%
[6] Sreedhar and Reddy[54]	alkyl, allyl or benzyl halides	NaN_3, cat. CuI, ultrasound, H_2O, rt, 15–30 min	52–95%
[7] Liang *et al.*[55]	alkyl, allyl or benzyl halides	NaN_3, cat. CuI, Na_2CO_3, [bmin][BF_3]–H_2O, rt, 4–10 h	76–99%
	aryl iodide	NaN_3, cat. CuI, L-proline, Na_2CO_3, [bmin][BF_3]–H_2O, 65–80 °C, 8–12 h	70–80%
[8] Nolan *et al.*[33]	alkyl or benzyl bromide	NaN_3, cat. Cu(SIMes)Br, H_2O, rt, 0.3–2 h	90–98%
[9] Kacprzak[56]	alkyl or benzyl bromides	i. NaN_3, DMSO, rt, 12–24 h; ii, alkyne, cat. $CuSO_4$, Na ascorbate, H_2O, rt, 3–18 h	60–98%
[10] Beckmann and Wittmann[57]	alkyl or benzyl amines	i. TfN_3, cat. $CuSO_4$, $NaHCO_3$, CH_2Cl_2–MeOH–H_2O, rt, 30 min ii. Na ascorbate, TBTA, microwave, 80–120 °C, 10–30 min	78–99%
[11] Moses *et al.*[58]	aryl amines	i. ^{t}BuONO, $TMSN_3$, MeCN, 0 °C→rt, 2 h ii. cat. $CuSO_4$, Na ascorbate, rt, 16 h	79–87%

Table 3.5: Conditions of one-pot synthesis of triazoles from halides or amines.

Azides can also be obtained from other sources such as alkenes. Carreira *et al.*[59] reported a cobalt-catalysed hydroazidation of a range of unactivated alkenes with high Markovnikov selectivity. Further study had shown that the resulting azide can be trapped *in situ* by CuAAC under a stepwise one-pot procedure to give a triazole. It was demonstrated with the synthesis of triazole **680** from the unactivated alkene **677** *via* azide **679** (Scheme 3.6).

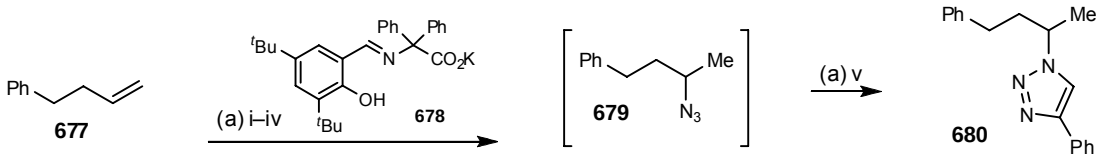

Reagents and conditions: (a) i. cat. $Co(BF_4)_2$•$6H_2O$, **678**, EtOH, rt, 30 min; ii. **677**, TsN_3, ^{t}BuOOH, rt, 10 min; iii. TMDSO, rt, 4 h; iv. H_2O, rt, 30 min; v. cat. $CuSO_4$, sodium ascorbate, phenylacetylene, H_2O, rt, 20 h, 60%.

Scheme 3.6: One-pot synthesis of triazole **680** from alkene **677** by Carreira *et al.*[59]

Alternatively, Chandrasekhar *et al*.[60] and Sreedhar *et al*.[61] generated allyl azides **684** *in situ* from alkyl acrylates **683**, which were in turn obtained by Baylis-Hillmann alkylation of aldehyde **681** using activated alkene **682**. The *in situ* azide **684** was subsequently trapped as triazole *via* CuAAC under one-pot conditions conducted in EtOH, H_2O or PEG (Scheme 3.7).

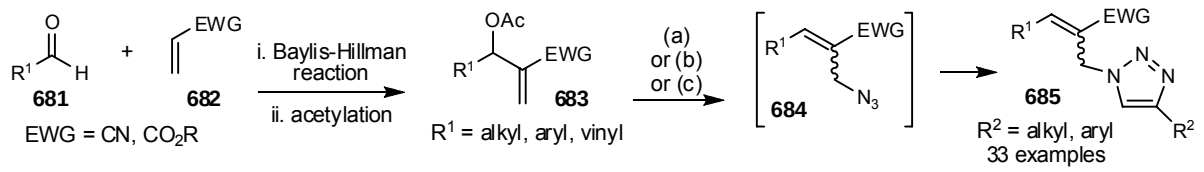

Reagents and conditions: (a) $R^2C{\equiv}CH$, NaN_3, copper turnings, cat. $CuSO_4$, EtOH–H_2O, reflux, 2 h, 72–91%; (b) $R^2C{\equiv}CH$, NaN_3, cat. CuI, NEt_3, H_2O, rt, 8–12 h, 50–80%; (c) $R^2C{\equiv}CH$, NaN_3, cat. CuI, PEG-400, rt, 6–8 h, 58–90%;

Scheme 3.7: One-pot synthesis of triazoles **685** from alkenes **683** by Chandrasekhar *et al*.[60] and Sreedhar *et al*.[61]

Aucagne and Leigh[62] reported a stepwise one-pot chemoselective synthesis of two distinct triazole moieties by successive copper and copper-silver-catalysed cycloaddition. The first step of this one-pot reaction involved a CuAAC of an azide to bis-acetylene **686** in which one of the terminal alkynes was masked by a TMS group. The second CuAAC was conducted in the presence of Ag(I) which deprotected the TMS-alkyne *in situ* to allow the formation of the subsequent triazole moiety without interim workup or purification (Scheme 3.8).

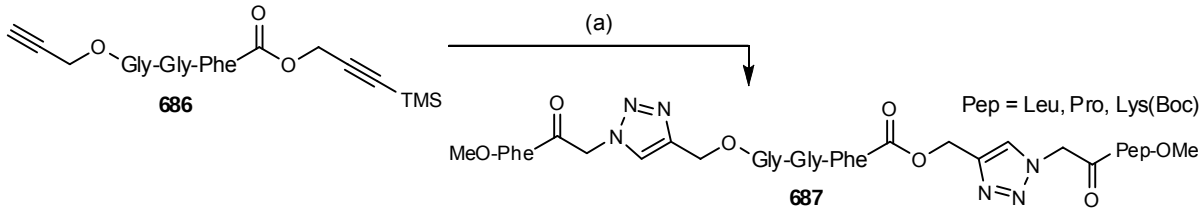

Reagents and conditions: (a) i. $MeOPheCOCH_2N_3$, cat. $CuSO_4$, sodium ascorbate, ^tBuOH–H_2O, 35 °C, 18 h; ii. $MeOPepCOCH_2N_3$, cat. $CuSO_4$, Na ascorbate, $AgPF_6$, ^tBuOH–H_2O, 35 °C, 18 h, 88–93%.

Scheme 3.8: One-pot synthesis of bis-triazoles **687** from mono-silylated bis-acetylene **686** by Aucagne and Leigh.[62]

3.4.7 Synthesis of 1,5-Disubstituted and 1,4,5-Trisubstituted Triazoles

1,5-Disubstituted and 1,4,5-trisubstituted triazole derivatives are not so well studied compared to their 1,4-disubstituted counterparts. Their progress had been hampered by syntheses that lacked regioselectivity and/or tolerance towards other functional groups.[63]

(a) 1,5-Disubstituted Triazoles

The 1,5-disubstituted triazole moiety is a stable isostere of the *cis*-peptide bond due to its intrinsic geometrical constraint and amide bond mimicry.[64] *cis*-Peptide bonds induce structural disruption and are important elements found in turns and loops of peptide secondary structures, where

proline is commonly involved.[1,65] However, unlike the 1,4-disubstituted triazoles, the number of 1,5-disubstituted derivatives is limited due to the lack of reliable and versatile synthetic methodology.[64]

1,5-Disubstituted triazoles moieties are commonly installed by the intramolecular cycloaddition of azides to alkynes. Appella *et al*.[64] utilised this "ring-constrained" Huigen's cycloaddition for the construction of structural scaffold **691**, which was subsequently incorporated into a peptoid oligomer backbone to induce a hairpin conformation. The synthesis started with the conversion of bromoacetyl chloride **688** to azidoacetamide **689**. Subsequent intramolecular cycloaddition gave 1,5-disubstituted bicyclic triazole **690** exclusively. Cleavage of the lactam and Fmoc protection furnished triazole scaffold **691** ready to be incorporated into peptoid oligomer **692** (Scheme 3.9).

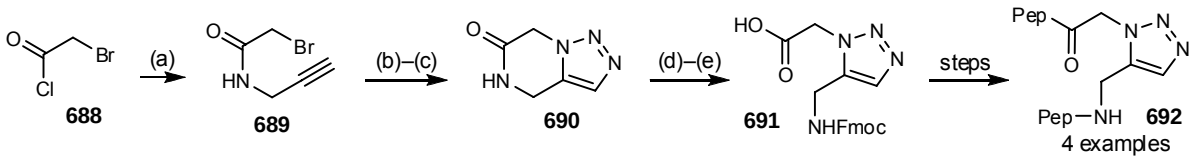

Reagents and conditions: (a) propargyl amine, DIPEA, CH_2Cl_2, -15 °C, 1.5 h, 67%; (b) NaN_3, DMF, rt, 18 h; (c) toluene, reflux, 1 d, 71% over 2 steps; (d) aq. HCl, H_2O, 80 °C, 16 h; (e) FmocOSu, K_2CO_3, dioxane–H_2O, 0 °C→rt, 4 h, 65% over 2 steps.

Scheme 3.9: Synthesis of 1,5-disubstituted triazole scaffold **691** *via* intramolecular cycloaddition by Appella *et al*.[64]

Hotha *et al*.[66] generated a library of carbohydrate-derived fused-ring analogues **695** and **698** which were produced from azido-acetylenes **694** and **697** using the intramolecular cycloaddition as a key step to generate the 1,5-disubstituted triazole moiety. These analogues then served as scaffolds for the synthesis of structurally diverse polycyclic molecules such as triazole fused glycosides **700** and nucleosides **702** (Scheme 3.10).

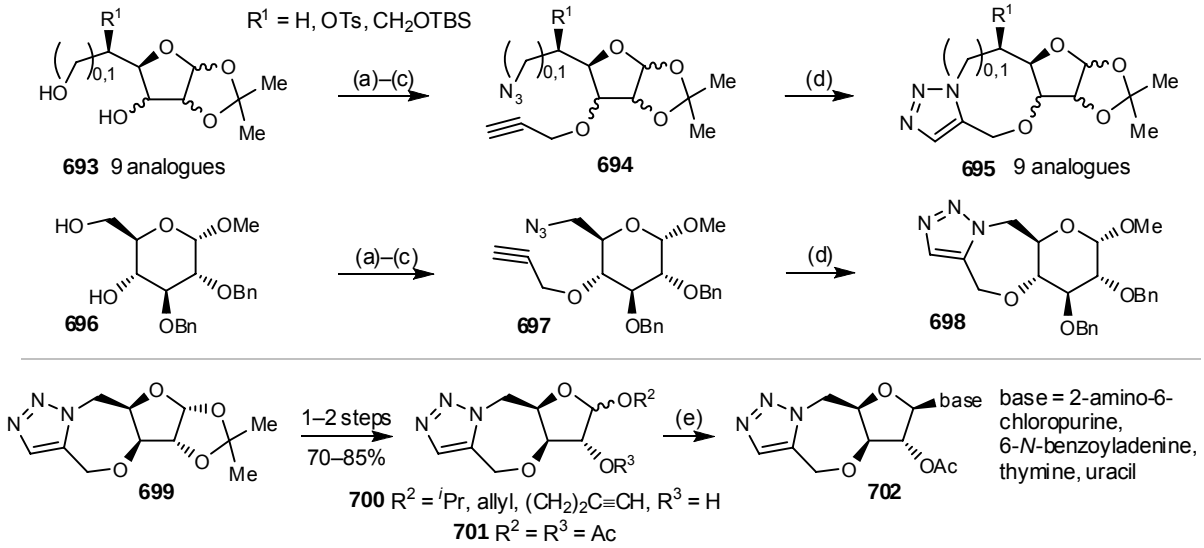

Reagents and conditions: (a) *p*-TsCl, pyridine, 0 °C→rt, 10–15 h, 86–91%; (b) NaN_3, DMF, 90–120 °C, 8 h, 92–95%; (c) propargyl bromide, NaH, DMF, 0 °C→rt, 2 h, 87–93%; (d) toluene, 100 °C, 2–6 h, 75–95%; (e) **701**, base, HMDS, TfOH, TMSCl, MeCN, rt–reflux, 8–10 h, 35–50%.

Scheme 3.10: Synthesis of carbohydrate-derived ring-fused analogues by Hotha *et al*.[66]

A regioselective intermolecular synthesis of a 1,5-disubstituted triazole was reported by Krasiński *et al*.[67] after re-examination and refining earlier work. The synthesis involved the cycloaddition of azide **705** to halomagnesium acetylide **704** generated *in situ* from terminal alkyne **703** and ethylmagnesium halide. 4-Halomagnesiotriazole intermediate **707** was then hydrolysed to yield the desired 1,5-disubstituted triazole **708**. Alternatively, intermediate **707** could be trapped by a range of appropriate electrophiles **709** giving 1,4,5-trisubstituted triazoles **710** regioselectively (Scheme 3.11). However, this method cannot be used for substrates that bear functionalities such as acidic protons or carbonyl groups which are sensitive to Grignard reagents.

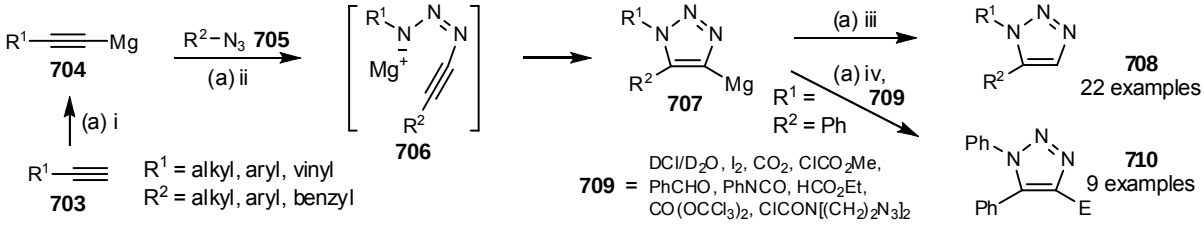

Reagents and conditions: (a) i. EtMgCl or EtMgBr, THF, rt→50 °C, 15 min; ii. **705**, neat or THF, rt→50 °C, 1–24 h; iii. aq. NH_4Cl, 63–100%; iv. **709**, neat or THF, 42–95%.

Scheme 3.11: Regioselective synthesis of 1,5-disubstitued triazoles **708** and 1,4,5-trisubstituted triazoles **710** under magnesium-mediated cycloaddition by Krasiński *et al*.[67]

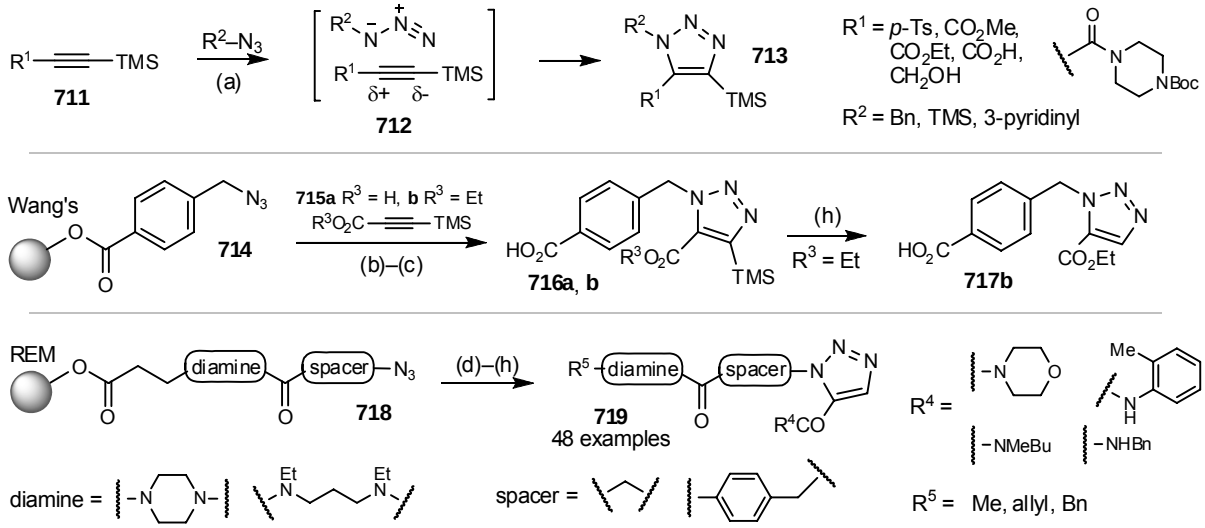

Reagents and conditions: (a) R^2N_3, toluene, reflux, 12–46 h, 42–82%; (b) **715**, BSA, toluene, reflux, 18 h; (c) TFA, CH_2Cl_2, rt, 1 h, 94–99% over 2 steps; (d) **715a**, BSA, xylene, 105 °C, 1 d; (e) R^4NH, PyBOP, DIPEA, DMF, rt, 1 d; (f) R^5X, DMSO, rt, 18 h; (g) DIPEA, CH_2Cl_2, rt, 6 h; (h) aq. HF, THF, rt, 4 h, 79% for **717b** or 27–100% overall yield calculated on the basis of the initial loading of REM resin.

Scheme 3.12: Synthesis of 1,5-disubstituted triazoles under TMS-directed cycloadditions by Hlasta *et al*.[68]

Hlasta *et al*.[68] synthesed 1,5-disubstitued triazoles regioselectively by using the bulky TMS as a directing group in both solution and solid phase reaction. Due to its steric hindrance and the ability of silicon to stabilise the developing partial positive charge on the alkyne β-carbon in the transition

state, the TMS group preferably resides at C4 position, leaving the other substituent resided at C5 position of the trisubstituted triazoles as seen in **713**. BSA was sometimes added to minimise the unwanted desilylation during solid phase cycloaddition. Subsequent cleavage from the resin and removal of the TMS group by aqueous HF yielded 1,5-disubstitued triazole **717b**. A small library of 1,5-disubstituted triazoles **719** was generated successfully using this method with REM resin (Scheme 3.12).

However, none of the above syntheses of complementary 1,5-triazoles is catalytic in nature to possibly mirror the success of CuAAC, until the discovery of ruthenium catalyst **722** by Fokin *et al*.[69] Ruthenium catalyst **722**, Cp*RuCl(PPh$_3$)$_2$, catalysed the cycloaddition of azides **720** to terminal alkynes **721** to afford 1,5-disubstituted triazoles **723** exclusively. Unlike CuAAC, this system also produces 1,4,5-trisubstituted triazole **726** by catalysing the cycloaddition of benzyl azide **(724)** to phenylacetylene **(725)**, a symmetrical internal alkyne. Therefore, the metal acetylide intermediate is not involved in the postulated ruthenium-catalytic cycle (Scheme 3.13).

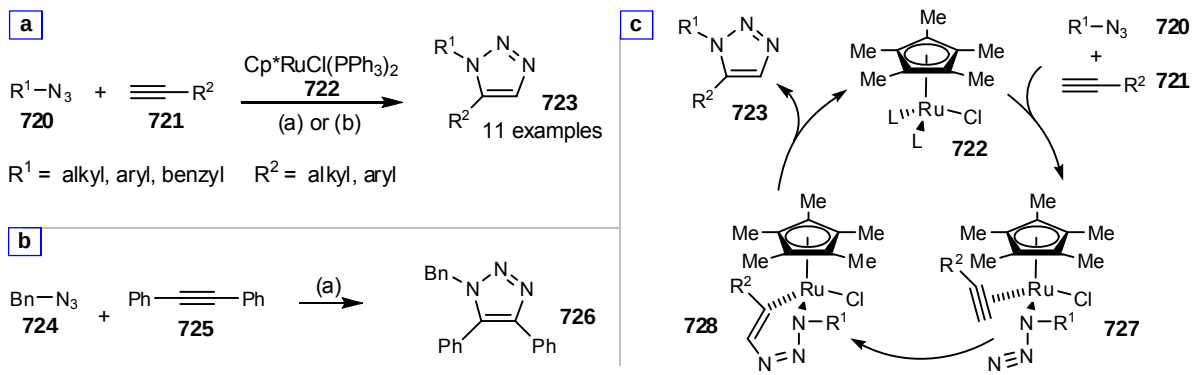

Reagents and conditions: (a) cat. **722**, benzene, 80 °C, 2–4 h, 80–94%; (b) cat. **722**, dioxane, 60 °C, 2–12 h, 80–94%.

Scheme 3.13: [a] Ruthenium-catalysed cycloaddition of azides **720** to terminal alkynes **721** gave 1,5-disubstituted triazoles **723**. [b] Ruthenium-catalysed cycloaddition of benzyl azide **(724)** to diphenylacetylene **(725)** produced trisubstituted triazole **726**. For the uncatalysed reaction, only trace amount of triazole **726** was detected after 1 day of reflux. [c] The ruthenium catalytic cycle proposed by Fokin *et al*.[69] The cycle began with the oxidative coupling of an azide and an alkyne on ruthenium to give a six-membered ruthenacycle **728**. Subsequent reductive-elimination of **728** yielded the desired triazole **723**. Unlike the catalytic cycle of CuAAC, metal acetylide was not involved.

Weinreb *et al*.[70] attempted to address the regiochemistry problem resulting from the ruthenium-catalysed cycloadditions when asymmetrical internal alkynes were used. Although the catalysis between azide and an internal alkyne was shown to be a general process, the regiochemistry varied depending on the substituents. For example, the carbonyl substituent preferred to reside at C4 position of triazole whereas the propargylic alcohol substituent preferred to reside at C5 position of triazole. Bulky substituents on either the alkyne or the azide resulted in a very slow reaction with low yield. The studies were unable to offer a mechanistic rationale for the regiochemical results (Scheme 3.14).

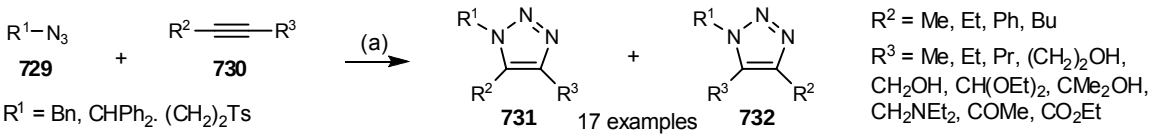

Reagents and conditions: (a) cat. **722**, benzene, 80 °C, 2.5–20 h, 65–100%.

Scheme 3.14: Ruthenium-catalysed cycloaddition of azides **729** to internal alkynes **730** by Weinreb *et al.*[70] The regiochemistry of the reaction varies depending on the substituents. Low yields (10–15%) were observed when a bulky substituent, such as *tert*-butyl or 1-adamantyl group, was found on either substrate.

(b) 1,4,5-Trisubstituted Triazoles

In addition to the syntheses illustrated in Scheme 3.11–3.14, 1,4,5-trisubstituted triazoles have been synthesised by variants of the popular CuAAC.[67-69] Wu *et al.*[71] conducted CuAAC in the presence of stoichiometric CuI and an electrophile which trapped 5-triazoyl-copper intermediate **651** *in situ*. This concept was similar to the electrophilic trapping of halomagnesiotriazole intermediate **707** that was previously discussed (Scheme 3.11).[67] A strong electrophile was required due to the lower nucleophilicity of triazoyl-copper intermediate **651** and only a moderate yield was obtained (Scheme 3.15).

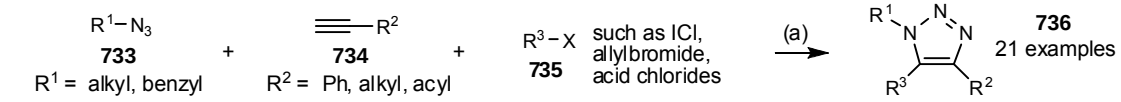

Reagents and conditions: (a) CuI, NEt_3, THF, rt, 20 h, 27–82%

Scheme 3.15: Synthesis of trisubstituted triazoles **736** using modified CuAAC by Wu *et al.*[71]

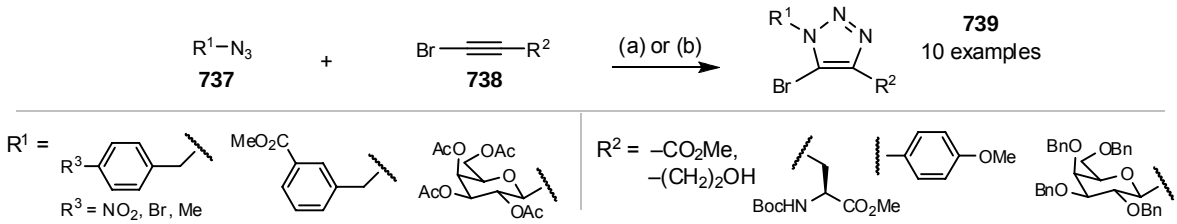

Reagents and conditions: (a) cat. CuI/$Cu(OAc)_2$ (1:1), THF, rt–50 °C, 16–50 h, 60–94% (+ 4–14% 5-iodotriazole); (b) cat. CuBr/$Cu(OAc)_2$ (1:1), THF, 50 °C, 16 h–7 d, 65–99%.

Scheme 3.16: Synthesis of trisubstitued 5-bromotriazoles **739** from azides **737** and bromoacetylene **738** catalysed by a mixture of CuX/$Cu(OAc)_2$ by Rutjes *et al.*[63]

Rutjes *et al.*[63] reported a versatile synthesis of trisubstituted 5-bromotriazoles **739** using azides **737** and stable bromoacetylenes **738** catalysed by a mixture Cu(I) and Cu(II). Two mixtures of catalyst were suggested: either CuI/$Cu(OAc)_2$ or CuBr/$Cu(OAc)_2$. When CuI was used, the reaction proceeded faster but a small amount of corresponding 5-iodotriazole was also formed. The formation of this iodo by-product was avoided if CuBr was used but the reaction proceeded significantly slower. The resulting 5-halo substituent provides a useful handle for metal-mediated derivatisations such as

palladium-catalysed cross-coupling or nucleophilic substitution *via* halogen-metal exchange. The synthesis of 5-iodotriazole starting from iodoacetylene was also attempted but failed due to the instability of iodoacetylene towards the reaction conditions. Compared to Wu's modified CuAAC, this method avoids the use of stoichiometric CuI as well as the use of hazardous and corrosive ICl (Scheme 3.16).[63]

The use of Cu(I)/Cu(II) mixture as the catalysts for the synthesis of 5-alkynyltriazoles **742** was reported by Porco *et al.*[72] The 1:1 mixture of Cu(I) and Cu(II) catalyst was generated *in situ* by the oxidation of Cu(I) complex using NMO. However, the proposed reaction conditions gave a variable mixture of trisubstituted and disubstituted triazoles **742** and **743** in variable quantities (Scheme 3.17).

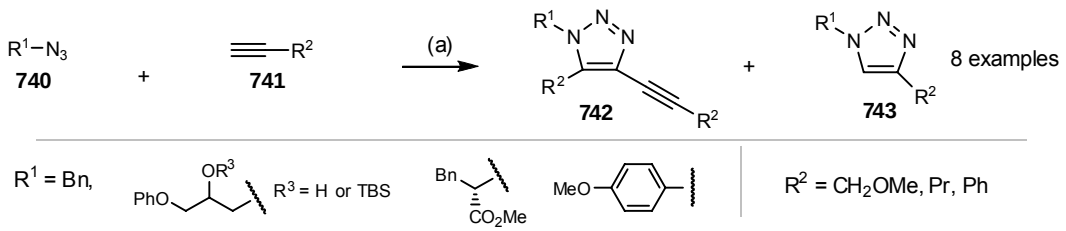

Reagents and conditions: (a) cat. $Cu(MeCN)_4PF_6$, TMEDA, NMO, DIEA, CH_2Cl_2, rt, **742**: 31–68%, **743**: 24–46%.

Scheme 3.17: Synthesis of trisubstitued 5-alkynyltriazoles **742** by Porco *et al.*[72]

During the investigation using histidine derivatives as the Cu(I) stabilising and rate accelerating agents of CuAAC (Table 3.4), Fukase *et al.*[41] also isolated 5-iodotriazole derivatives as the major product under prolonged reaction conditions. It was suggested that the presence of base and excess CuI facilitated the iodination of triazole after its formation, although the *in situ* trapping of the 5-triazoyl-copper intermediate **651** was also plausible (Scheme 3.18).

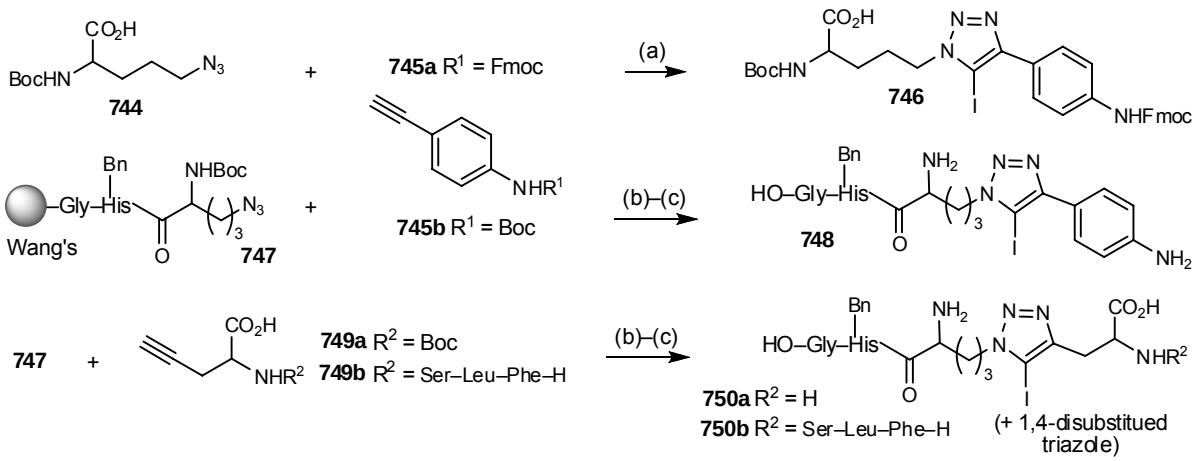

Reagents and conditions: (a) CuI, **644**, DMF, rt, 77%; (b) CuI, DMF, rt, 12 h; (c) TFA–TES–H_2O, rt, 30 min, yields over 2 steps: **748**: 100%, **750a**: 43% (+ 57% 1,4-disubstitued triazole), **750b**: 70% (+ 18% 1,4-disubstitued triazole).

Scheme 3.18: Synthesis of 5-iodo-1,4-disubstituted triazole derivatives by using excess CuI and prolonged reaction conditions by Fukase *et al.*[41]

A preliminary study conducted by Nolan *et al.*[33] discovered that highly reactive carbene coordination complex, Cu(SIMes)Br, also catalysed the cycloaddition of azides to internal alkynes. The carbene ligand was crucial for the catalysis and enabled the activation of internal alkyne by enhancing the π-coordination/backbonding of the copper complex (Scheme 3.19).

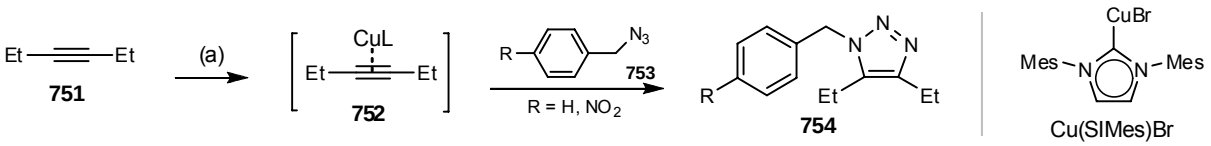

Reagents and conditions: (a) cat. Cu(SIMes)Br, neat, 70 °C, 48 h, 59–80%.

Scheme 3.19: Synthesis of trisubstituted triazoles **754** from azides **753** and 3-hexyne **(751)** catalysed by Cu(SIMes)Br.[33]

3.5 Alternative Use of Azides—Staudinger Reactions

Apart from its utilisation in cycloaddition, organic azides are also useful starting materials for various reactions which provide alternative routes for diversity oriented synthesis (DOS) starting from a common intermediate. Among those, the Staudinger reaction is one of the important examples and it usually refers to a mild reduction of azide **755** to amine **759** using phosphine as reducing agent. The mechanism of this reduction involves the hydrolysis of aza-ylide intermediate **758**, generated by the addition of phosphine to azide **755** with concomitant loss of nitrogen gas (Scheme 3.20). This reaction is a convenient metal free alternative to the metal-catalysed reduction/hydrogenation of azides.[73]

The Staudinger ligation, on the other hand, usually refers to the modified procedure in which aza-ylide intermediate **758** is trapped *in situ* by a non-aqueous electrophile such as a carboxylic acid, to give amide **760**. This procedure effectively ligates two molecules together through an amide bond with one bearing substituent originally carried by the azide and another one bearing a carbonyl group and its substituent. This latter reaction is commonly used in the peptide ligations and *N*-glycopeptides synthesis (Scheme 3.20).[73-77]

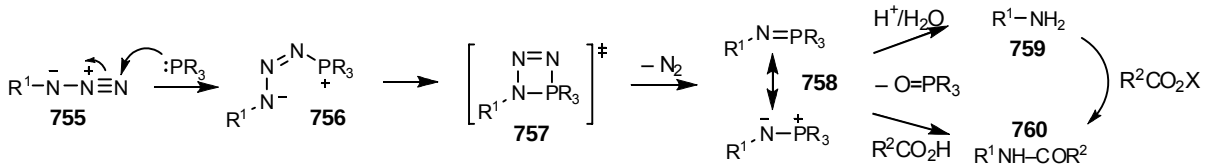

Scheme 3.20: The Staudinger reactions. Trapping of aza-ylide **758** by water gave amine **759** whereas trapping by a carboxylic acid gave amide **760**. The later is sometime referred as Staudinger ligation especially when one of the substituents is a peptide.[73-76]

N-Glycopeptides are usually synthesised by the condensation of a glycosyl amine with an activated amino acid derivative. The glycosyl amine intermediate, in turn, was generated from the reduction of glycosyl azide or other methods. However, the unstable glycosyl amine can undergo spontaneous dimerisation and can be easily hydrolysed under neutral or acidic conditions. The anomeric centre of the glycosyl amine also isomerises easily in the presence of an acid or a metal, giving a mixture of anomers regardless the stereochemistry of the starting material. This is why the Staudinger ligation, a direct one-step procedure that avoids the isolation of the glycosyl amine intermediate, was considered to be a superior alternative to the two-step condensation procedures for the synthesis of *N*-glycopeptides (Scheme 3.20).[73-77]

N-Glycosylation of the aspartic acid (Asp) side chain is of particular interest because the carboxylic acid side chain of aspartic acid serves as a connection point between glycosides and peptide aglycons in naturally occurring *N*-glycopeptides. Most of these connections are thermodynamically stable β-glycosidic linkages.[75,76,78-81]

3.5.1 Selected Examples of Staudinger Reaction/Ligation

Vilarrasa *et al*.[82] reported the first one-pot synthesis of amide **763** from unactivated carboxylic acid **761** and azide **762** using the Staudinger reaction, initially using PPh_3 as the reducing agent. However, it was later discovered that the use of more reactive PEt_3 provided better yields and faster reaction, thus allowing the use of milder reaction conditions. The water soluble $O{=}PEt_3$ by-product can easily be removed by aqueous work-up (Scheme 3.21).

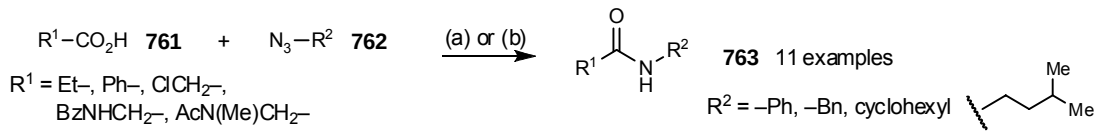

Reagents and conditions: (a) PPh_3, benzene, reflux, 12 h–5 d, 60–96%; (b) PEt_3, benzene, 80 °C, 5–15 h, 87–99%.

Scheme 3.21: Synthesis of amide **763** from carboxylic acid **761** and azide **762** by Vilarrasa *et al*.[82]

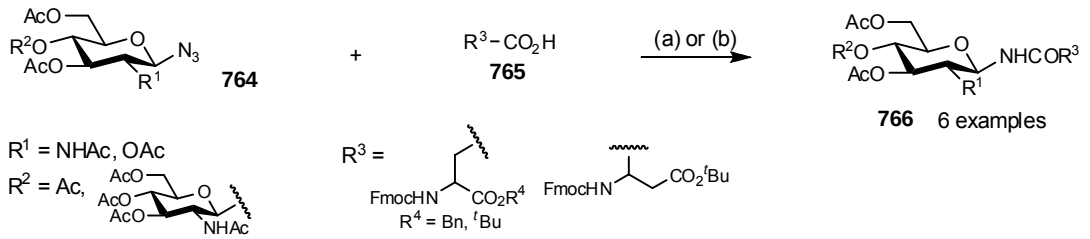

Reagents and conditions: (a) PEt_3, CH_2Cl_2, rt, 18 h, 23–88%; (b) i. PEt_3, CH_2Cl_2, -78 °C, (or MeCN, -30 °C), 18 h; ii. aq. citric acid wash, 66–100%.

Scheme 3.22: First synthesis of *N*-glycopeptide **766** from glycosyl azide **764** and carboxylic acid **765** by Inazu and Kobayashi.[78] Conducting the same reactions at lower temperature improved the yield.[79]

The first synthesis of *N*-glycopeptides **766** using the Staudinger reaction was reported by Inazu and Kobayashi[78] who demonstrated the direct coupling between glucosyl azides **764** and asparagine derivatives **765** in moderate yields. Subsequent optimisation studies revealed a dependence whereby lower reaction temperature resulted in improved yields (Scheme 3.22).[79]

N-Glycolipids can also be synthesised from glycosyl azides using the Staudinger reaction. Boullanger *et al*.[83] reported the use of reactive fatty acid chloride **768** to trap the aza-ylide intermediate **757** generated from a variety of glycosyl azide **767**. PPh_3 was chosen as the reducing agent due to its stability and ease of handling despite its lower reactivity compared to PBu_3 or PEt_3 (Scheme 3.23). This *N*-acylation of glycosides has limited usage in the synthesis of *N*-glycopeptides due to functional group intolerance.

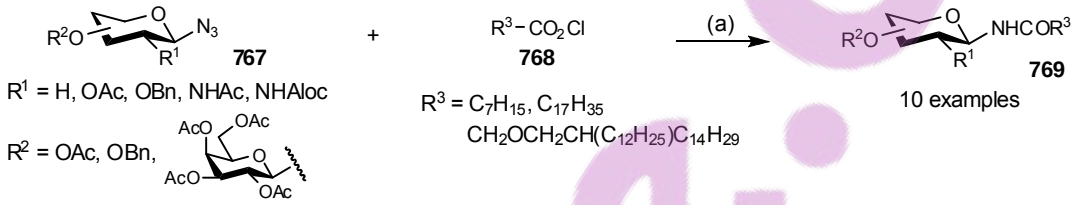

Reagents and conditions: (a) PPh_3, CH_2Cl_2 or benzene or toluene, rt, 52–95%.

Scheme 3.23: Synthesis of *N*-glycolipid **769** from corresponding glycosyl azide **767** and fatty acid chloride **768** by Boullanger *et al*.[83] α-*N*-Glycolipids were also synthesised similarly (not shown).

Bertozzi *et al*.[74] introduced an intramolecular two-component ("traceless") Staudinger ligation in which the acyl group, destined for the amide bond, was attached to the phosphine by a rigid but cleavable linkage as in **771** or **777**. Thereby, once aza-ylide intermediate **757** was generated, it was intramolecularly acylated concomitantly. The acylation also displaced the cleavable linkage leading to the detachment of the desired amide and phosphine oxide by-product **775** or **779** upon hydrolysis. Unlike most other coupling methods, this two-component ligation did not require the protection of hydroxyl groups or the exclusion of water during the reaction. However, extra synthetic steps were involved in order to prepare the functionalised phosphine **771** or **777** required for the coupling (Scheme 3.24).

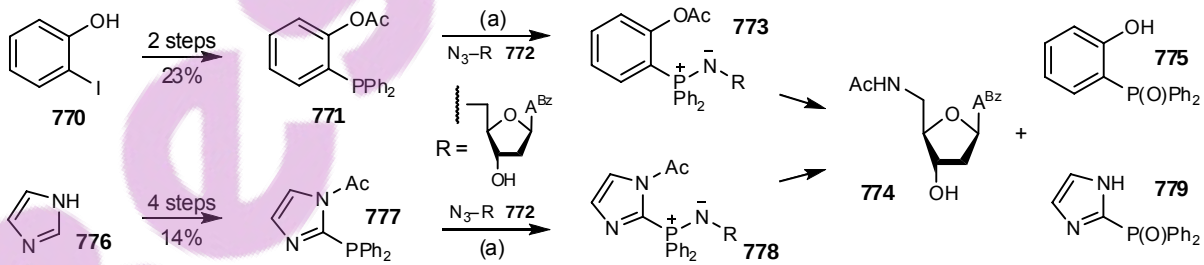

Reagents and conditions: (a) wet THF, rt, 3–4 d, 95%.

Scheme 3.24: Two-component ("traceless") Staudinger ligation by Bertozzi *et al*.[74]

Although natural *N*-glycopeptides are mostly β-linked, the unnatural and less stable α-linked *N*-glycopeptide are also studied for their synthesis and bioactivity.[75,76,78-81] Bianchi and Bernardi[80] applied this two-component Staudinger ligation to acylate α-azides of fructose, glucose and galactose derivatives **780**, **782** and **783**. α-Azides are prone to undergo anomerisation, but this mild acylation using functionalised phosphine **771** allowed the reaction to proceed without isomerisation and preserved their desired α-anomeric carbon (Scheme 3.25).

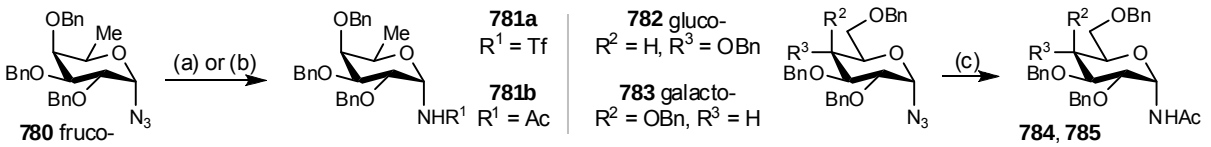

Reagents and conditions: (a) i. PMe_3, CH_2Cl_2, rt, 30 min; ii. Tf_2O, NEt_3, -78 °C, 3 h, **781a**: 76%; (b) **771**, CCl_4, 70 °C, 3 h, then 40 °C, 1 d, **771b**: 79%; (c) **771**, CCl_4, 70 °C, 1 d, 73–77%.

Scheme 3.25: Acetylation of α-glycosyl azides **781**, **784** and **785** by Bianchi and Bernardi.[80]

Bernardi *et al.*[81] then extended their investigations into the acylations using other alkyl functionalised phosphines **787** and those bearing an aspartic acid side chain such as **789** and **791**. Disappointingly, anomerisations occurred in all ligations conducted and the severity varied with the choice of solvents (16% in $CHCl_3$ and 5% in DMF) and complexity of the substrates. On the other hand, acylations using the stable β-glucosyl azides **793** and phosphines **771** or **789** were conducted without anomerisation albeit in moderate yield (Scheme 3.26).

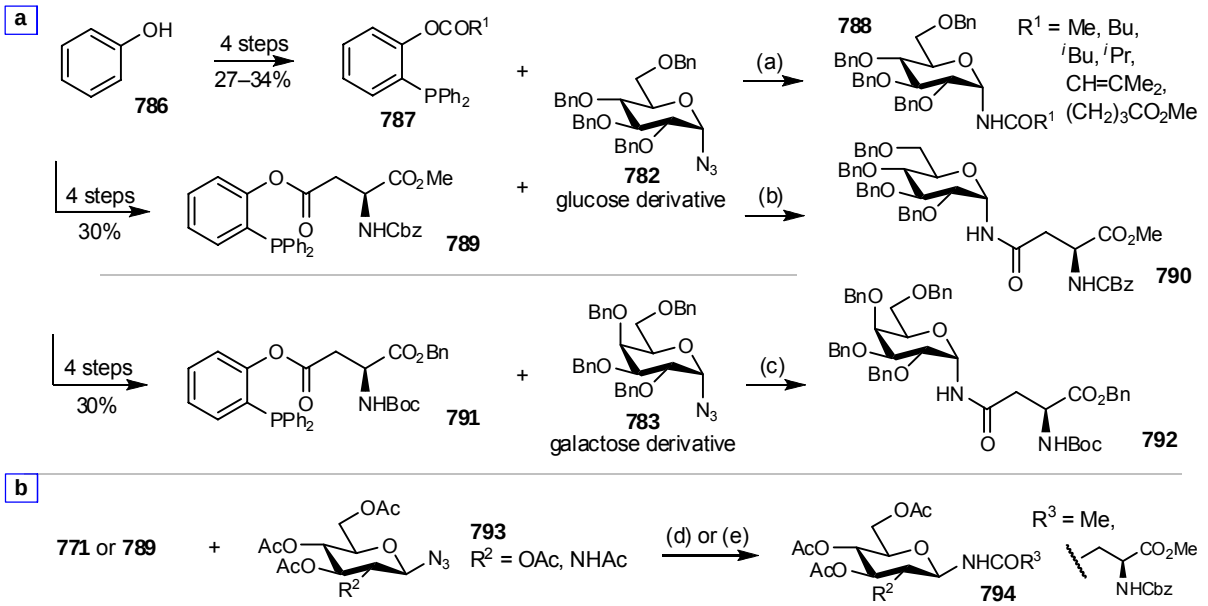

Reagents and conditions: (a) i. DMF, 70 °C, 20 h; ii. H_2O, 70 °C, 2 h, 54–81% (+ 2–6% β-anomer); (b) i. toluene, 70 °C, 18 h; ii. H_2O, 70 °C, 2 h, 65% (+ 10% β-anomer); (c) i. DMA–toluene, 70 °C, 4 h; ii. H_2O, 70 °C, 18 h, 48% (+ 23% β-anomer); (d) **771**, $CHCl_3$, 70 °C, 1 d, 81%; (e) i. **789**, DMA, 70 °C, 4 h; ii. H_2O, 70 °C, 18 h, 51–69%.

Scheme 3.26: Staudinger ligation between functionalised phosphines and various azides by Bernardi *et al.*[81] [a] α-glycosyl azides **782** and **783** were used. [b] β-glucosyl azide **793** was used.

Kiessling *et al.*[75] reported the synthesis of *β-N*-glycosyl amides *via* a two-component Staudinger ligation using peptide-derived C-terminal phosphinothioesters **796**, which were commonly used in peptide ligation to couple two peptide subunits together in a good yield.[84] Diphenyl and dialkyl phosphinothioesters **796** were synthesised by a general route *via* air stable phosphine-borane complexes. The resulting aspartic acid derived phosphinothioesters **796** then reacted with glycosyl azides **797** to give glycosyl amides **798** albeit in moderate yields (Scheme 3.27).[75]

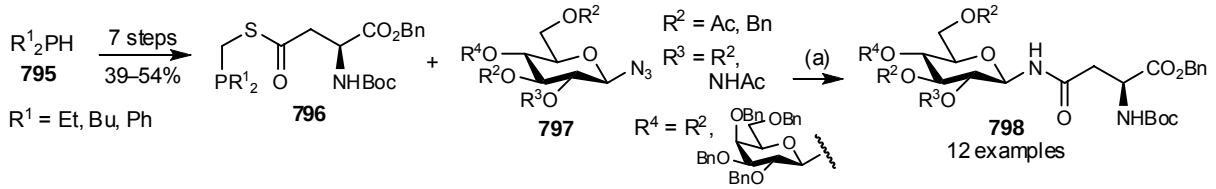

Reagents and conditions: (a) DMF or THF, rt, 12 h, 20–55%.

Scheme 3.27: Staudinger ligation between *β*-glycosyl azides **797** and phosphinothioesters **796** by Kiessling *et al.*[75]

Two-component Staudinger ligations often require a multi-step synthesis to generate the required functionalised phosphine and the coupling often affords moderate yields. As a result, Davis *et al.*[76] decided to concentrate and improve the existing three-component Staudinger ligation, which in theory, should have wider application and scope. In this synthesis, the carboxyl group in **799** was activated to enhance its electrophilicity, thus facilitating the trapping of the aza-ylide intermediate **757** which generated from PBu_3 and glycosyl azides **800**. This procedure was then successfully applied to the glycosylation of larger peptides such as **802** in a good yield (Scheme 3.28).

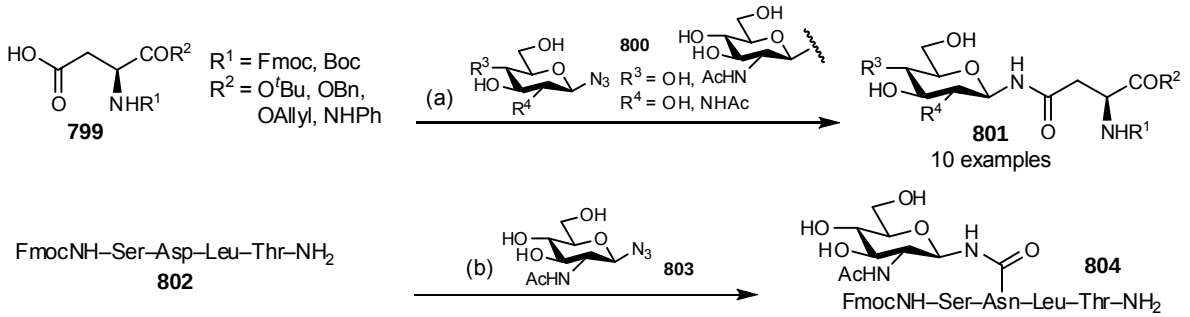

Reagents and conditions: (a) i. DCC, HOBt, MeCN, rt, 30 min; ii. **800**, PBu_3, rt, 16 h, 47–87%; (b) i. DCC, HOBt, DMF, rt, 30 min; ii. **803**, PBu_3, rt, 3 d, 77%.

Scheme 3.28: Synthesis of *N*-glycopeptides using *β*-glycosyl azides and activated carboxylic acids by Davis *et al.*[76]

3.6 Research Opportunities Based on Spiroacetal-Triazoles and Amino Acid Analogues

This chapter has provided an overview regarding the biology and chemistry of triazole and amino acid analogues supported with selected examples. As previously mentioned, we were interested in the chemical attachment between biologically useful subunits. With the structural features offered by 6,6-spiroacetals and the benefit of triazole and amino acid moieties, the hybrid of these motifs might lead to potentially interesting bioactivity. Both moieties can be, in theory, synthesised from a common azide intermediate and this represents a good opportunity for the diversity oriented synthesis.

The following chapters will discuss, in detail, the synthesis of these spiroacetal-triazoles and amino acids as well as spiroacetal-nucleobases. The aim of the current research will be first examined, followed by the model studies embarked for feasibility purpose, and finally the target hybrids that we were interested in.

3.7 References

1. N. A. Campbell and J. B. Reece, *Biology*, 7th edn., Benjamin Cummings, San Francisco, 2005.
2. J. E. McMurry, *Organic Chemistry*, 6th edn., Brooks/Cole, Pacific Grove, 2003.
3. H. C. Kolb and K. B. Sharpless, *Drug Discov. Today*, 2003, **8**, 1128-1137.
4. Maybridge, *Bioisosteres in Medicinal Chemistry*, Thermo Fisher Scientific, Cornwall.
5. V. D. Bock, H. Hiemstra and J. H. van Maarseveen, *Eur. J. Org. Chem.*, 2006, 51-68.
6. W. S. Horne, M. K. Yadav, C. D. Stout and M. R. Ghadiri, *J. Am. Chem. Soc.*, 2004, **126**, 15366-15367.
7. P. Wu and V. V. Fokin, *Aldrichimica Acta*, 2007, **40**, 7-17.
8. M. V. Gil, M. J. Arévalo and Ó. López, *Synthesis*, 2007, 1589-1620.
9. S. Dedola, S. A. Nepogodiev and R. A. Field, *Org. Biomol. Chem.*, 2007, **5**, 1006-1017; L. Yet, in *Progress in Heterocyclic Chemistry*, eds. G. W. Gribble and J. A. Joule, Elsevier, Oxford, 2007, vol. 18; L. Yet, in *Progress in Heterocyclic Chemistry*, eds. G. W. Gribble and J. A. Joule, Elsevier, Oxford, 2008, vol. 19.
10. R. G. Micetich, S. N. Maiti, P. Spevak, T. W. Hall, S. Yamabe, N. Ishida, M. Tanaka, T. Yamazaki, A. Nakai and K. Ogawa, *J. Med. Chem.*, 1987, **30**, 1469-1474; C. M. Perry and A. Markham, *Drugs*, 1999, **57**, 805-843.
11. L. V. Lee, M. L. Mitchell, S.-J. Huang, K. B. Sharpless, C.-H. Wong and V. V. Fokin, *J. Am. Chem. Soc.*, 2003, **125**, 9588-9589.
12. A. C. Cunha, J. M. Figueiredo, J. L. M. Tributino, A. L. P. Miranda, H. C. Castro, R. B. Zingali, C. A. M. Fraga, M. C. B. V. de Souza, V. F. Ferreira and E. J. Barreiro, *Bioorg. Med. Chem.*, 2003, **11**, 2051-2059.
13. A. Brik, J. Muldoon, Y.-C. Lin, J. H. Elder, D. S. Goodsell, A. J. Olson, V. V. Fokin, K. B. Sharpless and C.-H. Wong, *ChemBioChem*, 2003, **4**, 1246-1248; A. Brik, J. Alexandratos, Y.-C. Lin, J. H. Elder, A. J. Olson, A. Wlodawer, D. S. Goodsell and C.-H. Wong, *ChemBioChem*, 2005, **6**, 1167-1169.
14. V. D. Bock, R. Perciaccante, T. P. Jansen, H. Hiemstra and J. H. van Maarseveen, *Org. Lett.*, 2006, **8**, 919-922; V. D. Bock, D. Speijer, H. Hiemstra and J. H. van Maarseveen, *Org. Biomol. Chem.*, 2007, **5**, 971-975.

15. S. Groothuys, B. H. M. Kuijpers, P. J. L. M. Quaedflieg, H. C. P. F. Roelen, R. W. Wiertz, R. H. Blaauw, F. L. van Delft and F. P. J. T. Rutjes, *Synthesis*, 2006, 3146-3152.
16. S. A. Nepogodiev, S. Dedola, L. Marmuse, M. T. de Oliveira and R. A. Field, *Carbohydr. Res.*, 2007, **342**, 529-540.
17. A. Nuzzi, A. Massi and A. Dondoni, *QSAR Comb. Sci.*, 2007, **26**, 1191-1199.
18. C. Ornelas, J. R. Aranzaes, E. Cloutet, S. Alves and D. Astruc, *Angew. Chem. Int. Ed.*, 2007, **46**, 872-877.
19. H. C. Kolb, M. G. Finn and K. B. Sharpless, *Angew. Chem. Int. Ed.*, 2001, **40**, 2004-2021.
20. G. Patton, *Development and Applications of Click Chemistry*, Seminar report, University of Illinois, Urbana, 2004.
21. Q. Wang, S. Chittaboina and H. N. Barnhill, *Lett. Org. Chem.*, 2005, **2**, 293-301.
22. C. W. Tornøe, C. Christensen and M. Meldal, *J. Org. Chem.*, 2002, **67**, 3057-3064.
23. W. H. Binder and C. Kluger, *Curr. Org. Chem.*, 2006, **10**, 1791-1815.
24. V. V. Rostovtsev, L. G. Green, V. V. Fokin and K. B. Sharpless, *Angew. Chem. Int. Ed.*, 2002, **41**, 2596-2599.
25. F. Himo, T. Lovell, R. Hilgraf, V. V. Rostovtsev, L. Noodleman, K. B. Sharpless and V. V. Fokin, *J. Am. Chem. Soc.*, 2005, **127**, 210-216.
26. A. R. Katritzky, Y. Zhang and S. K. Singh, *Heterocycles*, 2003, **60**, 1225-1239.
27. D. Häbich, W. Barth and M. Rösner, *Heterocycles*, 1989, **29**, 2083-2088.
28. M. Yamashita, P. M. Reddy, Y. Kato, V. K. Reddy, K. Suzuki and T. Oshikawa, *Carbohydr. Res.*, 2001, **336**, 257-270.
29. A. R. Katritzky and S. K. Singh, *J. Org. Chem.*, 2002, **67**, 9077-9079.
30. A. Dondoni, P. P. Giovannini and A. Massi, *Org. Lett.*, 2004, **6**, 2929-2932.
31. P. Li and L. Wang, *Lett. Org. Chem.*, 2007, **4**, 23-26.
32. Y. L. Angell and K. Burgess, *Chem. Soc. Rev.*, 2007, **36**, 1474-1689.
33. S. Diéz-González, A. Correa, L. Cavallo and S. P. Nolan, *Chem. Eur. J*, 2006, **12**, 7558-7564.
34. B. H. Lipshutz and B. R. Taft, *Angew. Chem. Int. Ed.*, 2006, **45**, 8235-8238.
35. C. Girard, E. Önen, M. Aufort, S. Beauviére, E. Samson and J. Herscovici, *Org. Lett.*, 2006, **8**, 1689-1692.
36. K. R. Reddy, K. Rajgopal and M. L. Kantam, *Catal. Lett.*, 2007, **114**, 36-40.
37. F. Seela and V. R. Sirivolu, *Helv. Chim. Acta*, 2007, **90**, 535-552.
38. K. R. Reddy, K. Rajgopal and M. L. Kantam, *Synlett*, 2006, 957-959.
39. T. R. Chan, R. Hilgraf, K. B. Sharpless and V. V. Fokin, *Org. Lett.*, 2004, **6**, 2853-2855.
40. W. G. Lewis, F. G. Magallon, V. V. Fokin and M. G. Finn, *J. Am. Chem. Soc.*, 2004, **126**, 9152-9153.
41. K. Tanaka, C. Kageyama and K. Fukase, *Tetrahedron Lett.*, 2007, **48**, 6475-6479.
42. Y. Angell and K. Burgess, *Angew. Chem. Int. Ed.*, 2007, **46**, 3649-3651.
43. I. Bae, H. Han and S. Chang, *J. Am. Chem. Soc.*, 2005, **127**, 2038-2039.
44. M. P. Cassidy, J. Raushel and V. V. Fokin, *Angew. Chem. Int. Ed.*, 2006, **45**, 3154-3157; S. H. Cho, E. J. Yoo, I. Bae and S. Chang, *J. Am. Chem. Soc.*, 2005, **127**, 16046-16047.
45. E. J. Yoo, M. Ahlquist, S. H. Kim, I. Bae, V. V. Fokin, K. B. Sharpless and S. Chang, *Angew. Chem. Int. Ed.*, 2007, **46**, 1730-1733.
46. V. O. Rodionov, V. V. Fokin and M. G. Finn, *Angew. Chem. Int. Ed.*, 2005, **44**, 2210-2215; M. Ahlquist and V. V. Fokin, *Organometallics*, 2007, **26**, 4389-4391.
47. J. M. Casas-Solvas, A. Vargas-Berenguel, L. F. Capitan-Vallvey and F. Santoyo-Gonzalez, *Org. Lett.*, 2004, **6**, 3687-3690.
48. M. IJsselstijn and J.-C. Cintrat, *Tetrahedron*, 2006, **62**, 3837-3842.
49. A. K. Feldman, B. Colasson and V. V. Fokin, *Org. Lett.*, 2004, **6**, 3897-3899.
50. X. Zhang, R. P. Hsung and L. You, *Org. Biomol. Chem.*, 2006, **4**, 2679-2682.
51. P. Appukkuttan, W. Dehaen, V. V. Fokin and E. Van der Eycken, *Org. Lett.*, 2004, **6**, 4223-4225.
52. S. Chittaboina, F. Xie and Q. Wang, *Tetrahedron Lett.*, 2005, **46**, 2331-2336.
53. J. Andersen, S. Bolvig and X. Liang, *Synlett*, 2005, 2941-2947.
54. B. Sreedhar and P. S. Reddy, *Synth. Commun.*, 2007, **37**, 805-812.
55. Y.-B. Zhao, Z.-Y. Yan and Y.-M. Liang, *Tetrahedron Lett.*, 2006, **47**, 1545-1549.
56. K. Kacprzak, *Synlett*, 2005, 943-946.
57. H. S. G. Beckmann and V. Wittmann, *Org. Lett.*, 2007, **9**, 1-4.
58. K. Barral, A. D. Moorhouse and J. E. Moses, *Org. Lett.*, 2007, **9**, 1809-1811.

59. J. Waser, H. Nambu and E. M. Carreira, *J. Am. Chem. Soc.*, 2005, **127**, 8294-8295.
60. S. Chandrasekhar, D. Basu and C. Rambabu, *Tetrahedron Lett.*, 2006, **47**, 3059-3063.
61. B. Sreedhar, P. S. Reddy and N. S. Kumar, *Tetrahedron Lett.*, 2006, **47**, 3055-3058.
62. V. Aucagne and D. A. Leigh, *Org. Lett.*, 2006, **8**, 4505-4507.
63. B. H. M. Kuijpers, G. C. T. Dijkmans, S. Groothuys, P. J. L. M. Quaedflieg, R. H. Blaauw, F. L. van Delft and F. P. J. T. Rutjes, *Synlett*, 2005, 3059-3062.
64. J. K. Pokorski, L. M. M. Jenkins, H. Feng, S. R. Durell, Y. Bai and D. H. Appella, *Org. Lett.*, 2007, **9**, 2381-2383.
65. B. Alberts, A. Johnson, J. Lewis, M. Raff, K. Roberts and P. Walter, *Molecular Biology of the Cell*, 4th edn., Garland Science, New York, 2002; B. Alberts, D. Bray, J. Lewis, M. Raff, K. Roberts and J. D. Watson, *Molecular Biology of the Cell*, 3rd edn., Garland, New York, 1994.
66. S. Hotha, R. I. Anegundi and A. A. Natu, *Tetrahedron Lett.*, 2005, **46**, 4585-4588; R. I. Anegundi, V. G. Puranik and S. Hotha, *Org. Biomol. Chem.*, 2008, **6**, 779-786.
67. A. Krasiński, V. V. Fokin and K. B. Sharpless, *Org. Lett.*, 2004, **6**, 1237-1240.
68. S. J. Coats, J. S. Link, D. Gauthier and D. J. Hlasta, *Org. Lett.*, 2005, **7**, 1469-1472.
69. L. Zhang, X. Chen, P. Xue, H. H. Y. Sun, I. D. Williams, K. B. Sharpless, V. V. Fokin and G. Jia, *J. Am. Chem. Soc.*, 2005, **127**, 15998-15999.
70. M. M. Majireck and S. M. Weinreb, *J. Org. Chem.*, 2006, **71**, 8680-8683; A. H. Yap and S. M. Weinreb, *Tetrahedron Lett.*, 2006, **47**, 3035-3038.
71. Y.-M. Wu, J. Deng, Y. Li and Q.-Y. Chen, *Synthesis*, 2005, 1314-1318.
72. B. Gerard, J. Ryan, A. B. Beeler and J. A. Porco, Jr., *Tetrahedron*, 2006, **62**, 6405-6411.
73. L. Kürti and B. Czakó, *Strategic Applications of Named Reactions in Organic Synthesis*, 1st edn., Elsevier Academic Press, San Diego, 2005 and references cited therein.
74. E. Saxon, J. I. Armstrong and C. R. Bertozzi, *Org. Lett.*, 2000, **2**, 2141-2143.
75. Y. He, R. J. Hinklin, J. Chang and L. L. Kiessling, *Org. Lett.*, 2004, **6**, 4479-4482.
76. K. J. Doores, Y. Mimura, R. A. Dwek, P. M. Rudd, T. Elliott and B. G. Davis, *Chem. Comm.*, 2006, 1401-1403.
77. M. Mogemark and J. Kihlberg, in *The Organic Chemistry of Sugars*, eds. D. E. Levy and P. Fügedi, CRC Press, Boca Raton, 2006, pp. 755-803.
78. T. Inazu and K. Kobayashi, *Synlett*, 1993, 869-870.
79. M. Mizuno, I. Muramoto, K. Kobayashi, H. Yaginuma and T. Inazu, *Synthesis*, 1999, 162-165.
80. A. Bianchi and A. Bernardi, *Tetrahedron Lett.*, 2004, **45**, 2231-2234.
81. A. Bianchi, A. Russo and A. Bernardi, *Tetrahedron: Asymmetry*, 2005, **16**, 381-386; A. Bianchi and A. Bernardi, *J. Org. Chem.*, 2006, **71**, 4565-4577, references cited therein.
82. F. Urpĭ and J. Vilarrasa, *Tetrahedron Lett.*, 1986, **27**, 4623-4624; J. Garcia, F. Urpĭ and J. Vilarrasa, *Tetrahedron Lett.*, 1984, **25**, 4841-4844.
83. V. Maunier, P. Boullanger and D. Lafont, *J. Carbohydr. Chem.*, 1997, **16**, 231-235; P. Boullanger, V. Maunier and D. Lafont, *Carbohydr. Res.*, 2000, **324**, 97-106.
84. M. B. Soellner, B. L. Nilsson and R. T. Raines, *J. Org. Chem.*, 2002, **67**, 4993-4996; M. B. Soellner, B. L. Nilsson and R. T. Raines, *J. Am. Chem. Soc.*, 2006, **128**, 8820-8828 and references cited therein.

Chapter Four:

Aim of Present Research

The structural uniqueness and significant bioactivity of the 6,6-spiroacetals, together with our long standing interest in their synthesis, had prompted our research group to conduct a diversity oriented synthesis (DOS) towards their elaboration. Nucleobases, triazoles and amino acids were chemically attached to the spiroacetal scaffold. This elaboration generated a collection of small hybrid molecules that could be used as biological probes for broad phenotypic assays to screen for any potential functionality.

The aim of the research reported in this thesis was to develop a viable synthetic route to the novel nucleoside analogues **808** based on a 6,6-spiroacetal (1,7-dioxaspiro[5.5]undecane) ring system, which served as a surrogate for the sugar moiety in natural nucleosides (Figure 4.1). The 6,6-spiroacetal ring system was, in theory, conformationally locked in a *trans*-diaxial orientation by both ring oxygen atoms due to anomeric stabilisation. In this conformation, the ring system holds the hydroxymethyl substituent and the base in a particular spatial orientation ready to be processed by kinases and/or polymerases.

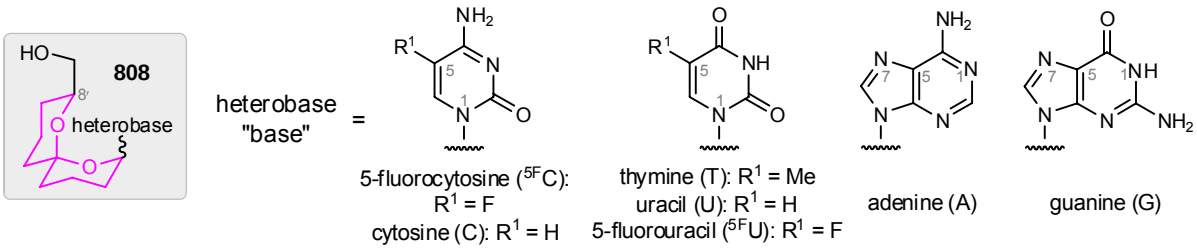

Figure 4.1: Target structures of spiroacetal-nucleosides **808**: 5-fluorocytidine, cytidine, thymidine, uridine, 5-fluorouridine, adenosine and guanosine.

Subsequently, we anticipated that the knowledge acquired during the synthesis of spiroacetal-nucleosides **808** would extend to the synthesis of spiroacetal-triazoles **809** and spiroacetal-amino acids **810**, thereby collectively constituting a small library of spiroacetal hybrids (Figure 4.2).

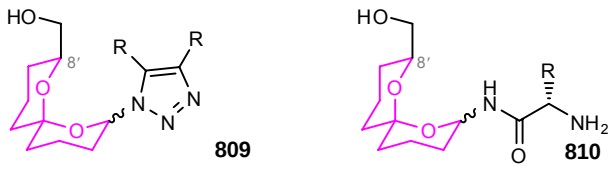

Figure 4.2: Target structures of spiroacetal-triazoles **809** and spiroacetal-amino acids **810**.

In order to expedite the synthesis of the novel spiroacetal targets **808**–**810**, the initial study was directed towards the synthesis of spiroacetal models **811** and **812**, all of which lack the C8′-hydroxymethyl group (Figure 4.3). The coupling between the spiroacetal ring and the heterocyclic moiety was investigated in order to generate a viable and efficient methodology. Once the prototype of the synthetic route to prepare simpler spiroacetal models **811** and **812** was established, the C8′-hydroxymethyl substituent was then introduced onto the spiroacetal ring system. The tactics developed using the model system was re-examined and adjusted accordingly in order to synthesise the desired spiroacetal targets **808**–**810**.

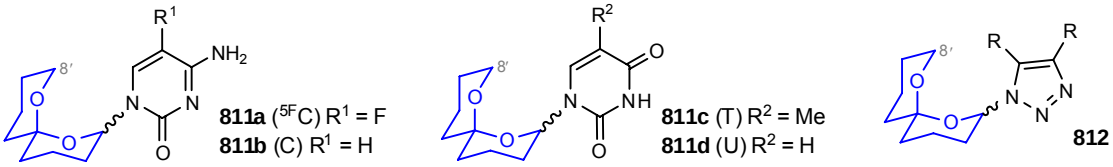

Figure 4.3: Model structures of spiroacetal-nucleosides **811** and spiroacetal-triazoles **812**.

Chapter Five:

Discussion: Synthesis of the Model Spiroacetals

5.1 Retrosynthetic Analysis of Spiroacetal Heterocycle Models 811 and 812

5.1.1 Retrosynthesis

As depicted in Figure 5.1, spiroacetals **813** were the targets of our intended study. In order to establish a viable route to these targets, initial synthesis was focused model spiroacetals **811** and **812** that lacked the C8′-hydroxymethyl group.

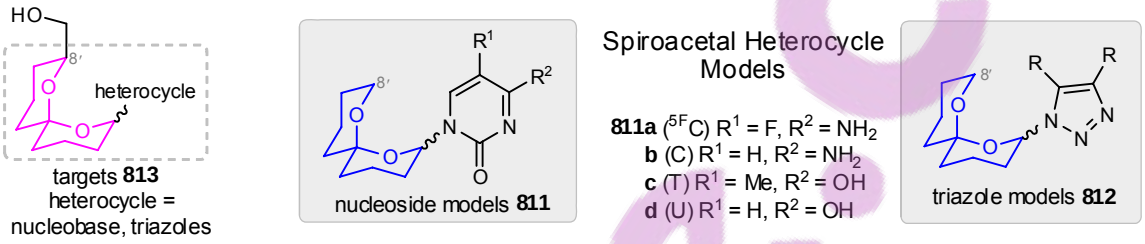

Figure 5.1: Spiroacetal heterocycle analogues: targets **813** (left) and models **811** and **812** (middle and right) which lack the C8′ hydroxymethyl group.

The overall aim of the present work is to elaborate the 6,6-spiroacetal framework by the incorporation of a range of bioactive motifs in order to achieve a diversity oriented synthesis (DOS). It is important that a flexible and convergent strategy is adopted in order to facilitate this diversity oriented synthetic approach. Towards this goal, derivatisation of a common intermediate would lead to the synthesis of spiroacetals bearing other motifs.

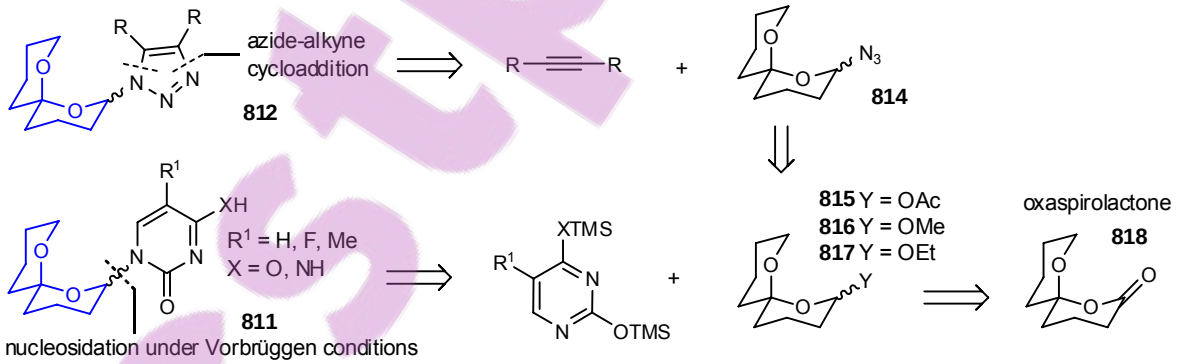

Scheme 5.1: Proposed retrosynthesis of spiroacetal-nucleoside models **811** and triazole models **812**.

The proposed retrosynthesis of spiroacetal models **811** and **812** hinges on the disconnection of the anomeric C–N bond that links the spiroacetal with the heterocycle. For nucleoside analogues, this connection is generated by the nucleosidation under Vorbrüggen conditions. In the presence of a Lewis acid, spiroacetals **815–817** bearing a leaving group at the anomeric position generate an oxonium ion which can be trapped by a persilylated heterobase. For triazole analogues, the

connection is generated by azide substitution of the leaving group present in spiroacetals **815–817**. Spiroacetals **815–817**, in turn, are prepared *via* reduction and protection of oxaspirolactone **818** (Scheme 5.1).

Oxaspirolactone **818** is generated from keto-acid **819**. Further disconnection of keto-acid **819** leads to commercially available δ-valerolactone **(820)** and protected butynol **821** (Scheme 5.2). This disconnection of oxaspirolactone **818** is based on personal communications from Kitching *et al.*[1] and a preliminary study conducted by Brimble *et al.*[2]

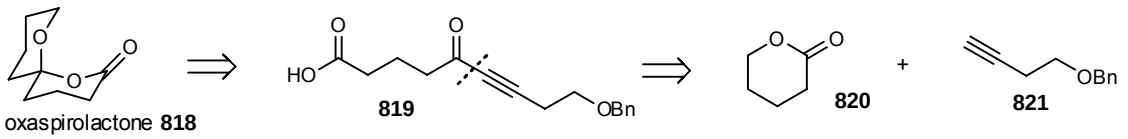

Scheme 5.2: Proposed retrosynthesis of oxaspirolactone **818**.[1,2]

5.1.2 Nucleophilic Addition to an Oxonium Ion Generated From an Activated Spiroacetal

To date, the synthesis of a 6,6-spiroacetal that bears a heterobase at the anomeric position, has not been reported. While the use of a glycosyl acetate as a precursor to an oxonium ion is well documented in nucleoside and carbohydrate chemistry, precedent for the successful generation of an oxonium ion from a spiroacetal bearing an anomeric leaving group, has only been reported for a few cases.[3-6]

Nevertheless, these literature examples have provided the rationale behind the major C-N bond disconnection and the adaptation of nucleosidation under Vorbrüggen conditions depicted in the above retrosynthesis. From these examples, studies conducted by Mead and Zemribo[4,6], Brimble *et al.*[5], Robertson and Dallimore[7], were particularly relevant to the present research.

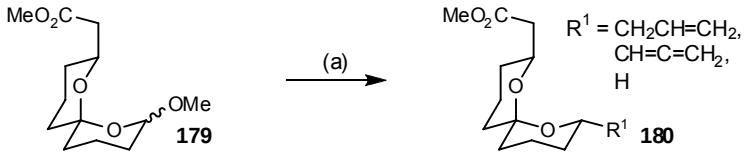

Reagents and Conditions: (a) allyltrimethylsilane or propargyltrimethylsilane or diphenylmethylsilane, TMSOTf, CH_2Cl_2, -50 °C, 1.0–1.5 h, 65–68%.

Scheme 5.3: Nucleophilic addition of a silane to an oxonium ion generated from methoxy-spiroacetal **179** by Mead and Zemribo.[4,6] More examples are depicted in Scheme 1.27 and 1.28.

Mead and Zemribo[4,6] conducted a series of studies on the nucleophilic addition of various silanes to an oxonium ion generated from spiroacetals bearing methoxy, hydroxyl and 4-nitrobenzoyl

groups at the anomeric position. These were the first systematic studies to demonstrate Lewis acid-catalysed substitution of the spiroacetals at the anomeric position that provided a direct route to useful derivatives (Scheme 5.3). The substitution reaction has previously been discussed in Chapter 1.5.1.

Brimble *et al.*[5] used acetate **822** in the presence of TMSOTf to generate an oxonium ion which was trapped by a range of allylstannanes **823**. Compared to Mead and Zemribo's studies,[4,6] only mild conditions were required for the generation of the oxonium ion due to stronger nucleophilicity of stannanes. The reaction proceeded *via* the axial addition of the stannane to the oxonium ion, followed by a ring flip of the substituted ring to relieve the unfavourable 1,3-diaxial interaction between the allyl group and C8 to give spiroacetals **825** (Scheme 5.4).

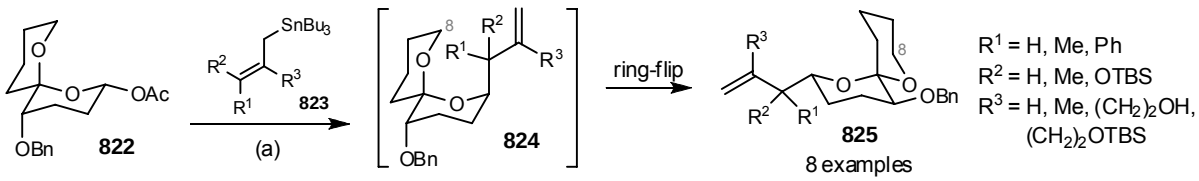

Reagents and Conditions: (a) **823**, TMSOTf, 4 Å MS, CH_2Cl_2, -78 °C→rt, 6–16 h, 28–72%.

Scheme 5.4: Nucleophilic addition of allylstannanes **823** to an oxonium ion generated from acetate **822** by Brimble *et al.*[5]

Encouraged by their earlier success, Robertson and Dallimore[7] used this oxonium trapping strategy for the attachment of an anomeric side-chain to the C7–C18 tricyclic spiroacetal core of the lituarines.[8] Both the model study using the simple 5,6-spiroacetal acetate **826** and enol ether **827** as well as the subsequent synthesis using tricyclic spiroacetal acetate **829** and the functionalised enol ether **830** successfully afforded the desired spiroacetals **828** and **831** in the presence of $SnBr_4$ (Scheme 5.5).

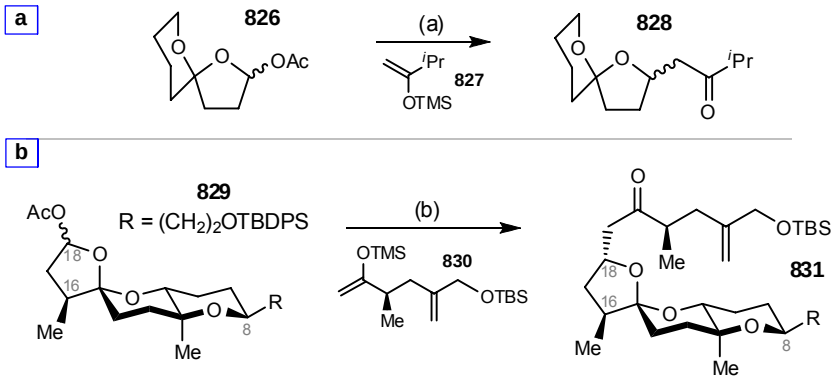

Reagents and Conditions: (a) **827**, $SnBr_4$, CH_2Cl_2, -78 °C, 5 min, 93% (1:1 *dr*); (b) **830**, $SnBr_4$, CH_2Cl_2, -78 °C, 20 min, 68%.

Scheme 5.5: [a] Model study using simple acetate **826**. [b] Synthesis of the C7–C18 tricyclic spiroacetal core **831** present in the lituarines by Robertson and Dallimore.[7]

5.2 Synthesis of Oxaspirolactone 818

5.2.1 Previous Synthesis of Oxaspirolactone 818

The first synthesis of the key intermediate oxaspirolactone **818** was carried out by Mioskowski *et al.*[9,10] using a Wittig coupling. Phosphonium salt **833** reacted with aldehyde **834** to generate enol ether **835** which was subsequently cyclised under acidic conditions to yield oxaspirolactone **818** (Scheme 5.6).

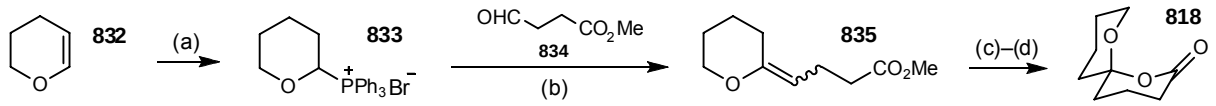

Reagents and conditions: (a) PPh_3, HBr, CH_2Cl_2, 0 °C, 85%; (b) i. BuLi, HMPA, THF, -78°C; ii. **834**, 70%; (c) LiOH, DME–H_2O; (d) pH 5, HCl, Et_2O, 75% over 2 steps.

Scheme 5.6: The first synthesis of oxaspirolactone **818** by Mioskowski *et al.*[9,10]

Kitching *et al.*[1] and Brimble *et al.*[2] adopted a similar approach towards the synthesis of oxaspirolactone **818** starting from 3-butyn-1-ol **(836)**. Acetylide, generated from benzylated butynol **821**, was added to valerolactone **820** and the resulting adduct was oxidised to give keto-acid **819**. Subsequent hydrogenation and cyclisation of **819** under acidic conditions yielded oxaspirolactone **818** (Scheme 5.7).

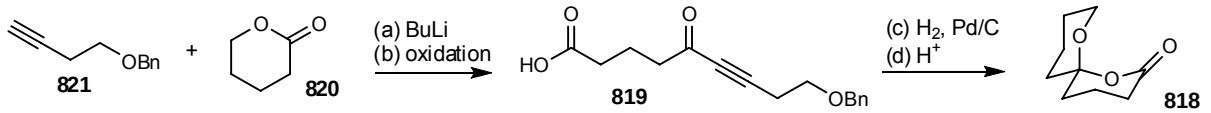

Reagents and conditions by Kitching et al.[1]*:* (a) i. BuLi, THF, -78→-50 °C, 20 min; ii. **820**, THF, -78→-65 °C, 2 h, 99%; (b) PDC, DMF, rt, 16 h, 61% or Jones' reagent, acetone, rt, 20 min, 82%; (c) i. H_2 (35 psi), cat. Pd/C, EtOAc, rt, 16 h; (d) SiO_2, Et_2O, rt, trace of **818** was obtained.

Reagents and conditions by Brimble et al.[2]*:* (a) i. BuLi, THF, -78→-50 °C, 30 min; ii. **820**, THF, -78 °C, 2 h, 53%; (b) Jones' reagent, acetone, rt, 74%; (c) i. H_2 (45 psi), cat. Pd/C, cat. AcOH, THF, rt, 1 d, 92%; (d) $MgSO_4$, CH_2Cl_2, rt, 17%.

Scheme 5.7: Synthesis of oxaspirolactone **818** by Kitching *et al.*[1] and Brimble *et al.*[2] Procedures by Kitching *et al.*[1] produced trace amount of **818** after five steps starting from butynol **836** whereas procedures by Brimble *et al.*[2] yielded 6% of **818**.

Due to the undesirable but necessary use of carcinogenic HMPA during Mioskowski's synthesis[9,10], the acetylide addition[1,2] was adopted for the preparation of oxaspirolactone **818**. This decision was based on several literature reports and past experience for the synthesis of structurally similar spiroacetals, particularly preliminary studies on oxaspirolacetone **818** carried our in this group.[2,11-14] However, both the studies by Kitching *et al.*[1] and Brimble *et al.*[2] produced oxaspirolactone **818** in a low yield (< 6% after five steps from butynol **836**), thus providing plenty of scope for improvement (Scheme 5.7).

Syntheses of oxaspirolactones of other ring sizes, such as 1,6-dioxaspiro[4.5]decan-2-one[7,15] and 1,6-dioxaspiro[4.4]decan-2-one[13,16,17], have also been extensively reported in the literature.

5.2.2 Synthesis of Keto-Acid 819

(a) Synthesis of Keto-Alcohol 837

The synthesis of keto-acid **819** started with the protection of 3-butyn-1-ol **(836)** as a benzyl ether following a procedure adapted from Burns *et al.*[18] Instead of using a distillation for purification employed by Burns *et al.*,[18] benzyl ether **821** was purified by chromatography to remove the impurities such as benzyl bromide and benzyl alcohol. The reaction proceeded smoothly using NaH in THF at 0 °C with an optimum yield of 99% (Scheme 5.8).

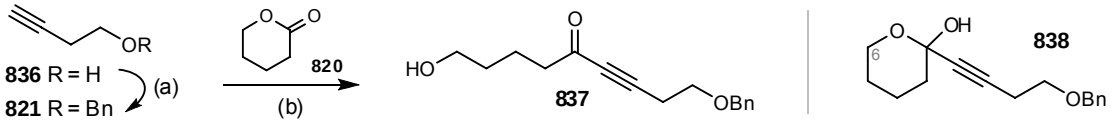

Reagents and conditions: (a) i. NaH, THF, 0 °C, 30 min; ii. BnBr, THF, 0 °C→rt, 18 h, 99%; (b) i. BuLi, THF, -78 °C, 30 min; ii. **820**, THF, -78 °C, 2 h, 87%.

Scheme 5.8: Synthesis of keto-alcohol **837**.

With benzyl ether **821** in hand, the subsequent coupling step was carried out. Lithium acetylide, generated *in situ* from alkyne **821**, was added to δ-valerolactone **(820)** in THF to give keto-alcohol **837** in 87% yield (Scheme 5.8). HMPA was not required as a co-solvent. The previously reported hemiacetal **838** was not detected as noted by the absence of the characteristic chemical shift of the hemiacetal carbon (*ca.* δ_C 90-100 ppm) and H6 resonance (*ca.* δ_H 3.6 ppm) in the ^{1}H and ^{13}C NMR spectra.[1,2]

(b) Oxidation of Keto-Alcohol 837

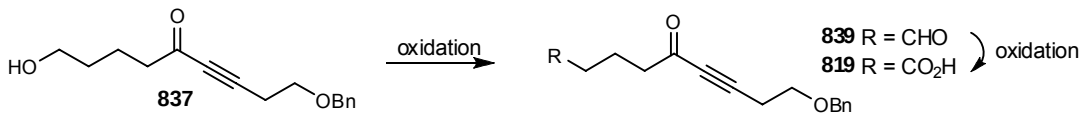

Scheme 5.9: Oxidation of keto-alcohol **837** to either aldehyde **839** or keto-acid **819**. See Table 5.1 for the reaction conditions.

The oxidation of keto-alcohol **837** was attempted using a variety of reagents and conditions (Scheme 5.9). Initially, the one step oxidation to keto-acid **819** using Jones' reagent[19] was investigated but only a moderate yield of 55% was obtained. Alternatively, the use of TEMPO/NaOCl in the presence of a phase-transfer quaternary ammonium salt[20] gave a variable mixture of aldehyde **839** and acid **819** which indicated an incomplete oxidation (Table 5.1).

Due to the above disappointing results, two-step oxidations *via* aldehyde **839** were subsequently investigated. Initial use of Swern[21] and TPAP[22] oxidation both produced a complex mixture due to the intolerance of the reactive ynone towards these oxidants. Use of mild oxidants such as modified PCC oxidation[23], Dess-Martin periodinane[24] and TEMPO/PhI(OAc)$_2$[25] successfully produced aldehyde **839** in various yields. After much experimentation, the best result was achieved *via* a two-step oxidation using TEMPO/PhI(OAc)$_2$ buffered in aqueous KH_2PO_4 followed by $NaClO_2$[26] to give the desired acid **819** in 92% yield (Table 5.1).

It was noticed that the use of TEMPO and $NaClO_2$ gave the best yield when aqueous buffer was used. This suggested the pH sensitivity of keto-alcohol **837** and aldehyde **839** that might account for the low yield observed in the Jones' oxidation as well as in the unbuffered TEMPO and PCC oxidation (Table 5.1).

Entry	*Reagents*		*Solvents*	*Conditions*	*% of Aldehyde 839*	*% of Acid 819*
1[19]	Jones' reagent		acetone	rt, 2 h	----	55%
2[20]	cat. TEMPO, aq. NaOCl, NaBr, $NaHCO_3$	cat. $BnEt_3N^+Cl$	CH_2Cl_2–H_2O	0 °C, 1–2 h	21–36%	47–56%
3		cat. $BnEt_3N^+Cl$ and Bu_4NCl^-	CH_2Cl_2–H_2O	0 °C, 5 d	61%	31%
4[21]	$(COCl)_2$, DMSO, NEt_3		CH_2Cl_2	-78 °C, 4 h	complex mixture	
5[22]	TPAP, NMO, 4 Å MS		CH_2Cl_2	rt. 20 h	complex mixture	
6	TPAP, NMO, 4 Å MS		MeCN	rt. 30 min–20 h	complex mixture	
7[23]	PCC, K_2CO_3		CH_2Cl_2	rt, 20 h	24%	----
8	PCC, NaOAc, silica		CH_2Cl_2	rt, 20 h	17%	----
9	PCC, alumina		CH_2Cl_2	rt, 2 h	58%	----
10	PCC, alumina		toluene	rt, 18 h	24%	----
11	PCC, NEt_3, alumina		toluene	ultrasound, rt, 6 h	28%	----
12	PCC, 2,6-lutidine, alumina		CH_2Cl_2	rt, 4 h	20%	----
13	PCC, NaOAc, NEt_3, Celite®		CH_2Cl_2	rt, 20 h	10%	----
14[24,26]	(a) Dess-Martin periodinane (b) $NaClO_2$, KH_2PO_4, cyclohexene		CH_2Cl_2 ^{t}BuOH–H_2O	rt, 21 h rt, 1 h	----	91% over 2 steps
15[25]	cat. TEMPO, PhI(OAc)$_2$		CH_2Cl_2	rt, 4 h	69%	----
16	cat. TEMPO, PhI(OAc)$_2$		MeCN	rt, 20 h	47%	----
17[25,26]	(a) cat. TEMPO, PhI(OAc)$_2$, KH_2PO_4 (b) $NaClO_2$, cyclohexene, KH_2PO_4		MeCN–H_2O ^{t}BuOH–H_2O	rt, 6 h rt, 2 h	----	92% over 2 steps

Table 5.1: Summary of reagents and conditions used for the oxidation of keto-alcohol **837**.

5.2.3 Synthesis of Oxaspirolactone 818

(a) Two-step Synthesis *via* Hydroxy-Acid 840

With the required keto-acid **819** in hand, the key transformation of **819** to oxaspirolactone **818** was then investigated. According to the studies by Kitching *et al.*[1] and Brimble *et al.*[2],

oxaspirolactone **818** was obtained *via* palladium-catalysed hydrogenation of keto-acid **819** followed by dehydrative cyclisation (Scheme 5.10). This cyclisation is postulated to be facilitated by acid as well as by the removal of water generated during the reaction.

Using the procedure developed by Brimble *et al.*,[2] debenzylation and hydrogenation of keto-acid **819** proceeded smoothly in the presence of catalytic acetic acid and palladium on carbon under an atmosphere of hydrogen to give crude intermediate hydroxy-acid **840**, required for the subsequent dehydrative cyclisation (Scheme 5.10).

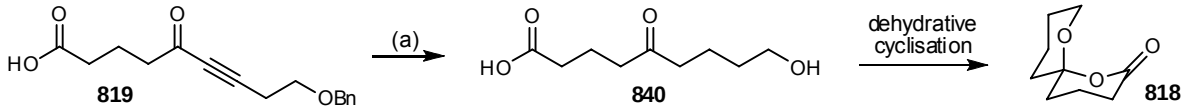

Reagents and conditions: (a) H_2, cat. Pd/C, cat. AcOH, THF, rt, 18 h, 94%.

Scheme 5.10: Hydrogenation of keto-acid **819** and subsequent cyclisation to oxaspirolactone **818**. See Table 5.3 for the cyclisation conditions.

Entry	*Reagents used by Kitching*[1]	*Results*	*Reagents used by Brimble*[2]	*Results*
1	Amberlyst-15, MeCN, rt	no reaction (TLC)	CSA, CH_2Cl_2, rt	complex mixture
2	Amberlyst-15, 3 Å MS, MeCN, rt	complex mixture	PPTS, CH_2Cl_2, rt	complex mixture
3	filtered through silica, Et_2O, rt	trace	BF_3•OEt_2, CH_2Cl_2, rt	complex mixture
4	PPTS, Dean-Stark trap, benzene, reflux	trace	*p*-TsOH, CH_2Cl_2, rt	complex mixture
5			*p*-TsOH, CH_2Cl_2, 4 Å MS, rt	complex mixture
6			*p*-TsOH, CH_2Cl_2, 4 Å MS, reflux	complex mixture
7			*p*-TsOH, pentane, 4 Å MS, reflux	complex mixture
8			*p*-TsOH, Dean-Stark trap, benzene, reflux	no reaction
9			*p*-TsOH, Et_2O, $MgSO_4$, rt	complex mixture
10			HCl, THF, rt	no reaction
11			HCl, Et_2O, rt	no reaction
12			filtered through $MgSO_4$, CH_2Cl_2, rt	17%

Table 5.2: Summary of the reagents and conditions previously used for the dehydrative cyclisation of oxaspirolactone **818** by Kitching *et al.*[1] and Brimble *et al.*[2]

Disappointingly, both communications reported major difficulties in the subsequent dehydrative cyclisation. The list of attempted cyclisation conditions used by Kitching *et al.*[1] and Brimble *et al.*[2] are summarised in Table 5.2 and these cyclisation often produced a complex mixture. Even if oxaspirolactone **818** were successfully produced by the reaction conditions, the yield observed was low and not reproducible. Hence, a reliable and efficient synthesis of oxaspirolactone **818** must be developed before the synthesis of nucleoside and triazole analogues can be developed.

Inspired by the preliminary study conducted by Brimble *et al.*[2], cyclisation using $MgSO_4$ as both a drying agent and a mild Lewis acid was initially attempted. However, these conditions failed to produce oxaspirolactone **818**. The addition of either the weak acid, PPTS or filtration through a pad of

$MgSO_4$ and silica in an attempt to facilitate the loss of water was also ineffective. Both filtration through a silica pad and flash chromatography using silica gel led to a mixture of unidentified compounds, possibly formed by degradation of the newly formed oxaspirolactone **818**, as suggested by Brimble *et al*.[2] An alternative method of cyclisation was therefore sought (Table 5.3).

Activation of acid **840** by DCC in the presence of catalytic DMAP produced a crude mixture of hydroxy-acid **840** and oxaspirolactone **818** as evidenced by NMR. Prolonged reaction times (up to five days) did not improve the yield. Moreover, attempted isolation of oxaspirolactone **818** from the mixture by flash chromatography on silica gel led to degradation, and only 3% of the desired product **818** was recovered. Decreasing the reaction time from five days to two days did not improve the results. Furthermore, the purification of the crude mixture contaminated with DCU was problematic (Table 5.3).

Entry	*Reagents*	*Solvents*	*Conditions*	*Results*	*Comments*
1	$MgSO_4$	CH_2Cl_2	rt, 1 d	no reaction	
2	i. $MgSO_4$ i. cat. PPTS, $MgSO_4$	CH_2Cl_2	rt, 1 d	complex mixture	
3	cat. PPTS, then filtered through a pad of $MgSO_4$ and silica	CH_2Cl_2	rt, 15 min	complex mixture	degradation on silica
4	i. $MgSO_4$; ii. cat. PPTS, $MgSO_4$ iii DCC, cat. DMAP	CH_2Cl_2	rt, 7 d	evidence in crude (NMR) 3% after column	degradation on silica
5	DCC, cat. DMAP, $MgSO_4$	CH_2Cl_2	rt, 2–5 d	evidence in crude (NMR)	degradation on silica
6	cat. HCl in dioxane	CH_2Cl_2	rt, 1–2 d	evidence in crude (NMR) 8% after column	degradation on alumina

Table 5.3: Summary of the reagents and conditions used for the attempted cyclisation of oxaspirolactone **818**.

Following the synthesis reported by Mioshowshi *et al.*[9], reactions using HCl in dioxane to effect cyclisation were next attempted. Despite the evidence of oxapirolactone **818** in the NMR of the crude reaction mixture, attempted purification by chromatography on alumina resulted in degradation, and only 8% of oxaspirolactone **818** was isolated (Table 5.3).

Several literature reports[7,13,17] have stated that the formation of simple oxaspirolactones from the corresponding lactol-ester or lactol-carboxylic acid can be problematic. The relatively low yields may be attributed to the volatility and instability of the oxaspirolactones.[13] Difficulties encountered for the simple lactonisation of other hydroxy-esters have also been reported.[27,28] The present findings appear to be consistent with these literature reports.

(b) One-Pot Synthesis

Serendipitously, a large scale (*ca.* 1 g) hydrogenation of keto-acid **819** followed by slow removal of acetic acid using a rotary evaporator (reduced pressure *ca*. 30 mmHg at 30 °C) produced a crude mixture of hydroxy-acid **840** and oxaspirolactone **818** in a ratio of 1:9. It was proposed that after

the removal of volatiles such as THF and CH_2Cl_2, the residual acetic acid from the hydrogenation reaction catalysed the cyclisation of hydroxy-acid **840**. The low pressure conditions and mild heating also helped to remove any water that was generated in the cyclisation step, thereby aiding the formation of oxaspirolactone **818**. Disappointingly, an attempt to purify oxaspirolactone **818** by chromatography on alumina led to degradation of the product.

Following on from the above encouraging observation, another large-scale hydrogenation reaction was carried out. While concentrating the reaction mixture using a rotary evaporator, acetic acid was added in three portions to replenish what was removed under vacuum and the water bath temperature was increased slightly to 35 °C. Gratifyingly, these conditions led to the isolation of crude material in 94% yield that was established to be pure oxaspirolactone **818** by NMR (Scheme 5.11). Due to its instability, crude oxaspirolactone **818** was used directly in the next step without further purification.

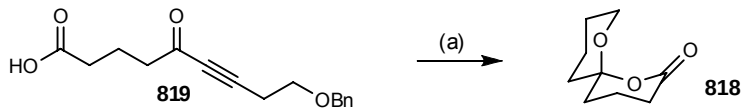

Reagents and conditions: (a) i. H_2, cat. Pd/C, cat. AcOH, THF, rt, 18 h; ii. AcOH, toluene, 30-35 °C, 30 mmHg, 94%.

Scheme 5.11: One-pot synthesis of oxaspirolactone **818** from keto-acid **819**.

Based on these findings, it is questionable as to whether or not oxaspirolactone **818** was formed in the initial hydrogenations or in the subsequent attempts to prepare this compound (Table 5.3). Insufficient time during the evaporation step and the presence of residual water may effect hydrolysis and degradation of the newly formed oxaspirolactone **818**. This observation may explain the variable and unpredictable results obtained from the previous cyclisations attempted.

(c) Thorpe-Ingold Effect (*gem*-Disubstituent Effect)

The Thorpe-Ingold effect is defined by the enhanced rate of cyclisation resulting from the introduction of substituents on the chain tethering the two reaction centres. One simple explanation that has been proposed is that the repulsion between the *gem*-dialkyl substituents in the open chain causes a compression of the internal angle which brings the reaction centres on the chain closer together, thus increasing the rate of cyclisation (Figure 5.2).[29,30]

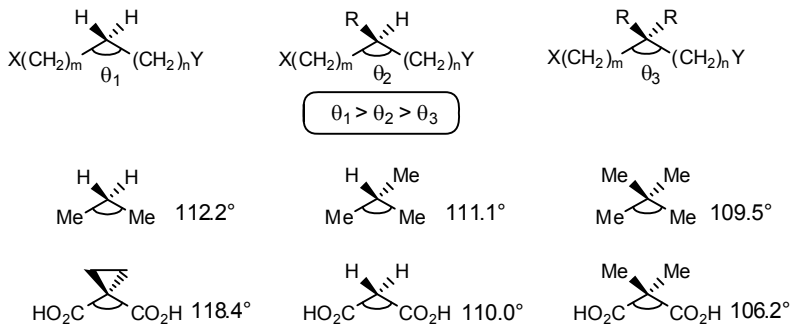

Figure 5.2: The Thorpe-Ingold effect and the effect of substitution on bond angles.[27]

An investigation on the effect of substituents on the hydrolysis of δ-valerolactones has shown an increase in both the equilibrium and rate constants for the unsubstituted δ-valerolactone **(820)** compared to its substituted counterpart. This represents a decrease in the rate of cyclisation due to the lack of ring stabilisation by the substituent and an increase in the rate of ring opening due to lack of steric shielding from hydrolysis. Both enthalpy and entropy of activation also became less favourable for the cyclisation of unsubstituted δ-valerolactone **(820)**.[30]

Because an unsubstituted spiroacetal was chosen as the model due to its simplicity, the Thorpe-Ingold effect cannot facilitate the lactonisation of hydroxy-acid **840**. This may the reason for the problematic cyclisation step and account for why the open-chain hydroxy-acid **840** is preferred over the cyclised oxaspirolactone **818** especially in the presence of water.

5.3 Synthesis of Spiroacetal Acetate 815 and Ethoxy-Spiroacetal 817

With the crucial oxaspirolactone **818** in hand, attention next turned to the synthesis of acetate **815** and acetals **816** and **817**, the precursors of spiroacetal-nucleosides **811** and triazoles **812** (Scheme 5.1).

5.3.1 Synthesis of Spiroacetal Acetate 815

It was envisaged that acetate **815** would be derived from the conceptionally simple reduction and acetylation of oxaspirolactone **818** *via* lactol intermediate **841** (Scheme 5.12).

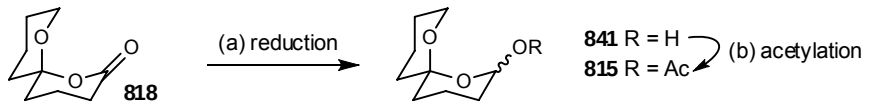

Scheme 5.12: Synthesis of spiroacetal acetate **815**. See Table 5.4 for reaction conditions.

DIBAL-H was employed for the reduction due to its ability to selectively reduce the lactone to the corresponding lactol under mild conditions. Unlike other hydride-based reducing agents such as $NaBH_4$ and $LiAlH_4$, over-reduction to the corresponding diol was not observed when the reaction was conducted at low temperature.[31] This DIBAL-H reduction–acetylation reaction has been well documented for the synthesis of the acetate precursors which were subsequently used for nucleosidations under Vorbrüggen conditions.[32-35]

Reduction of oxaspirolactone **818** using DIBAL-H and subsequent trapping of the resulting lactol **841** only gave a disappointingly poor yield of acetate **815**. The best yield was obtained using a two-step procedure in which oxapirolactone **818** was reduced by DIBAL-H (1 M in THF) in toluene at -78 °C for 15 min followed by the addition of MeOH to cleave the aluminium complex. Care was taken to avoid trace quantity of acid. The resulting lactol **841** was acetylated under standard conditions using Ac_2O, NEt_3 and catalytic DMAP in CH_2Cl_2 to give acetate **815** in 25% yield. The use of more reactive DIBAL-H in hexane or changing the reaction conditions such as varying the solvent or using a lower temperature did not improve the yield (Table 5.4).

Entry	*1 or 2-pot?*	*Reagents*	*Solvents*	*Conditions*	*Yields of 815*
1	1-pot	i. DIBAL-H in THF; ii. Ac_2O, pyridine, cat. DMAP	CH_2Cl_2 CH_2Cl_2	-78 °C, 1 h -78 °C→rt, 4 h	7%
2	1-pot	i. DIBAL-H in hexane; ii. Ac_2O, pyridine, cat. DMAP	CH_2Cl_2 CH_2Cl_2	-78 °C, 10 min -78 °C→rt, 18 h	18%
3	1-pot	i. DIBAL-H in hexane; ii. Ac_2O, pyridine	CH_2Cl_2 CH_2Cl_2	-78 °C, 10 min -78 °C→rt, 18 h	complex mixture
4	1-pot	i. DIBAL-H in hexane; ii. Ac_2O, NEt_3, cat. DMAP	CH_2Cl_2 CH_2Cl_2	-78 °C, 10 min -78 °C→rt, 18 h	23%
5	1-pot	i. DIBAL-H in hexane; ii. Ac_2O, NEt_3, cat. DMAP	toluene CH_2Cl_2	-100 °C, 10 min -78 °C→rt, 18 h	complex mixture
6	2-pot	(a) DIBAL-H in hexane (b) AcCl, NEt_3, cat. DMAP	toluene CH_2Cl_2	-78 °C, 30 min rt, 4 h	complex mixture
7	2-pot	(a) DIBAL-H in hexane (b) Ac_2O, NEt_3, cat. DMAP	toluene CH_2Cl_2	-78 °C, 30 min 0 °C→rt, 20 h	20%
8	2-pot	(a) DIBAL-H in THF (b) Ac_2O, NEt_3, cat. DMAP	toluene CH_2Cl_2	-78 °C, 15 min 0 °C→rt, 20 h	18%
9	2-pot	(a) i. DIBAL-H in THF; ii. MeOH (b) Ac_2O, NEt_3, cat. DMAP	toluene CH_2Cl_2	-78 °C, 15 min; -78 °C, 30 min 0 °C→rt, 20 h	25%

Table 5.4: Summary of the reagents and conditions used for the synthesis of acetate **815**.

It was observed that only approximately 60% of crude lactol **841** was recovered from the initial DIBAL-H reduction. This may be due to the water solubility of the resulting lactol **841** and its ring opened equivalents. It is also possible that these polar molecules become permanently bound to the aluminium salt. Unfortunately, the use of a one-pot procedure, by directly trapping the newly formed lactol **841** from its aluminium complex at low temperature, failed to improve the yield (Table 5.4).

The low yields may also be due to the instability of lactol **841** and the resulting acetate **815**. Furthermore, both **815** and **841** are volatile, thus further contributing to the low yields.[12,13,17,36] Unfortunately, this volatility problem has not been recognised until the synthesis of the structurally similar ethoxy-spiroacetal **817** and is one of the problems that required addressing in the present work (See Section 5.7).

5.3.2 Synthetic Routes to Ethoxy-Spiroacetal 817

Two possible synthetic routes to ethoxy-spiroacetal **817** were evaluated.

The first generation approach was based on the conceptionally simple reduction and protection of oxaspirolactone **818**. This route has proven to be feasible for the synthesis of acetate **815**, although more synthetic steps were involved and the yield was low (Scheme 5.13).

The second generation approach was proposed after close examination of the first synthetic route revealed a flaw in its design. The virtue of the oxidation step to give keto-acid **819** was effectively cancelled by the subsequent reduction to give spiroacetals **816** and **817**. Interestingly, lactol **841** has the same oxidation level as the saturated aldehyde **839**. Therefore, investigation of the direct hydrogenation of aldehyde **839** was embarked with caution. The resulting linear aldehyde is expected to spontaneously equilibrate *via* a carbonyl cascade cyclisation, to give lactol **841** which can subsequently be alkylated to give methoxy-spiroacetal **816** or ethoxy-spiroacetal **817** (Scheme 5.13).[4,6,37]

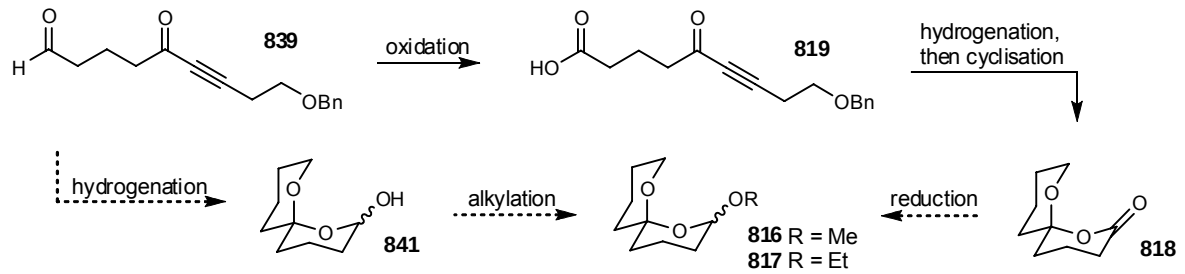

Scheme 5.13: The two proposed synthetic routes to alkoxy-spiroacetals **816** and **817**.

5.3.3 The First Approach to the Synthesis of Ethoxy-Spiroacetal 817 from Oxaspirolactone 818

Due to the low yields of acetate **815** obtained *via* reduction-acetylation of oxaspirolactone **818**, a change of reducing agent was attempted. Use of superhydride® ($LiBEt_3H$) in THF, followed by ethoxylation of the resulting lactol **841** under mild conditions, failed to yield acetal **817**.[38] Shortening the reduction time also failed to give any desired product, probably due to over-reduction by the powerful borohydride reagent (Scheme 5.14).[39]

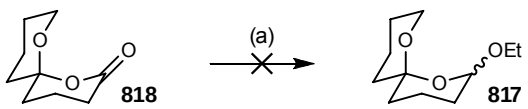

Reagents and conditions: (a) i. superhydride®, THF, -78 °C, 1–1.5 h; ii. PPTS, EtOH, -78 °C→rt, 18 h.

Scheme 5.14: Attempted synthesis of ethoxy-spiroacetal **817** from oxaspirolactone **818**.

5.3.4 The Second Approach to the Synthesis of Ethoxy-Spiroacetal 817 from Keto-Aldehyde 839

Using the same reaction conditions employed previously, hydrogenation of keto-aldehyde **839** in THF or EtOAc only gave a complex mixture. Using MeOH as the solvent also produced a mixture of products which presumably contained lactol **841**, methoxy-spiroacetal **816**, methoxypyran **842** and other mono or dimethoxy compounds. Attempts to equilibrate the complex mixture using PPTS, *p*-TsOH or 4 Å molecular sieves in CH_2Cl_2 failed. Fortunately, repeating the hydrogenation in the presence of *p*-TsOH followed by CSA-catalysed equilibration afforded a 51% yield of the desired product **816**, albeit as a 4:1 inseparable mixture of methoxypyran **842** : methoxy-spiroacetal **816** (Scheme 5.15 and Table 5.5).

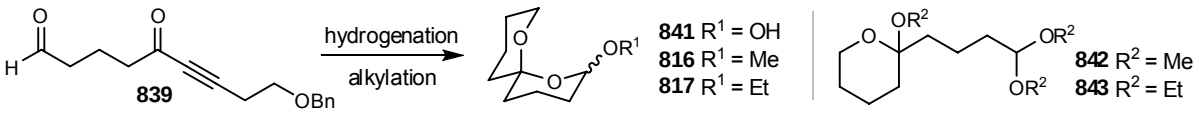

Scheme 5.15: Synthesis of spiroacetals **816**, **817** and **841** from keto-aldehyde **839**. Alkoxypyrans **842** and **843** were also isolated in variable quantities. See Table 5.5 for reaction conditions.

On the other hand, hydrogenation of keto-aldehyde **839** in EtOH with catalytic *p*-TsOH produced more promising results. Ethoxy-spiroacetal **817** was isolated in 33–65% yield using EtOH or in 36–40% yield using EtOH–CH_2Cl_2. Careful chromatography of the crude reaction mixture also allowed the isolation of ethoxypyran **843** and other related structures which could be converted to ethoxy-spiroacetal **817** under acidic conditions affording **817** in 79% yield over the two steps (Table 5.5).

Entry	*Reagents*	*Solvents*	*Conditions*	*Yields of 815–817*
1	H_2, cat. Pd/C, cat. AcOH	THF	rt, 18 h	complex mixture
2	H_2, cat. Pd/C	EtOAc	rt, 18 h	complex mixture
3	(a) H_2, cat. Pd/C (b) i. PPTS; ii. *p*-TsOH or (b) 4 Å MS	MeOH CH_2Cl_2 CH_2Cl_2	rt, 2 d rt, 21 h rt, 1 d	complex mixture
4	(a) H_2, cat. Pd/C, cat. *p*-TsOH (b) CSA	MeOH MeOH–benzene	rt, 18 h rt, 18 h	51% (inseparable 4:1 mixture of **842**:**816**)
5	H_2, cat. Pd/C, cat. *p*-TsOH	EtOH	rt, 18 h	**817**: 33–65%
6	H_2, cat. Pd/C, cat. *p*-TsOH	EtOH–CH_2Cl_2	rt, 18 h	**817**: 36–40%
7	H_2, cat. Pd/C, cat. *p*-TsOH	Ac_2O	rt, 18 h	saturation of alkyne but no debenzylation
8	(a) i. H_2, cat. Pd/C, cat. *p*-TsOH ii. chromatographic separation (b) *p*-TsOH, H_2O	EtOH–CH_2Cl_2 EtOH–CH_2Cl_2	rt, 18 h rt, 18 h	**817**: 79% over 2 steps

Table 5.5: Summary of the reagents and conditions used for the synthesis of spiroacetals **815**–**817**.

The presence of ethoxypyran **843** and other related structures was not surprising due to the weakly thermodynamically driven equilibrium of the carbonyl cascade cyclisation, thus resulting in a mixture of various half-cyclised products. The use of a separate equilibration step to obtain the desired alkoxy-spiroacetal after the initial deprotection step is commonly reported in the literature.[4,6,37]

Unfortunately, it was observed that ethoxy-spiroacetal **817** was volatile and part of the product was lost during the solvent removal step. This observation raised the question as to the volatility of other structurally similar spiroacetals such as acetate **815**, methoxy-spiroacetal **816** and lactol **841**. Attempts to reduce the quantity of EtOH used for the hydrogenation reaction by using a EtOH–CH_2Cl_2 mixture failed to improve the yield. This volatility problem is one of the major problems that required addressing in the present work (See Section 5.7).

Finally, attempts to synthesise lactol **841** or acetate **815** *via* the hydrogenation of keto-aldehyde **839** in Ac_2O (Table 5.5) or *via* nucleophilic substitution of ethoxy-spiroacetal **817** failed (Scheme 5.16).

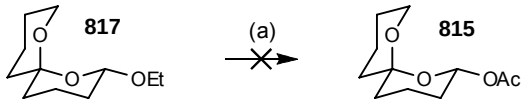

Reagents and conditions: (a) i. BF_3•OEt_2, CH_2Cl_2, -78 °C, 15 min; ii. KOAc, CH_2Cl_2, -78 °C→rt, 2 h; iii. Ac_2O, NEt_3, cat. DMAP, rt, 1 h.

Scheme 5.16: Attempted synthesis of acetate **815** from ethoxy-spiroacetal **817**.

5.3.5 NMR and Stereochemistry of Spiroacetal Acetate 815 and Ethoxy-Spiroacetal 817

(a) NMR Analysis

NMR analysis of both acetate **815** and acetal **817** revealed the characteristic anomeric H2 protons at δ_H 5.94 and 4.72 ppm, that resonated as doublet of doublets ($J_{2ax,3ax}$ 9.9–10.1 Hz) with a large 1,2-diaxial coupling. These characteristic couplings established that the C2 substituent (acetate or ethoxy group) adopted an equatorial position. Quaternary carbons resonated at δ_C 97.5–98.6 ppm were assigned to the spirocarbon C6, thus confirming the presence of the spiroacetal ring system (Table 5.6).

The ^{1}H and ^{13}C NMR chemical shifts for acetate **815** and acetal **817** were very similar to the corresponding C8-substituted spiroacetals **861** and **862**. These similarities were not surprising because the spiroacetals also adopted the thermodynamically-favoured *bis*-anomerically stabilised conformation as depicted in Table 5.6.

Atom number	***Chemical Shifts (δ in ppm)***			
	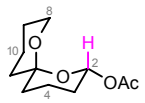 ***acetate 815***	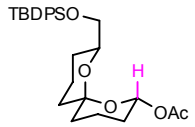 ***acetate 861***	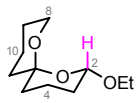 ***acetal 817***	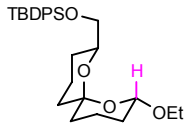 ***acetal 862***
H2	5.94 dd (*J* 10.1 and 2.6 Hz)	6.00 dd (*J* 10.1 and 2.6 Hz)	4.72 dd (*J* 9.9 and 2.2 Hz)	4.83 dd (*J* 10.0 and 2.3 Hz)
C2	90.0	90.2	96.5	96.6
C3	29.4	29.5	30.8	30.9
C4	17.5	17.4	17.8 / 18.5	17.8 / 18.5
C5	35.2	34.6	34.8 / 35.5	34.8 / 35.2
C6	98.6	99.1	97.5	98.1
C8	61.1	70.7	60.7	70.9
C9	25.0	26.6	25.3	27.0
C10	18.3	18.2	17.8 / 18.5	17.8 / 18.5
C11	34.6	34.9	34.8 / 35.5	34.8 / 35.2

Table 5.6: Characteristic ^{1}H and ^{13}C NMR chemical shifts of the spiroacetal unit present in acetate **815** and acetal **817**. The related C8-substituted spiroacetals **861** and **862** are depicted here for comparison.

(b) Stereochemistry

It was intriguing that only the equatorial substituted acetate **815** and acetal **817** were isolated from the synthesis. The equatorial isomer was presumably less stable than the corresponding axial isomer due to operation of the anomeric effect. However, the anomeric effect only offers *ca*. 1.4–1.5 kcal mol^{-1} of stabilisation energy[40] which could be overcome by opposing stereoelectronic effects. In this case, the alignment of 1,3-dipole moments between the substituent and the C–O bond of the unsubtituted ring as well as the steric clash between them may disfavour the formation of the axial isomer under the thermodynamically-controlled conditions used to effect the reaction.[14,41]

5.4 Synthesis of Spiroacetal-Nucleosides 811

With acetate **815** and acetal **817** in hand, the final step for the synthesis of the first spiroacetal hybrid, namely spiroacetal-nucleosides **811** was next undertaken.

It was planned to effect the nucleosidation under Vorbrüggen conditions. A persilylated heterobase was added to an oxonium ion generated from a spiroacetal bearing a leaving group at the anomeric position in the presence of a Lewis acid. TMSOTf was the first choice of Lewis acid due to its use for the successful generation of oxonium ions from similar spiroacetal-based systems (Scheme 5.1).[4-6]

5.4.1 Nucleosidation of Spiroacetal Acetate 815

Adapting the procedures from Mann *et al.*[32] and Paquette *et al.*[34,42], acetate **815** was successfully reacted with persilylated 5-fluorocytosine **845** in the presence of TMSOTf in CH_2Cl_2 at 0 °C. The reaction occurred at the less hindered N1 position to give spiroacetal 5-fluorocytidine **811a** in 39% yield after purification by chromatography. The (*Z*)-enamide **846*** by-product was also isolated in 24% yield. Persilylated 5-fluorocytosine **845**, in turn, was generated by heating 5-fluorocytosine **(844)** under reflux in *N*,*O*-bis(trimethylsilyl)acetimide (BSA, Scheme 5.17).

Unfortunately, attempts to improve the yield by substitution of CH_2Cl_2 with DCE, a solvent commonly used for nucleosidations, only produced a complex mixture (Scheme 5.17).

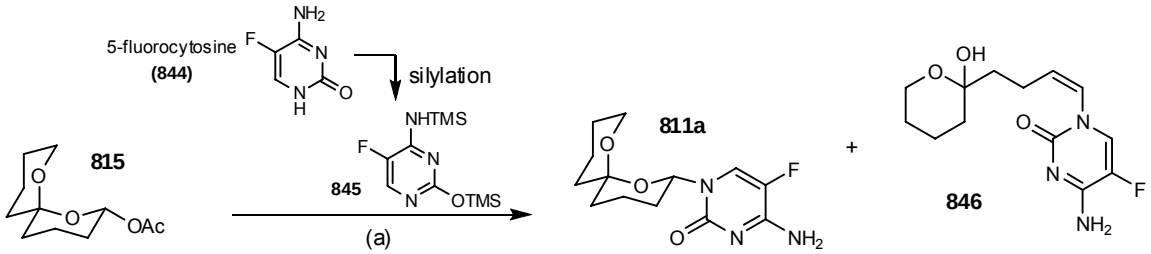

Reagents and conditions: (a) ^{5F}C, BSA, reflux, 1 h; (b) **845**, TMSOTf, CH_2Cl_2, 0 °C→rt, 20 h, **811a**: 39%, **846**: 24%.

Scheme 5.17: Nucleosidation under Vorbrüggen conditions of acetate **815** and persilylated 5-fluorocytosines **845**. Substitution of CH_2Cl_2 by DCE as solvent resulted in a complex mixture.

5.4.2 Nucleosidation of Ethoxy-Spiroacetal 817

Given the low yields of acetate **815** obtained from oxaspirolactone **818**, the use of acetal **817** for the nucleosidation step was an attractive option. Disappointingly, attempts to effect a similar nucleosidation using the reaction conditions developed above for acetate **815** failed. Changing the nature of the heterobase (such as ^{5F}C, C or T), the silylating agents (such as BSA or HMDS), Lewis

---

* The magnitude of the vinylic coupling constant (*J* 8.4 Hz) clearly established the *(Z)*-stereochemistry of the enamide **846**. A tentative mechanism was proposed by initial formation of nucleoside **847** in which the heterocyclic base occupied the more sterically hindered axial position. In the presence of a Lewis acid during the nucleosidation, the unstable spiroacetal **847** underwent an *β*-hydrogen elimination-ring opening sequence to give *(Z)*-enamide **846**. However, attempted conversion of spiroacetal **811a** to enamide **846** in the presence of TMSOTf only resulted in degradation of **811a**. The instability of enamide **846** was also observed during NMR studies.

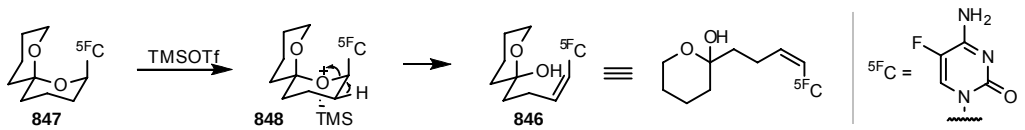

A similar acid-mediated *β*-hydrogen elimination-ring opening sequence of a 6,6-spiroacetal has also been observed by Porco *et al.*[43] to give a lactol by-product. Another similar acid-mediated *β*-hydrogen elimination-ring opening sequence was also observed during a synthetic study towards rubromycin analogues conducted by our group.[44]

acids (such as TMSOTF, $SnCl_4$, $Sc[OTf]_3$[45] or $MeSiCl_3$[46]) and solvent (e.g. CH_2Cl_2, MeCN or toluene) as well as varying the reaction conditions (e.g. use of a one or two-pot procedure) and temperature (e.g. < 0 °C or room temperature) were all unsuccessful to produce the desired spiroacetal nucleosides (Scheme 5.18).

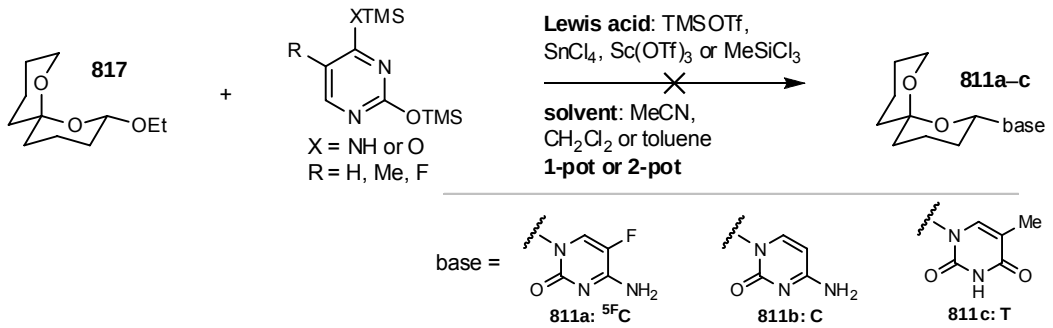

Scheme 5.18: Attempted nucleosidation under Vorbrüggen conditions of acetal **817** using persilylated heterobase. See Table 5.7 for reaction conditions.

Entry	*1 or 2-pot?*[a]	*Reagents*	*Solvents*	*Conditions*	*Results*
1	2-pot	(a) ^{5F}**C**, cat. $(NH_4)_2SO_4$ (b) TMSOTf	HMDS CH_2Cl_2	reflux, 1 h 0 °C→rt, 18 h	complex mixture
2	1-pot	i. ^{5F}**C**, BSA ii. TMSOTf	MeCN MeCN	rt, 2 h rt, 18 h	complex mixture
3	1-pot	i. ^{5F}**C**, BSA ii. TMSOTf	MeCN CH_2Cl_2	reflux, 1 h 0 °C→rt, 18 h	complex mixture
4	1-pot	i. ^{5F}**C**, BSA, 4 Å MS ii. TMSOTf	MeCN CH_2Cl_2	reflux, 1 h -40 °C→rt, 5 h	complex mixture
5	2-pot	(a) **C** (b) TMSOTf	BSA CH_2Cl_2	reflux, 1 h rt, 20 h	complex mixture
6	1-pot	i. **C**, BSA ii. TMSOTf	MeCN MeCN	reflux, 1 h reflux, 2 h	complex mixture
7	2-pot	(a) **T**, BSA (b) TMSOTf or $SnCl_4$	toluene CH_2Cl_2–MeCN	reflux, 1 h 0 °C→rt, 4 h	complex mixture
8	2-pot	(a) **T**, BSA (b) TMSOTf	toluene CH_2Cl_2 or MeCN	reflux, 1 h 0 °C→rt, 2 h	complex mixture
9	1-pot	i. **T**, BSA ii. TMSOTf	MeCN CH_2Cl_2	reflux, 1 h 0 °C→rt, 4 h	complex mixture
10	2-pot	(a) **T**, BSA (b) $SnCl_4$	toluene CH_2Cl_2	reflux, 1 h -78 °C, 45 min	complex mixture
11	2-pot	(a) **T**, BSA (b) $Sc(OTf)_3$	toluene CH_2Cl_2	reflux, 1 h rt, 18 h	complex mixture
12	2-pot	(a) **T** (b) TMSOTf	BSA CH_2Cl_2	reflux, 1 h -78 °C→rt, 1.5 h	complex mixture
13	2-pot	(a) **T**, BSA (b) $MeSiCl_3$	toluene CH_2Cl_2	reflux, 1 h 0 °C→rt, 18 h	complex mixture

Table 5.7: Summary of the reagents and conditions used for the attempted nucleosidation of acetal **817**.

[a] In two-pot reactions, the silylating agent was removed *in vacuo* and the persilylated heterobase was co-eluted with toluene before the addition of acetal **817** and the Lewis acid. These reactions are denoted by "(a)…(b)" in the column of reagents. In one-pot reactions, the silylating agent was not removed and these reaction are denoted by "i.…ii." in the column of reagents.

The failure to effect nucleosidation using persilylated cytosine, in particular, may be due to the formation of a strong σ-complex between the heterobase and the Lewis acid, thus preventing it from generating of the oxonium ion from the activated spiroacetal moiety. The formation of the complex is also commonly observed when other amino substituted heterobases (such as adenine and guanine) are used and can be avoided if less basic *N*-acylated aminoheterobases are used.[47]

Gratifyingly, one-pot nucleosidation of acetal **817** using persilylated uracil **850** in the presence of TMSOTf gave the desired spiroacetal uridine **811d** in 19% yield. No formation of enamide was observed. A similar two-pot nucleosidation also provided uridine **811d** in 13% yield (Scheme 5.19 and Table 5.8).

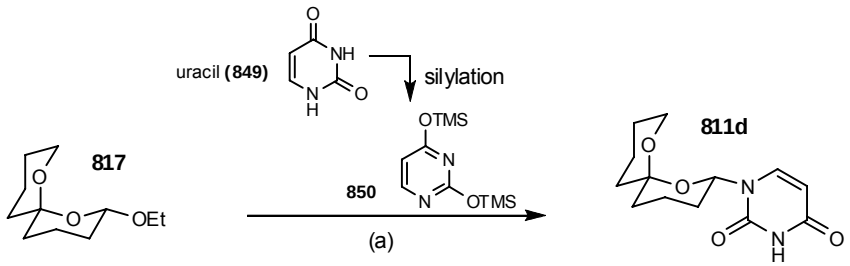

Reagents and conditions: (a) i. U, BSA, reflux, 1 h; ii. **850**, TMSOTf, CH_2Cl_2, 0 °C→rt, 19%.

Scheme 5.19: Nucleosidation of acetal **817** under Vorbrüggen conditions using persilylated uracil **850**.

Entry	*1 or 2-pot?*	*Reagents*	*Solvents*	*Conditions*	*Results*
1	2	(a) **U** (b) TMSOTf	BSA CH_2Cl_2	reflux, 1 h rt, 2.5 h	complex mixture
2	2	(a) **U**, cat. $(NH_4)_2SO_4$ (b) TMSOTf	HMDS CH_2Cl_2	reflux 0 °C→rt, 18 h	13%
3	1	i. **U**, BSA ii. TMSOTf	MeCN CH_2Cl_2	reflux, 1 h 0 °C→rt, 18 h	19%

Table 5.8: Summary of the reagents and conditions used for the nucleosidation of acetal **817** using persilylated uracil **850**.

5.4.3 Comparison of the Use of Spiroacetal Acetate 815 and Ethoxy-Spiroacetal 817 for Nucleosidation Reactions

After much experimentation, 5-fluorocytidine **811a** was synthesised from acetate **815** in 39% yield and uridine **811d** from acetal **817** in 19% yield. The lower yield observed for the nucleosidation of acetal **817** was probably due to the poorer leaving group ability of the ethoxy group compared to the acetate group.

A considerable amount of literature affirmed the use of glycosyl acetates to generate the required oxonium ions for nucleosidations.[47] When alkoxy glycosides were used, a stronger Lewis acid such as $TiCl_4$ was often required to effect the nucleosidation.[27,48] Alternatively, the alkoxy glycoside was converted to the more labile glycosyl acetate or halide prior to the nucleosidation.[49]

Unfortunately, acetal **817** was not compatible with the use of strong Lewis acids due to the sensitivity of the delicate spiroacetal ring.[4] Moreover, the conversion of acetal **817** to acetate **815** was also questionable as such a transformation is often conducted under strongly acidic conditions (such as a mixture of glacial acetic acid and sulfuric acid). The 6,6-spiroacetal ring is not expected to survive under these conditions.[49]

Both Mead and Zemribo[4,6] and Brimble *et al.*[5] have reported the nucleophilic addition to an oxonium ion generated from simple 6,6-spiroacetals in the presence of TMSOTf. It was therefore decided to test the ability of acetal **817** to generate an oxonium ion under similar conditions to the above used by Mead and Zemribo[4,6] and Brimble *et al.*[5]

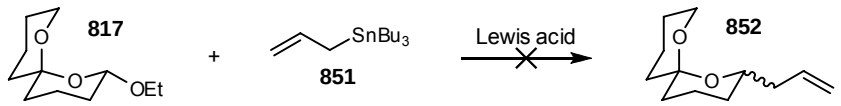

Scheme 5.20: Attempted allylation of acetal **817**.

Entry	*Lewis Acid*	*Additives*	*Solvents and Conditions*	*Results*
1	cat. TMSOTf	4 Å MS	CH_2Cl_2, -78 °C→rt, 18 h	complex mixture
2	TMSOTf (2 eq.)		CH_2Cl_2, 0 °C, 3 h	complex mixture
3	cat. BF_3•OEt_2		CH_2Cl_2, -78→-50 °C, 2.5 h	complex mixture

Table 5.9: Summary of the reagents and conditions used for the attempted allylation of acetal **817**.

It was envisaged that the oxonium ion, if generated, could be trapped *in situ* by allylstannane **851** which is a better nucleophile than the corresponding allylsilane.[4-6] However, treatment of acetal **817** with TMSOTf or BF_3•OEt_2 in the presence of allylstannane, failed to produce allyl-spiroacetal **852**. The use of a higher reaction temperature and the inclusion of molecular sieves also did not effect the desired allylation (Scheme 5.20 and Table 5.9).

In contrast, a similar substitution reaction effected by the treatment of acetal **817** with an excess of TMSOTf and $TMSN_3$ successfully afforded a mixture of diastereomeric azides **814** in 71% yield (Scheme 5.22).[†] As a result, it was suspected that the failure to effect the nucleosidation of acetal **817** was due to the inefficiency of **817** to generate the crucial oxonium ion intermediate under mild conditions. Therefore, use of a good nucleophile under forcing conditions (such as excess Lewis acid) is essential in order to effect the desired anomeric substitution reaction.

A dilemma was therefore apparent for the attempted nucleosidation of acetal **817**. It was known that the persilylated heterobase formed a σ-complex with the Lewis acid, thus decreasing its

[†] This particular procedure was adapted from Trost *et al.*[53] who used a large excess of TMSOTf (5 eq.) and $TMSN_3$ (10 eq.) at 0 °C to effect an azide substitution reaction during the synthesis of a highly oxygenated azide intermediate of mycalamide A.[50]

effective concentration. However, increasing the amount of Lewis acid degrades the fragile unsubstituted spiroacetal moiety. This dilemma is more problematic when the unsubstituted spiroacetals was used in this model study and required addressing in the present work (see Section 5.7).

5.4.4 NMR and Stereochemistry of Spiroacetal 5-Fluorocytidine 811a and Uridine 811d

(a) NMR Analysis

NMR analysis of both 5-fluorocytidine **811a** and uridine **811d** revealed the characteristic anomeric H2′ resonances at δ_H 5.95–6.03 ppm. The large 1,2-diaxial coupling constants ($J_{2ax,3ax}$ 10.9–11.2 Hz) were consistent with a dihedral angle of *ca*. 180°. This indicated that both of the nucleoside substituents adopted equatorial positions. In **811a**, the anomeric H2′ resonance also exhibited a long range J^5 coupling to the fluorine of the heterobase highlighting the connection between the two moieties. Quaternary carbons resonated at δ_C 98.5–98.6 ppm were assigned to the spirocarbon C6′, thus confirming the presence of the spiroacetal ring system.

A clear HMBC correlations between C2′–H6 and H2′–C6 confirmed the desired chemical connection between C2′ and N1, but not between the potentially competitive C2′ and N3. NOESY studies also confirmed the *bis*-anomerically stabilised confirmation of 5-fluorocytidine **811a** and uridine **811d** through observation of a correlation between H2′ and H8′. This correlations confirmed the adoption of the *bis*-anomerically stabilised spiroacetal conformation in which the basic substituent adopting an equatorial position. NOESY correlations between the H6 of the pyrimidines with H2′ and H3′ of the spiroacetal ring were also observed (Scheme 5.21).

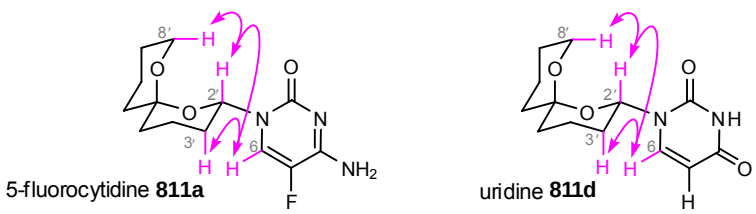

Scheme 5.21: Structures of 5-fluorocytidine **811a** and uridine **811d** showing the *bis*-anomerically stabilised spiroacetal rings and their pyrimidine equatorial substituents. NOESY correlations are denoted by arrows.

(b) Stereochemistry

Similar to their precursors (acetate **815** and acetal **817**), both 5-fluorocytidine **811a** and uridine **811d** were isolated as the equatorial isomer. It was postulated that steric interactions prevented the axial approach of the persilylated heterobase. The less electronegative nitrogen atom in the nucleobase also provided less anomeric stabilisation for the axial isomer. This effect together

with the disfavourable alignment of 1,3-dipole moments and steric interactions rendered the axial isomer less thermodynamically stable than the corresponding equatorial isomer.[51]

The reason for the absence of any axial isomer in the product mixture was not clear. The axial isomer may have failed to form under the reaction conditions or may have degraded during the reaction or subsequent work-up step. Similar stereoselective formation of the equatorial isomer from the nucleosidation of pyranosides or furanosides lacking a stereodirecting neighbouring group have also previously been reported in the literature.[35,52]

5.5 Synthesis of Spiroacetal Triazoles 812

Having successfully developed the methodology for the synthesis of spiroacetal nucleosides **811**, attention was next turned to the synthesis of a second series of spiroacetal hybrids, namely spiroacetal triazoles **812**. Triazoles **812** are available *via* cycloaddition of azide **814** to various alkynes (Scheme 5.1).

5.5.1 Preparation of Azido-Spiroacetal 814

Azide **814** was synthesised from acetal **817** using a procedure adapted from Trost *et al*.[53] Acetal **817** was reacted with TMSOTf in CH_2Cl_2 at 0 °C to generate an oxonium ion which was subsequently trapped by $TMSN_3$ to give diastereomeric azides **814a** and **814b** in 71% yield as a 1:3 inseparable mixture (Scheme 5.22). Due to the volatility of the azides, crude mixture of azides **814** was usually used without purification.

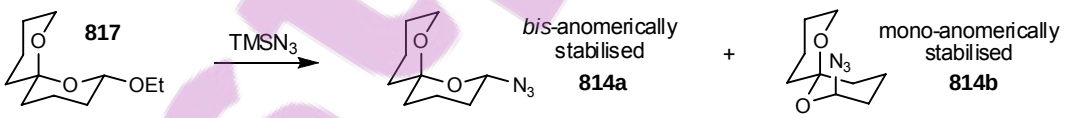

Reagents and conditions: (a) $TMSN_3$, TMSOTf, CH_2Cl_2, 0 °C, 3 h, 71% (**814a**:**814b** 1:3).

Scheme 5.22: Synthesis of azides **814** from acetal **817**.

The success of this previously problematic substitution reaction of acetal **817** is due to the excellent nucleophilicity and the small size of azide. Also because of the slender azide group, the stereodirecting effect contributed by the presence of the spiroacetal rings has little effect on the stereochemical outcome of the reaction, thus a mixture of isomers resulted.

5.5.2 NMR and Stereochemistry of Azido-Spiroacetals 814

(a) NMR analysis

NMR analysis of azides **814a** and **814b** revealed the characteristic anomeric H2′ resonances at δ_H 4.66–4.85 ppm. A larger 1,2-diaxial coupling was observed for azide **814a** (dd, $J_{2ax,3ax}$ 10.8 Hz) whereas a smaller 1,2-diequatorial coupling was observed for azide **814b** (t, $J_{2eq,3ax/3eq}$ 6.5 Hz). These characteristic coupling constants established that the azide substituent adopted an equatorial position in **814a** and the axial position in **814b**. Quaternary carbons resonated at δ_C 93.9 and 98.3 ppm were assigned to the spirocarbon C6′, thus confirming the presence of the spiroacetal ring system (Table 5.10).

Due to the significant differences observed between the chemical shifts of azides **814a** and **814b** in the ^{13}C NMR (noticably the signals observed for C11), it was apparent that **814a** and **814b** were not simple C2 anomers, but rather exhibit substantial conformational differences in their spiroacetal rings. The ^{1}H and ^{13}C NMR chemical shifts of azides **814a** and **814b** were, however, very similar to the corresponding C8-substituted spiroacetals **860a** and **860b**. These similarities were not surprising because the spiroacetal ring of azides **814a** and **860a** adopted the *bis*-anomerically stabilised conformation while the spiroacetal ring of azide **814b** and **860b** adopted the mono-anomerically stabilised conformation as depicted in Table 5.10.

The structure of azide **814a** was further supported by the close similarity of the ^{1}H and ^{13}C NMR chemical shifts to those observed for other spiroacetals adopting the *bis*-anomerically stabilised conformation, such as acetate **815** and acetal **817** (see Section 5.3.5).

Atom number	***Chemical Shifts (δ in ppm)***			
	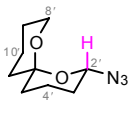 ***azide 814a***	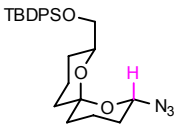 ***azide 860a***	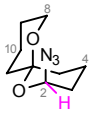 ***azide 814b***	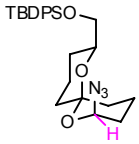 ***azide 860b***
H2	4.85 dd (*J* 10.8 and 2.5 Hz)	4.94 dd (*J* 10.8 and 2.5 Hz)	4.66 t (*J* 6.4 Hz)	4.61 t (*J* 6.4 Hz)
C2	83.3	83.2	77.8	77.8
C3	30.2	30.2	32.3	32.0
C4	17.8 / 18.3	17.8 / 18.3	18.8 / 19.0	18.7
C5	34.5	34.4 / 34.8	34.0	34.1
C6	98.3	98.6	93.9	92.3
C8	60.8	71.0	63.3	73.3
C9	29.7	26.7	24.7	26.8
C10	17.8 / 18.3	17.8 / 18.3	18.8 / 19.0	19.1
C11	35.2	34.4 / 34.8	39.1	39.8

Table 5.10: Characteristic ^{1}H and ^{13}C NMR chemical shifts of the spiroacetal unit present in azides **814a** and **814b**. The related C8-substituted spiroacetals **860a** and **860b** are depicted here for comparison.

(b) Stereochemistry

The predominance of the mono-anomerically stabilised azide **814b** was attributed to the unfavourable steric interactions between the protons attached to C8 and the axial azide substituent at C2. The formation of axial azide **814b** was postulated to take place *via* a ring-opening and subsequent ring-closing mechanism that was facilitated in the presence of a Lewis acid. More details of this mechanism will be discussed in Chapter 6.8.1 (Scheme 5.23).

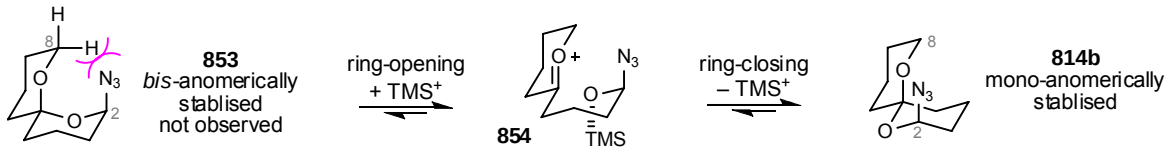

Scheme 5.23: Postulated mechanism for the formation of mono-anomerically stablised **814b**.

5.5.3 Cycloadditions of Azido-Spiroacetals 814

With azides **814** in hand, attention turned to the synthesis of triazole cycloadducts *via* reactions with alkynes. Both the thermally-promoted and highly popular copper-catalysed conditions were tested for the conversion of these spiroacetal-azides to a range of triazoles. Due to the volatility of the azide mixtures, crude starting material was used in order to minimise handling.

(a) Thermally-Promoted 1,3-Dipolar Cycloaddition

Use of a thermally-promoted 1,3-dipolar cycloaddition proved to be the optimum procedure when using activated electron deficient alkynes. The formation of regioisomers is avoided if symmetrical alkynes were used. Hence, the cycloaddition of crude mixture of azides **814a** and **814b** to dimethylacetylene dicarboxylate (DMAD, **855**) was attempted. After much experimentation, the thermally-promoted cycloaddition afforded triazole **812a** in 25% yield when the reaction was performed in neat DMAD at 80 °C. Conducting the same reaction with excess DMAD in toluene only produced triazole **812a** in 7% yield, while use of the highly activated maleic anhydride **(856)** for the cycloaddition failed to give the desired product **812b** (Scheme 5.24).

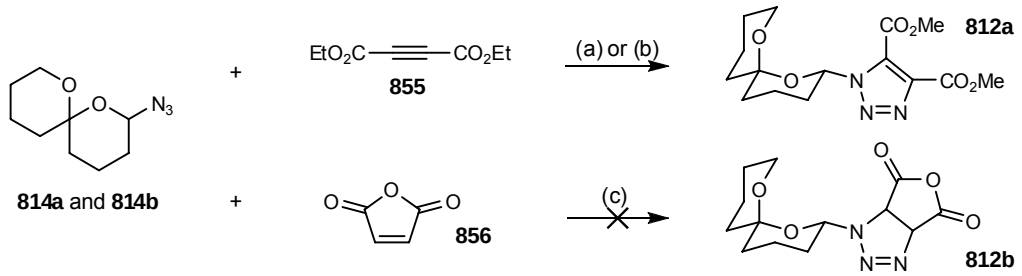

Reagents and conditions: (a) **855**, toluene, 80 °C, 5 h, 7%; (b) **855**, 80 °C, 3 h, 25%; (c) **856**, toluene, 65 °C, 4 h.

Scheme 5.24: Thermally-promoted 1,3-dipolar cycloaddition of crude mixture of azides **814a** and **814b** with DMAD **855** and maleic anhydride **856**.

(b) Copper-Catalysed Azide–Alkyne Cycloaddition (CuAAC)

CuAAC is a popular reaction due to its broad applicability and the popularity of triazole moiety. The reaction catalyses the cycloaddition of azides to terminal alkynes producing only 1,4-disubstitued triazoles.

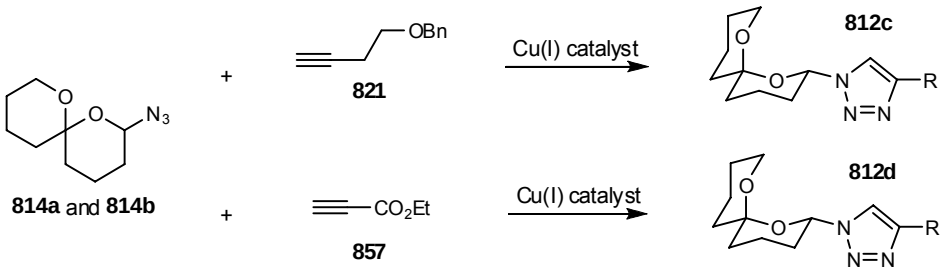

Scheme 5.25: CuAAC of crude mixture of azides **814a** and **814b** to terminal alkynes **821** and **857**. See Table 5.11 for reaction conditions.

Using the procedure adapted from Meldal *et al*.[54], the cycloaddition of alkyne **821** to the crude mixture of azides **814a** and **814b** only proceeded to completion after the addition excess CuI and DIPEA giving triazole **812c** in 10% yield. Secondly, use of the sodium ascorbate method adapted from the procedure by Sharpless *et al*.[55] was attempted but the reaction only produced triazole **812c** in 7% yield using alkyne **821** while no triazole **812d** was obtained using alkyne **857** under same conditions. Finally, use of a phophine-stabilised copper(I) salt[56] [CuI•P(OEt)$_3$] effected reaction of the crude mixture of azides **814a** and **814b** to afford triazole **812d** in 23% yield using an excess of alkyne **857** (Scheme 5.25 and Table 5.11).

Entry	*Alkyne*	*Reagents*	*Solvents*	*Conditions*	*Results*	Notes
1	OBn **821**	CuI, DIPEA	toluene	rt, 2 d	10%	catalytic CuI and DIPEA were used initially with excess reagents subsequently added
2		cat. Cu(OAc)$_2$ Na ascorbate	^{t}BuOH–H$_2$O	rt, 18 h	7%	
3	CO_2Et **857**	cat. Cu(OAc)$_2$ Na ascorbate	^{t}BuOH–H$_2$O	rt, 18 h	complex mixture	
4		cat. CuI•P(OEt)$_3$	toluene	rt, 18 h	2%	starting materials recovered
5		cat. CuI•P(OEt)$_3$	toluene	rt, 18 h	23%	excess alkyne **867** was used

Table 5.11: Summary of the reagents and conditions used for the attempted CuAAC of crude mixture of azides **814a** and **814b** with terminal alkynes **821** and **857**.

5.5.4 NMR and Stereochemistry of Triazoles 812

(a) NMR Analysis

NMR analysis of triazoles **812a**, **812c** and **812d** revealed the characteristic anomeric H2′ resonances at δ_H 5.96–6.15 ppm. The large 1,2-diaxial coupling constants ($J_{2ax,3ax}$ 10.7–11.1 Hz)

indicated that the triazole moieties adopted an equatorial position. Quaternary carbons resonated at δ_C 98.4–98.7 ppm also confirmed the presence of the spiroacetal ring system (Table 5.12).

NOESY studies confirmed the *bis*-anomerically stabilised structures of triazoles **812a**, **812c** and **812d** by observation of a correlation between H2′ and H8′ of the neighbouring rings. This correlation is only possible when the spiroacetal ring adopts a *bis*-anomerically stabilised conformation and the triazole substituent adopts an equatorial position.

The ^{1}H and ^{13}C NMR chemical shifts for triazoles **812a**, **812c** and **812d** were very similar to the corresponding C8-substituted spiroacetals **909f**, **909a** and **909e**. These similarities were not surprising since the spiroacetals adopted the thermodynamically-favoured *bis*-anomerically stabilised conformation as depicted in Table 5.12.

The 1,4-disubstitution in triazoles **812c** and **812d** cannot be confirmed unambiguously due to the absence of long range C2′–H5 or H2′–C5 correlations in the weak HMBC spectra. The 1,4-disubsitution of **812c** and **812d** was indirectly established by the close similarity of the ^{1}H and ^{13}C NMR chemical shifts with the closely related and structurally confirmed C8-substituted spiroacetals **909a** and **909e** (Table 5.12).

Atom number	***Chemical Shifts (δ in ppm)***					
	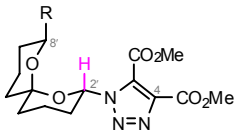		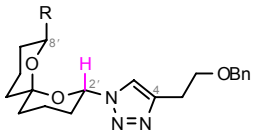		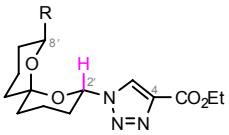	
	812a: R = H	**909f**: R = $CH_2OTBDPS$	**812c**: R = H	**909a**: R = $CH_2OTBDPS$	**812d**: R = H	**909e**: R = $CH_2OTBDPS$
H2′	6.15, dd (*J* 10.7 and 3.1 Hz)	6.18, dd (*J* 10.6 and 3.0 Hz)	5.96, dd (*J* 11.1 and 2.2 Hz)	6.01, dd (*J* 11.1 and 2.4 Hz)	6.05, dd (*J* 10.9 and 2.4 Hz)	6.07, dd (*J* 10.9 and 2.2 Hz)
H5	----	----	7.58	7.54	8.29	8.25
C2′	82.7	82.8	81.2	81.0	81.7	81.6
C3′	30.3	30.4	31.0	30.8	31.4	31.2
C4′	17.6	17.5	18.2	18.0	17.8	17.8
C5′	34.5 or 35.0	34.4	34.6	34.5	34.5 or 34.9	34.4
C6′	98.9	99.4	98.4	98.8	98.7	99.2
C8′	61.1	71.0	61.1	71.0	61.2	71.3
C9′	24.8	26.6	24.9	26.5	24.9	26.4
C10′	18.0	17.8	18.1	18.1	18.1	18.1
C11′	34.5 or 35.0	34.7	35.0	34.6	34.5 or 34.9	34.5

Table 5.12: Characteristic ^{1}H and ^{13}C NMR chemical shifts of the spiroacetal unit present in triazoles **812a**, **812c** and **812d**. Their related C8-substituted spiroacetals **909f**, **909a** and **909e** are depicted here for comparison.

(b) Stereochemistry

Only the equatorial triazoles, generated from the minor equatorial azide **814a** bearing the *bis*-anomerically stabilised spiroacetal, were isolated from all of the cycloaddition reactions that were conducted. The axial triazoles, generated from axial azide **814b** bearing the mono-anomerically stabilised spiroacetal, were believed to be unstable and degraded under the reaction conditions. The low and variable yields may also be due to the volatility of the initial azide mixtures and the use of crude starting materials. The exact ratio of equatorial and axial azides **814a** and **814b** present in the crude mixture was unknown and did vary between batches. Therefore, it was unclear whether or not any of the axial triazole that formed, in fact, equilibrated to the equatorial isomer.

5.6 Synthesis of Spiroacetal Nitrile 858

With the successful generation of spiroacetal-nucleosides and triazoles, the next diversity oriented synthesis was investigated. Due to its unique features, tetrazoles are isosteres of carboxylic acid and *cis*-peptides depending on the nature of its substituent[57] and they can be synthesised *via* the cycloaddition of nitriles to azides.

Using the procedure adapted from Trost *et al*.[53], acetal **817** was reacted with TMSOTf to generate an oxonium ion which was subsequently trapped by TMSCN to give nitrile **858** in 7% yield (Scheme 5.26). The observed ^{1}H and ^{13}C NMR chemical shifts indicated that nitrile **858** adopted a *bis*-anomerially stabilised structure with the cyano substituent adopting an equatorial position.

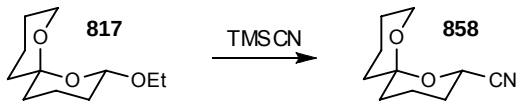

Reagents and conditions: (a) TMSOTf, TMSCN, CH_2Cl_2, 0 °C, 3 h, 7%.

Scheme 5.26: Synthesis of nitrile **858** from acetal **817**.

Although this reaction has not been optimised, the 7% yield is very low. This low yield together with the volatility of nitrile **858** rendered the use of nitrile **858** as a key intermediate for further synthetic works unusable and this approach was abandoned.

5.7 Summary and Conclusion

In conclusion, the yield obtained for oxaspirolactone **818** synthesis from butynol **836** has been successfully optimised to 75% over five steps, which was an improvement from the 6% yield

previously reported in literature.[2] Acetate **815** was also successfully prepared in two steps from oxaspirolactone **818** as planned. Modifications to the synthetic route afforded the alternative intermediate, namely acetal **817** in 79% over two steps *via* hydrogenation of aldehyde **839** (Scheme 5.27).

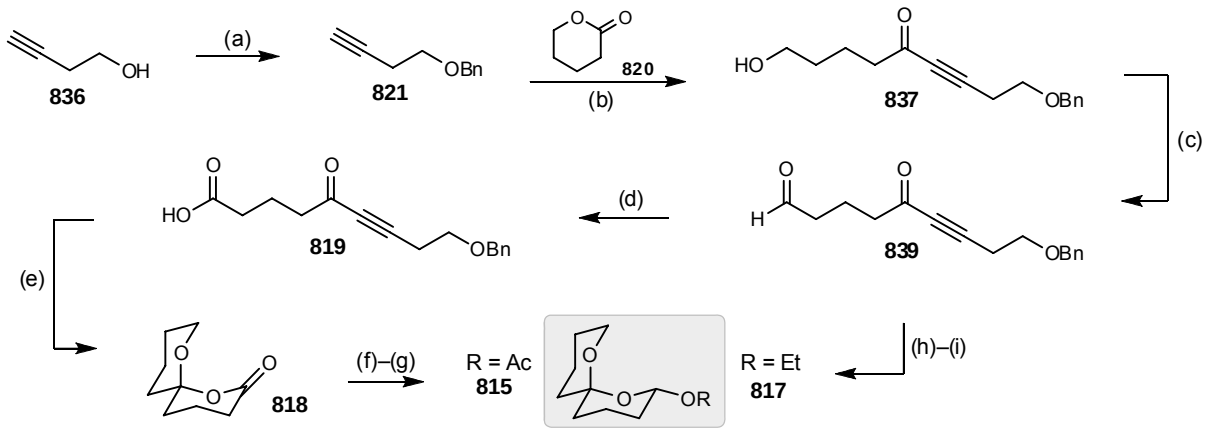

Reagents and conditions: (a) i. NaH, THF, 0 °C, 30 min; ii. BnBr, THF, 0 °C→rt, 18 h, 99%; (b) i. BuLi, THF, -78 °C, 30 min; ii. **820**, THF, -78 °C, 2 h, 87%; (c) cat. TEMPO, $PhI(OAc)_2$, KH_2PO_4, MeCN–H_2O, rt, 6 h; (d) $NaClO_2$, cyclohexene, KH_2PO_4, ^tBuOH–H_2O, rt, 2 h, 92% over 2 steps; (e) i. H_2, cat. Pd/C, cat. AcOH, THF, rt, 18 h; ii. AcOH, toluene, 30-35 °C, 30 mmHg, 94%; (f) i. DIBAL-H, toluene, -78 °C, 15 min; (g) Ac_2O, NEt_3, cat. DMAP, CH_2Cl_2, 0 °C→rt, 20 h, 25% over 2 steps; (h) H_2, cat. Pd/C, cat. *p*-TsOH, EtOH–CH_2Cl_2, rt, 18 h; (i) *p*-TsOH, aq. EtOH–CH_2Cl_2, rt, 18 h, 79% over 2 steps.

Scheme 5.27: Synthesis of the key intermediates: acetate **815** and acetal **817**.

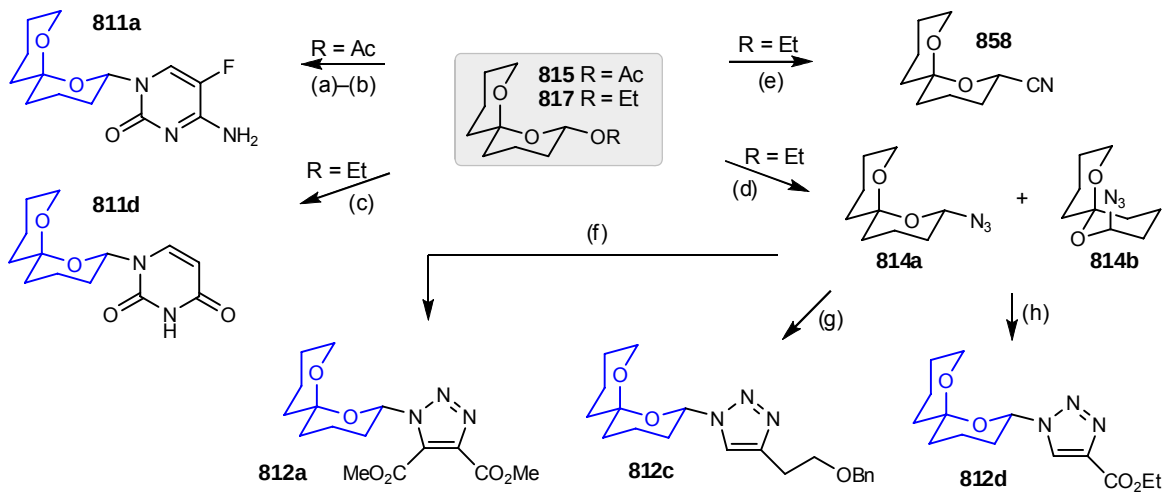

Reagents and conditions: (a) ^{5F}C, BSA, reflux, 1 h; (b) **815**, TMSOTf, CH_2Cl_2, 0 °C→rt, 20 h, 39%; (c) i. U, BSA, reflux, 1 h; ii. **817**, TMSOTf, CH_2Cl_2, 0 °C→rt, 19%; (d) **817**, $TMSN_3$, TMSOTf, CH_2Cl_2, 0 °C, 3 h, 71% (**814a**:**814b** 1:3); (e) **817**, TMSOTf, TMSCN, CH_2Cl_2, 0 °C, 3 h, 7%; (f) DMAD, 80 °C, 3 h, 25%; (g) **821**, CuI, DIPEA, toluene, rt, 2 d, 10%; (h) **858**, cat. CuI•$P(OEt)_3$, toluene, rt, 18 h, 23%.

Scheme 5.28: Synthesis of spiroacetal nucleosides **811** and triazoles **812**.

With the successful synthesis of acetate **815** and acetal **817** as key intermediates, spiroacetal nucleosides **811** and triazole derivatives **812** were next prepared (Scheme 5.28). Although the yields

of the derivatives obtained were moderate, this model study has demonstrated the feasibility and flexibility of the synthetic route.

The model study was designed to aid the subsequent synthesis of the C8′-hydroxymethyl substituted targets by providing significant quantities of spiroacetals with which to develop nucleosidation protocols as well as to gather information and experience during the synthetic investigation. The models themselves were synthesised, but not without problems. The unsubstituted spiroacetal structure is volatile and labile and readily undergoes ring-opening reactions. A slight change of structure such as the introduction of a substituent on the ring may well stabilise the spiroacetal and increase its boiling point, thus allowing a wider range of reagents and conditions to be used to effect subsequent reactions. It was, therefore, envisioned that the low yield reactions encountered in the model study may not be extended to the subsequent synthesis of targets bearing a C8′-hydroxymethyl substitutent. Moreover, the synthesis of these C8′-substituted targets may improve the volatility and stability of the spiroacetal structures.

The stereochemistry of the new spiroacetal analogues that generated adopted an equatorial position on anomeric centre rather than the axial position as initially desired. Despite this deviation in stereochemistry of the product obtained, this model study had, nevertheless, provided valuable information for the synthesis of the novel spiroacetal hybrids. Satisfied with the results achieved so far, it was envisioned that the synthetic method hitherto developed for the unsubstituted spiroacetal ring, could be extended to the synthesis of C8′-hydroxymethyl substituted targets. In the next chapter, efforts towards the synthesis of the C8′-hydroxymethyl substituted spiroacetal-nucleoside and triazole analogues are described.

5.8 References

1. W. Kitching, Personal Communication.
2. J. E. Robinson, Bachelor of Science (Honours) Dissertation, The University of Auckland, 2001.
3. R. E. Ireland and D. Häbich, *Chem. Ber.*, 1981, **114**, 1418-1427.
4. K. T. Mead and R. Zemribo, *Synlett*, 1996, 1063-1064.
5. M. A. Brimble, F. A. Fares and P. Turner, *J. Chem. Soc., Perkin Trans. 1*, 1998, 677-684.
6. R. Zemribo and K. T. Mead, *Tetrahedron Lett.*, 1998, **39**, 3895-3898; R. Zemribo and K. T. Mead, *Tetrahedron Lett.*, 1998, **39**, 3891-3894.
7. J. Robertson and J. W. P. Dallimore, *Org. Lett.*, 2005, **7**, 5007-5010.
8. J.-P. Vidal, R. Escale, J.-P. Girard, J.-C. Rossi, J.-M. Chantraine and A. Aumelas, *J. Org. Chem.*, 1992, **57**, 5857-5860.
9. J. B. Ousset, C. Mioskowski, Y.-L. Yang and J. R. Falck, *Tetrahedron Lett.*, 1984, **25**, 5903-5906.
10. S. V. Ley, B. Lygo, H. M. Organ and A. Wonnacott, *Tetrahedron*, 1985, **41**, 3825-3836.
11. R. Baker, A. L. Boyes and C. J. Swain, *J. Chem. Soc., Perkin Trans. 1*, 1990, 1415-1421; J. Chen, M. T. Fletcher and W. Kitching, *Tetrahedron: Asymmetry*, 1995, **6**, 967-972; Y. Q. Tu, A. Hubener, H. S. Zhang, C. J. Moore, M. T. Fletcher, P. Hayes, K. Dettner, W. Francke, C. S. P. McErlean and W. Kitching, *Synthesis*, 2000, 1956-1978; J. L. Koviach, M. D. Chappell and R. L. Halcomb, *J. Org. Chem.*, 2001, **66**, 2318-2326; J. W. Lane and R. L. Halcomb, *Tetrahedron*, 2001,

57, 6531-6538; J. W. Lane and R. L. Halcomb, *J. Org. Chem.*, 2002, **68**, 1348-1357; S. Cahill and M. O'Brien, *Tetrahedron Lett.*, 2006, **47**, 3665-3668; M. T. Crimmins and A. C. DeBaillie, *J. Am. Chem. Soc.*, 2006, **128**, 4936-4937; M. A. Brimble, G. M. Williams, R. Baker and M. James, *Tetrahedron Lett.*, 1990, **31**, 3043-3046; M. A. Brimble, G. M. Williams and R. Baker, *J. Chem. Soc., Perkin Trans. 1*, 1991, 2221-2227; P. R. Allen, M. A. Brimble and F. A. Fares, *J. Chem. Soc., Perkin Trans. 1*, 1998, 2403-2411; M. A. Brimble, J. H. Park and C. M. Taylor, *Tetrahedron*, 2003, **59**, 5861-5868; M. A. Brimble, J. E. Robinson, K. W. Choi and P. D. Woodgate, *Aust. J. Chem.*, 2004, **57**, 665-668; J. E. Robinson and M. A. Brimble, *Chem. Comm.*, 2005, 1560-1562; M. A. Brimble, C. L. Flowers, M. Trzoss and K. Y. Tsang, *Tetrahedron*, 2006, **62**, 5883-5896; M. A. Brimble and C. J. Bryant, *Chem. Comm.*, 2006, 4506-4508; M. A. Brimble and C. J. Bryant, *Org. Biomol. Chem.*, 2007, **5**, 2858-2866; J. E. Robinson and M. A. Brimble, *Org. Biomol. Chem.*, 2007, **5**, 2572-2582.

12. J. Doubský , L. Streinz, D. Šaman, J. Zedník and B. Koutek, *Org. Lett.*, 2004, **6**, 4909-4911.
13. M. A. Brimble, F. A. Fares and P. Turner, *Aust. J. Chem.*, 2000, **53**, 845-851.
14. P. R. Allen, M. A. Brimble and H. Prabaharan, *J. Chem. Soc., Perkin Trans. 1*, 2001, 379-389.
15. H. Fukuda, M. Takeda, Y. Sato and O. Mitsunobu, *Synthesis*, 1979, 368-370; M. Yamamoto, M. Yoshitake and K. Yamada, *J. Chem. Soc., Chem. Comm.*, 1983, 991-992; P. DeShong and D. R. Sidler, *J. Org. Chem.*, 1988, **53**, 4892-4894; P. Deshong and P. J. Rybczynski, *J. Org. Chem.*, 1991, **56**, 3207-3210.
16. D. H. Davies, J. Hall and E. H. Smith, *J. Chem. Soc., Perkin Trans. 1*, 1989, 837-838.
17. Y. Q. Tu, K. A. Byriel, C. H. L. Kennard and W. Kitching, *J. Chem. Soc., Perkin Trans. 1*, 1995, 1309-1315.
18. C. J. Burns, M. Gill and S. Saubern, *Aust. J. Chem.*, 1997, **50**, 1067-1079.
19. K. Bowden, I. M. Heilbron, E. R. H. Jones and B. C. L. Weedon, *J. Chem. Soc.*, 1946, 39-45; I. Heilbron, E. R. H. Jones and F. Sondheimer, *J. Chem. Soc.*, 1949, 604-607; A. Bowers, T. G. Halsall, E. R. H. Jones and A. J. Lemin, *J. Chem. Soc.*, 1953, 2548-2560.
20. P. L. Anelli, C. Biffi, F. Montanari and S. Quici, *J. Org. Chem.*, 1987, **52**, 2559-2562; M. R. Leanna, T. J. Sowin and H. E. Morton, *Tetrahedron Lett.*, 1992, **33**, 5029-5032.
21. K. Omura and D. Swern, *Tetrahedron*, 1978, **34**, 1651-1660; J. Sisko, J. R. Henry and S. M. Weinreb, *J. Org. Chem.*, 1993, **58**, 4945-4951.
22. W. P. Griffith, S. V. Ley, G. P. Whitcombe and A. D. White, *J. Chem. Soc., Chem. Comm.*, 1987, 1625-1627; W. P. Griffith and S. V. Ley, *Aldrichimica Acta*, 1990, **23**, 13-19.
23. E. J. Corey and J. W. Suggs, *Tetrahedron*, 1975, **16**, 2647-2650; Y.-S. Cheng, W.-L. Liu and S.-H. Chen, *Synthesis*, 1980, 223-224; D. Savoia, C. Trombini and A. Umani-Ronchi, *J. Org. Chem.*, 1982, **47**, 564-566; B. M. Trost, T. A. Grese and D. M. T. Chan, *J. Am. Chem. Soc.*, 1991, **113**, 7350-7362.
24. D. B. Dess and J. C. Martin, *J. Org. Chem.*, 1983, **48**, 4155-4156; D. B. Dess and J. C. Martin, *J. Am. Chem. Soc.*, 1991, **113**, 7277-7287; M. Frigerio, M. Santagostino and S. Sputore, *J. Org. Chem.*, 1999, **64**, 4537-4538.
25. A. De Mico, R. Margarita, L. Parlanti, A. Vescovi and G. Piancatelli, *J. Org. Chem.*, 1997, **62**, 6974-6977; I. Paterson, G. J. Florence, K. Gerlach, J. P. Scott and N. Sereinig, *J. Am. Chem. Soc.*, 2001, **123**, 9535-9544.
26. B. S. Bal, W. E. J. Childers and H. W. Pinnick, *Tetrahedron*, 1981, **37**, 2091-2096; C. A. Weir and C. M. Taylor, *J. Org. Chem.*, 1999, **64**, 1554-1558.
27. T. Murano, S. Muroyama, T. Yokomatsu and S. Shibuya, *Synlett*, 2002, 1657-1660; T. Murano, Y. Yuasa, S. Muroyama, T. Yokomatsu and S. Shibuya, *Tetrahedron*, 2003, **59**, 9059-9073.
28. A. H. Butt, J. M. Percy and N. S. Spencer, *Chem. Comm.*, 2000, 1691-1692.
29. R. M. Beesley, C. K. Ingold and J. F. Thorpe, *J. Chem. Soc.*, 1915, **107**, 1080-1106; C. K. Ingold, *J. Chem. Soc.*, 1921, **119**, 305-329; C. K. Ingold, S. Sako and J. F. Thorpe, *J. Chem. Soc.*, 1922, **121**, 1177-1198; J. Kaneti, A. J. Kirby, A. H. Koedjikov and I. G. Pojarlieff, *Org. Biomol. Chem.*, 2004, **2**, 1098-1103.
30. M. E. Jung and G. Piizzi, *Chem. Rev.*, 2005, **105**, 1735-1766.
31. P. Galatsis, in *e-EROS Encyclopedia of Reagents for Organic Synthesis*, ed. L. A. Paquette, Wiley Interscience, 2001.
32. M. G. B. Drew, S. Gorsuch, J. H. M. Gould and J. Mann, *J. Chem. Soc., Perkin Trans. 1*, 1999, 969-978.
33. C. Lescop and F. Huet, *Tetrahedron*, 2000, **56**, 2995-3003; S. Wendeborn, G. Binot, M. Nina and T. Winkler, *Synlett*, 2002, 1683-1687; L. A. Paquette, A. L. Kahane and C. K. Seekamp, *J. Org. Chem.*, 2004, **69**, 5555-5562; R. Alibés, A. Alvárez-Larena, P. de March, M. Figueredo, J. Font, T. Parella and A. Rustullet, *Org. Lett.*, 2006, **8**, 491-494; E. Rozners and Y. Liu, *J. Org. Chem.*, 2005, **70**, 9841-9848.

34. L. A. Paquette, R. T. Bibart, C. K. Seekamp and A. L. Kahane, *Org. Lett.*, 2001, **3**, 4039-4041; L. A. Paquette, D. R. Owen, R. T. Bibart and C. K. Seekamp, *Org. Lett.*, 2001, **3**, 4043-4045.
35. L. A. Paquette, C. K. Seekamp, A. L. Kahane, D. G. Hilmey and J. Gallucci, *J. Org. Chem.*, 2004, **69**, 7442-7447.
36. M. T. Fletcher, B. J. Wood, I. M. Brereton, J. E. Stok, J. J. De Voss and W. Kitching, *J. Am. Chem. Soc.*, 2002, **124**, 7666-7667; P. Hayes, M. T. Fletcher, C. J. Moore and W. Kitching, *J. Org. Chem.*, 2001, **66**, 2530-2533.
37. T. Lister and M. V. Perkins, *Angew. Chem. Int. Ed.*, 2006, **45**, 2560-2564; R. Zemribo and K. T. Mead, *Synlett*, 2000, 1569-1572; K. T. Mead and R. Zemribo, *Synlett*, 1996, 1065-1066; G. Vidari, G. Lanfranchi, N. Pazzi and S. Serra, *Tetrahedron Lett.*, 1999, **40**, 3063-3066; B. M. Trost and J. R. Corte, *Angew. Chem. Int. Ed.*, 1999, **38**, 3664-3666; M. de Greef and S. Z. Zard, *Org. Lett.*, 2007, **9**, 1773-1776.
38. Z.-Q. Xia, M. A. Costa, H. C. Pèlissier, L. B. Davin and N. G. Lewis, *J. Biol. Chem.*, 2001, **276**, 12614-12623.
39. M. Zaidlewicz and H. Brown, in *e-EROS Encyclopedia of Reagents for Organic Synthesis*, ed. L. A. Paquette, Wiley Interscience, 2001.
40. P. Deslongchamps, D. D. Rowan, N. Pothier, T. Sauvé and J. K. Saunders, *Can. J. Chem.*, 1981, **59**, 1105-1121.
41. M. A. Brimble, *Molecules*, 2004, **9**, 394-404; G. J. McGarvey and M. W. Stepanian, *Tetrahedron Lett.*, 1996, **37**, 5461-5464; G. J. McGarvey, M. W. Stepanian, A. R. Bressette and J. F. Ellena, *Tetrahedron Lett.*, 1996, **37**, 5465-5468.
42. L. A. Paquette, C. K. Seekamp and A. L. Kahane, *J. Org. Chem.*, 2003, **68**, 8614-8624.
43. B. A. Kulkarni, G. P. Roth, E. Lobkovsky and J. A. Porco, Jr., *J. Comb. Chem.*, 2002, **4**, 56-72.
44. K. Y. Tsang and M. A. Brimble, *Tetrahedron*, 2007, **63**, 6015-6034.
45. A. Ben, T. Yamauchi, T. Matsumoto and K. Suzuki, *Synlett*, 2004, 225-230; S. Kobayashi, *Eur. J. Org. Chem.*, 1999, 15-27.
46. C. Brocke, M. A. Brimble, D. S. H. Lin and M. D. McLeod, *Synlett*, 2004, 2359-2363; B. R. Buckley, P. C. B. Page, H. Heaney, E. P. Sampler, S. Carley, C. Brocke and M. A. Brimble, *Tetrahedron*, 2005, **61**, 5876-5888; M. A. Brimble and C. Brocke, *Eur. J. Org. Chem.*, 2005, 2385-2396; A. Lehmann, C. Brocke, D. Barker and M. A. Brimble, *Eur. J. Org. Chem.*, 2006, 3205-3215.
47. H. Vorbrüggen and C. Ruh-Pohlenz, *Org. React.*, 2000, **55**, 1-630; H. Vorbrüggen and C. Ruh-Pohlenz, *Handbook of Nucleoside Synthesis*, John Wiley & Sons, Inc., Chichester, UK, 2001.
48. N. Cohen, B. Schaer, G. Saucy, R. Borer, L. Todaro and A.-M. Chiu, *J. Org. Chem.*, 1989, **54**, 3282-3292.
49. J.-D. Ye, X. Liao and J. A. Piccirilli, *J. Org. Chem.*, 2005, **70**, 7902-7910; K. Van derpoorten and M. E. Migaud, *Org. Lett.*, 2004, **6**, 3461-3464.
50. N. B. Perry, J. W. Blunt, M. H. G. Munro and A. M. Thompson, *J. Org. Chem.*, 1990, **55**, 223-227; N. B. Perry, J. W. Blunt, M. H. G. Munro and L. K. Pannell, *J. Am. Chem. Soc.*, 1988, **110**, 4850-4851.
51. A. J. Kirby, *Stereoelectronic Effects*, 1st edn., Oxford University Press, Oxford, 1996.
52. M. Böhringer, H.-J. Roth, J. Hunziker, M. Göbel, R. Krishnan, A. Giger, B. Schweizer, J. Schreiber, C. Leumann and A. Eschenmoser, *Helv. Chim. Acta*, 1992, **75**, 1416-1477.
53. B. M. Trost, H. B. Yang and G. D. Probst, *J. Am. Chem. Soc.*, 2004, **126**, 48-49.
54. C. W. Tornøe, C. Christensen and M. Meldal, *J. Org. Chem.*, 2002, **67**, 3057-3064.
55. V. V. Fokin, V. V. Rostovtsev, L. G. Green and K. B. Sharpless, *Angew. Chem. Int. Ed.*, 2002, **41**, 2596-2599.
56. J. M. Casas-Solvas, A. Vargas-Berenguel, L. F. Capitan-Vallvey and F. Santoyo-Gonzalez, *Org. Lett.*, 2004, **6**, 3687-3690.
57. Maybridge, *Bioisosteres in Medicinal Chemistry*, Thermo Fisher Scientific, Cornwall; Z. P. Demko and K. B. Sharpless, *Angew. Chem. Int. Ed.*, 2002, **41**, 2110-2113; Z. P. Demko and K. B. Sharpless, *Angew. Chem. Int. Ed.*, 2002, **41**, 2113-2116.

Chapter Six:

6

Discussion: Synthesis of Functionalised Spiroacetals

6.1 Retrosynthetic Analysis of Spiroacetal Targets 808–810

Having successfully developed the methodology to synthesise the model spiroacetals **811** and **812**, attention next focused on the synthesis of spiroacetal-nucleosides **808** and spiroacetal-triazoles **809** bearing a C8′-hydroxymethyl substituent. Preliminary work towards the synthesis of spiroacetal-amino acids **810** will also be investigated, thus enabling the synthesis of a small library of spiroacetal hybrids (Figure 6.1).

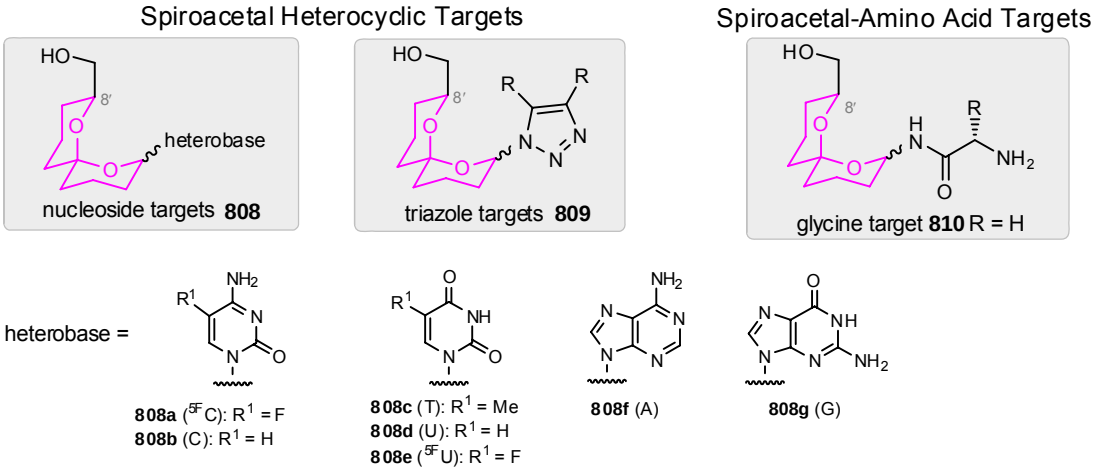

Figure 6.1: Spiroacetal-heterocycle targets **808** and **809** and amino acid targets **810** bearing a C8′-hydroxymethyl group.

The focus of this research has directed towards the elaboration of a 6,6-spiroacetal framework with bioactive motifs in order to achieve diversity oriented synthesis (DOS). Therefore, it is important that a flexible and convergent strategy is adopted to facilitate possible derivatisation of a common intermediate.

6.1.1 Retrosynthesis—the First Approach

Following the lead from the model study, the proposed retrosynthesis of spiroacetal targets **808–810** hinges on the disconnection of the anomeric C–N bond that links the spiroacetal with the heterocyclic or amino acid motifs. For nucleoside analogues **808**, this connection is initially generated by the nucleosidation under Vorbrüggen conditions of spiroacetals **861** and **862** bearing a leaving group at the anomeric position. For triazole analogues **809**, the spiroacetal–heterocycle connection is initially generated by conversion of the leaving group in spiroacetals **861** and **862** to an azide that can then act as a cycloaddition partner. For amino acid analogues, spiroacetal-glycine **810** was chosen as the initial target for this preliminary investigation. The spiroacetal-amino acid

connection is generated by the Staudinger ligation of an activated glycine derivative and azide **860** which is also a precursor used in the synthesis of triazoles **809**. Spiroacetals **861** and **862**, in turn, are prepared *via* reduction and protection of oxaspirolactone **863** (Scheme 6.1).

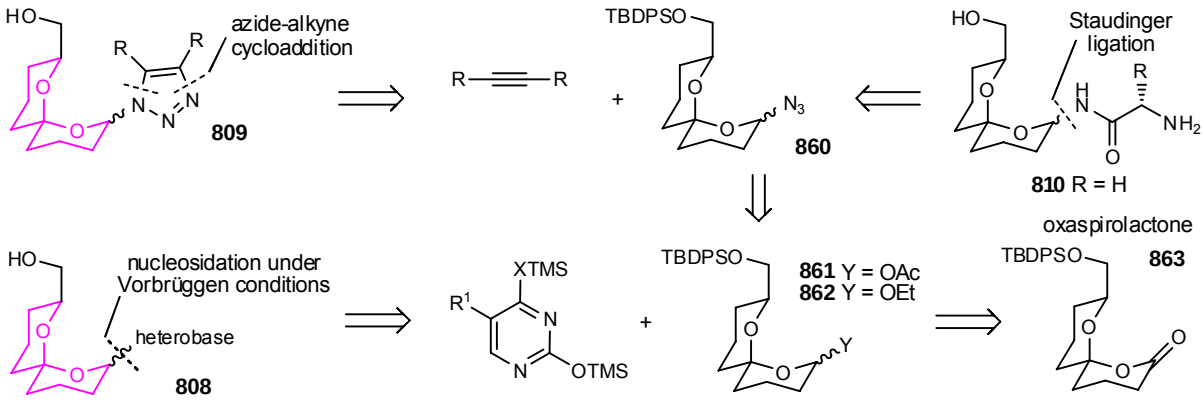

Scheme 6.1: Proposed retrosynthesis of spiroacetal targets (nucleosides **808**, triazoles **809** and amino acids **810**) from oxaspirolacetone **863**.

Oxaspirolactone **863** is envisaged to be cyclised from carboxylic acid **864**. Further disconnection of **864** leads to valerolactone **865** and silylated butynol **866** (Scheme 6.2). The syntheses of **865** and **866** have been previously described in the literature.[1,2]

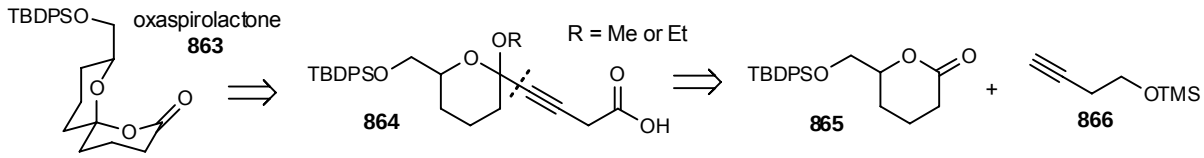

Scheme 6.2: Proposed retrosynthesis of oxaspirolactone **863**.

6.1.2 Retrosynthesis—the Second Approach

Given the potential failures and flaws of the attempted synthesis towards oxaspirolactone **863** as observed in the model study reported in Chapter 5, a second and more direct approach is also proposed.

The revised retrosynthesis directly targeted spiroacetal acetate **861** and ethoxy-spiroacetal **862**, thus bypassing the use of the problematic oxaspirolactone **863** as an intermediate. Based on the model study, acetate **861** and acetal **862** can be obtained *via* deprotection-cyclisation of ketone **867** (Scheme 6.3).

Further disconnection of ketone **867** gives valerolactone **865** and Grignard reagent **868**. The use of Grignard reagent **868** is an alternative to the four-carbon synthon equivalent to the protected

butynols **821** and **866**. This revised synthetic route bypasses the acetylide addition step, thus avoiding the reactive ynone functionality and the need for subsequent hydrogenation. Grignard reagent **868** is chosen specifically to carry a masked aldehyde functionality in order to avoid the necessity of potentially problematic oxidation later in the synthesis. Grignard reagent **868** was generated from bromide **869** which was, in turn, synthesised from either butyrolactone **870** or tetrahydrofuran (Scheme 6.3).

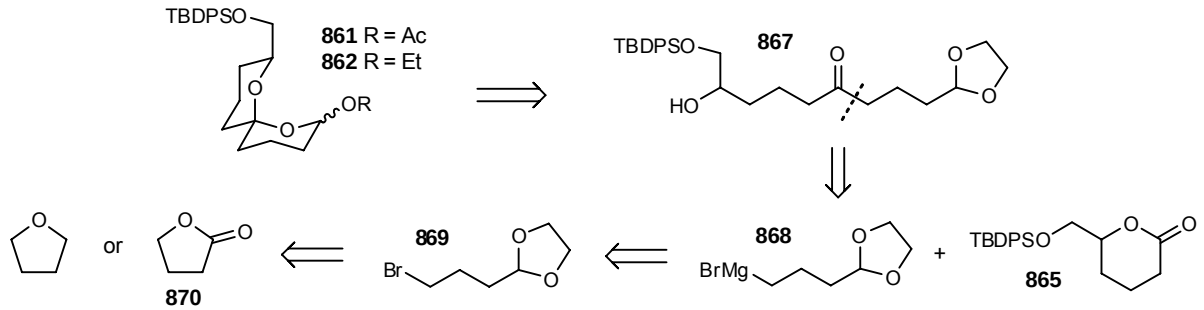

Scheme 6.3: Revised retrosynthesis of acetate **861** and ethoxy-spiroacetal **862**.

6.2 Previous Synthesis of Similar Structures

To date, the synthesis of a 6,6-spiroacetal that bears a heterobase, triazole or amino acid at the anomeric position, has not been reported, reflecting the novelty of these hybrid structures. Several molecules of similar structure have been reported in the literature and are discussed below.

(a) Nucleosides

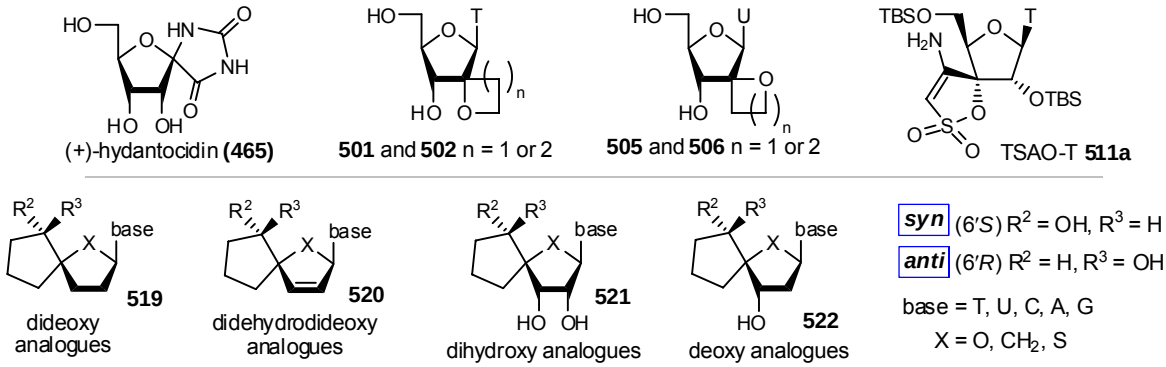

Scheme 6.4: [Top] 1′-, 2′- and 3′-spirocyclic nucleosides. [Bottom] Paquette's 4′-spirocyclic nucleosides. The syntheses of these spirocyclic nucleosides were discussed in Chapter 2.6.

The syntheses of several spirocyclic nucleosides have been previously described in Chapter 2.6. In particular, 4′-spirocyclic nucleosides **519–522** synthesised by Paquette's group[3] bear

some similarity to our target spiroacetal nucleosides **808** with respect to the spirocyclic structure (Scheme 6.4).

(b) Triazoles and Amides

Ley *et al*.[4] described a diversity oriented synthesis (DOS) based on 6,6-spiroacetal scaffolds. In particular, spiroacetal-triazole **254** bears a striking resemblance to our targets **809**. Spiroacetal-triazole **254** was prepared *via* cycloaddition of phenyl acetylene to azide **871** which, in turn, was obtained from spiroacetal **248**. The synthesis of **248** was described in Chapter 1.5.3. Oxidation of alcohol **248**, followed by the coupling of the resultant acid **253** with 2-picolyl amine, gave spiroacetal **255** (Scheme 6.5).

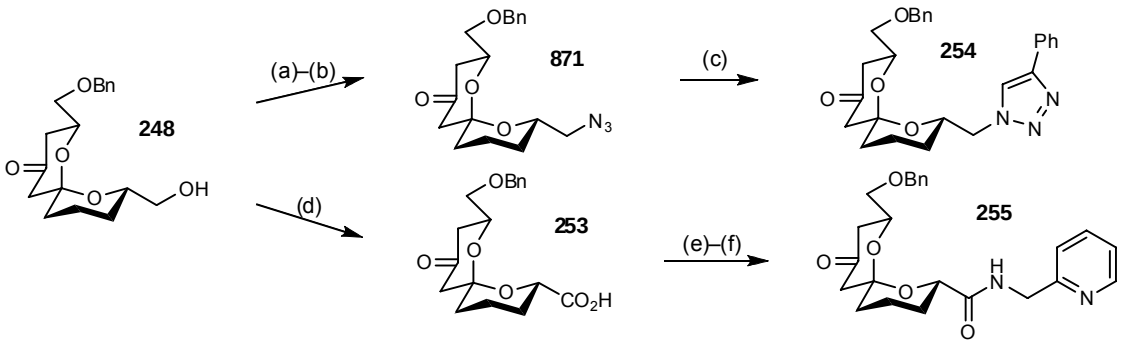

Reagents and conditions: (a) Tf_2O, pyridine, CH_2Cl_2, -78 °C→rt, 30 min; (b) NaN_3, DMF, rt, 1 h, 100% over 2 steps; (c) phenyl acetylene, cat. $CuSO_4$, sodium ascorbate, H_2O–^{t}BuOH, rt, 3 h, 100%; (d) PDC, DMF, rt, 18 h; (e) *p*-nitrophenyl chloroformate, pyridine, THF, rt, 20 min; (f) 2-picolyl amine, rt, 10 min, 90% over 3 steps.

Scheme 6.5: Synthesis of spiroacetal-triazole **254** and amide **255** by Ley *et al*.[4] Syntheses of other 6,6-spiroacetal based analogues from the same study were discussed in Chapter 1.5.3.

During the structure-activity studies (SAR) of TSAO analogues, it was discovered that the glycoside spirocyclic moiety of TSAO is crucial for the observed antiviral activity due to its interaction with the reverse transcriptase. On the other hand, the heterobase moiety is not strictly recognised by the enzyme, thus suggesting that possible structural modification of this moiety could also be used to modulate the cytotoxicity of TSAO analogues.[5]

Based on these foundings, Camarasa *et al*.[5] synthesised a range of TSAO-triazole analogues during their SAR studies to determine the role of the heterobase in the interaction between TSAO derivatives and the target enzymes. From the range of TSAO triazole analogues synthesised and tested, **874a–c** and **875d** were shown to exhibit interesting activity (EC_{50} = 0.06–0.92 μM and CC_{50} = 20–165 μM). The synthesis of triazoles **874** and **875** started with the conversion of acetate **872** to azide **873** and subsequent thermally-promoted cycloaddition with the appropriate alkyne to give a mixture of TSAO-triazoles **874a–c** and **875a–c**. Treatment of the regioisomeric mixture of **874c** and **875c** with dimethylamine afforded **874d** and **875d** (Scheme 6.6).

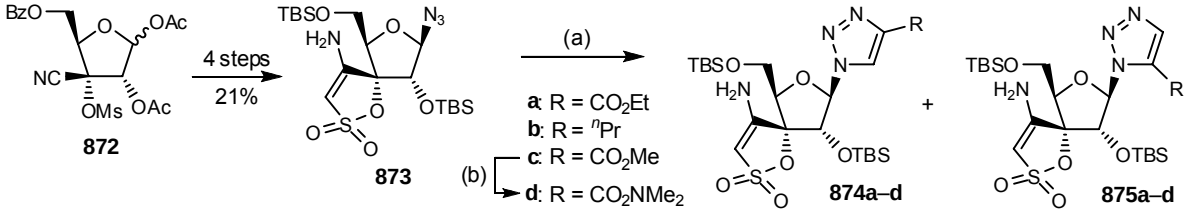

Reagents and conditions: (a) HC≡CR, toluene, reflux, 18 h–2 d, **874a–c**: 26–67%, **875a–c**: 18–25%; (b) **874c** and **875c** (3:1), $NHMe_2$, EtOH, rt, 8 h, **874d**: 58%, **875d**: 19%.

Scheme 6.6: Synthesis of anti-HIV TSAO-triazole analogues **874** and **875** by Camarasa *et al.*[5]

6.3 Attempted Syntheses of Oxaspirolactone 863

The initial strategy for the synthesis of oxaspirolactone **863** is based on an extension from the model study. The proposed synthesis relies on the key dehydrative cyclisation of acids **864** which can be obtained from the oxidation of alcohols **876**. Acetals **876** are cyclised from a keto-alcohol adduct obtained from the coupling between valerolactone **865**[1] and alkyne **866**[2] (Scheme 6.7).

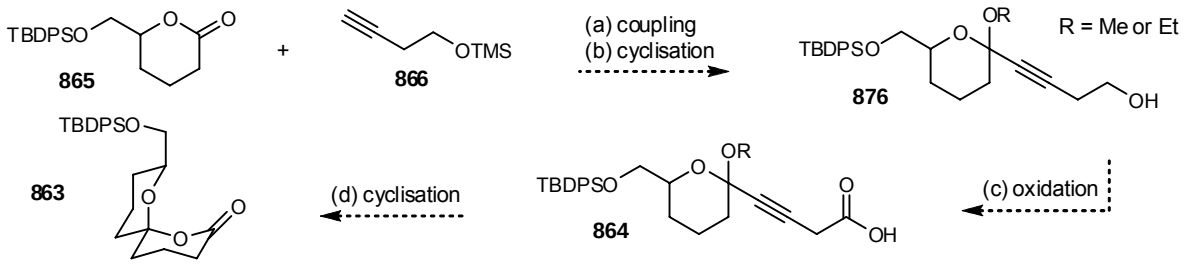

Scheme 6.7: Proposed synthesis of oxaspirolactone **863**.

6.3.1 Synthesis of Valerolactone 865

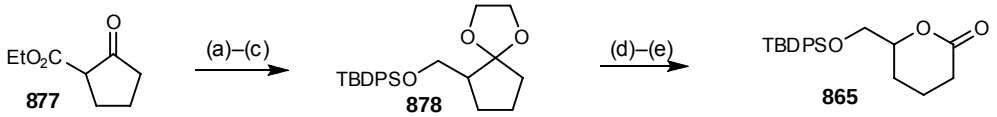

Reagents and conditions: (a) ethylene glycol, *p*-TsOH, CH_2Cl_2, reverse Dean-Stark apparatus, reflux, 18 h, 100%; (b) $LiAlH_4$, Et_2O, reflux, 4 h, 98%; (c) TBDPSCl, cat. DMAP, NEt_3, CH_2Cl_2, rt, 18 h, 92%; (d) cat. PPTS, aq. acetone, reflux, 4 h, 99%; (e) *m*-CPBA, $NaHCO_3$, CH_2Cl_2, rt, 3 h, 97%.

Scheme 6.8: Synthesis of valerolactone **865** adapted from Taylor *et al.*[1]

The synthesis of oxaspirolactone **863** started with the preparation of valerolactone **865** from ethyl 2-oxocyclopentanecarboxylate **(877)** using the procedures adapted from Taylor *et al.*[1] Under these adapted procedures, valerolactone **865** was obtained in five steps with an overall yield of 87%

(Scheme 6.9). Although shorter syntheses[6,7] with three or four steps may be possible, the current five step procedure proved to be reproducible, high yielding and scalable to *ca.* 15 g, thus the shorter routes were not investigated further.

6.3.2 Attempted Synthesis (1)—via Keto-diol 879

With the starting materials in hand, the first synthetic route to oxaspirolactone **863** was investigated. Lithium acetylide, generated from protected alkyne **866**[2], was added to valerolactone **865** in THF using the protocol developed in the model study to afford keto-diol **879**. However, the subsequent cyclisation of **879** using either Amberlite IR118 in MeOH or PPTS in EtOH failed to yield methoxy or ethoxy-spiroacetals **876** and only starting material **879** was recovered. The failure to effect the cyclisation step may be due to the steric hindrance exerted by the TBDPS group (Scheme 6.9).

In the hope that the bulky TBDPS group would exert some steric hindrance over the neighbouring secondary alcohol, an attempt was made to selectively oxidised the primary hydroxy group of keto-diol **879** using Dess-Martin periodinane.[8] Disappointingly, this oxidation only gave a complex mixture (Scheme 6.9).

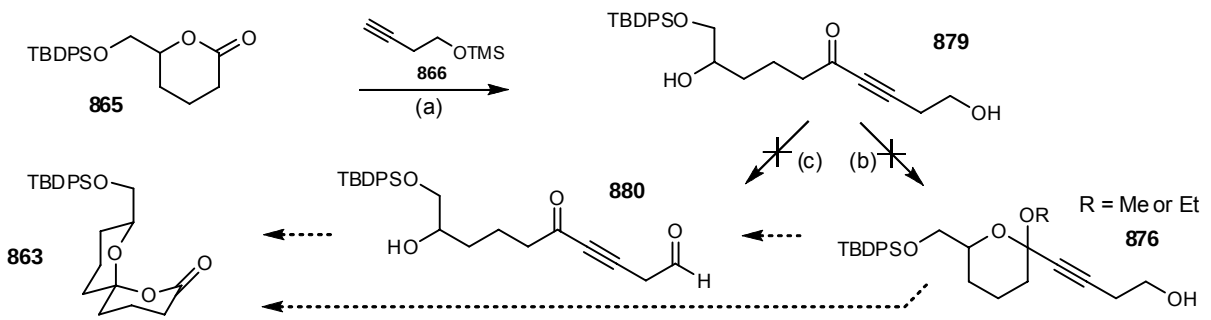

Reagents and conditions: (a) i. **866**, BuLi, THF, -78 °C, 45 min; ii. **865**, THF, -78 °C→rt, 2 h, 65%; (b) Amberlite IR118, MeOH, rt, 2–3 h; or PPTS, EtOH, rt, 18 h; (c) Dess-Martin periodinane, pyridine, CH_2Cl_2, rt, 18 h.

Scheme 6.9: Attempted synthesis of oxaspirolactone **863** *via* keto-diol **879**.

6.3.3 Attempted Synthesis (2)—via Spiroacetal 883

Given the steric bulk of the TBDPS group and the uncertainty as to whether it is possible to oxidise the labile acetals **876**, modifications to the current synthetic route were made in order to circumvent these problems. Given the unsuccessful synthesis of oxaspirolactone **863** *via* the oxidation of diol **879**, the sequence of the reaction steps was rearranged such that the troublesome oxidation was executed after cyclisation of the linear precursor to spiroacetal (Scheme 6.10).

Lithium acetylide, generated from protected alkyne **821**,[9] was added to valerolactone **865** in THF using the protocol developed in the model study to afford keto-alcohol **881**. The subsequent cyclisation of **881** failed to give acetal **882** and only starting material was recovered (Scheme 6.10).

One-pot hydrogenation-cyclisation of ynone **881** to spiroacetal **883** proceeded smoothly under acidic conditions. However, the subsequent ruthenium-catalysed oxidation[10-12] of spiroacetal **883** failed to give oxaspirolactone **863** regardless of the reaction conditions used. Variations in the number of equivalent of the ruthenium catalyst used, the nature of the solvent, the reaction temperature or the addition sequence did not give the desired result and only starting material **883** was recovered from all the oxidations attempted. The bulky TBDPS group may pose a problem preventing the oxidation from taking place.[11] Due to the potential instability of the resultant lactone **863** under aqueous conditions, over-oxidation may have occurred, presumably *via* the lactol intermediate (Scheme 6.10).[12]

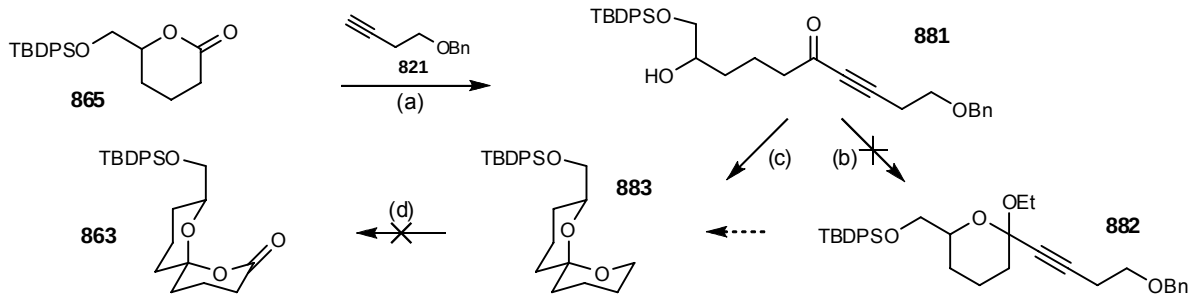

Reagents and conditions: (a) i. **821**, BuLi, THF, -78 °C, 30 min; ii. **865**, THF, -78 °C, 2 h, 73%; (b) PPTS, EtOH, rt, 18 h; (c) H_2, cat. Pd/C, *p*-TsOH, THF, rt, 18 h, 71%; (d) $NaIO_4$, cat. $RuCl_4$, CCl_4–MeCN–H_2O, rt–40 °C, 18 h.

Scheme 6.10: Attempted synthesis of oxaspirolactone **863** *via* spiroacetal **882**.

6.3.4 Attempted Synthesis (3)—via Protected Butynal 885

In the third synthetic route investigated, the problematic oxidation step was carried out at the beginning of the synthetic route. In this new route, the alkyne contained a protected aldehyde that was then coupled to valerolactone **865** (Scheme 6.11).

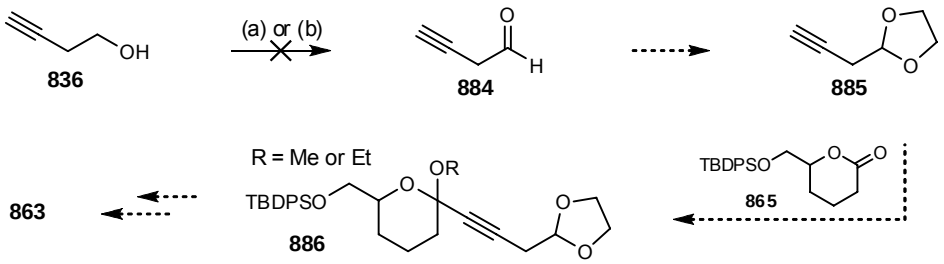

Reagents and conditions: (a) PCC, CH_2Cl_2, rt, 3.5 h; (b) Dess-Martin periodinane, pyridine, CH_2Cl_2, rt, 18 h.

Scheme 6.11: Attempted synthesis of oxaspirolactone **865** *via* protected butynal **885**.

Oxidation of butynol **836** using PCC[13] or Dess-Martin periodinane[8] was attempted but only a complex mixture was obtained from the reaction (Scheme 6.11). Surprisingly, there is no literature precedent for this seemingly simple oxidation. This problem together with the associated cost of butynol **836** forced us to abandon this route.

All three of the above synthetic routes have suffered the same design flaw as the model study. The virtue of the oxidation was effectively cancelled by the subsequent reduction of oxaspirolactone **863**. This disappointing situation prompted the investigation of a second approach in order to circumvent these problems.

6.4 Synthesis of Ketone 867 and 892 —the Spiroacetal Precursor

The second generation strategy for the synthesis of acetate **861** and acetal **862** is based on the knowledge accumulated from the model study and the ill-fated synthesis of oxaspirolactone **863**. This proposed strategy involved the synthesis of bromide **869** from either butyrolactone **870** or tetrahydrofuran. Bromide **869** is then converted to Grignard reagent **868**, followed by a key monoaddition to valerolactone **865**. Subsequent deprotection of ketone **867**, followed by cyclisation and trapping of the resulting lactol would then afford the desired spiroacetal acetate **861** and ethoxy-spiroacetal **862** (Scheme 6.12).

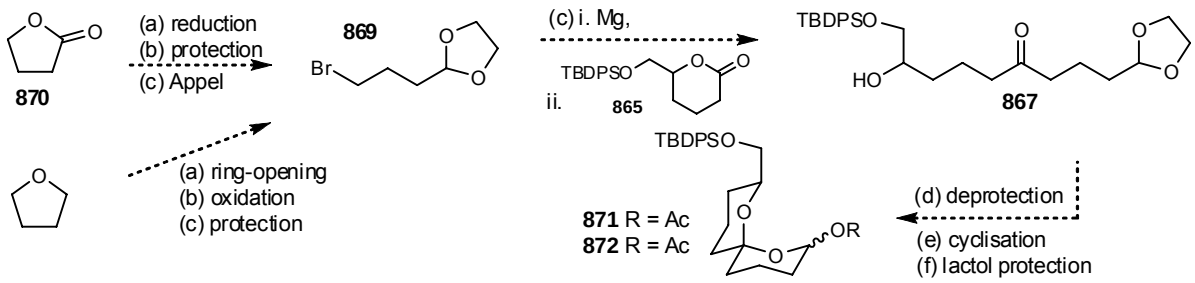

Scheme 6.12: Proposed synthesis of acetate **861** and acetal **862**.

6.4.1 Synthesis of Bromide 869

The revised synthesis hinges on the synthesis of bromide **869** bearing a protected aldehyde moiety and is proposed to be synthesised from either butyrolactone **870** or tetrahydrofuran.

(a) From Butyrolactone 870

The synthesis started with the DIBAL-H reduction of butytolactone **870** to lactol **887**. Attempts to trap the resulting aldehyde failed to yield the desired dioxolane **888**, but protected lactol **889** was isolated instead. Further attempts to equilibrate protected lactol **889** to the desired dioxolane **888** failed using either acidic or basic conditions, probably due to the lack of thermodynamic or kinetic driving force for the equilibration. Therefore, bromide **869** was unable to be synthesised from butyrolactone **870** and an alternative preparation from tetrahydrofuran was subsequently pursued (Scheme 6.13).

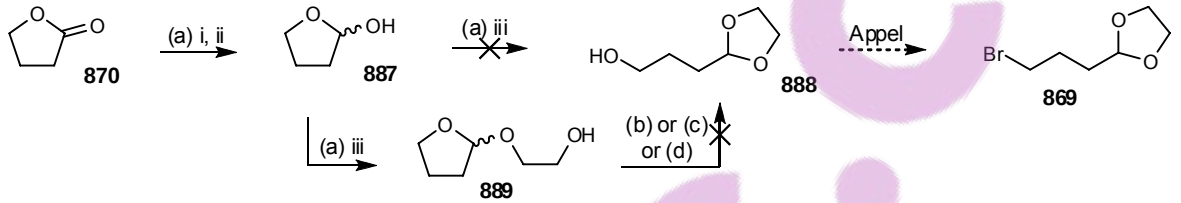

Reagents and conditions: (a) i. DIBAL-H, CH_2Cl_2, -78 °C, 1.5 h; ii. *p*-TsOH, CH_2Cl_2, -78 °C→rt, 30 min; iii. ethylene glycol, *p*-TsOH, reverse Dean-Stark apparatus, reflux, 18 h, **889**: 62%; (b) K_2CO_3, aq. MeOH, rt, 18 h; (c) *p*-TsOH, CH_2Cl_2 or EtOH, rt, 18 h; (d) Amberlite IR118, ethylene glycol, rt or 100 °C, 18 h.

Scheme 6.13: Attempted synthesis of bromide **869** from butyrolactone **870**.

(b) From Tetrahydrofuran

The alternative synthesis of bromide **869** began with the acidic cleavage of tetrahydrofuran to give bromo-alcohol **890** using previously reported procedures.[14,15] PCC oxidation of **890** and subsequent protection of the unstable aldehyde successfully afforded bromide **869** using the literature procedures.[1,15,16]

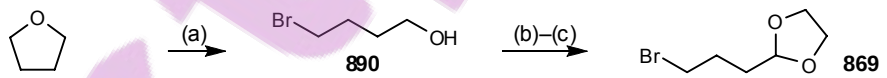

Reagents and conditions: (a) HBr (48% w/w), THF, reflux, 4 h, 33%; (b) PCC, CH_2Cl_2, rt, 45 min; (c) ethylene glycol, *p*-TsOH, CH_2Cl_2, reverse Dean-Stark apparatus, reflux, 18 h, 77% over 2 steps.

Scheme 6.14: Synthesis of bromide **869** from THF.

There are several other ways to synthesise bromide **869**, for example starting from readily available 4-bromobutyric acid ester.[17] However, the synthetic route starting from tetrahydrofuran was shown to be reproducible, scalable (up to *ca*. 13 g) with lower cost of materials, thus other synthetic routes were not investigated further at this stage.

6.4.2 Coupling between Bromide 869 and Valerolactone 865

With bromide **869** and valerolactone **865** in hand, attention next turned to the generation of Grignard reagent **868** and its monoaddition to valerolactone **865** (Scheme 6.15). In general, Grignard reagents react with lactones to afford a double-addition product due to the higher susceptibility of the ketone intermediate to undergo a second nucleophilic addition. However, the monoaddition product can be obtained when the reaction temperature is kept below -78 °C.[18]

Grignard reagent **868** was prepared using the procedure adapted from the literature in which bromide **869** was stirred with activated magnesium before the addition of the electrophile.[16,19,20] Despite a range of conditions used, an unknown mixture resulted in all cases (Table 6.1). Attempts to equilibrate the unknown mixture to ethoxy-spiroacetal **862** by unmasking the aldehyde in ethanol under acidic conditions (Amberlite IR 118 or CSA) failed.

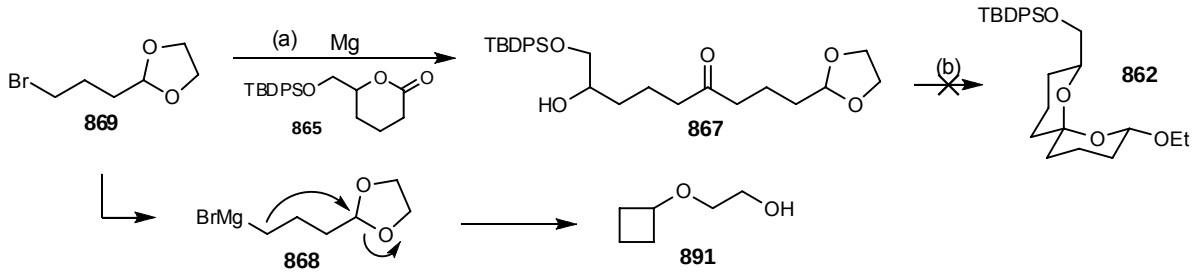

Reagents and conditions: (a) See Table 6.1 for reaction conditions; (b) Amberlite IR 118 or CSA, EtOH, rt, 18 h.

Scheme 6.15: [Top] Attempted synthesis of keto-alcohol **867** from valerolactone **865** and Grignard reagent **868** generated from bromide **869**. See Table 6.1 for reaction conditions. [Bottom] Spontaneous ring closure side reaction/degradation of Grignard reagent **868** that led to the formation of alcohol **891** by-product.[19]

Entry	*Reagents*	*Solvents*	*Conditions*	*Yields*
1	i. Mg, cat. I_2, $(CH_2Br)_2$ ii. **869**, iii. **865**	THF	rt rt→reflux, 1 h -78 °C, 2 h	complex mixture
2	i. Mg, **869**, cat. I_2, $(CH_2Br)_2$ ii. **865**	THF	rt, 15 min -78 °C, 6 h	complex mixture
3	i. Mg, **869**, cat. I_2, $(CH_2Br)_2$ ii. **865**	THF	rt, 15 min -78 °C, 18 h	complex mixture
4	i. Mg, cat. I_2, $(CH_2Br)_2$ ii. **869**, iii. **865**	Et_2O	rt rt, 15 min -78 °C, 2 h	complex mixture
5	i. Mg, cat. I_2, $(CH_2Br)_2$ ii. **869**, iii. **865**	Et_2O	rt rt, 1 h -78 °C, 2 h	complex mixture

Table 6.1: Summary of reagents and conditions used for the attempted synthesis of keto-alcohol **867**.

Forbes *et al.*[19] reported that the formation of Grignard reagent **868** from bromide **869** was liable to effect a spontaneous ring closure side-reaction which led to the formation of alcohol **891** after

work-up (Scheme 6.15). Generation of the Grignard reagent **868** under thermal conditions also accelerated this degradation, thus use of excess Grignard reagent **868** was often required. While the loss of reagent can be minimised by conducting the generation of Grignard reagent **868** at a high concentration, it also encouraged the dimerisation of the reagent through Wurtz coupling. The use of concentrated or excess reagent also leads to undesired double addition to valerolactone **865**. It was decided that in order to ensure successful of monoaddition, valerolactone **865** should be converted to Weinreb amide **892** prior to the coupling step.

6.4.3 Coupling between Bromide 869 and Weinreb Amide 892

(a) Conversion of Valerolactone 865 to Weinreb Amide 892

Conversion of valerolactone **865** to Weinreb amide **893** proceeded smoothly using the procedures adapted from Weinreb *et al*.[21] and Hodgetts *et al*.[22] The reaction was effected using an aluminium amide intermediate generated from trimethylaluminium and *N*,*O*-dimethyl-hydroxylamine hydrochloride with the concomitant release of methane gas. The crude alcohol was used in the subsequent protection step without further purification (Scheme 6.16).

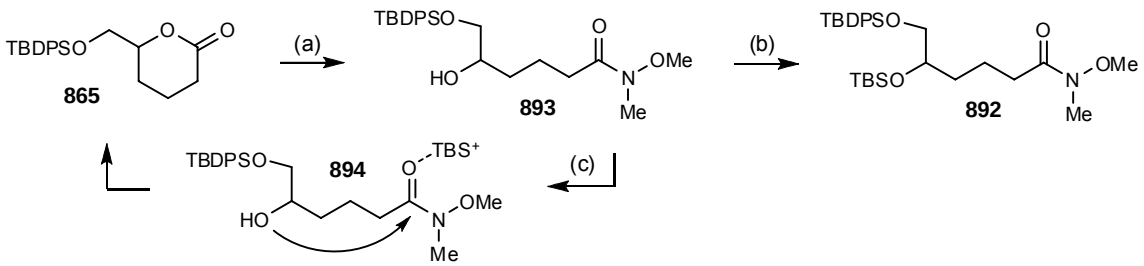

Reagents and conditions: (a) i. *N,O*-dimethylhydroxylamine hydrochloride, $AlMe_3$, CH_2Cl_2, 0 °C, 20 min; ii. **865**, CH_2Cl_2, 0 °C→rt, 2 h; (b) TBSCl, imidazole, cat. DMAP, CH_2Cl_2, rt, 3 d, 85% over 2 steps (+ 12% **865**); (c) TBSOTf, 2,6-lutidine, CH_2Cl_2, -78 °C, 30 min, 49% (+ 10% **892**).

Scheme 6.16: Synthesis of Weinreb amide **892** from valerolactone **865**. See Table 6.2 for the silylation conditions.

The next step involved protection of alcohol **893** as a TBS ether. After much experimentation, the best yield was obtained when alcohol **893** was silylated by TBSCl in the presence of imidazole and catalytic DMAP to give TBS ether **892** in 85% yield over two steps (Scheme 6.16). Due to the hindered nature of the secondary hydroxyl group, the silylation only proceeded to completion under concentrated conditions.

Interestingly, the starting material, valerolactone **865** was isolated in various amounts depending on the reaction conditions and scale used for the reaction. It was suspected that the steric

hindrance exerted by the neighbouring TBDPS group obstructed the nucleophilic attack of the hydroxyl group on the silylating agent. Instead, the silylating agent acted as a Lewis acid coordinating with the carbonyl group, thus promoting intramolecular cyclisation to give valerolactone **865**. This side-reaction was more pronounced when the strong Lewis acid and silylating agent, TBSOTf was used in a large scale reaction to afford valerolactone **865** as the major product in 49% yield (Table 6.2).

Entry	*Reagents*	*Solvents*	*Conditions*	*Yields of 892*
1	TBSCl, imidazole	CH_2Cl_2	rt, 2 d	68% (+ 18% **865**)
2	TBSCl, NEt_2, cat. DMAP	CH_2Cl_2	rt, 2 d	31%
3	TBSCl, imidazole, cat. DMAP	CH_2Cl_2	rt, 3 d	85% (+ 12% **865**)
4	TBSOTf, 2,6-lutidine (small scale)	CH_2Cl_2	-78→0 °C, 2 h	57%
5	TBSOTf, 2,6-lutidine (large scale)	CH_2Cl_2	-78 °C, 30 min	10% (+ 49% **865**)

Table 6.2: Summary of reagents and conditions used for the silylation of Weinreb amide **892**.

(b) Addition of the Grignard Reagent 868 to Weinreb Amide 892

With Weinreb amide **892** and bromide **869** in hand, attention next focussed on their union *via* the generation of Grignard reagent **868**. Due to the instability of Grignard reagent **868**, the use of Barbier conditions was considered. Under Barbier conditions, Grignard reagent was generated and immediately trapped by the electrophile *in situ*. These conditions have been successfully applied in several examples conducted by our research group.[23]

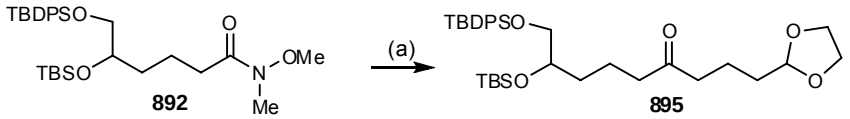

Reagents and conditions: (a) i. Mg, cat. I_2, $(CH_2Br)_2$, THF, rt, 1 h; ii. **892**, THF, rt, 5 min; iii. **869**, 33 °C, 2 h, 80%.

Scheme 6.17: Synthesis of ketone **895** from Weinreb amide **892** *via* Grignard reagent **868**.

Using a procedure adapted from the literature,[19,23,24] magnesium turnings were pre-washed with dilute aqueous HCl and water then dried *in vacuo* with a heat gun. After activation of the magnesium turnings with iodine and 1,2-dibromoethane, Weinreb amide **892** and bromide **869** were added sequentially and the reaction was triggered with the addition of iodine. The reaction initially afforded ketone **895** successfully in 42–65% yield when the reaction temperature was not controlled. However, it was later found that a higher yield (78–80%) was obtained when the reaction was conducted under concentrated conditions with the temperature lower than 33 °C in order to minimise the degradation of Grignard reagent **868** (Scheme 6.17). The use of magnesium powder was also attempted, but this reagent only afforded ketone **895** in 12% yield.

6.5 Synthesis of Spiroacetal Acetate 861 and Ethoxy-Spiroacetal 862

In light of the successful preparation of ketone **895**, the synthesis of spiroacetal acetate **861** and ethoxy-spiroacetal **862** was next pursued as previously stated (Scheme 6.12).

6.5.1 Synthesis of Ethoxy-Spiroacetal 862

The synthesis of acetal **862** from ketone **895** was first investigated. It was envisaged that acetal **862** can be obtained from the simultaneous unmasking of the aldehyde and the secondary alcohol followed by cyclisation and subsequent ethoxylation of the resulting lactol (Scheme 6.18).

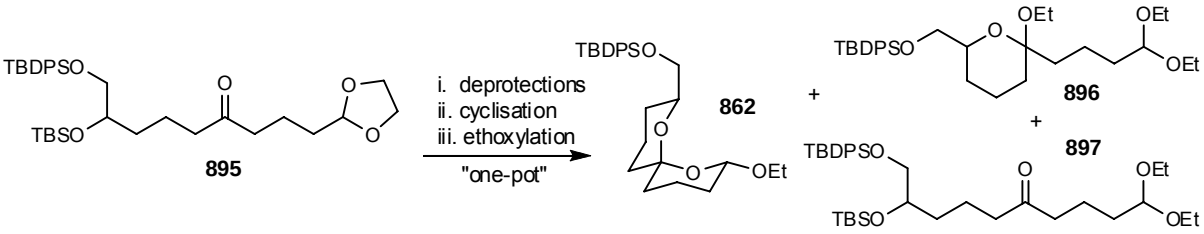

Scheme 6.18: Synthesis of acetal **862** from ketone **895**. Various amounts of **896** and **897** were also produced and were subsequently isolated and recycled. See Table 6.3 for reaction conditions.

(a) Previous Synthesis of Structurally Similar Alkoxy-acetals

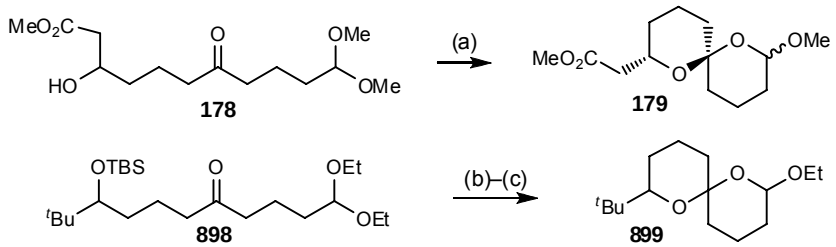

Reagents and conditions: (a) cat. BF_3•OEt_2, CH_2Cl_2, -5 °C, 78%; (b) TBAF, THF, reflux, 6 h; (c) Amberlyst-15, CH_2Cl_2, 0 °C→rt, 19 h, 57% over 2 steps.

Scheme 6.19: Examples of structurally similar alkoxy-spiroacetals **179** and **899** synthesised *via* a carbonyl cascade cyclisation under acidic conditions by Mead and Zemribo.[25] and de Greef and Zard.[26]

Ideally, the double-deprotection, cyclisation and ethoxylation can all be effected using a one-pot acidic reaction conditions. Although there has been no previous synthesis of acetal **862**, the preparation of structurally similar spiroacetals **179** and **899** from their linear precursors **178** and **898** had been described *via* a carbonyl cascade cyclisation executed under acidic conditions. Mead and

Zemribo[25] reported a one-pot cyclisation of keto-alcohol **178** to methoxy-spiroacetal **179** in the presence of BF_3•OEt_2. On the other hand, de Greef and Zard[26] were unable to simultaneously deprotect and cyclise ketone **898**. Therefore, a two-step procedure was employed to give ethoxy-spiroacetal **899** (Scheme 6.19).

(b) Optimisation of the Deprotection and Cyclisation

A variety of reagents and conditions were attempted in order to optimise the one-pot deprotection, cyclisation and ethoxylation reactions (Table 6.3).

Firstly, mildly acidic PPTS was used but the reaction only afforded acetal **862** in 26% yield after heating in aqueous EtOH–THF under reflux. The use of more equivalents of PPTS led to a complex mixture (Table 6.3).

Secondly, the reaction was performed in the presence of *p*-TsOH in a range of solvent mixtures and conditions. The best yield (40%) was produced when the reaction was carried out in the presence of *p*-TsOH (2 equiv.) in aqueous EtOH at room temperature. The use of more equivalents of acid and/or higher reaction temperatures led to a complex mixture (Table 6.3).

Entry	*Reagents (equiv.)*	*Solvents*	*Conditions*	*Yields*
1	cat. PPTS (0.3)	aq. EtOH–THF	60 °C, 2 h	no reaction
2	PPTS (1)	aq. EtOH–THF	reflux, 18 h	26%
3	PPTS (2)	EtOH	reflux, 18 h	complex mixture
4	cat. *p*-TsOH (0.1)	aq. EtOH–CH_2Cl_2	rt, 18 h	no reaction
5	cat. *p*-TsOH (0.5)	aq. EtOH–CH_2Cl_2	rt, 2 h	no reaction
6	cat. *p*-TsOH (0.5)	aq. EtOH	rt, 2 d	complex mixture
7	cat. *p*-TsOH (0.5)	aq. EtOH	reflux, 3 h	complex mixture
8	*p*-TsOH (2)	aq. EtOH–toluene	reflux, 3 h	complex mixture
9	*p*-TsOH (2)	aq. EtOH–CH_2Cl_2	rt, 18 h	40%
10	*p*-TsOH (2)	aq. EtOH	rt, 18 h	36%
11	*p*-TsOH (3)	aq. EtOH–CH_2Cl_2	rt, 18 h	complex mixture
12	CSA (2)	aq. EtOH–CH_2Cl_2	rt, 6 h	12% (+ **896**: 59% and **897**: 19%)
13	CSA (2)	aq. EtOH–CH_2Cl_2	rt, 18 h	complex mixture
14	CSA (2)	EtOH–MeCN	rt, 18 h	33%
15	CSA (2)	EtOH	rt, 4–5 h	56–59% (+ **896**: 11% and **897**: 5%)
16	CSA (2)	aq. EtOH	rt, 18 h	56–68%
17	CSA (2)	aq. EtOH	40 °C, 6 h	45%
18	CSA (2)	aq. EtOH	rt, 3 h	50–61% (85–86% after 3 x recycling)

Table 6.3: Summary of reagents and conditions used for the synthesis of acetal **862** (Scheme 6.18).

Finally, inspired by the methoxylation of lactol carried out by Mead and Zemribo[27], the use of CSA (2 equiv.) was investigated. Gratifyingly, acetal **862** was produced in most cases despite the

variations in the conditions used. Semi-cyclised intermediates **896** and **897** were also isolated after careful chromatography. After much experimentation, the best yield resulted when ketone **895** was stirred in the presence of CSA in aqueous EtOH at room temperature for 3 hours. Acetal **862** was then carefully isolated by flash chromatography from the crude product that also contained unreacted ketone **895**, semi-cyclised intermediates **896** and **897** and other degraded materials. The crude residue was recycled by subjecting it to the same cyclisation conditions (CSA in aqueous EtOH) to give 85–86% yield of acetal **862** after the third recycling step. The NMR and stereochemistry of acetal **862** are discussed in Section 6.5.3.

Consistent with the observations from the model study, acetal **862** was shown to be a poor glycosyl donor in nucleosidation reactions (see Section 6.6.1). It was important to obtain spiroacetal acetate **861** that is a better glycosyl donor and therefore crucial for the success of the desired nucleosidation (see Section 6.6.2).

6.5.2 Synthesis of Spiroacetal Acetate 861

There are two possible starting materials for the synthesis of acetate **861**, starting from either ketone **895** or acetal **862**.

(a) From Ketone 895

It was envisaged that acetate **861** can be synthesised from ketone **895** after double-deprotection and cyclisation under acidic conditions to give lactol **900**. Subsequent acetylation under standard conditions then afforded acetate **861** (Scheme 6.20). Similar acid-catalysed deprotection–cyclisations of a ketone to a spirolactol have been reported by Trost and Corte[28] and Vidari *et al.*[29] for the synthesis of the spiroacetal unit present in the saponacelolides.

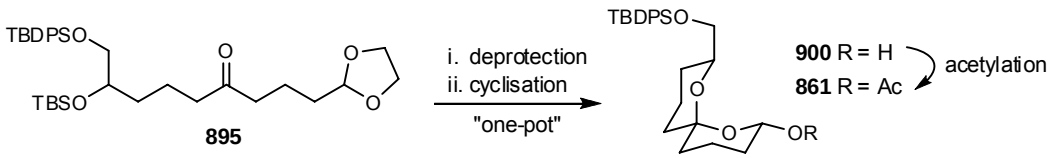

Scheme 6.20: Synthesis of acetate **861** from ketone **895**. See Table 6.4 for reaction conditions.

A variety of reagents and conditions were attempted in order to optimise the synthesis of lactol **900** and subsequently the synthesis of acetate **861**. Initially, *p*-TsOH in aqueous THF was used but this only gave acetate **861** in 15% yield under catalytic conditions at 40 °C overnight. The use of CSA, AcOH, $PdCl_2(MeCN)_2$,[30] HCl,[28,29] and CAN[31] all failed to yield the desired lactol **900** under various conditions. Finally, the use of PPTS[32] in aqueous acetone under reflux successfully produced acetate **861** albeit in 30–35% yield over two steps (Table 6.4).

Entry	*Reagents (equiv.)*	*Solvents*	*Conditions*	*Yields of 861 (after Acetylation*)*
1	*p*-TsOH (0.05–0.15)	aq. THF	rt, 3 d	no reaction
2	*p*-TsOH (0.1)	aq. THF	40 °C, 18 h	15%
3	*p*-TsOH (0.05)	aq. THF	microwave, 120 °C, 10 min	complex mixture
4	*p*-TsOH (excess)	aq. THF	40 °C, 18 h	complex mixture
5	CSA (0.1–0.15)	aq. THF	rt, 1 d	complex mixture
6	CSA (1)	aq. THF	microwave, 80–130 °C, 5–30 min	complex mixture
7	AcOH (excess)	aq. THF	microwave, 65–100 °C, 10–90 min	complex mixture
8	$PdCl_2(MeCN)_2$ (0.01)	aq. acetone	reflux, 18 h	complex mixture
9	aq. HCl (0.2)	aq. THF	rt, 3 h	no reaction
10	CAN (1.6)	MeOH	0 °C→rt, 18 h	complex mixture
11	CAN (2)	MeOH	rt, 18 h	complex mixture
12	PPTS (0.2)	aq. acetone	microwave, 80 °C, 2 h	23%
13	PPTS (0.2), LiCl (0.2)	aq. acetone	reflux, 18 h	16–26%
14	PPTS (0.2–1)	aq. acetone	reflux, 6 h–1 d	30–35%

* *Reagents and conditions:* Ac_2O, cat. DMAP, NEt_3, CH_2Cl_2, rt, 2 h.

Table 6.4: Summary of reagents and conditions used for the synthesis of acetate **861** from ketone **895**.

During the synthesis, a mixture of by-products was also obtained along with the desired acetate **861**. Although the structure of the by-products was not confirmed, the presence of the TBDMS group was observed. Hence, it was suspected that the poor yield obtained may be due to the inefficiency of the TBDMS deprotection step under the conditions used. This problem together with the premature exposure of the reactive keto-aldehyde moiety under acidic conditions led to a number of possible side-reactions.

(b) From Ethoxy-Spiroacetal 862

In light of the disappointing results obtained for the synthesis of acetate **861** from ketone **895**, the focus was turned towards the synthesis of acetate **861** starting from the related acetal **862** which lacked the potentially problematic TBDMS group (Scheme 6.21).

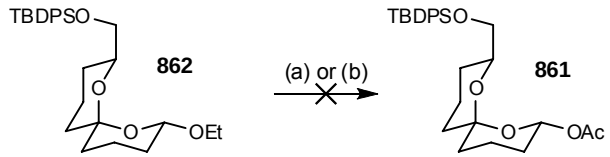

Reagents and conditions: (a) TMSOAc, TIPSOTf or TMSOTf, CH_2Cl_2, rt, 18 h; (b) TMSOAc, CH_2Cl_2, rt, 18 h.

Scheme 6.21: Synthesis of acetate **861** from acetal **862**.

Firstly, the direct conversion of acetal **862** to acetate **861** was attempted. The reaction hinged on the successful trapping of the oxonium intermediate by TMSOAc. Disappointly, only a complex mixture resulted presumably due to the insufficient nucleophilicity of the TMSOAc (Scheme 6.21).

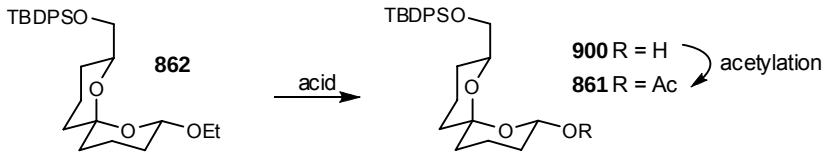

Scheme 6.22: Synthesis of acetate **861** from acetal **862**. See Table 6.5 for reaction conditions.

Next, the synthesis of acetate **861**, *via* the intermediate lactol **900**, was attempted using a variety of reagents and conditions (Scheme 6.22). Use of aqueous acetic acid under reflux gave a complex mixture whereas use of either aqueous HCl or PPTS produced a low yield of acetate **861** (6% and 21% after acetylation, respectively). Deprotection using *p*-TsOH gave a variable yield of acetate **861** (17–52%). Finally after much experimentation, the use of CSA to convert acetal **862** to lactol **900** proceeded with consistent yields of 58–66% after the acetylation step (Table 6.5).

Entry	*Reagents (equiv.)*	*Solvents*	*Conditions*	*Yields of 861 (after Acetylation*)*
1	AcOH (excess)	aq. AcOH	70 °C, 3 h	complex mixture
2	aq. HCl (excess)	aq. THF	rt, 1.5 h	6%
3	PPTS (0.5)	aq. THF	45 °C, 18 h	21%
4	*p*-TsOH (cat.)	aq. THF	35 °C, 1 d	52%
5	*p*-TsOH (0.2)	aq. THF	40 °C, 1 d	16% (larger scale)
6	*p*-TsOH (0.4)	aq. THF	40 °C, 2 d	47% (larger scale)
7	CSA (0.1)	aq. THF	40–50 °C, 18 h	19%
8	CSA (0.3)	aq. THF	45 °C, 1 d	41%
9	CSA (0.45)	aq. THF	rt, 2 d then 50 °C, 4 h	42%
10	CSA (0.4)	aq. THF	40 °C, 18 h	58–66%

* *Reagents and conditions:* Ac_2O, cat. DMAP, NEt_3, CH_2Cl_2, rt, 2 h.

Table 6.5: Summary of reagents and conditions used for the synthesis of acetate **861** from acetal **862** (Scheme 6.22).

6.5.3 NMR and Stereochemistry of Ethoxy-Spiroacetal 862 and Spiroacetal Acetate 861

(a) NMR Analysis

Similar to the model study, NMR analysis of both acetate **861** and acetal **862** revealed the characteristic anomeric H2 acetal resonances at δ_H 6.00 and 4.83 ppm, respectively. These resonated as doublet of doublets with a characteristic large 1,2-diaxial coupling constant ($J_{2ax,3ax}$ 10.0–10.1 Hz). This indicated that both the ethoxy and acetyl substituent adopted equatorial positions. Quaternary carbons resonating at δ_C 98.1–99.1 ppm were assigned to the spirocarbon C6, thus confirming the presence of the spiroacetal ring system.

NOESY studies also confirmed the *bis*-anomerically stabilised conformation of both acetate **861** and acetal **862** as indicated by a correlation between H2 and H8. This correlation confirmed the adoption of the *bis*-anomerically stabilised spiroacetal conformation in which both the TBDPS-protected hydroxymethyl and acetyl/ethoxy substituents adopted equatorial positions on their associated tetrahydropyran rings. NOESY correlations between H2 on the spiroacetal ring and the ethoxy or acetate substituent were also observed (Figure 6.2a).

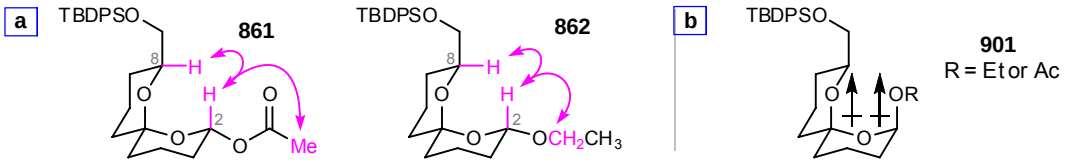

Figure 6.2: [a] Structures of acetate **861** and acetal **862** showing the *bis*-anomerically stabilised spiroacetal rings and their equatorial substituents. NOESY correlations are denoted by arrows. [b] Axial substituted spiroacetals **901** showing the unfavourable alignment of dipole 1,3-moments.

Stereochemistry

Similar to the model study, only the equatorial substituted acetate **861** and acetal **862** were isolated from the synthesis. The equatorial isomer was supposingly less stable than the corresponding axial isomer due to operation of the anomeric effect. However, the anomeric effect only offers *ca*. 1.4–1.5 kcal mol^{-1} of stabilisation energy[33] which could be overcome by other opposing stereoelectronic effects if they are additively significant. In this particular case, the bulky TBDPS-protected hydroxymethyl group may exert a destabilising steric interaction if the ethoxy or acetate substituent occupied an axial position. The alignment of 1,3-dipole moments between the ethoxy or acetate substituents and the C–O bond of the neighbouring ring may also disfavour the formation of the axial isomer under the thermodynamically-controlled conditions used to effect the reaction used (Figure 6.2b).[34]

6.5.4 X-ray Crystallography of Acetate 861

Recrystallisation of acetate **861** from hexane (with a small amount of dichloromethane) afforded white prisms that allowed structural determination by X-ray crystallography. The results were consistent with the above NMR analysis which established that the spiroacetal rings adopted a *bis*-anomerically stabilised structure. As expected, both the acetate and TBDPS-protected hydroxymethyl substituents occupied equatorial positions on their respective tetrahydropyran ring, thus minimising unfavourable steric interactions and 1,3-dipolar effects (Figure 6.3).

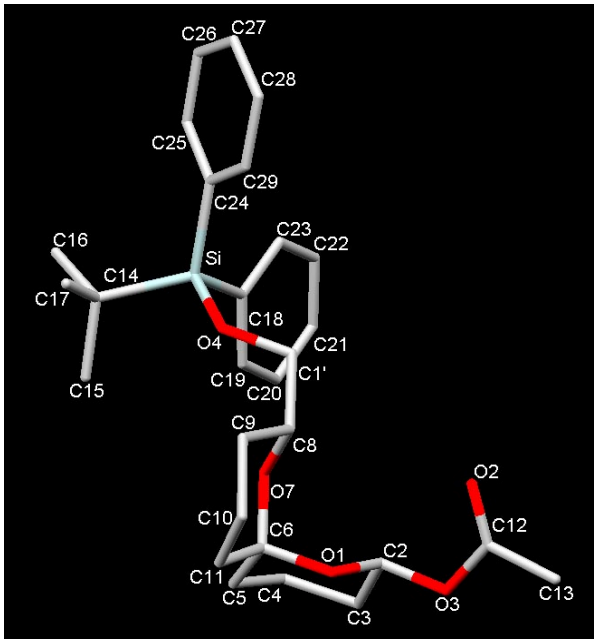

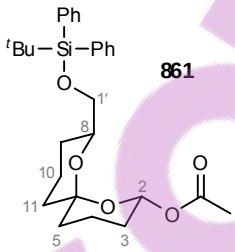

Figure 6.3: X-ray crystal structure of acetate **861**. The crystal structure data is listed in Appendix A.

6.6 Synthesis of Spiroacetal-Nucleosides 902

With acetate **862** and acetal **861** in hand, the synthesis of the spiroacetal hybrids, namely spiroacetal-nucleosides **902** was next investigated. As an extension from the model study, the nucleosidation under Vorbrüggen conditions was used. A persilylated heterobase was added to an oxonium ion generated in the presence of a Lewis acid, from a spiroacetal bearing a leaving group at the anomeric position (see Section 6.1.1). TMSOTf was the first choice of Lewis acid due to successful oxonium ion generation observed in the model study described in Chapter 5 and with other structurally similar spiroacetal systems reported in the literature.[25,27,35]

6.6.1 Nucleosidation of Ethoxy-Spiroacetal 862

Nucleosidation of ethoxy-spiroacetal **862** was first carried out because acetal **862** was obtained in higher yield in less synthetic steps than acetate **861**. Despite the problematic nucleosidation of structurally similar ethoxy-spiroacetal **862** in the model study, reaction of acetal **862** with persilylated 5-fluorocytosine was attempted using TMSOTf (Scheme 6.23).

Two commonly used silylation reaction conditions were evaluated. The use of BSA effected faster silylation of the nucleobase but the acetamide by-product interfered with the nucleosidation reaction (Scheme 6.23). The use of HMDS with catalytic $(NH_4)_2SO_4$ effected cleaner reaction but silylation of the nucleobase was much slower, particularly for the purines used in subsequent nucleosidations (see Section 6.6.2).

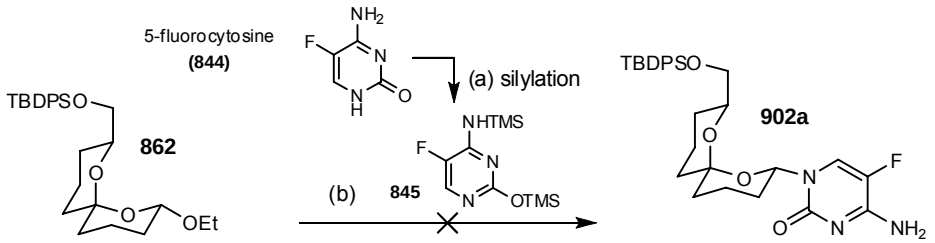

Reagents and conditions: (a) 5-FC, BSA, reflux, 45 min or 5-FC, HMDS, cat. $(NH_4)_2SO_4$, reflux, 45 min; (b) **862**, TMSOTf, CH_2Cl_2, rt, 3–20 h.

Scheme 6.23: Attempted nucleosidation of acetal **862** with persilylated 5-fluorocytosine **845** under Vorbrüggen conditions.

Unfortunately, nucleosidation of acetal **862** with persilylated 5-fluorocytosine **845** using a two-pot Vorbrüggen conditions only gave a trace amount (< 1%) of the desired spiroacetal 5-fluorocytidine **902a** as identified by NMR spectroscopy. Acetal **862** (> 50%) was also recovered from the reaction together with a complex mixture of degraded material.

The recovery of starting material was consistent with the observations from the model study in which model acetal **817** was found to be only a weak glycosyl donor for nucleosidation under Vorbrüggen conditions. This result was attributed to the poor ability of acetals **817** and **862** to generate the corresponding oxonium ions under the conditions used.

6.6.2 Nucleosidation of Spiroacetal Acetate 861

With the failure to effect nucleosidation using acetal **861** as the oxonium ion precursor, the use of acetate **861** bearing a better leaving group was next investigated (Scheme 6.24).

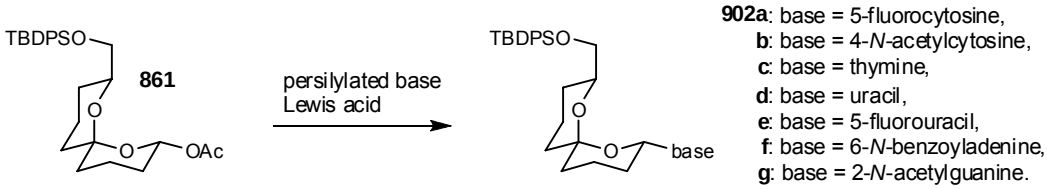

Scheme 6.24: Nucleosidation of acetate **861** with persilylated nucleobase under Vorbrüggen conditions. See Table 6.6–6.8 for silylation and reaction conditions.

(a) Nucleosidation with Pyrimidine Bases

Firstly, nucleosidation of acetate **861** using presilylated pyrimidines was investigated using a two-pot Vorbrüggen procedure (Scheme 6.24). The silylation was effected using HMDS with catalytic $(NH_4)_2SO_4$ which avoided the use of BSA and the subsequent formation of the acetamide by-product. Using these reaction conditions adapted from the model study, nucleosidation reactions using

5-fluorocytosine, 4-*N*-acetylcytosine, thymine, uracil and 5-fluorouracil were carried out in the presence of TMSOTf in CH_2Cl_2 at room temperature. Gratifyingly, spiroacetal-nucleosides **902a–e** were successfully produced in 20–45% yield (Table 6.6).

Entry	*Persilylated Bases*	*Silylation Conditions*	*Nucleosidation Conditions*	*Products*	*Yields*
1	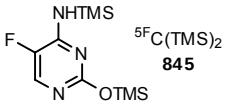 **845**	HMDS, cat. $(NH_4)_2SO_4$, reflux, 1.5 h	TMSOTf, CH_2Cl_2, rt, 3 h	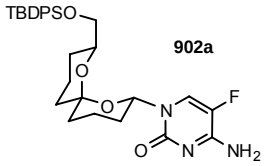 **902a**	22%
2	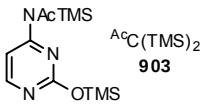 **903**	HMDS, cat. $(NH_4)_2SO_4$, reflux, 3 h	TMSOTf, CH_2Cl_2, rt, 2 h	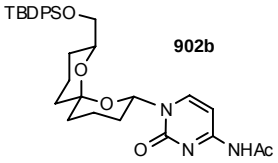 **902b**	46%
3	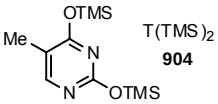 **904**	HMDS, cat. $(NH_4)_2SO_4$, reflux, 4 h	TMSOTf, CH_2Cl_2, rt, 3 h	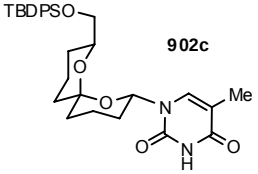 **902c**	45%
4	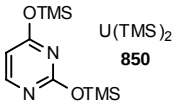 **850**	HMDS, cat. $(NH_4)_2SO_4$, reflux, 1 h	TMSOTf, CH_2Cl_2, rt, 3 h	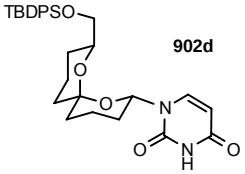 **902d**	36%
5	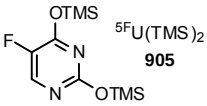 **905**	HMDS, cat. $(NH_4)_2SO_4$, reflux, 1 h	TMSOTf, CH_2Cl_2, rt, 3 h	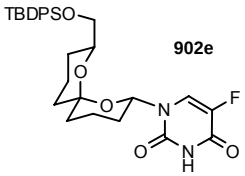 **902e**	20%

Table 6.6: Summary of reagents and conditions used for the nucleosidation of acetate **861** with persilylated pyrimidines using two-pot Vorbrüggen conditions (Scheme 6.24).

(b) Optimisation

Although the nucleosidations of acetate **861** with several pyrimidines were successful, the yields obtained for the reactions were moderate. Hence, an optimisation study of the nucleosidation was conducted using the synthesis of thymidine **902c** as a model reaction (Scheme 6.25).

A variety of reagents and conditions were evaluated as summarised in Table 6.7. Nucleosidation reactions using either one-pot conditions, BSA, $SnCl_4$, BF_3•OEt_2 or MeCN only proceeded in lower yield. An equivalent yield (45%) was obtained using TIPSOTf[36] in CH_2Cl_2 at room temperature with the reaction taking longer to proceed under the same conditions (18 hours versus 3 hours using TMSOTf).

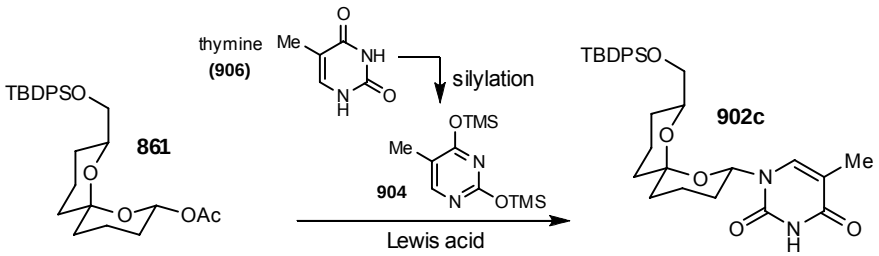

Scheme 6.25: Optimisation of nucleosidation by studying the synthesis of thymidine **902c**. See Table 6.7 for reaction conditions.

Entry	*1/2-pot?*	*Silylating Agent*	*Lewis acids*	*Solvents*	*Conditions*	*Yields*
1	2-pot	HMDS	TMSOTf	CH_2Cl_2	rt, 3 h	45%
2	2-pot	HMDS	$SnCl_4$	CH_2Cl_2	rt, 3 h	24%
3	2-pot	HMDS	$SnCl_4$	MeCN	rt, 3 h	complex mixture
4	2-pot	HMDS	TIPSOTf	CH_2Cl_2	rt, 18 h	45%
5	2-pot	HMDS	$BF_3{\bullet}OEt_2$	CH_2Cl_2	rt, 3 h	complex mixture
6	1-pot	BSA	TMSOTf	MeCN	rt, 3 h	33%

Table 6.7: Summary of reagents and conditions used for the optimisation study of the nucleosidation under two-pot Vorbrüggen conditions (Scheme 6.24).

According to Dalla *et al.*[36], TIPSOTf is a stronger Lewis acid than TMSOTf and has better air and moisture stability due to its steric bulk. Therefore, they suggested that TIPSOTf provides a good alternative to the use of TMSOTf reagent and such a suggestion was consistent with the present results observed for the nucleosidation of acetate **861** with thymine under Vorbrüggen conditions. However, attempts to extend the use of TIPSOTf to other nucleosidations using the pyrimidine bases, namely uracil and 5-fluorouracil, only gave lower yield than the use of TMSOTf (Table 6.8). It was, therefore, established that the use of TMSOTf in CH_2Cl_2 at room temperature was, in fact, the preferred method for the nucleosidation of acetate **861** with persilylated pyrimidines due to its wide versatility and tolerance for various substrates.

Entry	*Persilylated Bases*	*Silylation Conditions*	*Nucleosidation Conditions*	*Products*	*Yields*
1	$U(TMS)_2$	BSA, reflux, 1 h	TIPSOTf, CH_2Cl_2, rt, 18 h	spiroacetal uridine **902d**	9% (36%)
2	$^{5F}U(TMS)_2$	BSA, reflux, 1 h	TIPSOTf, CH_2Cl_2, rt, 18 h	spiroacetal 5-fluorouridine **902e**	complex mixture (20%)
3	$^{5F}U(TMS)_2$	HMDS, cat. $(NH_4)_2SO_4$, reflux, 1 h	TIPSOTf, CH_2Cl_2, rt, 18 h	spiroacetal 5-fluorouridine **902e**	complex mixture (20%)

Table 6.8: Summary of reagents and conditions used for the nucleosidation of acetate **861** with persilylated uracil or 5-fluorouracil under two-pot Vorbrüggen conditions (Scheme 6.24). The percentages in parenthesis represent the yields obtained when TMSOTf was used for the nucleosidation (Table 6.6).

(c) Nucleosidation with Purine Bases

With the nucleosidation of acetate **861** using pyrimidines established, the problematic nucleosidations using purine bases were next investigated. Purines have several nitrogens available for possible alkylation. However unlike the pyrimidines, the difference in the steric hindrance exerted by the neighbouring groups near the nitrogens is not significant enough to allow for selective alkylation. Alkylation of purines are, therefore, rarely regioselective and a mixture of N7 and N9 regioisomers are commonly isolated for guanosine and some adenosine derivatives.[37]

Nevertheless, the nucleosidation of acetate **861** with *N*-acylated adenine or guanine was carried out. The silylation step was carried out using BSA under reflux after discovering that the use of HMDS was too slow within the reaction timeframe. Later, the silylation step was effected by heating the base with a mixture of BSA, HMDS and toluene under reflux, thus producing cleaner persilylated purines. TIPSOTf was used to generate the oxonium required for the nucleosidation due to its better air and moisture stability (Scheme 6.26).

Gratifyingly, the nucleosidation of acetate **861** with persilylated *N*-benzoyladenine gave the desired N9-substituted spiroacetal-adenosine **902f** in 35–37% yield as the only regioisomer. On the other hand, nucleosidation of persilylated *N*-acetylguanine gave a mixture of N9-guanosine **902g** and N7-guanosine **902h** in 20% and 11% yield, respectively (Scheme 6.26). Preparative thin layer chromatography (PLC) was required to separate the N7 and N9 regioisomers.

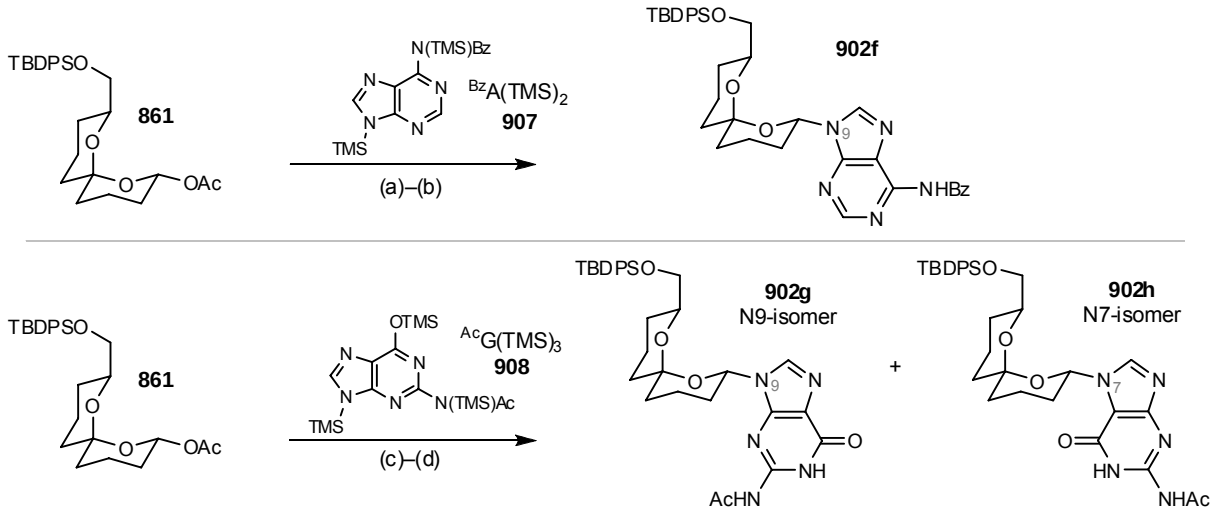

Reagents and conditions: (a) *N*-benzoyladenine, HMDS–BSA–toluene, reflux, 1 h; (b) **861**, TIPSOTf, CH_2Cl_2, rt, 18 h, **861**: 35–37%; (c) *N*-acetylguanine, HMDS–BSA–toluene, reflux, 1 h; (d) **861**, TIPSOTf, CH_2Cl_2, rt, 18 h, **902g**: 20%, **902h**: 11%.

Scheme 6.26: Nucleosidation of acetate **861** with persilylated purines using a two-pot Vorbrüggen procedure.

6.6.3 NMR and Stereochemistry of Spiroacetal-Nucleosides 902

(a) NMR Analysis

Similar to the model study, NMR analysis of nucleoside analogues **902a–h** revealed the characteristic anomeric H2′ resonances at δ_H 5.85–6.22 ppm. These resonated as doublet of doublets with a large characteristic 1,2-diaxial coupling constant ($J_{2ax,3ax}$ 10.6–11.1 Hz). This indicated that the nucleoside substituent in analogues **902a–h** adopted equatorial positions. Quaternary carbon resonating at δ_C 98.8–99.3 ppm were assigned to the spirocarbon C6, thus confirming the presence of the spiroacetal ring system (Figure 6.4).

Characteristic NOESY correlations were observed for pyrimidines **902a–e** between H2′–H8′, H2′–H6 and H3′–H6 and for purines **902f–h** between H2′–H8′, H2′–H8 and H3′–H8. These correlations confirmed the adoption of the *bis*-anomerically stabilised spiroacetal conformation in which both the TBDPS-protected hydroxymethyl and basic substituents adopting equatorial positions on their associated tetrahydropyran rings (Figure 6.4).

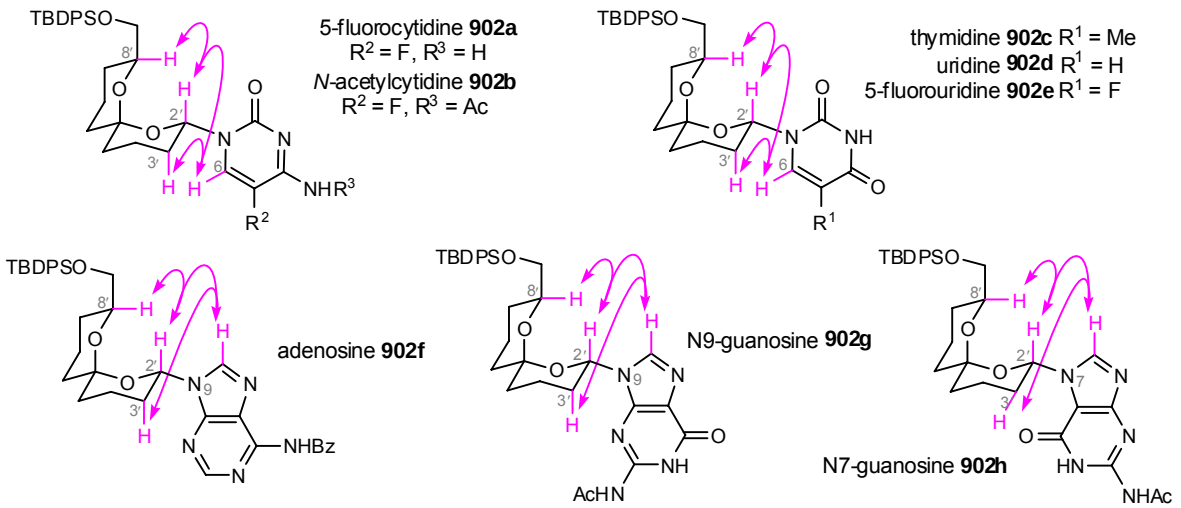

Figure 6.4: Structures of pyrimidine analogues **902a–e** and purine analogues **902f–h** showing the *bis*-anomerically stabilised spiroacetal rings and their equatorial substituents. NOESY correlations are denoted by arrows.

In pyrimidine analogues **902a–e**, long range HMBC correlations between C2′–H6 and H2′–C6 confirmed the desired linkage between C2′ of the spiroacetal ring and N1 of the heterobase.

In purine analogues **902f–h**, the desired linkages between C2′ of the spiroacetal unit and the purine were confirmed by a clear HMBC correlation between H2′ and C8. The N9–C2′ connection in adenosine **902f** and N9-guanosine **902g** was established by HMBC correlations between H2′ and C4. The N7–C2′ connection in N7-guanosine **902h** was also established by a clear HMBC correlation between H2′ and C5.

(b) Stereochemistry

Similar to the model study in which spiroacetals **811a** and **811d** were prepared, only the equatorial substituted nucleoside analogues **902a–h** were isolated from the nucleosidation step. This result may be due to the destabilising steric interaction exerted by the bulky TBDPS-protected hydroxymethyl group if the nucleoside occupied an axial position. The alignment of 1,3-dipole moments between the basic substituent and the C–O bond of the neighbouring ring may also disfavour formation of the axial isomer. Therefore, under the thermodynamically controlled conditions used in this nucleosidation step, only equatorial isomers **809a–h** were, in fact, formed.[34]

Mead and Zemribo[25] conducted systematic studies that involved nucleophilic addition to an oxonium ion generated on a closely related 6,6-spiroacetal ring system. The results were consistent with the current study in which Lewis acid-mediated substitution of acetal **179** gave the *bis*-anomerically stabilised spiroacetals **180** in which both substituents were equatorial (Scheme 6.27).

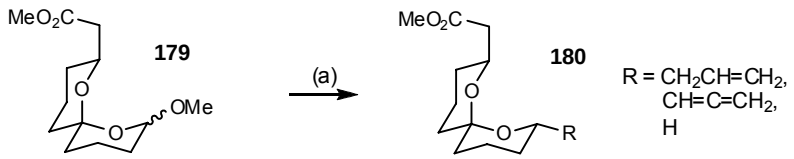

Reagents and conditions: (a) allyl-trimethylsilane or propargyltrimethylsilane or diphenylmethylsilane, TMSOTf, CH_2Cl_2, -50 °C, 1.0–1.5 h, 65–68%.

Scheme 6.27: Lewis acid-mediated substitution reaction of methoxy-spiroacetal **179** by Mead and Zemribo[25] See Scheme 1.30 for the synthesis of methoxy-spiroacetal **179** and other related examples.

Mead and Zemribo[25] rationalised the observed *bis*-equatorial substitution by carrying out *ab initio* calculations on the oxonium ion intermediate involved in the reaction. The lowest energy was achieved when the oxonium ion containing ring adopted a half chair conformation in order to minimise 1,3-diaxial repulsions. Thus, the resulting conformation was only mono-anomerically stabilised due to the pseudo-axially disposed ring oxygens. Nucleophilic addition from the less hindered face, *anti* to the ring oxygen of the other ring, resulted in overall equatorial substitution (Figure 6.5).

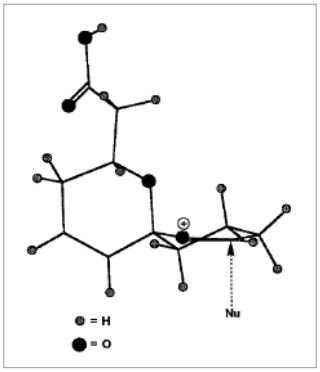

Figure 6.5: Lowest energy conformation of the proposed oxonium ion intermediate by *ab initio* calculations at the STO-3G level conducted by Mead and Zemribo[25]

Due to the close resemblance of the substrates used in the present work to those studies by Mead and Zemribo[25] as well as the similarity of the reaction conditions and reagents used, the above explanation may well be used to explain the observed equatorial substitution of nucleoside analogues **902a–h**. Similar exclusive production of the equatorial isomer from the nucleosidation of

pyranosides or furanosides lacking a stereodirecting neighbouring group have also been reported in the literature.[38]

6.6.4 X-ray Crystallography of Uridine 902d

Recrystallisation of uridine **902d** from dichloromethane–hexane afforded pale yellow needles that allowed structural determination by X-ray crystallography.[39] The results were consistent with the above NMR analysis which established that the spiroacetal rings adopted a *bis*-anomerically stabilised conformation. As expected, both the uracil and TBDPS-protected hydroxymethyl substituent occupied equatorial positions on their respective tetrahydropyran ring, thus minimising unfavourable steric interactions and 1,3-dipolar effects (Figure 6.6).

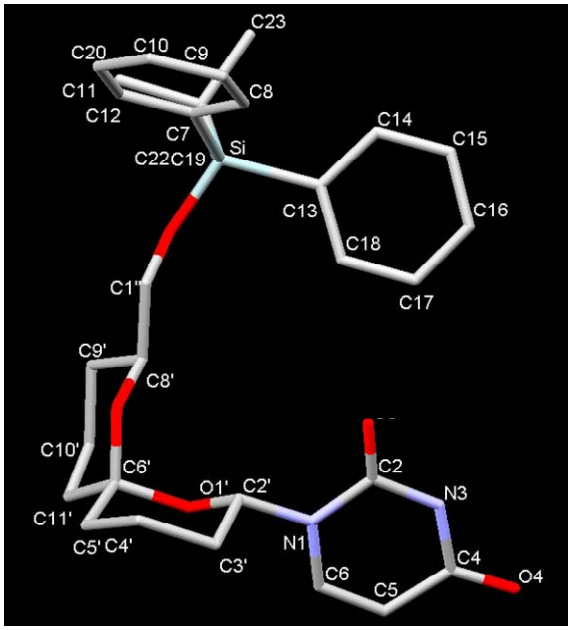

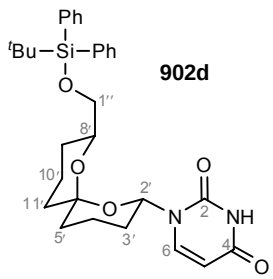

Figure 6.6: X-ray crystal structure of uridine **902d**. The crystal structure data is listed in Appendix B.[39]

In the solid state structure of uridine **902d**, the basic substituent adopted an orientation in which the C2 carbonyl pointed in the same direction (*syn*) as H2′.[39] This conformation was adopted possibly to minimise repulsive interactions between the lone pair of electrons on the C2 carbonyl group and the axial H3′ hydrogen (Figure 6.6).

6.7 Synthesis of Spiroacetal-Triazoles 909

With the successful nucleosidation of acetate **961** accomplished, attention next turned to the synthesis of spiroacetals containing triazole moieties. This work began with the initial preparation of azide **860** adopting the retrosynthesis depicted in Scheme 6.1 (see page 129).

6.7.1 Preparation of Azido-Spiroacetal 860

Using the procedure developed in the model study, azide **860** was synthesised from acetal **862** using TMSOTf and $TMSN_3$ in CH_2Cl_2 at -10 °C. A diastereomeric mixture of azides **860a** and **860b** was afforded in 36% and 15% yield respectively that were carefully separated by flash chromatography (Scheme 6.28). The stereochemistry of azides **860a** and **860b** was established by NMR spectroscopy (see Section 6.7.2).

Treating axial azide **860b** with TMSOTf and $TMSN_3$ in CH_2Cl_2 at -10 °C led to epimerisation of **860b** into a separable 2.2:1 mixture of equatorial azide **860a** and axial azide **860b** in 63% yield. Together with the initial substitution reaction, the recyclisation afforded equatorial and axial azides **860a** and **860b** in 42% and 3% yield over two steps from acetal **862**. No epimerisation occurred when the reaction was conducted in the absence of TMSOTf or when using $Sc(OTf)_3$ as the Lewis acid (Scheme 6.28).

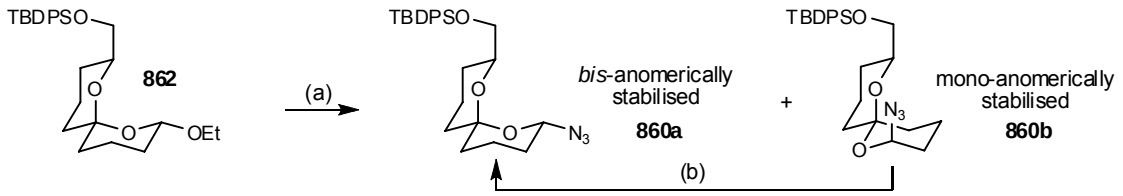

Reagents and conditions: (a) $TMSN_3$, TMSOTf, CH_2Cl_2, -10 °C, 3 h, **860a**: 36%, **860b**: 15%, **862**: 5%; (b) $TMSN_3$, TMSOTf, CH_2Cl_2, -10 °C, 3 h, **860a**: 43%, **860b**: 20%.

Scheme 6.28: Synthesis of azides **860a** and **860b** from acetal **862**.

Similar to the model study, a diastereomeric mixture of *bis*-anomerically stabilised azide **860a** and mono-anomerically stabilised azide **860b** resulted from the substitution reaction. Although the diastereomers were separable, equatorial azide **860a** was obtained in higher quantity whereas axial azide **814b** was the major product in the model system that lacked the protected C8-hydroxymethyl substituent. This result indicated that the bulky TBDPS-protected hydroxymethyl exerted a prominent steric effect that outweighed any anomeric stabilisation and hindered an axial approach of the azide nucleophile to the oxonium ion. The axial azide would also be destabilised by unfavourable steric interactions with the protected hydroxymethyl group at C8.

Stereochemistry

Mono-anomerically stabilised azide **860b** was postulated to be formed from the *bis*-anomerically stabilised axial azide **910** *via* a ring-opening and closing mechanism that proceeded in the presence of Lewis acid. This conversion is driven by relief of unfavourable steric interactions between the axial azide and TBDPS-protected hydroxymethyl substituents (Scheme 6.29).

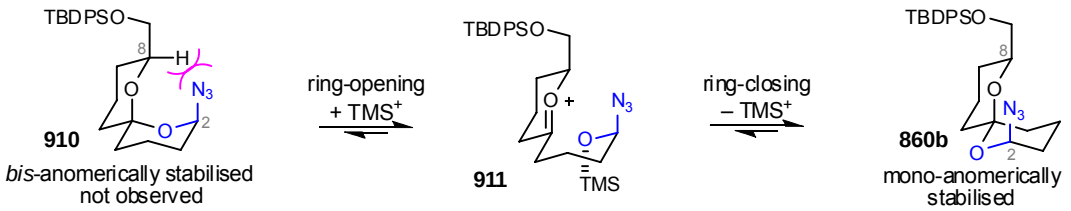

Scheme 6.29: Postulated formation of mono-anomerically stabilised azide **860b** *via* a ring-opening and closing mechanism.

6.7.2 NMR Analysis of Azido-Spiroacetals 860

Similar to the model study, NMR analysis of azides **860a** and **860b** revealed the characteristic anomeric H2 resonances at δ_H 4.61–4.94 ppm. A larger 1,2-diaxial coupling was observed for azide **860a** (dd, $J_{2ax,3ax}$ 10.8 Hz) whereas a smaller 1,2-diequatorial coupling was observed for azide **860b** (t, $J_{2eq,3ax/3eq}$ 6.4 Hz). These characteristic coupling constants established that the azide substituent adopted an equatorial position in **860a** and an axial position in **860b**. Quaternary carbons resonating at δ_C 93.2 ppm were assigned to the spirocarbon C6, thus confirming the presence of the spiroacetal ring system.

Due to the significant differences observed between the chemical shifts of azides **860a** and **860b** in the ^{13}C NMR (noticably the signals for C5 and C11), it was apparent that **860a** and **860b** were not simple C2 anomers, but rather exhibit substantial conformational differences in their spiroacetal rings.

For azide **860a**, NOESY spectra confirmed the *bis*-anomerically stabilised conformation through an observation of a correlation between H2 and H8. This correlation confirmed the adoption of the *bis*-anomerically stabilised spiroacetal conformation in which both the TBDPS-protected hydroxymethyl and azide substituents adopt equatorial positions on their associated tetrahydropyran rings (Figure 6.7).

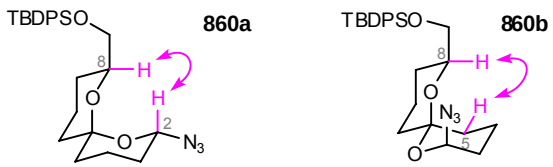

Figure 6.7: Structures of azide **860a** and **860b** showing the anomerically stabilised spiroacetal rings and their substituents. NOESY correlations are denoted by arrows.

For azide **860b**, NOESY spectra confirmed the adoption of a mono-anomerically stabilised conformation through an observation of a correlation between the H5 and H8 (Figure 6.7).

6.7.3 Cycloaddition of Azido-Spiroacetals 860 to Alkynes

With azides **860a** and **860b** in hand, attention next focused on their subsequent cycloaddition to a range of alkynes in order to prepare spiroacetal-triazoles **909**. Both the highly popular copper-catalysed and thermally-promoted conditions were used for the conversion of these spiroacetal-bearing azides to a small library of triazole containing spiroacetals **909** (Scheme 6.30).

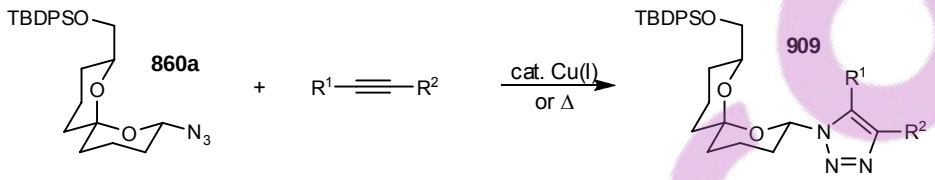

Scheme 6.30: Cycloadditions of azides **860a** to a range of alkynes under copper(I)-catalysed or thermally-promoted conditions. See Table 6.9 for reaction conditions.

Using the reagents and conditions developed in the model study, cycloaddition of equatorial azide **860a** to alkynes was first carried out using a catalytic phophine-stabilised copper(I) salt[40] [CuI•P(OEt)$_3$]. Gratifyingly, all the cycloadditions performed well using an excess of alkyne in toluene under reflux to afford spiroacetal-triazoles **909a** and **909c–e** in excellent yield (83–98%, Table 6.9).

For the thermally-promoted cycloaddition of azide **860a**, similar use of the reagents and conditions as developed earlier for the model study were investigated. Disappointingly, heating azide **860a** and neat dimethylacetylene-dicarboxylate **855** at 110 °C only afforded a complex mixture (Table 6.9).

Subsequently, minor adjustment of the reaction conditions, in which the cycloaddition of azide **860a** was conducted using an excess of alkynes in toluene at 110 °C, successfully afforded spiroacetal triazoles **909f–h** in good yield (64–84%, Table 6.9).

The thermal-promoted cycloaddition was completed within an hour of reflux in toluene using the highly activated dienophile, dimethylacetylene dicarboxylate **855**. On the other hand, prolonged heating in a sealed tube with a large excess of alkyne was required for the cycloadditions using unactivated alkynes **915** and **916** (Table 6.9).

Entry	*Alkynes*	*Reagents and Conditions*	*Products*	*Yields*
1	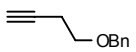 **821**	cat. CuI•P(OEt)$_3$, toluene, reflux, 1 h	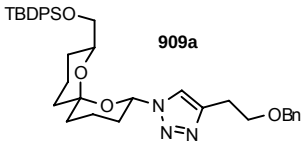 **909a**	98%
2	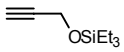 **912**	cat. CuI•P(OEt)$_3$, toluene, reflux, 1 h	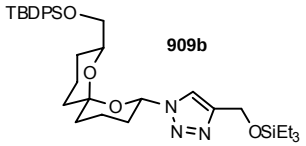 **909b**	4%* (+ 4% **909c** and 60% **860a**)
3	 **913**	cat. CuI•P(OEt)$_3$, toluene, reflux, 1 h	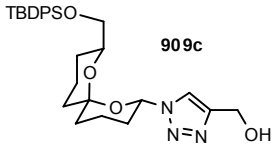 **909c**	83%
4	**914**	cat. CuI•P(OEt)$_3$, toluene, reflux, 1 h	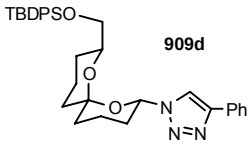 **909d**	96%
5	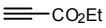 **857**	cat. CuI•P(OEt)$_3$, toluene, reflux, 1 h	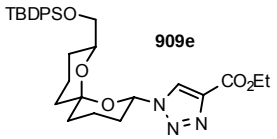 **909e**	84%
6	 **855**	neat, 110 °C, 1 h toluene, reflux, 1 h	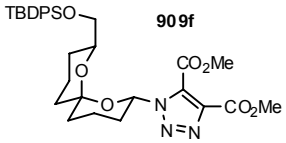 **909f**	complex mixture 78%
7	**915**	toluene, sealed tube, reflux, 2 d	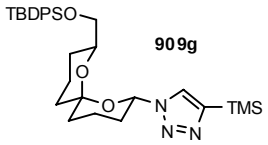 **909g**	64%# (+ 36% **860a**)
8	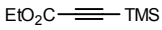 **916**	toluene, sealed tube, reflux, 2 d	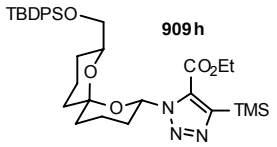 **909h**	84%

Table 6.9: Summary of reagents and conditions used for the cycloaddition of azide **860a** (Scheme 6.30).

*Low yield due to the instability of the TES-protected alkyne **912** in the presence of the copper(I) catalyst. The silyl residue may poison the copper(I) catalyst leading to the recovery of azide starting material **860a** (60%).

#Azide starting material **860a** was recovered from the cycloaddition due to the high volatility of trimethylsilyl-acetylene **915** despite using a large excess of the alkyne in a sealed tube.

The regio-directing effect of the silyl substituent in alkynes **915** and **916** was clearly observed with 4-trimethylsilyl substituted triazoles **909g** and **909h**[41] being obtained from the cycloadditions (Table 6.9). This regioselectivity resulted from the steric bulk exerted by the trimethylsilyl substituent and the ability of silicon to stabilise the developing partial positive charge on the alkyne β-carbon in the transition state for the reaction. Mono-substituted triazole **809g** together with 1,5-disubstituted

triazole **809h** were then obtained upon removal of the 4-trimethylsilyl substituent in **909g** and **909h** (see Section 6.9.1). A 1,5-disubstituted triazole is a stable isostere of a *cis*-peptide bond commonly found in turns and loops of peptide secondary structures (see Chapter 3.4.7).[42]

For all the cycloadditions performed using equatorial azide **860a**, only the corresponding equatorial triazoles **909a–h** resulted from the reaction with no epimerisation at the anomeric or spiro-centre being observed as confirmed by NMR studies (see Section 6.7.4). No work-up was required for all of the cycloadditions carried out and the crude reaction mixture was directly purified by chromatography. Due to the satisfactory yield obtained and the ease of purification, no optimisation was carried out at this stage.

The cycloaddition of axial azide **860b** to alkynes **821** and **914** was attempted however only complex mixtures were obtained in both cases. It was suspected that the steric clash between the newly formed axial triazole substituent and the TBDPS-protected hydroxymethyl substituent destabilised the resulting triazole **912** leading to its degradation, resulting in a complex mixture of product (Scheme 6.31).

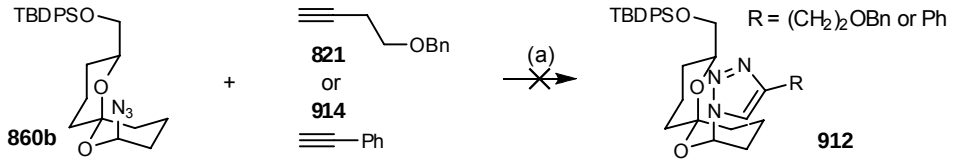

Reagents and conditions: (a) alkyne **821** or **914**, cat. CuI•P(OEt)$_3$, toluene, reflux, 1 h, complex mixture.

Scheme 6.31: Attempted cycloaddition of azides **860b** to alkynes **821** or **914**.

6.7.4 NMR Analysis of Triazoles 909

Similar to the previously mentioned spiroacetals, NMR analysis of triazoles **909a–g** revealed the characteristic anomeric H2 resonances at δ_H 6.01–6.18 ppm. The characteristic deshielded nature of H2′ resonance of **909h** (δ_H 6.65 ppm) was due to the through-space electron withdrawing effect and anisotropic effect exerted by the neighbouring carbonyl group at C5 of the triazole ring (Figure 6.8). In all triazole analogues **909a–h**, the large 1,2-diaxial coupling constants ($J_{2ax,3ax}$ 10.6–11.3 Hz) indicated that the triazole moieties adopted equatorial positions. Quaternary carbons resonating at δ_C 98.8–99.4 ppm were assigned to the spirocarbon C6, thus confirming the presence of the spiroacetal ring system (Figure 6.9).

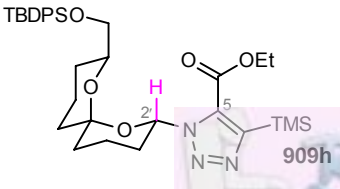

Figure 6.8: Trisubstituted triazole **909h** showing the electron withdrawing effect exerted by the neighbouring carbonyl group.

Characteristic NOESY correlations were observed for the 1,4-disubstitued triazoles **909a–e** and **909g** between H2′–H8′, H2′–H5 and H3′–H5 and for the trisubstituted triazole **909f** and **909h** between H2′–H8′. These correlations confirmed the adoption of the *bis*-anomerically stabilised spiroacetal conformation in which both the TBDPS-protected hydroxymethyl and triazole substituents adopting equatorial positions on their associated tetrahydropyran rings (Figure 6.9).

Figure 6.9: Structures of 1,4-disubstituted triazole analogues **909a–e** and **909g** and trisubstituted triazole analogues **909f** and **909f** showing the *bis*-anomerically stabilised spiroacetal rings with equatorial substitutions. NOESY correlations are denoted by arrows.

Long range HMBC correlations between H2′ and C5 confirmed the desired 1,4-disubstitution pattern of the triazole ring in analogues **909a–e** and **909g**. This correlation also supported formation of the chemical linkage between C2′ of the spiroacetal ring and N1 of the triazole in spiroacetals **909a–e** and **909g**.

6.8 Synthesis of Spiroacetal-Amino Acid 913

With analogues of spiroacetal-nucleoside and triazole successfully synthesised, attention next focused on hybridisation of spiroacetal moiety with an amino acid. Glycine analogue **913** was initially chosen as a representative target for this preliminary investigation of the synthesis of spiroacetal amino acids. The retrosynthesis used is depicted in Scheme 6.1.

As part of a diversity oriented synthesis (DOS) approach to elaborate a 6,6-spiroacetal system, it was initially intended to utilise azide **860a**, from the synthesis of triazole analogues **909**, to synthesise spiroacetal-glycine **913** using a Staudinger ligation (Scheme 6.32).

The Staudinger ligation procedure used for the synthesis of spiroacetal-glycine **913** from azide **860a** was adapted from Doores *et al.*[43]. This one-pot/three-component procedure reduces a glycosyl azide to an aza-ylide intermediate, which is then trapped *in situ* by an activated carboxylic acid derivative to give the desired amide. This mild reductive-coupling method avoids isolation of the unstable and easily epimerised hemiaminal/glycosyl amine intermediate (see Chapter 3.5).

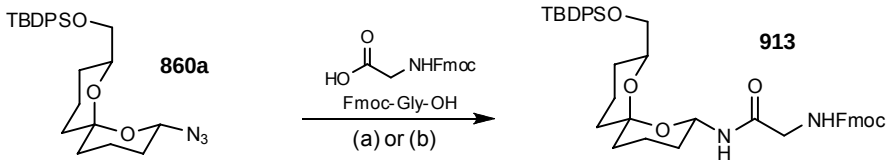

Reagents and conditions: (a) i. Fmoc-Gly-OH, DCC, HOBt•H_2O, MeCN, rt, 30 min; ii. **860a**, PBu_3, MeCN, rt, 4 h, 19%; (b) i. Fmoc-Gly-OH, DIC, HOBt, MeCN, rt, 30 min; ii. **860a**, PBu_3, MeCN, rt, 18 h, 32%.

Scheme 6.32: Synthesis of spiroacetal-glycine **913** from azide **860a** using the Staudinger reaction.

Initially, Fmoc-protected glycine was activated using DCC and hydrous HOBt. The adduct was then reacted with azide **860a** in the presence of tributylphosphine to give spiroacetal-glycine **913** albeit in 19% yield. The crude product from this reaction was also contaminated with DCU, rendering purification difficult. Subsequently, use of DIC and anhydrous HOBt for activation of the amino acid with subsequent addition of azide **860a** and tributylphosphine, gave spiroacetal-glycine **913** in an improved 32% yield (Scheme 6.32).

Similar to the other spiroacetal analogues synthesised in this series, the structure of spiroacetal-glycine **913** (as depicted in Scheme 6.32) was confirmed by the NMR analysis. **913** bears the *bis*-anomerically stabilised spiroacetal conformation with both the TBDPS-protected hydroxymethyl and amino acid substituents adopting equatorial positions on their respective tetrahydropyran rings.

Although the improved yield (32%) was still disappointing, it was, nevertheless, an acceptable result for this preliminary study. Hybridisation of the spiroacetal moiety with an amino acid has been demonstrated to be feasible and there is plenty of scope for future derivatisation to generate a library of spiroacetal-amino acid analogues.

6.9 Deprotection of Spiroacetal Analogues

With the protected spiroacetal analogues, nucleosides **902**, triazoles **909** and amino acid **913** successfully synthesised. The final stage of this study was focused on the final deprotection of these derivatives in order to unmask the 8′-hydroxymethyl substituent on the spiroacetal.

6.9.1 Desilylation of Spiroacetal-Triazoles 909

The desilylation of TBDPS-protected spiroacetal-triazoles **909a–h** and 4-silylated triazoles **909g** and **909h** were envisaged to take place using fluoride-based reagents (Scheme 6.33).

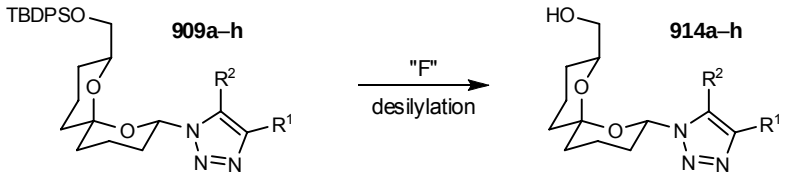

Scheme 6.33: Desilylations of TBDPS-protected triazoles **909a–h** and 4-silylated triazoles **909g** and **909h**. See Table 6.10 for reaction conditions.

Entry	*TBDPS ether*	*Reagents and Conditions*	*Products*	*Yields*
1	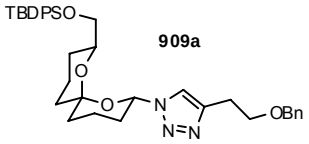	TBAF, 3 Å MS, THF, rt, 4 h	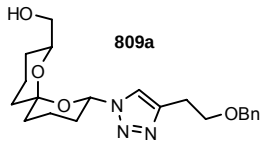	74%
2		HF•pyridine, THF, rt, 18 h		72–75%
3		3HF•NEt_3, THF, rt, 2 d		99%
4	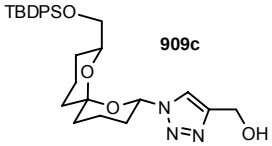	HF•pyridine, THF, rt, 18 h	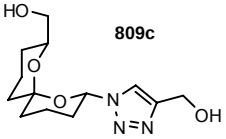	71%
5	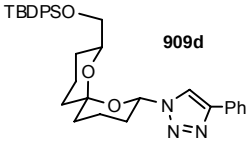	TBAF, 3 Å MS, THF, rt, 1 h	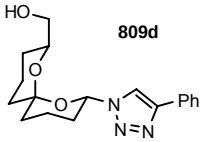	82%
6	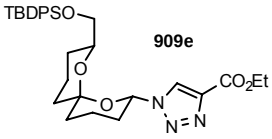	HF•pyridine, THF, rt, 18 h	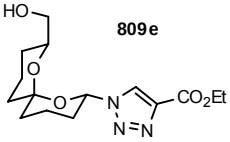	70%
7	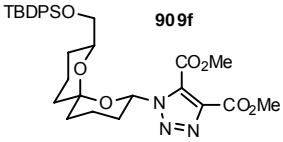	TBAF, 3 Å MS, THF, rt, 3 h	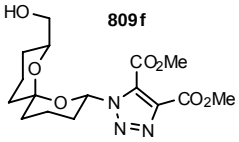	complex mixture
8		HF•pyridine, THF, rt, 1 d		23%
9		3HF•NEt_3, THF, rt, 2.5 d		69%
10	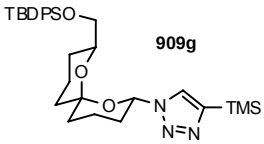	HF•pyridine, THF, rt, 18 h	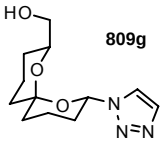	26%
11		3HF•NEt_3, THF, rt, 18 h		86%
12	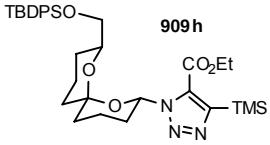	TBAF, THF, rt, 1 h	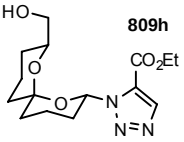	complex mixture
13		3HF•NEt_3, THF, rt–40 °C, 2 d		complex mixture
14		3HF•NEt_3, NEt_3, THF, 40 °C, 2.5 d		93%
15		AcCl, MeOH–CH_2Cl_2, rt, 2 h		complex mixture

Table 6.10: Summary of reagents and conditions used for the desilylations of TBDPS-protected triazoles **909a–h** and 4-silylated triazoles **909g** and **909h** (Scheme 6.33).

Firstly, the desilylations of TBDPS ethers **909a** and **909d** was effected using TBAF in the presence of molecular sieves to give triazoles **809a** and **809d** in 74% and 82% yield, respectively. However, the use of TBAF could not be extended to the desilylation of TBDPS ethers **909f** and **909h** which yielded complex mixtures, possibly due to the basicity of the fluoride reagent used (Table 6.10).

Secondly, the less basic reagent, HF•pyridine was used to successfully effect desilylation of TBDPS ethers **909c** and **909e** in 70–71% yield. The use of HF•pyridine for the deprotection of TBDPS ethers **909a** gave a comparable yield (72–75%) to that observed using TBAF (74%). However, the use of HF•pyridine was found to be too harsh for the deprotection of TBDPS ethers **909f** and **909g** which only afforded triazoles **809f** and **809g** in 23–26% yield (Table 6.10).

Finally, use of a very mild reagent, namely HF•triethylamine[44] was used to effect desilylation of the sensitive triazoles **909f**–**h**. Using the deprotection of TBDPS ether **909a** as a trial reaction, desilylation using HF•triethylamine in THF at room temperature afforded triazole **809a** in 99% yield although a long reaction time was required (2 days). Satisfied the high yield obtained for this reaction, the desilylation of **909f** and **909g** using HF•triethylamine also proceeded successfully to afford triazoles **809f** and **809g** in 69% and 86% yield, respectively. The 4-silyl group in **909g** was also simultaneously removed to give the monosubstituted compound **809g** (Table 6.10).

Disappointingly, use of HF•triethylamine was found to be too harsh to effect the deprotection of **909h** and only a complex mixture was obtained. Subsequently, excess triethylamine was added to buffer the reaction, and gratifyingly, the desired triazole **809h** was afforded in 93% yield. The 4-silyl group in **909h** was also simultaneously removed to give the 1,5-disubstituted compound **809h** (Table 6.10).

The use of non-fluoride based desilylation reagents was also attempted. However, use of catalytic HCl[45], generated *in situ* from the addition of acetyl chloride to methanol, failed to give triazole **809h** and only a complex mixture resulted (Table 6.10).

No epimerisation of the C6′ spirocentre or the C2′/C8′ anomeric centre was observed during the desilylation reactions. Similar to other spiroacetal analogues synthesised in this series, the structures of spiroacetal-triazoles **809a**–**h** were confirmed by the NMR analysis. **809a**–**h** bear the *bis*-anomerically stabilised spiroacetal conformation with both the hydroxymethyl and triazole substituents adopting equatorial positions on their respective tetrahydropyran rings.

The characteristic deshielded nature of H2′ (δ_H 6.74 ppm) in the ^{1}H NMR spectra of the 1,5-disubstituted triazole **809h** was also observed. This observation was due to the electron withdrawing effect exerted by the neighbouring carbonyl group at C5 of the triazole ring, similar to that observed for TBDPS-protected triazole **909h** (Figure 6.8).

6.9.2 Desilylation and Deacylation of Spiroacetal-Nucleosides 902

In light of the successful desilylation of spiroacetal-triazoles **909** described above, deprotection of spiroacetal-nucleosides **902a**–**i** was next carried out. In addition to removal of the

TBDPS group to unmask the 8′-hydroxymethyl group in **902a**–i, *N*-deacylation was also required for nucleosides **902b**, **902f** and **808f**–**h** to afford unmasked nucleosides **808b**, **902i** and **808i**–**k**.

(a) Desilylation

As an extension to the deprotection of triazole analogues, the desilylation of TBDPS-protected spiroacetal-nucleosides **902a**–**i** was carried out primarily using HF•triethylamine (Scheme 6.34).

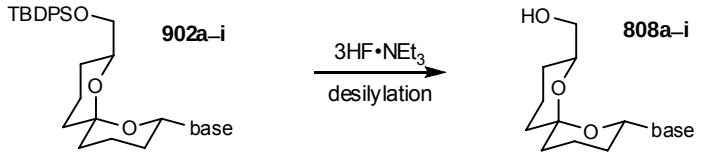

Scheme 6.34: Desilylations of TBDPS-protected nucleosides **902a**–**i**. See Table 6.11 for reaction conditions.

Gratifyingly, the desilylation of TBDPS ethers **902a**–**i** proceeded successfully in the presence of HF•triethylamine to give nucleosides **808a**–**i** in 69–95% yield. The reactions were very sluggish at room temperature and required use of prolonged reaction times and excess reagents. The deprotection were, therefore, carried out at 40 °C (Table 6.11).

Entry	*TBDPS ether*	*Reagents and Conditions*	*Products*	*Yields*
1	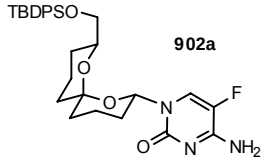	3HF•NEt$_3$, THF, 40 °C, 2 d	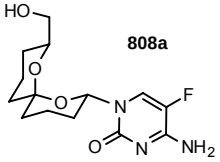	77%
2	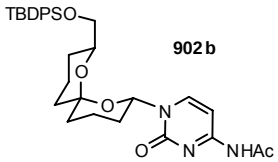	3HF•NEt$_3$, THF, 40 °C, 1 d	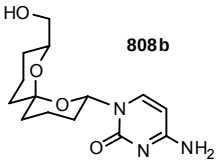	69%*
3	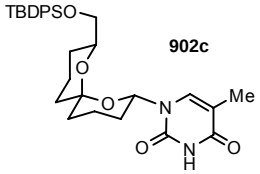	3HF•NEt$_3$, THF, 40 °C, 2 d	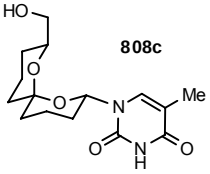	76–79%
4		$CeCl_3$•H_2O, NaI, MeCN, reflux, 3 h		complex mixture
5	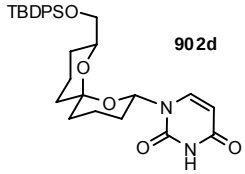	3HF•NEt$_3$, THF, 40 °C, 2 d	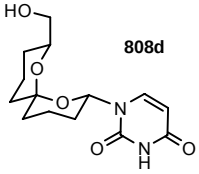	73%
6	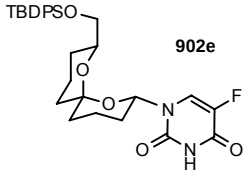	3HF•NEt$_3$, THF, 40 °C, 1 d	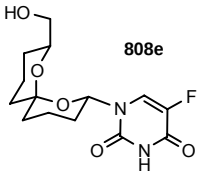	65%

7	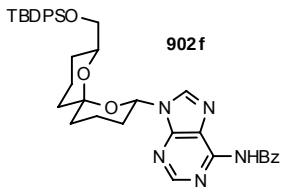 **902f**	3HF•NEt$_3$, THF, 40 °C, 2 d	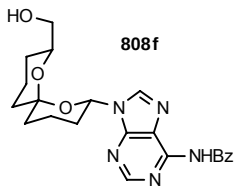 **808f**	85%
8	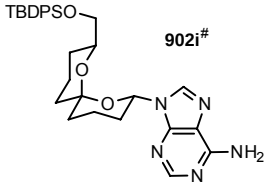 **902i**[#]	3HF•NEt$_3$, THF, 40 °C, 2 d	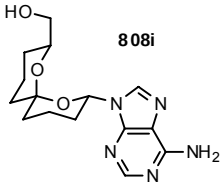 **808i**	92%
9	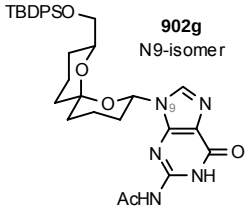 **902g** N9-isomer	3HF•NEt$_3$, THF, 40 °C, 2 d	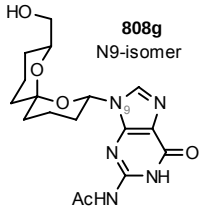 **808g** N9-isomer	91%
10	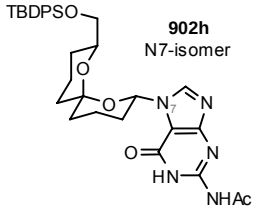 **902h** N7-isomer	3HF•NEt$_3$, THF, 40 °C, 2 d	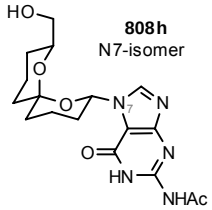 **808h** N7-isomer	95%

Table 6.11: Summary of reagents and conditions used for the desilylations of TBDPS-protected nucleosides **902a–i** (Scheme 6.34).

* One-pot desilylation/*N*-deacetylation was achieved for this particular reaction.

[#] Synthesised *via N*-debenzoylation of adenosine **902f**. See Table 6.12 for reaction conditions.

Attempts to desilylate protected thymidine **902c** using a non-fluoride based reagent, cesium(III) chloride and sodium iodide in MeCN[46] failed to give thymidine **808c** and only a complex mixture resulted (Table 6.11).

Under the current reaction conditions (HF•triethylamine at 40 °C), the *N*-deacetylation of protected cytidine **902b** also occurred concomitantly to give the desired cytidine **808b** in 69% yield. However, deacylation was not observed for the reaction of adenosine and guanosines **902f–h** with HF•triethylamine under the same conditions (Table 6.11). Therefore, a separate *N*-deacylation step was required for these protected nucleosides.

(b) *N*-Deacylation of Nucleosides 808f–h and 902f

A mild *N*-deacylation reaction was required in order to unmask the purine moiety in protected spiroacetal nucleosides **808f–h** and **902f** without effecting cleavage of the sensitive spiroacetal ring and the pseudo *N*-glycosidic bond (Scheme 6.35).

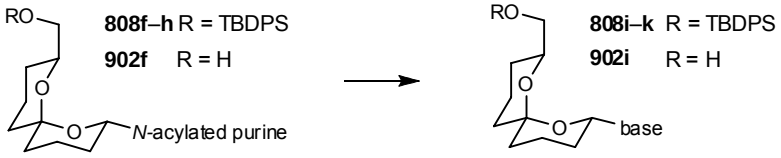

Scheme 6.35: *N*-Deacylation of protected purines **808f–h** and **902f**. See Table 6.12 for reaction conditions.

Entry	*N*-Acylated Nucleosides	*Reagents and Conditions*	*Products*	*Yields*
1	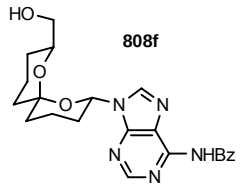	$ZnBr_2$, MeOH–$CHCl_3$, rt, 3 d	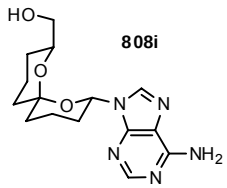	complex mixture
2	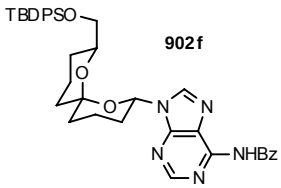	aq. MeOH–NEt_3, microwave, 120 °C, 30 min	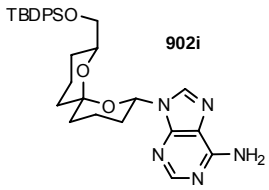	90%*
3	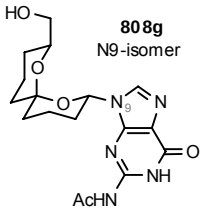	aq. MeOH–NEt_3, microwave, 100 °C, 30 min	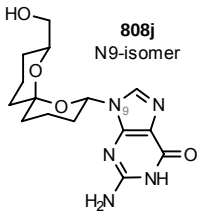	93%
4	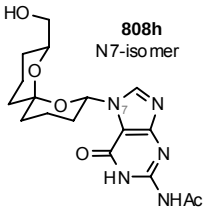	aq. MeOH–NEt_3, microwave, 100 °C, 30 min	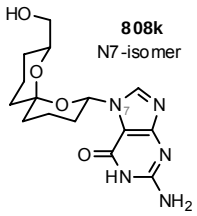	86%

Table 6.12: Summary of reagents and conditions used for the *N*-deacylation of protected purines **808f–h** and **902f** (Scheme 6.35).

* Adenosine **902i** was then desilylated using HF•triethylamine. See Table 6.11 for reaction conditions.

Use of the mild reagent, zinc(II) bromide in MeOH–$CHCl_3$[47] failed to effect *N*-deacylation of protected purine **808f** and only a complex mixture resulted. This result was attributed to the undesired coordination of zinc(II) ion to the spiroacetal ring oxygens instead of the purine N1, thus initiating several ring-opening side reactions. Given the metal-coordinating ability of spiroacetals in general, metal based *N*-deacylation was decreed inappropriate (Table 6.12).

N-Deacylation using non-metal based reagents was next examined. Gratifyingly, protected purine **808g**, **808h** and **902f** was heated at 100–120 °C under microwave irradiation in a mixture of NEt_3–H_2O–MeOH[48] to successfully afford nucleosides **808j**, **808k** and **902i** in 86–93% yield (Table 6.12).

No epimerisation of the C6′ spirocentre or the C2′/C8′ anomeric centre was observed during the desilylation and *N*-deacylation reactions. Similar to other spiroacetal analogues synthesised in this series, the structures of spiroacetal-nucleosides **808a–k** were confirmed by the NMR analysis. **808a–k** bear the *bis*-anomerically stabilised spiroacetal conformation with both the hydroxymethyl and basic substituents adopting equatorial positions on their respective tetrahydropyran rings.

6.9.3 Attempted Deprotection of Spiroacetal-Glycine 913

With the unmasking of the 8′-hydromethyl substituent successfully accomplished for the nucleoside and triazole analogues, attention finally turned to the deprotection of the spiroacetal-amino acid, namely spiroacetal-glycine **913**.

The deprotection of Fmoc group is commonly carried out under basic conditions using an excess of piperidine. Therefore, it is possible that removal of the TBDPS and Fmoc group can be conducted in a stepwise one-pot procedure.

Attempted desilylation of TBDPS ether **913** in the presence of HF•triethylamine at room temperature only gave spiroacetal-glycine **917** in 14% yield after stirring for 3 days with 80% of the starting material being recovered. A second attempt at this desilylation step was conducted successfully using HF•triethylamine in THF at 40–45 °C for 2 days (Scheme 6.36).

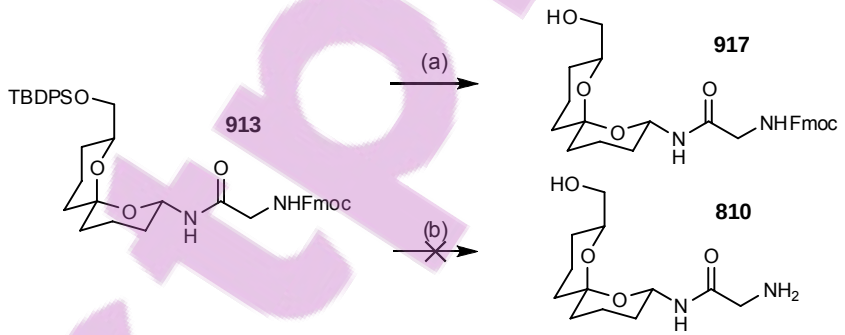

Reagents and conditions: (a) 3HF•NEt_3, THF, rt, 3 d, 14%, (+ **913**: 80%); (b) i. 3HF•NEt_3, THF, 40–45 °C, 2 d, 14%; ii. piperidine, rt, 3 h, complex mixture.

Scheme 6.36: Attempted deprotections of spiroacetal-glycine **913**.

After the disappearance of TBDPS ether **913** was confirmed during the HF•triethylamine reaction, excess piperidine was added to effect neutralisation of the reaction and to effect removal of the Fmoc group. Unfortunately, this addition led to a complex mixture. It was possible that deprotected spiroacetal-glycine **810** was in a form that was too unstable to survive the work-up and chromatography steps (Scheme 6.36).

It is known that amines are often unstable and are therefore often isolated as salts such as salts of ammonium chloride. Despite of the unsuccessful attempt to effect this deprotection step, there is plenty of scope to improve the deprotection and isolation of spiroacetal-glycine **810**, thus providing opportunities for future investigation.

6.10 Summary and Conclusion

To conclude this study, the elaboration of 6,6-spiroacetal with nucleoside, triazole and amino acid bioactive motifs has been successfully accomplished after considerable amount of experimentation with constant revision of the synthetic strategy adopted.

Similar to the model study, acetal **862** served as a key intermediate for this work although its synthesis was different from that described previously. Firstly, lactone **865**[1] was converted to Weinreb amide **892** which was then reacted with Grignard reagent **868** generated from bromide **869**.[15,16] Double deprotection and cyclisation of the resulting ketone **895** under acidic conditions gave the desired acetal **862** over four steps in 58% overall yield (Scheme 6.37).

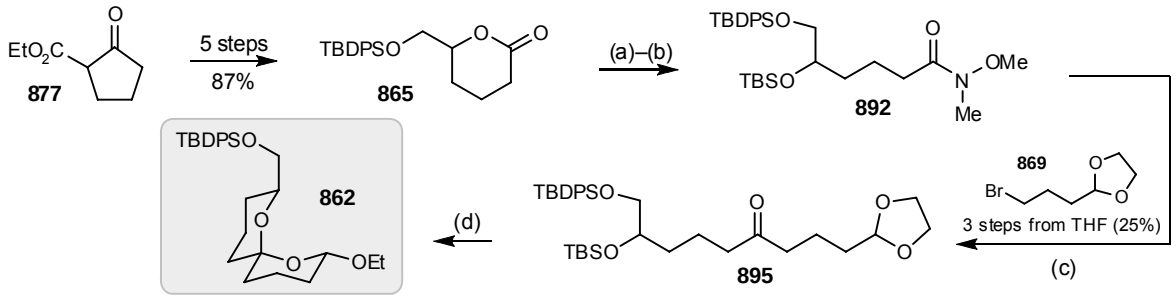

Reagents and conditions: (a) i. N,O-dimethylhydroxylamine hydrochloride, $AlMe_3$, CH_2Cl_2, 0 °C, 20 min; ii. **865**, CH_2Cl_2, 0 °C→rt, 2 h; (b) TBSCl, imidazole, cat. DMAP, CH_2Cl_2, rt, 3 d, 85% over 2 steps (+ 12% **865**); (c) i. Mg, cat. I_2, $(CH_2Br)_2$, THF, rt, 1 h; ii. **892**, THF, rt, 5 min; iii. **869**, 33 °C, 2 h, 80%; (d) CSA, aq. EtOH, rt, 3 h, 85–86% (after 3 x recycling).

Scheme 6.37: Synthesis of acetal **869**.

For the synthesis of spiroacetal-nucleoside analogues, acetal **862** was next converted to acetate **891**. Nucleosidation under Vorbrüggen conditions of acetate **891** gave eight spiroacetal-nucleosides after deprotection of the silyl group. The nucleosides successfully prepared were 5-fluorocytidine **808a**, cytidine **808b**, thymidine **808c**, uridine **808d**, 5-fluorouridine **808e**, adenosine **808i**, N9-guanosine **808j** and N7-guanosine **808k** (Scheme 6.38).

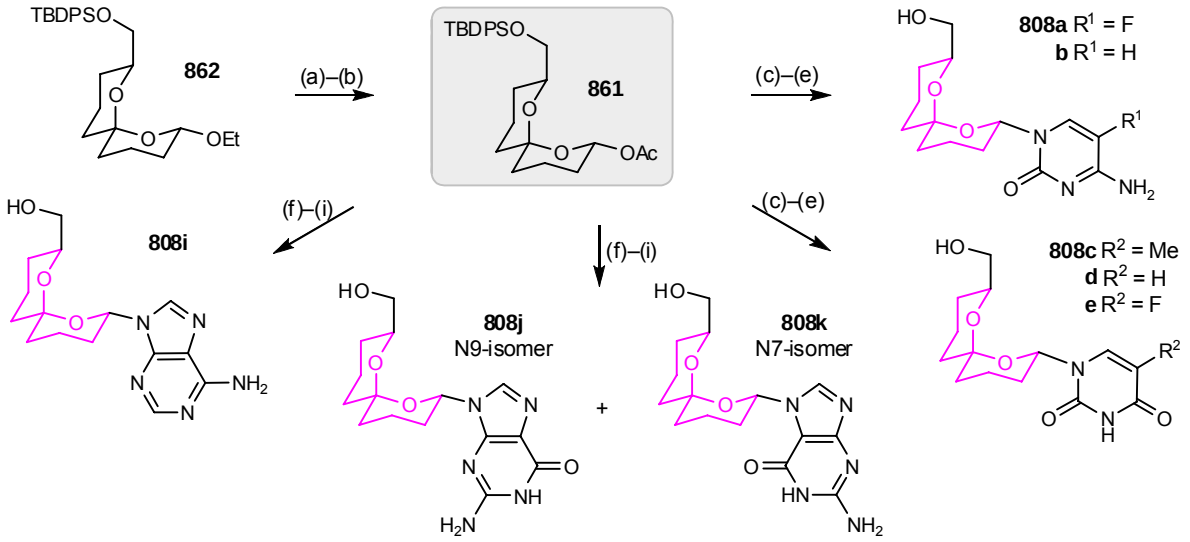

Reagents and conditions: (a) CSA, aq. THF, 40 °C, 18 h; (b) Ac_2O, cat. DMAP, NEt_3, CH_2Cl_2, rt, 2 h, 58–66%; (c) pyrimidine (^{5F}C, ^{Ac}C, T, U and ^{5F}U), cat. $(NH_4)_2SO_4$, HMDS, reflux, 1–4 h; (d) **861**, TMSOTf, CH_2Cl_2, rt, 2–3 h, 20–45%; (e) 3HF•NEt_3, THF, 40 °C, 1–2 d, 65–79%; (f) purine (^{Bz}A and ^{Ac}G), HMDS–BSA–toluene, reflux, 1 h; (g) **861**, TIPSOTf, CH_2Cl_2, rt, 18 h, 33–37%; (h) 3HF•NEt_3, THF, 40 °C, 2 d, 85–95%; (i) aq. MeOH–NEt_3, microwave, 120 °C, 30 min; 86–93%

Scheme 6.38: Synthesis of spiroacetal–nucleosides **808**.

For the synthesis of spiroacetal-triazole analogues, acetal **862** was converted to azide **860a**. Cycloaddition of **860a** to a range of alkynes, either catalysed by copper(I) or promoted thermally, gave seven spiroacetal-triazoles after deprotection of the silyl group. The triazoles successfully prepared were 1,4-disubstitued triazoles **809a–e**, trisubstituted triazole **809f**, monosubstituted triazole **809g** and 1,5-disubstitued triazole **809h** (Scheme 6.39).

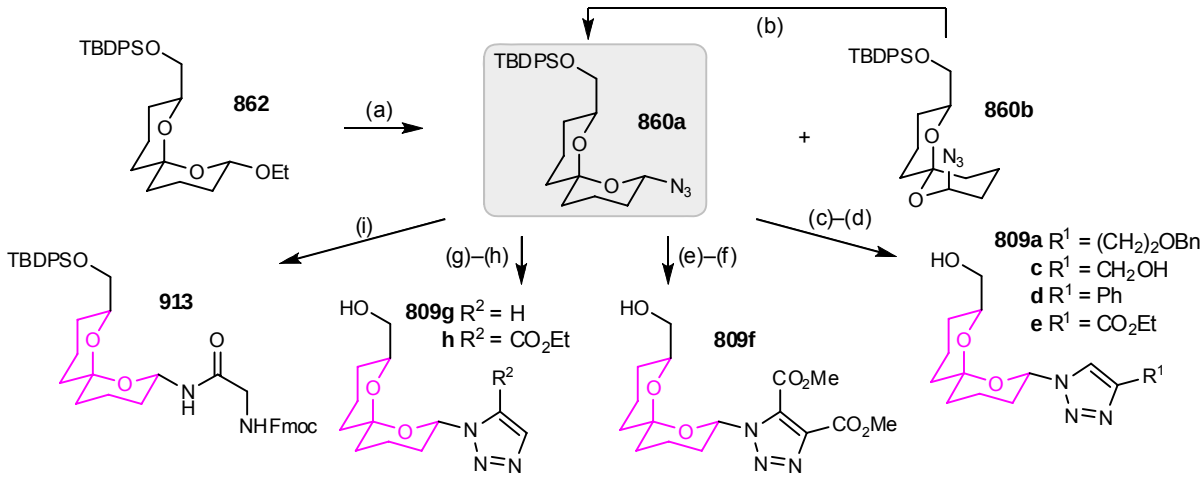

Reagents and conditions: (a) $TMSN_3$, TMSOTf, CH_2Cl_2, -10 °C, 3 h, **860a**: 36%, **860b**: 15%, **862**: 5%; (b) $TMSN_3$, TMSOTf, CH_2Cl_2, -10 °C, 3 h, **860a**: 43%, **860b**: 20%; (c) alkyne, cat. CuI•$P(OEt)_3$, toluene, reflux, 1 h, 84–98%; (d) either 3HF•NEt_3, THF, rt, 2 d, **809a**: 99% or HF•pyridine, THF, rt, 18 h, **809c**: 71%, **809e**: 70% or TBAF, 3 Å MS, THF, rt, 1 h, **809d**: 82%; (e) DMAD, toluene, reflux, 1 h, 78%; (f) 3HF•NEt_3, THF, rt, 2.5 d, 69%; (g) alkyne, toluene, seal tube, reflux, 2 d, 64–84%; (h) either 3HF•NEt_3, THF, rt, 18 h, **809f**: 86%, **809g**: 86% or 3HF•NEt_3, NEt_3, THF, 40 °C, 2.5 d, **809h**: 93%; (i) i. Fmoc-Gly-OH, DIC, HOBt, MeCN, rt, 30 min; ii. **860a**, PBu_3, MeCN, rt, 18 h, 32%.

Scheme 6.39: Synthesis of spiroacetal–triazoles **809** and spiroacetal–glycine **913**.

For the preliminary investigation of spiroacetal-amino acid analogues, spiroacetal-glycine **810** was targeted as a representative example. Using the Staudinger ligation, spiroacetal **913** was synthesised from azide **860a** and an activated glycine derivative in the presence of a phosphine (Scheme 6.39). Due to the time constraints, the deprotection of spiroacetal-glycine **913** was attempted but not completed. Suggestions for future work will be discussed in the following section (see Section 6.11).

All of the spiroacetal analogues synthesised in the present work (except for azide **860b**) bear the *bis*-anomerically stabilised spiroacetal conformation with both the C8′-hydroxymethyl and C2′-substituents adopting equatorial positions on their associated tetrahydropyran rings. The conformation was adopted to minimise the unfavourable steric interactions and 1,3-dipole effects.

During the nucleophilic addition to an oxonium ion generated from acetate **861** or acetal **862**, the possible adoption of a half chair conformation in the oxonium ion containing ring may also lead to the addition from the less hindered face, resulting in overall equatorial substitution.[25]

It is also noted that the present synthetic route afforded a racemic mixture of spiroacetal analogues due to the use of racemic starting material, namely valerolactone **865**. Stereospecific synthesis of spiroacetal analogues, therefore, provides opportunities for future investigation (see Section 6.11.3).

Compared to the model study, spiroacetals bearing a 8′-hydroxymethyl substituent were found to be easier to handle in general. The volatility and stability problems encountered during the model study, were not observed in the present work.

To date, a small collection of novel spiroacetal hybrids have been synthesised. The knowledge gained in this study will be beneficial for future elaboration of 6,6-spiroacetals with other biologically active motifs. As a result, a large number of derivatives can be generated and used as biological probes for future broad phenotypic assays to screen for any potential functionality.

6.11 Future Work

6.11.1 Spiroacetal-Amino Acids and Spiroacetal-Peptides 918

Firstly, optimisation of the Staudinger ligation used for the synthesis of spiroacetal-amino acid derivatives is required. This work may be achieved by using alternative coupling agents and/or phosphines. The successful conditions that developed can then be applied to the synthesis of other amino acid or peptide derivatives (Scheme 6.40).

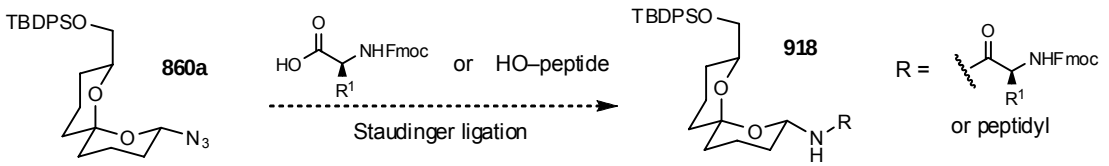

Scheme 6.40: Staudinger ligations between azide **860a** and other amino acids or peptide chains.

Secondly, removal of the TBDPS and Fmoc groups are required to complete the synthesis of spiroacetal-amino acid derivative. It was envisaged that the removal of the TBDPS group could be accomplished using HF•triethylamine by adjusting previously used reaction conditions. On the other hand, removal of the Fmoc group using piperidine or morpholine requires further investigation. Isolation of the free amine as its ammonium salt could also be beneficial (Scheme 6.41).

Alternatively, removal of Fmoc alone may enable further coupling of the spiroacetal derivative to a peptide chain and rapidly generate a range of spiroacetal-peptide analogues (Scheme 6.41).

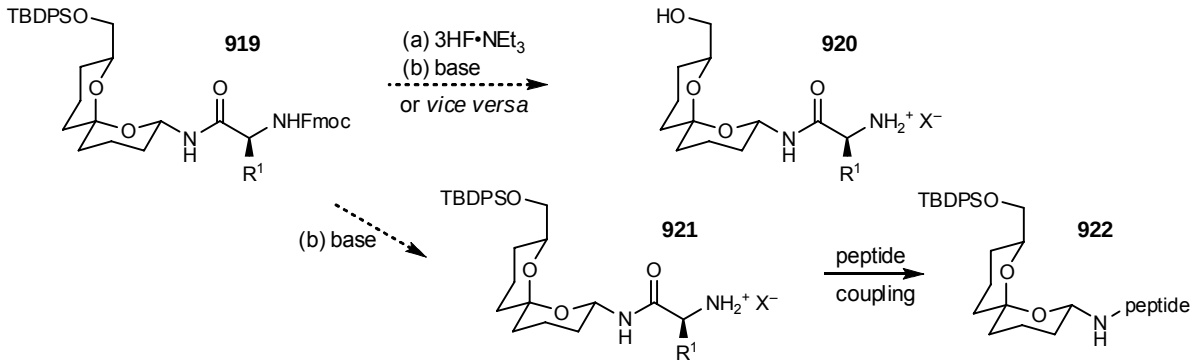

Scheme 6.41: Deprotection of spiroacetal-amino acid analogues **919**. Removal of Fmoc in **921** gives **922** which may be subsequently coupled to a peptide.

6.11.2 Spiroacetal-Triazoles 925 and Spiroacetal-Tetrazoles 926

In light of the successful synthesis of spiroacetal-triazoles **809** *via* the cycloaddition of azide **860a** to alkynes, the complementary triazole analogues **925** and tetrazole analogues **926** may be worthwhile to investigate. With the C–C connection between the spiroacetal and triazole/tetrazole moiety, these novel analogues **925** and **926** may provide better stability against hydrolytic cleavage (Scheme 6.42). As previously mentioned, the tetrazole moiety is an isostere of a carboxylic acid and a *cis*-peptide bond depending on the nature of its substituent (see Chapter 5.6).[49]

It is envisaged that spiroacetal-triazoles **925** and tetrazoles **926** can be obtained *via* the cycloaddition of an azide to spiroacetal-acetylene **923** or nitrile **924**. Alkyne **923** and nitrile **824**, in turn,

are synthesised from either acetate **861** or acetal **862** using procedures adapted from the literature (Scheme 6.42).[50]

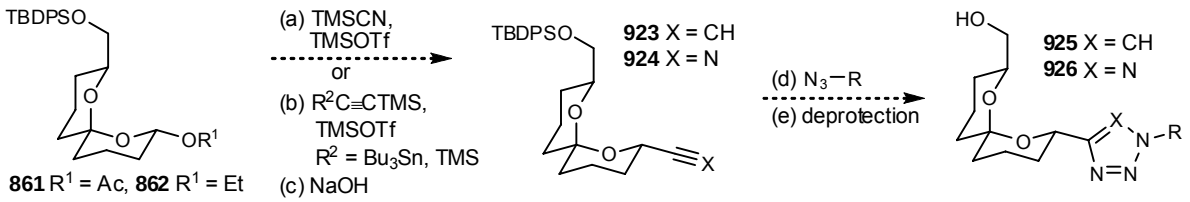

Scheme 6.42: Proposed synthesis of spiroacetal-triazoles **925** and tetrazoles **926** from acetate **861** or acetal **862**.

6.11.3 Stereoselective Synthesis of Ethoxy-Spiroacetal 862

It should be noted that the spiroacetal analogues synthesised in this study are all racemic. The stereoselective synthesis of the spiroacetal derivatives would be interesting, both chemically and biologically.

It is envisaged that the stereochemistry of the spiroacetal analogues can be controlled using enantiomerically pure lactone **865**. The use of *(S)*-lactone **865** in the synthesis would give *(S,S,S)*-acetal **862** whereas the use of *(R)*-lactone **865** would give *(R,R,R)*-acetal **862**. The preparation of *(S)*-lactone **865** has previously been described by Forsyth *et al.*[7] starting from *(R)*-glycidol **(244)** (Scheme 6.43). Although the stereospecific synthesis of *(R)*-lactone **865** was not described in the literature, it is expected that *(R)*-lactone **865** can be prepared from *(S)*-glycidol **(244)** using the same transformation as its enantiomeric *(S)*-lactone **865** (Scheme 6.44).

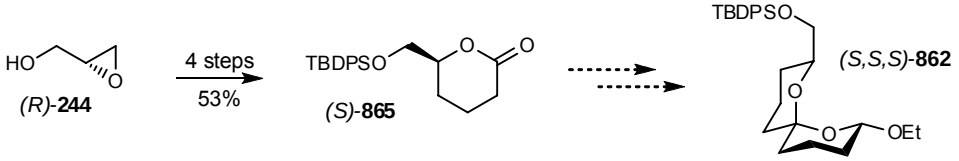

Scheme 6.43: Proposed synthesis of *(S,S,S)*-acetal **862** from *(R)*-glycidol **(244)** *via (S)*-lactone **865**, which was previously synthesised by Forsyth *et al.*[7]

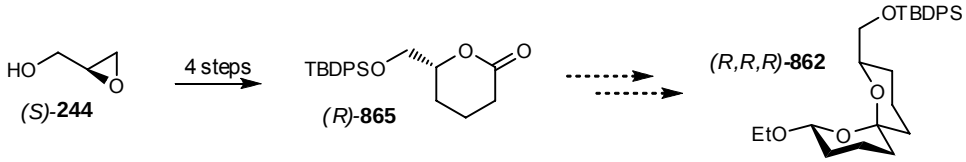

Scheme 6.44: Proposed synthesis of *(R,R,R)*-acetal **862** from *(S)*-glycidol **(244)** *via (R)*-lactone **865**.[7]

6.12 References

1. R. J. K. Taylor, K. Wiggins and D. H. Robinson, *Synthesis*, 1990, 589-590.
2. R. J. Anderson, H. R. Chinn, K. Gill and C. A. Henrick, *J. Chem. Ecol.*, 1979, **5**, 919-927; M. A. Brimble, M. K. Edmonds and G. M. Williams, *Tetrahedron*, 1992, **48**, 6455-6466.
3. L. A. Paquette, *Aust. J. Chem.*, 2004, **57**, 7-17 and references cited therein; S. Dong and L. A. Paquette, *J. Org. Chem.*, 2005, **70**, 1580-1596 and references cited therein; R. Hartung and L. A. Paquette, *J. Org. Chem.*, 2005, **70**, 1597-1604; R. E. Hartung and L. A. Paquette, *Synthesis*, 2005, 3209-3218; L. A. Paquette and S. Dong, *J. Org. Chem.*, 2005, **70**, 5655-5664; R. E. Hartung and L. A. Paquette, *Heterocycles*, 2006, **67**, 75-78; S. Dong and L. A. Paquette, *J. Org. Chem.*, 2006, **71**, 1647-1652.
4. G. Zinzalla, L.-G. Milroy and S. V. Ley, *Org. Biomol. Chem.*, 2006, **4**, 1977-2002.
5. R. Alvarez, S. Velázquez, A. San-Félix, S. Aquaro, E. De Clercq, C.-F. Perno, A. Karlsson, J. Balzarini and M. J. Camarasa, *J. Med. Chem.*, 1994, **37**, 4185-4194.
6. Q. Chen, H. Deng, J. Zhao, Y. Lu, M. He and H. Zhai, *Tetrahedron*, 2005, **61**, 8390-8393.
7. A. B. Dounay, R. A. Urbanek, V. A. Frydrychowski and C. J. Forsyth, *J. Org. Chem.*, 2001, **66**, 925-938; A. B. Dounay and C. J. Forsyth, *Org. Lett.*, 1999, **1**, 451-453.
8. D. B. Dess and J. C. Martin, *J. Org. Chem.*, 1983, **48**, 4155-4156; D. B. Dess and J. C. Martin, *J. Am. Chem. Soc.*, 1991, **113**, 7277-7287; M. Frigerio, M. Santagostino and S. Sputore, *J. Org. Chem.*, 1999, **64**, 4537-4538.
9. C. J. Burns, M. Gill and S. Saubern, *Aust. J. Chem.*, 1997, **50**, 1067-1079.
10. L. A. Paquette, D. R. Owen, R. T. Bibart, C. K. Seekamp, A. L. Kahane, J. C. Lanter and M. A. Corral, *J. Org. Chem.*, 2001, **66**, 2828-2834; W. G. Dauben and A. F. Cunningham, *J. Org. Chem.*, 1983, **48**, 2842-2847; H.-J. Liu and W.-L. Yeh, *Heterocycles*, 1996, **42**, 493-497; P. H. J. Carlsen, T. Katsuki, V. S. Martin and K. B. Sharpless, *J. Org. Chem.*, 1981, **46**, 3936-3938.
11. K. Mori and M. Miyake, *Tetrahedron*, 1987, **43**, 2229-2239.
12. A. B. Smith, III and R. M. Scarborough, *Synth. Commun.*, 1980, **10**, 205-211.
13. E. J. Corey and J. W. Suggs, *Tetrahedron*, 1975, **16**, 2647-2650; Y.-S. Cheng, W.-L. Liu and S.-H. Chen, *Synthesis*, 1980, 223-224; D. Savoia, C. Trombini and A. Umani-Ronchi, *J. Org. Chem.*, 1982, **47**, 564-566; B. M. Trost, T. A. Grese and D. M. T. Chan, *J. Am. Chem. Soc.*, 1991, **113**, 7350-7362.
14. P. C. Wälchli and C. H. Eugster, *Helv. Chim. Acta*, 1978, **61**, 885-898.
15. E. Vedejs, M. J. Arnost and J. P. Hagen, *J. Org. Chem.*, 1979, **44**, 3230-3238; M. Segi, M. Takahashi, T. Nakajima, S. Suga and N. Sonoda, *Synth. Commun.*, 1989, **19**, 2431-2439.
16. D. Wenkert, S. B. Ferguson, B. Porter, A. Qvarnstrom and A. T. McPhail, *J. Org. Chem.*, 1985, **50**, 4114-4119.
17. D. Enders, B. Nolte, G. Raabe and J. Runsink, *Tetrahedron: Asymmetry*, 2002, **13**, 285-291.
18. R. Shintani and G. C. Fu, *Org. Lett.*, 2002, **4**, 3699-3702; D. Castagnolo, I. Breuer and P. M. Pihko, *J. Org. Chem.*, 2007, **72**, 10081-10087; P. M. Pihko and J. E. Aho, *Org. Lett.*, 2004, **6**, 3849-3852.
19. C. P. Forbes, G. L. Wenteler and A. Wiechers, *J. Chem. Soc., Perkin Trans. 1*, 1977, 2353-2355.
20. S. A. Bal, A. Marfat and P. Helquist, *J. Org. Chem.*, 1982, **47**, 5045-5050.
21. J. I. Levin, E. Turos and S. M. Weinreb, *Synth. Commun.*, 1982, **12**, 989-993.
22. K. J. Hodgetts, *ARKIVOC*, 2001, 74-79.
23. K. Meilert and M. A. Brimble, *Org. Biomol. Chem.*, 2006, **4**, 2184-2192; K. Meilert and M. A. Brimble, *Org. Lett.*, 2005, **7**, 3497-3500; M. A. Brimble and D. P. Furkert, *Org. Biomol. Chem.*, 2004, **2**, 3573-3583.
24. B. S. Bal, W. E. J. Childers and H. W. Pinnick, *Tetrahedron*, 1981, **37**, 2091-2096.
25. K. T. Mead and R. Zemribo, *Synlett*, 1996, 1063-1064.
26. M. de Greef and S. Z. Zard, *Org. Lett.*, 2007, **9**, 1773-1776.
27. R. Zemribo and K. T. Mead, *Tetrahedron Lett.*, 1998, **39**, 3891-3894.
28. B. M. Trost and J. R. Corte, *Angew. Chem. Int. Ed.*, 1999, **38**, 3664-3666.
29. G. Vidari, G. Lanfranchi, N. Pazzi and S. Serra, *Tetrahedron Lett.*, 1999, **40**, 3063-3066.

30. N. S. Wilson and B. A. Keay, *J. Org. Chem.*, 1996, **61**, 2918-2919; B. H. Lipshutz, D. Pollart, J. Monforte and H. Kotsuki, *Tetrahedron Lett.*, 1985, **26**, 705-708.
31. G. Barone, E. Bedini, A. Iadonisi, E. Manzo and M. Parrilli, *Synlett*, 2002, 1645-1648; A. DattaGupta, R. Singh and V. K. Singh, *Synlett*, 1996, 69-71.
32. C. Prakash, S. Saleh and I. A. Blair, *Tetrahedron Lett.*, 1989, **30**, 19-22.
33. P. Deslongchamps, D. D. Rowan, N. Pothier, T. Sauvé and J. K. Saunders, *Can. J. Chem.*, 1981, **59**, 1105-1121.
34. P. R. Allen, M. A. Brimble and H. Prabaharan, *J. Chem. Soc., Perkin Trans. 1*, 2001, 379-389; M. A. Brimble, *Molecules*, 2004, **9**, 394-404; G. J. McGarvey and M. W. Stepanian, *Tetrahedron Lett.*, 1996, **37**, 5461-5464; G. J. McGarvey, M. W. Stepanian, A. R. Bressette and J. F. Ellena, *Tetrahedron Lett.*, 1996, **37**, 5465-5468.
35. R. Zemribo and K. T. Mead, *Tetrahedron Lett.*, 1998, **39**, 3895-3898; M. A. Brimble, F. A. Fares and P. Turner, *J. Chem. Soc., Perkin Trans. 1*, 1998, 677-684.
36. R. Ben Othman, T. Bousquet, A. Fousse, M. Othman and V. Dalla, *Org. Lett.*, 2005, **7**, 2825-2828.
37. H. Vorbrüggen and C. Ruh-Pohlenz, *Org. React.*, 2000, **55**, 1-630; H. Vorbrüggen and C. Ruh-Pohlenz, *Handbook of Nucleoside Synthesis*, John Wiley & Sons, Inc., Chichester, UK, 2001; K. Izawa and H. Shiragami, *Pure Appl. Chem.*, 1998, **70**, 313-318.
38. M. Böhringer, H.-J. Roth, J. Hunziker, M. Göbel, R. Krishnan, A. Giger, B. Schweizer, J. Schreiber, C. Leumann and A. Eschenmoser, *Helv. Chim. Acta*, 1992, **75**, 1416-1477; L. A. Paquette, C. K. Seekamp, A. L. Kahane, D. G. Hilmey and J. Gallucci, *J. Org. Chem.*, 2004, **69**, 7442-7447.
39. K. W. Choi, M. A. Brimble and T. Groutso, *Acta Crystallogr. Sect. E: Struct. Rep. Online*, 2008, **64**, O715-U1424.
40. J. M. Casas-Solvas, A. Vargas-Berenguel, L. F. Capitan-Vallvey and F. Santoyo-Gonzalez, *Org. Lett.*, 2004, **6**, 3687-3690.
41. C. S. Kraihanzel and M. L. Losee, *J. Org. Chem.*, 1968, **33**, 1983-1986; J. Cossy, A. Schmitt, C. Cinquin, D. Buisson and D. Belotti, *Bioorg. Med. Chem. Lett.*, 1997, **7**, 1699-1700; P. J. Dunn and C. W. Rees, *J. Chem. Soc., Perkin Trans. 1*, 1987, 1579-1584.
42. S. J. Coats, J. S. Link, D. Gauthier and D. J. Hlasta, *Org. Lett.*, 2005, **7**, 1469-1472.
43. K. J. Doores, Y. Mimura, R. A. Dwek, P. M. Rudd, T. Elliott and B. G. Davis, *Chem. Comm.*, 2006, 1401-1403.
44. M. C. Pirrung, S. W. Shuey, D. C. Lever and L. Fallon, *Bioorg. Med. Chem. Lett.*, 1994, **4**, 1345-1346; D. K. Ress, S. N. Baytas, Q. Wang, E. M. Munoz, K. Tokuzoki, H. Tomiyama and R. J. Linhardt, *J. Org. Chem.*, 2005, **70**, 8197-8200.
45. A. T. Khan and E. Mondal, *Synlett*, 2003, 694-698.
46. G. Bartoli, M. Bosco, E. Marcantoni, L. Sambri and E. Torregiani, *Synlett*, 1998, 209-211.
47. R. Kierzek, H. Ito, R. Bhatt and K. Itakura, *Tetrahedron Lett.*, 1981, **22**, 3761-3764.
48. E. Söderberg, J. Westman and S. Oscarson, *J. Carbohydr. Chem.*, 2001, **20**, 397-410.
49. Maybridge, *Bioisosteres in Medicinal Chemistry*, Thermo Fisher Scientific, Cornwall; Z. P. Demko and K. B. Sharpless, *Angew. Chem. Int. Ed.*, 2002, **41**, 2110-2113; Z. P. Demko and K. B. Sharpless, *Angew. Chem. Int. Ed.*, 2002, **41**, 2113-2116.
50. N. Cohen, B. Schaer, G. Saucy, R. Borer, L. Todaro and A.-M. Chiu, *J. Org. Chem.*, 1989, **54**, 3282-3292; S. D. Rychnovsky and L. R. Takaoka, *Angew. Chem. Int. Ed.*, 2003, **42**, 818-820; T. Nishikawa, M. Ishikawa and M. Isobe, *Synlett*, 1999, 123-125; M. Isobe, R. Nishizawa, S. Hosokawa and T. Nishikawa, *Chem. Comm.*, 1998, 2665-2676; A. Dondoni, G. Mariotti and A. Marra, *J. Org. Chem.*, 2002, **67**, 4475-4486.

Chapter Seven:

7 Experimental

7.1 General Details

Reaction Conditions

Experiments requiring anhydrous conditions were performed under a dry nitrogen or argon atmosphere using oven- or flame-dried apparatus and standard techniques in handling air- and/or moisture-sensitive materials unless otherwise stated. Anhydrous dichloromethane (CH_2Cl_2), triethylamine (NEt_3), dimethyl sulfoxide (DMSO), hexane and acetonitrile (MeCN) were distilled from calcium hydride; anhydrous tetrahydrofuran (THF) and diethyl ether (Et_2O) was distilled from sodium wire; anhydrous dry toluene was distilled from sodium wire. Solvents used (except for Et_2O) for reactions, work-up extractions and chromatographic purifications were distilled, unless otherwise stated. Commercial reagents were analytical grade or were purified by standard procedures prior to use.[1] Aqueous solutions of sodium chloride (brine), sodium bicarbonate and ammonium chloride were saturated. Reactions performed at room temperature were carried out at *ca.* 20 °C and reaction temperatures from -78 °C to 0 °C were obtained using the following cryostats: acetone/dry ice, -78 °C; acetonitrile/dry ice, -40 °C; NaCl/ice, -15 °C; water/ice, 0 °C.

Microwave reactions were conducted in sealed reaction vessels using a Discover® LabMate microwave synthesiser (CEM Corporation) at the temperature stated.

The progress of reactions was monitored by analytical thin layer chromatography (TLC) using Keiselgel F_{254} 0.2 m (Merck) silica plates or aluminium oxide N/UV_{254} 0.2 mm (Macherey-Nagel) alumina plates as stated, with visualisation by ultraviolet irradiation (365 nm) followed by staining with either ethanolic vanillin or phosphomolybdic acid (PMA) solution.

Separation of mixtures was performed by flash chromatography using Kieselgel S 63–100 μm (Riedel-de-Hahn) silica gel with the indicated eluent. The relevant fractions were combined and the solvents were removed *in vacuo*.

Physical Characterisation

Melting points were recorded on a Kofler hot-stage apparatus and are uncorrected.

Mass spectra were recorded on a VG-70SE mass spectrometer at a nominal accelerating voltage of 70 eV for low resolution and at a nominal resolution of 5000 to 10000 as appropriate for high resolution. Ionisation was effected using electron impact (EI^+), desorption electron impact (DEI^+), fast atom bombardment (FAB^+) using 3-nitrobenzyl alcohol as the matrix or chemical ionisation (CI^+) using ammonia as a carrier gas. Major and significant fragments are quoted in the form x (y), where x is the mass to charge ratio (*m/z*) and y is the percentage abundance relative to the base peak (100%).

Spectroscopic Characterisation

Infrared spectra were obtained using a Perkin Elmer Spectrum 1000 Fourier Transform Infrared spectrometer as a thin film between sodium chloride plates. Absorption peaks are reported as wavenumbers (ν, cm^{-1}).

^{1}H NMR spectra were recorded on either a Bruker DRX300 spectrophotometer operating at 300 MHz or a Bruker DRX400 spectrophotometer operating at 400 MHz at ambient temperature. ^{1}H NMR chemical shifts are reported in parts per million (ppm) relative to the tetramethylsilane peak (δ 0.00 ppm). ^{1}H NMR values are reported as chemical shift δ, relative integral, multiplicity (s, singlet; d, doublet; t, triplet; q, quartet; quintet; m, multiplet), coupling constant (*J*, Hz) and assignment. Coupling constants were taken directly from the spectra. Decoupled ^{13}C NMR spectra were recorded on either a Bruker DRX300 spectrophotometer operating at 75 MHz or a Bruker DRX400 spectrophotometer operating at 100 MHz at ambient temperature. ^{13}C NMR chemical shifts are reported in ppm relative to the peak of $CDCl_3$ (δ 77.0 ppm) or CD_3OD (δ 49.0 ppm). ^{13}C NMR values are reported as chemical shift δ, multiplicity and assignment. Assignments were made with the aid of DEPT, COSY, HSQC, HMBC and NOESY experiments. Decoupled ^{19}F NMR spectra were recorded on a Bruker DRX300 spectrophotometer operating at 282 MHz and data are expressed in ppm relative to $CFCl_3$ peak (δ 0.00 ppm).

7.2 Experimental Data–Spiroacetal Models

7.2.1 Synthesis of Acetylene Starting Materials

1-(Benzyloxy)but-3-yne (821)[2]

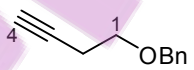

This procedure is an adaptation of that reported by Burns *et al.*[2]

To a suspension of NaH (2.13 g, 89.1 mmol, 95% mineral oil dispersion) in anhydrous THF (100 mL) at 0 °C was added 3-butyn-1-ol (5.40 mL, 71.3 mmol) dropwise. After 30 min, a solution of benzyl bromide (8.91 mL, 74.9 mmol) in anhydrous THF (66 mL) was added dropwise and the mixture was stirred at room temperature overnight. Ice-cold brine (50 mL) was added and the aqueous phase was extracted with EtOAc (3 x 100 mL). The combined organic extracts were dried over $MgSO_4$ and concentrated *in vacuo*. Purification by flash chromatography using hexane–Et_2O (1:0 to 4:1) as eluent yielded the title benzyl ether **821** as a yellow oil (11.3 g, 99%). The spectral data were in agreement with that reported in the literature.[2]

HRMS (FAB): found MH^+, 161.0957, $C_{11}H_{13}O$ requires 161.0966.

ν_{max} (film)/cm^{-1}: 3295 (≡C–H), 2916, 2863 (C–H), 2120 (C≡C), 1453, 1363, 1104 (C–O), 738, 698.

δ_H (300 MHz; $CDCl_3$): 2.00 (1 H, t, $J_{4,2}$ 2.7, 4-H), 2.51 (2 H, td, $J_{2,1}$ 6.9 and $J_{2,4}$ 2.7, 2-H), 3.61 (2 H, t, $J_{1,2}$ 6.9, 1-H), 4.57 (2 H, s, OC*H*$_2$Ph), 7.26–7.37 (5 H, m, Ph).

δ_C (75 MHz; $CDCl_3$): 19.9 (CH_2, C-2), 68.1 (CH_2, C-1), 69.3 (C, C-3), 73.0 (CH_2, O*CH*$_2$Ph), 81.2 (CH, C-4), 127.7 (2 x CH, Ph), 128.4 (CH, Ph), 138.0 (C, Ph).

***m/z* (CI):** 178 (MH + NH_3, 44%), 161 (MH^+, 20), 159 (M – H, 32), 105 (22), 91 (Bn, 100).

1-(Trimethylsilyloxy)but-3-yne (866)[3]

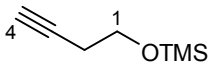

To a solution of 3-butyn-1-ol (3.24 mL, 42.8 mmol) and NEt_3 (11.9 mL, 85.6 mmol) in anhydrous THF (75 mL) at room temperature was added TMSCl (5.47 mL, 42.8 mmol) dropwise. After 24 h, water (10 mL) was added and the aqueous phase was extracted with Et_2O (3 x 10 mL). The combined organic extracts were dried over $MgSO_4$ then concentrated *in vacuo*. Purification by flash chromatography using pentane–Et_2O (19:1 to 9:1) as eluent yielded the title acetylene **866** (4.20 g, 69%) as a colourless oil. The spectral data were in agreement with that reported in the literature.[3]

ν_{max} (film)/cm^{-1}: 3312 (≡C–H), 2957 (C–H), 2122 (C≡C), 1252 (C–O), 1103 (C–O), 919, 842, 749, 635.

δ_H (300 MHz; $CDCl_3$): 0.14 (9 H, s, $OSiMe_3$), 1.98 (1 H, t, $J_{4,2}$ 2.7, 4-H), 2.42 (2 H, td, $J_{2,1}$ 7.1 and $J_{2,4}$ 2.7, 2-H), 3.72 (2 H, t, $J_{1,2}$ 7.1, 1-H).

δ_C (75 MHz; $CDCl_3$): -0.5 (CH_3, $OSiMe_3$), 22.7 (CH_2, C-2), 61.1 (CH_2, C-1), 69.4 (CH, C-4), 81.4 (C, C-3).

Ethyl Propiolate (857)[4]

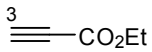

To a solution of propiolic acid (879 μL, 14.2 mmol) and anhydrous ethanol (1.65 mL, 28.4 mmol) in anhydrous Et_2O (10 mL) at -40 °C was added an ice-cold mixture of DCC (3.24 g, 15.7 mmol) and DMAP (121 mg, 994 μmol) in Et_2O (30 mL) dropwise. The mixture was warmed to room temperature. After 18 h, the mixture was filtered, washed with ice-cold aqueous HCl solution (2 x 30 mL, 1.0 mol L^{-1}) and brine (30 mL). The combined aqueous phases were extracted with Et_2O (30 mL). The combined organic extracts were dried over $MgSO_4$ and concentrated *in vacuo*. Purification by distillation under reduced pressure yielded the title acetylene **857** (598 mg, 43%) as a colourless oil. The spectral data were in agreement with that reported in the literature.[5]

B.p.: 43 °C at 70 mmHg (literature b.p.[5]: 116–118 °C)

δ_H (300 MHz; $CDCl_3$): 1.33 (3 H, t, J_{CH_3,CH_2} 7.1, OCH_2CH_3), 2.89 (1 H, s, 3-H), 4.26 (2 H, q, J_{CH_3,CH_2} 7.1, OCH_2CH_3).

δ_C (75 MHz; $CDCl_3$): 13.9 (CH_3, OCH_2CH_3), 62.3 (CH_2, OCH_2CH_3), 74.3 (CH, C-3), 74.8 (C, C-2), 152.6 (C, C-1).

Ethyl 3-Trimethylsilylpropiolate (916)[6,7]

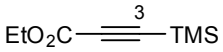

To a solution of trimethylsilylacetylene (719 μL, 5.09 mmol) in anhydrous THF (15 mL) at -78 °C was added BuLi (3.50 mL, 1.6 mol L^{-1} in hexane, 5.60 mmol) dropwise. After 30 min, ethyl chloroformate (581 μL, 6.11 mmol) was added dropwise. After 3 h, saturated NaCl solution (10 mL) was added and the mixture was warmed to room temperature. The aqueous phase was extracted with Et_2O (3 x 10 mL). The combined organic extracts were dried over $MgSO_4$ and concentrated *in vacuo*. Purification by flash chromatography using hexane–EtOAc (1:0 to 99:1) as eluent yielded the title acetylene **916** (627 mg, 72%) as a colourless oil. The spectral data were in agreement with that reported in the literature.[7]

ν_{max} (film)/cm^{-1}: 2964 (C–H), 2182 (C≡C), 1713, 1366, 1228 (C–O), 1028, 954, 849, 702.

δ_H (400 MHz; $CDCl_3$): 0.25 (9 H, s, $OSiMe_3$), 1.32 (3 H, t, J_{CH_3,CH_2} 7.2, OCH_2CH_3), 4.23 (2 H, q, J_{CH_3,CH_2} 7.2, OCH_2CH_3).

δ_C (100 MHz; $CDCl_3$): -0.91 (CH_3, $OSiMe_3$), 14.0 (CH_3, OCH_2CH_3), 62.0 (CH_2, OCH_2CH_3), 93.6 (C, C-2), 94.7 (C, C-3), 153.0 (C, C-1).

7.2.2 Synthesis of Oxaspirolactone 818

1-Benzyloxy-9-hydroxynon-3-yn-5-one (837)[8]

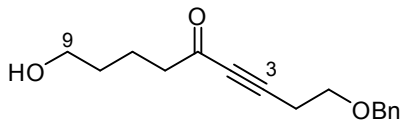

This procedure is an adaptation of that reported by Koutek *et al.*[8]

To a solution of 1-(benzyloxy)but-3-yne **(821)** (5.08 g, 31.7 mmol) in anhydrous THF (100 mL) at -78 °C was added BuLi (36.2 mL, 1.0 mol L^{-1} in hexane, 36.2 mmol) dropwise. After 30 min, a solution of δ-valerolactone **(820)** (3.24 mL, 34.9 mmol) in anhydrous THF (20 mL) was added dropwise. After 2 h, water (70 mL) was added. The mixture was warmed to room temperature and the aqueous phase was extracted with EtOAc (3 x 100 mL). The combined organic extracts were dried over $MgSO_4$ and concentrated *in vacuo*. Purification by flash chromatography using hexane–Et_2O (2:3, 1:4 to 0:1) as eluent yielded the title keto-alcohol **837** (7.18 g, 87%) as a yellow oil. The spectral data were in agreement with that reported in the literature.[8]

HRMS (CI): found MH^+, 261.1488, $C_{16}H_{21}O_3$ requires 261.1491.

ν_{max} (film)/cm^{-1}: 3438br (O–H), 2938 (C–H), 2869 (C–H), 2214 (C≡C), 1729 (C=O), 1670, 1453, 1362, 1164 (C–O), 1101 (C–O), 739, 699.

δ_H (400 MHz; $CDCl_3$): 1.53–1.63 (2 H, m, 8-H), 1.61–1.64 (1 H, br s, OH), 1.71–1.89 (2 H, m, 7-H), 2.59 (2 H, t, $J_{6,7}$ 7.2, 6-H), 2.67 (2 H, t, $J_{2,1}$ 6.7, 2-H), 3.61 (2 H, t, $J_{9,8}$ 7.2, 9-H), 3.64 (2 H, t, $J_{1,2}$ 6.7, 1-H), 4.56 (2 H, s, O*CH*$_2$Ph), 7.28–7.37 (5 H, m, Ph).

δ_C (100 MHz; $CDCl_3$): 20.1 (CH_2, C-2), 20.5 (CH_2, C-7), 31.9 (CH_2, C-8), 45.0 (CH_2, C-6), 62.3 (CH_2, C-9), 67.2 (CH_2, C-1), 73.1 (CH_2, O*CH*$_2$Ph), 81.4 (C, C-4), 90.9 (C, C-3), 127.7 (CH, Ph), 127.8 (CH, Ph), 128.5 (CH, Ph), 137.7 (C, Ph), 188.0 (C, C-5).

***m/z* (CI):** 278 (MH + NH_3, 22%), 261 (MH^+, 16), 243 (M – OH, 100), 199 (22), 159 ($C_{11}H_{11}O$, 13), 153 (20), 118 (19), 101 ($C_5H_9O_2$, 16), 91 (Bn, 15).

9-Benzyloxy-5-oxonon-6-ynal (839)[9]

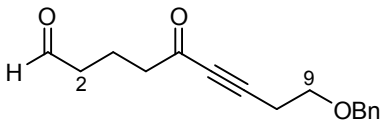

Method A: Dess-Martin Periodinane Oxidation[9,10]

To a solution of keto-alcohol **837** (50.0 mg, 19.2 μmol) in anhydrous CH_2Cl_2 (5.0 mL) was added Dess-Martin periodinane[10] (122 mg, 288 μmol) and the resulting mixture stirred at room temperature overnight followed by the addition of a second portion of Dess-Martin periodinane (25.0 mg, 59.0 μmol). After 1 h, the reaction was poured into a mixture of CH_2Cl_2 (5 mL), saturated $NaHCO_3$ solution (5 mL) and aqueous $Na_2S_2O_5$ (3 mL, 10% w/v) then stirred vigorously for 15 min. The aqueous phase was extracted with CH_2Cl_2 (3 x 10 mL). The combined organic extracts were dried over $MgSO_4$ and concentrated *in vacuo* to yield the crude title aldehyde **839** as a pale yellow oil. This unstable aldehyde **839** was used directly in the sodium chlorite oxidation described below without further purification.

Method B: TEMPO Oxidation[11]

To a solution of keto-alcohol **837** (1.00 g, 3.84 mmol) and TEMPO (60.0 mg, 38.4 μmol) in MeCN (25 mL) at room temperature was added a solution of KH_2PO_4 (2.61 g, 19.2 mmol) in water (5.0 mL) and iodobenzene diacetate (1.86 g, 5.76 mmol). After 1 h, a second portion of iodobenzene diacetate (619 mg, 1.92 mmol) was added. After 1 h, CH_2Cl_2 (25 mL) and aqueous $Na_2S_2O_5$ (20 mL, 10% w/v) were added and the mixture was stirred vigorously for 15 min. The aqueous phase was extracted with CH_2Cl_2 (3 x 25 mL). The combined organic extracts were dried over $MgSO_4$ and concentrated *in vacuo* to yield the crude title aldehyde **839** as a pale yellow oil. This unstable aldehyde **839** was used directly in the sodium chlorite oxidation described below without further purification.

Method C: PCC Oxidation on Alumina[12]

To a solution of keto-alcohol **837** (1.00 g, 3.84 mmol) in anhydrous CH_2Cl_2 (40 mL) at room temperature was added PCC on alumina[12] (10.7 g, 0.82 mmol g^{-1}, 8.83 mmol). After 2 h, the mixture was filtered through a short column of silica and the remaining slurry was washed repeatedly with CH_2Cl_2 (20 mL) until no more aldehyde **839** was eluted from the column. The combined extracts were concentrated *in vacuo* and purification by flash chromatography using hexane–Et_2O (7:3) as eluent yielded the title aldehyde **839** (571 mg, 58%) as a pale yellow oil. The spectral data were in agreement with that obtained in personal communications.[9]

HRMS (CI): found MH^+, 259.1329, $C_{16}H_{19}O_3$ requires 259.1334.

ν_{max} (film)/cm^{-1}: 2935 (C–H), 2869, 2214 (C≡C), 1723 (C=O), 1673 (C=O), 1363, 1161, 1102 (C–O), 741, 699.

δ_H (400 MHz; $CDCl_3$): 1.97 (2 H, tt, $J_{3,2}$ = $J_{3,4}$ 7.2, 3-H), 2.50 (2 H, td, $J_{2,3}$ 7.2 and $J_{2,1}$ 1.2, 2-H), 2.61 (2 H, t, $J_{4,3}$ 7.2, 4-H), 2.67 (2 H, t, $J_{8,9}$ 6.7, 8-H), 3.63 (2 H, t, $J_{9,8}$ 6.8, 9-H), 4.56 (2 H, s, OCH_2Ph), 7.27–7.38 (5 H, m, Ph), 9.76 (1 H, t, $J_{1,2}$ 1.2, 1-H).

δ_C (100 Hz; $CDCl_3$): 16.2 (CH_2, C-3), 20.5 (CH_2, C-8), 42.7 (CH_2, C-4), 44.2 (CH_2, C-2), 67.1 (CH_2, C-9), 73.1 (CH_2, OCH_2Ph), 81.2 (C, C-6), 91.2 (C, C-7), 127.7 (CH, Ph), 127.9 (CH, Ph), 128.5 (CH, Ph), 137.7 (C, Ph), 186.8 (C, C-5), 201.4 (CH, C-1).

***m/z* (CI):** 276 (MH + NH_3, 100%), 259 (MH^+, 64), 238 (16), 143 (16), 116 (12), 108 (18), 91 (Bn, 31).

9-Benzyloxy-5-oxonon-6-ynoic Acid (819)[9]

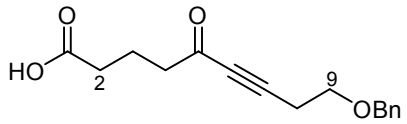

Method A: Jones' Oxidation of Keto-Alcohol **837**

To a solution of keto-alcohol **837** (200 mg, 770 μmol) in acetone (10 mL) at room temperature was added Jones' reagent[13] dropwise until the orange colour persisted. After 18 h, the mixture was filtered through a pad of Celite® and concentrated *in vacuo*. Water (15 mL) and EtOAc (15 mL) were added to the residue oil and the aqueous phase extracted with EtOAc (3 x 15 mL). The combined organic extracts were washed with brine, dried over $MgSO_4$ and concentrated *in vacuo*. Purification by flash chromatography using CH_2Cl_2–Et_2O (19:1 to 1:1) as eluent yielded the title keto-acid **819** (117 mg, 55%) as a pale yellow oil.

Method B: Sodium Chlorite Oxidation of Keto-Aldehyde **839**

To a solution of crude keto-aldehyde **839** (4.03 mmol) in ^{t}BuOH (25 mL) and cyclohexene (2.0 mL) at room temperature was added a solution of $NaClO_2$ (3.65 g, 40.3 mmol) and KH_2PO_4 (4.12 g, 30.2 mmol) in water (15 mL) dropwise. The resulting biphasic mixture was stirred vigorously for 2 h. Aqueous $Na_2S_2O_5$ (40 mL, 15% w/v) was added dropwise and solid NaCl was added to

saturate the aqueous phase. The mixture was extracted with Et_2O (4 × 80 mL). The combined organic extracts were dried over $MgSO_4$ and concentrated *in vacuo*. Purification by flash chromatography using CH_2Cl_2–Et_2O (19:1 to 1:1) as eluent yielded the title keto-acid **819** (1.02 g, 92% over 2 steps) as a pale yellow oil. The spectral data were in agreement with that obtained in personal communications.[9]

HRMS (CI): found MH^+, 275.1282, $C_{16}H_{19}O_4$ requires 275.1283.

ν_{max} (film)/cm^{-1}: 3439br (O–H), 2936 (C–H), 2870 (C–H), 2215 (C≡C), 1731 (C=O), 1673 (C=O), 1454, 1362, 1164 (C–O), 1100 (C–O), 739, 699.

δ_H (400 MHz; $CDCl_3$): 1.97 (2 H, quintet, $J_{3,2}$ = $J_{3,4}$ 7.3, 3-H), 2.40 (2 H, t, $J_{2,3}$ 7.3, 2-H), 2.64 (2 H, t, $J_{4,3}$ 7.3, 4-H), 2.67 (2 H, t, $J_{8,9}$ 6.8, 8-H), 3.64 (2 H, t, $J_{9,8}$ 6.8, 9-H), 4.56 (2 H, s, OCH_2Ph), 7.27–7.36 (5-H, m, Ph).

δ_C (75 MHz; $CDCl_3$): 18.7 (CH_2, C-3), 20.4 (CH_2, C-2), 32.6 (CH_2, C-8), 44.1 (CH_2, C-4), 67.1 (CH_2, C-9), 73.1 (CH_2, OCH_2Ph), 81.2 (C, C-6), 91.2 (C, C-7), 127.7 (CH, Ph), 127.8 (CH, Ph), 128.4 (CH, Ph), 137.6 (C, Ph), 178.4 (C, C-1), 186.8 (C, C-5).

***m/z* (CI):** 292 (MH + NH_3, 5%), 275 (MH^+, 9), 257 (M – OH, 7), 249 (12), 195 (11), 159 ($C_{11}H_{11}O$, 11), 108 (16), 105 (33), 91 (Bn, 100), 81 (11).

1,7-Dioxaspiro[5.5]undecan-2-one (818)[9,14]

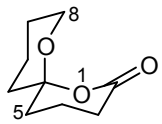

A solution of keto-acid **819** (602 mg, 2.19 mmol), acetic acid (1.20 mL) and Pd/C (192 mg, 10% w/w) in anhydrous THF (25 mL) at room temperature was stirred vigorously under an atmosphere of hydrogen. After 18 h, the mixture was filtered through a pad of Celite® and concentrated *in vacuo*. Additional acetic acid was added (3 x 0.50 mL) then slowly removed *in vacuo* at 40 °C. After 3 h, the excess acetic acid was removed completely *in vacuo* by azeotroping with toluene (3 x 2 mL) to yield the crude title oxaspirolactone **818** (350 mg, 94%) as a pale yellow oil. The unstable oxaspirolactone **818** was used directly in the DIBAL-H reduction described below without further purification. The spectral data were in agreement with that obtained in personal communications.[9]

HRMS (EI): found $M^{+\bullet}$, 170.0945, $C_9H_{14}O_3$ requires 170.0943.

ν_{max} (film)/cm^{-1}: 2943 (C–H), 1711 (C=O), 1412, 1247, 1177, 1083, 1036 (C–O), 981.

δ_H (300 MHz; $CDCl_3$): 1.53–1.79 (6 H, m, 4-H_A, 5-H_A, 9-H_A, 9-H_B, 10-H_A and 11-H_A), 1.85–1.95 (2 H, m, 5-H_B and 11-H_B), 1.98–2.21 (2 H, m, 10-H_B and 4-H_B), 2.35–2.52 (1 H, m, 3-H_A), 2.59–2.70 (1 H, m, 3-H_B), 3.68–3.80 (1 H, m, 8-H_A), 3.84–3.99 (1 H, m, 8-H_B).

δ_C (75 MHz; $CDCl_3$): 15.2 (CH_2, C-4), 17.8 (CH_2, C-10), 24.6 (CH_2, C-9), 29.3 (CH_2, C-3), 33.2 (CH_2, C-5), 34.8 (CH_2, C-10), 62.4 (CH_2, C-8), 102.7 (C, C-6), 171.6 (C, C-2).

***m/z* (EI):** 170 ($M^{+\bullet}$, 12%), 126 (13), 115 (81), 114 (18), 101 (64), 98 (100), 87 (43), 83 (40), 70 (22), 60 (38), 55 (69).

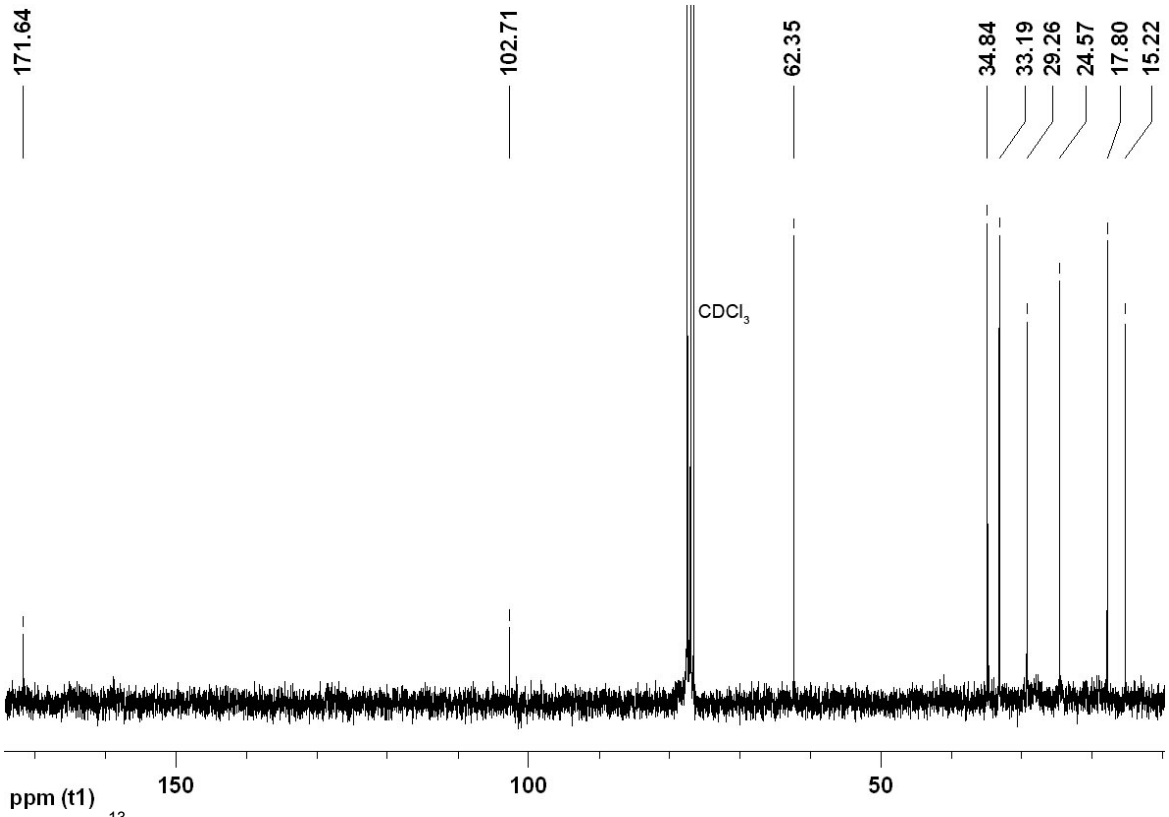

Figure 7.1: ^{13}C NMR spectrum (75 MHz; $CDCl_3$) of oxaspirolactone **818**.

7.2.3 Synthesis of Spiroacetals 815–817 and Spiroacetal Nitrile 858

(2*R,6*S**)-2-Acetoxy-1,7-dioxaspiro[5.5]undecane (815)**

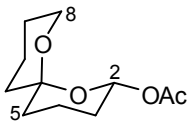

To a solution of crude oxaspirolactone **818** (80.0 mg, 470 μmol) in anhydrous toluene (2.0 mL) at -78 °C was added dropwise DIBAL-H (611 μL, 1.0 mol L^{-1} in THF, 611 μmol). After 15 min, MeOH (0.2 mL) was added. After 30 min, EtOAc (5 mL) and saturated $NaHCO_3$ (1 mL) were added and the mixture was warmed to room temperature. The aqueous phase was extracted with EtOAc (2 x 5 mL). The combined organic extracts were dried over $MgSO_4$ and concentrated *in vacuo* to yield the crude lactol as a pale yellow oil. This unstable lactol was used directly in the acetylation described below without further purification.

To a solution of crude lactol, DMAP (6.20 mg, 50.6 μmol) and NEt_3 (70.5 μL, 506 μmol) in anhydrous CH_2Cl_2 (5.0 mL) at 0 °C was added a solution of Ac_2O (33.5 μL, 354 μmol) in CH_2Cl_2 (1.0 mL) dropwise. After 2 h, the reaction was warmed to room temperature and stirred overnight. The organic phase was washed with saturated NH_4Cl solution (5 mL) followed by saturated $NaHCO_3$ solution (5 mL), dried over $MgSO_4$ and concentrated *in vacuo*. Purification by flash chromatography using hexane–EtOAc–NEt_3 (98:1:1) yielded the *title compound* **815** (256 mg, 25%) as a pale yellow oil.

HRMS (EI): $M^{+\bullet}$, 214.1205, $C_{11}H_{18}O_4$ requires 214.1205.

ν_{max} (film)/cm^{-1}: 2949 (C–H), 1751(C=O), 1368, 1239, 1228, 1199 (C–O), 1082 (C–O), 1043, 982.

δ_H (300 MHz; $CDCl_3$): 1.39–1.75 (8 H, m, 3-H_A, 4-H_A, 5-H_A, 9-H_A, 9-H_B, 10-H_A, 11-H_A and 11-H_B), 1.75–2.01 (4 H, m, 3-H_B, 4-H_B, 5-H_B and 10-H_B), 2.10 (3 H, s, $COCH_3$), 3.62–3.69 (1 H, m, 8-H_A), 3.97–4.07 (1 H, m, 8-H_B), 5.94 (1 H, dd, $J_{2ax,3ax}$ 10.1 and $J_{2ax,3eq}$ 2.6, 2-H_{ax}).

δ_C (75 MHz; $CDCl_3$): 17.5 (CH_2, C-4), 18.3 (CH_2, C-10), 21.3 (CH_3, CO*CH_3*), 25.0 (CH_2, C-9), 29.4 (CH_2, C-3), 34.6 (CH_2, C-11), 35.2 (CH_2, C-5), 61.1 (CH_2, C-8), 90.0 (CH, C-2), 98.6 (C, C-6), 169.6 (C=O, *CO*CH_3).

***m/z* (EI):** 214 ($M^{+\bullet}$, 2%), 126 (20), 101 (27), 98 (100), 99 (14), 83 (16), 70 (10), 60 (11), 55 (33), 45 (12), 43 (70), 41 (23).

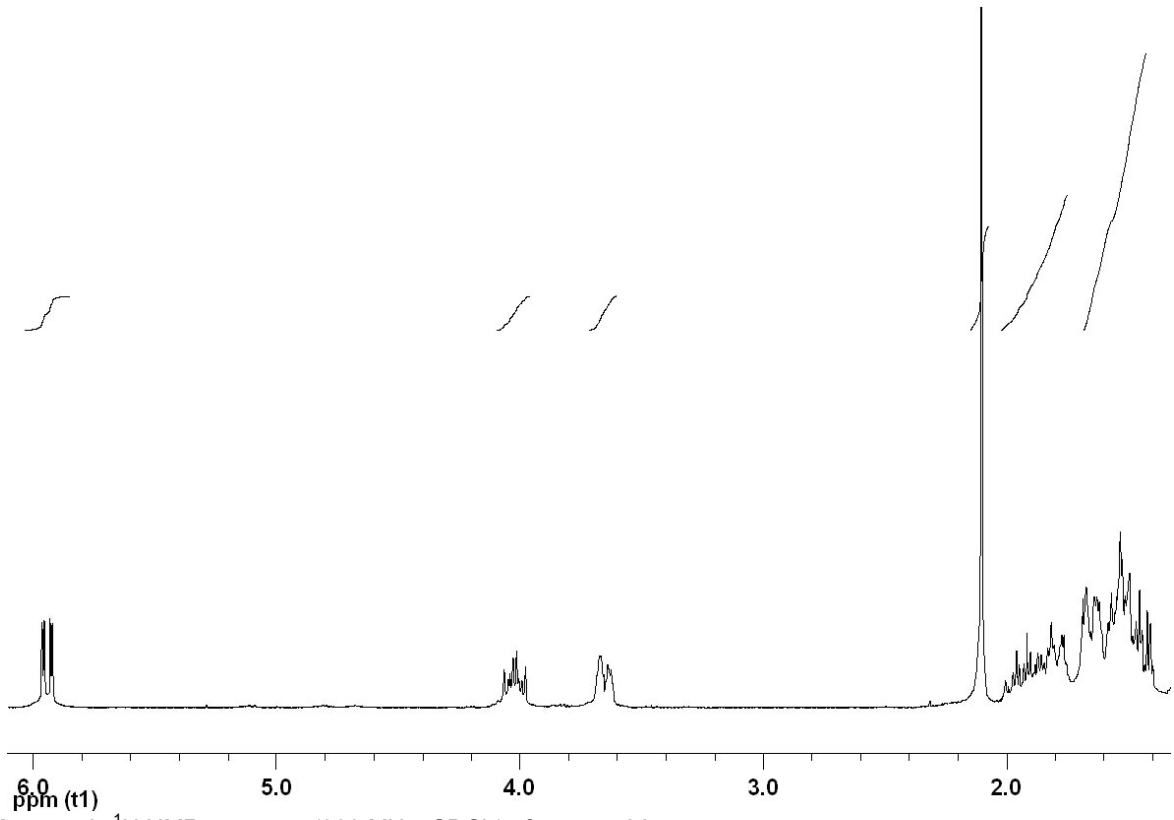

Figure 7.2: ^{1}H NMR spectrum (300 MHz; $CDCl_3$) of acetate **815**.

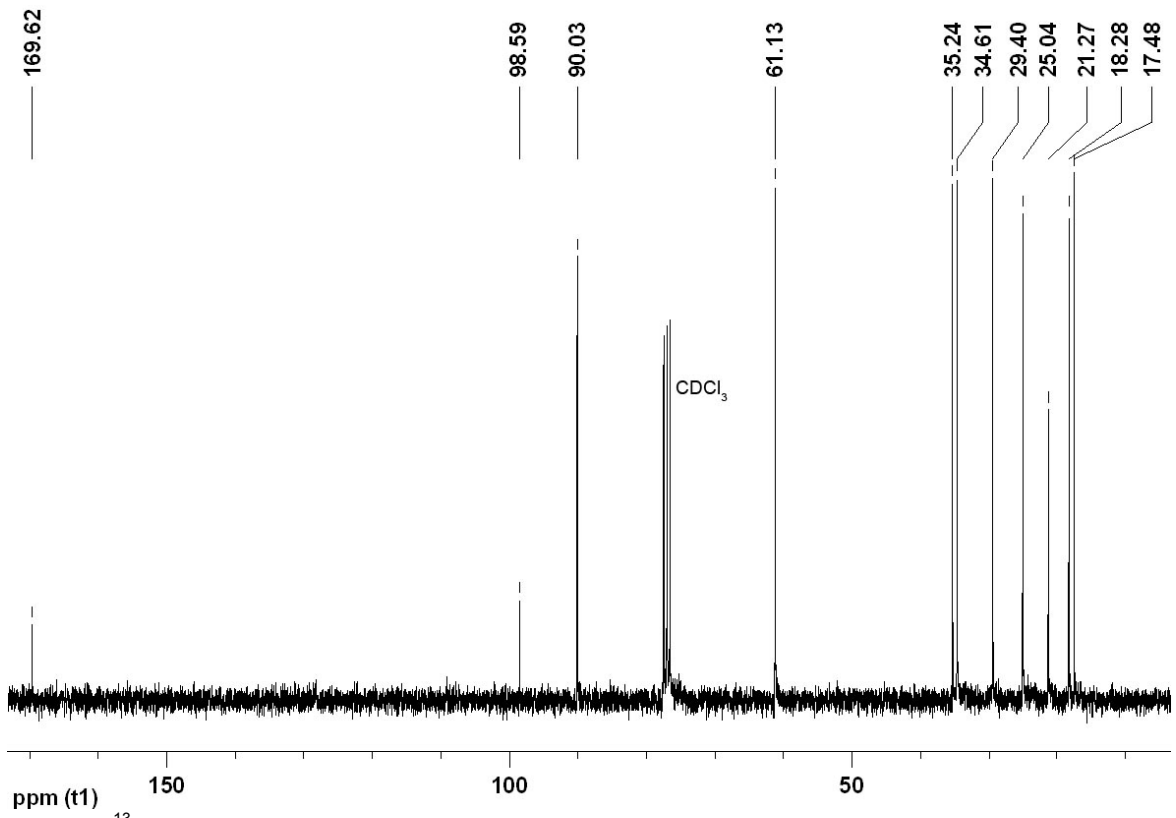

Figure 7.3: ^{13}C NMR spectrum (75 MHz; $CDCl_3$) of acetate **815**.

2-(4′,4′-Dimethoxybutyl)-2-methoxytetrahydro-2*H*-pyran (842) and (2*S,6*S**)-2-Methoxy-1,7-dioxaspiro[5.5]undecane (816)**

Major isomer **842**

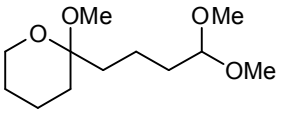

Minor isomer **816**

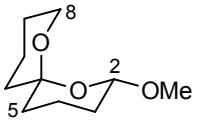

To a solution of aldehyde **839** (100 mg, 387 μmol) in MeOH (3.0 mL) at room temperature was added *p*-toluenesulfonic acid monohydrate (3.33 mg, 19.4 μmol). After 2 h, Pd/C (40.0 mg, 10% w/w) was added and the mixture was flushed with hydrogen for 5 min followed by vigorous stirring overnight under an atmosphere of hydrogen. The mixture was filtered through a pad of Celite® and concentrated *in vacuo*. Further filtration through a pad of K_2CO_3 followed by concentration *in vacuo* yielded a dark yellow oil which was used directly in the following cyclisation without further purification.

To a solution of the above crude material in a 1:1 mixture of MeOH–benzene (3.0 mL) at room temperature was added (+)-10-camphorsulfonic acid monohydrate (4.86 mg, 19.4 μmol). After 18 h, the mixture was filtered through a pad of K_2CO_3 and concentrated *in vacuo*. Further filtration through a pad of silica followed by concentration *in vacuo* afforded an oil. Purification by flash chromatography using pentane–Et_2O (4:1 to 1:1) as eluent yielded the *title compounds* (30.2 mg, 51%) as an inseparable 4:1 mixture of methoxy-pyran **842** : acetal **816**.

HRMS (CI): found $[M_A - OMe]^+$, 201.1475, $C_{11}H_{21}O_3$ requires 201.1491; found M_BH^+, 187.1329, $C_{10}H_{19}O_3$ requires 187.1334.

ν_{max} (film)/cm^{-1}: 2948 (C–H), 2872, 1460, 1362, 1193 (C–O), 1127 (C–O), 1091, 1059, 1028, 980, 946, 884, 868.

δ_H (400 MHz; $CDCl_3$): †1.31–2.00 (14.4 H, m, 3-H, 4-H, 5-H, 1′-H, 2′-H, 3′-H, 3-H*, 4-H*, 5-H*, 9-H*, 10-H* and 11-H*), 3.17 (3 H, s, OMe), 3.31 (3 H, s, OMe), 3.32 (3 H, s, OMe), 3.54 (0.58 H, s, OMe*), 3.58–3.65 (2 H, m, 6-H), 3.65–3.68 (0.19 H, m, 8-H_A*), 3.74–3.82 (0.19 H, m, 8-H_B*), 4.36 (1 H, t, $J_{4',3'}$ 5.8, 4′-H), 4.62 (0.19 H, dd, $J_{2ax^*,3ax^*}$ 9.8 and $J_{2ax^*,3eq^*}$ 2.3, 2-H_{ax}*).

δ_C (100 MHz; $CDCl_3$): 17.7 (CH_2, C-10*), 18.5 (CH_2, C-2′), 18.5 (CH_2, C-4*), 18.6 (CH_2, C-4), 25.2 (CH_2, C-5), 25.3 (CH_2, C-9*), 30.6 (CH_2, C-3*), 32.6 (2 x CH_2, C-3 and C-3′), 34.8 (CH_2, C-5* or C-11*), 35.6 (CH_2, C-5* or C-11*), 36.1 (CH_2, C-1′), 47.2 (CH_3, OCH_3), 52.6 (CH_3, OCH_3), 52.7 (CH_3, OCH_3), 56.0 (CH_3, OCH_3*), 60.7 (CH_2, C-8*), 61.2 (CH_2, C-6), 97.5 (C, C-6*), 97.8 (CH, C-2*), 98.8 (C, C-2), 104.4 (CH, C-4′).

***m/z* (CI):** 201 (8%), 169 (100), 154 (13), 137 (78), 110 (18), 75 (11), 71 (12).

(2*S,6*S**)-2-Ethoxy-1,7-dioxaspiro[5.5]undecane (817)**

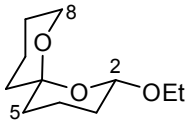

To a solution of keto-aldehyde **839** (423 mg, 1.64 mmol) in EtOH (20 mL) at room temperature was added *p*-toluenesulfonic acid monohydrate (14.1 mg, 82.0 μmol). After 2 h, Pd/C (150 mg, 10% w/w) was added and the mixture was flushed with hydrogen for 5 min followed by vigorous stirring under an atmosphere of hydrogen overnight. NEt_3 (3 drops) was added and the mixture filtered through a pad of Celite® then concentrated *in vacuo*. Purification by flash chromatography using pentane–Et_2O (19:1 to 4:1) as eluent yielded the *title compound* (177 mg, 54%) as a pale yellow oil together with a mixture of starting materials (146 mg). The recovered starting materials were subjected to the above hydrogenation conditions to yield the *title compound* **817** (258 mg, 79% overall yield after 2 cycles) after purification.

HRMS (CI): found MH^+, 201.1497, $C_{11}H_{21}O_3$ requires 201.1491.

ν_{max} (film)/cm^{-1}: 2941 (C–H), 2870 (C–H), 1441, 1209, 1177, 1141 (C–O), 1092 (C–O), 1045, 980, 949.

δ_H (400 MHz; $CDCl_3$): 1.27 (3 H, t, J_{CH_3,CH_2} 7.1, OCH_2CH_3), 1.36–1.48 (3 H, m, 3-H_A, 5-H_A and 11-H_A), 1.49–1.65 (5 H, m, 4-H_A, 5-H_B or 11-H_B, 9-H_A, 9-H_B and 10-H_A), 1.68–1.98 (4 H, m, 3-H_B, 4-H_B, 5-H_B or 11-H_B and 10-H_B), 3.56 (1 H, dq, J_{AB} 9.2 and J_{CH_2,CH_3} 7.1, $OCH_AH_BCH_3$), 3.62–3.68 (1 H, m, 8-H_A), 3.76 (1 H, ddd, J_{AB} 11.4, $J_{8ax,9ax}$ 11.2 and $J_{8ax,9eq}$ 2.9, 8-H_B), 4.03 (1 H, dq, J_{AB} 9.2 and J_{CH_2,CH_3} 7.1, $OCH_AH_BCH_3$), 4.72 (1 H, dd, $J_{2ax,3ax}$ 9.9 and $J_{2ax,3eq}$ 2.2, 2-H_{ax}).

† Resonances assigned to the minor product, methoxy-spiroacetal **816**, are designated with an asterisk *.

δ_C (100 MHz; $CDCl_3$): 15.2 (CH_3, OCH_2CH_3), 17.8 (CH_2, C-4 or C-10), 18.5 (CH_2, C-4 or C-10), 25.3 (CH_2, C-9), 30.8 (CH_2, C-3), 34.8 (CH_2, C-5 or C-11), 35.5 (CH_2, C-5 or C-11), 60.7 (CH_2, C-8), 64.2 (CH_2, OCH_2CH_3), 96.5 (CH, C-2), 97.5 (C, C-6).

***m/z* (CI):** 201 (MH^+, 4%), 199 (M – H, 13), 185 (24), 183 (24), 155 (M – OEt, 100), 139 (16), 137 (76).

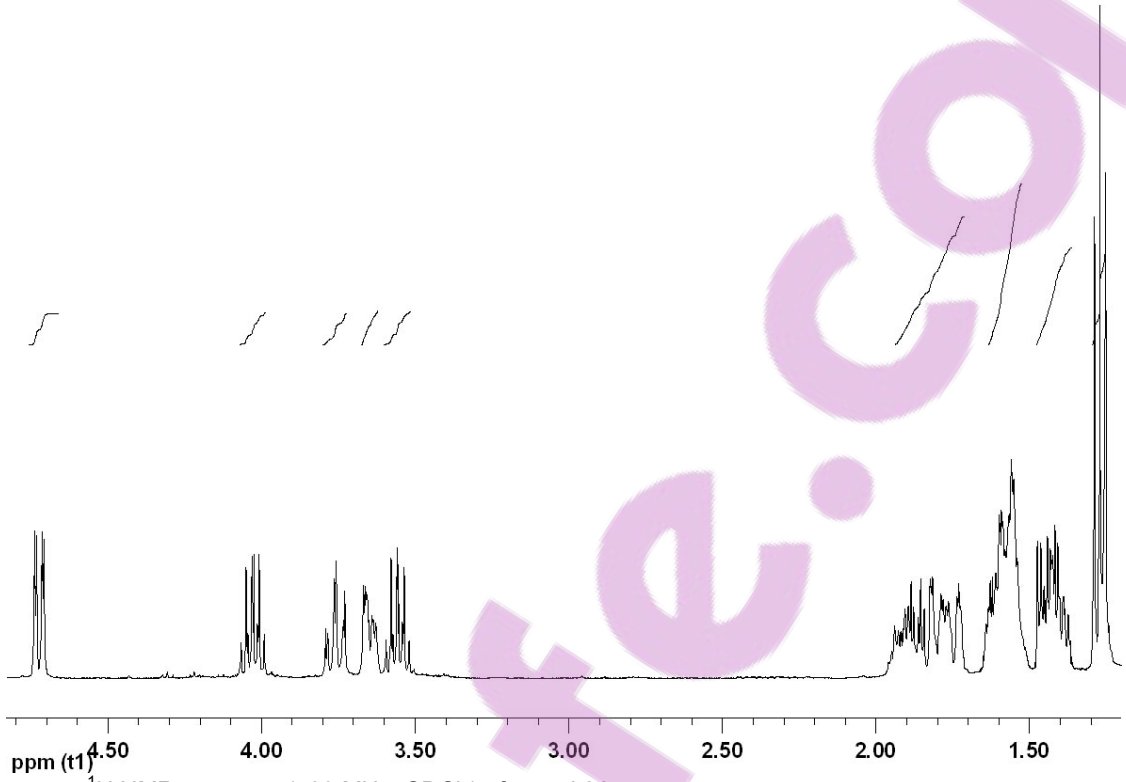

Figure 7.4: ^1H NMR spectrum (400 MHz; $CDCl_3$) of acetal **817**.

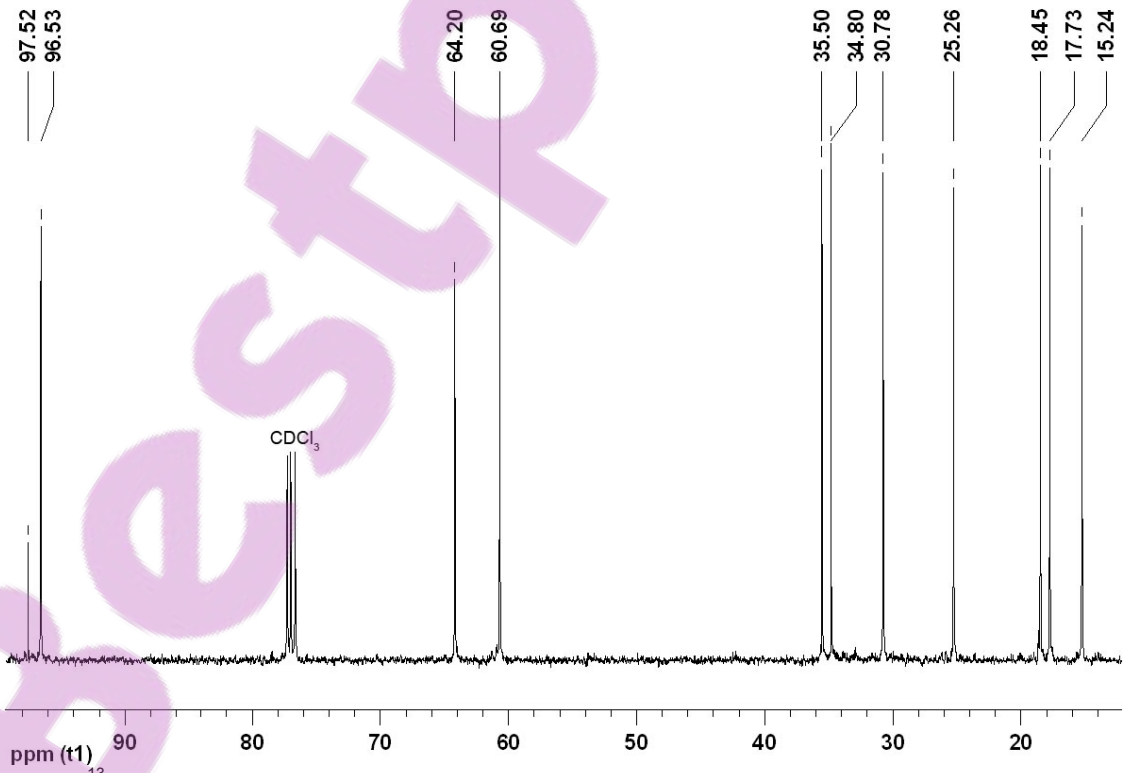

Figure 7.5: ^{13}C NMR spectrum (100 MHz; $CDCl_3$) of acetal **817**.

(2*S,6*R**)-2-Azido-1,7-dioxaspiro[5.5]undecane (814b) and (2*S**,6*S**)-2-Azido-1,7-dioxaspiro[5.5]undecane (814a)**

Major isomer:
Axial (2*S**,6*R**)-**814b**

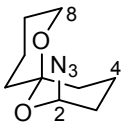

Minor isomer:
Equatorial (2*S**,6*S**)-**814a**

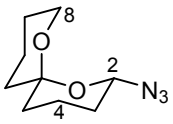

To a solution of ethoxy-spiroacetal **817** (30.0 mg, 150 μmol) and $TMSN_3$ (99.4 μL, 749 μmol) in anhydrous CH_2Cl_2 (3.0 mL) at 0 °C was added freshly prepared TMSOTf solution (375 μL, 0.80 mol L^{-1} in CH_2Cl_2, 300 μmol). After 2 h, a second portion of TMSOTf solution (187 μL, 150 μmol) was added to the mixture dropwise. After 1 h, saturated $NaHCO_3$ solution (3 mL) was added and the aqueous phase was extracted with Et_2O (3 x 10 mL). The combined organic extracts were dried over $MgSO_4$ and concentrated *in vacuo*. Purification by flash chromatography using pentane–Et_2O (19:1) as eluent yielded the *title compounds* (20.8 mg, 71%) as an inseparable 3:1 mixture of axial azido-spiroacetal **814b** : equatorial azido-spiroacetal **814a** as a pale yellow oil.

ν_{max} (film)/cm^{-1}: 2947 (C–H), 2873, 2103 (N_3), 1454, 1245 (C–O), 1208 (C–O), 1046, 868.

δ_H (400 MHz; $CDCl_3$): ‡1.18–1.95 (15.6 H, m, 3-H, 4-H, 5-H, 9-H, 10-H, 11-H, 3-H*, 4-H*, 5-H*, 9-H*, 10-H*, 11-H*), 3.78–3.82 (2 H, m, 8-H), 3.87–3.94 (0.61 H, m, 8-H*), 4.66 (1 H, t, $J_{2,3}$ 6.5, 2_{eq}-H), 4.85 (0.30 H, dd, $J_{2ax^*,3ax^*}$ 10.8 and $J_{2ax^*,3eq^*}$ 2.4, 2-H_{ax}*).

δ_C (100 MHz; $CDCl_3$): 17.8 (CH_2, C-4* or C-10*), 18.3 (CH_2, C-4* or C-10*), 18.8 (CH_2, C-4 or C-10), 19.0 (CH_2, C-4 or C-10), 24.7 (CH_2, C-9), 29.7 (CH_2, C-9*), 30.2 (CH_2, C-3*), 32.3 (CH_2, C-3), 34.0 (CH_2, C-5), 34.5 (CH_2, C-5*), 35.2 (CH_2, C-11*), 39.6 (CH_2, C-11), 60.8 (CH_2, C-8*), 63.3 (CH_2, C-8), 77.8 (CH, C-2), 83.3 (CH, C-2*), 93.9 (C, C-6), 98.3 (C, C-6*).

***m/z* (CI):** 170 ($MH^+ - N_2$, 30%), 155 ($M - N_3$, 100), 152 (45), 141 (17), 137 (20), 98 (16), 85 (17).

(2*S,6*S**)-2-Cyano-1,7-dioxaspiro[5.5]undecane (858)**

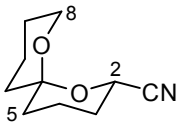

To a solution of ethoxy-spiroacetal **817** (30.0 mg, 150 μmol) and TMSCN (100 μL, 749 μmol) in anhydrous CH_2Cl_2 (3.0 mL) at 0 °C was added freshly prepared TMSOTf solution (375 μL, 0.80 mol L^{-1} in CH_2Cl_2, 300 μmol). After 3 h, saturated $NaHCO_3$ solution (3 mL) was added and the aqueous phase was extracted with Et_2O (4 x 4 mL). The combined organic extracts were dried over $MgSO_4$ and concentrated *in vacuo*. Purification by flash chromatography using pentane–Et_2O (19:1) as eluent yielded the *title compound* **858** (2.00 mg, 7%) as a pale yellow oil.

HRMS (EI): found $M^{+\bullet}$, 181.1109, $C_{10}H_{15}NO_2$ requires 181.1103.

‡ Resonances assigned to the minor product, equatorial azido-spiroacetal **814a**, are designated with an asterisk *.

δ_H (400 MHz; $CDCl_3$): 1.41–1.49 (1 H, m, 3-H_A), 1.57–1.93 (11 H, m, 3-H_B, 4-H_A, 4-H_B, 5-H_A, 5-H_B, 9-H_A, 9-H_B, 10-H_A, 10-H_B, 11-H_A and 11-H_B), 3.63–3.67 (2 H, m, 8-H), 4.53 (1 H, dd, $J_{2ax,3ax}$ 11.7 and $J_{2ax,3eq}$ 2.5, 2-H_{ax}).

δ_C (100 MHz; $CDCl_3$): 17.7 (CH_2, C-4 or C-10), 18.1 (CH_2, C-4 or C-10), 24.8 (CH_2, C-9), 29.3 (CH_2, C-3), 34.4 (CH_2, C-5 or C-11), 34.9 (CH_2, C-5 or C-11), 61.0 (CH_2, C-8), 65.6 (CH, C-2), 97.9 (C, C-6), 117.6 (C, CN).

***m/z* (EI):** 181 ($M^{+\bullet}$, 17%), 126 (100), 125 (57), 123 (74), 98 (87), 85 (59), 84 (40), 83 (31), 80 (35). 71 (23).

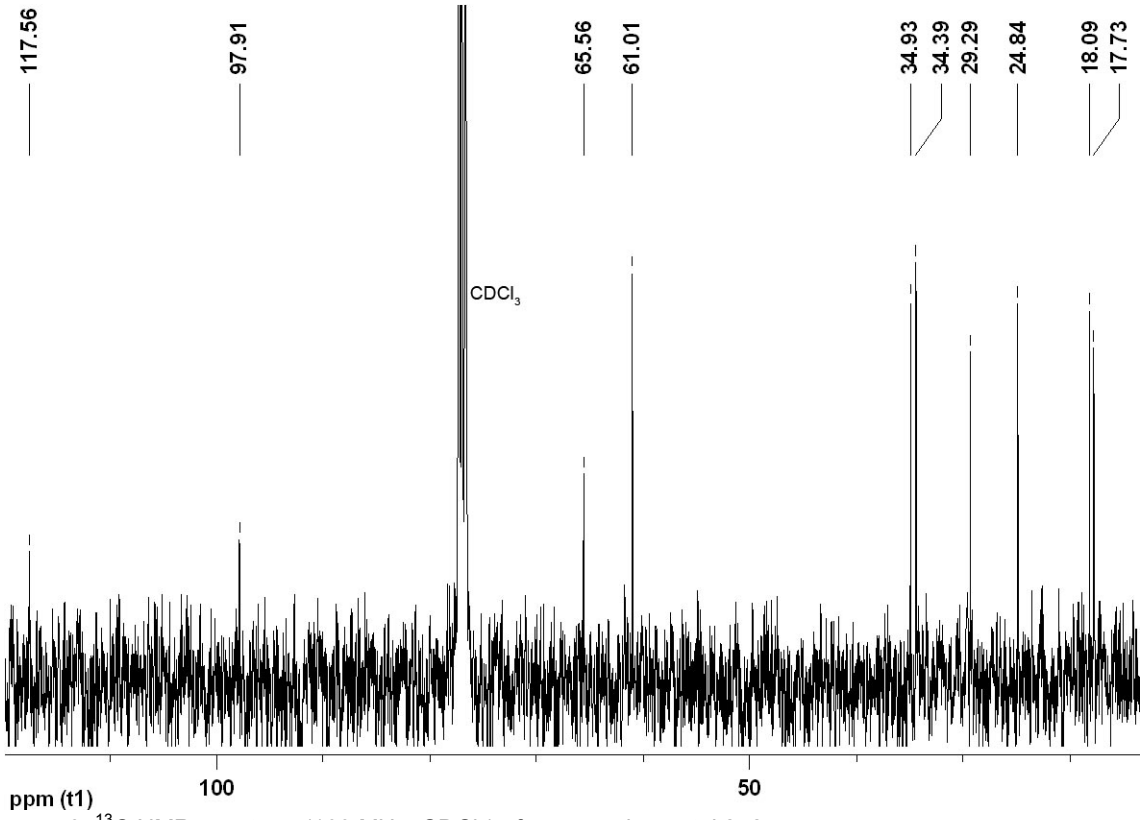

Figure 7.6: ^{13}C NMR spectrum (100 MHz; $CDCl_3$) of cyano-spiroacetal **858**.

7.2.4 Synthesis of Spiroacetal Nucleoside-Models 811

1-([2′*S,6′*S**]-1′,7′-Dioxaspiro[5.5]undecan-2′-yl)-5-fluorocytidine (811a)**

Spiroacetal 5-fluorocytidine **811a**

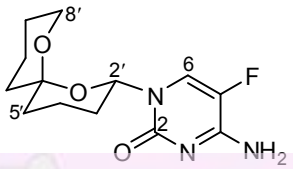

Enamide impurity **846**

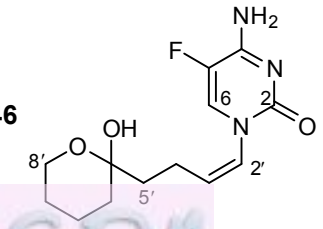

This procedure is an adaptation of that reported by Vorbrüggen *et al.*[15]

A suspension of 5-fluorocytosine (43.5 mg, 337 μmol) in *N*,*O*-bis(trimethylsilyl)acetamide (0.33 mL) was heated to reflux until the white solid dissolved. After 2 h, the mixture was concentrated *in vacuo* to a thick yellow oil. Acetate **815** (42.3 mg, 198 μmol) in CH_2Cl_2 (2.5 mL) was added to this oil and the mixture cooled to 0 °C. TMSOTf (35.8 μL, 198 μmol) was added dropwise. The mixture was stirred at 0 °C for 2 h then warmed to room temperature. After 18 h, saturated $NaHCO_3$ solution (2 mL) was added and the mixture stirred for 15 min. The aqueous phase was extracted with CH_2Cl_2 (3 x 3 mL). The combined organic extracts were dried over $MgSO_4$ and concentrated *in vacuo*. Purification by flash chromatography using hexane–EtOAc–MeOH (1:1:0, 0:1:0 to 0:19:1) as eluent followed by PLC using CH_2Cl_2–MeOH (99:1) as eluent yielded the *title compound* **811a** (21.9 mg, 39%) and the enamide impurity **846** (13.3 mg, 24%) as pale yellow oils.

Spiroacetal 5-fluorocytidine **811a**

HRMS (FAB): found MH^+, 284.1412, $C_{13}H_{19}FN_3O_3$ requires 284.1410.

ν_{max} (film)/cm^{-1}: 3342 (N–H), 3048 (N–H), 2936 (C–H), 1693 (C=O), 1644, 1514, 1406, 1278 (C–O), 1035, 977, 772.

δ_H (300 MHz; $CDCl_3$ with a drop of CD_3OD): 1.27–1.35 (1 H, m, 3′-H_A), 1.36–1.47 (1 H, m, 5′-H_A), 1.47–1.61 (4 H, m, 9′-H_A, 9′-H_B, 10′-H_A and 11′-H_A), 1.65–1.83 (4 H, m, 4′-H_A, 5′-H_B, 10′-H_B and 11′-H_B), 1.97–2.13 (2 H, m, 3′-H_B and 4′-H_B), 2.82 (2 H, br s, NH_2), 3.64–3.77 (2 H, m, 8′-H), 6.03 (1 H, ddd, $J_{2'ax,3'ax}$ 10.9, $J_{2'ax,3'eq}$ 2.3 and $J_{2'ax,5F}$ 2.1, 2′-H_{ax}), 7.55 (1 H, d, $J_{6,5F}$ 6.3, 6-H).

δ_C (100 MHz; $CDCl_3$ with a drop of CD_3OD): 17.8 (CH_2, C-4′), 18.1 (CH_2, C-10′), 24.7 (CH_2, C-9′), 30.6 (CH_2, C-3′), 34.6 (CH_2, C-5′), 35.1 (CH_2, C-11′), 60.9 (CH_2, C-8′), 77.5 (CH, C-2′), 98.5 (C, C-6′), 125.3 (CH, d, $J_{6,5F}$ 31.4, C-6), 136.6 (C, d, $J_{5,5F}$ 242.5, C-5), 154.1 (C, C-2), 157.6 (C, $J_{4,5F}$ 13.6, C-4).

δ_F (282 MHz; $CFCl_3$): -169.2 (CF, 5-F).

***m/z* (FAB):** 284 (MH^+, 18%), 165 (12), 155 ($C_9H_{15}O_2$, 100), 130 (63), 120 (31), 111 (19).

Enamide impurity **846**

δ_H (300 MHz; $CDCl_3$): 1.20–2.13 (12 H, m, 3′-H, 4′-H, 5′-H, 9′-H, 10′-H and 11′-H,), 3.95–4.12 (2 H, m, 8′-H), 4.74–4.89 (1 H, m, 2′-H), 5.27 (1 H, d, $J_{2',3'}$ 8.4, 2′-H), 7.38 (1 H, d, $J_{6,5F}$ 5.4, 6-H).

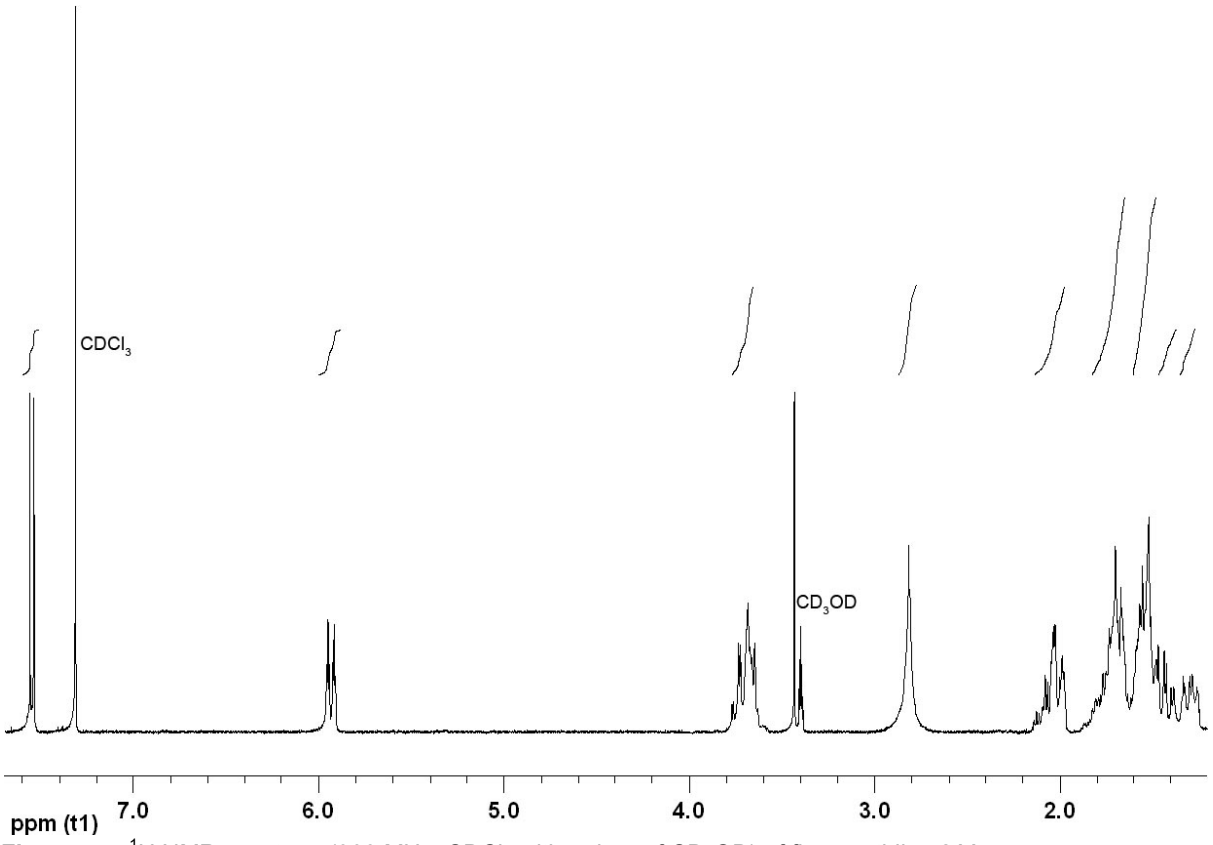

Figure 7.7: ^{1}H NMR spectrum (300 MHz; $CDCl_3$ with a drop of CD_3OD) of fluorocytidine **811a**.

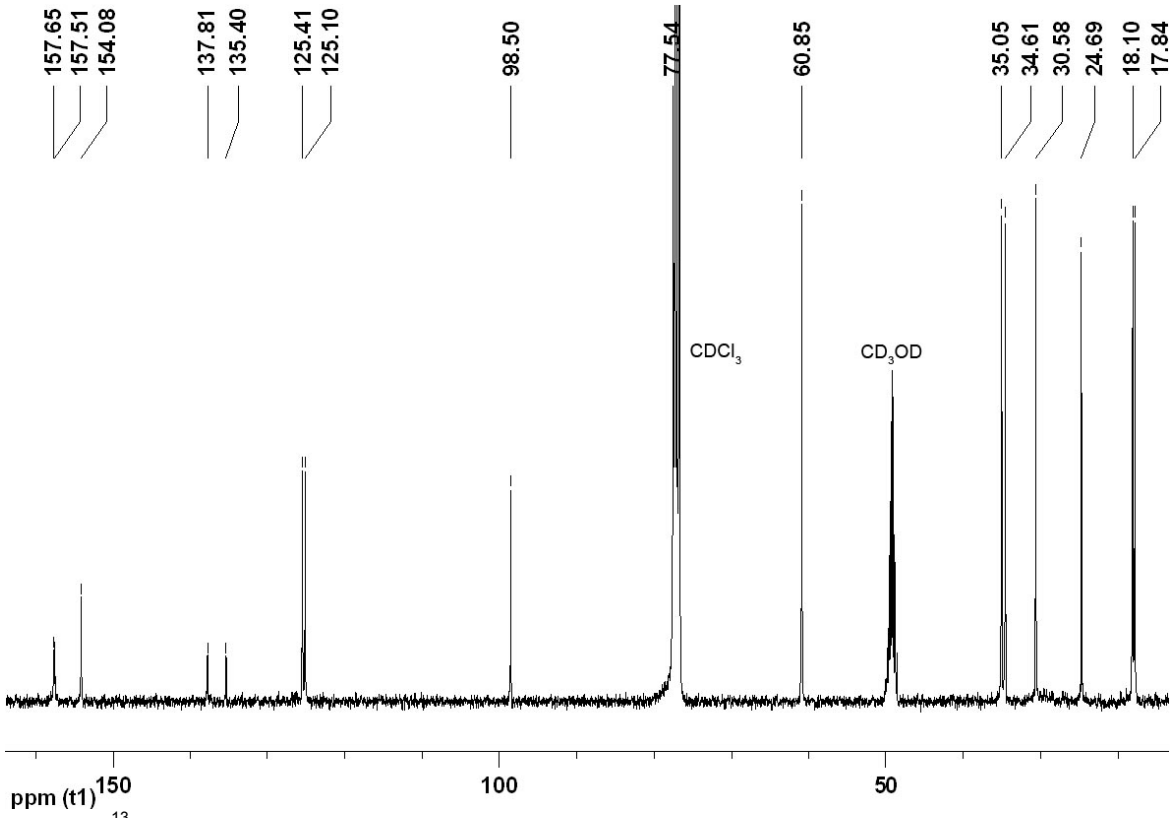

Figure 7.8: ^{13}C NMR spectrum (100 MHz; $CDCl_3$ with a drop of CD_3OD) of fluorocytidine **811a**.

1-([2′*S,6′*S**]-1′,7′-Dioxaspiro[5.5]undecan-2′-yl)uridine (811d)**

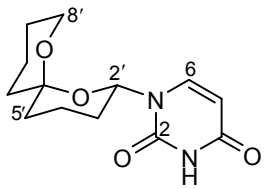

This procedure is an adaptation of that reported by Vorbrüggen *et al.*[15]

A suspension of uracil (28.0 mg, 255 μmol) in *N*,*O*-bis(trimethylsilyl)acetamide (125 μL, 510 μmol) and MeCN (1.0 mL) was heated to reflux until the white solid dissolved. After 2 h, ethoxy acetal **817** (30.0 mg, 150 μmol) in CH_2Cl_2 (1.0 mL) was added and the mixture was cooled to 0 °C. TMSOTf (29.8 μL, 165 μmol) was added dropwise. The mixture was stirred at 0 °C for 2 h then warmed to room temperature. After 18 h, saturated $NaHCO_3$ solution (2 mL) was added and the mixture was stirred for 15 min. The aqueous phase was extracted with EtOAc (3 x 7 mL). The combined organic extracts were dried over $MgSO_4$ and concentrated *in vacuo*. Purification by flash chromatography using hexane–EtOAc (1:1) as eluent followed by PLC using hexane–EtOAc (1:1) as eluent yielded the *title compound* **811d** (7.50 mg, 19%) as a colourless oil.

HRMS (EI): found $M^{+\bullet}$, 266.1273, $C_{13}H_{18}N_2O_4$ requires 266.1267.

ν_{max} (film)/cm^{-1}: 3196br (N–H), 3059br (N–H), 2944 (C–H), 1693 (C=O), 1457, 1269 (C–O), 1204, 1072, 985.

δ_H (400 MHz; $CDCl_3$): 1.39–1.58 (6 H, m, 3′-H_A, 5′-H_A, 9′-H_A, 9′-H_B, 10′-H_A and 11′-H_A), 1.66–1.84 (4 H, m, 4′-H_A, 5′-H_B, 10′-H_B and 11′-H_B), 1.86–1.92 (1 H, m, 3′-H_B), 2.00–2.12 (1 H, m, 4′-H_B), 3.66–3.77 (2 H, m, 8′-H), 5.75 (1 H, dd, $J_{5,6}$ 8.1 and J 2.2, 5-H). 5.95 (1 H, dd, $J_{2'ax,3'ax}$ 11.2, $J_{2'ax,3'eq}$ 2.5, 2′-H_{ax}), 8.1 (1 H, d, $J_{6,5}$ 8.1, 6-H), 2.49 (1 H, br s, NH).

δ_C (100 MHz; $CDCl_3$): 18.0 (CH_2, C-4′), 18.2 (CH_2, C-10′), 24.8 (CH_2, C-9′), 30.2 (CH_2, C-3′), 34.6 (CH_2, C-5′), 35.1 (CH_2, C-11′), 61.0 (CH_2, C-8′), 76.5 (CH, C-2′), 98.6 (C, C-6′), 102.3 (CH, C-5), 140.3 (CH, C-6), 150.0 (C, C-2), 162.9 (C, C-4).

***m/z* (EI):** 266 ($M^{+\bullet}$, 2%), 155 ($C_9H_{15}O_2$, 100), 138 (13), 126 (17), 111 (21), 108 (10), 98 (93), 95 (13), 55 (23).

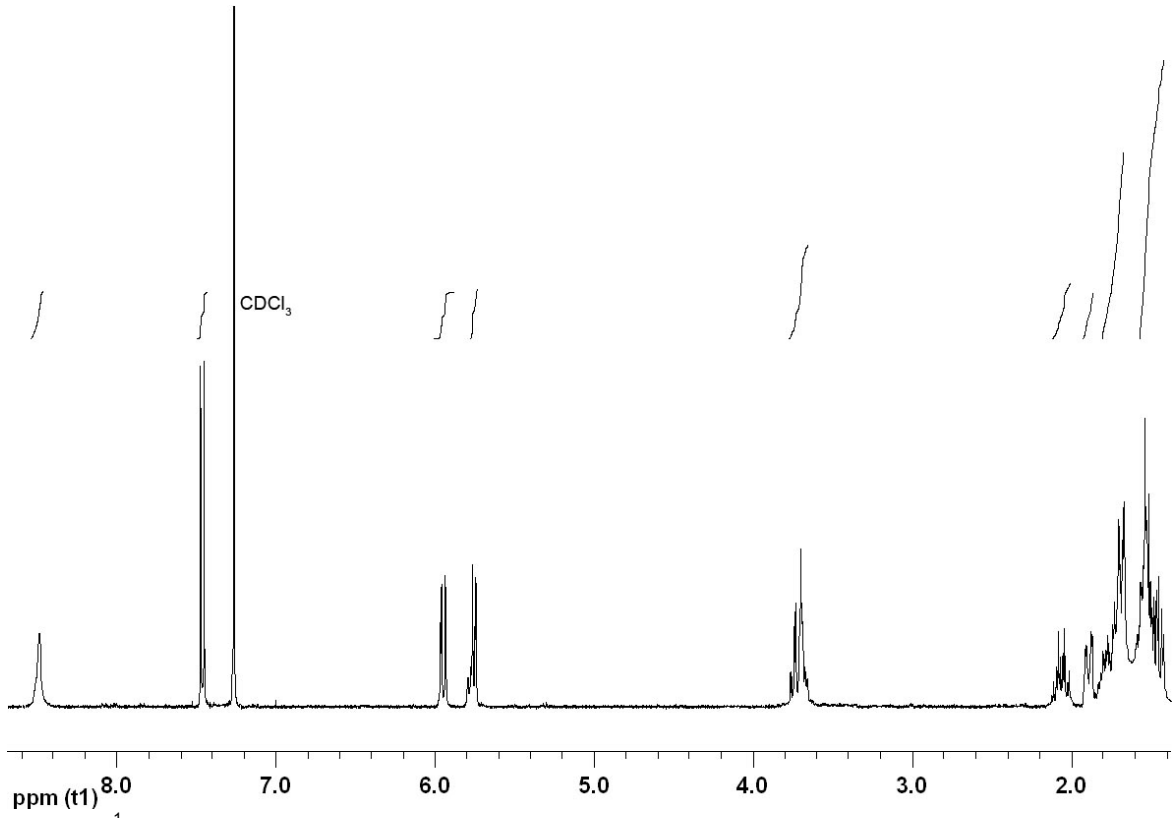

Figure 7.9: ^{1}H NMR spectrum (400 MHz; $CDCl_3$) of uridine **811d**.

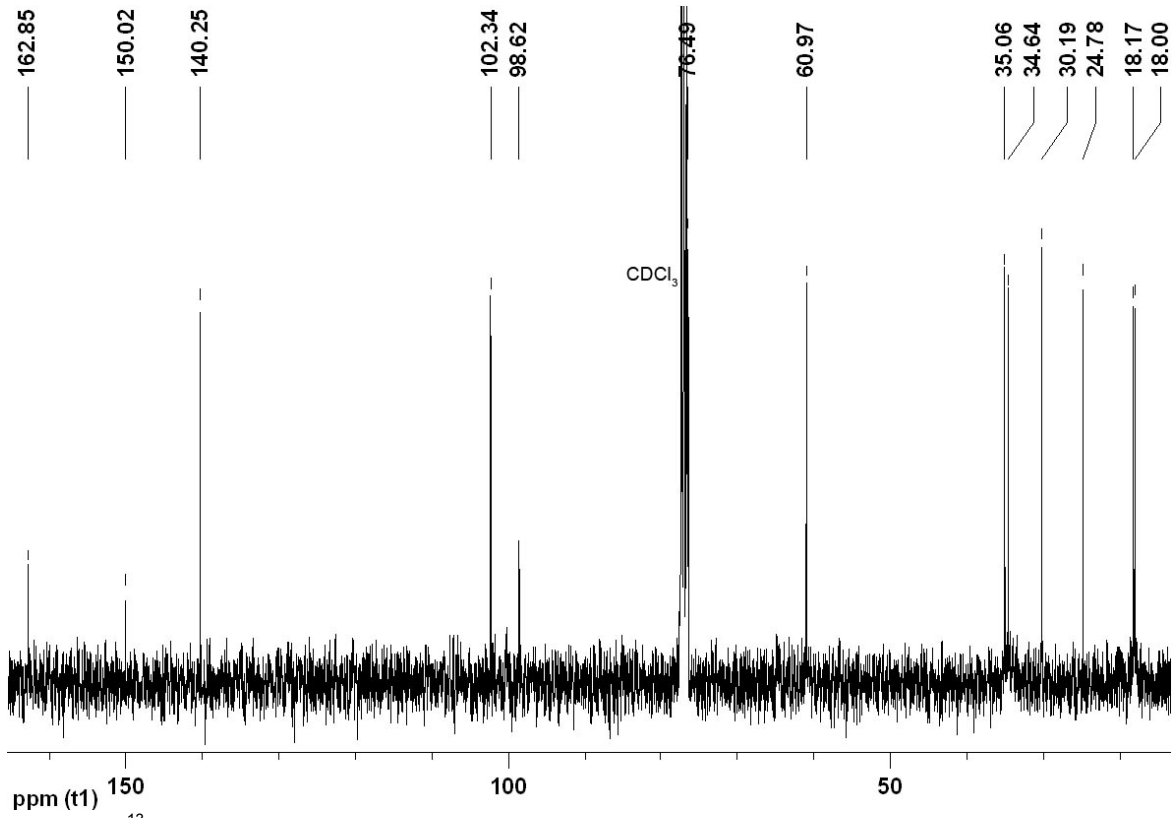

Figure 7.10: ^{13}C NMR spectrum (100 MHz; $CDCl_3$) of uridine **811d**.

7.2.5 Synthesis of Spiroacetal Triazole-Models 812

Dimethyl 1-([2′*S,6′*S**]-1′,7′-Dioxaspiro[5.5]undec-2′-yl)-1*H*-1,2,3-triazole-4,5-dicarboxylate (812a)**

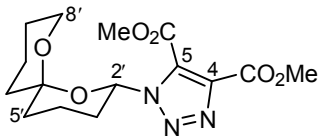

A 3:1 mixture of azide **814b** and **814a** (30.0 mg, 152 μmol) in dimethylacetylene dicarboxylate (190 μL, 1.52 mmol) was stirred at 70 °C for 3 h. The reaction mixture was purified directly by flash chromatography using hexane–EtOAc (4:1) as eluent to give the *title compound* **812a** (12.0 mg, 24%) as a pale yellow oil.

HRMS (EI): found $M^{+\bullet}$, 339.1427, $C_{15}H_{21}N_3O_6$ requires 339.1430.

ν_{max} (film)/cm^{-1}: 2954 (C–H), 1735 (C=O), 1458, 1212 (C–O), 1103 (C–O), 984.

δ_H (300 MHz; $CDCl_3$): 1.49–1.62 (6 H, m, 3′-H_A, 5′-H_A, 9′-H_A, 9′-H_B, 10′-H_A and 11′-H_A), 1.64–1.83 (4 H, m, 4′-H_A, 10′-H_B, 5′-H_B and 11′-H_B), 2.02–2.09 (1 H, m, 4′-H_B), 2.12–2.31 (2 H, m, 3′-H_B), 3.67–3.72 (2 H, m, 8′-H), 3.96 (3 H, s, OCH_3), 3.99 (3 H, s, OCH_3), 6.15 (1 H, dd, $J_{2'ax,3'ax}$ 10.7 and $J_{2'ax,3'eq}$ 3.1, 2′-H_{ax}).

δ_C (75 MHz; $CDCl_3$): 17.6 (CH_2, C-4′), 18.0 (CH_2, C-10′), 24.8 (CH_2, C-9′), 30.3 (CH_2, C-3′), 34.5 (CH_2, C-5′ or C-11′), 35.0 (CH_2, C-5′ or C-11′), 52.5 (CH_3, OCH_3), 53.4 (CH_3, OCH_3), 61.1 (CH_2, C-8′), 82.7 (CH, C-2′), 98.9 (C, C-6′), 133.4 (C, C-5), 138.3 (C, C-4), 160.0 (C, C=O), 160.3 (C, C=O).

***m/z* (EI$^+$):** 339 ($M^{+\bullet}$, 3%), 280 (M – CO_2Me, 5), 155 ($C_9H_{15}O_2$, 24), 154 (67), 126 (25), 98 (100), 55 (46).

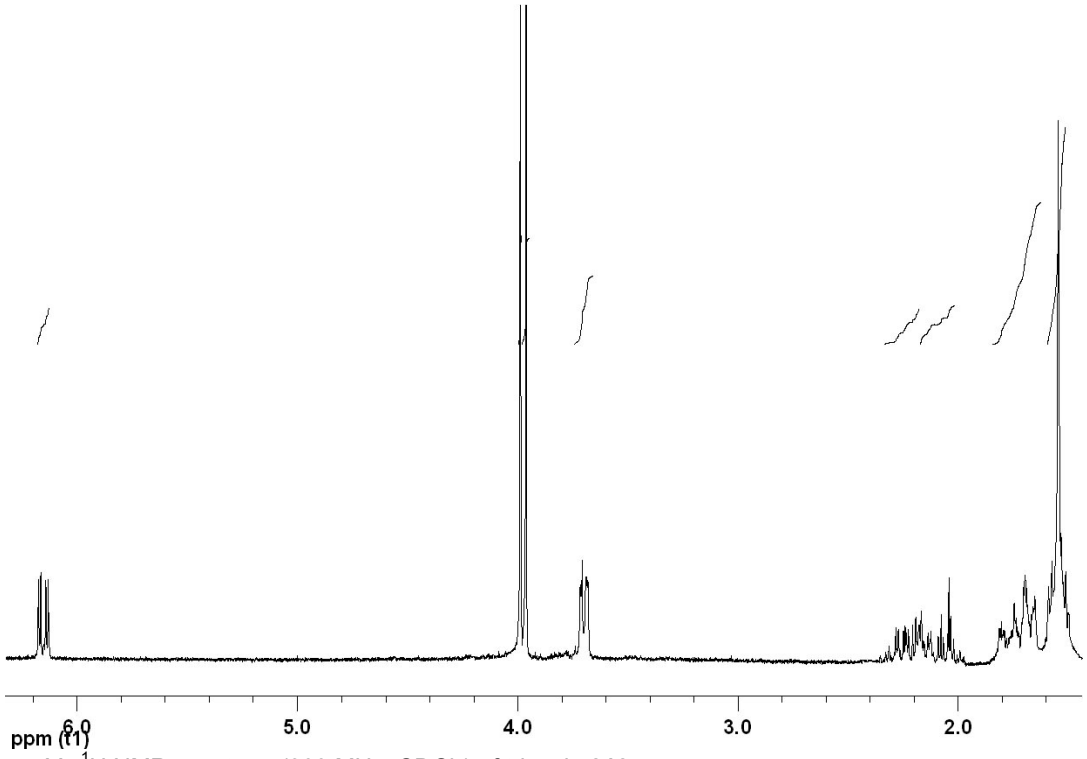

Figure 7.11: ^{1}H NMR spectrum (300 MHz; $CDCl_3$) of triazole **812a**.

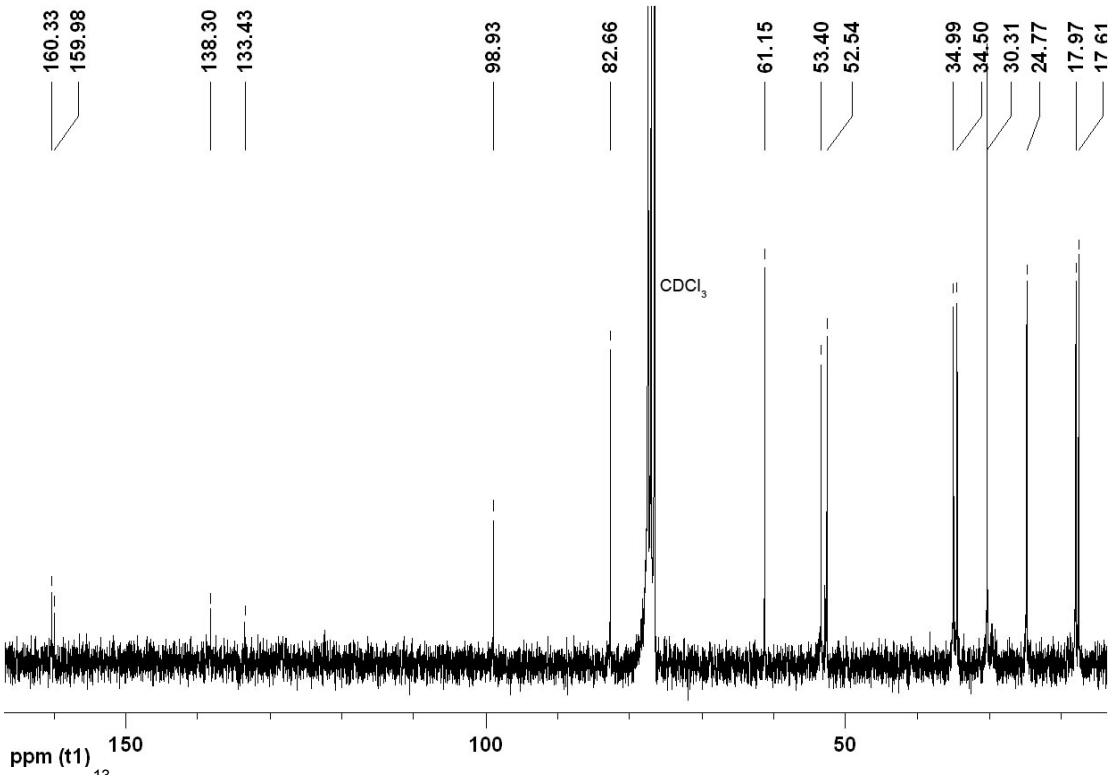

Figure 7.12: ^{13}C NMR spectrum (75 MHz; $CDCl_3$) of triazole **812a**.

4-[2″-(Benzyloxy)ethyl]-1-([2′*S,6′*S**]-1′,7′-dioxaspiro[5.5]undecan-2′-yl)-1*H*-1,2,3-triazole (812c)**

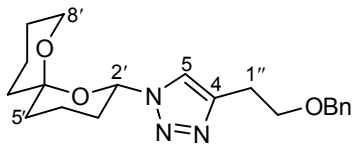

This procedure is an adaptation of that reported by Tornøe *et al.*[16]

To a 3:1 mixture of azide **814b** and **814a** (30.0 mg, 152 μmol) and 1-(benzyloxy)but-3-yne **(821)** (29.2 mg, 183 μmol) in anhydrous toluene (500 μL) at room temperature was added CuI (5.79 mg, 30.4 μmol) and DIPEA (26.5 μL, 152 μmol). After 18 h, a second portion of CuI (24.0 mg, 126 μmol) and DIPEA (104 μL, 597 μmol) were added. After 18 h, the mixture was filtered through Celite® and concentrated *in vacuo*. Purification by flash chromatography using CH_2Cl_2–EtOAc (9:1) as eluent yielded the *title compound* **812c** (5.70 mg, 10%) as a pale yellow oil.

HRMS (EI): found $M^{+\bullet}$, 357.2056, $C_{20}H_{27}N_3O_3$ requires 357.2052.

ν_{max} (film)/cm^{-1}: 2921 (C–H), 2869, 1604, 1495, 1455, 1209 (C–O), 4417, 1081 (C–O), 1030, 729, 694.

δ_H (400 MHz; $CDCl_3$): 1.48–1.62 (5 H, m, 5′-H_A, 9′-H_A, 9′-H_B, 10′-H_A and 11′-H_A), 1.70–1.82 (4 H, m, 4′-H_A, 5′-H_B, 10′-H_B and 11′-H_B), 1.82–1.92 (1 H, m, 3′-H_A), 2.03–2.15 (2 H, m, 3′-H_B and 4′-H_B), 3.08 (2 H, t, $J_{1'',2''}$ 6.6, 1″-H), 3.74–3.84 (2 H, m, 8′-H), 3.79 (2 H, t, $J_{2'',1''}$ 6.6, 2″-H), 4.55 (2 H, s, OCH_2Ph), 5.96 (1 H, dd, $J_{2'_{ax},3'_{ax}}$ 11.1 and $J_{2'_{ax},3'_{eq}}$ 2.2, 2′-H_{ax}), 7.27–7.36 (5 H, m, Ph), 7.58 (1 H, s, 5-H).

δ_C (100 MHz; $CDCl_3$): 18.1 (CH_2, C-10′), 18.2 (CH_2, C-4′), 24.9 (CH_2, C-9′), 26.6 (CH_2, C-1″), 31.0 (CH_2, C-3′), 34.6 (CH_2, C-5′), 35.0 (CH_2, C-11′), 61.1 (CH_2, C-8′), 69.1 (CH_2, C-2″), 73.0 (CH_2,

O*CH*$_2$Ph), 81.2 (CH, C-2′), 98.4 (C, C-6′), 119.8 (CH, C-5), 127.7 (2 x CH, Ph), 128.4 (CH, Ph), 138.3 (C, Ph), 145.1 (C, C-4).

***m/z* (EI):** 357 ($M^{+\bullet}$, 1%), 204 (14), 155 ($C_9H_{15}O_2$, 15), 136 (64), 97 (66), 91 (100, Bn), 79 (11), 65 (13), 55 (15).

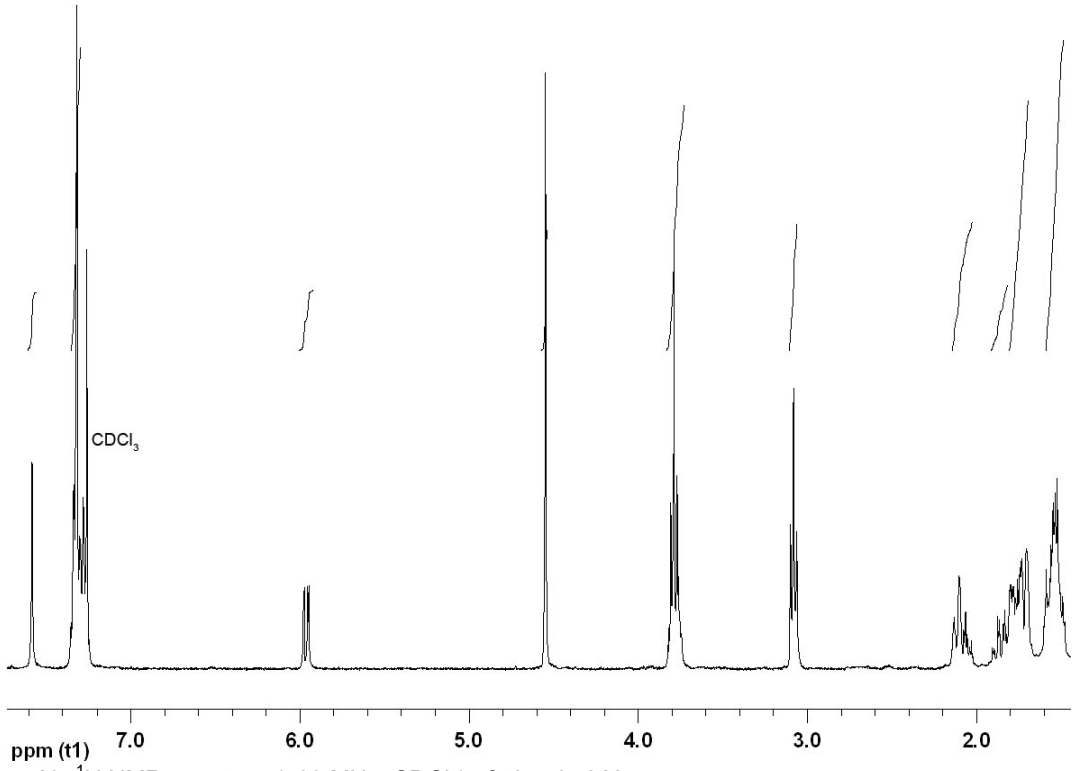

Figure 7.13: ^{1}H NMR spectrum (400 MHz; $CDCl_3$) of triazole **812c**.

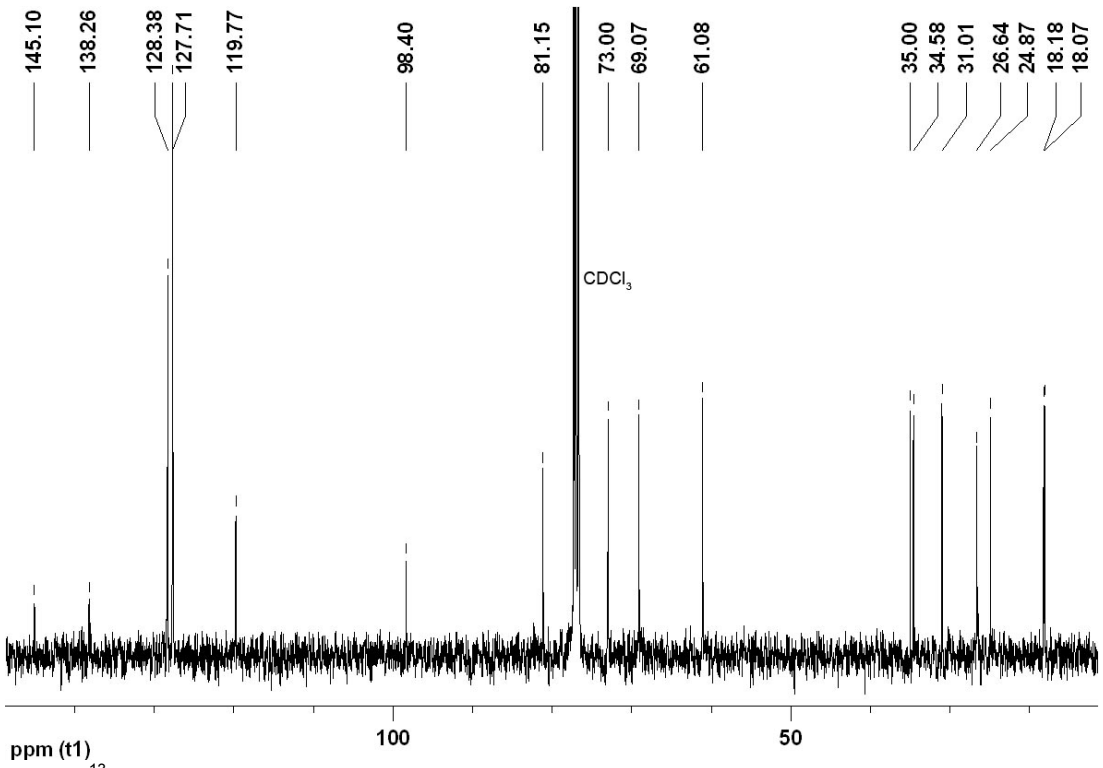

Figure 7.14: ^{13}C NMR spectrum (100 MHz; $CDCl_3$) of triazole **812c**.

Ethyl 1-([2′*S,6′*S**]-1′,7′-Dioxaspiro[5.5]undecan-2′-yl)-1*H*-1,2,3-triazole-4-carboxylate (812d)**

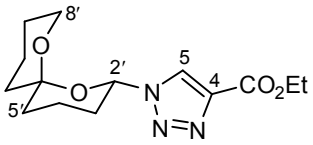

This procedure is an adaptation of that reported by Vargas-Berenguel *et al.*[17]

To a 3:1 mixture of azide **814b** and **814a** (49.3 mg, 250 μmol) in anhydrous toluene (500 μL) at room temperature under an atmosphere of argon was added CuI•[P(OEt)$_3$] (8.92 mg, 25.0 μmol) and ethyl propiolate **(857)** (5 x 25.3 μL, 1.25 mmol in total) in 5 portions at 30 min intervals. The resulting mixture was stirred overnight and was purified directly by flash chromatography using CH_2Cl_2–EtOAc (1:0 to 19:1) as eluent to give the *title compound* **812d** (17.0 mg, 23%) as a pale yellow oil.

HRMS (EI): found $M^{+\bullet}$, 295.1530, $C_{14}H_{21}N_3O_4$ requires 295.1532.

ν_{max} (film)/cm^{-1}: 2941 (C–H), 1731 (C=O), 1214 (C–O), 1032 (C–O).

δ_H (400 MHz; CDCl$_3$): 1.42 (3 H, t, J_{CH_3,CH_2} 7.1, OCH$_2$*CH$_3$*), 1.49–1.61 (5 H, m, 5′-H$_A$, 9′-H$_A$, 9′-H$_B$, 10′-H$_A$ and 11′-H$_A$), 1.73–1.87 (5 H, m, 3′-H$_A$, 4′-H$_A$, 5′-H$_B$, 10′-H$_B$ and 11′-H$_B$), 2.10 (1 H, m, 4′-H$_B$), 2.18–2.24 (1 H, m, 3′-H$_B$), 3.72–3.77 (2 H, m, 8′-H), 4.44 (2 H, q, J_{CH_2,CH_3} 7.1, O*CH$_2$*CH$_3$), 6.05 (1 H, dd, $J_{2'ax,3'ax}$ 10.9 and $J_{2'ax,3'eq}$ 2.4, 2′-H$_{ax}$), 8.29 (1 H, s, 5-H).

δ_C (100 MHz; CDCl$_3$): 14.3 (CH$_3$, OCH$_2$*CH$_3$*), 17.8 (CH$_2$, C-4′), 18.1 (CH$_2$, C-10′), 24.7 (CH$_2$, C-9′), 31.4 (CH$_2$, C-3′), 34.5 (CH$_2$, C-5′ or C-11′), 34.9 (CH$_2$, C-5′ or C-11′), 61.2 (CH$_2$, C-8′), 61.3 (CH$_2$, O*CH$_2$*CH$_3$), 81.7 (CH, C-2′), 98.7 (C, C-6′), 125.6 (CH, C-5), 140.1 (C, C-4), 160.8 (C, C=O).

***m/z* (EI):** 295 ($M^{+\bullet}$, 2%), 222 (M – CO$_2$Et, 3), 155 ($C_9H_{15}O_2$, 41), 126 (59), 111 (17), 98 (CH≡CCO$_2$Et, 100), 96 (25), 55 (27), 43 (15), 41 (24).

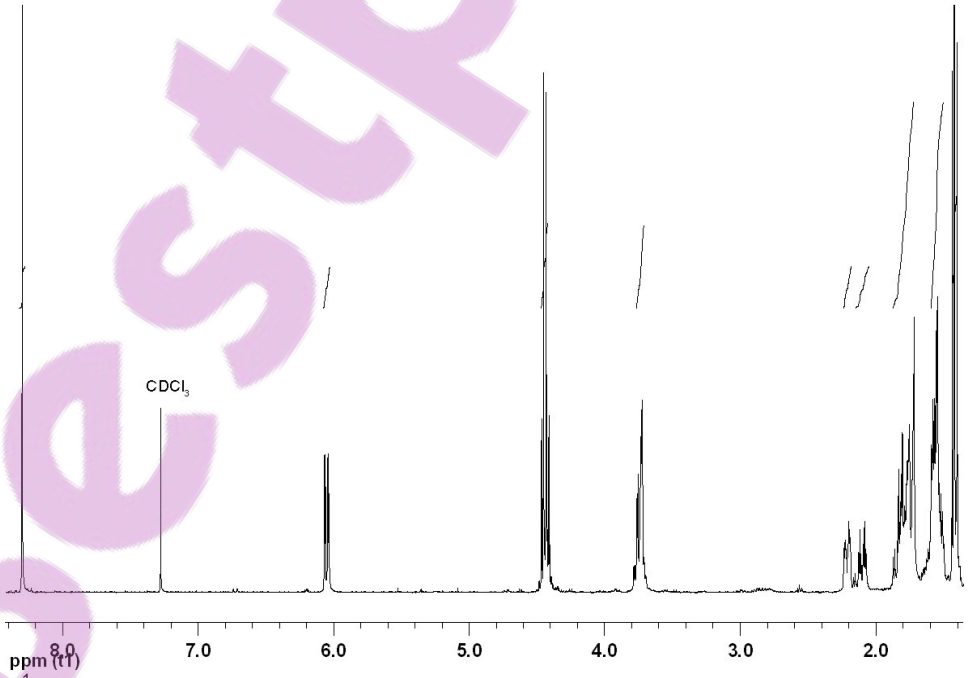

Figure 7.15: ^{1}H NMR spectrum (400 MHz; CDCl$_3$) of triazole **812d**.

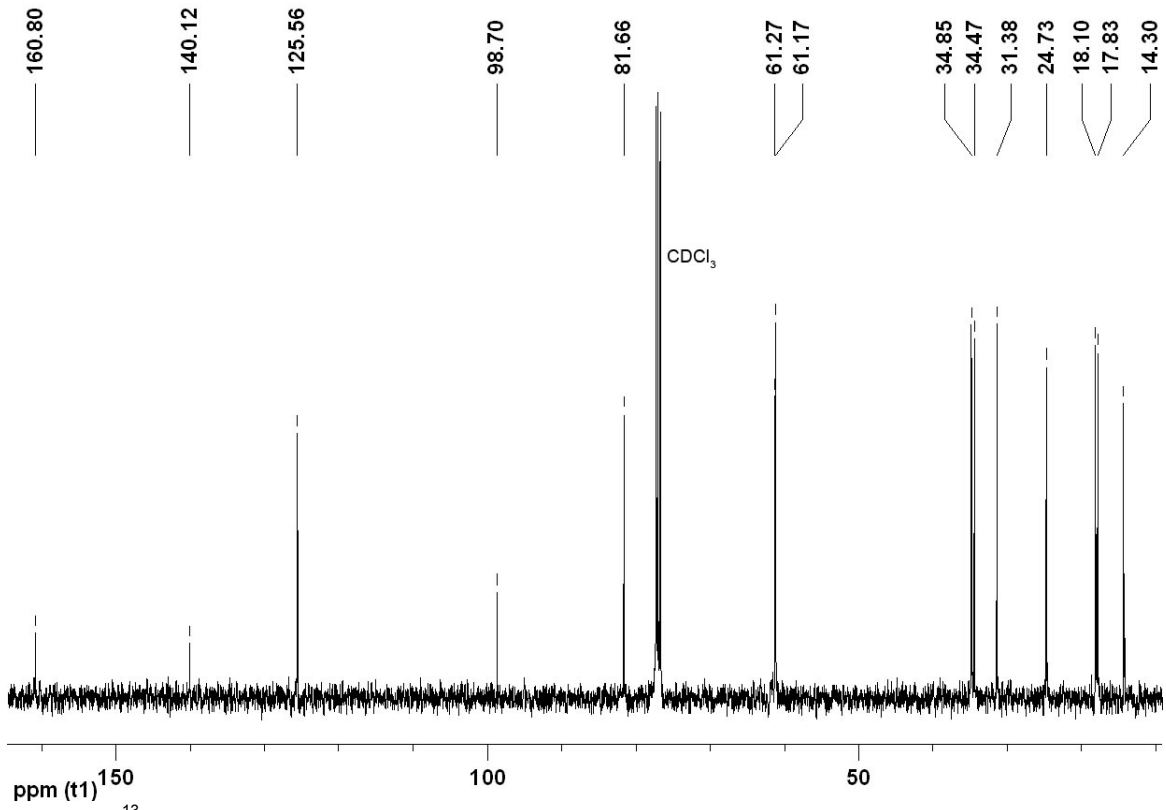

Figure 7.16: ^{13}C NMR spectrum (100 MHz; $CDCl_3$) of triazole **812d**.

7.3 Experimental Data–Spiroacetals Bearing a Hydroxymethyl Substituent

7.3.1 Synthesis of Valerolactone 865

Ethyl 1,4-Dioxaspiro[4.4]nonane-6-carboxylate (927)[18-20]

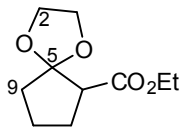

This procedure is an adaptation of that reported by Taylor *et al.*[20]

A solution of ethyl 2-oxocyclopentanecarbocylate **(877)** (4.74 mL, 32.0 mmol), *p*-toluenesulfonic acid monohydrate (121 mg, 640 μmol) and ethylene glycol (2.14 mL, 38.4 mmol) in CH_2Cl_2 (100 mL) was heated to reflux under a reverse Dean-Stark apparatus. After 18 h, the organic phase was washed with saturated $NaHCO_3$ solution (2 x 20 mL) and brine (20 mL). The resulted mixture was dried over $MgSO_4$ and concentrated *in vacuo* to give the title acetal **927** (6.40 g, 100%) as a pale yellow oil which was used in the $LiAlH_4$ reduction described below without further purification. The spectral data were in agreement with that reported in the literatures.[18,19]

HRMS (CI): found MH^+, 201.1123, $C_{10}H_{17}O_4$ requires 201.1127.

δ_H (400 MHz; $CDCl_3$): 1.27 (3 H, t, J_{CH_3,CH_2} 7.1, OCH_2CH_3), 1.60–1.71 (1 H, m, 8-H_A), 1.78–1.87 (2 H, m, 8-H_B and 9-H_A), 1.88–1.97 (2 H, m, 9-H_B and 7-H_A), 2.13 (1 H, dq, J_{AB} 13.2 and $J_{7_B,6} = J_{7_B,8_A} = J_{7_B,8_B}$ 7.4, 7-H_B), 2.90 (1 H, dd, $J_{6,7_A}$ 8.9 and $J_{6,7_B}$ 7.0, 6-H), 3.86–3.98 (3 H, m, 2-H and 3-H_A), 3.99–4.06 (1 H, m, 3-H_B), 4.14 (1 H, dq, J_{AB} 10.9 and J_{CH_2,CH_3} 7.1, $OCH_AH_BCH_3$), 4.20 (1 H, dq, J_{AB} 10.9 and J_{CH_2,CH_3} 7.1, $OCH_AH_BCH_3$).

δ_C (100 MHz; $CDCl_3$): 14.2 (CH_3, OCH_2CH_3), 22.0 (CH_2, C-8), 26.8 (CH_2, C-7), 36.7 (CH_2, C-9), 52.2 (CH, C-6), 60.3 (CH_2, OCH_2CH_3), 64.4 (CH_2, C-3), 65.1 (CH_2, C-2), 118.3 (C, C-5), 172.3 (C, C=O).

***m/z* (CI):** 201 (MH^+, 30%), 200 (M^+, 9), 155 (M – OEt, 57), 100 (27), 99 (100).

6-Hydroxymethyl-1,4-dioxaspiro[4.4]nonane (928)[18-21]

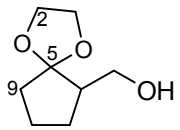

This procedure is an adaptation of that reported by Taylor *et al.*[20]

To a slurry of $LiAlH_4$ (469 mg, 12.4 mmol) in anhydrous Et_2O (10 mL) was added a solution of crude ester **927** (3.30 g, 16.5 mmol) in anhydrous Et_2O (15 mL) dropwise and the mixture was heated to reflux for 2 h. Additional $LiAlH_4$ (250 mg, 6.59 mmol) was added and the mixture was heated to reflux for another 2 h. The reaction was cooled to room temperature and MeOH was added dropwise until fizzing stopped. The resulting slurry was filtered through a pad of Celite®. Saturated Rochelle's salt solution (40 mL) was added to the filtrate and the mixture was stirred vigorously for 30 min. The aqueous phase was extracted with ether (3 x 30 mL) and the combined organic extracts were dried over $MgSO_4$. Concentration *in vacuo* and re-filtration through a pad of Celite® yielded the title alcohol **928** as an orange oil (2.55 g, 98%) which was used in the hydroxyl protection step described below without further purification. Purification by flash chromatography was performed using hexane–EtOAc (7:3) as eluent. The spectral data were in agreement with that reported in the literatures.[19,21]

HRMS (EI): found $M^{+\bullet}$, 158.0944, $C_8H_{14}O_3$ requires 158.0943.

δ_H (400 MHz; $CDCl_3$): 1.51–1.72 (3 H, m, 7-H_A and 8-H), 1.72–1.80 (2 H, m, 9-H), 1.81–1.91 (1 H, m, 7-H_A), 2.14 (1 H, tt, $J_{6,7}$ 7.9 and $J_{6,6\text{-}CH_2}$ 5.6, 6-H), 2.67 (1 H, br s, OH), 3.64 (2 H, d, $J_{6\text{-}CH_2,6}$ 5.6, 6-CH_2O), 3.87–4.01 (4 H, m, 2-H and 3-H).

δ_C (100 MHz; $CDCl_3$): 21.0 (CH_2, C-8), 25.7 (CH_2, C-7), 35.5 (CH_2, C-9), 46.9 (CH, C-6), 62.2 (CH_2, 6-CH_2O), 63.8 (CH_2, C-2), 64.3 (CH_2, C-3), 118.7 (C, C-5).

***m/z* (EI):** 158 ($M^{+\bullet}$, 10%), 149 (20), 141 (M – OH, 8), 129 (25), 99 (100), 81 (26), 69 (34), 41 (31).

6-(*tert*-Butyldiphenylsilyloxymethyl)-1,4-dioxaspiro[4,4]nonane (878)[20]

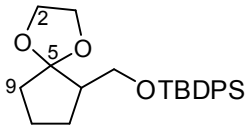

To a solution of crude alcohol **928** (2.55 g, 16.1 mmol), NEt_3 (2.70 mL, 19.4 mmol) and DMAP (393 mg, 3.22 mmol) in anhydrous CH_2Cl_2 (50 mL) at room temperature was added TBDPSCl (4.40 mL, 16.9 mmol) dropwise. After 18 h, saturated NH_4Cl solution (100 mL) was added and the aqueous phase was extracted with Et_2O (3 x 40 mL). The combined organic extracts were dried over $MgSO_4$ and concentrated *in vacuo*. Purification by flash chromatography using hexane–CH_2Cl_2 (4:1 to 2:3) as eluent yielded the title silyl ether **878** (5.89 g, 92%) as a colourless oil. The spectral data were in agreement with that reported in the literature.[20]

HRMS (CI): found MH^+, 397.2207, $C_{24}H_{33}O_3Si$ requires 397.2199.

δ_H (300 MHz; $CDCl_3$): 1.04 (9 H, s, $OSiPh_2{}^tBu$), 1.50–1.71 (3 H, m, 7-H_A, 8-H_A and 8-H_B), 1.72–1.80 (2 H, m, 9-H), 1.87–2.00 (1 H, m, 7-H_B), 2.14–2.25 (1 H, m, 6-H), 3.56 (1 H, dd, J_{AB} 10.2 and $J_{6\text{-}CH_2,6}$ 7.8, 6-CH_AH_BO), 3.71–3.86 (5 H, m, 2-H, 3-H and 6-CH_AH_BO), 7.33–7.44 (6 H, m, Ph), 7.66–7.71 (4 H, m, Ph).

δ_C (75 MHz; $CDCl_3$): 19.2 (C, $OSiPh_2{}^tBu$), 21.1 (CH_2, C-8), 26.9 (CH_3, $OSiPh_2{}^tBu$), 27.6 (CH_2, C-7), 36.5 (CH_2, C-9), 48.4 (CH, C-6), 63.8 (CH_2, 6-CH_2O), 64.1 (CH_2, C-2), 64.8 (CH_2, C-3), 117.8 (C, C-5), 127.6 (CH, Ph), 129.5 (CH, Ph), 134.0 (C, Ph), 134.1 (C, Ph), 135.6 (CH, Ph), 135.6 (CH, Ph).

***m/z* (CI):** 397 (MH^+, 100%), 339 (M – ^{t}Bu, 12), 319 (M – Ph, 12), 195 (41), 275 (33), 141 (31), 62 (40).

2-(*tert*-Butyldiphenylsilyloxymethyl)cyclopentanone (929)[20]

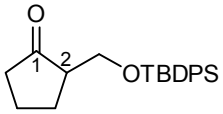

A solution of acetal **878** (5.00 g, 12.6 mmol) and PPTS (797 mg, 3.17 mmol) in acetone (80 mL) and water (30 mL) was heated to reflux. After 4 h, Et_2O (80 mL) and solid NaCl were added until the aqueous phase was saturated. The aqueous phase was extracted with Et_2O (3 x 80 mL). The combined organic extracts were washed with saturated $NaHCO_3$ solution (2 x 40 mL), dried over $MgSO_4$ and concentrated *in vacuo*. Purification by flash chromatography using hexane–Et_2O (9:1 to 1:1) as eluent followed by recrystallisation from hot hexane yielded the title ketone **929** (4.39 g, 99%) as a white powder. The spectral data were in agreement with that reported in the literature.[20]

M.p.: 70.8–72.1 °C (lit. m.p.[20]: 71.2–72.4 °C).

HRMS (CI): found MH^+, 353.1932, $C_{22}H_{29}O_2Si$ requires 353.1937.

ν_{max} (film)/cm^{-1}: 2930 (C–H), 1728 (C=O), 1427, 1113 (C–O), 821, 701.

δ_H (400 MHz; $CDCl_3$): 1.02 (9 H, s, $OSiPh_2{}^tBu$), 1.76–1.85 (1 H, m, 3-H_A), 2.0–2.34 (6 H, m, 2-H, 3-H_B, 4-H_A, 4-H_B, 5-H_A and 5-H_B), 3.76 (1 H, dd, J_{AB} 10.0 and $J_{2\text{-}CH_2,2}$ 3.0, 2-CH_AH_BO), 3.95 (1 H, dd, J_{AB} 10.0 and $J_{2\text{-}CH_2,2}$ 4.5, 2-CH_AH_BO), 7.35–7.42 (6 H, m, Ph), 7.63–7.76 (4 H, m, Ph).

δ_C (100 MHz; $CDCl_3$): 19.3 (C, $OSiPh_2{}^tBu$), 21.0 (CH_2, C-3), 16.5 (CH_2, C-4), 26.8 (CH_3, $OSiPh_2{}^tBu$), 39.2 (CH_2, C-5), 50.8 (CH, C-2), 62.6 (CH_2, 2-CH_2O), 127.7 (CH, Ph), 129.6 (CH, Ph), 133.2 (C, Ph), 133.5 (C, Ph), 135.5 (CH, Ph), 135.6 (CH, Ph).

***m/z* (CI):** 370 (MH + NH_3, 2%), 353 (MH^+, 1), 295 (M – ^{t}Bu, 24), 275 (M – Ph, 100), 217 (7), 196 (7).

6-(*tert*-Butyldiphenylsilyloxymethyl)tetrahydro-2*H*-pyran-2-one (865)[20,22]

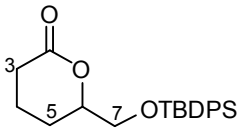

This procedure is an adaptation of that reported by Taylor *et al.*[20] and Uenishi *et al.*[22]

To a solution of ketone **929** (8.01 g, 22.7 mmol) in CH_2Cl_2 (110 mL) at room temperature was added $NaHCO_3$ (3.82 g, 45.4 mmol) and *m*-CPBA (9.52 g, 70%, 38.6 mmol). After 3 h, saturated $Na_2S_2O_3$ solution (30 mL) and water (30 mL) were added and stirred for 20 min. The organic phase was washed with saturated $NaHCO_3$ solution (2 x 100 mL). The combined organic phase was dried over $MgSO_4$ and concentrated *in vacuo*. Purification by flash chromatography using hexane–EtOAc (9:1 to 7:3) as eluent yielded the title valerolactone **865** (8.14 g, 97%) as a cream solid. Further purification by recrystallisation from hot hexane yielded cream needles The spectral data were in agreement with that reported in the literature.[20]

M.p.: 93.7–94.9 °C (lit. m.p.[20]: 94.0–94.7 °C).

HRMS (CI): found MH^+, 369.1888, $C_{22}H_{29}O_3Si$ requires 369.1886.

ν_{max} (film)/cm^{-1}: 2923 (C–H), 1731 (C=O), 1248, 1108 (C–O), 707.

δ_H (400 MHz; $CDCl_3$): 1.06 (9 H, s, $OSiPh_2{}^tBu$), 1.73–1.87 (2 H, m, 4-H_A and 5-H_A), 1.93–2.00 (2 H, m, 4-H_B and 5-H_B), 2.45 (1 H, ddd, J_{AB} 17.9, $J_{3A,4A}$ 8.8 and $J_{3A,4B}$ 6.5, 3-H_A), 2.69 (1 H, m, 3-H_B), 3.75 (1 H, dd, J_{AB} 10.6 and $J_{7A,6}$ 5.0, 7-H_A), 3.79 (1 H, dd, J_{AB} 10.6 and $J_{7B,6}$ 3.9, 7-H_B), 4.39 (1 H, m, 6-H), 7.37–7.46 (6 H, m, Ph), 7.66 (4 H, m, Ph).

δ_C (100 MHz; $CDCl_3$): 18.3 (CH_2, C-4), 19.2 (C, $OSiPh_2{}^tBu$), 24.4 (CH_2, C-4), 26.7 (CH_3, $OSiPh_2{}^tBu$), 29.9 (CH_2, C-3), 65.5 (CH_2, C-7), 80.2 (CH, C-6), 127.7 (CH, Ph), 129.8 (CH, Ph), 132.9 (C, Ph), 133.0 (C, Ph), 135.5 (CH, Ph), 135.6 (CH, Ph), 171.2 (C, C=O).

***m/z* (CI):** 386 (MH + NH_3, 18%), 369 (MH^+, 4), 311 (M – ^{t}Bu, 57), 291 (M – Ph, 100), 233 (52).

7.3.2 Synthesis of Spiroacetal 883

1-(Benzyloxy)-10-(*tert*-butyldiphenylsilyloxy)-9-hydroxydec-3-yn-5-one (881)

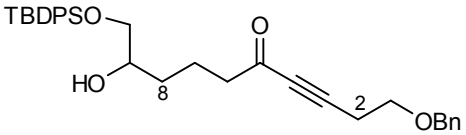

To a solution of 1-(benzyloxy)but-3-yne **(821)** (198 mg, 1.24 mmol) in anhydrous THF (4.0 mL) at -78 °C was added BuLi (930 μL, 1.6 mol L^{-1} in hexane, 1.49 mmol) dropwise. After 30 min, a solution of valerolactone **865** (500 mg, 1.36 mmol) in anhydrous THF (2.0 mL) was added dropwise. After 2 h, saturated NH_4Cl solution (3 mL) was added. The mixture was warmed to room temperature and the aqueous phase extracted with EtOAc (3 x 4 mL). The combined organic extracts were dried over $MgSO_4$ and concentrated *in vacuo*. Purification by flash chromatography using hexane–Et_2O (4:1) as eluent yielded the *title compound* **881** (478 mg, 73%) as a pale yellow oil together with the benzyl ether **821** (52.7 mg, 27%).

HRMS (FAB): found $[M – OH]^+$, 511.2664, $C_{33}H_{39}O_3Si$ requires 511.2669.

ν_{max} (film)/cm^{-1}: 3478br (O–H), 2930 (C–H), 2858 (C–H), 2215 (C≡C), 1732 (C=O), 1673, 1471, 1428, 1361, 1240, 1112 (C–O), 740, 702.

δ_H (300 MHz; $CDCl_3$): 1.06 (9 H, s, $OSiPh_2{}^tBu$), 1.35–1.44 (2 H, m, 8-H), 1.61–1.73 (1 H, m, 7-H_A), 1.73–1.86 (1 H, m, 7-H_B), 2.48 (1 H, br s, OH), 2.54 (2 H, t, $J_{6,7}$ 7.3, 6-H), 2.65 (2 H, t, $J_{2,1}$ 6.8, 2-H), 3.47 (1 H, dd, J_{AB} 9.9 and $J_{10_A,9}$ 7.3, 10-H_A), 3.62 (2 H, t, $J_{1,2}$ 6.8, 1-H), 3.61–3.66 (1 H, m, 10-H_B), 3.66–3.74 (1 H, m, 9-H), 4.54 (2 H, s, OCH_2Ph), 7.26–7.44 (11 H, m, $OSiPh_2{}^tBu$ and OCH_2Ph), 7.63–7.68 (4 H, m, $OSiPh_2{}^tBu$),.

δ_C (75 MHz; $CDCl_3$): 19.2 (C, $OSiPh_2{}^tBu$), 20.0 (CH_2, C-7), 20.4 (CH_2, C-2), 26.8 (CH_3, $OSiPh_2{}^tBu$), 31.9 (CH_2, C-8), 45.2 (CH_2, C-6), 67.2 (CH_2, C-1), 67.9 (CH_2, C-10), 71.5 (CH, C-9), 73.1 (CH_2, OCH_2Ph), 81.4 (C, C-4), 90.6 (C, C-3), 127.7 (CH, OCH_2Ph), 127.8 (CH, OCH_2Ph and $OSiPh_2{}^tBu$), 128.5 (CH, OCH_2Ph), 129.8 (CH, $OSiPh_2{}^tBu$), 133.1 (C, $OSiPh_2{}^tBu$), 135.5 (CH, $OSiPh_2{}^tBu$), 137.7 (C, OCH_2Ph), 187.7 (C, C-5).

***m/z* (FAB):** 511 ($[M – OH]^+$, 17%), 471 (M – ^tBu, 3), 451 (M – Ph, 2), 421 (M – OBn, 1), 239 ($SiPh_2{}^tBu$, 5), 207 (18), 199 (45), 197 (37), 139 (18), 137 (34), 135 (67), 91 (Bn, 100).

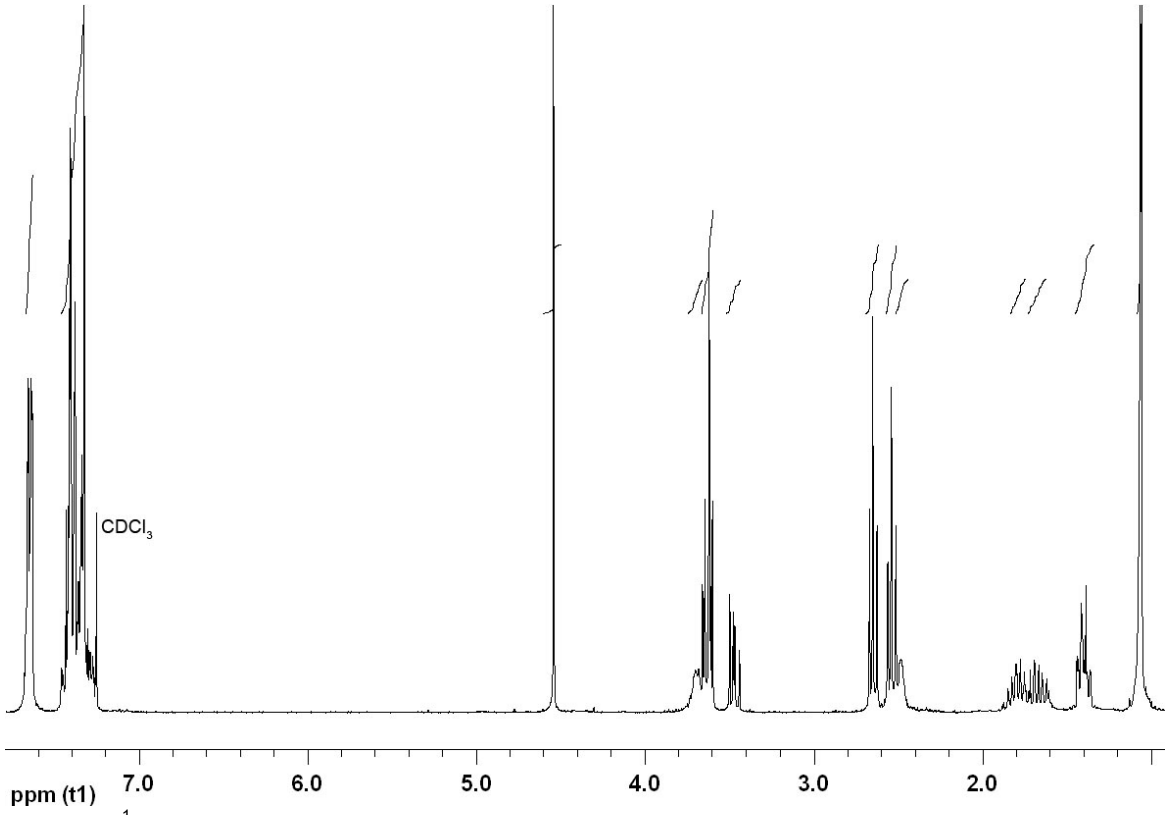

Figure 7.17: ^{1}H NMR spectrum (300 MHz; $CDCl_3$) of keto-alcohol **881**.

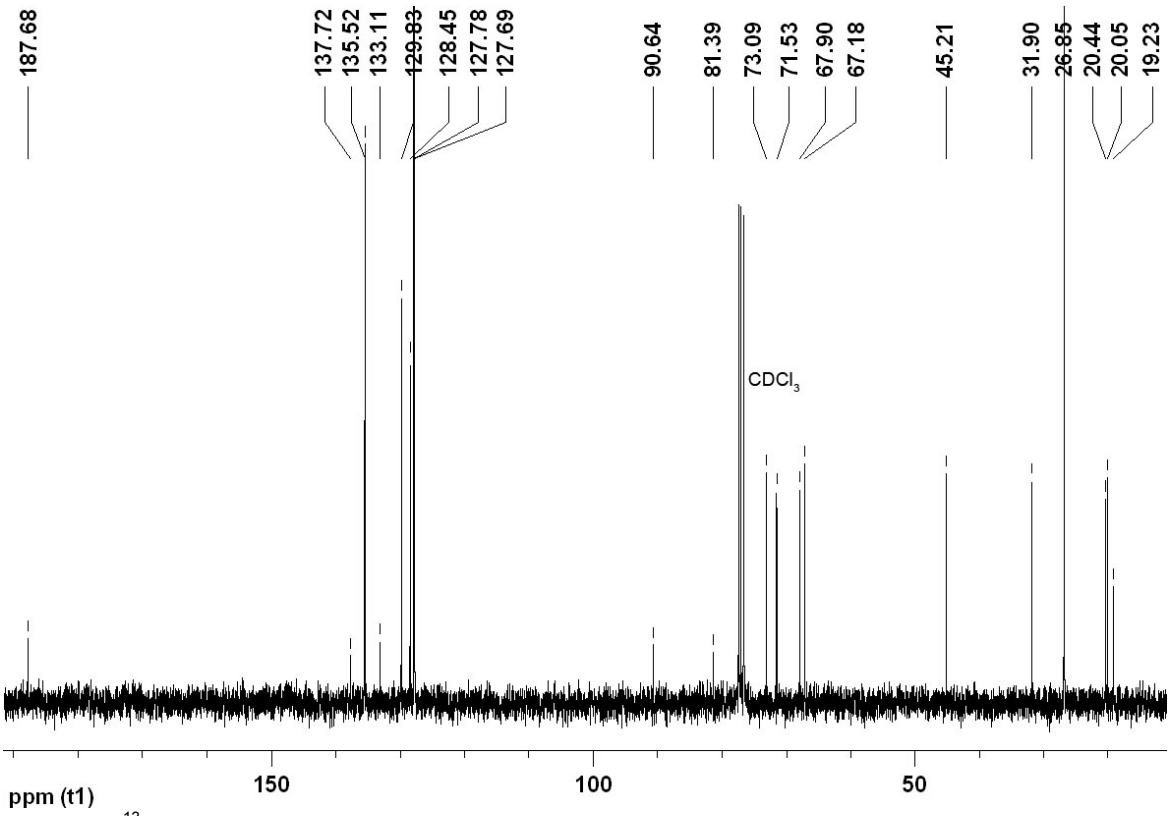

Figure 7.18: ^{13}C NMR spectrum (75 MHz; $CDCl_3$) of keto-alcohol **881**.

2-(*tert*-Butyldiphenylsilyloxymethyl)-1,7-dioxaspiro[5.5]undecane (883)

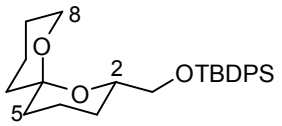

To a solution of keto-alcohol **881** (230 mg, 435 μmol) in THF (20 mL) was added *p*-tolenesulfonic acid monohydrate (3.75 mg, 21.8 mmol) and Pd/C (35.0 mg, 10% w/w) and the mixture was stirred under an atmosphere of hydrogen. After 18 h, NEt_3 (6 drops) was added. The mixture was filtered through a pad of Celite® and concentrated *in vacuo*. Purification by flash chromatography using pentane–Et_2O (19:1) as eluent yielded the *title compound* **883** (131 mg, 71%) as a colourless oil.

HRMS (EI): found $M^{+\bullet}$, 424.2423, $C_{26}H_{36}O_3Si$ requires 424.2434.

ν_{max} (film)/cm^{-1}: 2936 (C–H), 1428, 1228, 1112 (C–O), 993, 823, 800, 701, 501.

δ_H (300 MHz; $CDCl_3$): 1.05 (9 H, s, $OSiPh_2{}^tBu$), 1.16–1.28 (1 H, m, 3-H_A), 1.31–1.40 (1 H, m, 5-H_A or 11-H_A), 1.40–1.67 (8 H, m, 3-H_B, 4-H_A, 5-H_A or 11-H_A, 5-H_B, 9-H_A, 9-H_B, 10-H_A and 11-H_B), 1.78–1.98 (2 H, m, 4-H_B and 10-H_B), 3.53–3.62 (2 H, m, 8-H_A and 2-CH_AH_BO), 3.66–3.84 (3 H, m, 2-H, 8-H_B and 2-CH_AH_BO), 7.34–7.45 (6 H, m, Ph), 7.69–7.77 (4 H, m, Ph).

δ_C (75 MHz; $CDCl_3$): 18.5 (2 x CH_2, C-4 and C-10), 19.2 (C, $OSiPh_2{}^tBu$), 25.3 (CH_2, C-9), 26.7 (CH_3, $OSiPh_2{}^tBu$), 27.1 (CH_2, C-3), 35.4 (CH_2, C-5 or C-11), 35.7 (CH_2, C-5 or C-11), 60.2 (CH_2, C-8), 67.4 (CH_2, 2-CH_2O), 70.1 (CH, C-2), 94.4 (C, C-6), 127.5 (CH, Ph), 127.6 (CH, Ph), 129.5 (CH, Ph), 129.5 (CH, Ph), 133.8 (C, Ph), 133.9 (C, Ph), 135.6 (CH, Ph), 135.7 (CH, Ph).

***m/z* (EI):** 424 ($M^{+\bullet}$, 1%), 367 (M – ^{t}Bu, 100), 199 (98), 155 ($C_9H_{15}O_2$, 28), 111 (40), 55 (31), 41 (29).

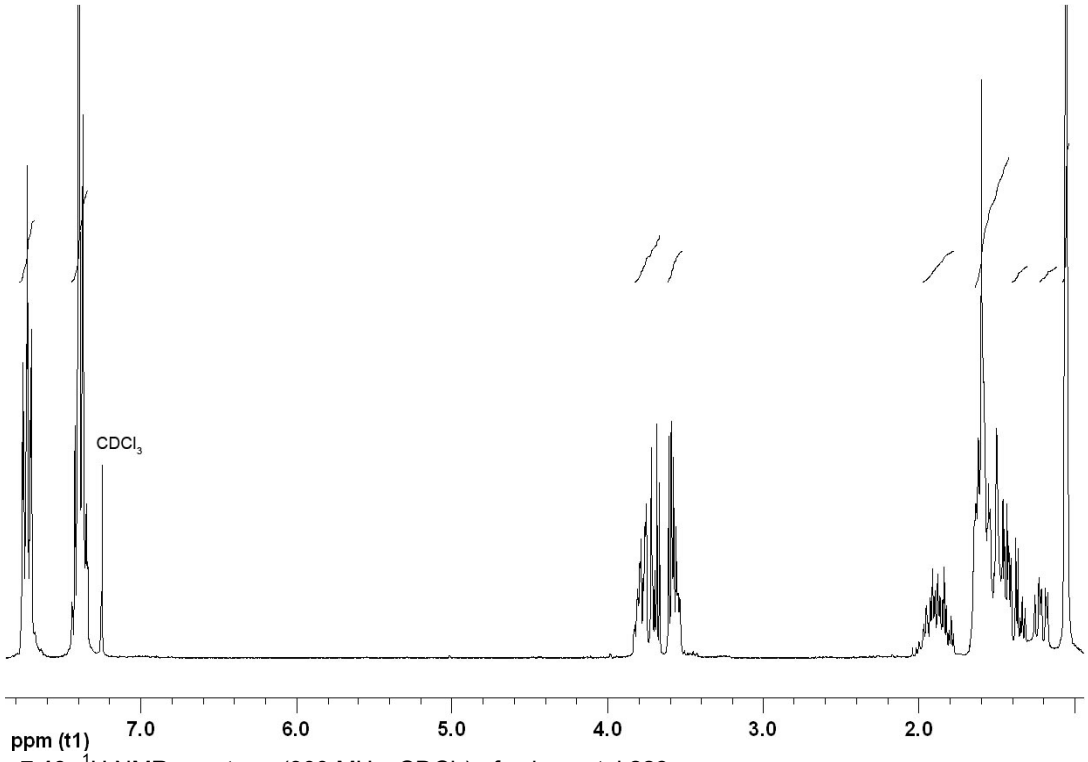

Figure 7.19: ^{1}H NMR spectrum (300 MHz; $CDCl_3$) of spiroacetal **883**.

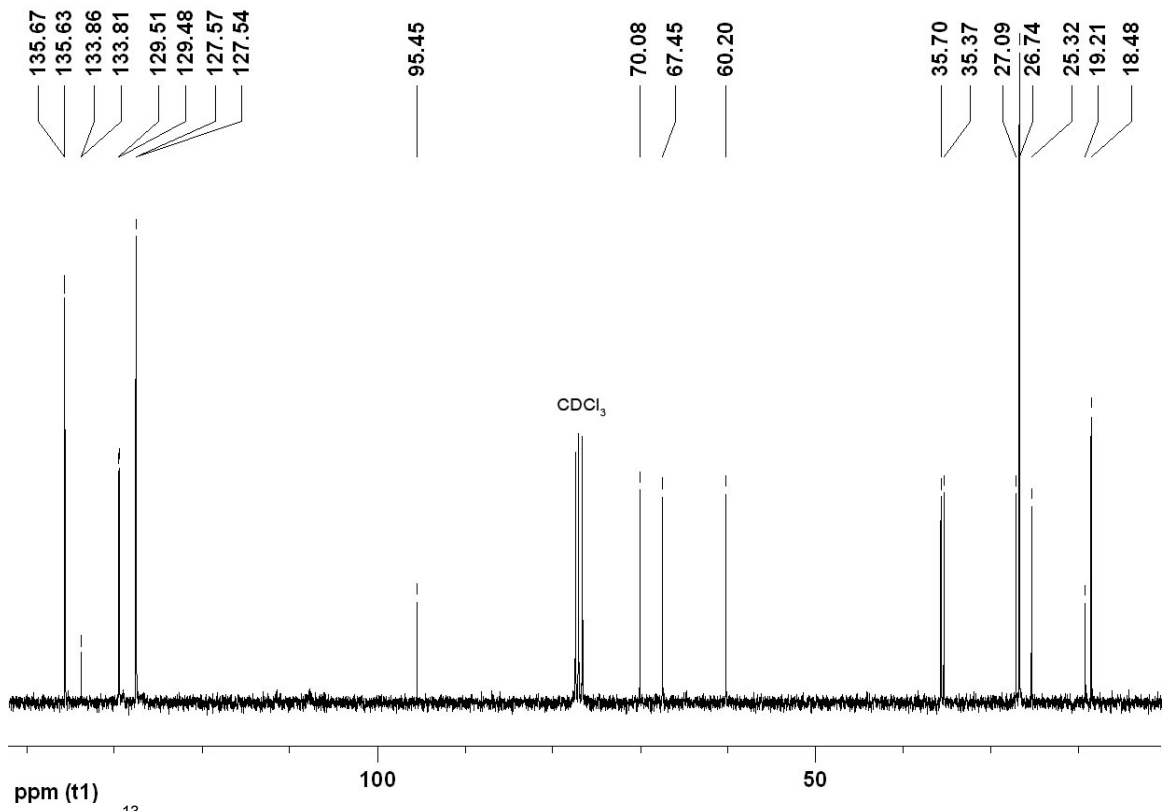

Figure 7.20: ^{13}C NMR spectrum (75 MHz; $CDCl_3$) of spiroacetal **883**.

10-(*tert*-Butyldiphenylsilyloxy)-1,9-dihydroxydec-3-yn-5-one (879)

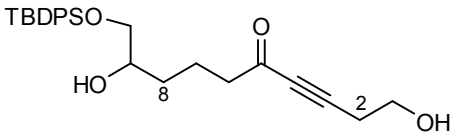

To a solution of 1-(trimethylsilyloxy)but-3-yne **(866)** (148 mg, 1.04 mmol) in anhydrous THF (4.0 mL) at -78 °C was added BuLi (975 μL, 1.6 mol L^{-1} in hexane, 1.56 mmol) dropwise. After 45 min, a solution of valerolactone **865** (383 mg, 1.04 mmol) in anhydrous THF (2.0 mL) was added dropwise. After 2 h, saturated NH_4Cl solution (2 mL) was added. The mixture was warmed to room temperature and the aqueous phase was extracted with EtOAc (3 x 4 mL). The combined organic extracts were dried over $MgSO_4$ and concentrated *in vacuo*. Purification by flash chromatography using hexane–EtOAc (9:1 to 1:1) as eluent yielded the *title compound* **879** (295 mg, 65%) as a pale yellow oil.

HRMS (FAB): found $[M – OH]^+$, 421.2203, $C_{26}H_{33}O_3Si$ requires 421.2199.

ν_{max} (film)/cm^{-1}: 3403br (O–H), 2930 (C–H), 2857 (C–H), 2214 (C≡C), 1719 (C=O), 1670, 1427, 1113 (C–O), 1076 (C–O), 703.

δ_H (400 MHz; $CDCl_3$): 1.06 (9 H, s, $OSiPh_2{}^tBu$), 1.33–1.48 (2 H, m, 8-H), 1.64–1.76 (1 H, m, 7-H_A), 1.81–1.93 (1 H, m, 7-H_B), 2.54 (2 H, t, $J_{6,7}$ 7.2, 6-H), 2.61 (2 H, t, $J_{2,1}$ 6.1, 2-H), 3.48 (1 H, dd, J_{AB} 10.3 and $J_{10_A,9}$ 7.7, 10-H_A), 3.64 (1 H, dd, J_{AB} 10.3 and $J_{10_B,9}$ 3.4, 10-H_B), 3.69–3.76 (1 H, m, 9-H), 3.78 (2 H, t, $J_{1,2}$ 6.1, 1-H), 7.37–7.46 (6 H, m, Ph), 7.62–7.67 (4 H, m, Ph).

δ_C (100 MHz; $CDCl_3$): 19.2 (C, $OSiPh_2{}^tBu$), 20.2 (CH_2, C-7), 23.4 (CH_2, C-2), 26.8 (CH_3, $OSiPh_2{}^tBu$), 31.8 (CH_2, C-8), 45.1 (CH_2, C-6), 60.1 (CH_2, C-1), 65.9 (CH_2, C-10), 71.6 (CH, C-9), 81.7 (C, C-4), 91.2 (C, C-3), 127.8 (CH, Ph), 129.9 (CH, Ph), 133.0 (C, Ph), 133.0 (C, Ph), 135.5 (CH, Ph), 188.1 (C, C-5).

***m/z* (FAB):** 439 (MH^+, 2%), 421 (M – OH, 45), 381 (M – ^{t}Bu, 15), 361 (M – Ph, 11), 239 ($SiPh_2{}^t$Bu, 7), 207 (40), 199 (M – $SiPh_2{}^t$Bu, 72), 197 (33), 167 (35), 147 (39), 139 (40), 137 (100), 136 (79), 135 (86).

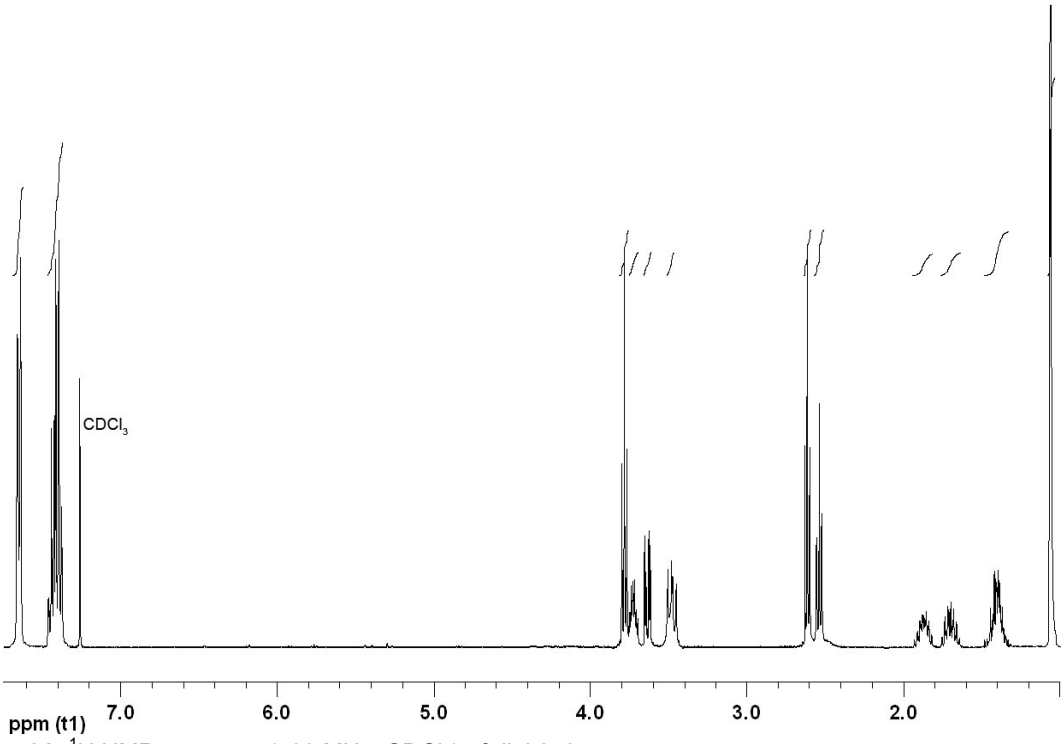

Figure 7.21: ^{1}H NMR spectrum (400 MHz; $CDCl_3$) of diol **879**.

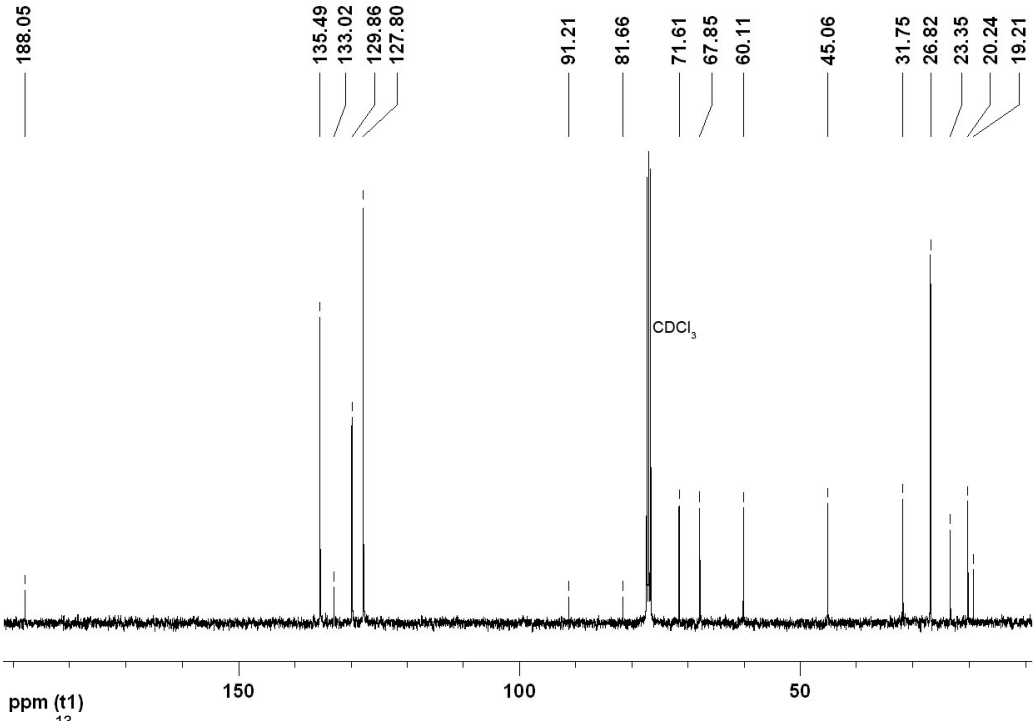

Figure 7.22: ^{13}C NMR spectrum (100 MHz; $CDCl_3$) of diol **879**.

7.3.3 Synthesis of Linear Spiroacetal Precursor 895

4-Bromobutan-1-ol (890)[23,24]

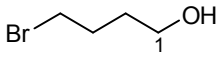

To THF (13.5 mL, 167 mmol) heated under reflux was added aqueous HBr (9.06 g, 48% w/w, 53.8 mmol) dropwise *via* a syringe pump over 2 h. The resulting mixture was heated under reflux for 2 h then cooled to room temperature. Solid $NaHCO_3$ was added in small portions until the aqueous phase was saturated. The aqueous phase was extracted with Et_2O (3 x 10 mL) and the combined organic extracts were dried over $MgSO_4$ and concentrated *in vacuo*. Purification by distillation under reduced pressure yielded the title bromoalcohol **890** (2.70 g, 33%) as a colourless liquid. The spectral data were in agreement with that reported in the literature.[24]

B.p.: 70–71 °C at 1.0 mmHg (lit. b.p.: 73–74 °C at 3.1 mmHg[23], 75–76 °C at 12 mmHg[24]).

ν_{max} (film)/cm^{-1}: 3303br (O–H), 2943 (C–H), 1438, 1244, 1057 (C–O), 1028, 916, 891.

δ_H (300 MHz; $CDCl_3$): 1.68–1.79 (2 H, m, 2-H), 1.91–2.01 (2 H, m, 3-H), 3.46 (2 H, t, $J_{4,3}$ 6.6, 4-H), 3.71 (2 H, t, $J_{1,2}$ 6.4, 1-H), 4.80 (1 H, s, OH).

δ_C (75 MHz; $CDCl_3$): 29.0 (CH_2, C-3), 30.7 (CH_2, C-2), 33.5 (CH_2, C-4), 61.7 (CH_2, C-1).

***m/z* (EI):** 153 ([M – H]$^+$, 2%), 151 ([M – H]$^+$, 3), 137 (M – OH, 23), 135 (M – OH, 24), 129 (55), 99 (16), 55 (100), 42 (29).

2-(3′-Bromopropyl)-1,3-dioxolane (869)[23,25]

To a solution of PCC (21.2 g, 98.2 mmol) in anhydrous CH_2Cl_2 (80 mL) at room temperature was added a solution of 4-bromobutan-1-ol **(890)** (10.0 g, 65.4 mmol) in anhydrous CH_2Cl_2 (40 mL). After 45 min, Et_2O (40 mL) was added and the mixture was filtered through a short column of silica. The dark slurry was extracted repeatedly with Et_2O (40 mL each) and filtered through a short column of silica until no more aldehyde was eluted from the filtration column. The combined extracts were concentrated *in vacuo* to yield the crude aldehyde as a yellow oil which was used in the following step without further purification.

To a solution of crude aldehyde in CH_2Cl_2 (240 mL) was added ethylene glycol (4.38 mL, 78.5 mmol) and *p*-toluenesulfonic acid monohydrate (1.87 g, 9.81 mmol). The reaction was heated to reflux under a reverse Dean-Stark apparatus. After 24 h, the organic phase was washed with saturated $NaHCO_3$ solution (2 x 160 mL) and brine (160 mL). The resulted mixture was dried over $MgSO_4$ and concentrated *in vacuo*. Purification by distillation under reduced pressure yielded the title bromide **869** (9.82 g, 77%) as a colourless liquid which was stored over molecular sieves. The spectral data were in agreement with that reported in the literature.[25]

B.p.: 60–62 °C at 0.70 mmHg (lit. b.p.[25]: 45–51 °C at 0.025 mmHg).

HRMS (CI): found MH^+, 196.9990, $C_6H_{12}{}^{81}BrO_2$ requires 197.0000; found MH^+, 195.0015, $C_6H_{12}{}^{79}BrO_2$ requires 195.0021.

ν_{max} (film)/cm^{-1}: 2957 (C–H), 1439, 1409, 1251 (C–O), 1039 (C–O), 943, 885.

δ_H (300 MHz; $CDCl_3$): 1.77–1.86 (2 H, m, 1′-H), 1.95–2.06 (2 H, m, 2′-H), 3.46 (2 H, t, $J_{3',2'}$ 6.8, 3′-H), 3.82–3.91 (2 H, m, 4-H), 3.91–3.99 (2 H, m, 5-H), 4.90 (1 H, t, $J_{2,1'}$ 4.5, 2-H).

δ_C (75 MHz; $CDCl_3$): 27.1 (CH_2, C-2′), 32.2 (CH_2, C-1′), 33.4 (CH_2, C-3′), 64.9 (CH_2, C-4 and C-5), 103.6 (CH, C-2).

***m/z* (CI):** 197 (MH^+, 7%), 195 (MH^+, 9), 149 (18), 137 (83), 135 (86), 87 (35), 73 (100), 71 (33).

6-(*tert*-Butyldiphenylsilyloxy)-5-hydroxy-*N*-methoxy-*N*-methylhexanamide (893)

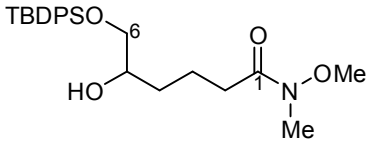

This procedure is an adaptation of that reported by Weinreb *et al.*[26] and Hodgett *et al.*[27]

To a suspension of *N,O*-dimethylhydroxylamine (2.20 g, 22.5 mmol) in anhydrous CH_2Cl_2 (80 mL) at 0 °C was added dropwise a solution of $AlMe_3$ (11.3 mL, 2.0 mol L^{-1} in toluene, 22.5 mmol). The mixture was stirred until the solid dissolved. A solution of valerolactone **865** (3.97 g, 10.8 mmol) in anhydrous CH_2Cl_2 (40 mL) was added and the mixture was warmed to room temperature. After 3 h, the reaction was carefully poured into an ice-cold 1:1 solution mixture of saturated NH_4Cl and Rochelle's salt (80 mL). The resulting mixture was stirred vigorously for 30 min with warming to room temperature. The aqueous phase was extracted with Et_2O (3 x 60 mL). The combined organic extracts were dried over $MgSO_4$ and concentrated *in vacuo* to yield the crude *title compound* **893** as a yellow oil (4.85 g, 100%) that was used in the hydroxyl protection step without further purification. Purification by flash chromatography was performed using hexane–EtOAc (7:3 to 3:2) as eluent to yield the *title compound* **893** as a colourless oil.

HRMS (CI): found MH^+, 430.2415, $C_{24}H_{36}NO_4Si$ requires 430.2414.

ν_{max} (film)/cm^{-1}: 3430br (O–H), 2931 (C–H), 1651 (C=O), 1427, 1112 (C–O), 703.

δ_H (300 MHz; $CDCl_3$): 1.07 (9 H, s, $OSiPh_2{}^tBu$), 1.47 (2 H, dt, $J_{4,5}$ 7.7 and $J_{4,3}$ 6.5, 4-H), 1.62–1.83 (2 H, m, 3-H), 2.43 (2 H, t, $J_{2,3}$ 7.4, 2-H), 2.64 (1 H, br s, OH), 3.16 (3 H, s, NMe), 3.51 (1 H, dd, J_{AB} 10.0 and $J_{6A,5}$ 7.4, 6-H_A), 3.66 (1 H, dd, J_{AB} 10.0 and $J_{6B,5}$ 3.6, 6-H_B), 3.66 (3 H, s, OMe), 3.71–3.77 (1 H, m, 5-H), 7.35–7.47 (6 H, m, Ph), 7.63–7.68 (4 H, m, Ph).

δ_C (75 MHz; $CDCl_3$): 19.2 (C, $OSiPh_2{}^tBu$), 20.5 (CH_2, C-3), 26.8 (CH_3, $OSiPh_2{}^tBu$), 31.6 (CH_2, C-2), 32.2 (CH_3, NMe), 32.4 (CH_2, C-4), 61.1 (CH_3, OMe), 68.0 (CH_2, C-6), 71.6 (CH, C-5), 127.7 (CH, Ph), 129.8 (CH, Ph), 133.2 (C, Ph), 135.5 (CH, Ph), 174.3 (C, C=O).

***m/z* (CI):** 430 (MH^+, 38%), 412 (M – OH, 3), 372 (M – ^{t}Bu, 22), 353 (26), 352 (M – Ph, 100), 322 (52), 291 (31), 264 (17), 199 (29), 78 (24).

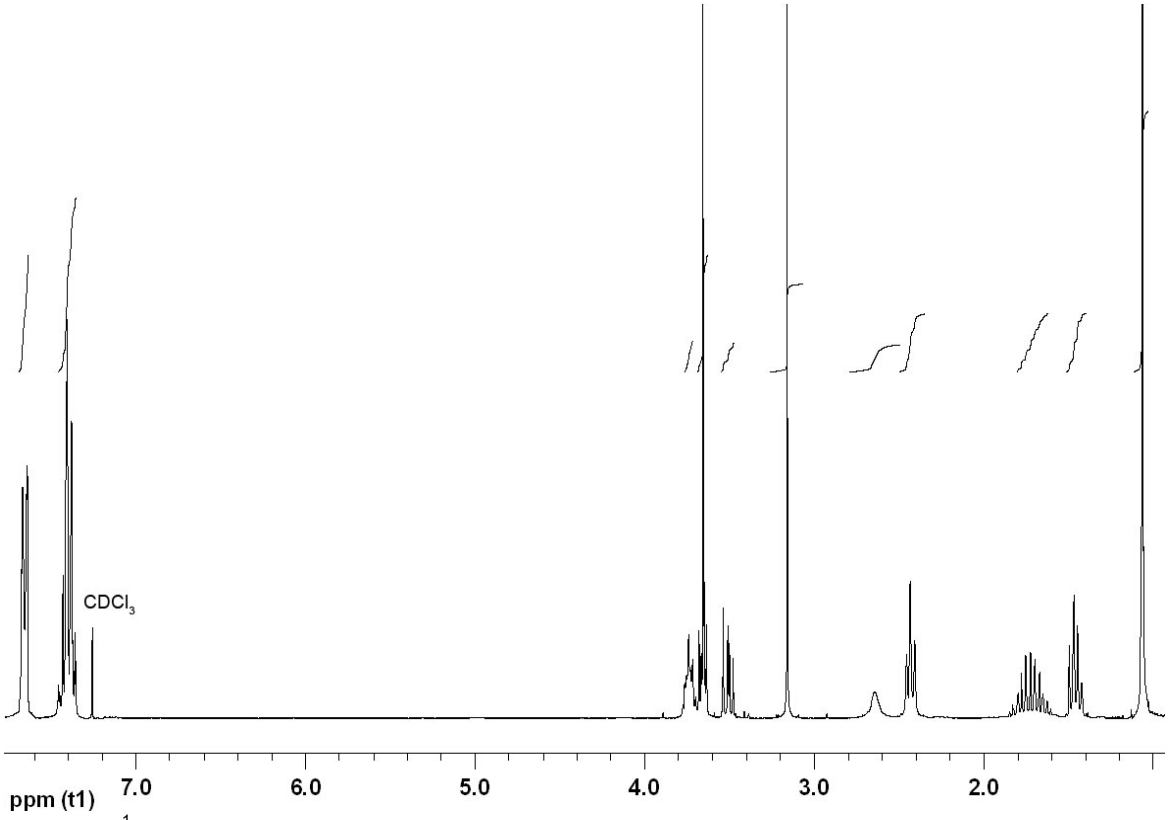

Figure 7.23: ^{1}H NMR spectrum (300 MHz; $CDCl_3$) of Weinreb amide **893**.

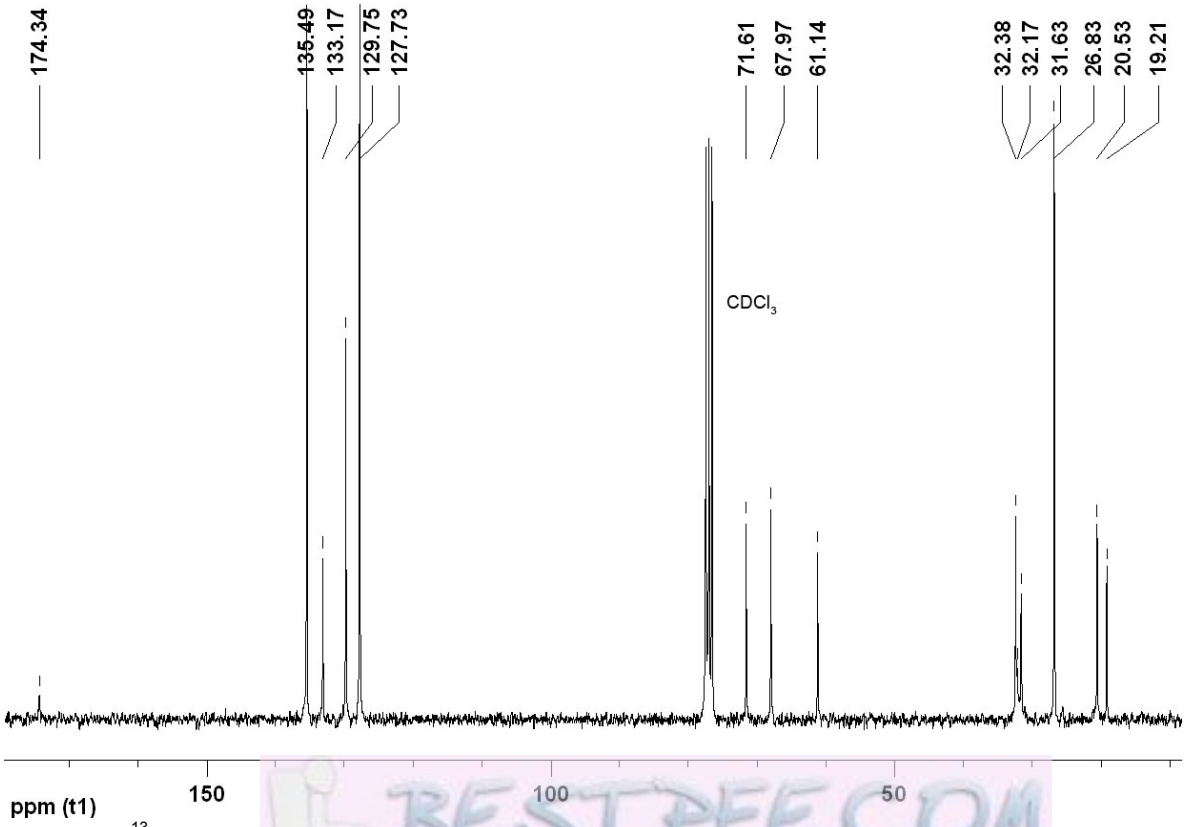

Figure 7.24: ^{13}C NMR spectrum (75 MHz; $CDCl_3$) of Weinreb amide **893**.

5-(*tert*-Butyldimethylsilyloxy)-6-(*tert*-butyldiphenylsilyloxy)-*N*-methoxy-*N*-methylhexanamide (892)

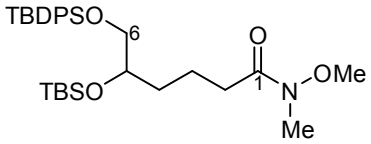

To a solution of crude alcohol **893** (*ca.* 4.85 g, 10.8 mmol) in anhydrous CH_2Cl_2 (50 mL) at room temperature was added imidazole (1.69 g, 24.9 mmol), DMAP (276 mg, 2.26 mmol) and TBSCl (1.87 g, 12.4 mmol). After 24 h, a second portion of TBSCl (170 mg, 1.13 mmol) was added and the mixture was concentrated *in vacuo* to half of its volume. After 2 h, saturated $NaHCO_3$ solution (25 mL) was added. The aqueous phase was extracted with Et_2O (3 x 25 mL) and the combined organic extracts were dried over $MgSO_4$ and concentrated *in vacuo*. Purification by flash chromatography (twice) using hexane–EtOAc (19:1 to 3:2) as eluent yielded the *title compound* **892** (4.80 g, 82% from valerolactone **865** over 2 steps) as a colourless oil and valerolactone **865** (0.56 g, 14%).

HRMS (FAB): found MH^+, 544.3273, $C_{30}H_{50}NO_4Si_2$ requires 544.3278.

ν_{max} (film)/cm^{-1}: 2930 (C–H), 1667 (C=O), 1428, 1254 (C–O), 1112 (C–O), 702.

δ_H (400 MHz; $CDCl_3$): -0.08 (3 H, s, OSi*Me*$_2$^{t}Bu), 0.00 (3 H, s, OSi*Me*$_2$^{t}Bu), 0.83 (9 H, s, OSiMe$_2$^{t}*Bu*), 1.04 (9 H, s, OSiPh$_2$^{t}*Bu*), 1.45–1.55 (1 H, m, 4-H$_A$), 1.58–1.77 (3 H, m, 3-H and 4-H$_B$), 2.43 (2 H, m, 2-H), 3.17 (3 H, s, NMe), 3.47 (1 H, dd, J_{AB} 10.0 and $J_{6A,5}$ 6.7, 6-H$_A$), 3.57 (1 H, dd, J_{AB} 10.0 and $J_{6B,5}$ 5.1, 6-H$_B$), 3.66 (3 H, s, OMe), 3.68–3.79 (1 H, m, 5-H), 7.34–7.42 (6 H, m, Ph), 7.64–7.68 (4 H, m, Ph).

δ_C (100 MHz; $CDCl_3$): -4.83 (CH_3, OSi*Me*$_2$^{t}Bu), -4.48 (CH_3, OSi*Me*$_2$^{t}Bu), 18.0 (C, OSiMe$_2$^{t}*Bu*), 19.2 (C, OSiPh$_2$^{t}*Bu*), 20.3 (CH_2, C-3), 25.8 (CH_3, OSiMe$_2$^{t}*Bu*), 26.8 (CH_3, OSiPh$_2$^{t}*Bu*), 32.3 (CH_3 and CH_2, NMe and C-2), 34.1 (CH_2, C-4), 61.1 (CH_3, OMe), 67.5 (CH_2, C-6), 72.6 (CH, C-5), 127.6 (CH, Ph), 129.6 (CH, Ph), 133.6 (C, Ph), 133.6 (C, Ph), 135.6 (CH, Ph), 174.6 (C, C=O).

***m/z* (FAB):** 544 (MH^+, 20%), 528 (M – Me, 5), 486 (M – ^{t}Bu, 72), 412 (M – OTBDMS, 39), 217 (25), 209 (50), 197 (45), 193 (30), 147 (23), 135 (100), 73 (98).

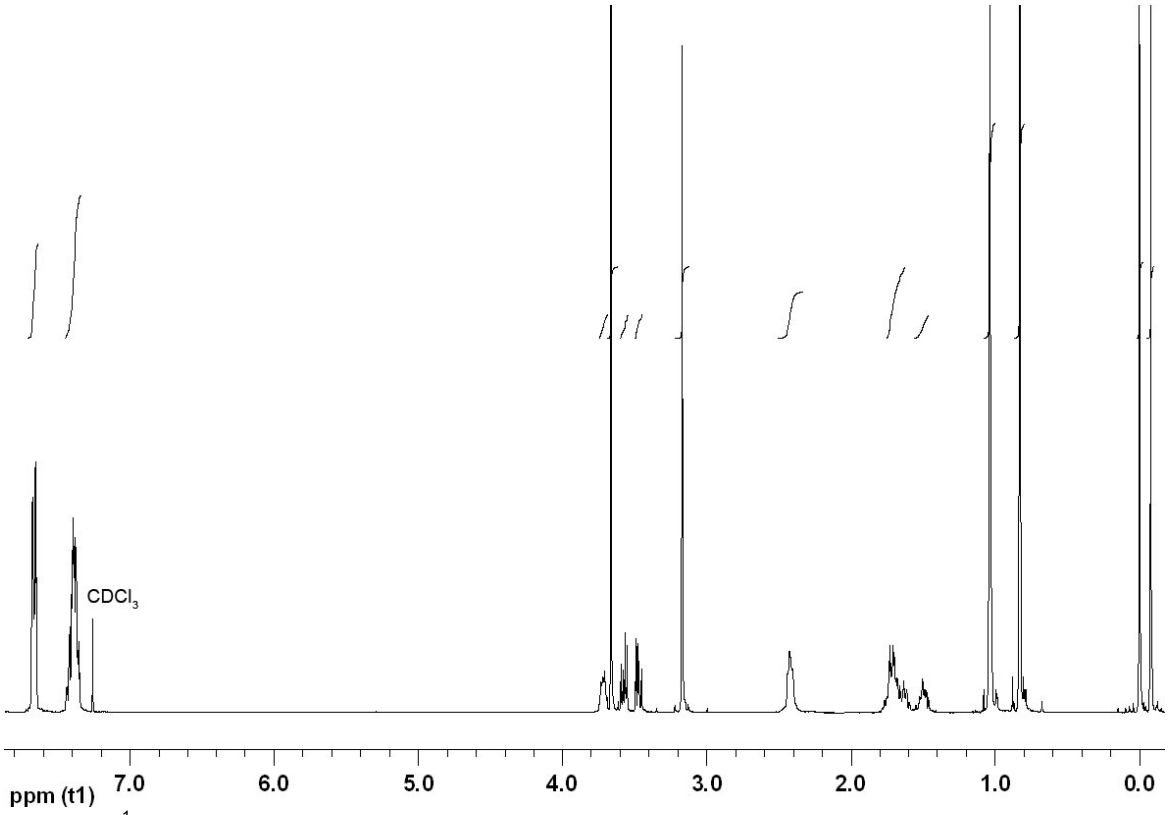

Figure 7.25: ^{1}H NMR spectrum (400 MHz; $CDCl_3$) of Weinreb amide **892**.

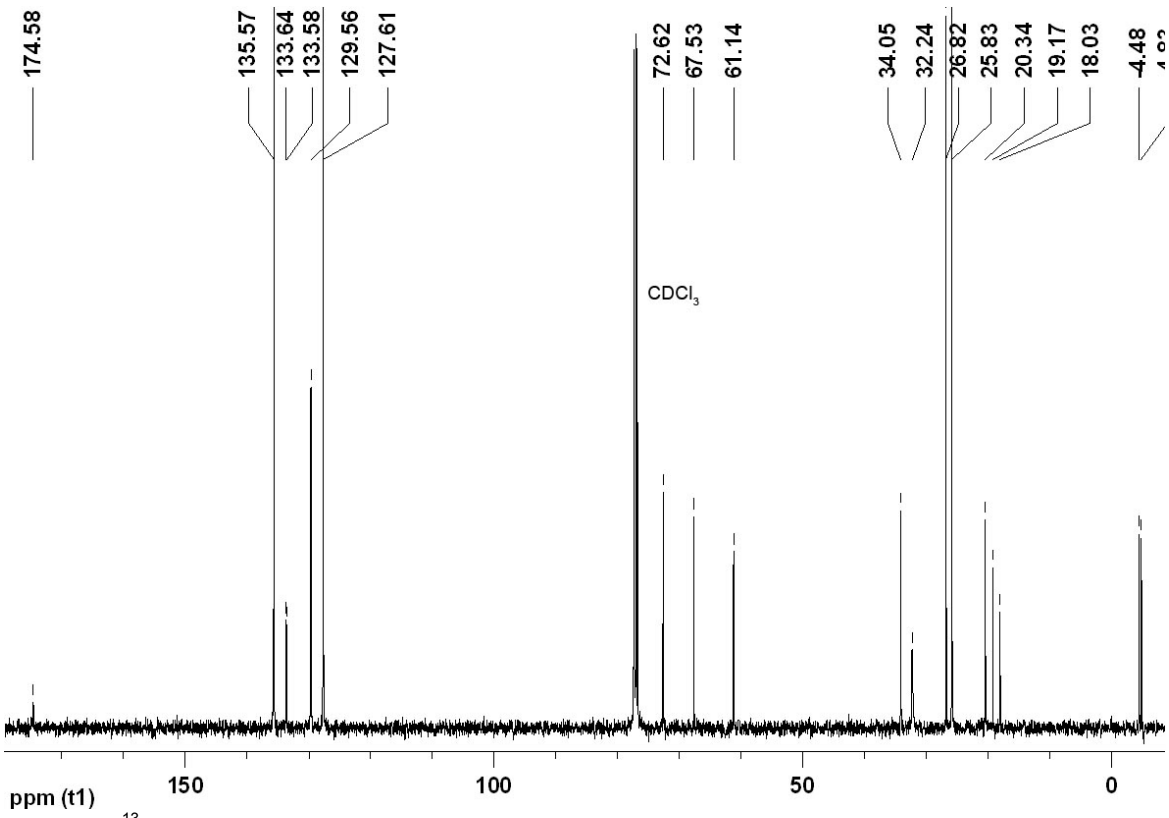

Figure 7.26: ^{13}C NMR spectrum (100 MHz; $CDCl_3$) of Weinreb amide **892**.

8′-(*tert*-Butyldimethylsilyloxy)-9′-(*tert*-butyldiphenylsilyloxy)-1′-(1,3-dioxolan-2-yl)nonan-4′-one (895)

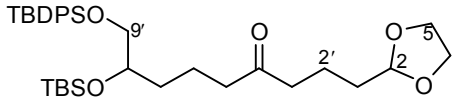

To a mixture of Mg turnings[§] (1.07 g, 44.0 mmol) in THF (5.0 mL) at room temperature under an atmosphere of argon was added I_2 (1 crystal) and 1,2-dibromoethane (228 μL, 2.64 mmol). The mixture was stirred until the yellow colour faded. Weinreb amide **892** (4.79 g, 8.80 mmol) in THF (31 mL) was added to the above activated magnesium *via* cannula followed by addition of bromide **867** (2.87 mL, 17.6 mmol) dropwise. The reaction was initiated with the addition of I_2 (1 crystal) and the internal reaction temperature was regulated carefully below 33 °C. After 1 h, a second portion of bromide **867** (1.44 mL, 8.80 mmol) was added dropwise. After 1 h, saturated $NaHCO_3$ solution (30 mL) was added and the aqueous phase was extracted with Et_2O (3 x 50 mL). The combined organic extracts were dried over $MgSO_4$ and concentrated *in vacuo*. Purification by flash chromatography using hexane-EtOAc (19:1 to 9:1) as eluent yielded the *title compound* **895** (4.23 g, 80%) as a pale yellow oil.

HRMS (CI): found MH^+, 599.3562, $C_{34}H_{55}O_5Si_2$ requires 599.3588.

ν_{max} (film)/cm^{-1}: 2930 (C–H), 1714 (C=O), 1428, 1254 (C–O), 1112 (C–O), 836, 703.

δ_H (300 MHz; $CDCl_3$): -0.08 (3 H, s, OSi*Me*$_2$^{t}Bu), -0.01 (3 H, s, OSi*Me*$_2$^{t}Bu), 0.83 (9 H, s, OSiMe$_2$^{t}*Bu*), 1.04 (9 H, s, OSiPh$_2$^{t}*Bu*), 1.40–1.46 (1 H, m, 7′-H_A), 1.60–1.78 (7 H, m, 1′-H_A, 1′-H_B, 2′-H_A, 2′-H_B, 6′-H_A, 6′-H_B and 7′-H_B), 2.38 (2 H, t, $J_{5',6'}$ 6.9, 5′-H), 2.45 (2 H, t, $J_{3',2'}$ 7.1, 3′-H), 3.45 (1 H, dd, J_{AB} 10.0 and $J_{9'A,8'}$ 6.8, 9′-H_A), 3.57 (1 H, dd, J_{AB} 10.0 and $J_{9'B,8'}$ 5.0, 9′-H_B), 3.64–3.74 (1 H, m, 8′-H), 3.81–3.89 (2 H, m, 4-H), 3.89–3.98 (2 H, m, 5-H), 4.85 (1 H, t, $J_{2,1'}$ 4.4, 2-H), 7.34–7.44 (6 H, m, Ph), 7.64–7.68 (4 H, m, Ph).

δ_C (75 MHz; $CDCl_3$): -4.81 (CH_3, OSi*Me*$_2$^{t}Bu), -4.46 (CH_3, OSi*Me*$_2$^{t}Bu), 18.0 (C, OSiMe$_2$^{t}*Bu*), 18.2 (CH_2, C-2′), 19.2 (C, OSiPh$_2$^{t}*Bu*), 19.5 (CH_2, C-6′), 25.8 (CH_3, OSiMe$_2$^{t}*Bu*), 26.9 (CH_3, OSiPh$_2$^{t}*Bu*), 33.1 (CH_2, C-1′), 33.9 (CH_2, C-7′), 42.2 (CH_2, C-3′), 43.1 (CH_2, C-5′), 64.8 (2 x CH_2, C-4 and C-5), 67.5 (CH_2, C-9′), 72.6 (CH, C-8′), 104.3 (CH, C-2), 127.6 (CH, Ph), 129.6 (CH, Ph), 133.7 (C, Ph), 135.6 (CH, Ph), 210.5 (C, C=O).

***m/z* (CI):** 599 (MH^+, 17%), 541 (26), 412 (M – OSiMe$_2$^{t}Bu, 100), 343 (M – OSiPh$_2$^{t}Bu, 11), 211 (27), 197 (16), 149 (20), 135 (24), 121 (36), 99 (40), 91 (20), 78 (37), 73 (94).

[§] The Mg turnings were pre-washed with aqueous HCl (0.10 mol L^{-1}) and water then flame-dried *in vacuo*.

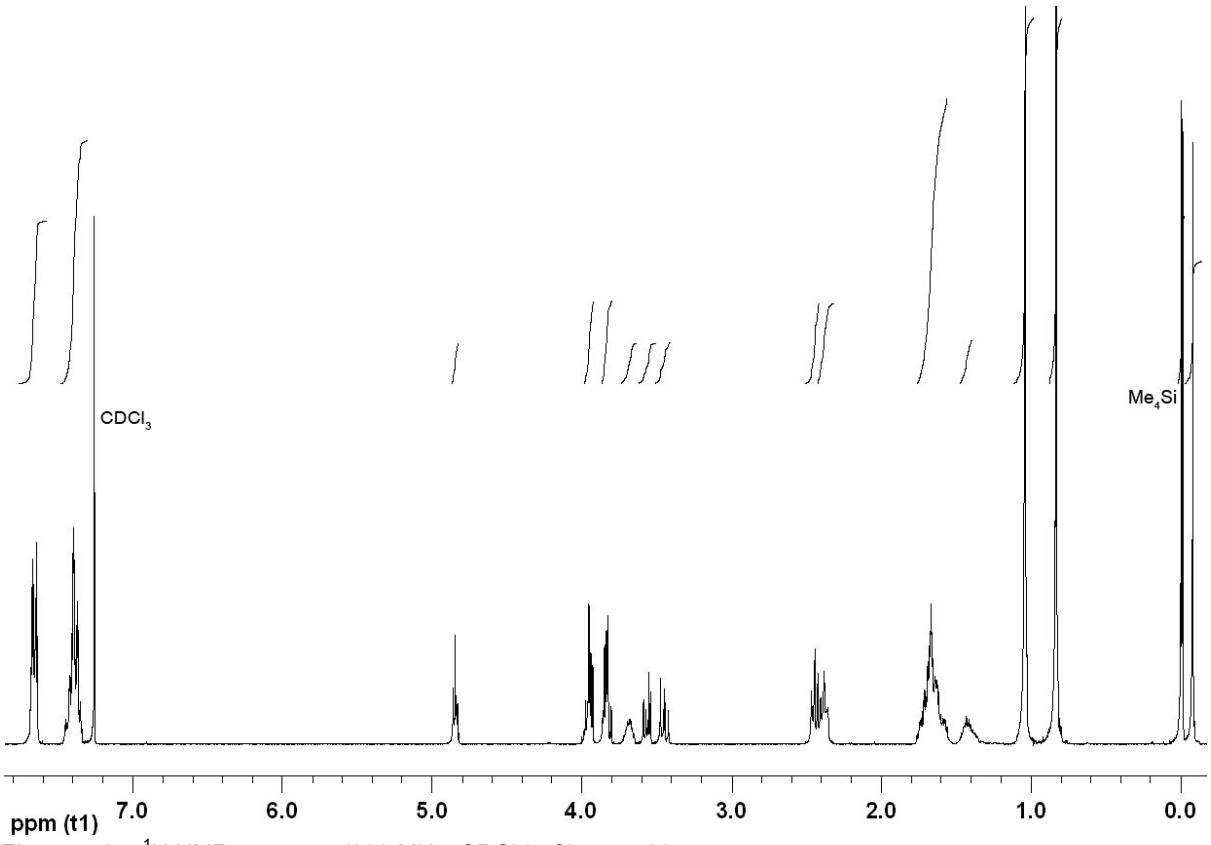

Figure 7.27: ^{1}H NMR spectrum (300 MHz; $CDCl_3$) of ketone **895**.

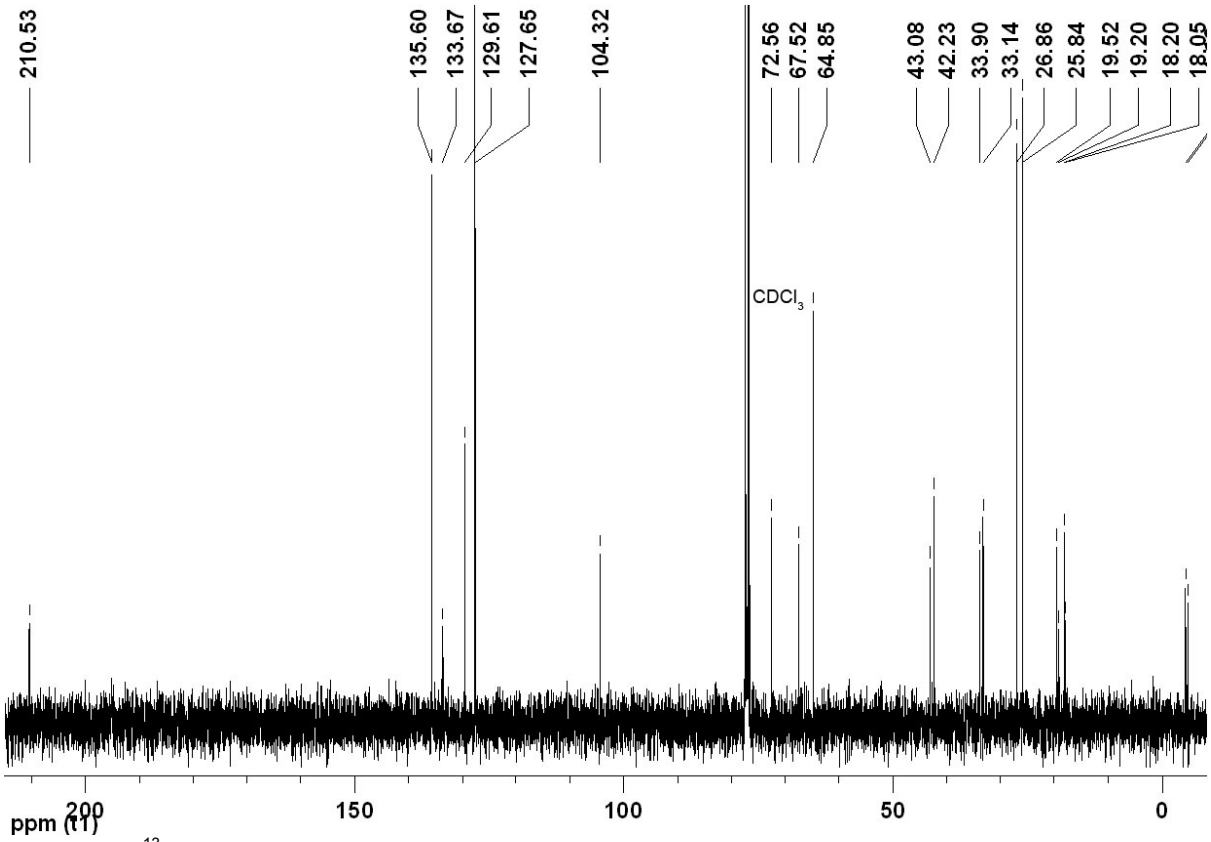

Figure 7.28: ^{13}C NMR spectrum (75 MHz; $CDCl_3$) of ketone **895**.

7.3.4 Synthesis of Spiroacetals 860–862

(2*S,6*S**,8*S**)-8-(*tert*-Butyldiphenylsilyloxymethyl)-2-ethoxy-1,7-dioxaspiro[5.5]undecane (862)**

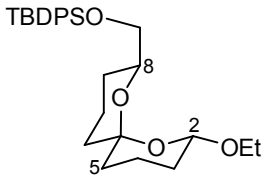

To a solution of ketone **895** (750 mg, 1.25 mmol) in a 99:1 mixture of EtOH–H_2O (15 mL) at room temperature was added (+)-10-camphorsulfonic acid monohydrate (628 mg, 2.51 mmol) in small portions. After 3 h, solid $NaHCO_3$ (220 mg, 2.63 mmol) was added and the mixture was concentrated *in vacuo*. The resulting thick yellow oil was dissolved in saturated $NaHCO_3$ solution (10 mL) and Et_2O (10 mL) and the aqueous phase was extracted with Et_2O (3 x 10 mL). The combined organic extracts were dried over $MgSO_4$ and concentrated *in vacuo*. Purification by flash chromatography using hexane–EtOAc (99:1, 97:3 to 9:1) as eluent yielded the *title compound* **862** (356 mg, 61%) as a pale yellow oil and a mixture of starting materials (264 mg). The recovered starting materials were subjected to the above reaction cycle several times to yield the *title compound* **862** (503 mg, 86% overall yield after 3 cycles) after purification.

HRMS (FAB): found MH^+, 467.2618, $C_{28}H_{39}O_4Si$ requires 467.2618.

ν_{max} (film)/cm^{-1}: 2934 (C–H), 1428, 1221, 1187, 1112 (C–O), 1083 (C–O), 973, 955, 702.

δ_H (300 MHz; $CDCl_3$): 1.05 (9 H, s, $OSiPh_2{}^tBu$), 1.17–1.22 (1 H, m, 9-H_A), 1.26 (3 H, t, J_{CH_3,CH_2} 7.1, OCH_2CH_3), 1.33–1.50 (3 H, m, 3-H_A, 5-H_A and 11-H_A), 1.56–1.66 (4 H, m, 4-H_A, 5-H_B or 11-H_B, 9-H_B and 10-H_A), 1.71–1.81 (2 H, m, 3-H_B and 5-H_B or 11-H_B), 1.87–2.06 (2 H, m, 4-H_B and 10-H_B), 3.53 (1 H, dq, J_{AB} 9.4 and J_{CH_2,CH_3} 7.1, $OCH_AH_BCH_3$), 3.59 (1 H, dd, J_{AB} 10.4 and $J_{8\text{-}CH_2,8}$ 4.2, 8-CH_AH_BO), 3.68 (1 H, dd, J_{AB} 10.4 and $J_{8\text{-}CH_2,8}$ 6.5, 8-CH_AH_BO), 3.86–3.95 (1 H, m, 8-H), 4.00 (1 H, dq, J_{AB} 9.4 and J_{CH_2,CH_3} 7.1, $OCH_AH_BCH_3$), 4.83 (1 H, dd, $J_{2_{ax},3_{ax}}$ 10.0 and $J_{2_{ax},3_{eq}}$ 2.3, 2-H_{ax}), 7.33–7.46 (6 H, m, Ph), 7.69–7.76 (4 H, m, Ph).

δ_C (75 MHz; $CDCl_3$): 15.3 (CH_3, OCH_2CH_3), 17.8 (CH_2, C-4 or C-10), 18.5 (CH_2, C-4 or C-10), 19.2 (C, $OSiPh_2{}^tBu$), 26.7 (CH_3, $OSiPh_2{}^tBu$), 27.0 (CH_2, C-9), 30.9 (CH_2, C-3), 34.8 (CH_2, C-5 or C-11), 35.2 (CH_2, C-5 or C-11), 64.3 (CH_2, OCH_2CH_3), 67.5 (CH_2, 8-CH_2O), 70.9 (CH, C-8), 96.6 (CH, C-2), 98.1 (C, C-6), 127.6 (CH, Ph), 127.6 (CH, Ph), 129.5 (CH, Ph), 129.6 (CH, Ph), 133.8 (C, Ph), 133.8 (C, Ph), 135.6 (CH, Ph), 135.7 (CH, Ph).

***m/z* (FAB):** 467 (MH^+, 3%), 423 (M – OEt, 27), 411 (M – ^{t}Bu, 10), 391 (M – Ph, 11), 365 (25), 207 (33), 199 (65), 197 (47), 167 (22), 149 (37), 137 (35), 135 (98), 85 (100), 75 (22).

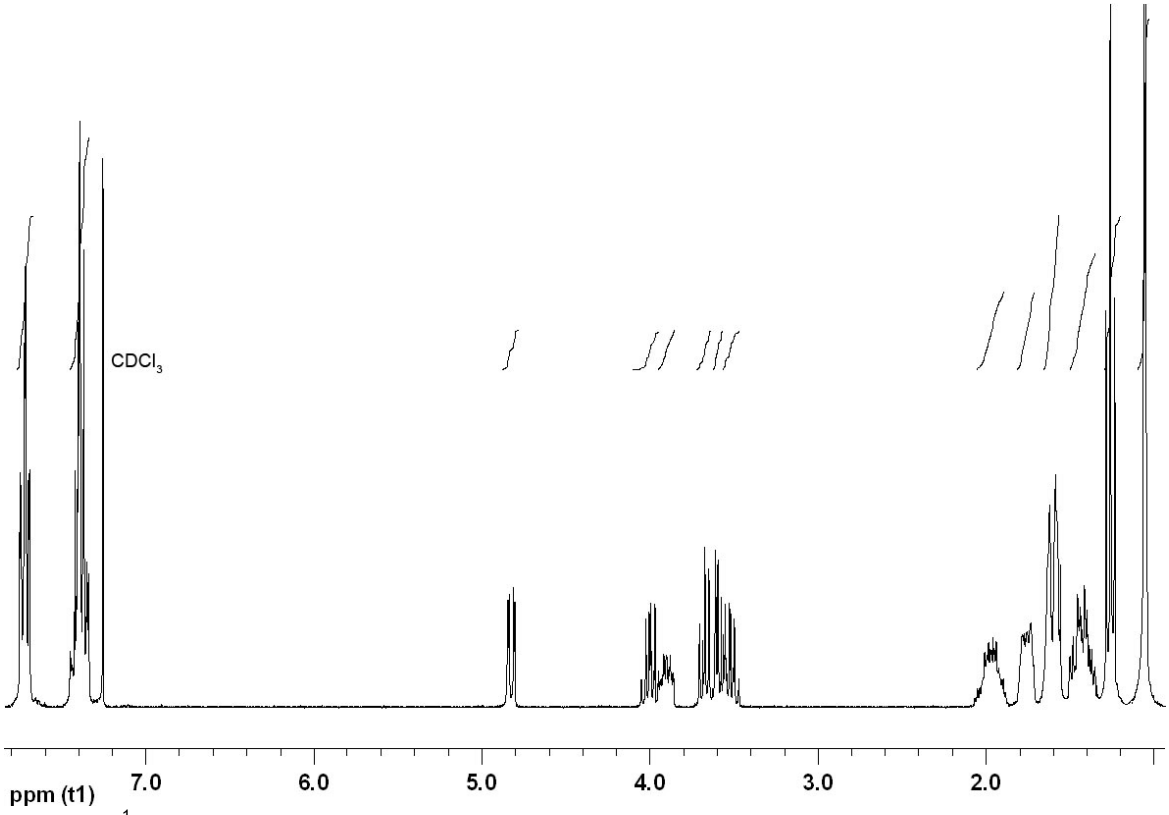

Figure 7.29: ^{1}H NMR spectrum (300 MHz; $CDCl_3$) of acetal **862**.

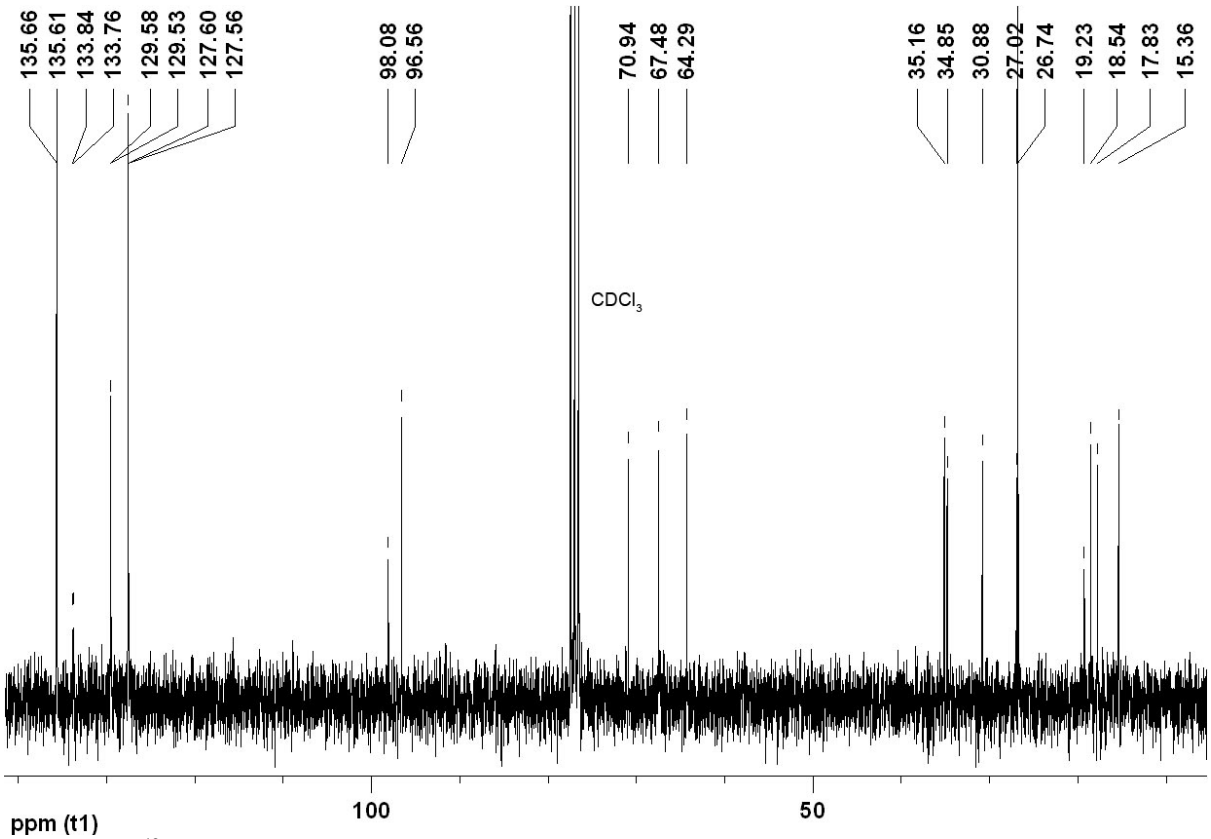

Figure 7.30: ^{13}C NMR spectrum (75 MHz; $CDCl_3$) of acetal **862**.

(2*R,6*S**,8*S**)-8-(*tert*-Butyldiphenylsilyloxymethyl)-2-acetoxy-1,7-dioxaspiro[5.5]undecane (861)**

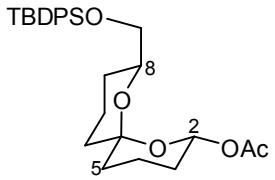

Method A: Using Ketone **895** as the Starting Material

A solution of ketone **895** (100 mg, 167 μmol) and PPTS (8.39 mg, 33.4 μmol) in a 2:1 mixture of acetone–water (3.0 mL) was heated to reflux. After 24 h, saturated $NaHCO_3$ solution (3 mL) and toluene (3 mL) were added and the aqueous phase was extracted with Et_2O (3 x 3 mL). The combined organic extracts were dried over $MgSO_4$ and concentrated *in vacuo* to yield the crude lactol as a pale yellow oil. This unstable lactol was used directly in the acetylation described below without further purification.

To a solution of crude lactol in anhydrous CH_2Cl_2 (1.5 mL) at room temperature was added DMAP (4.08 mg, 33.4 μmol), NEt_3 (23.3 μL, 167 μmol) and Ac_2O (13.3 μL, 134 μmmol). After 2 h, brine (2 mL) was added and the aqueous phase was extracted with CH_2Cl_2 (3 x 3 mL). The combined organic extracts were dried over $MgSO_4$ and concentrated *in vacuo*. Purification by flash chromatography using hexane–Et_2O–EtOAc (99:1:0, 99:0:1 to 97:0:3) yielded the *title compound* **861** (27.5 mg, 34% over 2 steps) as a white powder. Recrystallisation of acetate **861** from hexane–CH_2Cl_2 afforded white prisms.

Method B: Using Ethoxy-Spiroacetal **862** as the Starting Material

To a solution of ethoxy-spiroacetal **862** (485 mg, 1.04 mmol) in a 4:1 mixture of THF–water (18 mL) was added (+)-10-camphorsulfonic acid monohydrate (104 mg, 414 μmol) and the mixture was stirred at 40 °C overnight. Saturated $NaHCO_3$ solution (20 mL) and Et_2O (20 mL) were added and the aqueous phase was extracted with Et_2O (3 x 30 mL). The combined organic extracts were dried over $MgSO_4$ and concentrated *in vacuo* to yield the lactol as a pale yellow oil. The unstable lactol was used directly in the acetylation described below without further purification.

To a solution of crude lactol in anhydrous CH_2Cl_2 (9.0 mL) at room temperature was added DMAP (25.3 mg, 207 μmol), NEt_3 (216 μL, 1.55 mmol) and Ac_2O (117 μL, 1.24 mmol). After 3 h, the mixture was filtered through a pad of silica and the eluent was concentrated *in vacuo*. Purification by flash chromatography using hexane–Et_2O–EtOAc (99:1:0, 99:0:1 to 97:0:3) yielded the *title compound* **861** (298 mg, 58% over 2 steps) as a white powder. Recrystallisation of acetate **861** from hexane–CH_2Cl_2 afforded white prisms.

Melting Point: 106.9–108.5 °C

HRMS (FAB): $[M – H]^+$, 481.2407, $C_{28}H_{37}O_5Si$ requires 481.2410.

ν_{max} (film)/cm^{-1}: 2932 (C–H), 1754(C=O), 1428, 1367, 1226, 1199, 1113 (C–O), 1078 (C–O), 973, 702.

δ_H (400 MHz; $CDCl_3$): 1.05 (9 H, s, $OSiPh_2{}^tBu$), 1.31–1.40 (1 H, m, 9-H_A), 1.40–1.54 (3 H, m, 3-H_A, 5-H_A and 11-H_A), 1.59–1.72 (4 H, m, 4-H_A, 5-H_B, 9-H_B and 10-H_A), 1.72–1.82 (2 H, m, 3-H_B and 11-H_B), 1.87–1.96 (1 H, m, 10-H_B), 1.96–2.07 (1 H, m, 4-H_B), 2.11 (3 H, s, $COCH_3$), 3.64 (1 H, dd, J_{AB} 10.4 and $J_{2\text{-}CH_2,2}$ 4.2, 8-CH_AH_BO), 3.69 (1 H, dd, J_{AB} 10.4 and $J_{2\text{-}CH_2,2}$ 5.8, 8-CH_AH_BO), 4.16–4.23 (1 H, m, 8-H), 6.00 (1 H, dd, $J_{2ax,3ax}$ 10.1 and $J_{2ax,3eq}$ 2.6, 2-H_{ax}), 7.36–7.44 (6 H, m, Ph), 7.72–7.77 (4 H, m, Ph).

δ_C (100 MHz; $CDCl_3$): 17.4 (CH_2, C-4), 18.2 (CH_2, C-10), 19.2 (C, $OSiPh_2{}^tBu$), 21.3 (CH_3, $COCH_3$), 26.6 (CH_2, C-9), 26.7 (CH_3, $OSiPh_2{}^tBu$), 29.5 (CH_2, C-3), 34.6 (CH_2, C-5), 34.9 (CH_2, C-11), 67.2 (CH_2, 8-CH_2O), 70.7 (CH, C-8), 90.2 (CH, C-2), 99.1 (C, C-6), 127.5 (CH, Ph), 129.4 (CH, Ph), 129.4 (CH, Ph), 133.9 (C, Ph), 135.7 (CH, Ph), 135.7 (CH, Ph), 169.3 (C=O, $COCH_3$).

***m/z* (FAB):** 481 ([M – H]$^+$, 1%), 423 (M – OAc, 66), 405 (M – Ph, 4), 365 (59), 241 (33), 207 (55), 199 (55), 197 (36), 167 (32), 149 (29), 137 (76), 135 (100), 121 (41).

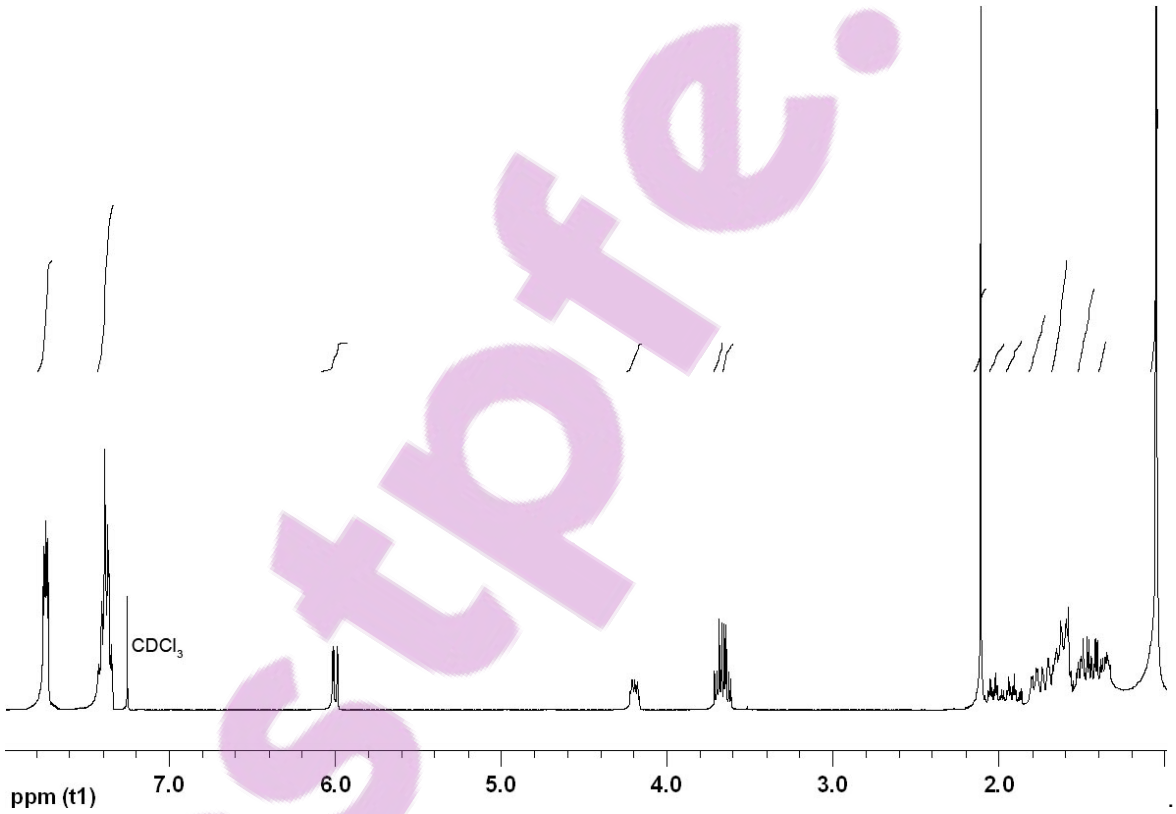

Figure 7.31: ^{1}H NMR spectrum (400 MHz; $CDCl_3$) of spiroacetal-acetate **861**.

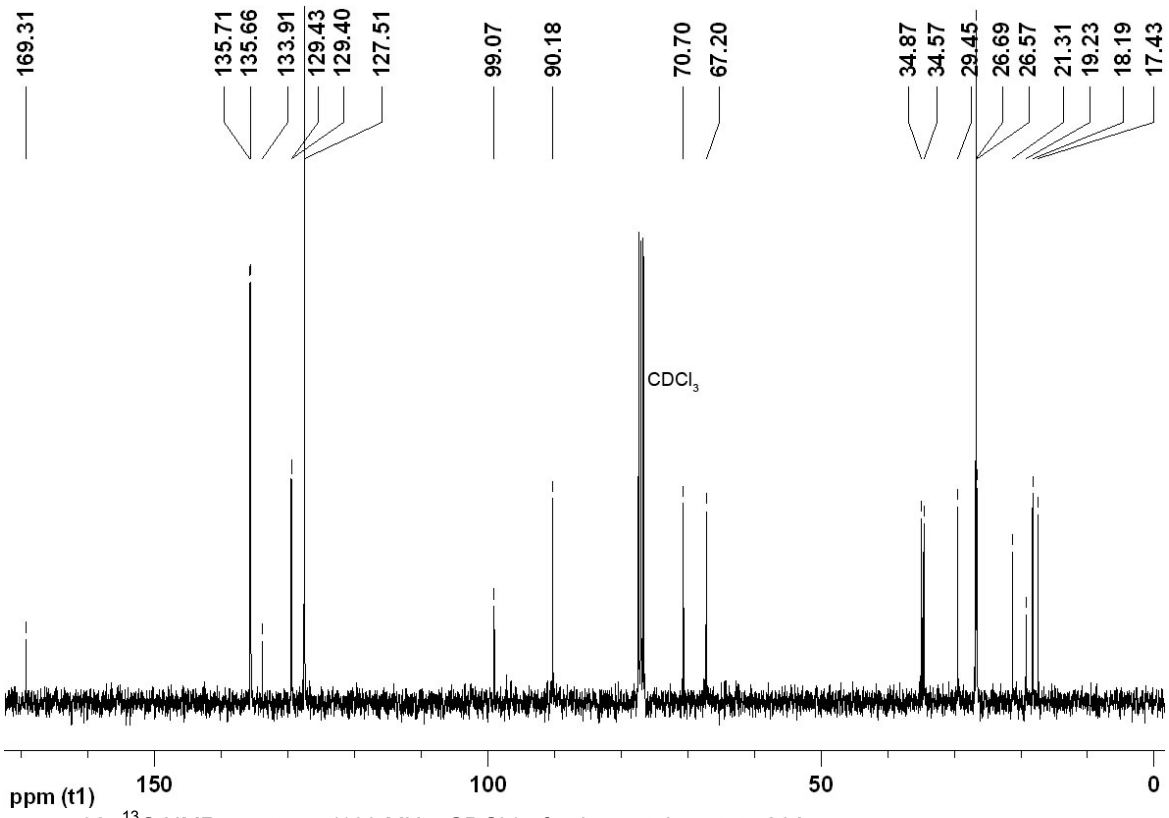

Figure 7.32: ^{13}C NMR spectrum (100 MHz; $CDCl_3$) of spiroacetal-acetate **861**.

(2*S,6*S**,8*S**)-2-Azido-8-(*tert*-butyldiphenylsilyloxymethyl)-1,7-dioxaspiro[5.5]undecane (860a) and (2*S**,6*R**,8*S**)-2-Azido-8-(*tert*-butyldiphenylsilyloxymethyl)-1,7-dioxaspiro[5.5]undecane (860b)**

Major isomer:
equatorial
(2*S**,6*S**,8*S**)-**860a**

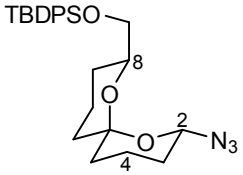

Minor isomer:
axial
(2*S**,6*R**,8*S**)-**860b**

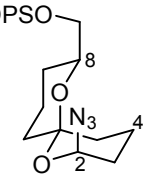

To a solution of ethoxy-spiroacetal **862** (293 mg, 624 μmol) and $TMSN_3$ (414 μL, 3.12 mmol) in anhydrous CH_2Cl_2 (9.7 mL) at -10 °C was added freshly prepared TMSOTf solution (1.16 mL, 0.70 mol L^{-1} in CH_2Cl_2, 811 μmol) dropwise. After 3 h, ice-cold saturated $NaHCO_3$ solution (3 mL) was added and the mixture was warmed to room temperature. Saturated $NaHCO_3$ (10 mL) and CH_2Cl_2 (10 mL) were added and the aqueous phase was extracted with CH_2Cl_2 (3 x 10 mL). The combined organic extracts were filtered through a pad of silica and concentrated *in vacuo*. Purification by flash chromatography using hexane–Et_2O–EtOAc (99:1:0, 49:1:0 to 97:0:3) as eluent yielded the *title equatorial azido-spiroacetal* **860a** (106 mg, 36%) and *axial azido-spiroacetal* **860b** (42.9 mg, 15%) as pale yellow oils. Unreacted ethoxy-spiroacetal **862** (13.6 mg, 5%) was also recovered.

Epimerisation of azido-spiroacetal **860b**:

To a solution of azido-spiroacetal **860b** (50 mg, 107 μmol) and $TMSN_3$ (71 μL, 535 μmol) in anhydrous CH_2Cl_2 (2.0 mL) at -10 °C was added freshly prepared TMSOTf solution (0.2 mL,

0.70 mol L^{-1} in CH_2Cl_2, 139 μmol) dropwise. After 3 h, ice-cold saturated $NaHCO_3$ solution (1.5 mL) was added and the mixture was warmed to room temperature. Saturated $NaHCO_3$ (2 mL) and CH_2Cl_2 (2 mL) were added and the aqueous phase was extracted with CH_2Cl_2 (3 x 4 mL). The combined organic extracts were filtered through a pad of silica and concentrated *in vacuo*. Purification by flash chromatography using hexane–Et_2O–EtOAc (99:1:0, 49:1:0 to 97:0:3) as eluent yielded the *title equatorial azido-spiroacetal* **860a** (21.5 mg, 43%) and *axial azido-spiroacetal* **860b** (10.1 mg, 20%) as pale yellow oils.

Equatorial azido-spiroacetal **860a**:

HRMS (FAB): found $[M - N_3]^+$, 423.2351, $C_{26}H_{35}O_3Si$ requires 423.2356.

ν_{max} (film)/cm^{-1}: 2929 (C–H), 2104 (N_3), 1428, 1248 (C–O), 1112 (C–O), 702.

δ_H (400 MHz; $CDCl_3$): 1.05 (9 H, s, $OSiPh_2{}^tBu$), 1.16–1.26 (1 H, m, 9-H_A), 1.37–1.48 (3 H, m, 3-H_A, 5-H_A and 11-H_A), 1.58–1.66 (4 H, m, 4-H_A, 5-H_B or 11-H_B, 9-H_B, and 10-H_A), 1.71–1.77 (2 H, m, 3-H_B and 5-H_B or 11-H_B), 1.90–2.02 (2 H, m, 4-H_B and 10-H_B), 3.58 (1 H, dd, J_{AB} 10.5 and $J_{8\text{-}CH_2,8}$ 4.2, 8-CH_AH_BO), 3.66 (1 H, dd, J_{AB} 10.5 and $J_{8\text{-}CH_2,8}$ 6.6, 8-CH_AH_BO), 3.81–3.87 (2 H, m, 8-H), 4.94 (1 H, dd, $J_{2ax,3ax}$ 10.8 and $J_{2ax,3eq}$ 2.5, 2-H_{ax}), 7.35–7.44 (6 H, m, Ph), 7.68–7.74 (4 H, m, Ph).

δ_C (75 MHz; $CDCl_3$): 17.8 (CH_2, C-4 or C-10), 18.3 (CH_2, C-4 or C-10), 19.2 (C, $OSiPh_2{}^tBu$), 26.7 (CH_2, C-9), 26.7 (CH_3, $OSiPh_2{}^tBu$), 30.2 (CH_2, C-3), 34.4 (CH_2, C-5 or C-11), 34.8 (CH_2, C-5 or C-11), 67.2 (CH_2, 8-CH_2O), 71.0 (CH, C-8), 83.2 (CH, C-2), 98.4 (C, C-6), 127.6 (CH, Ph), 127.6 (CH, Ph), 129.6 (CH, Ph), 129.6 (CH, Ph), 133.7 (C, Ph), 135.6 (CH, Ph).

***m/z* (FAB):** 423 ($[M - N_3]^+$, 13%), 199 (57), 197 (39), 139 (18), 137 (35), 135 (100), 105 (16), 91(17), 75(17).

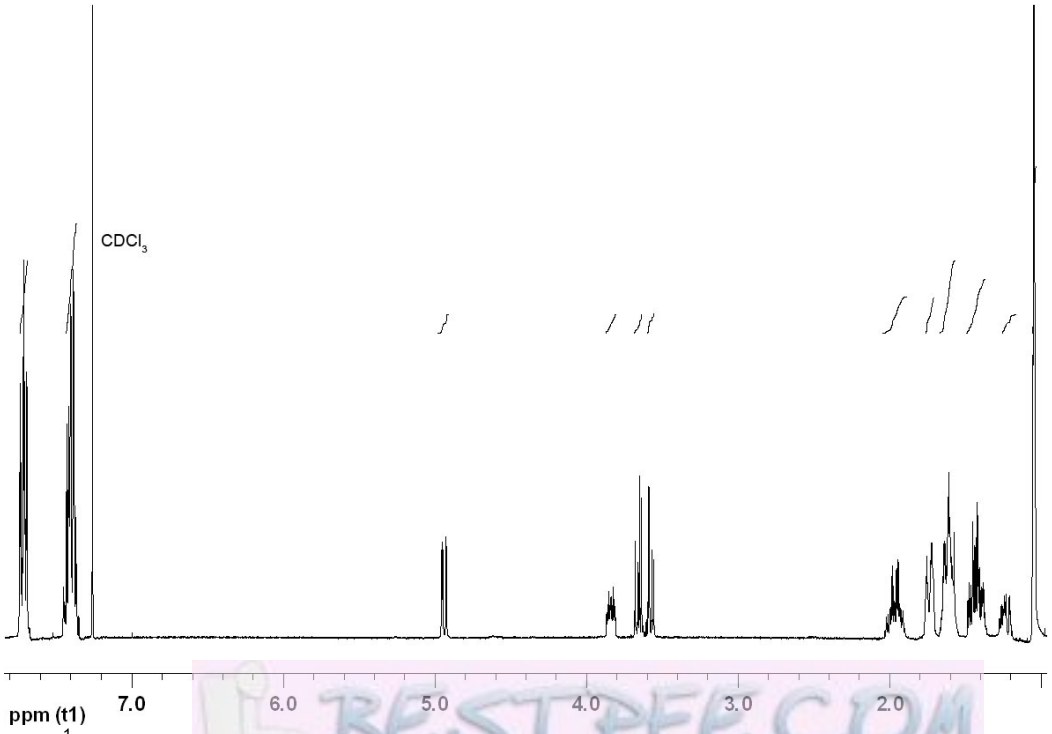

Figure 7.33: ^{1}H NMR spectrum (400 MHz; $CDCl_3$) of equatorial azido-spiroacetal **860a**

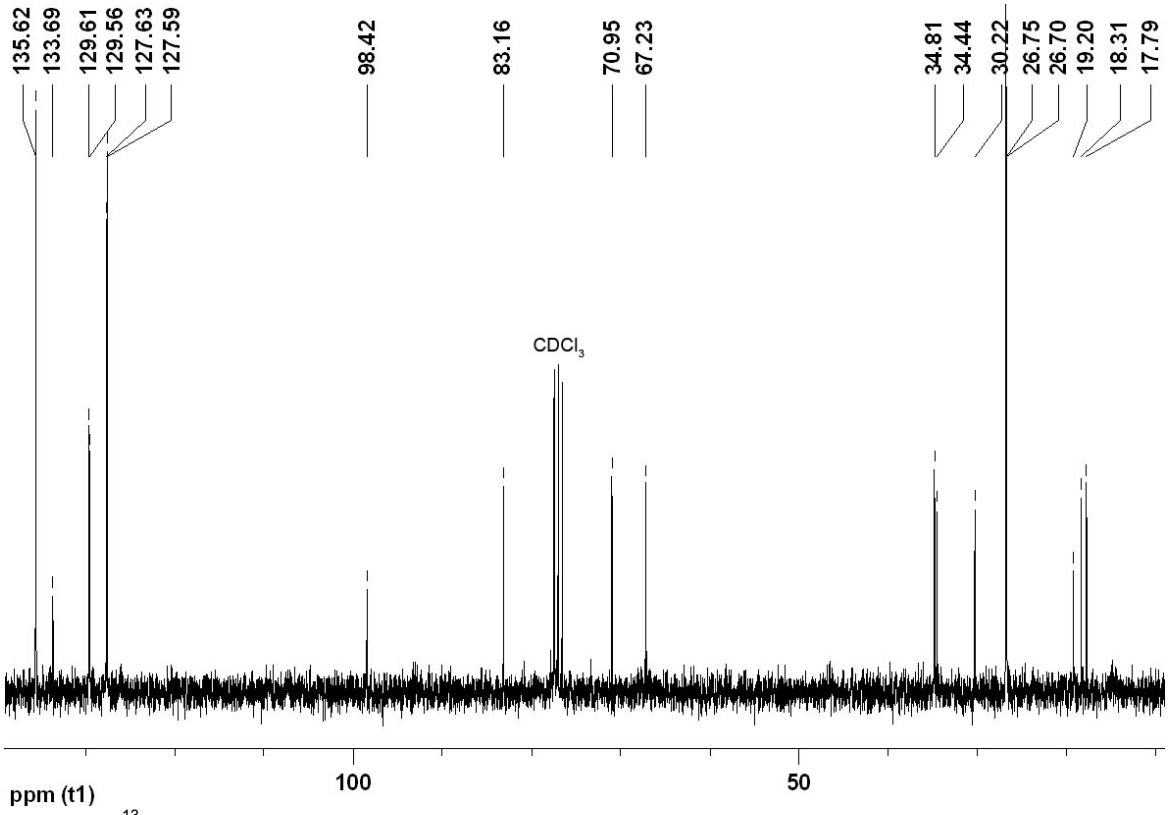

Figure 7.34: ^{13}C NMR spectrum (75 MHz; $CDCl_3$) of equatorial azido-spiroacetal **860a**.

Axial azido-spiroacetal **860b**:

HRMS (FAB): found MH^+, 466.2513, $C_{26}H_{36}N_3O_3Si$ requires 466.2526.

ν_{max} **(film)/cm^{-1}:** 2956 (C–H), 2858, 2105 (N_3), 1428, 1250 (C–O), 1113 (C–O), 1072, 847, 702.

δ_H **(300 MHz; $CDCl_3$):** 1.06 (9 H, s, $OSiPh_2{}^tBu$), 1.19–1.32 (1 H, m, 9-H_A), 1.32–1.44 (1 H, m, 3-H_A), 1.53–1.63 (3 H, m, 3-H_B, 10-H_A and 10-H_B), 1.65–1.81 (7 H, m, 4-H_A, 4-H_B, 5-H_A, 5-H_B, 9-H_B, 11-H_A and 11-H_B), 3.54 (1 H, dd, J_{AB} 10.5 and $J_{8\text{-}CH_2,8}$ 4.8, 8-CH_AH_BO), 3.62 (1 H, dd, J_{AB} 10.5 and $J_{8\text{-}CH_2,8}$ 5.3, 8-CH_AH_BO), 3.85–3.94 (2 H, m, 8-H), 4.61 (1 H, t, $J_{2,3}$ 6.4, 2-H_{eq}), 7.35–7.44 (6 H, m, Ph), 7.66–7.74 (4 H, m, Ph).

δ_C **(75 MHz; $CDCl_3$):** 18.7 (CH_2, C-4), 19.1 (CH_2, C-10), 19.3 (C, $OSiPh^tBu$), 26.8 (CH_2, C-9), 26.8 (CH_3, $OSiPh^tBu$), 32.0 (CH_2, C-3), 34.1 (CH_2, C-5), 39.8 (CH_2, C-11), 67.0 (CH_2, 8-CH_2O), 73.3 (CH, C-8), 77.8 (CH, C-2), 93.2 (C, C-6), 127.6 (CH, Ph), 129.6 (CH, Ph), 133.6 (C, Ph), 133.7 (C, Ph), 135.6 (CH, Ph).

m/z **(FAB):** 466 (MH^+, 1%), 423 (M – N_3, 2), 239 ($SiPh_2{}^tBu$, 7), 214 (32), 207 (13), 199 (38), 197 (37), 183 (13), 137 (24), 135 (100), 121 (14), 105 (14).

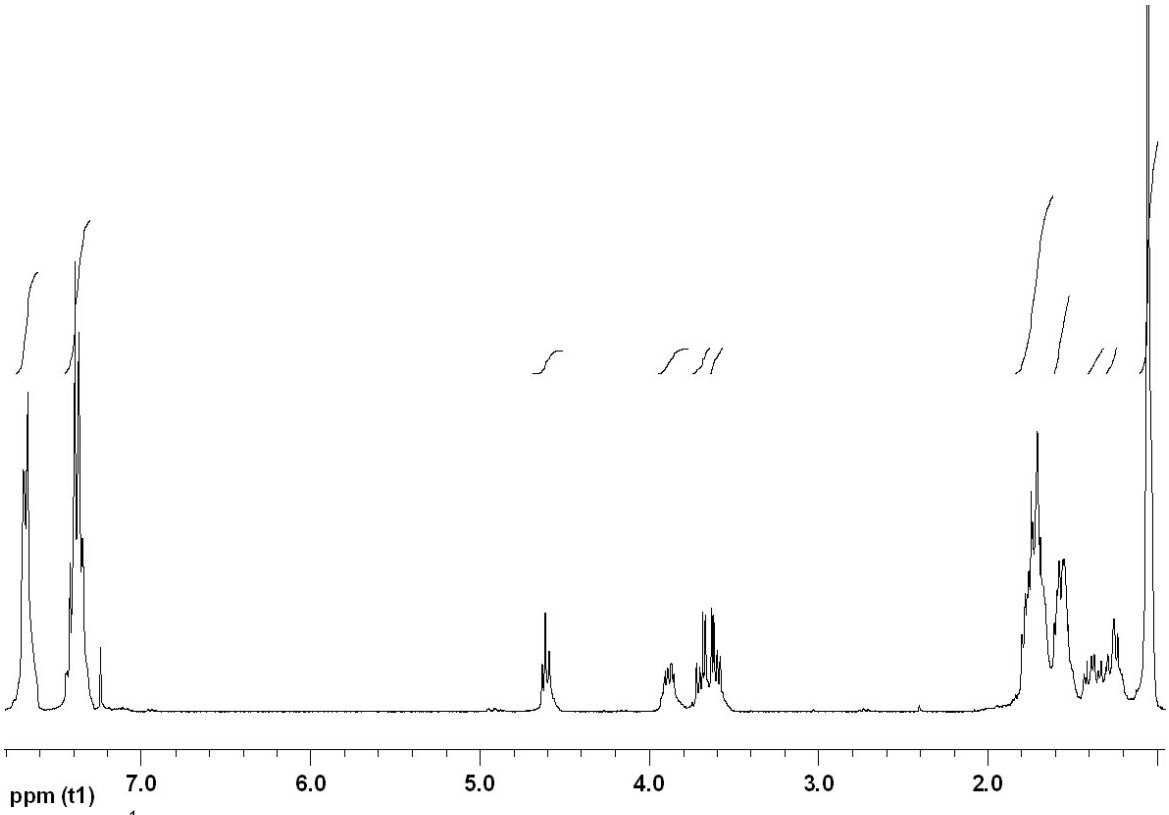

Figure 7. 35: ^{1}H NMR spectrum (300 MHz; $CDCl_3$) of axial azido-spiroacetal **860b**.

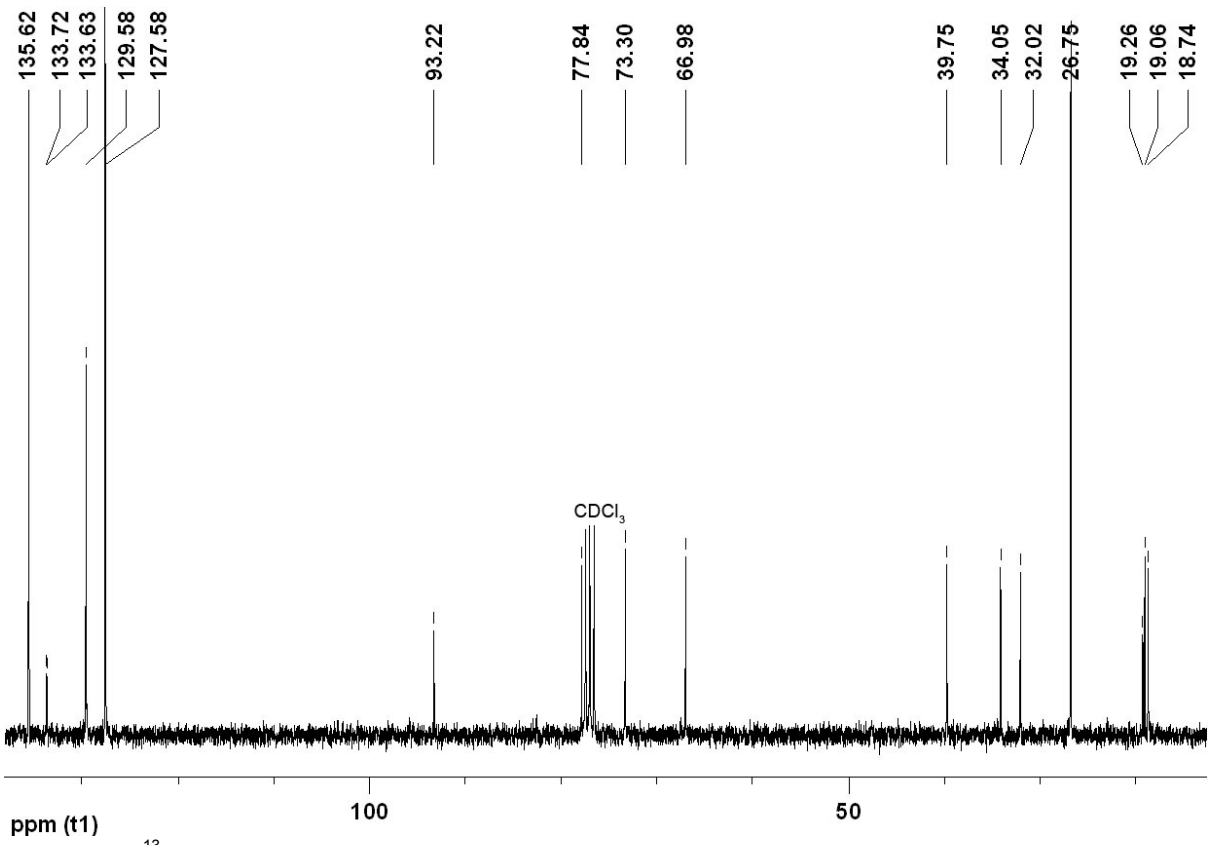

Figure 7.36: ^{13}C NMR spectrum (75 MHz; $CDCl_3$) of axial azido-spiroacetal **860b**.

7.3.5 Synthesis of Spiroacetal-Nucleosides 902

General Procedures for Nucleosidation under Vorbrüggen Conditions [28]

Method A: Nucleosidation with Pyrimidine Bases

This procedure is an adaptation of that reported by Vorbrüggen *et al.*[15]

To a suspension of the pyrimidine base (1.2–2.0 equiv.) in HMDS (0.50–1.0 mL) under an atmosphere of argon was added ammonium sulfate (2 crystals) and the mixture was heated to reflux until the white solid dissolved. After 3–4 h, the mixture was concentrated *in vacuo* to a thick yellow oil. Acetate **861** in CH_2Cl_2 (1.0–1.1 mL) was transferred to the yellow oil *via* cannula. Freshly prepared TMSOTf solution (1.6–2.2 equiv., 0.70 mol L^{-1} in CH_2Cl_2) was added dropwise. After 3 h, saturated $NaHCO_3$ solution (2 mL) and CH_2Cl_2 (2 mL) were added and the mixture was stirred for 15 min. The aqueous phase was extracted with CH_2Cl_2 (3 x 4 mL). The combined organic extracts were dried over $MgSO_4$ and concentrated *in vacuo*. Purification by flash chromatography using hexane–EtOAc as eluent yielded the spiroacetal nucleoside.

Method B: Nucleosidation with Purine Bases

This procedure is an adaptation of that reported by Vorbrüggen *et al.*[15]

To a suspension of the purine base (1.3 equiv.) in a 1:4:5 mixture of *N*,*O*-bis(trimethylsilyl)acetamide–HMDS–toluene (1.0 mL) under an atmosphere of argon was heated to reflux until the white solid dissolved. After 2 h, the mixture was concentrated *in vacuo* to a thick yellow oil. Acetate **861** in CH_2Cl_2 (1.5 mL) was transferred to the yellow oil *via* cannula. Freshly prepared TIPSOTf solution (1.4 equiv., 0.52 mol L^{-1} in CH_2Cl_2) was added dropwise. After 18 h, saturated $NaHCO_3$ solution (2 mL) and CH_2Cl_2 (2 mL) were added and stirred for 15 min. The aqueous phase was extracted with CH_2Cl_2 (3 x 4 mL). The combined organic extracts were dried over $MgSO_4$ and concentrated *in vacuo*. Purification by flash chromatography using hexane–EtOAc as eluent yielded the spiroacetal nucleoside.

1-{(2′*S,6′*S**,8′*S**)-8′-(*tert*-Butyldiphenylsilyloxymethyl)-1′,7′-dioxaspiro[5.5]undecan-2′-yl}-5-fluorocytidine (902a)**

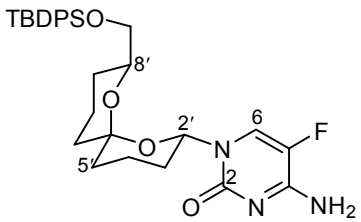

Method A: The *title compound* **902a** (6.10 mg, 22%) was prepared as a pale yellow oil from 5-fluorocytosine (12.4 mg, 97.0 μmol), acetate **861** (24.0 mg, 49.7 μmol) and TMSOTf solution (159 μL, 111 μmol) using the general procedure (method A) described above. Purification was carried out by flash chromatography using hexane–EtOAc (19:1, 1:1 to 1:4) as eluent.

HRMS (FAB): found MH^+, 552.2688, $C_{30}H_{39}FN_3O_4Si$ requires 552.2694.

ν_{max} (film)/cm^{-1}: 3297 (N–H), 3072 (N–H), 2931 (C–H), 1688 (C=O), 1626, 1514, 1112 (C–O), 982, 703.

δ_H (300 MHz; $CDCl_3$): 1.06 (9 H, s, $OSiPh_2{}^tBu$), 1.21–1.25 (1 H, m, 3′-H_A), 1.41–1.52 (3 H, m, 5′-H_A, 9′-H_A and 11′-H_A), 1.56–1.74 (5 H, m, 4′-H_A, 5′-H_B, 9′-H_B, 10′-H_A and 11′-H_B), 1.80–1.88 (1 H, m, 10′-H_B), 2.05–2.12 (2 H, m, 3′-H_B and 4′-H_B), 3.65 (1 H, dd, J_{AB} 10.2 and $J_{8'CH_2,8'}$ 4.8, 8′-CH_AH_BO), 3.72 (1 H, dd, J_{AB} 10.2 and $J_{8'\text{-}CH_2,8'}$ 4.2, 8′-CH_AH_BO), 3.74–3.85 (1 H, m, 8′-H), 5.87 (1 H, ddd, $J_{2'ax,3'ax}$ 10.8, $J_{2'ax,3'eq}$ 2.3 and $J_{2'ax,5F}$ 2.0, 2′-H_{ax}), 7.33–7.42 (6 H, m, Ph), 7.54 (1 H, d, $J_{6,5F}$ 6.4, 6-H), 7.68–7.74 (4 H, m, Ph).

δ_C (75 MHz; $CDCl_3$): 17.9 (CH_2, C-4′), 18.1 (CH_2, C-10′), 19.3 (C, $OSiPh_2{}^tBu$), 26.6 (CH_2, C-9′), 26.8 (CH_3, $OSiPh_2{}^tBu$), 30.9 (CH_2, C-3′), 34.9 (CH_2, C-5′ or C-11′), 35.0 (CH_2, C-5′ or C-11′), 66.9 (CH_2, 8′-CH_2O), 70.4 (CH, C-8′), 77.8 (CH, C-2′), 99.1 (C, C-6′), 125.6 (CH, d, $J_{6,5F}$ 31.3, C-6), 127.5 (CH, Ph), 127.6 (CH, Ph), 129.5 (CH, Ph), 133.9 (C, Ph), 133.9 (C, Ph), 135.6 (CH, Ph), 135.7 (CH, Ph), 136.3 (C, d, $J_{5,5F}$ 241.3, C-5), 153.4 (C, C-2), 157.5 (C, $J_{4,5F}$ 13.6, C-4).

δ_F (282 MHz; $CFCl_3$): -170.2 (CF, 5-F).

***m/z* (FAB):** 552 (MH^+, 1%), 494 (M – ^{t}Bu, 7), 474 (M – Ph, 1), 423 ($C_{26}H_{35}O_3Si$, 27), 239 ($SiPh_2{}^tBu$, 7), 207 (29), 197 (35), 135 (100), 130 (31), 105 (18).

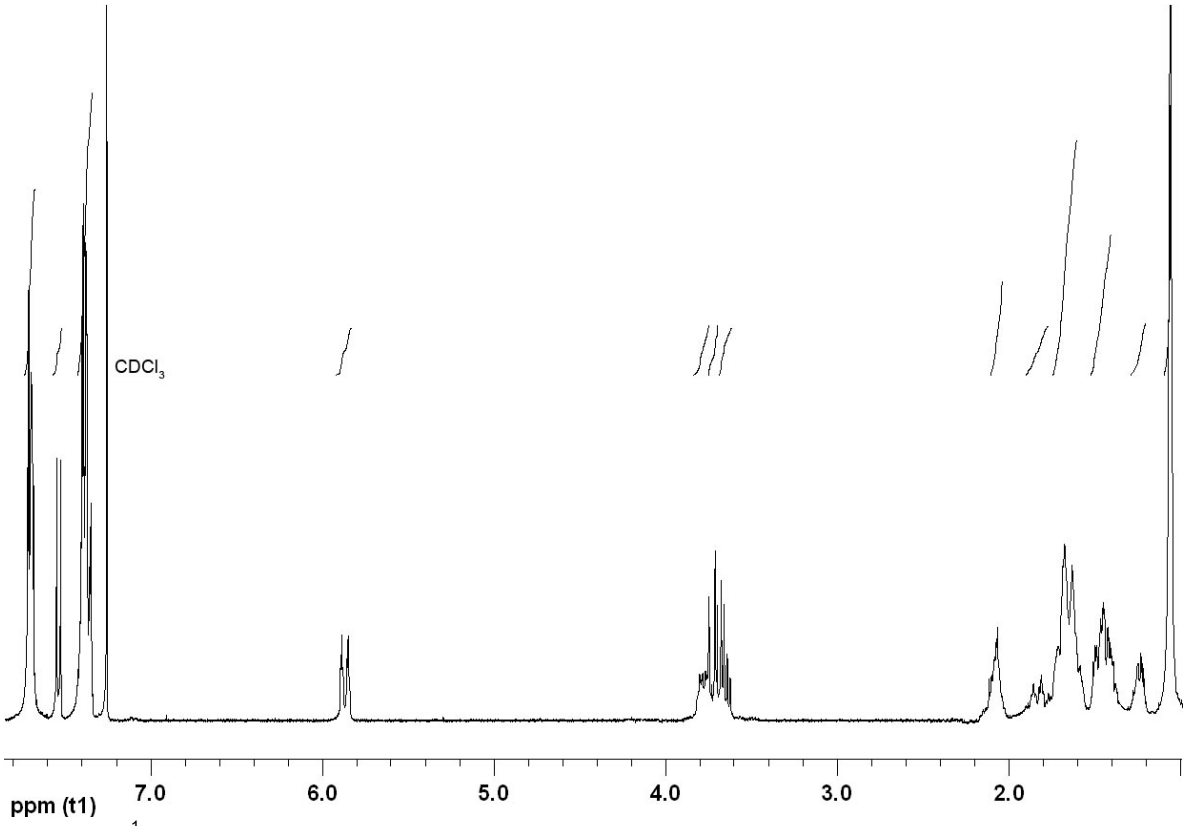

Figure 7.37: ^{1}H NMR spectrum (300 MHz; $CDCl_3$) of fluorocytidine **902a**.

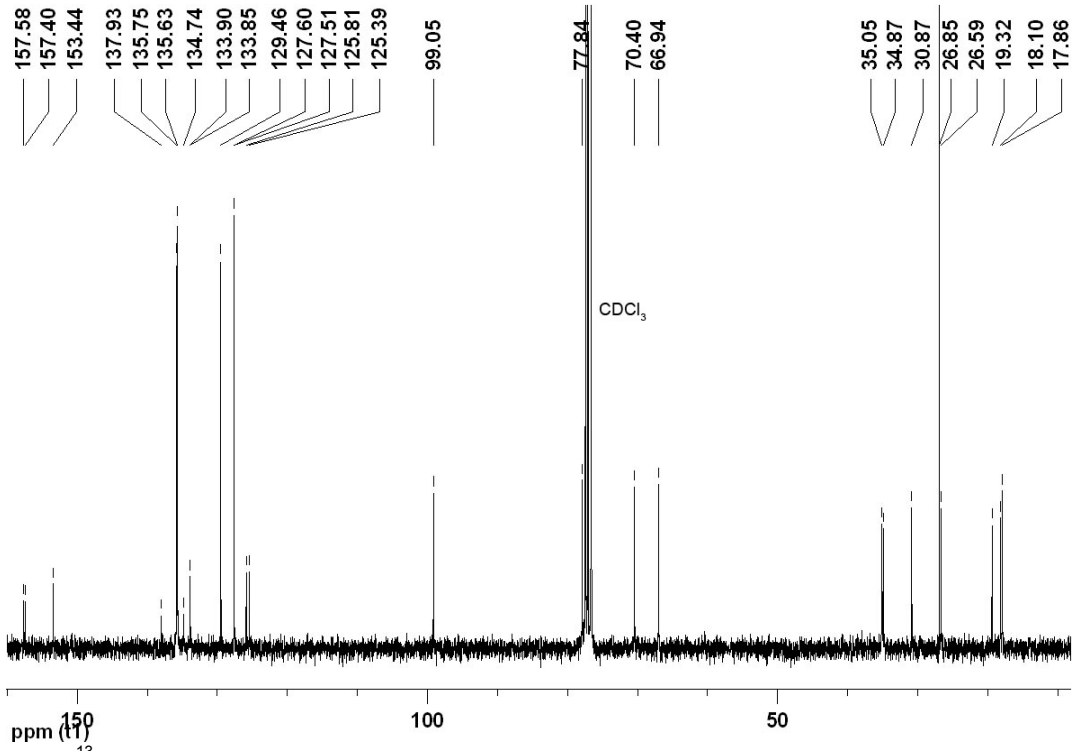

Figure 7.38: ^{13}C NMR spectrum (75 MHz; $CDCl_3$) of fluorocytidine **902a**.

4-*N*-Acetyl-1-{(2′*S,6′*S**,8′*S**)-8′-(*tert*-butyldiphenylsilyloxymethyl)-1′,7′-dioxaspiro[5.5]undecan-2′-yl}cytidine (902b)**

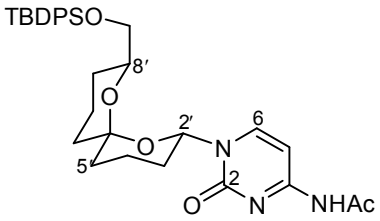

Method A: The *title compound* **902b** (14.3 mg, 46%) was prepared as a colourless oil from 4-*N*-acetylcytosine (9.86 mg, 64.4 μmol), acetate **861** (25.9 mg, 53.7 μmmol) and TMSOTf solution (123 μL, 86.4 μmol) using the general procedure (method A) described above. Purification was carried out by flash chromatography using hexane–EtOAc (9:1 to 1:1) as eluent.

HRMS (FAB): found MH^+, 576.2895, $C_{32}H_{42}N_3O_5Si$ requires 576.2894.

ν_{max} (film)/cm^{-1}: 3232 (N–H), 2932 (C–H), 1716 (C=O), 1668 (C=O), 1626, 1563, 1495, 1113 (C–O), 984, 703.

δ_H (400 MHz; $CDCl_3$): 1.06 (9 H, s, $OSiPh_2{}^tBu$), 1.18–1.24 (1 H, m, 3′-H_A), 1.24–1.44 (3 H, m, 5′-H_A, 9′-H_A and 11′-H_A), 1.47–1.75 (6 H, m, 4′-H_A, 5′-H_B, 9′-H_B, 10′-H_A, 10′-H_B and 11′-H_B), 1.96–2.07 (2 H, m, 3′-H_B and 4′-H_B), 2.17 (3 H, s, $COCH_3$), 3.52 (1 H, dd, J_{AB} 10.2 and $J_{8'\text{-}CH_2,8'}$ 4.8, 8′-CH_AH_BO), 3.61 (1 H, dd, J_{AB} 10.2 and $J_{8'CH_2\text{-}8'}$ 4.8, 8′-CH_AH_BO), 3.63–3.69 (1 H, m, 8′-H), 5.85 (1 H, dd, $J_{2'ax,3'ax}$ 10.7 and $J_{2'ax,3'eq}$ 2.0, 2′-H_{ax}), 7.24–7.34 (7 H, m, Ph and 5-H), 7.58–7.62 (4 H, m, Ph), 7.81 (1 H, d, $J_{6,5}$ 7.5, 6-H), 9.76 (1 H, br s, NH).

δ_C (100 MHz; $CDCl_3$): 17.8 (CH_2, C-4′), 18.0 (CH_2, C-10′), 19.2 (C, $OSiPh_2{}^tBu$), 24.9 (CH_3, CO*CH₃*), 26.6 (CH_2, C-9′), 26.8 (CH_3, $OSiPh_2{}^tBu$), 31.1 (CH_2, C-3′), 34.8 (CH_2, C-5′ or C-11′), 35.0 (CH_2, C-5′ or C-11′), 66.9 (CH_2, 8′-CH_2O), 70.6 (CH, C-8′), 78.4 (CH, C-2′), 96.6 (CH, C-5), 99.2 (C, C-6′), 127.5 (CH, Ph), 127.6 (CH, Ph), 129.5 (CH, Ph), 133.8 (C, Ph), 135.6 (CH, Ph), 135.7 (CH, Ph), 144.7 (CH, C-6), 154.6 (C, C-2), 162.4 (C, C-4), 170.9 (C, N*CO*CH_3).

***m/z* (FAB):** 576 (MH^+, 6%), 518 (18), 423 ($C_{26}H_{35}O_3Si$, 42), 405 (21), 207 (40), 199 (29), 197 (33), 154 (80), 135 (100), 121 (18).

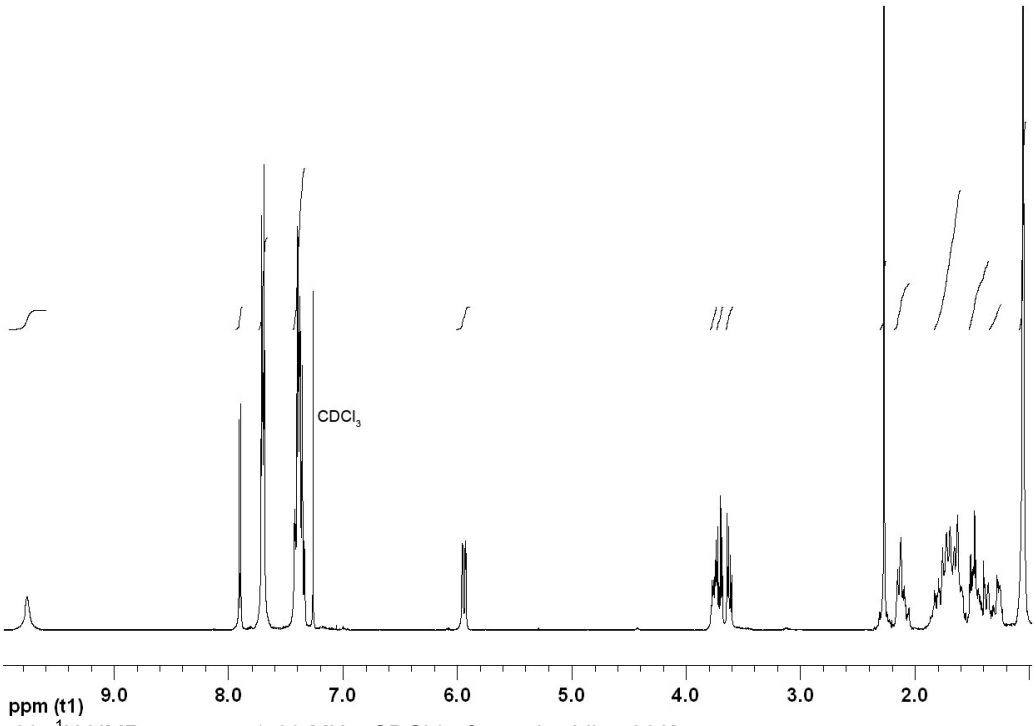

Figure 7.39: ^1H NMR spectrum (400 MHz; $CDCl_3$) of acetylcytidine **902b**.

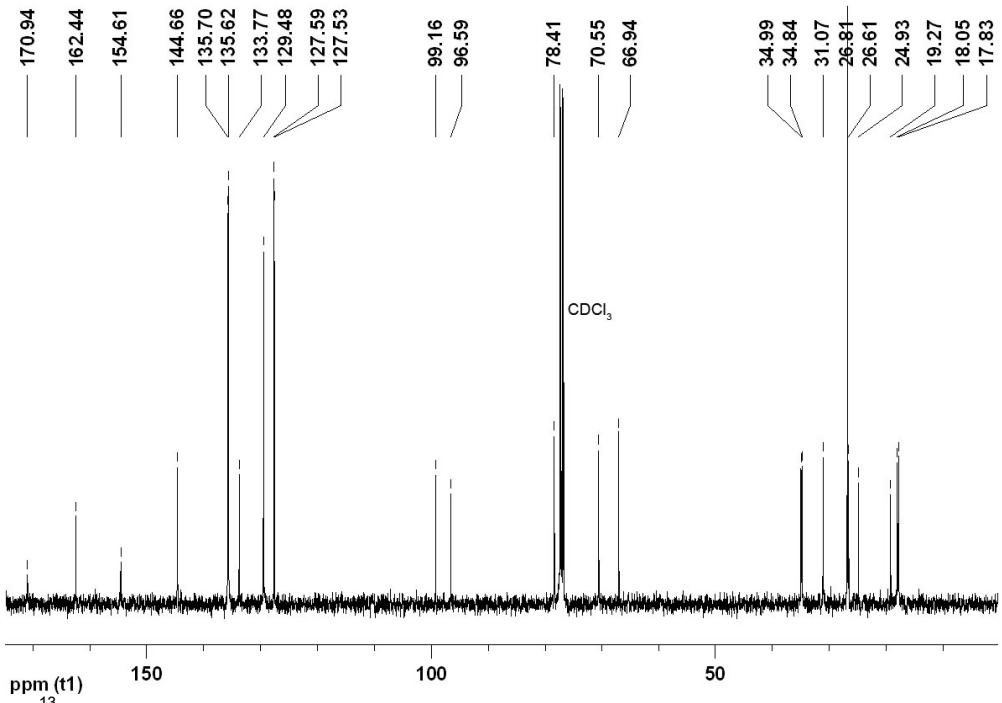

Figure 7.40: ^{13}C NMR spectrum (100 MHz; $CDCl_3$) of acetylcytidine **902b**.

1-{(2′*S,6′*S**,8′*S**)-8′-(*tert*-Butyldiphenylsilyloxymethyl)-1′,7′-dioxaspiro[5.5]undecan-2′-yl}thymidine (902c)**

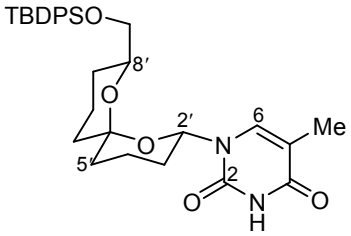

Method A**: The *title compound* **902c** (10.5 mg, 45%) was prepared as a pale yellow oil from thymine (8.49 mg, 67.3 μmol), acetate **861** (20.4 mg, 42.3 μmol) and TMSOTf solution (104 μL, 72.5 μmol) using the general procedure (method A) described above. Purification was carried out by flash chromatography using hexane–EtOAc (19:1, 9:1 to 4:1) as eluent.

HRMS (FAB): found MH^+, 549.2784, $C_{31}H_{41}N_2O_5Si$ requires 549.2785.

ν_{max} (film)/cm^{-1}: 3180 (N–H), 2930 (C–H), 1713 (C=O), 1694 (C=O), 1428, 1270 (C–O), 1112 (C–O), 981, 702.

δ_H (300 MHz; $CDCl_3$): 1.06 (9 H, s, $OSiPh_2{}^tBu$), 1.35–1.43 (1 H, m, 9′-H_A), 1.43–1.53 (3 H, m, 3′-H_A, 5′-H_A and 11′-H_A), 1.54–1.76 (5 H, m, 4′-H_A, 5′-H_B, 9′-H_B, 10′-H_A and 11′-H_B), 1.79–1.90 (2 H, m, 3′-H_B and 10′-H_B), 1.95 (3 H, d, $J_{5\text{-}CH_3,6}$ 1.2, 5-CH_3), 2.06–2.16 (1 H, m, 4′-H_B), 3.65 (1 H, dd, J_{AB} 10.5 and $J_{8'\text{-}CH_2,8'}$ 4.5, 8′-CH_AH_BO), 3.71 (1 H, dd, J_{AB} 10.5 and $J_{8'\text{-}CH_2,8'}$ 5.2, 8′-CH_AH_BO), 3.85–3.93 (1 H, m, 8′-H), 5.95 (1 H, dd, $J_{2'ax,3'ax}$ 11.1 and $J_{2'ax,3'eq}$ 2.5, 2′-H_{ax}), 7.25 (1 H, d, $J_{6,5\text{-}CH_3}$ 1.2, 6-H), 7.33–7.46 (6 H, m, Ph), 7.71–7.76 (4 H, m, Ph), 8.29 (1 H, br s, NH).

δ_C (75 MHz; $CDCl_3$): 12.6 (CH_3, 5-CH_3), 18.0 (CH_2, C-4′), 18.1 (CH_2, C-10′), 19.3 (C, $OSiPh_2{}^tBu$), 26.5 (CH_2, C-9′), 26.8 (CH_3, $OSiPh_2{}^tBu$), 30.1 (CH_2, C-3′), 34.7 (CH_2, C-5′ or C-11′), 34.8 (CH_2, C-5′ or C-11′), 67.0 (CH_2, 8′-CH_2O), 70.6 (CH, C-8′), 76.5 (CH, C-2′), 99.0 (C, C-6′), 110.4 (C, C-5), 127.5 (CH, Ph), 127.6 (CH, Ph), 129.5 (CH, Ph), 133.8 (C, Ph), 135.7 (CH, Ph), 135.7 (CH, Ph), 136.1 (CH, C-6), 146.9 (C, C-2), 163.6 (C, C-4).

***m/z* (FAB):** 549 (MH^+, 1%), 491 (M – ^{t}Bu, 14), 471(M – Ph, 3), 423 ($C_{26}H_{35}O_3Si$, 17), 207 (19), 199 (38), 197 (38), 165 (22), 135 (100), 122 (21).

** Under the equivalent conditions, the yield of 45% and 24% were achieved respectively when TIPSOTf (0.52 mol L^{-1}, 1.4 equiv.) and $SnCl_4$ (0.63 mol L^{-1}, 1.3 equiv.) was used in the place of TMSOTf.

A yield a 33% was achieved when the reaction was carried out under one-pot condition in which CH_2Cl_2 and HMDS were substituted with MeCN and *N*,*O*-bis(trimethylsilyl)acetamide and *bis*-silylated thymine was not isolated.

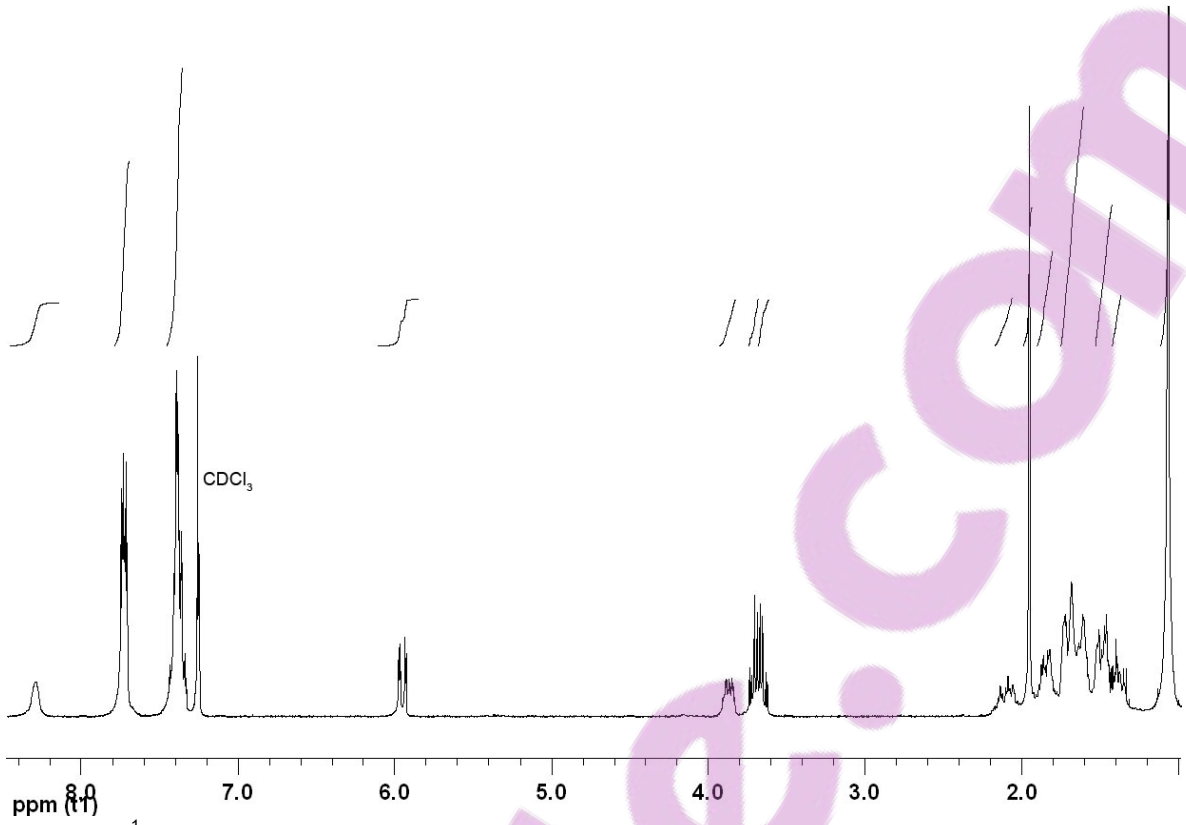

Figure 7.41: ^{1}H NMR spectrum (300 MHz; $CDCl_3$) of thymidine **902c**.

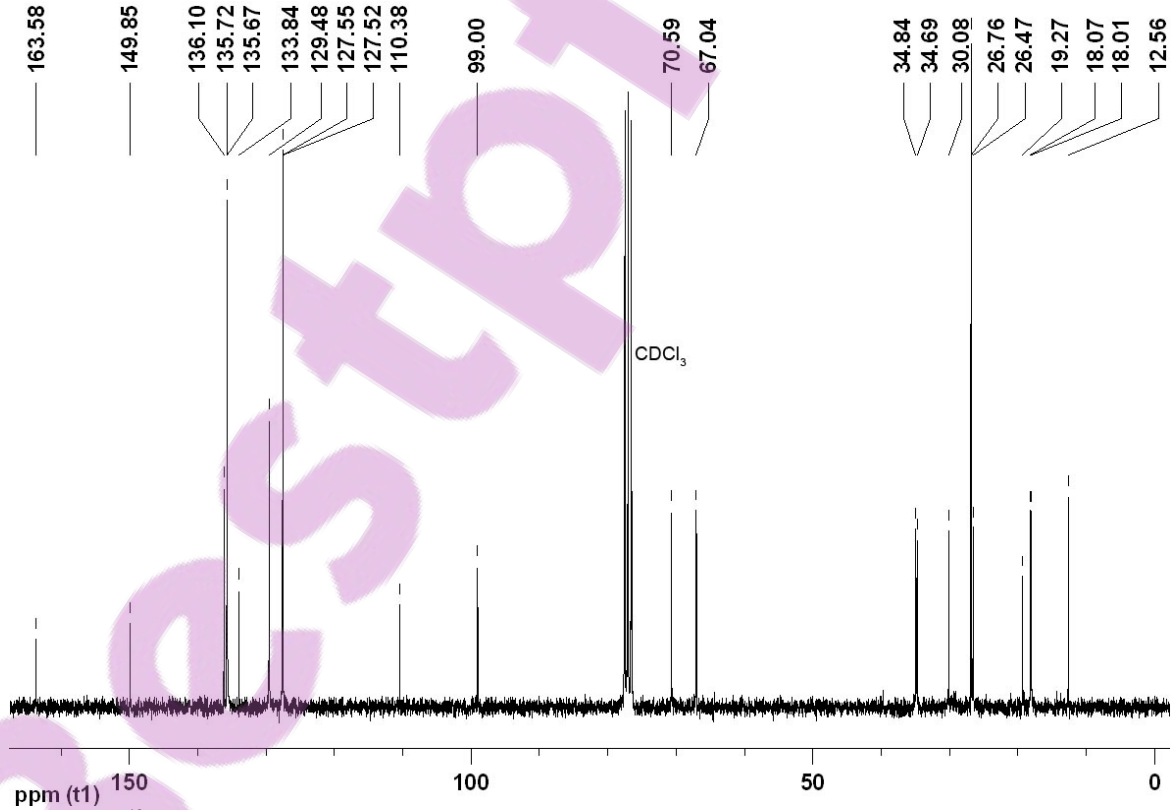

Figure 7.42: ^{13}C NMR spectrum (75 MHz; $CDCl_3$) of thymidine **902c**.

1-{(2′*S,6′*S**,8′*S**)-8′-(*tert*-Butyldiphenylsilyloxymethyl)-1′,7′-dioxaspiro[5.5]undecan-2′-yl}uridine (902d)**

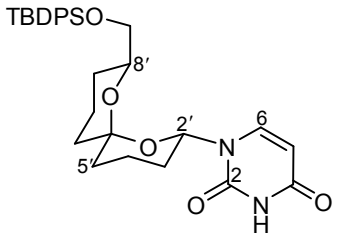

Method A: The *title compound* **902d** (7.50 mg, 36%) was prepared as a cream-coloured powder from uracil (6.95 mg, 61.9 μmol), acetate **861** (18.8 mg, 38.9 μmol) and TMSOTf solution (95.4 μL, 66.8 μmol) using the general procedure (method A) described above. Purification was carried out by flash chromatography using hexane–EtOAc (19:1 to 7:3) as eluent and recrystallisation of acetate **861** from hexane–CH_2Cl_2 afforded pale yellow needles.

Melting Point: 208.3–210.1 °C.

HRMS (FAB): found MH^+, 535.2633, $C_{30}H_{39}N_2O_5Si$ requires 535.2628.

ν_{max} (film)/cm^{-1}: 3376 (N–H), 2919 (C–H), 1689 (C=O), 1668 (C=O), 1456, 1377, 1267 (C–O), 1103 (C–O), 982, 699.

δ_H (300 MHz; $CDCl_3$): 1.07 (9 H, s, $OSiPh_2{}^tBu$), 1.31–1.38 (1 H, m, 9′-H_A), 1.41–1.51 (3 H, m, 3′-H_A, 5′-H_A and 11′-H_A), 1.56–1.76 (5 H, m, 4′-H_A, 5′-H_B, 9′-H_B, 10′-H_A and 11′-H_B), 1.80–1.94 (2 H, m, 3′-H_B and 10′-H_B), 2.07–2.16 (1 H, m, 4′-H_B), 3.63 (1 H, dd, J_{AB} 10.4 and $J_{8'\text{-}CH_2,8'}$ 4.5, 8′-CH_AH_BO), 3.72 (1 H, dd, J_{AB} 10.4 and $J_{8'\text{-}CH_2,8'}$ 5.3, 8′-CH_AH_BO), 3.82–3.89 (1 H, m, 8′-H), 5.73 (1 H, d, $J_{5,6}$ 8.2, 5-H), 5.94 (1 H, dd, $J_{2'ax,3'ax}$ 11.1 and $J_{2'ax,3'eq}$ 2.5, 2′-H_{ax}), 7.33–7.42 (6 H, m, Ph), 7.46 (1 H, d, $J_{6,5}$ 8.2, 6-H), 7.70–7.76 (4 H, m, Ph), 8.17 (1 H, br s, NH).

δ_C (75 MHz; $CDCl_3$): 17.9 (CH_2, C-4′), 18.0 (CH_2, C-10′), 19.3 (C, $OSiPh_2{}^tBu$), 26.5 (CH_2, C-9′), 26.8 (CH_3, $OSiPh_2{}^tBu$), 30.3 (CH_2, C-3′), 34.7 (CH_2, C-5′), 34.8 (CH_2, C-11′), 67.0 (CH_2, 8′-CH_2O), 70.7 (CH, C-8′), 76.8 (CH, C-2′), 99.1 (C, C-6′), 102.1 (CH, C-5), 127.6 (CH, Ph), 129.5 (CH, Ph), 129.5 (CH, Ph), 133.8 (C, Ph), 135.7 (CH, Ph), 135.7 (CH, Ph), 140.3 (CH, C-6), 149.7 (C, C-2), 162.8 (C, C-4).

***m/z* (FAB):** 535 (MH^+, 3%), 477 (M – ^{t}Bu, 11), 457 (M – Ph, 3), 423 ($C_{26}H_{35}O_3Si$, 19), 239 ($SiPh_2{}^tBu$, 8), 199 (35), 197 (35), 135 (100), 105 (32), 91 (73).

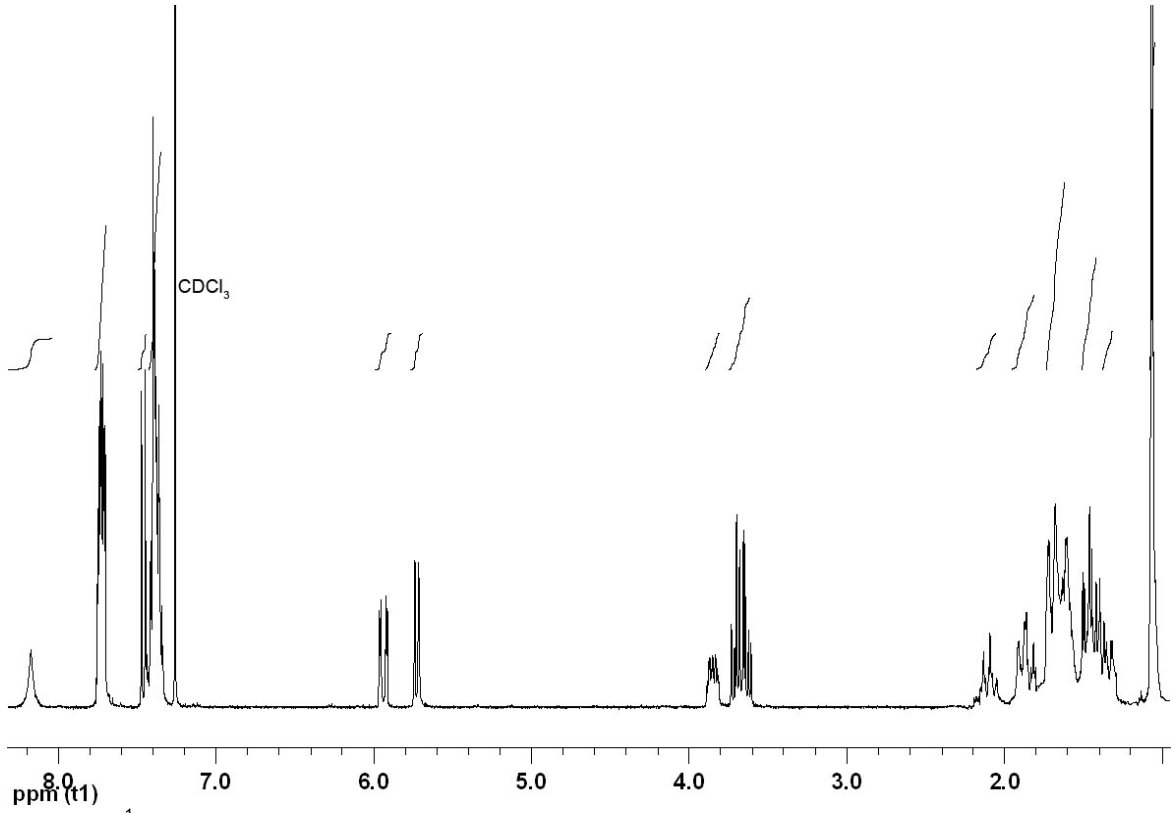

Figure 7.43: ^{1}H NMR spectrum (300 MHz; $CDCl_3$) of uridine **902d**.

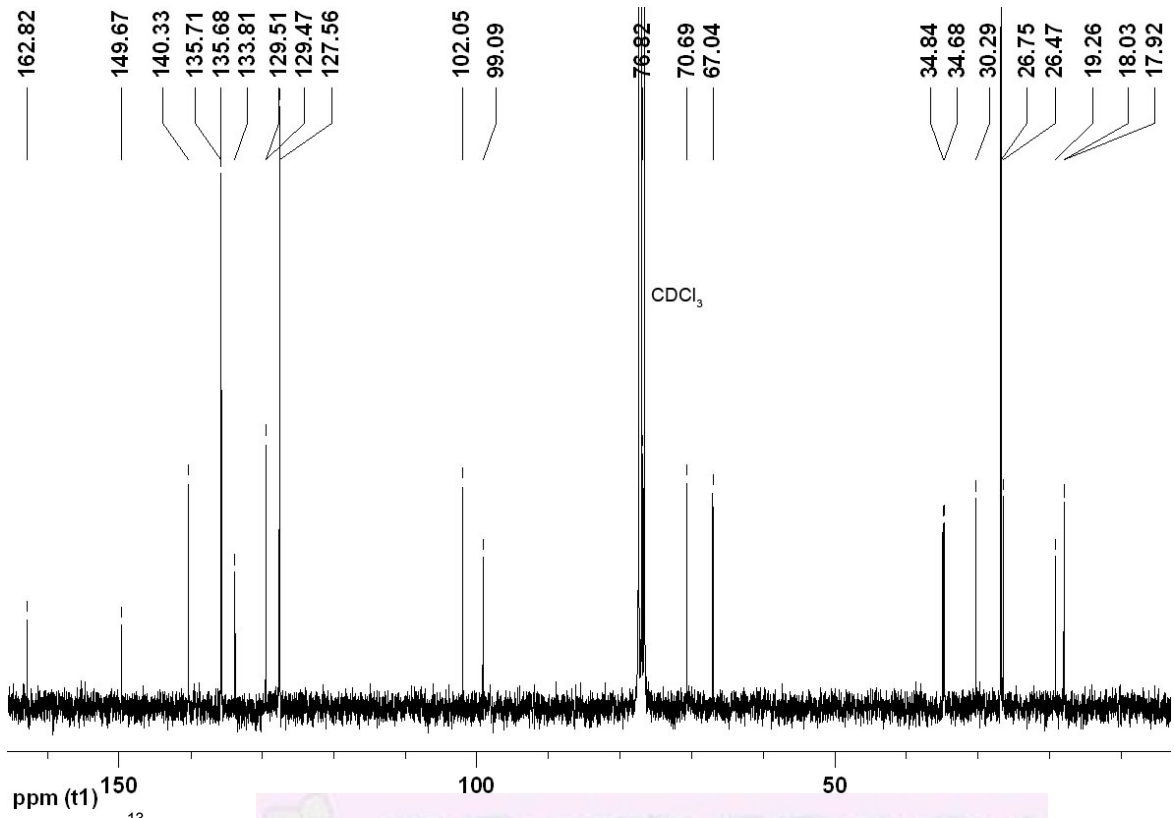

Figure 7.44: ^{13}C NMR spectrum (75 MHz; $CDCl_3$) of uridine **902d**.

1-{(2′*S,6′*S**,8′*S**)-8′-(*tert*-Butyldiphenylsilyloxymethyl)-1′,7′-dioxaspiro[5.5]undecan-2′-yl}-5-fluorouridine (902e)**

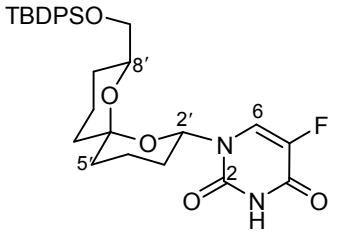

Method A: The *title compound* **902e** (4.00 mg, 19%) was prepared as a pale yellow oil from 5-fluorouracil (7.75 mg, 59.6 μmol), acetate **861** (18.0 mg, 37.2 μmol) and TMSOTf solution (92.0 μL, 64.4 μmol) using the general procedure (method A) described above. Purification was carried out by flash chromatography using hexane–EtOAc (19:1, 4:1 to 7:3) as eluent.

HRMS (FAB): found MH^+, 553.2540, $C_{30}H_{38}FN_2O_5Si$ requires 553.2534.

ν_{max} (film)/cm^{-1}: 3187 (N–H), 3063 (N–H), 2918 (C–H), 1712 (C=O), 1694 (C=O), 1673 (C=O), 1260 (C–O), 1112 (C–O), 987, 700.

δ_H (300 MHz; $CDCl_3$): 1.06 (9 H, s, $OSiPh_2{}^tBu$), 1.28–1.37 (1 H, m, 9′-H_A), 1.37–1.52 (3 H, m, 3′-H_A, 5′-H_A and 11′-H_A), 1.57–1.75 (5 H, m, 4′-H_A, 5′-H_B, 9′-H_B, 10′-H_A and 11′-H_B), 1.75–1.96 (2 H, m, 3′-H_B and 10′-H_B), 2.03–2.17 (1 H, m, 4′-H_B), 3.62 (1 H, dd, J_{AB} 10.5 and $J_{8'\text{-}CH_2,8'}$ 4.5, 8′-CH_AH_BO), 3.70 (1 H, dd, J_{AB} 10.5 and $J_{8'\text{-}CH_2,8'}$ 5.5, 8′-CH_AH_BO), 3.79–3.88 (1 H, m, 8′-H), 5.92 (1 H, ddd, $J_{2'ax,3'ax}$ 11.0, $J_{2'ax,3'eq}$ 2.4 and $J_{2',5F}$ 2.3, 2′-H_{ax}), 7.34–7.44 (6 H, m, Ph), 7.52 (1 H, d, $J_{6,5F}$ 6.3, 6-H), 7.70–7.75 (4 H, m, Ph), 8.45 (1 H, br s, NH).

δ_C (100 MHz; $CDCl_3$): 17.8 (CH_2, C-4′), 18.0 (CH_2, C-10′), 19.2 (C, $OSiPh_2{}^tBu$), 26.4 (CH_2, C-9′), 26.7 (CH_3, $OSiPh_2{}^tBu$), 30.2 (CH_2, C-3′), 34.6 (CH_2, C-5′ or C-11′), 34.8 (CH_2, C-5′ or C-11′), 67.0 (CH_2, 8′-CH_2O), 70.8 (CH, C-8′), 77.2 (CH, C-2′), 99.3 (C, C-6′), 124.6 (CH, d, $J_{6,5F}$ 33.6, C-6), 127.6 (CH, Ph), 129.5 (CH, Ph), 129.5 (CH, Ph), 133.7 (C, Ph), 135.7 (CH, Ph), 140.3 (C, d, $J_{5,5F}$ 236.5, C-5), 148.2 (C, C-2), 156.6 (C, $J_{4,5F}$ 26.7, C-4).

δ_F (282 MHz; $CFCl_3$): -165.8 (CF, F-5).

***m/z* (FAB):** 553 (MH^+, 4%), 495 (M – ^{t}Bu, 23), 475 (M – Ph, 7), 423 ($C_{26}H_{35}O_3Si$, 48), 207 (20), 199 (45), 197 (42), 169 (22), 135 (100), 121 (33), 105 (26), 89 (41).

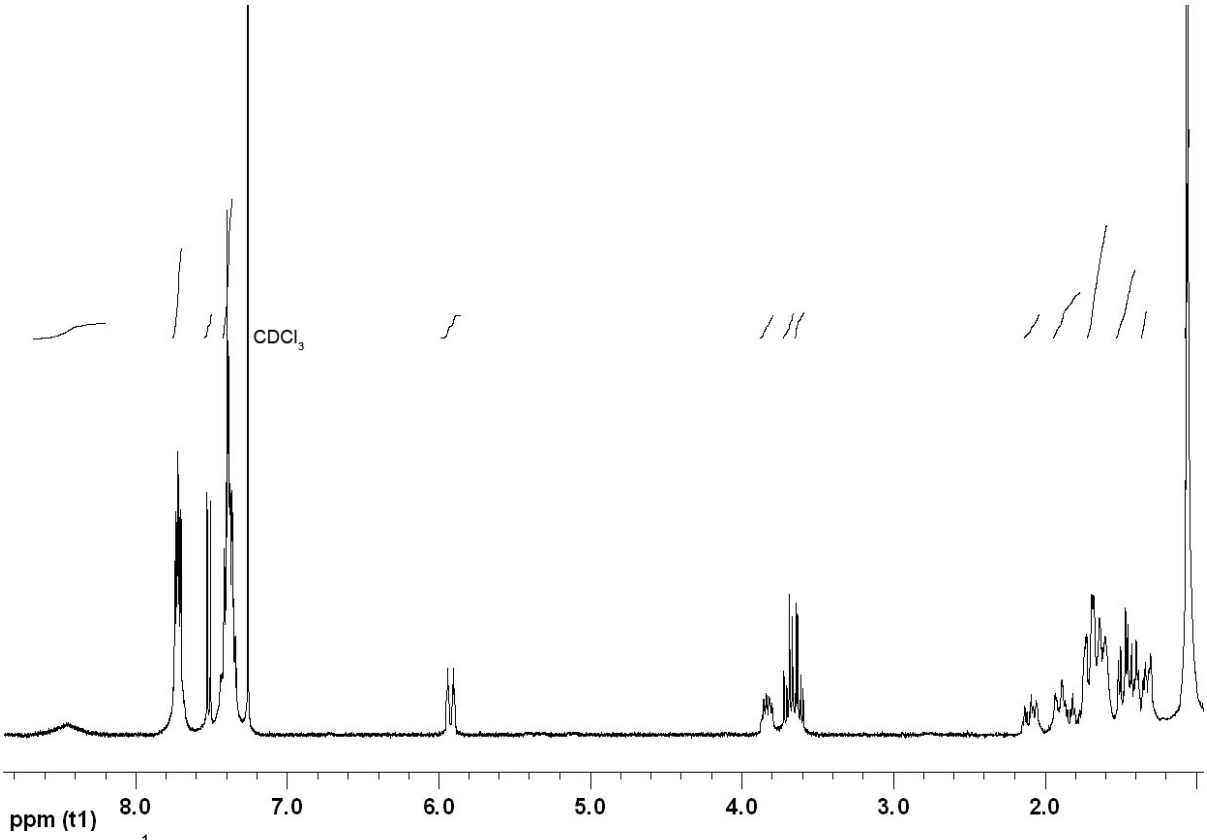

Figure 7.45: ^{1}H NMR spectrum (300 MHz; $CDCl_3$) of fluorouridine **902e**.

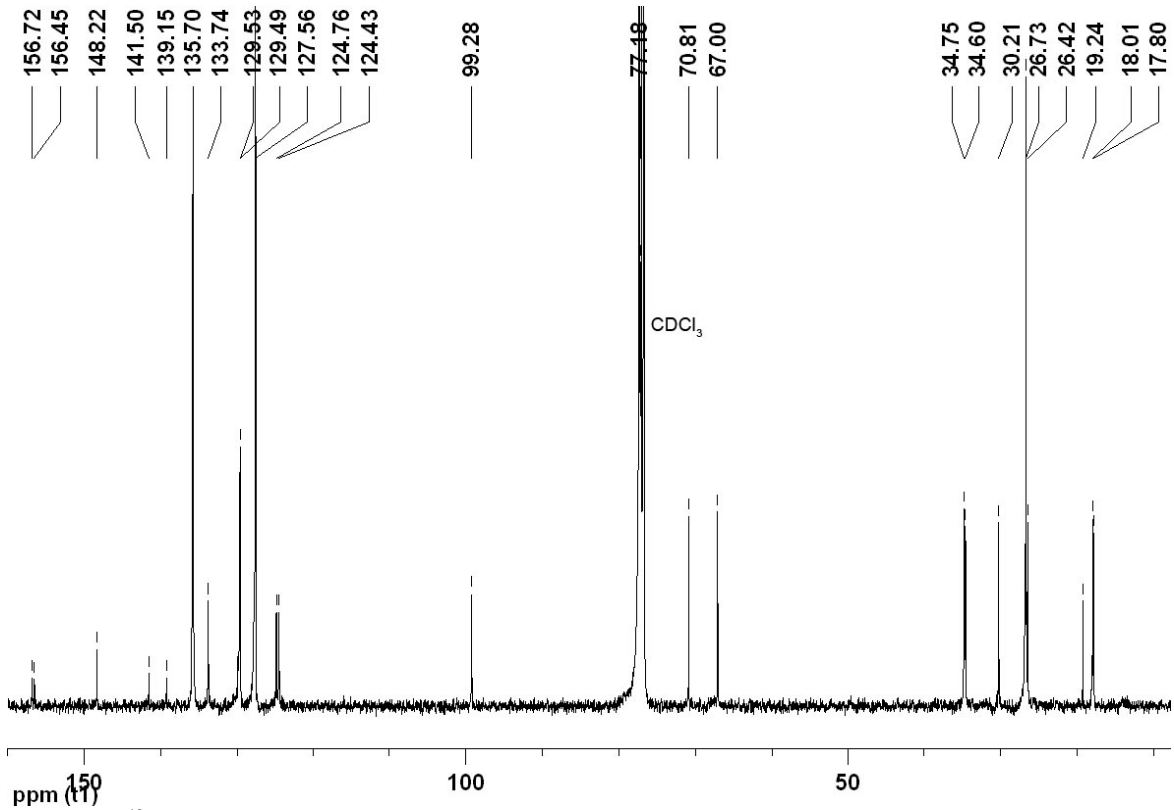

Figure 7.46: ^{13}C NMR spectrum (100 MHz; $CDCl_3$) of fluorouridine **902e**.

6-*N*-Benzoyl-9-{(2′*S,6′*S**,8′*S**)-8′-(*tert*-butyldiphenylsilyloxymethyl)-1′,7′-dioxaspiro[5.5]undecan-2′-yl}adenosine (902f)**

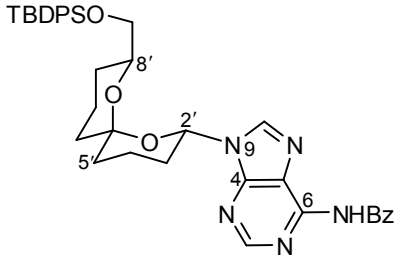

Method B: The *title compound* **902f** (14.5 mg, 35%) was prepared as a pale yellow oil from 6-*N*-benzoyladenine (19.3 mg, 80.8 μmol), acetate **861** (30.0 mg, 62.2 μmol) and TIPSOTf (167 μL, 86.9 μmol) using the general procedure (method B) described above. Purification was carried out by flash chromatography (twice) using hexane–EtOAc (19:1, 9:1 to 1:1) as eluent.

HRMS (FAB): found MH^+, 662.3162, $C_{38}H_{44}N_5O_4Si$ requires 662.3163.

ν_{max} (film)/cm^{-1}: 3070 (N–H), 2929 (C–H), 1696 (C=O), 1610, 1582, 1256, 1112 (C–O), 980, 704.

δ_H (400 MHz; $CDCl_3$): 1.09 (9 H, s, OSiPh$_2$*^{t}Bu*), 1.28–1.34 (1 H, m, 9′-H$_A$), 1.46–1.54 (1 H, m, 11′-H$_A$), 1.55–1.66 (3 H, m, 5′-H$_A$, 9′-H$_B$ and 10′-H$_A$), 1.73–1.85 (4 H, m, 4′-H$_A$, 5′-H$_B$, 10′-H$_B$ and 11′-H$_B$), 2.02–2.11 (1 H, m, 3′-H$_A$), 2.12–2.18 (1 H, m, 3′-H$_B$), 2.19–2.28 (1 H, m, 4′-H$_B$), 3.68 (1 H, dd, J_{AB} 10.4 and $J_{8'\text{-}CH_2,8'}$ 4.3, 8′-*CH$_A$*H$_B$O), 3.77 (1 H, dd, J_{AB} 10.4 and $J_{8'CH_2\text{-}8'}$ 6.2, 8′-CH$_A$*H$_B$*O), 4.05–4.11 (1 H, m, 8′-H), 6.22 (1 H, dd, $J_{2'ax,3'ax}$ 11.1 and $J_{2'ax,3'eq}$ 2.6, 2′-H$_{ax}$), 7.36–7.44 (6 H, m, OSi*Ph*$_2$^{t}Bu), 7.53 (2 H, t, *J* 7.4, COPh), 7.62 (1 H, t, *J* 7.4 COPh), 7.74–7.80 (4 H, m, OSi*Ph*$_2$^{t}Bu), 8.05 (2 H, d, *J* 7.4, COPh), 8.22 (1 H, s, 8-H), 8.78 (1 H, s, 2-H), 9.05 (1 H, s, NH).

δ_C (100 MHz; $CDCl_3$): 18.1 (CH$_2$, C-10′), 18.2 (CH$_2$, C-4′), 19.3 (C, OSiPh$_2$*^{t}Bu*), 26.6 (CH$_2$, C-9′), 26.8 (CH$_3$, OSiPh$_2$*^{t}Bu*), 30.8 (CH$_2$, C-3′), 34.6 (CH$_2$, C-5′), 34.7 (CH$_2$, C-11′), 67.2 (CH$_2$, 8′-CH$_2$O), 71.0 (CH, C-8′), 76.4 (CH, C-2′), 98.9 (C, C-6′), 123.0 (CH, C-5), 127.6 (CH, OSi*Ph*$_2$^{t}Bu), 127.9 (CH, CO*Ph*), 128.8 (CH, CO*Ph*), 129.5 (CH, OSi*Ph*$_2$^{t}Bu), 129.6 (CH, OSi*Ph*$_2$^{t}Bu), 132.7 (CH, CO*Ph*), 133.8 (2 x C, OSi*Ph*$_2$^{t}Bu and CO*Ph*), 135.7 (CH, OSi*Ph*$_2$^{t}Bu), 141.1 (CH, C-8), 149.3 (C, C-6), 151.7 (C, C-4), 152.6 (CH, C-2), 164.7 (C, *C*OPh).

***m/z* (FAB):** 662 (MH^+, 6%), 604 (M – ^{t}Bu, 5), 584 (M – Ph, 1), 423 ($C_{26}H_{35}O_3Si$, 3), 240 (100), 199 (12), 197 (15), 135 (41), 105 (29).

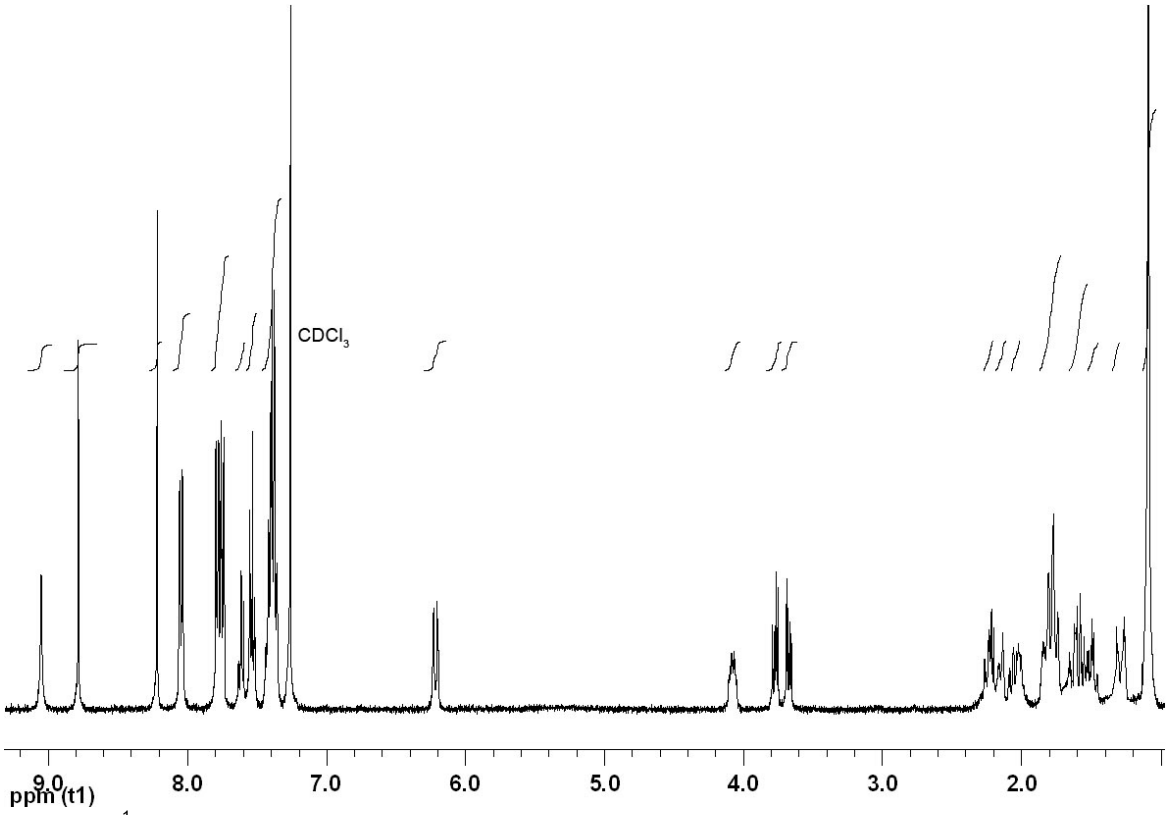

Figure 7.47: ^{1}H NMR spectrum (400 MHz; $CDCl_3$) of benzoyladenosine **902f**.

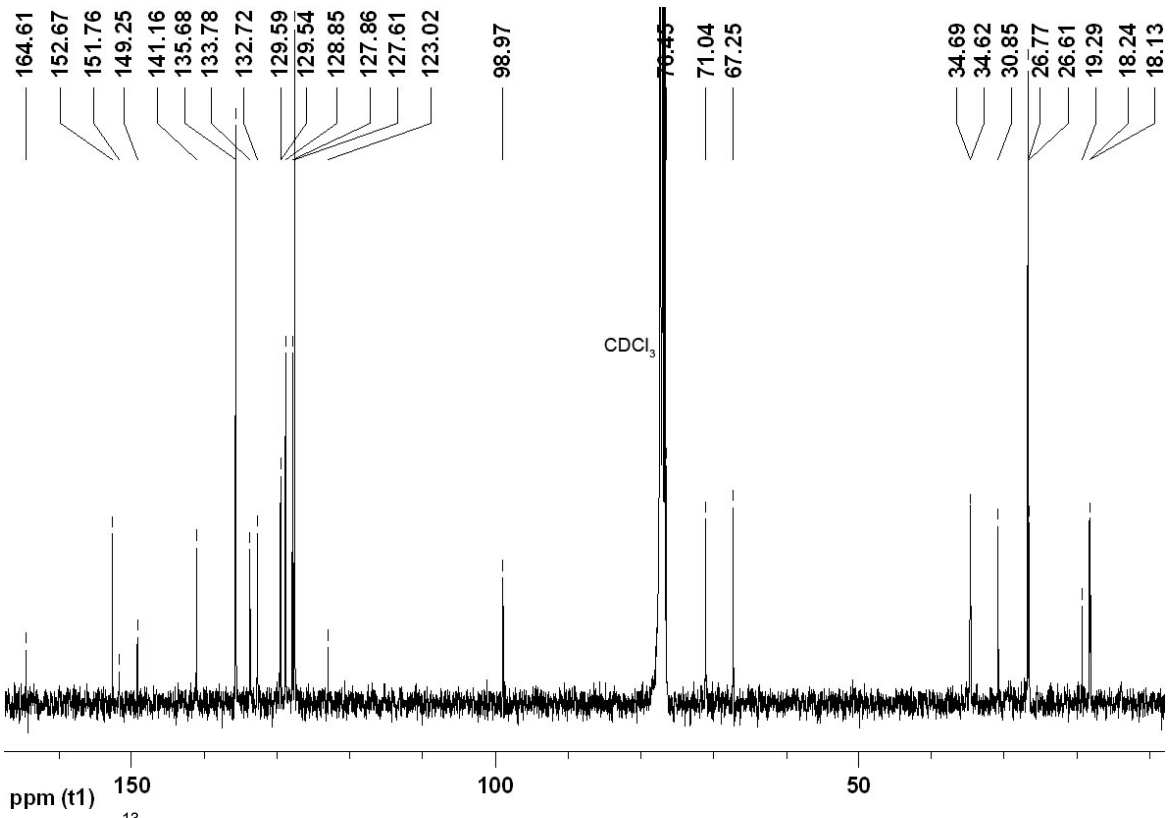

Figure 7.48: ^{13}C NMR spectrum (100 MHz; $CDCl_3$) of benzoyladenosine **902f**.

2-*N*-Acetyl-9-{(2′*S,6′*S**,8′*S**)-8′-(*tert*-butyldiphenylsilyloxymethyl)-1′,7′-dioxaspiro[5.5]undecan-2′-yl}guanosine (902g) and (2*S**,6*S**,8*S**)-2-*N*-Acetyl-7-{8′-(*tert*-butyldiphenylsilyloxymethyl)-1′,7′-dioxaspiro[5.5]undecan-2′-yl}guanosine (902h)**

Major isomer:
N9-Guanosine
902g

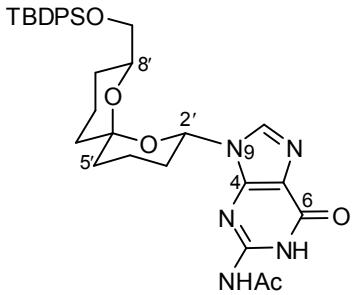

Minor isomer:
N7-Guanosine
902h

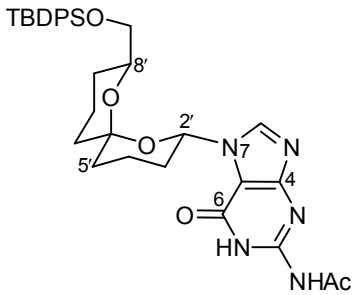

Method B: The *title N9-guanosine* **902g** (7.72 mg, 20%) and *N7-guanosine* **902h** (3.98 mg, 11%) were prepared as colourless oils from 2-*N*-acetylguanine (15.6 mg, 80.8 μmol), acetate **861** (30.0 mg, 62.2 μmol) and TIPSOTf (167 μL, 87.1 μmol) using the general procedure (method B) described above. Purification was carried out by flash chromatography using hexane–EtOAc (19:1, 3:2, 1:4 to 0:1) as eluent followed by PLC using hexane–EtOAc (1:1) as eluent.

N9-Guanosine **902g**:

HRMS (FAB): found MH^+, 616.2958, $C_{33}H_{42}N_5O_5Si$ requires 616.2955.

ν_{max} (film)/cm^{-1}: 3148 (N–H), 3049 (N–H), 2932 (C–H), 1682 (C=O), 1613, 1556, 1257, 1233, 1112 (C–O), 979, 703.

δ_H (300 MHz; $CDCl_3$): 1.13 (9 H, s, $OSiPh_2{}^tBu$), 1.29–1.34 (1 H, m, 9′-H_A), 1.46–1.66 (4 H, m, 5′-H_A, 9′-H_B, 10′-H_A and 11′-H_A), 1.73–1.89 (4 H, m, 4′-H_A, 5′-H_B, 10′-H_B and 11′-H_B), 1.80 (3 H, s, $COCH_3$), 1.90–2.02 (2 H, m, 3′-H), 2.16–2.30 (1 H, m, 4′-H_B), 3.69 (1 H, dd, J_{AB} 10.4 and $J_{8'\text{-}CH_2,8'}$ 3.7, 8′-CH_AH_BO), 3.80 (1 H, dd, J_{AB} 10.4 and $J_{8'CH_2\text{-}8'}$ 7.2, 8′-CH_AH_BO), 3.94–4.03 (1 H, m, 8′-H), 6.00 (1 H, dd, $J_{2'ax,3'ax}$ 10.6 and $J_{2'ax,3'eq}$ 2.6, 2′-H_{ax}), 7.34–7.44 (6 H, m, Ph), 7.50 (1 H, br s, NH), 7.74–7.80 (4 H, m, Ph), 7.90 (1 H, br s, 8-H), 11.76 (1 H, br s, NH).

δ_C (75 MHz; $CDCl_3$): 18.0 (CH_2, C-10′), 18.3 (CH_2, C-4′), 19.5 (C, $OSiPh_2{}^tBu$), 24.0 (CH_3, $COCH_3$), 26.6 (CH_2, C-9′), 27.0 (CH_3, $OSiPh_2{}^tBu$), 31.5 (CH_2, C-3′), 34.5 (CH_2, C-5′), 34.6 (CH_2, C-11′), 67.7 (CH_2, 8′-CH_2O), 71.1 (CH, C-8′), 76.0 (CH, C-2′), 98.8 (C, C-6′), 121.1 (C, C-5), 127.9 (CH, Ph), 129.9 (CH, Ph), 133.9 (C, Ph), 134.3 (C, Ph), 135.4 (CH, Ph), 137.1 (CH, C-8), 146.6 (C, C-2), 147.5 (C, C-4), 155.5 (C, C-6), 170.8 (C, N*C*OMe).

***m/z* (FAB):** 616 (MH^+, 15%), 538 (M – Ph, 1), 423 ($C_{26}H_{35}O_3Si$, 51), 207 (32), 198 (28), 194 (100), 136 (43), 135 (87), 121 (17), 91 (15).

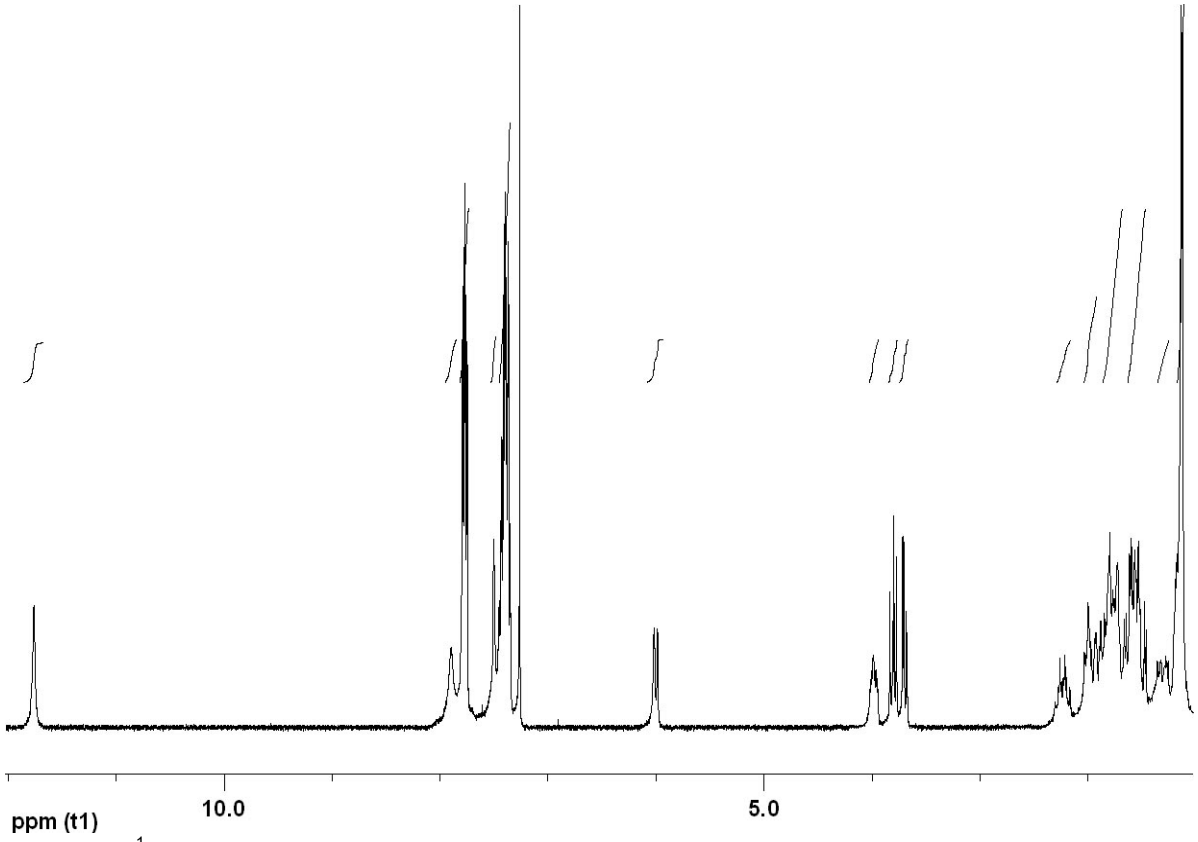

Figure 7.49: ^{1}H NMR spectrum (300 MHz; $CDCl_3$) of N9-guanosine **902g**.

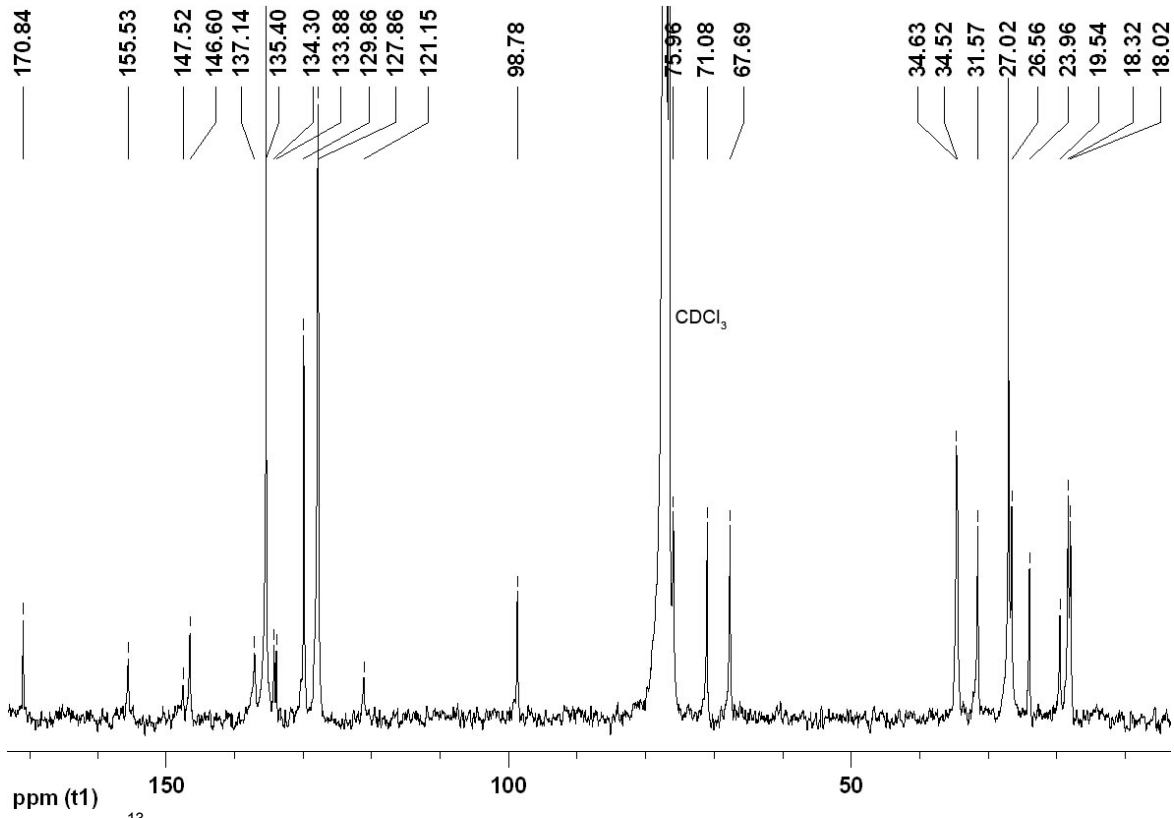

Figure 7.50: ^{13}C NMR spectrum (100 MHz; $CDCl_3$) of N9-guanosine **902g**.

N7-Guanosine **902h**:

HRMS (FAB): found MH^+, 616.2949, $C_{33}H_{42}N_5O_5Si$ requires 616.2955.

ν_{max} (film)/cm^{-1}: 3134 (N–H), 3070 (N–H), 2931 (C–H), 1694 (C=O), 1621, 1547, 1257, 1212, 1112 (C–O), 981, 703.

δ_H (300 MHz; $CDCl_3$): 1.07 (9 H, s, $OSiPh_2{}^tBu$), 1.42–1.50 (1 H, m, 9′-H_A), 1.52–1.70 (4 H, m, 5′-H_A, 9′-H_B, 10′-H_A and 11′-H_A), 1.70–1.89 (5 H, m, 3′-H_A, 4′-H_A, 5′-H_B, 10′-H_B and 11′-H_B), 2.14–2.35 (2 H, m, 3′-H_B and 4′-H_B), 2.38 (3 H, s, $COCH_3$), 3.70 (1 H, dd, J_{AB} 10.4 and $J_{8'\text{-}CH_2,8'}$ 4.7, 8′-CH_AH_BO), 3.78 (1 H, dd, J_{AB} 10.4 and $J_{8'CH_2\text{-}8'}$ 4.8, 8′-CH_AH_BO), 3.85–4.92 (1 H, m, 8′-H), 6.11 (1 H, dd, $J_{2'_{ax},3'_{ax}}$ 10.8 and $J_{2'_{ax},3'_{eq}}$ 2.1, 2′-H_{ax}), 7.34–7.43 (6 H, m, Ph), 7.70–7.78 (4 H, m, Ph), 8.05 (1 H, s, 8-H), 10.87 (1 H, br s, NH). 12.23 (1 H, br s, NH),

δ_C (75 MHz; $CDCl_3$): 17.9 (CH_2, C-4′), 18.1 (CH_2, C-10′), 19.3 (C, $OSiPh_2{}^tBu$), 24.6 (CH_3, $COCH_3$), 26.6 (CH_2, C-9′), 26.8 (CH_3, $OSiPh_2{}^tBu$), 32.4 (CH_2, C-3′), 34.7 (CH_2, C-5′), 34.9 (CH_2, C-11′), 67.0 (CH_2, 8′-CH_2O), 70.8 (CH, C-8′), 79.5 (CH, C-2′), 99.1 (C, C-6′), 111.3 (C, C-5), 127.6 (CH, Ph), 129.5 (CH, Ph), 133.8 (C, Ph), 135.7 (CH, Ph), 135.7 (CH, Ph), 141.0 (CH, C-8), 147.8 (C, C-2), 152.6 (C, C-6), 156.8 (C, C-4), 173.0 (C, N*CO*Me).

***m/z* (FAB):** 616 (MH^+, 9%), 558 (12), 538 (M – Ph, 3), 423 ($C_{26}H_{35}O_3Si$, 17), 405 (19), 207 (17), 197 (21), 194 (100), 136 (33), 135 (65), 121 (10), 91 (10).

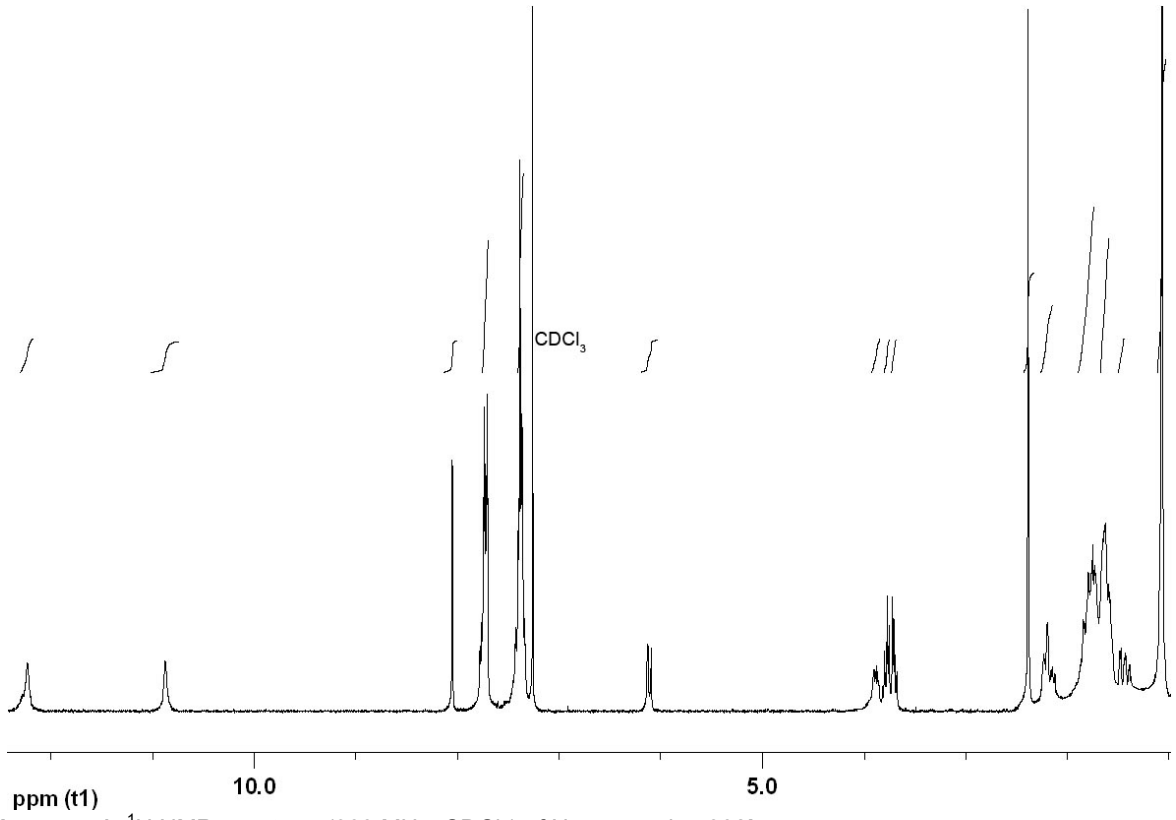

Figure 7.51: ^{1}H NMR spectrum (300 MHz; $CDCl_3$) of N7-guanosine **902h**

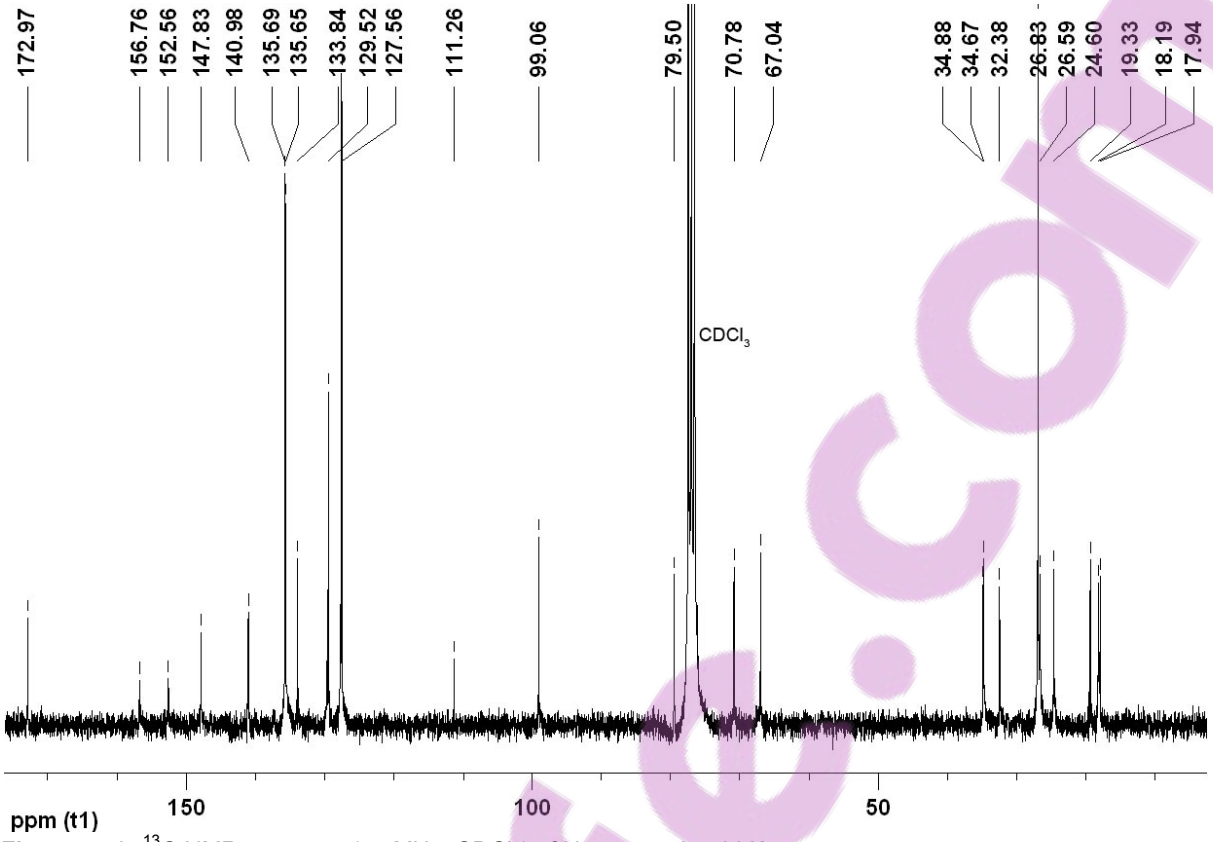

Figure 7.52: ^{13}C NMR spectrum (75 MHz; $CDCl_3$) of N7-guanosine **902h**.

7.3.6 Synthesis of Spiroacetal-Triazoles 909

General Procedures for 1,3-Dipolar Cycloaddition of Azide 860a to Alkynes[29]

Method A: For Terminal Alkynes with Catalysis by CuI•[P(OEt)$_3$]

This procedure is an adaptation of that reported by Vargas-Berenguel *et al.*[17]

To a solution of azide **860a** and alkyne (50.0–100 μL) in anhydrous toluene (250–500 μL) under an atmosphere of argon was added CuI•[P(OEt)$_3$] (0.10–0.12 equiv.). The resulting mixture was heated to reflux for 1 h. After cooling to room temperature, the mixture was purified directly by flash chromatography using hexane–EtOAc as eluent to give the spiroacetal containing a 1,4-disubstituted triazole substituent.

Method B: For Symmetrical Internal Alkynes

A solution of azide **860a** and alkyne (100 μL) in anhydrous toluene (500 μL) was heated to reflux for 1 h. The reaction mixture was purified directly by flash chromatography using hexane–EtOAc as eluent to give the spiroacetal containing a 1,4,5-trisubstituted triazole substituent.

Method C: For Internal Trimethylsilylacetylene

This procedure is an adaptation of that reported by Hlasta *et al.*[30]

A solution of azide **860a** and trimethylsilylacetylene (50.0–100 μL) in anhydrous toluene (500 μL) was heated at 110 °C in a sealed vessel. If the cycloaddition was not complete in 18 h (TLC), a second portion of trimethylsilylacetylene (50.0–100 μL) was added and the mixture was heated at 110 °C overnight. The reaction mixture was purified directly by flash chromatography using hexane–EtOAc as eluent to give the spiroacetal containing a 1,4,5-trisubstituted triazole substituent.

4-[2″-(Benzyloxy)ethyl]-1-{(2′*S,6′*S**,8′*S**)-8′-(*tert*-butyldiphenylsilyloxymethyl)-1′,7′-dioxaspiro[5.5]undecan-2′-yl}-1*H*-1,2,3-triazole (909a)**

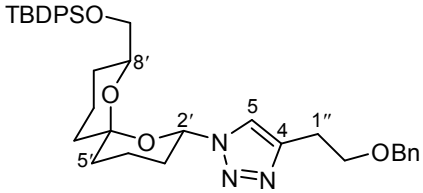

Method A: The *title compound* **909a** (39.3 mg, 98%) was prepared as a pale yellow oil from azide **860a** (30.0 mg, 64.4 μmmol), 1-(benzyloxy)but-3-yne **(821)** (100 μL) and CuI•[P(OEt)$_3$] (2.53 mg, 7.10 μmol) in toluene (500 μL) using the general procedure (method A) described above. Purification was carried out by flash chromatography using hexane–EtOAc (19:1, 7:3 to 1:1) as eluent.

HRMS (FAB): found MH$^+$, 626.3413, $C_{37}H_{48}N_3O_4Si$ requires 626.3414.

ν_{max} (film)/cm^{-1}: 2931 (C–H), 1455, 1427, 1222 (C–O), 1112 (C–O), 979, 702.

δ_H (400 MHz; CDCl$_3$): 1.06 (9 H, s, OSiPh$_2$^{t}*Bu*), 1.25–1.31 (1 H, m, 9′-H$_A$), 1.42–1.51 (1 H, m, 11′-H$_A$), 1.54–1.62 (3 H, m, 5′-H$_A$, 9′-H$_B$ and 10′-H$_B$), 1.70–1.81 (3 H, m, 4′-H$_A$, 5′-H$_B$ and 11′-H$_B$), 1.81–1.96 (2 H, m, 3′-H$_A$ and 10′-H$_B$), 2.05–2.18 (2 H, m, 3′-H$_B$ and 4′-H$_B$), 3.08 (2 H, t, $J_{1'',2''}$ 6.7, 1″-H), 3.63 (1 H, dd, J_{AB} 10.5 and $J_{8'\text{-}CH_2,8'}$ 4.0, 8′-*CH$_A$*H$_B$O), 3.72 (1 H, dd, J_{AB} 10.5 and $J_{8'CH_2,8'}$ 6.3, 8′-CH$_A$*H$_B$*O), 3.79 (2 H, t, $J_{2'',1''}$ 6.7, 2″-H), 3.87–3.94 (1 H, m, 8′-H), 4.55 (2 H, s, O*CH$_2$*Ph), 6.01 (1 H, dd, $J_{2'ax,3'ax}$ 11.1 and $J_{2'ax,3'eq}$ 2.4, 2′-H$_{ax}$), 7.27–7.34 (5 H, m, OCH$_2$*Ph*), 7.34–7.43 (6 H, m, OSi*Ph$_2$*^{t}Bu), 7.54 (1 H, s, 5-H), 7.72–7.75 (4 H, m, OSi*Ph$_2$*^{t}Bu).

δ_C (75 MHz; CDCl$_3$): 18.0 (CH$_2$, C-4′), 18.1 (CH$_2$, C-10′), 19.2 (C, OSiPh$_2$^{t}*Bu*), 26.5 (CH$_2$, C-9′), 26.6 (CH$_2$, C-1″), 26.8 (CH$_3$, OSiPh$_2$^{t}*Bu*), 30.8 (CH$_2$, C-3′), 34.5 (CH$_2$, C-5′), 34.6 (CH$_2$, C-11′), 67.2 (CH$_2$, 8′-CH$_2$O), 69.1 (CH$_2$, C-2″), 71.0 (CH, C-8′), 73.0 (CH$_2$, O*CH$_2$*Ph), 81.0 (CH, C-2′), 98.8 (C, C-6′), 119.9 (CH, C-5), 127.6 (CH, OSi*Ph$_2$*^{t}Bu and OCH$_2$*Ph*), 127.6 (CH, OCH$_2$*Ph*), 128.4 (CH, OCH$_2$*Ph*), 129.5 (CH, OSi*Ph$_2$*^{t}Bu), 129.6 (CH, OSi*Ph$_2$*^{t}Bu), 133.6 (C, OSi*Ph$_2$*^{t}Bu), 133.7 (C, OSi*Ph$_2$*^{t}Bu), 135.6 (CH, OSi*Ph$_2$*^{t}Bu), 135.6 (CH, OSi*Ph$_2$*^{t}Bu), 138.2 (C, OCH$_2$*Ph*), 144.8 (C, C-4).

***m/z* (FAB):** 626 (MH$^+$, 6%), 423 ($C_{26}H_{35}O_3Si$, 55), 405 (31), 386 (M – OSiPh$_2$^{t}Bu, 8), 239 (SiPh$_2$^{t}Bu, 12), 207 (54), 204 (51), 197 (35), 154 (19), 135 (100), 105 (22), 91 (83).

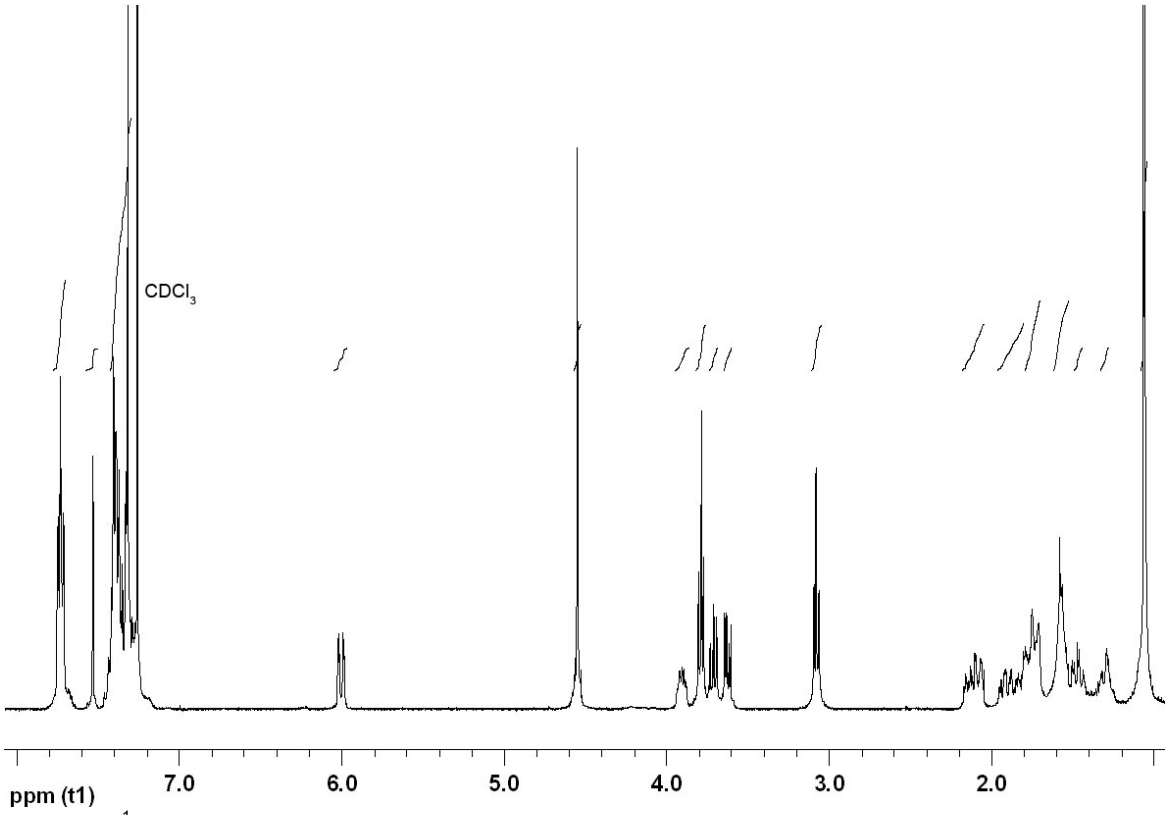

Figure 7.53: ^{1}H NMR spectrum (400 MHz; $CDCl_3$) of triazole **909a**.

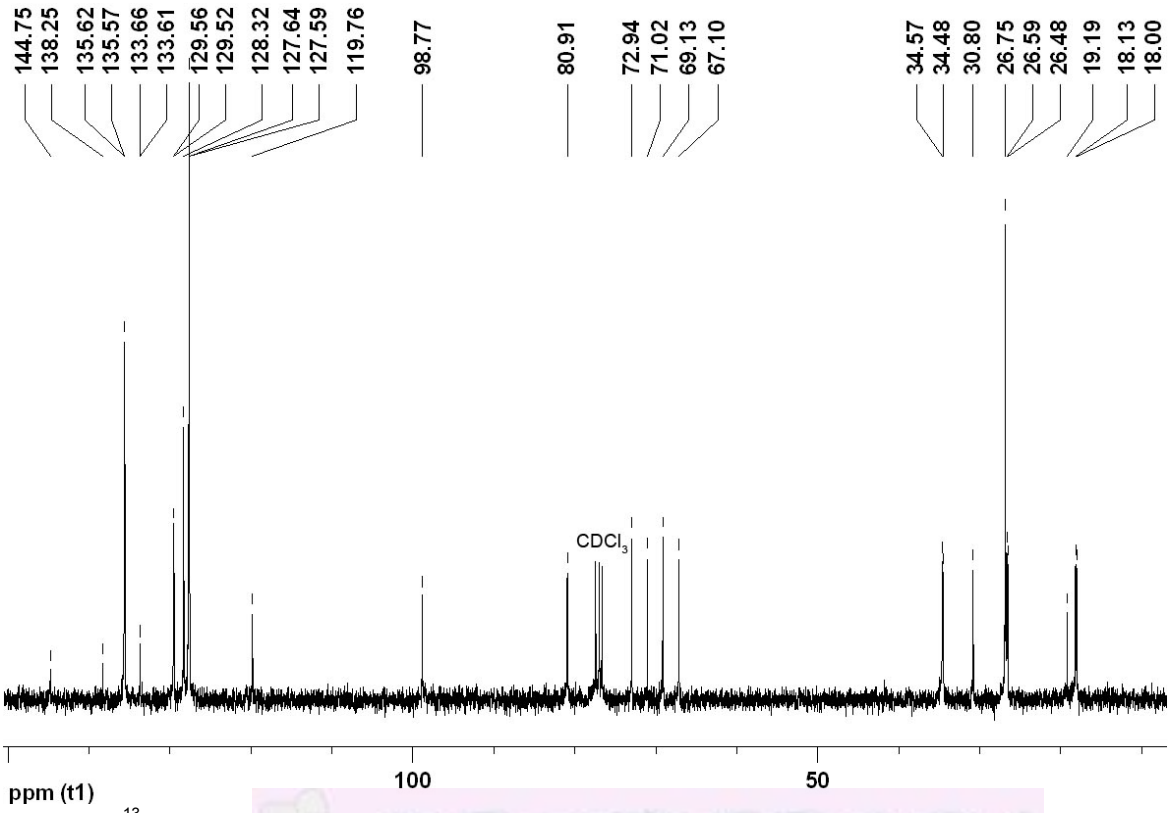

Figure 7.54: ^{13}C NMR spectrum (75 MHz; $CDCl_3$) of triazole **909a**.

1-{(2′*S,6′*S**,8′*S**)-8′-(*tert*-Butyldiphenylsilyloxymethyl)-1′,7′-dioxaspiro[5.5]undecan-2-yl}-4-(triethylsilyloxymethyl)-1*H*-1,2,3-triazole (909b)**

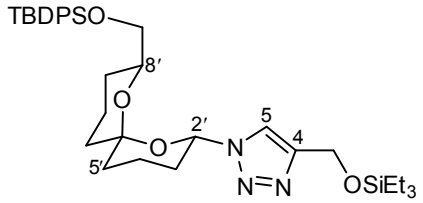

Method A: The *title compound* **909b** (1.20 mg, 4%) and the deprotected hydroxymethyl-triazole **909c** (1.00 mg, 4%) were prepared as pale yellow oils from azide **860a** (20.0 mg, 42.9 μmol), 1-(triethylsilyloxy)prop-3-yne (60.0 μL) and CuI•[P(OEt)$_3$] (1.53 mg, 4.29 μmol) in toluene (300 μL) using the general procedure (method A) described above. Purification was carried out by flash chromatography using hexane–EtOAc (99:1 to 19:1) as eluent. Unreacted azide **860a** (12.0 mg, 60%) was also recovered.

HRMS (FAB): found MH$^+$, 636.3666, $C_{35}H_{54}N_3O_4Si_2$ requires 636.3653.

ν_{max} (film)/cm^{-1}: 2931 (C–H), 2856, 1428, 1388, 1222, 1202, 1113 (C–O), 1091, 1071 (C–O), 1026, 980, 702.

δ_H (300 MHz; CDCl$_3$): 0.69 (6 H, q, Si(CH_2CH$_3$)$_3$), 1.00 (9 H, t, Si(CH$_2$$CH_3$)$_3$), 1.09 (9 H, s, OSiPh^t*Bu*), 1.26–1.35 (1 H, m, 9′-H$_A$), 1.45–1.54 (1 H, m, 11′-H$_A$), 1.57–1.66 (3 H, m, 5′-H$_A$, 9′-H$_B$ and 10′-H$_A$), 1.74–1.87 (4 H, m, 4′-H$_A$, 5′-H$_B$, 10′-H$_B$ and 11′-H$_B$), 1.95–2.03 (1 H, m, 3′-H$_A$), 2.10–2.22 (2 H, m, 3′-H$_B$ and 4′-H$_B$), 3.65 (1 H, dd, J_{AB} 10.5 and $J_{8'\text{-}CH_2,8'}$ 4.2, 8′-CH_AH$_B$O), 3.74 (1 H, dd, J_{AB} 10.5 and $J_{8'\text{-}CH_2,8'}$ 6.4, 8′-CH$_A$$H_B$O), 3.91–3.98 (1 H, m, 8′-H), 4.90 (2 H, s, CH$_2$O), 6.06 (1 H, dd, $J_{2'ax,3'ax}$ 11.0 and $J_{2'ax,3'eq}$ 2.5, 2′-H$_{ax}$), 7.39–7.47 (6 H, m, Ph), 7.69 (1 H, s, 5-H), 7.74–7.88 (4 H, m, Ph).

δ_C (100 MHz; CDCl$_3$): 4.33 (CH$_2$, OSi[CH_2CH$_3$]$_3$), 6.71 (CH$_3$, OSi[CH$_2$$CH_3$]$_3$), 18.0 (CH$_2$, C-4′), 18.1 (CH$_2$, C-10′), 19.2 (C, OSiPh$_2$^{t}*Bu*), 26.5 (CH$_2$, C-9′), 26.8 (CH$_3$, OSiPh$_2$^{t}*Bu*), 30.8 (CH$_2$, C-3′), 34.5 (CH$_2$, C-5′), 34.6 (CH$_2$, C-11′), 57.5 (CH$_2$, CH$_2$O), 67.1 (CH$_2$, 8′-CH$_2$O), 71.1 (CH, C-8′), 81.0 (CH, C-2′), 98.9 (C, C-6′), 119.9 (CH, C-5), 127.6 (CH, Ph), 129.6 (CH, Ph), 129.6 (CH, Ph), 133.6 (C, Ph), 133.6 (C, Ph), 135.6 (CH, Ph), 135.7 (CH, Ph), 148.0 (C, C-4).

***m/z* (FAB):** 636 (MH$^+$, 1%), 578 (M – ^{t}Bu, 1), 423 ($C_{26}H_{35}O_3Si$, 56), 239 (SiPh$_2$^{t}Bu, 9), 207 (31), 199 (37), 197 (38), 137 (28), 135 (100).

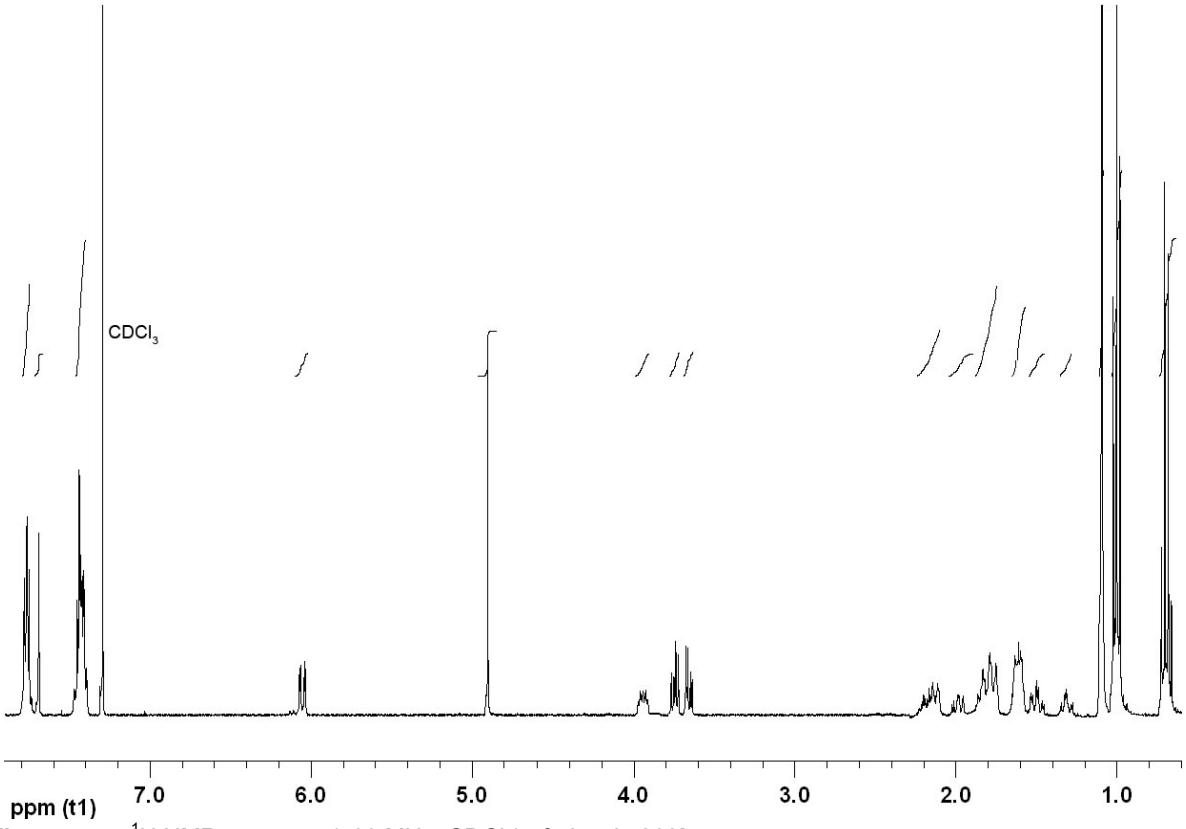

Figure 7.55: ^{1}H NMR spectrum (400 MHz; $CDCl_3$) of triazole **909b**.

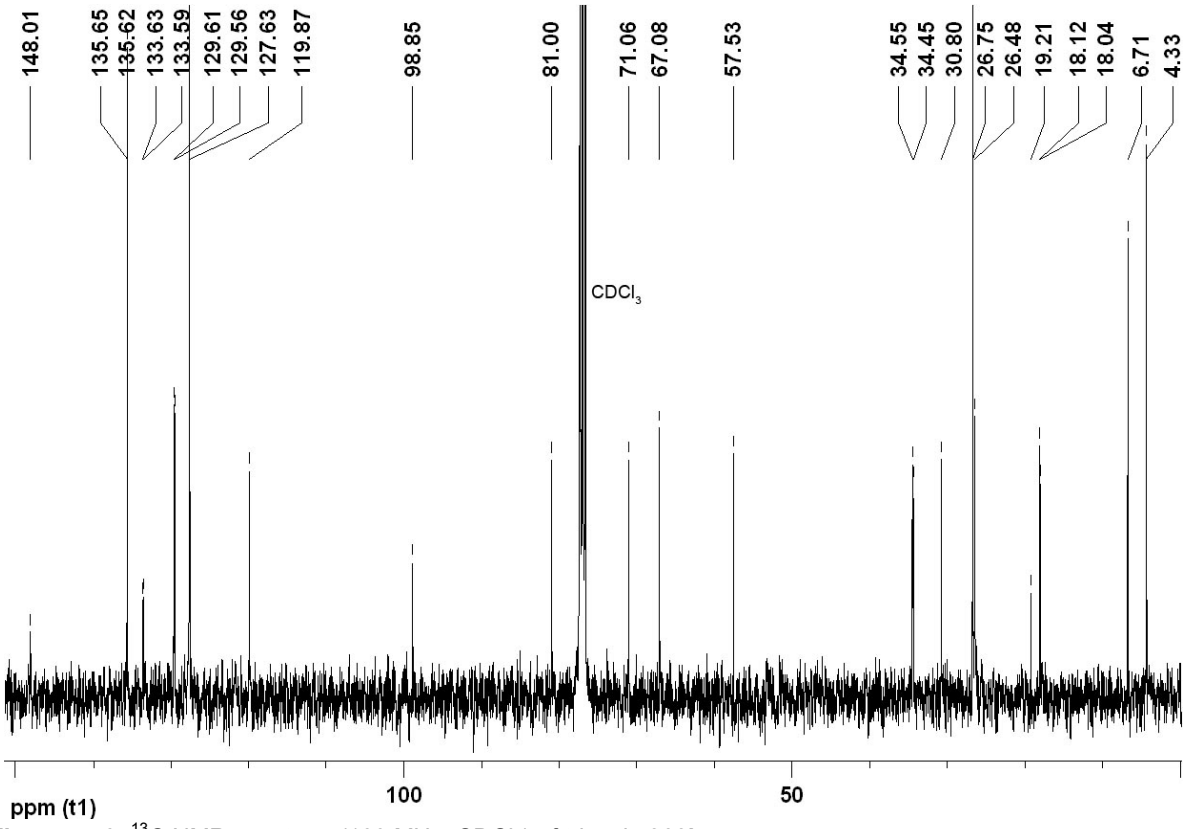

Figure 7.56: ^{13}C NMR spectrum (100 MHz; $CDCl_3$) of triazole **909b**.

1-{(2′*S,6′*S**,8′*S**)-8′-(*tert*-Butyldiphenylsilyloxymethyl)-1′,7′-dioxaspiro[5.5]undecan-2′-yl}-4-hydroxymethyl-1*H*-1,2,3-triazole (909c)**

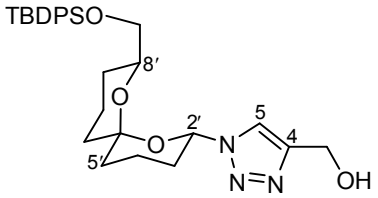

Method A: The *title compound* **909c** (13.9 mg, 83%) was prepared as a pale yellow oil from azide **860a** (15.0 mg, 32.2 μmol), prop-2-yn-1-ol (100 μL) and CuI•[P(OEt)$_3$] (1.15 mg, 3.22 μmol) in toluene (500 μL) using the general procedure (method A) described above. Purification was carried out by flash chromatography using hexane–EtOAc (9:1 to 3:2) as eluent.

HRMS (FAB): found MH$^+$, 522.2797, $C_{29}H_{40}N_3O_4Si$ requires 522.2788.

ν_{max} (film)/cm^{-1}: 3369 (O–H), 2930 (C–H), 2856, 1428, 1222, 1112 (C–O), 1091 (C–O), 980, 703.

δ_H (300 MHz; $CDCl_3$): 1.07 (9 H, s, OSiPh$_2$^{t}*Bu*), 1.29–1.36 (1 H, m, 9′-H$_A$), 1.41–1.51 (1 H, m, 11′-H$_A$), 1.51–1.64 (3 H, m, 5′-H$_A$, 9′-H$_B$ and 10′-H$_A$), 1.68–1.87 (5 H, m, 4′-H$_A$, 5′-H$_B$, 10′-H$_B$, 11′-H$_B$ and OH), 1.87–1.99 (1 H, m, 3′-H$_A$), 2.07–2.21 (2 H, m, 3′-H$_B$ and 4′-H$_B$), 3.63 (1 H, dd, J_{AB} 10.5 and $J_{8'\text{-}CH_2,8'}$ 4.2, 8′-C*H$_A$*H$_B$O), 3.83 (1 H, dd, J_{AB} 10.5 and $J_{8'\text{-}CH_2,8'}$ 6.3, 8′-CH$_A$*H$_B$*O), 3.84–3.95 (1 H, m, 8′-H), 4.82 (2 H, s, 4-*CH$_2$*OH), 6.03 (1 H, dd, $J_{2'ax,3'ax}$ 11.0 and $J_{2'ax,3'eq}$ 2.4, 2′-H$_{ax}$), 7.34–7.45 (6 H, m, Ph), 7.68 (1 H, s, 5-H), 7.70–7.76 (4 H, m, Ph).

δ_C (75 MHz; $CDCl_3$): 18.0 (CH$_2$, C-4′), 18.2 (CH$_2$, C-10′), 19.2 (C, OSiPh$_2$^{t}*Bu*), 26.5 (CH$_2$, C-9′), 26.8 (CH$_3$, OSiPh$_2$^{t}*Bu*), 30.9 (CH$_2$, C-3′), 34.5 (CH$_2$, C-5′), 34.6 (CH$_2$, C-11′), 56.7 (CH$_2$, 4-CH$_2$OH), 67.1 (CH$_2$, 8′-CH$_2$O), 71.2 (CH, C-8′), 81.2 (CH, C-2′), 98.9 (C, C-6′), 119.9 (CH, C-5), 127.6 (CH, Ph), 129.6 (CH, Ph), 129.6 (CH, Ph), 133.6 (C, Ph), 133.7 (C, Ph), 135.6 (CH, Ph), 135.6 (CH, Ph), 147.2 (C, C-4).

***m/z* (FAB):** 522 (MH$^+$, 3%), 464 (M – ^{t}Bu, 7), 423 ($C_{26}H_{35}O_3Si$, 82), 365 (11), 239 (SiPh$_2$^{t}Bu, 9), 207 (31), 199 (38), 197 (35), 137 (29), 135 (100).

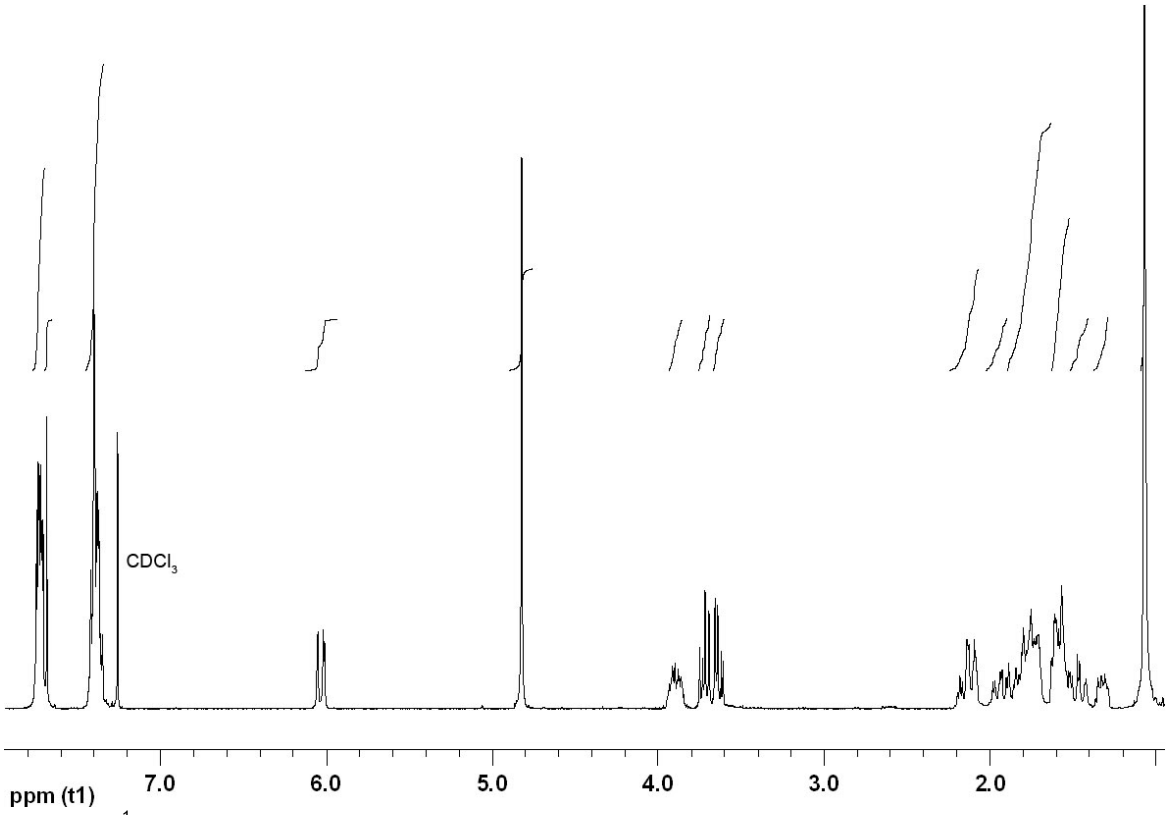

Figure 7.57: ^{1}H NMR spectrum (300 MHz; $CDCl_3$) of triazole **909c**.

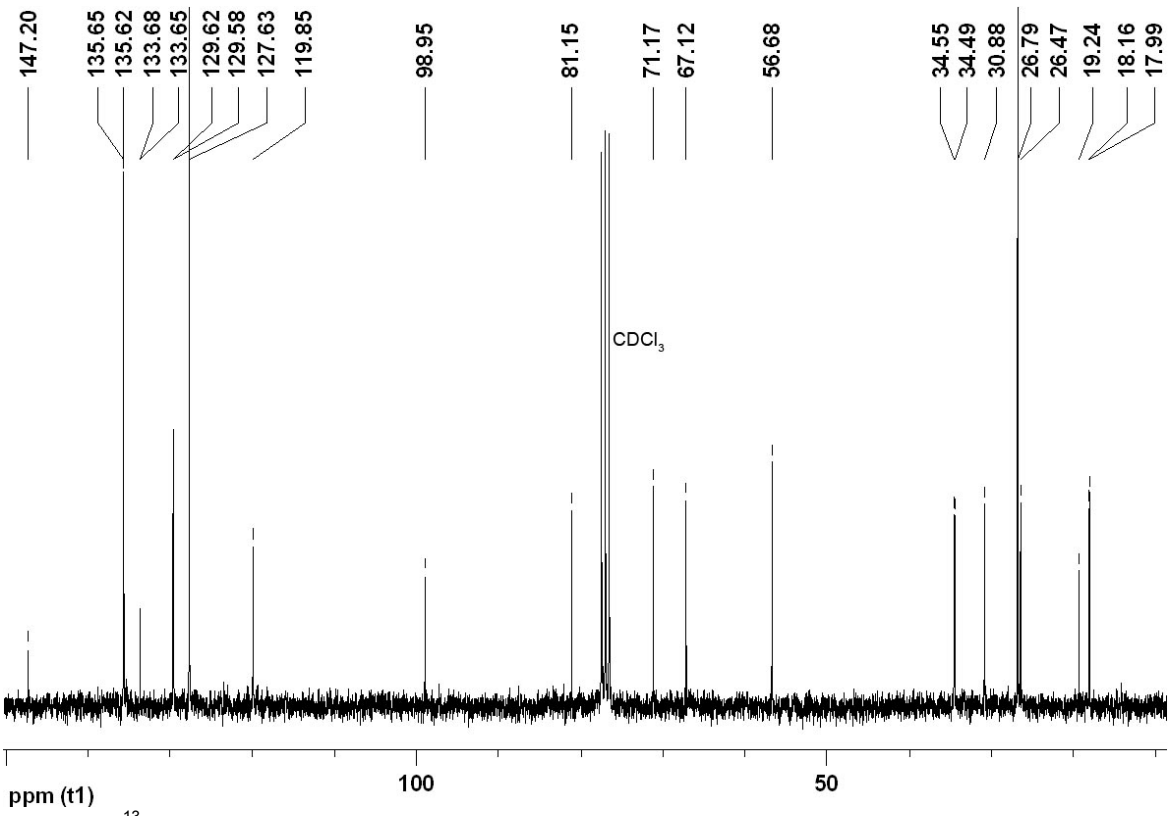

Figure 7.58: ^{13}C NMR spectrum (75 MHz; $CDCl_3$) of triazole **909c**.

1-{(2′*S,6′*S**,8′*S**)-8′-(*tert*-Butyldiphenylsilyloxymethyl)-1′,7′-dioxaspiro[5.5]undecan-2′-yl}-4-phenyl-1*H*-1,2,3-triazole (909d)**

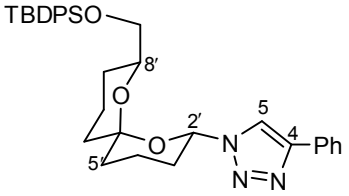

Method A: The *title compound* **909d** (14.2 mg, 96%) was prepared as a pale yellow oil from azide **860a** (12.0 mg, 25.8 μmol), phenylacetylene (50.0 μL) and CuI•[P(OEt)$_3$] (1.07 mg, 3.00 μmol) in toluene (250 μL) using the general procedure (method A) described above. Purification was carried out by flash chromatography using hexane–EtOAc (99:1 to 19:1) as eluent.

HRMS (FAB): found MH$^+$, 568.3001, $C_{34}H_{42}N_3O_3Si$ requires 568.2996.

ν_{max} (film)/cm^{-1}: 2932 (C–H), 2857, 1428, 1390, 1220, 1112 (C–O), 1074 (C–O), 1024, 979, 702.

δ_H (300 MHz; $CDCl_3$): 1.08 (9 H, s, OSiPh$_2$^{t}*Bu*), 1.27–1.34 (1 H, m, 9′-H$_A$), 1.44–1.55 (1 H, m, 11′-H$_A$), 1.56–1.65 (3 H, m, 5′-H$_A$, 9′-H$_B$ and 10′-H$_A$), 1.73–1.89 (4 H, m, 4′-H$_A$, 5′-H$_B$, 10′-H$_B$ and 11′-H$_B$), 1.92–2.04 (1 H, m, 3′-H$_A$), 2.10–2.26 (2 H, m, 3′-H$_B$ and 4′-H$_B$), 3.65 (1 H, dd, J_{AB} 10.5 and $J_{8'\text{-}CH_2,8'}$ 4.2, 8′-*CH$_A$*H$_B$O), 3.74 (1 H, dd, J_{AB} 10.5 and $J_{8'\text{-}CH_2,8'}$ 6.3, 8′-CH$_A$*H$_B$*O), 3.89–3.98 (1 H, m, 8′-H), 6.01 (1 H, dd, $J_{2'ax,3'ax}$ 11.1 and $J_{2'ax,3'eq}$ 2.4, 2′-H$_{ax}$), 7.32–7.47 (9 H, m, OSi*Ph*$_2$^{t}Bu and Ph), 7.72–7.78 (4 H, m, OSi*Ph*$_2$^{t}Bu), 7.84–7.89 (2 H, m, Ph), 7.90 (1 H, s, 5-H).

δ_C (75 MHz; $CDCl_3$): 18.0 (CH$_2$, C-4′), 18.2 (CH$_2$, C-10′), 19.3 (C, OSiPh$_2$^{t}*Bu*), 26.5 (CH$_2$, C-9′), 26.8 (CH$_3$, OSiPh$_2$^{t}*Bu*), 31.1 (CH$_2$, C-3′), 34.5 (CH$_2$, C-5′), 34.6 (CH$_2$, C-11′), 67.2 (CH$_2$, 8′-CH$_2$O), 71.2 (CH, C-8′), 81.2 (CH, C-2′), 99.0 (C, C-6′), 117.7 (CH, C-5), 125.8 (CH, Ph), 127.7 (CH, OSi*Ph*$_2$^{t}Bu), 128.1 (CH, Ph), 128.8 (CH, Ph), 129.6 (CH, OSi*Ph*$_2$^{t}Bu), 129.6 (CH, OSi*Ph*$_2$^{t}Bu), 130.8 (C, Ph), 133.7 (C, OSi*Ph*$_2$^{t}Bu), 135.6 (CH, OSi*Ph*$_2$^{t}Bu), 135.7 (CH, OSi*Ph*$_2$^{t}Bu), 147.5 (C, C-4).

***m/z* (FAB):** 568 (MH$^+$, 3%), 510 (M – ^{t}Bu, 7), 423 ($C_{26}H_{35}O_3Si$, 45), 239 (SiPh$_2$^{t}Bu, 8), 207 (38), 199 (31), 197 (37), 137 (21), 135 (100), 121 (16), 91 (18).

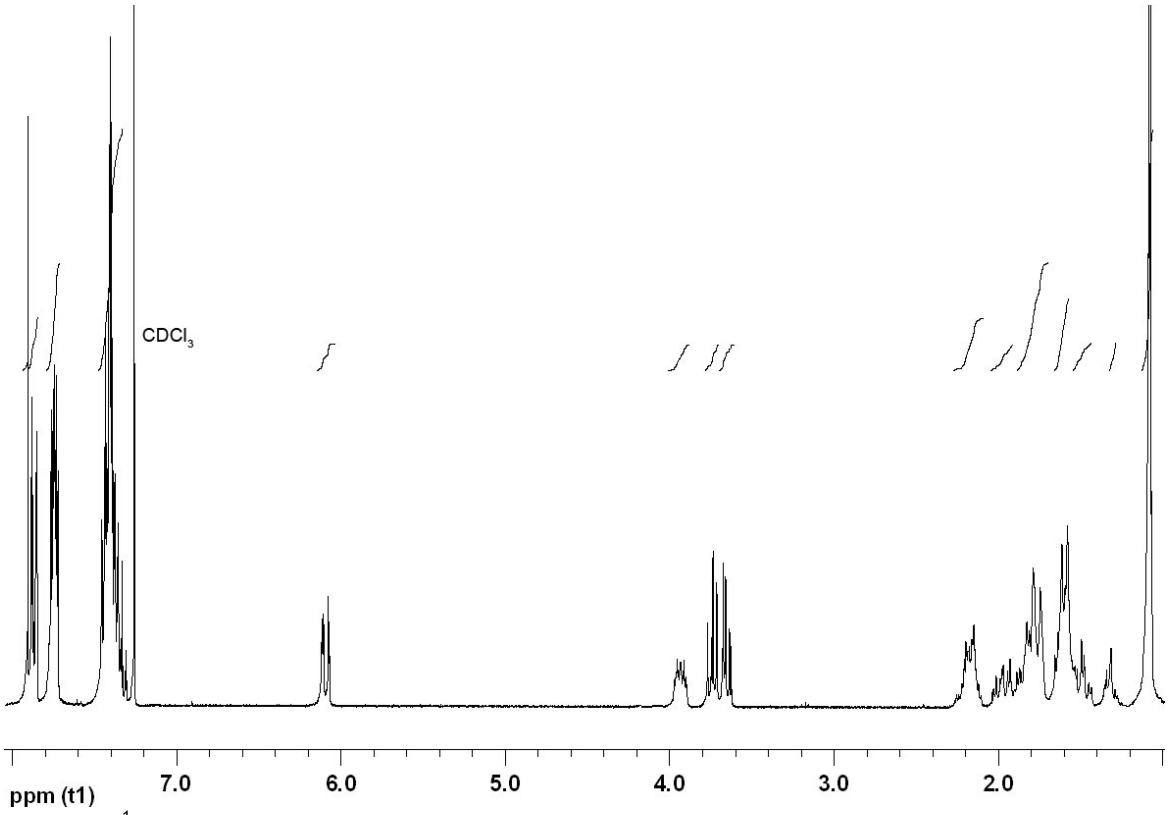

Figure 7.59: ^{1}H NMR spectrum (300 MHz; $CDCl_3$) of triazole **909d**.

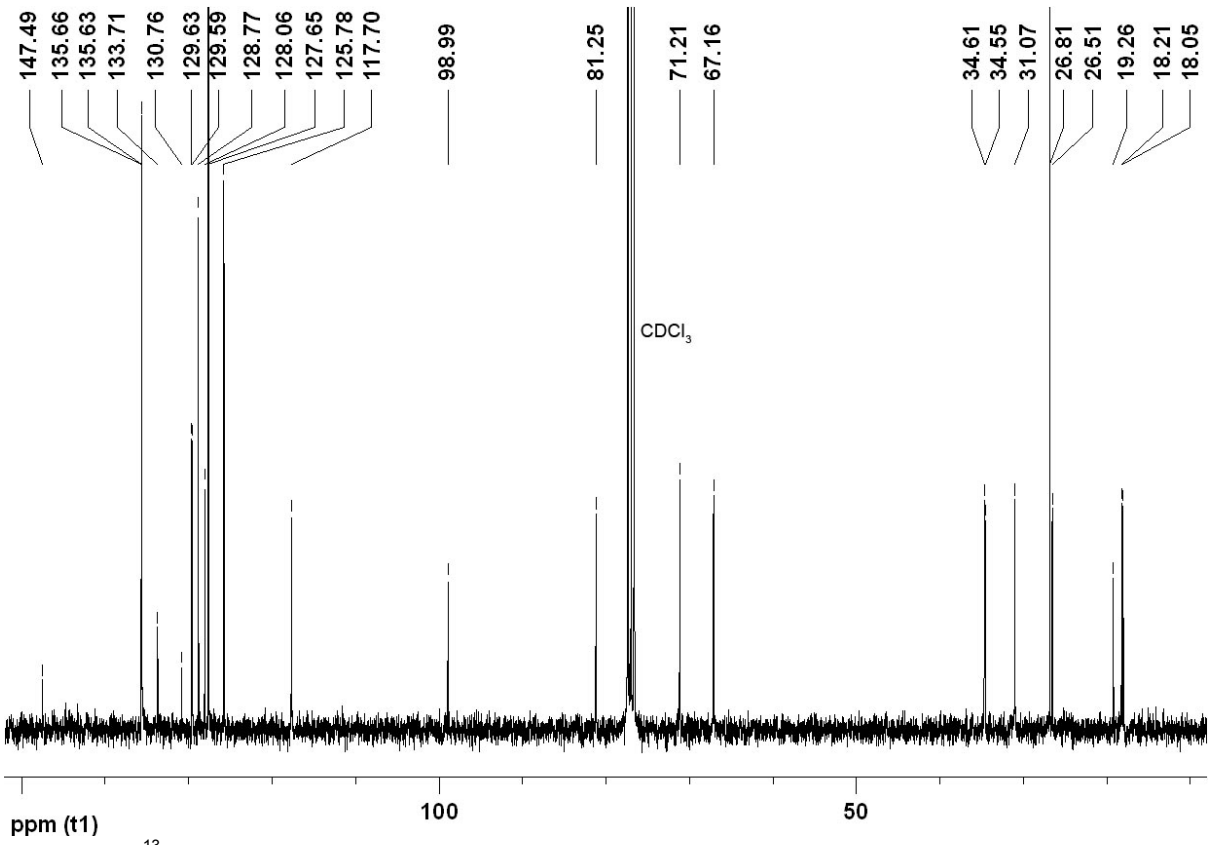

Figure 7.60: ^{13}C NMR spectrum (75 MHz; $CDCl_3$) of triazole **909d**.

Ethyl 1-{(2′*S,6′*S**,8′*S**)-8′-(*tert*-Butyldiphenylsilyloxymethyl)-1′,7′-dioxaspiro[5.5]undecan-2′-yl}-1*H*-1,2,3-triazole-4-carboxylate (909e)**

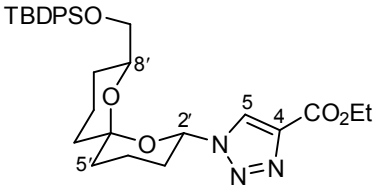

Method A: The *title compound* **909e** (9.00 mg, 84%) was prepared as a pale yellow oil from azide **860a** (9.00 mg, 19.3 μmol), ethyl propiolate **(857)** (50.0 μL) and CuI•[P(OEt)$_3$] (0.71 mg, 2.00 μmol) in toluene (250 μL) using the general procedure (method A) described above. Purification was carried out by flash chromatography using hexane–EtOAc (19:1 to 9:1) as eluent.

HRMS (FAB): found MH$^+$, 564.2892, $C_{31}H_{42}N_3O_5Si$ requires 564.2894.

ν_{max} (film)/cm^{-1}: 2932 (C–H), 1742 (C=O), 1428, 1221 (C–O), 1113 (C–O), 980, 703.

δ_H (300 MHz; CDCl$_3$): 1.06 (9 H, s, OSiPh$_2$*^{t}Bu*), 1.28–1.35 (1 H, m, 9′-H$_A$), 1.42 (3 H, t, J_{CH_3,CH_2} 7.1, OCH$_2$*CH$_3$*), 1.46–1.55 (1 H, m, 11′-H$_A$), 1.55–1.65 (3 H, m, 5′-H$_A$, 9′-H$_B$ and 10′-H$_A$), 1.69–1.92 (5 H, m, 3′-H$_A$, 4′-H$_A$, 5′-H$_B$, 10′-H$_B$ and 11′-H$_B$), 2.11–2.23 (2 H, m, 3′-H$_B$ and 4′-H$_B$), 3.62 (1 H, dd, J_{AB} 10.5 and $J_{8'\text{-}CH_2,8'}$ 4.2, 8′-*CH$_A$*H$_B$O), 3.72 (1 H, dd, J_{AB} 10.5 and $J_{8\text{-}CH_2,8'}$ 6.3, 8′-CH$_A$*H$_B$*O), 3.82–3.89 (1 H, m, 8′-H), 4.45 (2 H, t, J_{CH_2,CH_3} 7.1, O*CH$_2$*CH$_3$), 6.07 (1 H, dd, $J_{2'ax,3'ax}$ 10.9 and $J_{2'ax,3'eq}$ 2.2, 2′-H$_{ax}$), 7.34–7.44 (6 H, m, Ph), 7.69–7.75 (4 H, m, Ph), 8.25 (1 H, s, 5-H).

δ_C (75 MHz; CDCl$_3$): 14.1 (CH$_3$, OCH$_2$*CH$_3$*), 17.8 (CH$_2$, C-4′), 18.1 (CH$_2$, C-10′), 19.2 (C, OSiPh$_2$*^{t}Bu*), 26.4 (CH$_2$, C-9′), 26.8 (CH$_3$, OSiPh$_2$*^{t}Bu*), 31.2 (CH$_2$, C-3′), 34.4 (CH$_2$, C-5′), 34.5 (CH$_2$, C-11′), 61.2 (CH$_2$, O*CH$_2$*CH$_3$), 67.1 (CH$_2$, 8′-CH$_2$O), 71.3 (CH, C-8′), 81.6 (CH, C-2′), 99.2 (C, C-6′), 125.7 (CH, C-5), 127.6 (CH, Ph), 129.6 (CH, Ph), 129.6 (CH, Ph), 133.6 (C, Ph), 133.6 (C, Ph), 135.6 (CH, Ph), 135.6 (CH, Ph), 140.0 (C, C-4), 160.9 (C, C=O).

***m/z* (FAB):** 564 (MH$^+$, 0.5%), 518 (M – OEt, 2), 506 (M – ^{t}Bu, 5), 486 (M – Ph, 2), 423 ($C_{26}H_{35}O_3Si$, 69), 365 (18), 239 (SiPh$_2$^{t}Bu, 10), 207 (49), 199 (34), 197 (32), 135 (100), 121 (22).

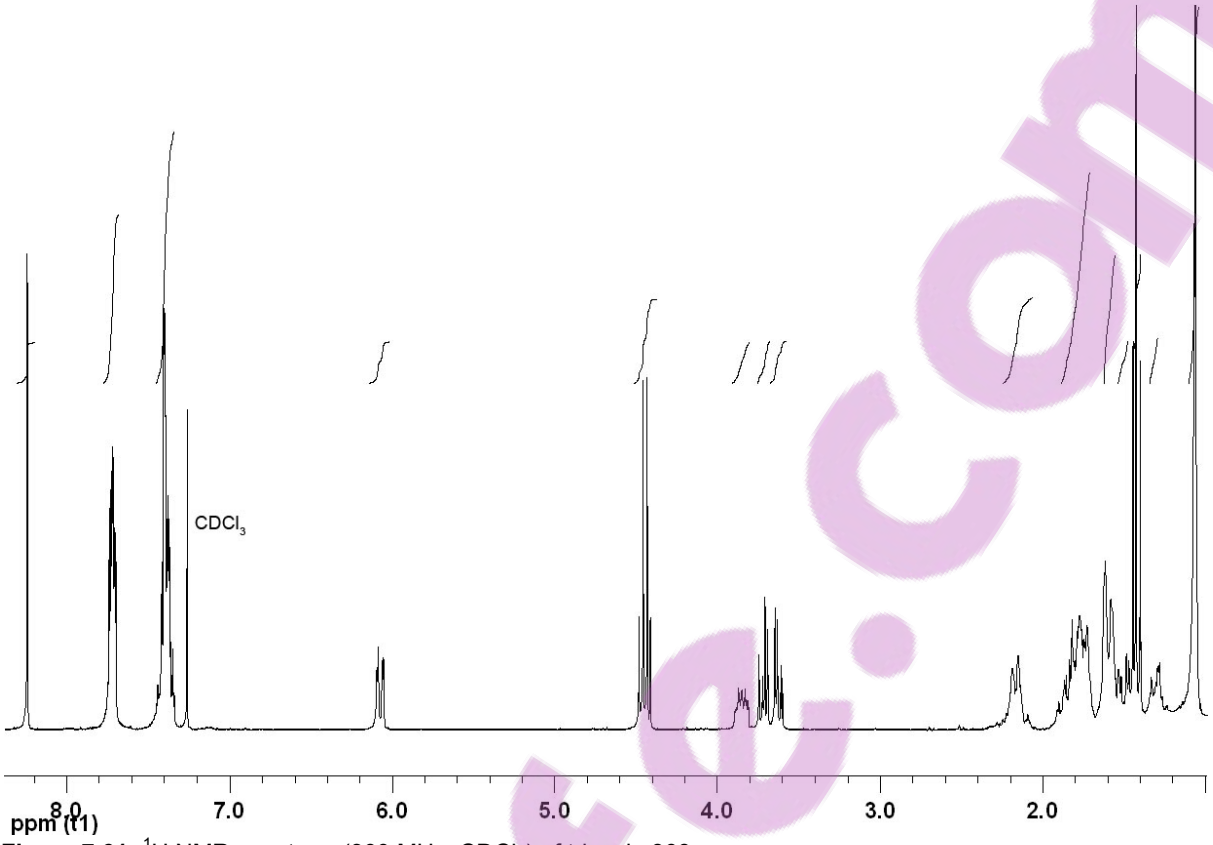

Figure 7.61: ^{1}H NMR spectrum (300 MHz; $CDCl_3$) of triazole **909e**.

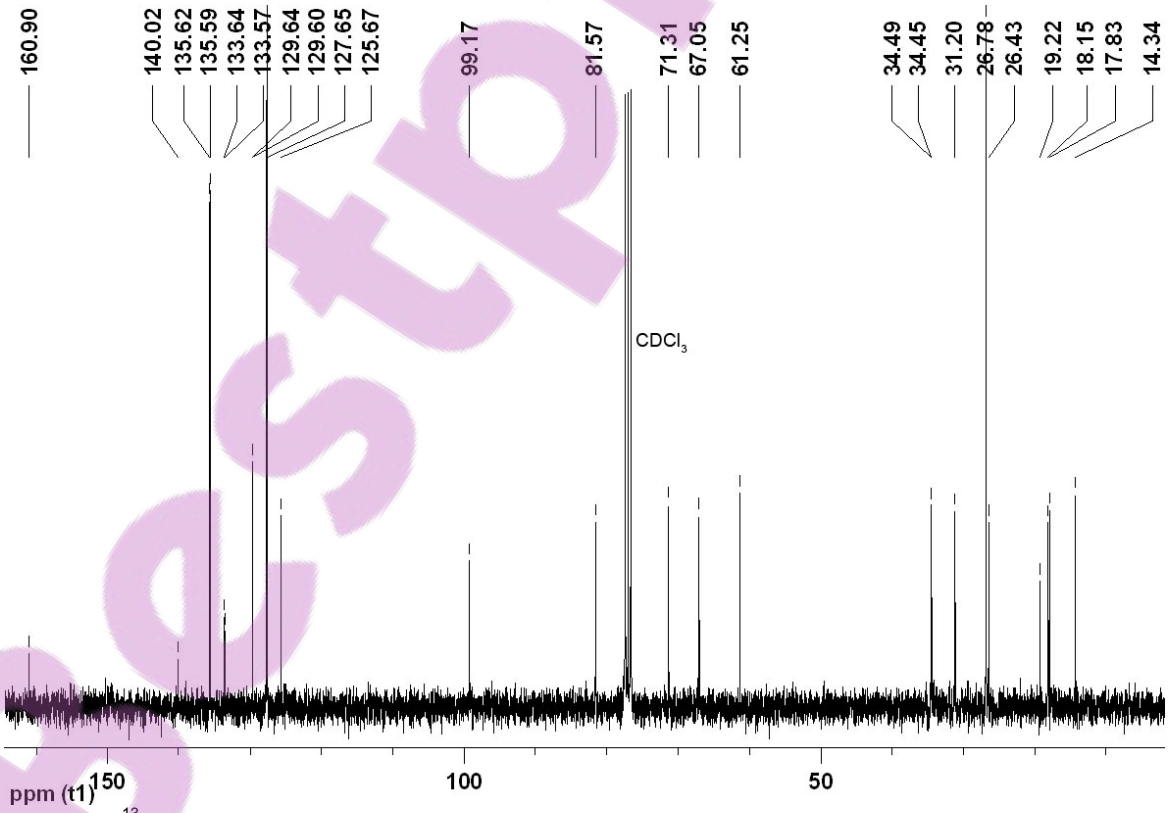

Figure 7.62: ^{13}C NMR spectrum (75 MHz; $CDCl_3$) of triazole **909e**.

Dimethyl 1-{(2′*S,6′*S**,8′*S**)-8′-(*tert*-Butyldiphenylsilyloxymethyl)-1′,7′-dioxaspiro[5.5]undecan-2′-yl}-1*H*-1,2,3-triazole-4,5-dicarboxylate (909f)**

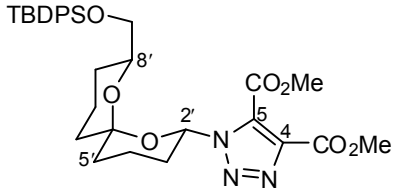

Method B: The *title compound* **909f** (8.30 mg, 78%) was prepared as a pale yellow oil from azide **860a** (8.20 mg, 17.6 μmol) and dimethylacetylene dicarboxylate (100 μL) in toluene (500 μL) using the general procedure (method B) described above. Purification was carried out by flash chromatography using hexane–EtOAc (19:1 to 9:1) as eluent.

HRMS (FAB): found [M – ^{t}Bu]$^+$, 550.2010, $C_{28}H_{32}N_3O_7Si$ requires 550.2010.

ν_{max} (film)/cm^{-1}: 2929 (C–H), 1741 (C=O), 1428, 1098 (C–O), 703.

δ_H (400 MHz; $CDCl_3$): 1.07 (9 H, s, OSiPh$_2$^{t}*Bu*), 1.27–1.33 (1 H, m, 9′-H$_A$), 1.41–1.51 (1 H, m, 11′-H$_A$), 1.54–1.80 (7 H, m, 4′-H$_A$, 5′-H$_A$, 5′-H$_B$, 9′-H$_B$, 10′-H$_A$, 10′-H$_B$ and 11′-H$_B$), 2.03–2.27 (3 H, m, 3′-H$_A$, 3′-H$_B$ and 4′-H$_B$), 3.60 (1 H, dd, J_{AB} 10.3 and $J_{8'\text{-}CH_2,8'}$ 4.8, 8′-*CH$_A$*H$_B$O), 3.71 (1 H, dd, J_{AB} 10.3 and $J_{8'\text{-}CH_2,8'}$ 5.8, 8′-CH$_A$*H$_B$*O), 3.77–3.83 (1 H, m, 8′-H), 3.96 (6 H, s, 2 x OMe), 6.18 (1 H, dd, $J_{2'ax,3'ax}$ 10.6 and $J_{2'ax,3'eq}$ 3.0, 2′-H$_{ax}$), 7.34–7.44 (6 H, m, Ph), 7.68–7.74 (4 H, m, Ph).

δ_C (100 MHz; $CDCl_3$): 17.5 (CH$_2$, C-4′), 17.8 (CH$_2$, C-10′), 19.3 (C, OSiPh$_2$^{t}*Bu*), 26.6 (CH$_2$, C-9′), 26.8 (CH$_3$, OSiPh$_2$^{t}*Bu*), 30.4 (CH$_2$, C-3′), 34.4 (CH$_2$, C-5′), 34.7 (CH$_2$, C-11′), 52.6 (CH$_3$, OMe), 53.4 (CH$_3$, OMe), 66.9 (CH$_2$, 8′-CH$_2$O), 71.0 (CH, C-8′), 82.8 (CH, C-2′), 99.4 (C, C-6′), 127.6 (CH, Ph), 129.6 (CH, Ph), 129.6 (CH, Ph), 131.8 (C, C-5), 133.5 (C, Ph), 133.6 (C, Ph), 135.6 (CH, Ph), 135.6 (CH, Ph), 138.0 (C, C-4), 160.1 (C, C=O), 160.3 (C, C=O).

***m/z* (FAB):** 550 ([M – ^{t}Bu]$^+$, 2%), 423 ($C_{26}H_{35}O_3Si$, 52), 207 (42), 199 (35), 197 (33), 137 (23), 135 (100).

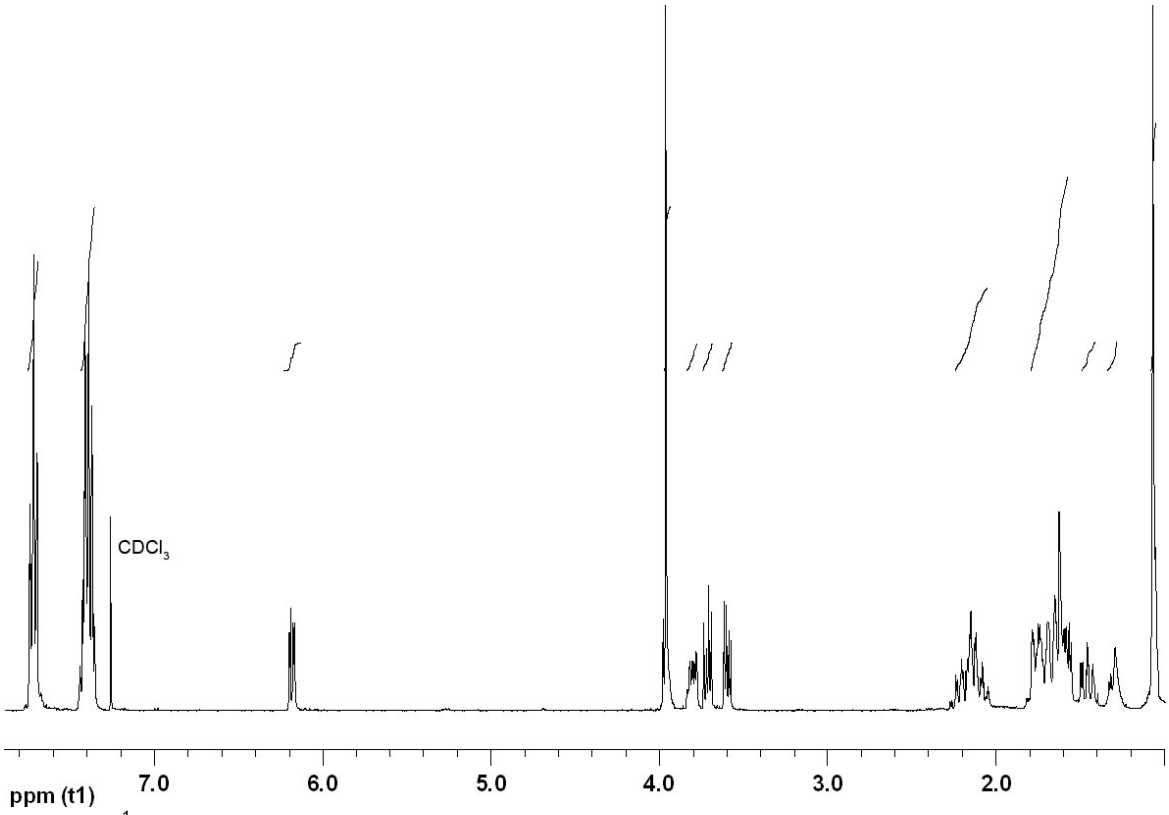

Figure 7.63: ^{1}H NMR spectrum (400 MHz; $CDCl_3$) of triazole **909f**.

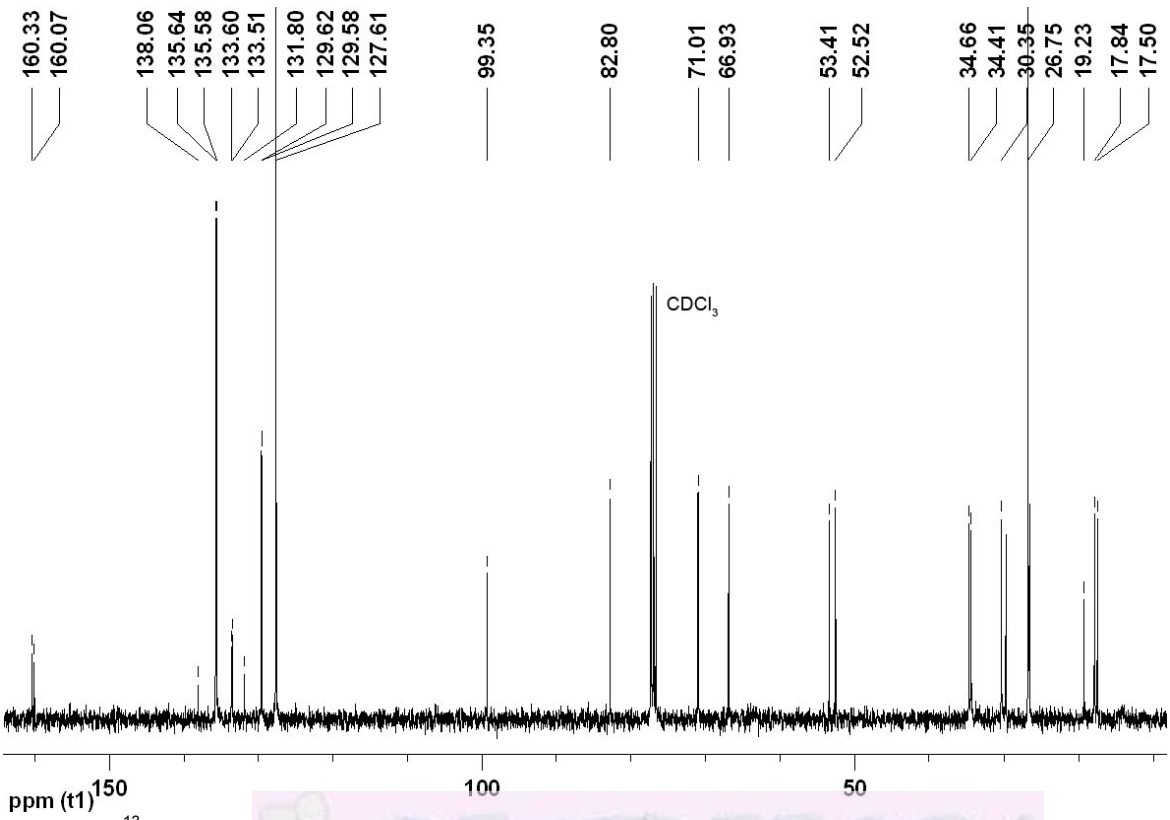

Figure 7.64: ^{13}C NMR spectrum (100 MHz; $CDCl_3$) of triazole **909f**.

1-{(2′*S,6′*S**,8′*S**)-8′-(*tert*-Butyldiphenylsilyloxymethyl)-1′,7′-dioxaspiro[5.5]undecan-2′-yl}-4-(trimethylsilyl)-1*H*-1,2,3-triazole (909g)**

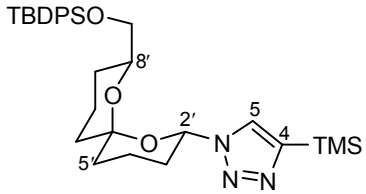

Method C: The *title compound* **909g** (7.80 mg, 64%) was prepared as a pale yellow oil from azide **860a** (10.1 mg, 21.6 μmmol) and trimethylsilylacetylene (2 x 100 μL) in toluene (500 μL) using the general procedure (method C) described above. Purification was carried out by flash chromatography using hexane–EtOAc (99:1 to 9:1) as eluent. Unreacted azide **860a** (3.60 mg, 36%) was also recovered.

HRMS (FAB): found MH^+, 564.3079, $C_{31}H_{46}N_3O_3Si_2$ requires 564.3078.

ν_{max} (film)/cm^{-1}: 2951 (C–H), 1428, 1249 (C–O), 1113 (C–O), 980, 842, 702.

δ_H (300 MHz; $CDCl_3$): 0.34 (9 H, s, $SiMe_3$), 1.07 (9 H, s, $OSiPh_2{}^tBu$), 1.26–1.34 (1 H, m, 9′-H_A), 1.40–1.53 (1 H, m, 11′-H_A), 1.53–1.64 (3 H, m, 5′-H_A, 9′-H_B and 10′-H_A), 1.70–1.80 (3 H, m, 4′-H_A, 5′-H_B and 11′-H_B), 1.80–1.99 (2 H, m, 3′-H_A and 10′-H_B), 2.06–2.25 (2 H, m, 3′-H_B and 4′-H_B), 3.63 (1 H, dd, J_{AB} 10.5 and $J_{8'\text{-}CH_2,8'}$ 4.2, 8′-C$H_A$$H_B$O), 3.72 (1 H, dd, J_{AB} 10.5 and $J_{8'\text{-}CH_2,8'}$ 6.3, 8′-$CH_A$$H_B$O), 3.88–3.96 (1 H, m, 8′-H), 6.11 (1 H, dd, $J_{2'ax,3'ax}$ 11.0 and $J_{2'ax,3'eq}$ 2.5, 2′-H_{ax}), 7.35–7.43 (6 H, m, Ph), 7.66 (1 H, s, 5-H), 7.70–7.76 (4 H, m, Ph).

δ_C (75 MHz; $CDCl_3$): -1.1 (CH_3, $SiMe_3$), 18.1 (CH_2, C-4′), 18.2 (CH_2, C-10′), 19.2 (C, $OSiPh_2{}^tBu$), 26.5 (CH_2, C-9′), 26.8 (CH_3, $OSiPh_2{}^tBu$), 31.2 (CH_2, C-3′), 34.6 (CH_2, C-5′), 34.7 (CH_2, C-11′), 67.2 (CH_2, 8′-CH_2O), 71.1 (CH, C-8′), 80.7 (CH, C-2′), 98.9 (C, C-6′), 126.9 (CH, C-5), 127.6 (CH, Ph), 129.6 (CH, Ph), 129.6 (CH, Ph), 133.7 (C, Ph), 135.6 (CH, Ph), 135.7 (CH, Ph), 146.1 (C, C-4).

***m/z* (FAB):** 564 (MH^+, 4%), 423 ($C_{26}H_{35}O_3Si$, 74), 405 (15), 239 ($SiPh_2{}^tBu$, 10), 207 (37), 197 (36), 142 (23), 135 (100), 73 (52).

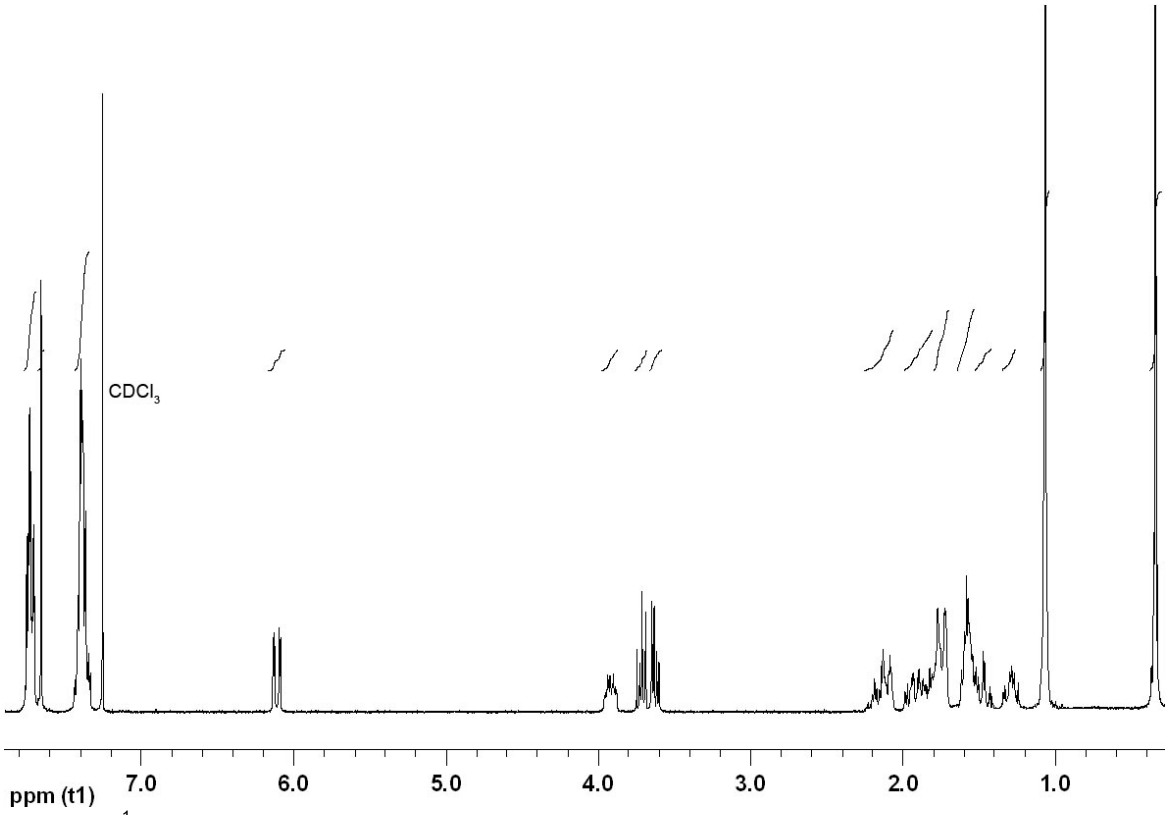

Figure 7.65: ^{1}H NMR spectrum (300 MHz; $CDCl_3$) of triazole **909g**

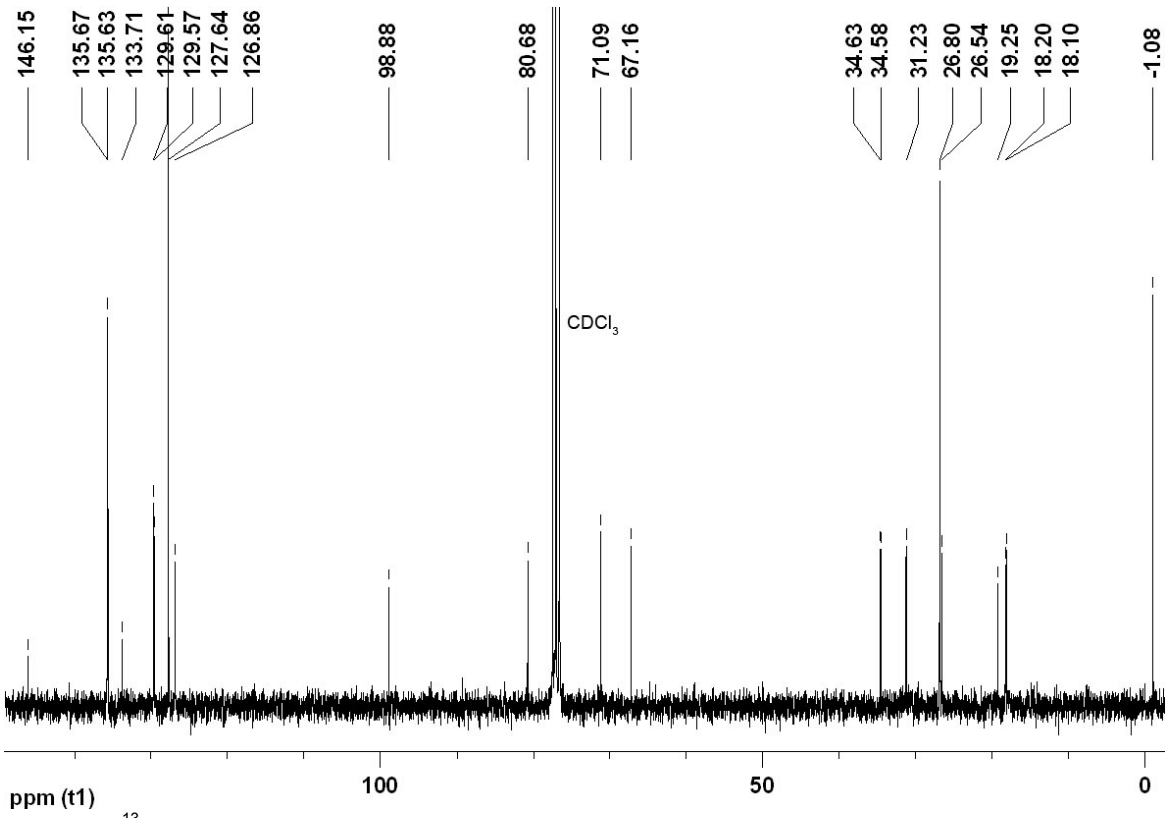

Figure 7.66: ^{13}C NMR spectrum (75 MHz; $CDCl_3$) of triazole **909g**.

Ethyl 1-{(2′*S,6′*S**,8′*S**)-8′-(*tert*-Butyldiphenylsilyloxymethyl)-1′,7′-dioxaspiro[5.5]undecan-2′-yl}-4-(trimethylsilyl)- 1*H*-1,2,3-triazole-5-carboxylate (909h)**

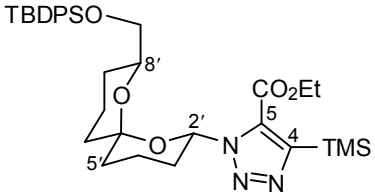

Method C: The *title compound* **909h** (9.10 mg, 84%) was prepared as a pale yellow oil from azide **860a** (8.00 mg, 17.2 μmol) and ethyl 3-(trimethylsilyl)propiolate **(916)** (2 x 50.0 μL) in toluene (500 μL) using the general procedure (method C) described above. Purification was carried out by flash chromatography using hexane–EtOAc (97:3, 19:1 to 9:1) as eluent.

HRMS (FAB): found MH^+, 636.3293, $C_{34}H_{50}N_3O_5Si_2$ requires 636.3289.

ν_{max} (film)/cm^{-1}: 2955 (C–H), 2857, 1728 (C=O), 1428, 1192, 1112 (C–O), 1079 (C–O), 847, 703.

δ_H (300 MHz; $CDCl_3$): 0.39 (9 H, s, $SiMe_3$), 1.08 (9 H, s, $OSiPh_2{}^tBu$), 1.30–1.40 (1 H, m, 9′-H_A), 1.36 (3 H, t, J_{CH_3,CH_2} 7.2, OCH_2CH_3), 1.41–1.49 (1 H, m, 11′-H_A), 1.50–1.61(1 H, m, 10′-H_A), 1.62–1.84 (6 H, m, 4′-H_A, 5′-H_A, 5′-H_B, 9′-H_B, 10′-H_B and 11′-H_B), 1.94–2.03 (1 H, m, 3′-H_A), 2.03–2.21 (1 H, m, 4′-H_B), 2.51–2.66 (1 H, m, 3′-H_B), 3.66 (1 H, dd, J_{AB} 10.0 and $J_{8'\text{-}CH_2,8'}$ 5.6, 8′-CH_AH_BO), 3.83 (1 H, dd, J_{AB} 10.0 and $J_{8'\text{-}CH_2,8'}$ 4.9, 8′-CH_AH_BO), 4.02–4.11 (1 H, m, 8′-H), 4.28–4.44 (2 H, m, OCH_2CH_3), 6.65 (1 H, dd, $J_{2'ax,3'ax}$ 11.3 and $J_{2'ax,3'eq}$ 2.6, 2′-H_{ax}), 7.35–7.46 (6 H, m, Ph), 7.74–7.80 (4 H, m, Ph).

δ_C (75 MHz; $CDCl_3$): -1.1 (CH_3, $SiMe_3$), 14.2 (CH_3, OCH_2CH_3), 18.1 (CH_2, C-4′ and C-10′), 19.3 (C, $OSiPh_2{}^tBu$), 26.8 (CH_3, $OSiPh_2{}^tBu$), 27.1 (CH_2, C-9′), 29.7 (CH_2, C-3′), 34.8 (CH_2, C-5′), 35.0 (CH_2, C-11′), 61.8 (CH_2, OCH_2CH_3), 67.1 (CH_2, 8′-CH_2O), 70.4 (CH, C-8′), 80.3 (CH, C-2′), 99.0 (C, C-6′), 127.5 (CH, Ph), 129.5 (CH, Ph), 129.5 (CH, Ph), 133.1 (C, C-5), 133.8 (C, Ph), 134.0 (C, Ph), 135.7 (CH, Ph), 135.7 (CH, Ph), 150.1 (C, C-4), 159.8 (C, C=O).

***m/z* (FAB):** 636 (MH^+, 1%), 578 (M – ^{t}Bu, 3), 558 (M – Ph, 1), 423 ($C_{26}H_{35}O_3Si$, 39), 214 (22), 207 (27), 199 (33), 197 (38), 135 (100), 73 (45).

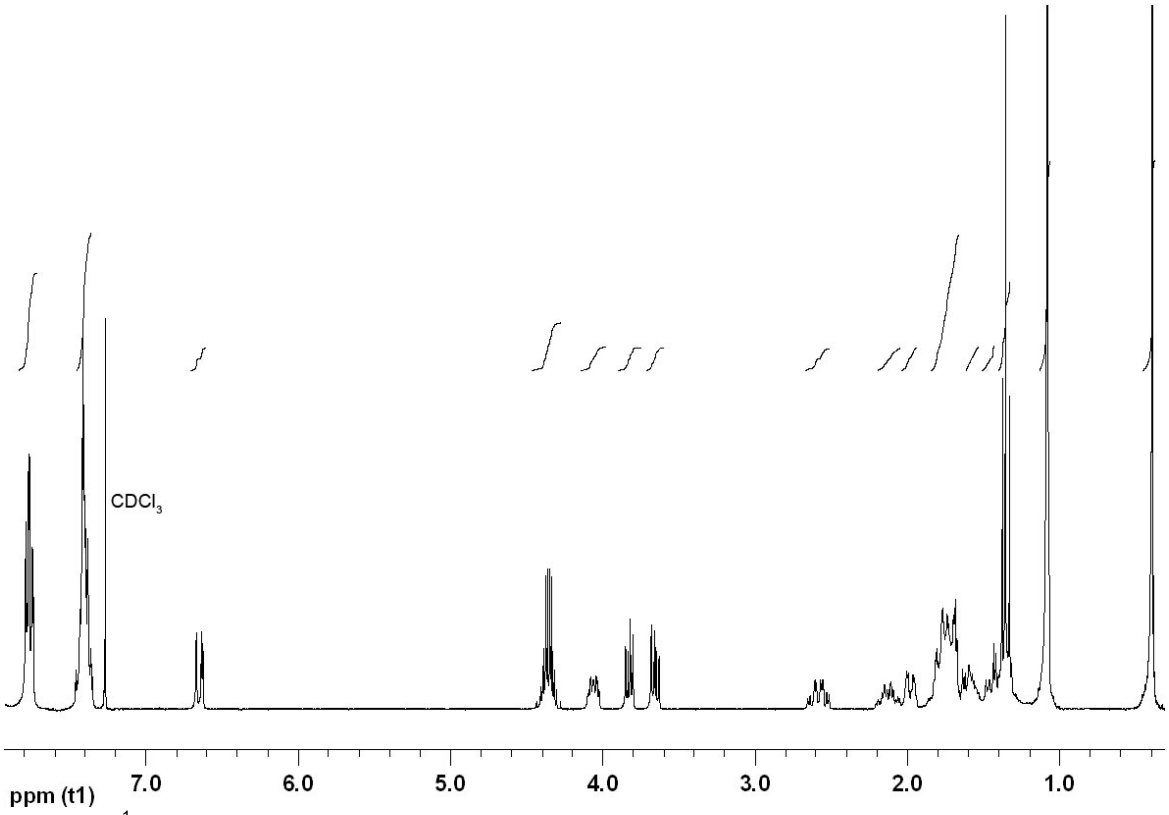

Figure 7.67: ^{1}H NMR spectrum (300 MHz; $CDCl_3$) of triazole **909h**.

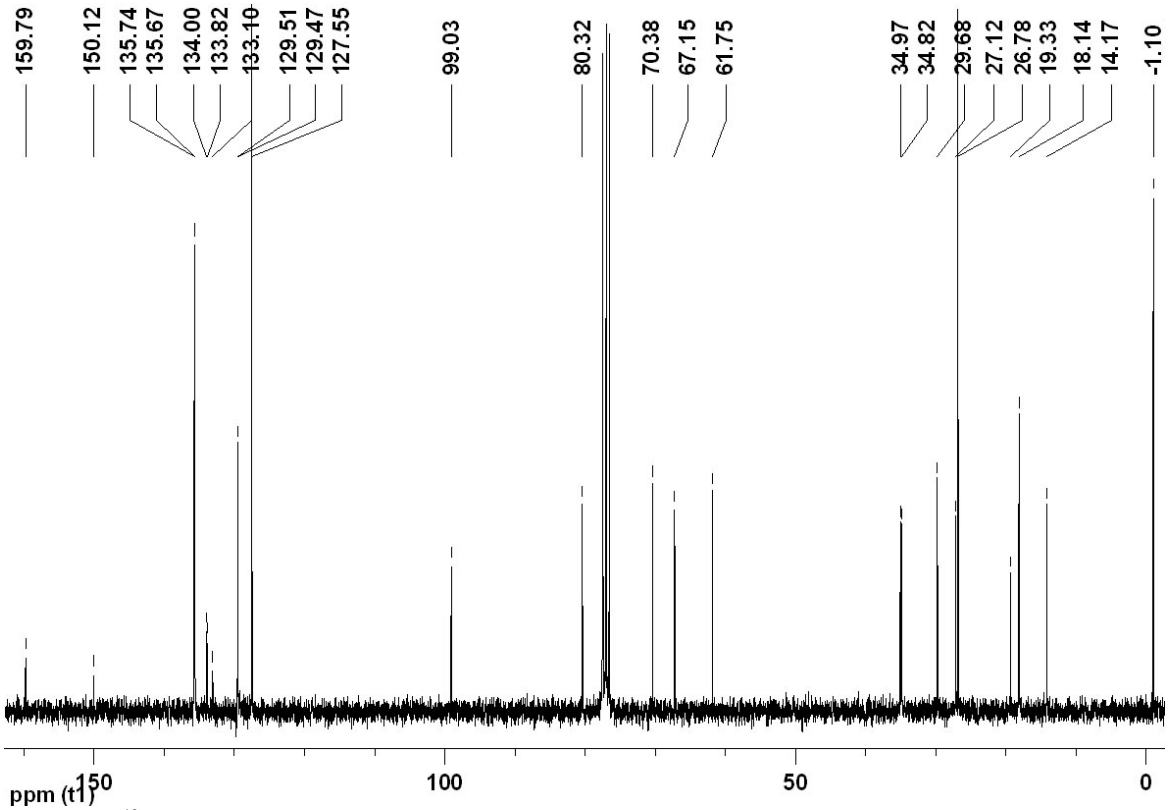

Figure 7.68: ^{13}C NMR spectrum (75 MHz; $CDCl_3$) of triazole **909h**.

7.3.7 Synthesis of Spiroacetal-Amino Acid 913

(2*S,6*S**,8*S**)-8-(*tert*-Butyldiphenylsilyloxymethyl)-*N*-[*N*-(9-fluorenylmethoxycarbonyl)glycyl]-1,7-dioxaspiro[5.5]undecan-2-ylamine (913)**

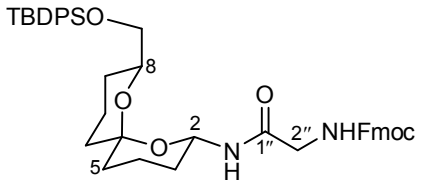

This procedure is an adaptation of that reported by Davis *et al.*[31]

To a solution of Fmoc-Gly-OH (13.2 mg, 44.4 μmol) and anhydrous HOBt [††] (6.00 mg, 44.4 μmol) in anhydrous MeCN (1.0 mL) at room temperature was added DIC (5.60 mg, 44.4 μmol). After 30 min, azide **860a** (18.8 mg, 40.4 μmol) in anhydrous MeCN (500 μL) was transferred to the mixture *via* cannula and Bu_3P (11.1 μL, 44.4 μmol) was added dropwise. After 18 h, saturated $NaHCO_3$ solution (2 mL) was added. The aqueous phase was extracted with Et_2O (3 x 3 mL) and the combined organic extracts were concentrated *in vacuo*. Purification by flash chromatography using hexane–EtOAc (9:1 to 3:2) as eluent followed by PLC using hexane–EtOAc (3:2) as eluent yielded the *title compound* **913** (9.20 mg, 32%) as a white foam.

Melting Point: 66.9–68.1 °C

HRMS (FAB): found MH^+, 719.3516, $C_{43}H_{51}N_2O_6Si$ requires 719.3516.

ν_{max} (film)/cm^{-1}: 3320br (N–H), 2931 (C–H), 2855, 1682 (C=O), 1539, 1228, 1111 (C–O), 1084 (C–O), 739, 702.

δ_H (400 MHz; $CDCl_3$): 1.06 (9 H, s, $OSiPh_2{}^tBu$), 1.31–1.46 (4 H, m, 3-H_A, 5-H_A, 9-H_A and 11-H_A), 1.57–1.88 (6 H, m, 3-H_B, 4-H_A, 5-H_B, 9-H_B, 10-H_A and 11-H_B), 1.85–1.97 (1 H, m, 10-H_B), 2.00–2.12 (1 H, m, 4-H_B), 3.69 (1 H, dd, J_{AB} 10.3 and $J_{8\text{-}CH_2,8}$ 3.8, 8-CH_AH_BO), 3.72 (1 H, dd, J_{AB} 10.3 and $J_{8\text{-}CH_2,8}$ 5.0, 8-CH_AH_BO), 3.91 (2 H, d, $J_{2'',2''\text{-}NH}$ 5.0, 2″-H), 4.11–4.18 (1 H, m, 8-H), 4.22 (1 H, t, $J_{9',9'\text{-}CH_2}$ 7.0, 9′-H_{Fmoc}), 4.42 (2 H, d, $J_{9'\text{-}CH_2,9'}$ 7.0, 9′-CH_2O_{Fmoc}), 5.46 (1 H, br s, 2″-NH), 5.52 (1 H, ddd, $J_{2ax,3ax}$ 11.3, $J_{2,2\text{-}NH}$ 9.2 and $J_{2ax,3eq}$ 2.4, 2-H_{ax}), 6.10 (1 H, d, $J_{2\text{-}NH,2}$ 9.2, 2-NH), 7.30 (2 H, tt, *J* 7.4 and 1.2, Fmoc), 7.34–7.43 (8 H, m, Fmoc and Ph), 7.59 (2 H, d, *J* 7.4, Fmoc), 7.74–7.78 (6 H, m, Fmoc and Ph).

δ_C (100 MHz; $CDCl_3$): 18.2 (CH_2, C-4), 18.3 (CH_2, C-10), 19.3 (C, $OSiPh_2{}^tBu$), 26.5 (CH_2, C-9), 26.8 (CH_3, $OSiPh_2{}^tBu$), 30.7 (CH_2, C-3), 34.6 (CH_2, C-5 or C-11), 35.0 (CH_2, C-5 or C-11), 44.5 (CH_2, C-2″), 47.1 (CH, C-9′$_{Fmoc}$), 67.2 (2 x CH_2, 8-CH_2O and 9′-CH_2O_{Fmoc}), 70.4 (CH, C-8), 72.0 (CH, C-2), 97.9 (C, C-6), 120.0 (CH, Fmoc), 125.0 (CH, Fmoc), 127.1 (CH, Fmoc), 127.5 (CH, Ph), 127.7 (CH, Fmoc),

[††] Water of crystallisation from hydrous HOBt was removed by azeotropic distillation with MeCN (3 x 10 mL) *in vacuo*.

129.4 (CH, Ph), 134.0 (C, Ph), 134.0 (C, Ph), 135.7 (CH, Ph), 135.8 (CH, Ph), 141.3 (C, Fmoc), 143.7 (C, Fmoc), 156.4 (C, C=O_{Fmoc}), 167.9 (C, C-1″).

***m/z* (FAB):** 719 (MH^+, 4%), 701 (M – OH, 6), 423 ($C_{26}H_{35}O_3Si$, 26), 239 ($SiPh_2{}^tBu$, 8), 207 (25), 199 (29), 197 (31), 179 (100), 149 (32), 137 (42), 135 (95), 121 (24), 91 (22).

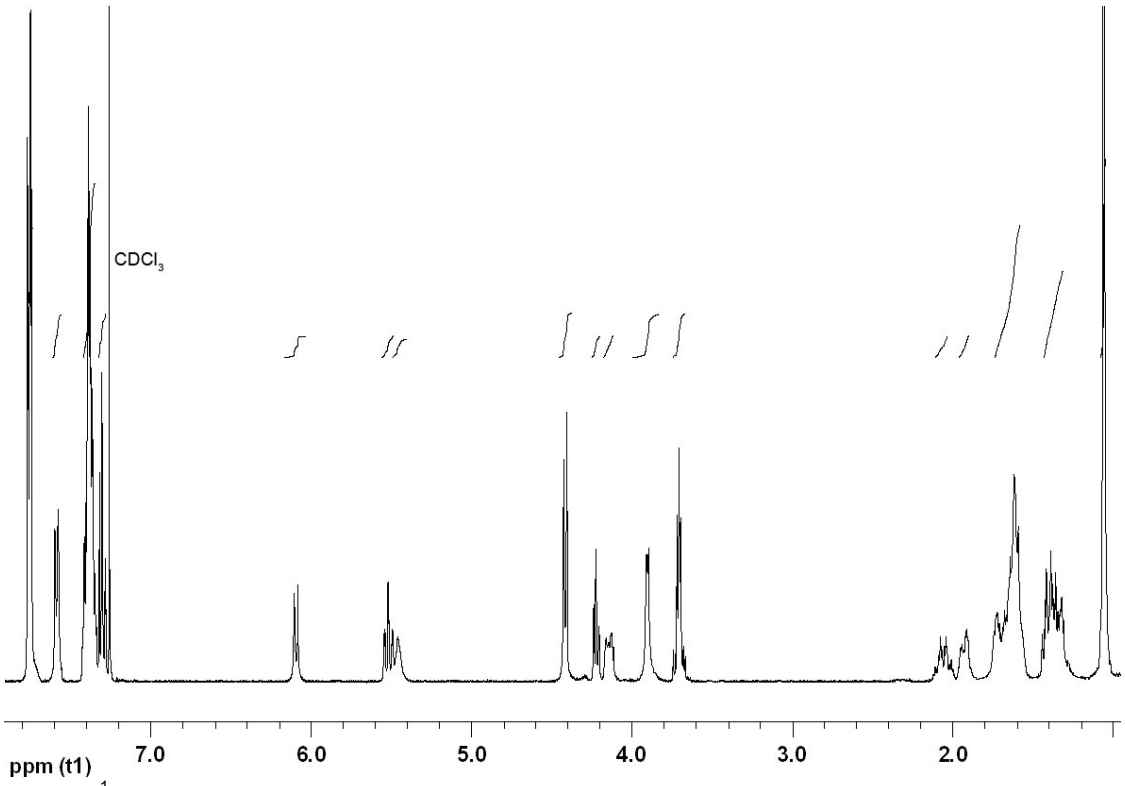

Figure 7.69: ^{1}H NMR spectrum (400 MHz; $CDCl_3$) of glycyl-spiroacetal **913**.

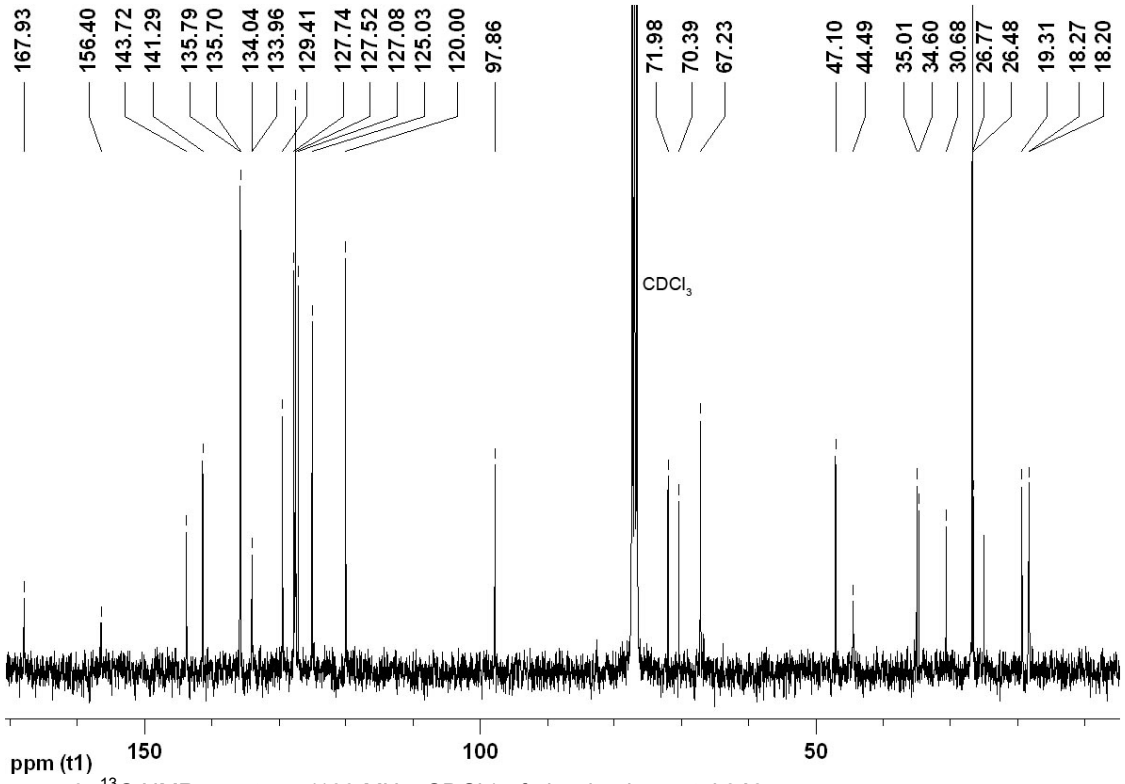

Figure 7.70: ^{13}C NMR spectrum (100 MHz; $CDCl_3$) of glycyl-spiroacetal **913**.

7.4 Deprotection of Spiroacetal Analogues

7.4.1 Deprotection of Spiroacetal-Triazoles 909

General Procedures for Deprotection of Spiroacetal-Triazoles 909

Method A: Desilylation using TBAF

To a solution of TBDPS-protected triazole **909** in anhydrous THF (1.0 mL) under an atmosphere of argon at room temperature was added activated molecular sieves (0.20 g) and TBAF solution (1.0 mol L^{-1} in THF, 2.0–10 equiv.). After 1–3 h, saturated NH_4Cl solution (1 mL) was added. The aqueous phase was extracted with Et_2O (3 x 2 mL) and the combined organic extracts were concentrated *in vacuo*. Purification by flash chromatography using the appropriate eluent yielded hydroxymethyl spiroacetal-triazole **809**.

Method B: Desilylation using HF•pyridine

To a solution of TBDPS-protected triazole **909** in anhydrous THF (1.0–2.0 mL) in a plastic vial under an atmosphere of argon was added HF•pyridine (1.5–3.4 μL per micromole of triazole) and the mixture was stirred at room temperature. If the desilylation was not complete within 18 h (TLC), a second portion of HF•pyridine (1.3–2.0 μL per micromole of triazole) was added and the mixture was stirred at room temperature for another 18 h. Saturated $NaHCO_3$ solution (4 mL) was added dropwise. The aqueous phase was extracted with Et_2O (4 x 4 mL) and the combined organic extracts were concentrated *in vacuo*. Purification by flash chromatography using the appropriate eluent yielded hydroxymethyl spiroacetal-triazole **809**.

Method C: Desilylation using $3HF•NEt_3$[32]

A solution of TBDPS-protected triazole **909** and $3HF•NEt_3$ (2.0–3.0 μL per micromole of triazole) in anhydrous THF (300 μL–1.0 mL) was stirred at room temperature under an atmosphere of argon. If the desilylation was not complete within 18 h (TLC), a second portion of $3HF•NEt_3$ (2.0–2.5 μL per micromole of triazole) was added and the mixture was stirred at room temperature for another 18 h. Saturated $NaHCO_3$ solution (4 mL) was added dropwise. The aqueous phase was extracted with Et_2O (4 x 4 mL) and the combined organic extracts were concentrated *in vacuo*. Purification by flash chromatography using the appropriate eluent yielded hydroxymethyl spiroacetal-triazole **809**.

Method D: Desilylation using $3HF•NEt_3$ and Buffered with NEt_3

A solution of TBDPS-protected triazole **909**, $3HF•NEt_3$ (2.0 μL per micromole of triazole) and NEt_3 (2.5 μL per micromole of triazole) in anhydrous THF (700 μL) was stirred at 40 °C for 48 h under

an atmosphere of argon. A second portion of 3HF•NEt_3 (1.0 μL micromole of triazole) and NEt_3 (1.3 μL per micromole of triazole) were added and the mixture was stirred at 40 °C for 18 h. Saturated $NaHCO_3$ solution (2 mL) was added dropwise. The aqueous phase was extracted with EtOAc (3 x 3 mL) and the combined organic extracts were concentrated *in vacuo*. Purification by flash chromatography using hexane–EtOAc as eluent yielded hydroxymethyl spiroacetal-triazole **809**.

4-[2″-(Benzyloxy)ethyl]-1-{(2′*S,6′*S**,8′*S**)-8′-(hydroxymethyl)-1′,7′-dioxaspiro[5.5]undecan-2′-yl}-1*H*-1,2,3-triazole (809a)**

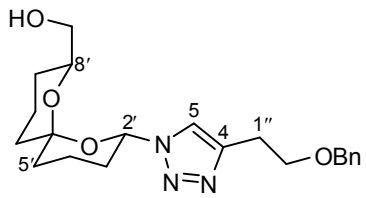

Method C[‡‡]: The *title compound* **809a** (13.7 mg, 99%) was prepared as a pale yellow oil from TBDPS-protected triazole **909a** (22.3 mg, 35.6 μmol) and 3HF•NEt_3 (2 x 72.0 μL) in anhydrous THF (1.0 mL) using the general procedure (method C) described above. Purification was carried out by flash chromatography using hexane–EtOAc (9:1, 1:1 to 0:1) as eluent.

HRMS (FAB): found MH^+, 388.2244, $C_{21}H_{30}N_3O_4$ requires 388.2236.

ν_{max} (film)/cm^{-1}: 3400 (O–H), 2942 (C–H), 2870, 1455, 1387, 1223 (C–O), 1099 (C–O), 1048, 980, 737.

δ_H (400 MHz; $CDCl_3$): 1.33–1.42 (1 H, m, 9′-H_A), 1.42–1.52 (2 H, m, 9′-H_B and 11′-H_A), 1.53–1.62 (2 H, m, 5′-H_A and 10′-H_A), 1.72–1.87 (5 H, m, 4′-H_A, 5′-H_B, 10′-H_B, 11′-H_B and OH), 1.87–2.04 (1 H, m, 3′-H_A), 2.06–2.16 (2 H, m, 3′-H_B and 4′-H_B), 3.06 (2 H, t, $J_{1'',2''}$ 6.6, 1″-H), 3.56 (1 H, dd, J_{AB} 11.6 and $J_{8'\text{-}CH_2,8'}$ 6.2, 8′-CH_AH_BO), 3.69 (1 H, dd, J_{AB} 11.6 and $J_{8'CH_2,8'}$ 3.3, 8′-CH_AH_BO), 3.78 (2 H, t, $J_{2'',1''}$ 6.6, 2″-H), 3.83–3.90 (1 H, m, 8′-H), 4.55 (2 H, s, OCH_2Ph), 5.94 (1 H, dd, $J_{2'ax,3'ax}$ 11.2 and $J_{2'ax,3'eq}$ 2.3, 2′-H_{ax}), 7.27–7.36 (5 H, m, Ph).

δ_C (100 MHz; $CDCl_3$): 17.9 (CH_2, C-10′), 18.1 (CH_2, C-4′), 26.0 (CH_2, C-9′), 26.6 (CH_2, C-1″), 30.8 (CH_2, C-3′), 34.4 (CH_2, C-5′), 34.7 (CH_2, C-11′), 66.0 (CH_2, 8′-CH_2O), 69.1 (CH_2, C-2″), 70.7 (CH, C-8′), 73.0 (CH_2, OCH_2Ph), 81.0 (CH, C-2′), 98.9 (C, C-6′), 119.9 (CH, C-5), 127.6 (CH, Ph), 127.7 (CH, Ph), 128.4 (CH, Ph), 138.2 (C, Ph), 145.0 (C, C-4).

***m/z* (FAB):** 388 (MH^+, 8%), 204 (100), 186 (87), 185 ($C_{10}H_{17}O_3$, 45), 121 (18), 99 (23), 91 (51).

[‡‡] A yield of 74% and 75% were achieved when method A and method B were used respectively.

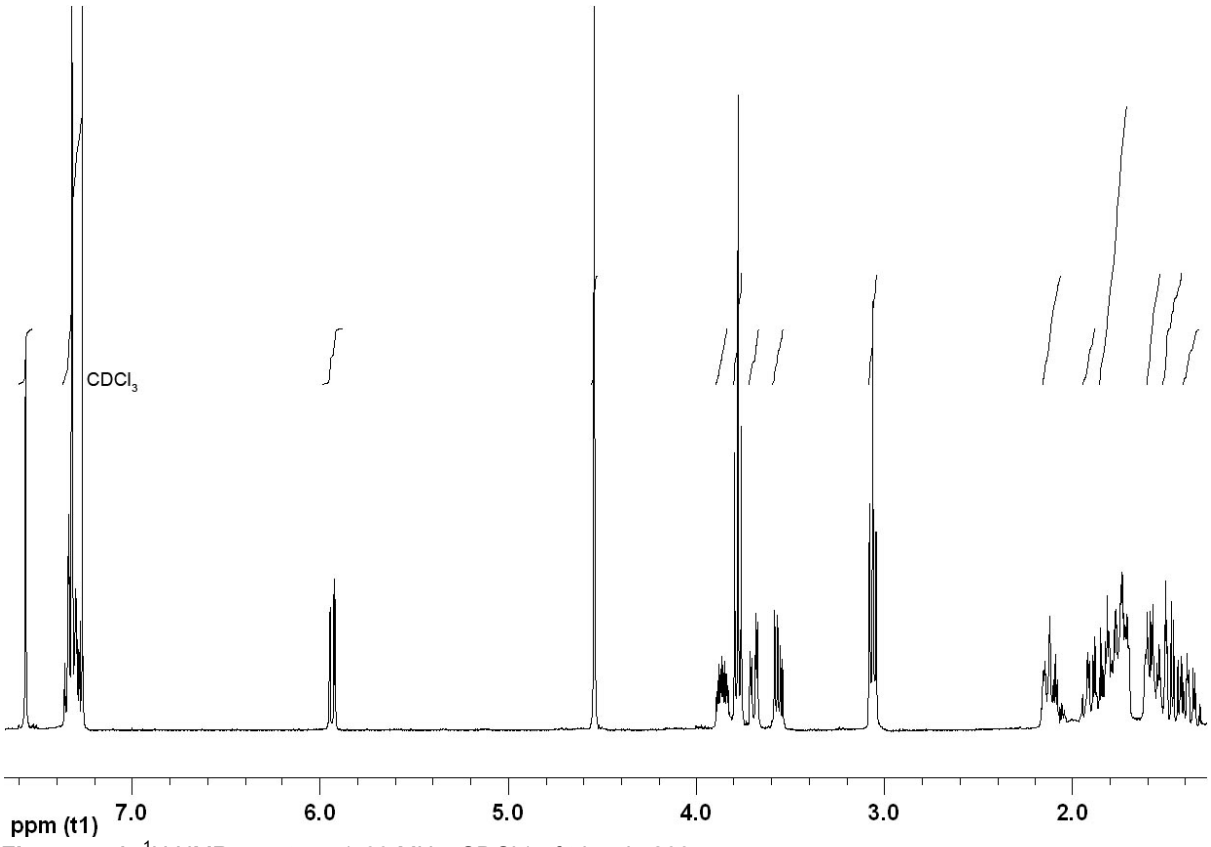

Figure 7.71: ^{1}H NMR spectrum (400 MHz; $CDCl_3$) of triazole **809a**.

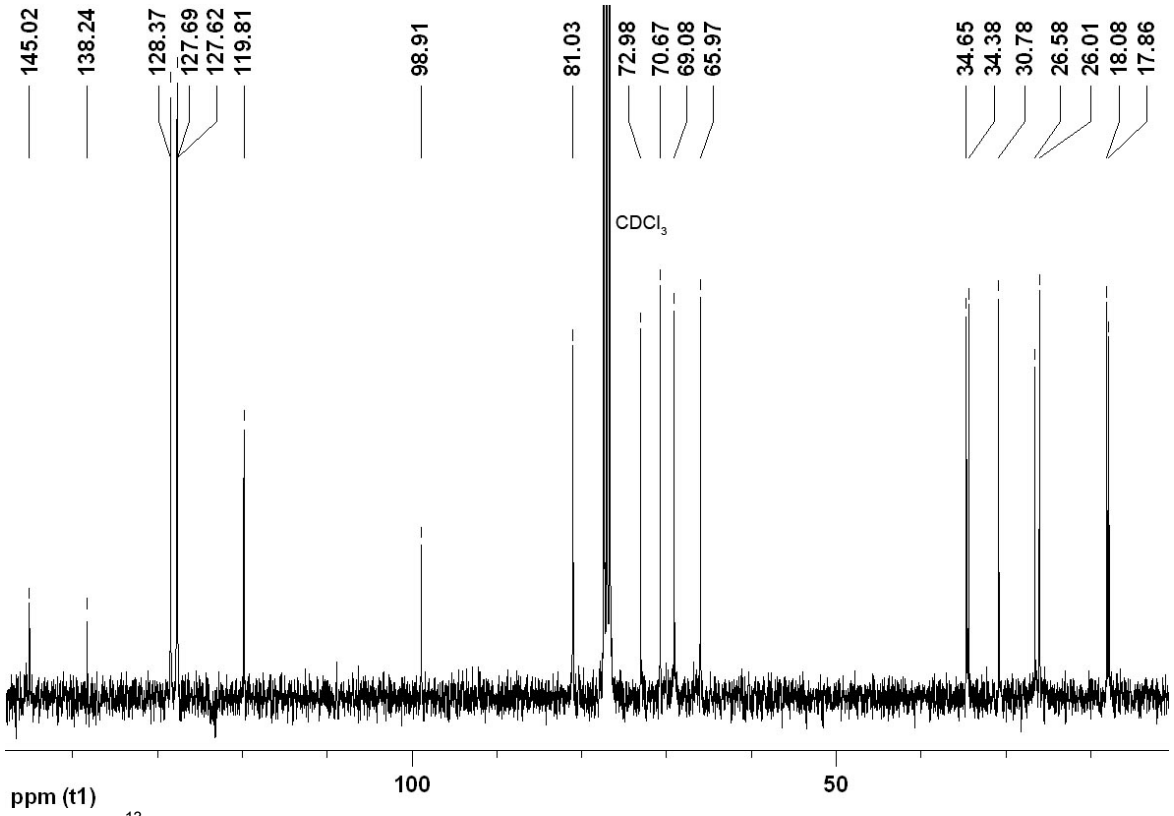

Figure 7.72: ^{13}C NMR spectrum (100 MHz; $CDCl_3$) of triazole **809a**.

1-{(2′*S,6′*S**,8′*S**)-8′-(Hydroxymethyl)-1′,7′-dioxaspiro[5.5]undecan-2-yl}-4-hydroxymethyl-1*H*-1,2,3-triazole (809c)**

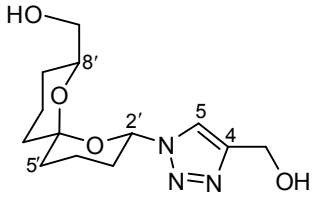

Method B: The *title compound* **809c** (4.80 mg, 71%) was prepared as a pale yellow oil from TBDPS-protected triazole **909c** (12.5 mg, 24.0 μmol) and HF•pyridine (60.0 μL) in anhydrous THF (1.5 mL) using the general procedure (method B) described above. Purification was carried out by flash chromatography using hexane–Et_2O–MeOH (4:1:0, 0:1:0 to 0:19:1) as eluent.

HRMS (FAB): found MH^+, 284.1618, $C_{13}H_{22}N_3O_4$ requires 284.1610.

ν_{max} (film)/cm^{-1}: 3375 (O–H), 2933 (C–H), 2872, 1456, 1440, 1223 (C–O), 1099 (C–O), 1047, 1017, 979.

δ_H (300 MHz; $CDCl_3$): 1.33–1.43 (1 H, m, 9′-H_A), 1.46–1.64 (4 H, m, 5′-H_A, 9′-H_B, 10′-H_A and 11′-H_A), 1.70–1.95 (5 H, m, 3′-H_A, 4′-H_A, 5′-H_B, 10′-H_B and 11′-H_B), 2.05–2.21 (3 H, m, 3′-H_B, 4′-H_B and OH), 2.46 (1 H, br s, OH), 3.57 (1 H, dd, J_{AB} 11.6 and $J_{8'\text{-}CH_2,8'}$ 6.3, 8′-C$H_A$$H_B$O), 3.69 (1 H, dd, J_{AB} 11.6 and $J_{8'\text{-}CH_2,8'}$ 3.3, 8′-$CH_A$$H_B$O), 3.82–3.90 (1 H, m, 8′-H), 4.81 (2 H, s, 4-CH_2OH), 5.97 (1 H, dd, $J_{2'ax,3'ax}$ 11.0 and $J_{2'ax,3'eq}$ 2.3, 2′-H_{ax}), 7.74 (1 H, s, 5-H).

δ_C (100 MHz; $CDCl_3$): 17.9 (CH_2, C-10′), 18.0 (CH_2, C-4′), 26.0 (CH_2, C-9′), 30.8 (CH_2, C-3′), 34.4 (CH_2, C-5′), 34.6 (CH_2, C-11′), 56.6 (CH_2, 4-CH_2OH), 66.0 (CH_2, 8′-CH_2O), 70.8 (CH, C-8′), 81.2 (CH, C-2′), 99.0 (C, C-6′), 119.9 (CH, C-5), 147.4 (C, C-4).

***m/z* (FAB):** 284 (MH^+, 12%), 185 ($C_{10}H_7O_3$, 45), 155 (40), 149 (37), 138 (52), 137 (100), 120 (20), 91 (26).

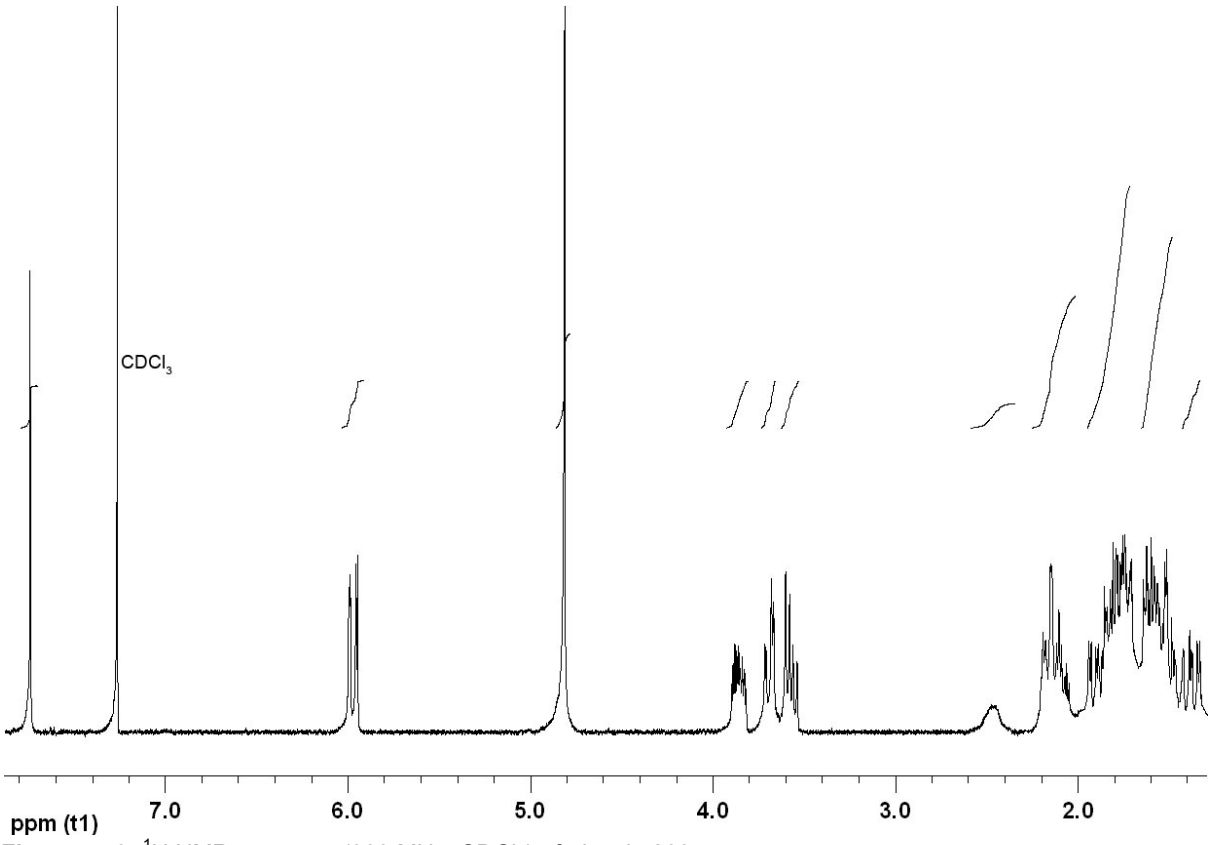

Figure 7.73: ^{1}H NMR spectrum (300 MHz; $CDCl_3$) of triazole **809c**.

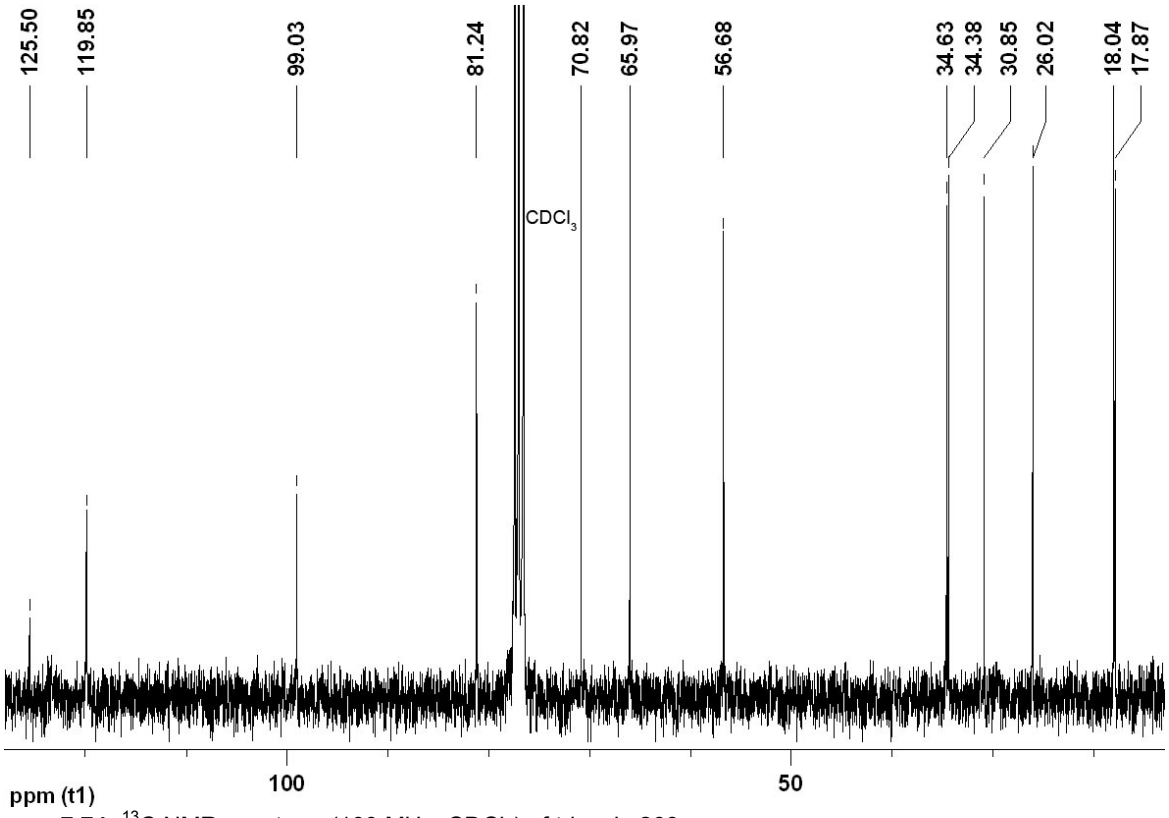

Figure 7.74: ^{13}C NMR spectrum (100 MHz; $CDCl_3$) of triazole **809c**

1-{(2′*S,6′*S**,8′*S**)-8′-(Hydroxymethyl)-1′,7′-dioxaspiro[5.5]undecan-2′-yl}-4-phenyl-1*H*-1,2,3-triazole (809d)**

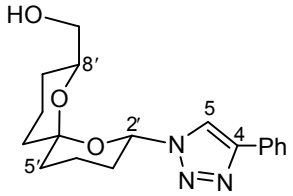

Method A: The *title compound* **809d** (7.10 mg, 81%) was prepared as a pale yellow oil from TBDPS-protected triazole **909d** (15.0 mg, 26.4 μmol) and TBAF solution (264 μL, 264 μmol) in anhydrous THF (1.0 mL) using the general procedure (method A) described above. Purification was carried out by flash chromatography using hexane–EtOAc (9:1 to 7:3) as eluent.

HRMS (EI): found $M^{+\bullet}$, 329.1735, $C_{18}H_{23}N_3O_3$ requires 329.1739.

ν_{max} (film)/cm^{-1}: 3389 (O–H), 2944 (C–H), 2873, 1438, 1391, 1234, 1202 (C–O), 1076 (C–O), 1046, 1019, 978, 766, 695.

δ_H (300 MHz; $CDCl_3$): 1.39–1.47 (1 H, m, 9′-H_A), 1.47–1.68 (4 H, m, 5′-H_A, 9′-H_B, 10′-H_A and 11′-H_A), 1.74–1.97 (4 H, m, 4′-H_A, 5′-H_B, 10′-H_B and 11′-H_B), 1.98–2.11 (2 H, m, 3′-H_A and OH), 2.11–2.26 (2 H, m, 3′-H_B and 4′-H_B), 3.57–3.67 (1 H, m, 8′-CH_AH_BO), 3.72 (1 H, d, J_{AB} 11.3, 8′-CH_AH_BO), 3.86–3.95 (1 H, m, 8′-H), 6.03 (1 H, dd, $J_{2'ax,3'ax}$ 11.0 and $J_{2'ax,3'eq}$ 2.4, 2′-H_{ax}), 7.30–7.36 (1 H, m, Ph), 7.40–7.46 (2 H, m, Ph), 7.84–7.88 (2 H, m, Ph), 7.95 (1 H, s, 5-H).

δ_C (100 MHz; $CDCl_3$): 17.9 (CH_2, C-10′), 18.1 (CH_2, C-4′), 26.0 (CH_2, C-9′), 31.0 (CH_2, C-3′), 34.4 (CH_2, C-5′), 34.7 (CH_2, C-11′), 66.0 (CH_2, 8′-CH_2O), 70.8 (CH, C-8′), 81.3 (CH, C-2′), 99.1 (C, C-6′), 117.7 (CH, C-5), 125.8 (CH, Ph), 128.1 (CH, Ph), 128.8 (CH, Ph), 130.6 (C, Ph), 147.6 (C, C-4).

***m/z* (EI):** 329 ($M^{+\bullet}$, 4%), 298 (M – CH_2OH, 2), 185 ($C_{10}H_{17}O_3$, 55), 145 (100), 128 (15), 121 (22), 117 (18), 99 (36), 71 (25), 57 (15), 55 (29), 43 (15), 41 (26).

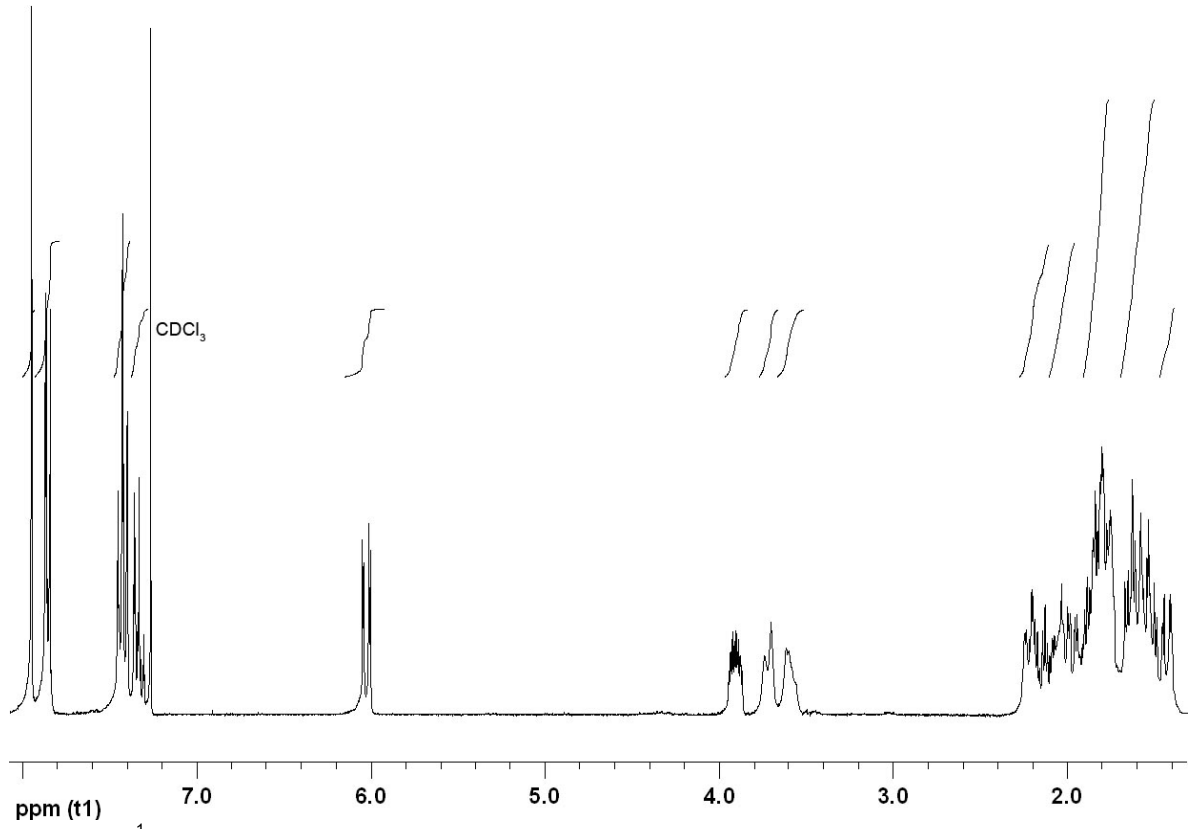

Figure 7.75: ^{1}H NMR spectrum (300 MHz; $CDCl_3$) of triazole **809d**.

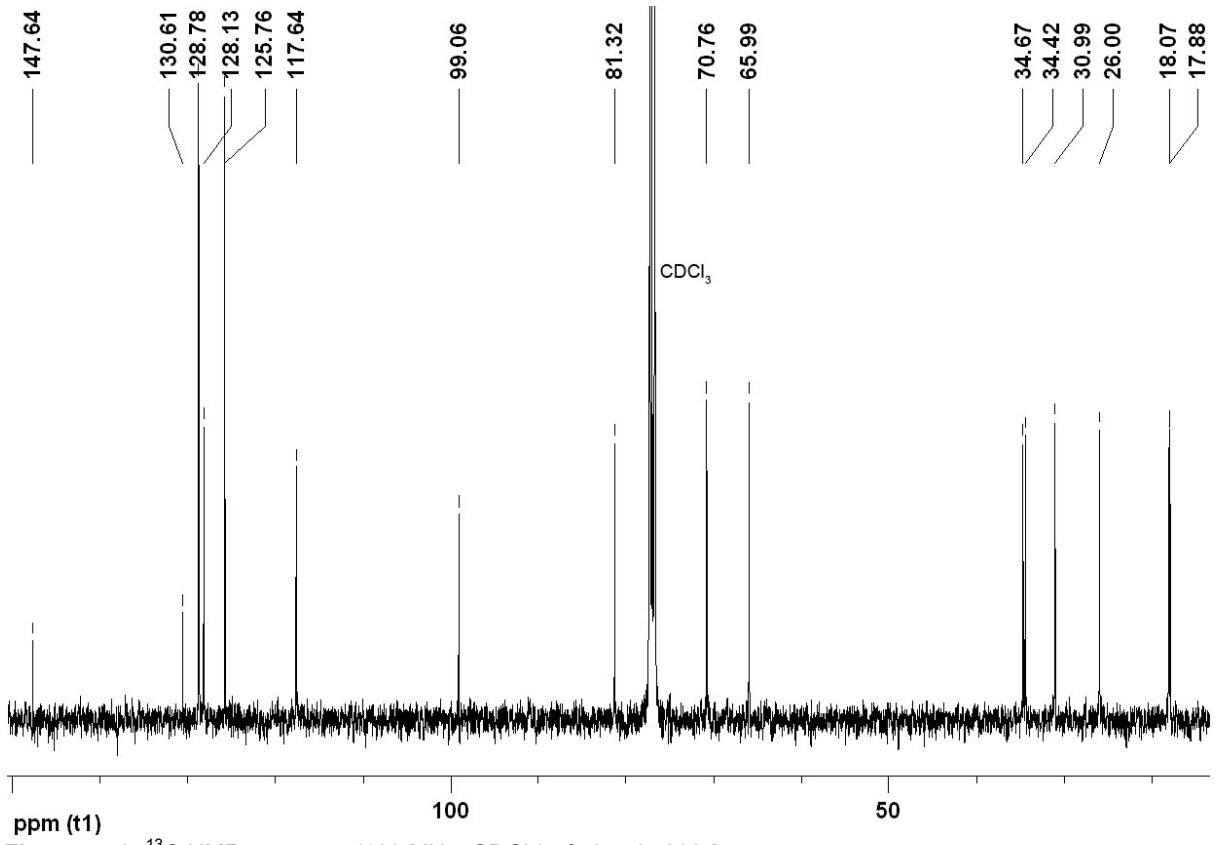

Figure 7.76: ^{13}C NMR spectrum (100 MHz; $CDCl_3$) of triazole **809d**.

Ethyl 1-{(2′*S,6′*S**,8′*S**)-8′-(Hydroxymethyl)-1′,7′-dioxaspiro[5.5]undecan-2′-yl}-1*H*-1,2,3-triazole-4-carboxylate (809e)**

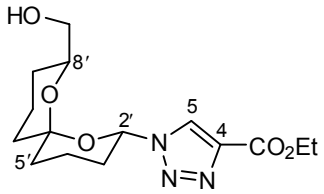

Method B: The *title compound* **809e** (3.50 mg, 70%) was prepared as a pale yellow oil from TBDPS-protected triazole **909e** (8.70 mg, 15.4 μmol) and HF•pyridine (2 x 50.0 μL) in anhydrous THF (1.0 mL) using the general procedure (method B) described above. Purification was carried out by flash chromatography using hexane–EtOAc (9:1 to 1:4) as eluent.

HRMS (EI): found $M^{+\bullet}$, 325.1638, $C_{15}H_{23}N_3O_5$ requires 325.1638.

ν_{max} (film)/cm^{-1}: 3412 (O–H), 2941 (C–H), 1733 (C=O), 1376, 1222 (C–O), 1044 (C–O), 980.

δ_H (300 MHz; $CDCl_3$): 1.38–1.45 (1 H, m, 9′-H_A), 1.42 (3 H, t, J_{CH_3,CH_2} 7.1, OCH_2CH_3), 1.48–1.58 (2 H, m, 9′-H_B and 11′-H_A), 1.58–1.66 (2 H, m, 5′-H_A and 10′-H_A), 1.73–1.94 (6 H, m, 3′-H_A, 4′-H_A, 5′-H_B, 10′-H_B, 11′-H_B and OH), 2.05–2.17 (1 H, m, 4′-H_B), 2.17–2.28 (1 H, m, 3′-H_B), 3.52–3.63 (1 H, m, 8′-CH_AH_BO), 3.63–3.76 (1 H, m, 8′-CH_AH_BO), 3.79–3.88 (1 H, m, 8′-H), 4.44 (2 H, t, J_{CH_2,CH_3} 7.1, OCH_2CH_3), 6.02 (1 H, dd, $J_{2'ax,3'ax}$ 10.8 and $J_{2'ax,3'eq}$ 2.5, 2′-H_{ax}), 8.28 (1 H, s, 5-H).

δ_C (100 MHz; $CDCl_3$): 14.3 (CH_3, OCH_2CH_3), 17.8 (CH_2, C-10′), 17.9 (CH_2, C-4′), 25.9 (CH_2, C-9′), 31.2 (CH_2, C-3′), 34.4 (CH_2, C-5′), 34.6 (CH_2, C-11′), 61.3 (CH_2, OCH_2CH_3), 65.9 (CH_2, 8′-CH_2O), 70.9 (CH, C-8′), 81.7 (CH, C-2′), 99.3 (C, C-6′), 125.7 (CH, C-5), 140.2 (C, C-4), 160.8 (C, C=O).

***m/z* (EI):** 325 ($M^{+\bullet}$, 5%), 294 (M – CH_2OH, 2), 280 (M – OEt, 3), 252 (M – CO_2Et, 2), 185 ($C_{10}H_{17}O_3$, 43), 156 (60), 128 (100), 114 (25), 99 (69), 96 (67), 70 (49), 55 (47), 41 (50).

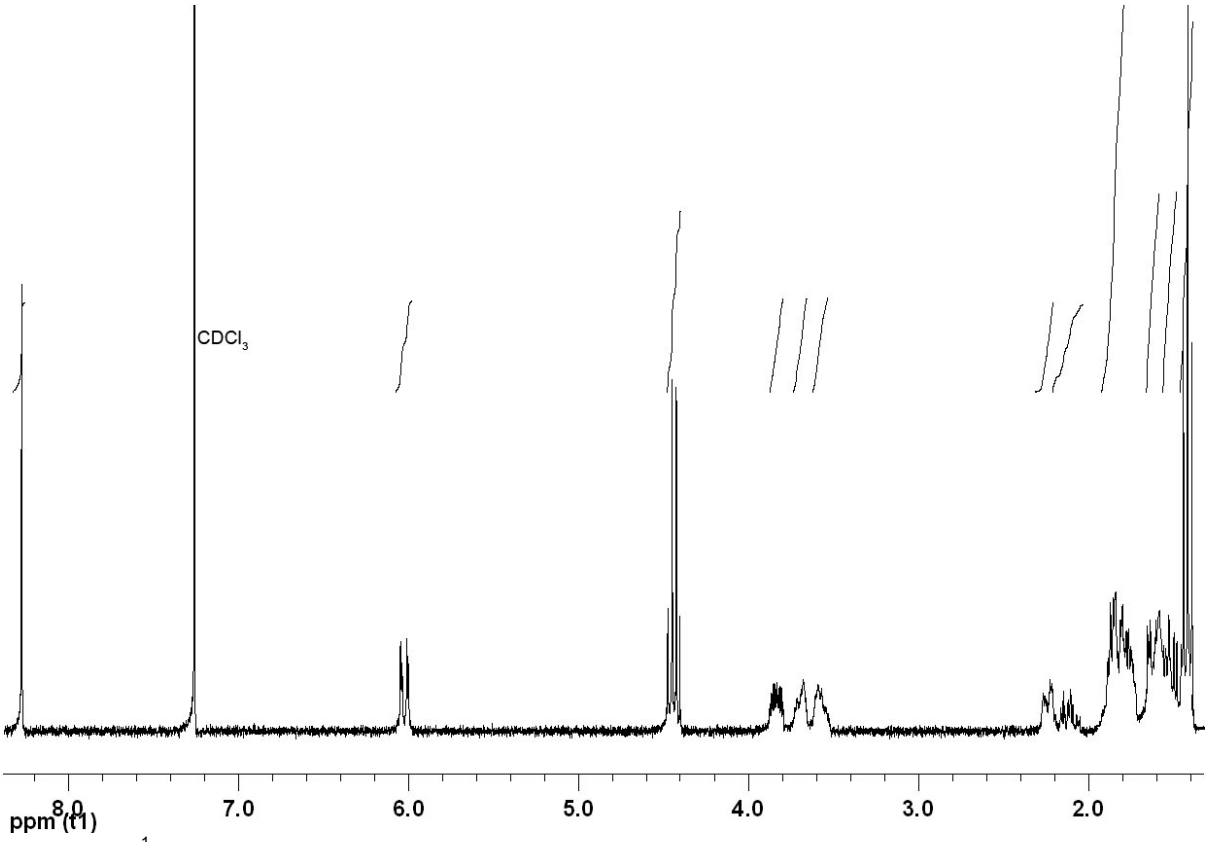

Figure 7.77: ^{1}H NMR spectrum (300 MHz; $CDCl_3$) of triazole **809e**.

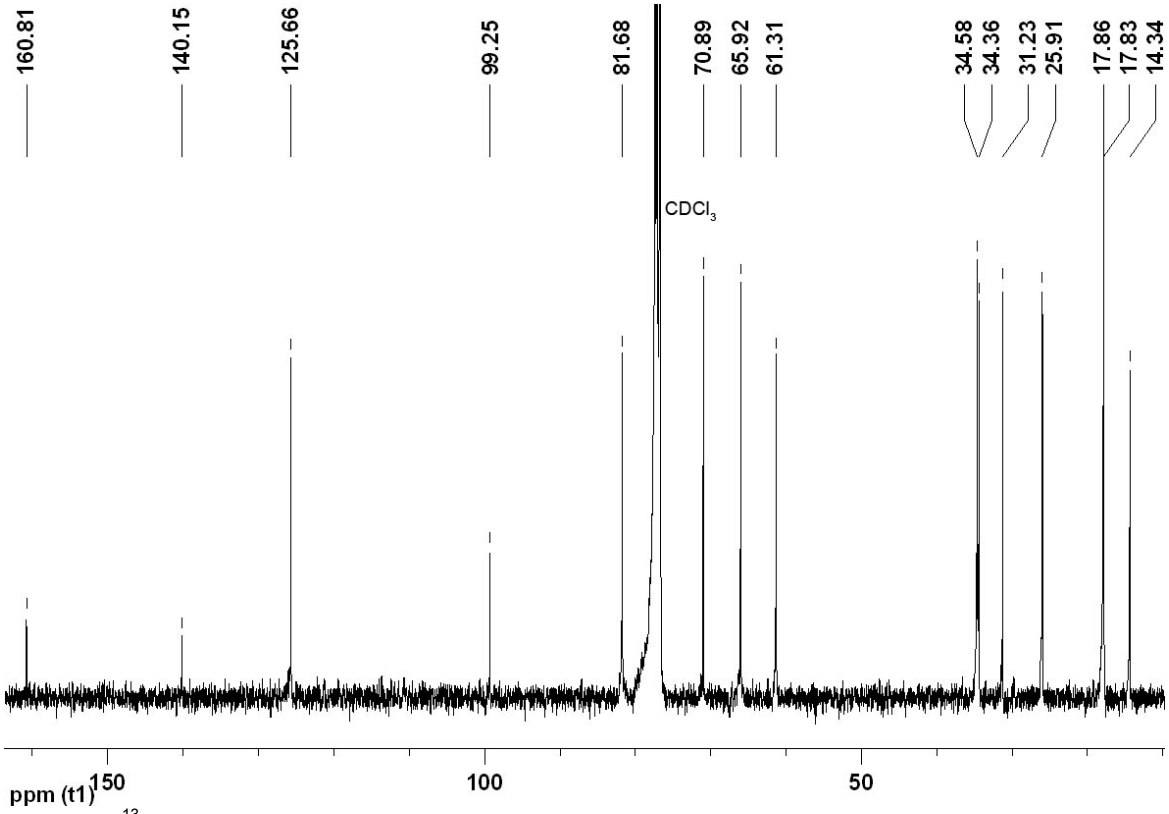

Figure 7.78: ^{13}C NMR spectrum (100 MHz; $CDCl_3$) of triazole **809e**.

Dimethyl 1-{(2′*S,6′*S**,8′*S**)-8′-(Hydroxymethyl)-1′,7′-dioxaspiro[5.5]undecan-2′-yl}-1*H*-1,2,3-triazole-4,5-dicarboxylate (809f)**

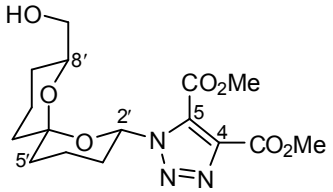

Method C[§§]: The *title compound* **809f** (3.50 mg, 69%) was prepared as a pale yellow oil from TBDPS-protected triazole **909f** (8.30 mg, 13.7 mmol) and 3HF•NEt_3 (3 x 34 μL) in anhydrous THF (300 μL) using the general procedure (method C) described above. Purification was carried out by flash chromatography using hexane–EtOAc (4:1, 1:1 to 0:1) as eluent followed by PLC using Et_2O as eluent.

HRMS (FAB): found MH^+, 370.1615, $C_{16}H_{24}N_3O_7$ requires 370.1614.

ν_{max} (film)/cm^{-1}: 3439br (O–H), 2953 (C–H), 1739 (C=O), 1462, 1290, 1258, 1229, 1204 (C–O), 1105 (C–O), 984.

δ_H (400 MHz; $CDCl_3$): 1.31–1.39 (1 H, m, 9′-H_A), 1.45–1.55 (2 H, m, 9′-H_B and 11′-H_A), 1.55–1.65 (2 H, m, 5′-H_A and 10′-H_A), 1.68–1.90 (5 H, m, 4′-H_A, 5′-H_B, 10′-H_B, 11′-H_B and OH), 2.05–2.19 (2 H, m, 3′-H_A and 4′-H_B), 2.28–2.40 (1 H, m, 3′-H_B), 3.56–3.60 (1 H, m, 8′-CH_AH_BO), 3.68 (1 H, d, J_{AB} 11.7, 8′-CH_AH_BO), 3.76–3.82 (1 H, m, 8′-H), 3.97 (3 H, s, OMe), 4.00 (3 H, s, OMe), 6.15 (1 H, dd, $J_{2'ax,3'ax}$ 11.2 and $J_{2'ax,3'eq}$ 2.7, 2′-H_{ax}).

δ_C (100 MHz; $CDCl_3$): 17.8 (2 x CH_2, C-4′ and C-10′), 26.0 (CH_2, C-9′), 30.1 (CH_2, C-3′), 34.3 (CH_2, C-5′), 34.6 (CH_2, C-11′), 52.6 (CH_3, OMe), 53.6 (CH_3, OMe), 66.0 (CH_2, 8′-CH_2O), 71.0 (CH, C-8′), 82.2 (CH, C-2′), 99.5 (C, C-6′), 131.5 (C, C-5), 138.5 (C, C-4), 159.9 (C, C=O), 160.3 (C, C=O).

***m/z* (FAB):** 370 (MH^+, 3%), 354 (M – Me, 2), 185 ($C_{10}H_{17}O_3$, 100), 149 (61), 137 (29), 127 (27), 121 (18), 95 (18), 85 (41), 71 (76).

[§§] A yield of 23% was achieved when method B was used.

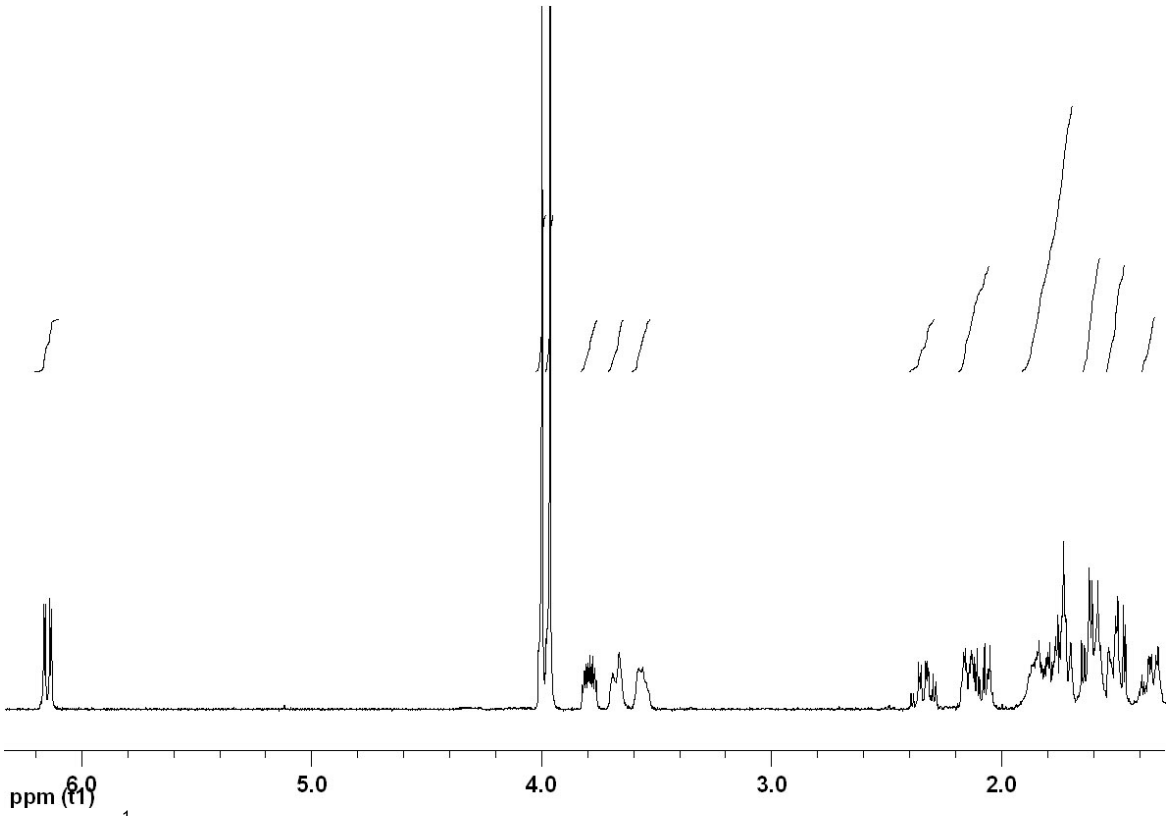

Figure 7.79: ^{1}H NMR spectrum (400 MHz; $CDCl_3$) of triazole **809f**.

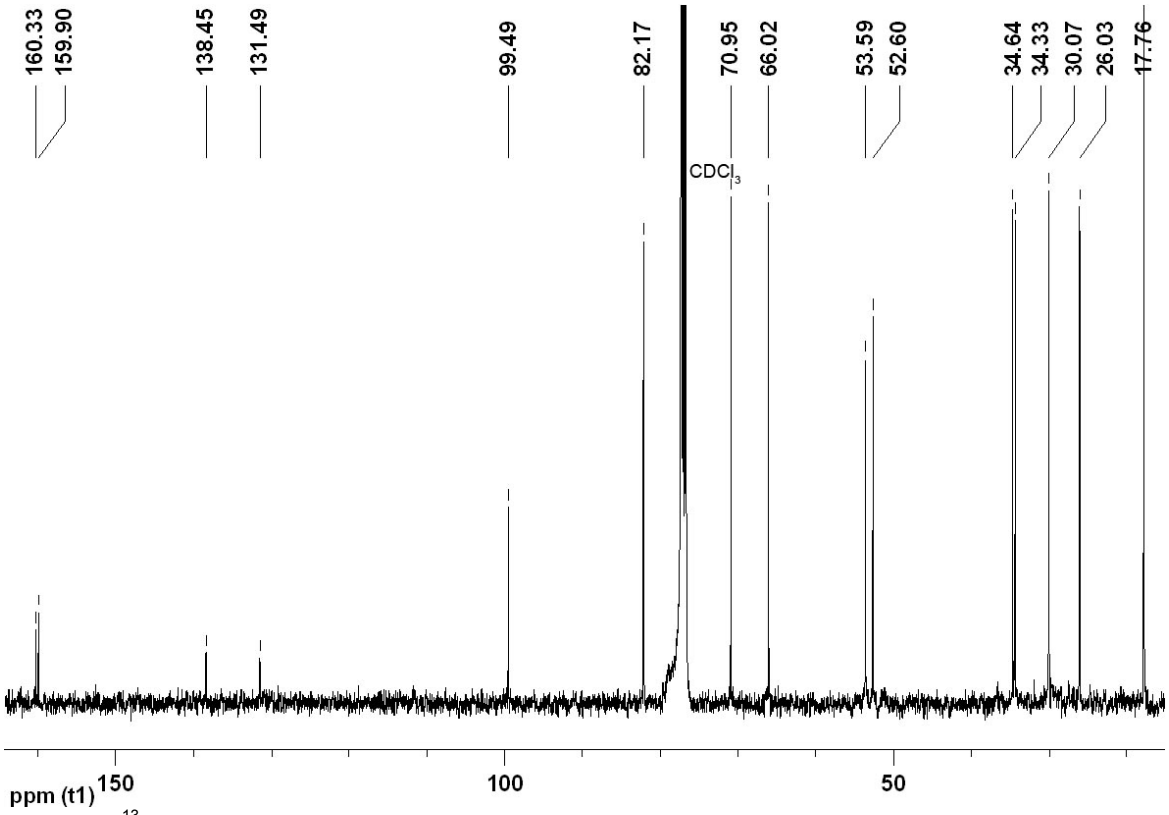

Figure 7.80: ^{13}C NMR spectrum (100 MHz; $CDCl_3$) of triazole **809f**.

1-{(2′*S,6′*S**,8′*S**)-8′-(Hydroxymethyl)-1′,7′-dioxaspiro[5.5]undecan-2′-yl}-1*H*-1,2,3-triazole (809g)**

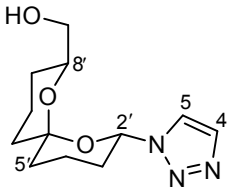

Method C***: The *title compound* **809g** (3.00 mg, 86%) was prepared as a pale yellow oil from TBDPS-protected triazole **909g** (7.80 mg, 13.8 μmol) and 3HF•NEt_3 (41.0 μL) in anhydrous THF (300 μL) using the general procedure (method C) described above. Purification was carried out by flash chromatography using hexane–EtOAc (4:1, 1:1 to 0:1) as eluent.

HRMS (EI): found $M^{+\bullet}$, 253.1427, $C_{12}H_{19}N_3O_3$ requires 253.1426.

ν_{max} (film)/cm^{-1}: 3390 (O–H), 2944 (C–H), 2873, 1456, 1387, 1220, 1201 (C–O), 1066 (C–O), 1047, 979.

δ_H (400 MHz; $CDCl_3$): 1.34–1.43 (1 H, m, 9′-H_A), 1.44–1.64 (4 H, m, 5′-H_A, 9′-H_B, 10′-H_A and 11′-H_A), 1.72–1.86 (4 H, m, 4′-H_A, 5′-H_B, 10′-H_B and 11′-H_B), 1.88–2.03 (2 H, m, 3′-H_A and OH), 2.07–2.21 (2 H, m, 3′-H_B and 4′-H_B), 3.58 (1 H, dd, J_{AB} 11.3 and $J_{8'\text{-}CH_2,8'}$ 6.2, 8′-CH_AH_BO), 3.71 (1 H, d, J_{AB} 11.3, 8′-CH_AH_BO), 3.85–3.91 (1 H, m, 8′-H), 6.03 (1 H, dd, $J_{2'ax,3'ax}$ 11.0 and $J_{2'ax,3'eq}$ 2.5, 2′-H_{ax}), 7.74 (1 H, d, $J_{4,5}$ 9.7, 4-H), 7.74 (1 H, d, $J_{5,4}$ 9.7, 5-H).

δ_C (100 MHz; $CDCl_3$): 17.9 (CH_2, C-10′), 18.1 (CH_2, C-4′), 26.0 (CH_2, C-9′), 30.9 (CH_2, C-3′), 34.4 (CH_2, C-5′), 34.6 (CH_2, C-11′), 66.0 (CH_2, 8′-CH_2O), 70.8 (CH, C-8′), 81.1 (CH, C-2′), 99.0 (C, C-6′), 121.5 (CH, C-5), 133.7 (CH, C-4).

***m/z* (EI):** 253 ($M^{+\bullet}$, 9%), 222 (M – CH_2OH, 7), 185 ($C_{10}H_{17}O_3$, 29), 156 (57), 128 (100), 109 (20), 99 (39), 97 (62), 95 (32), 80 (27), 70 (64), 67 (40), 55 (50), 41 (94).

*** A yield of 26% was achieved when method B was used.

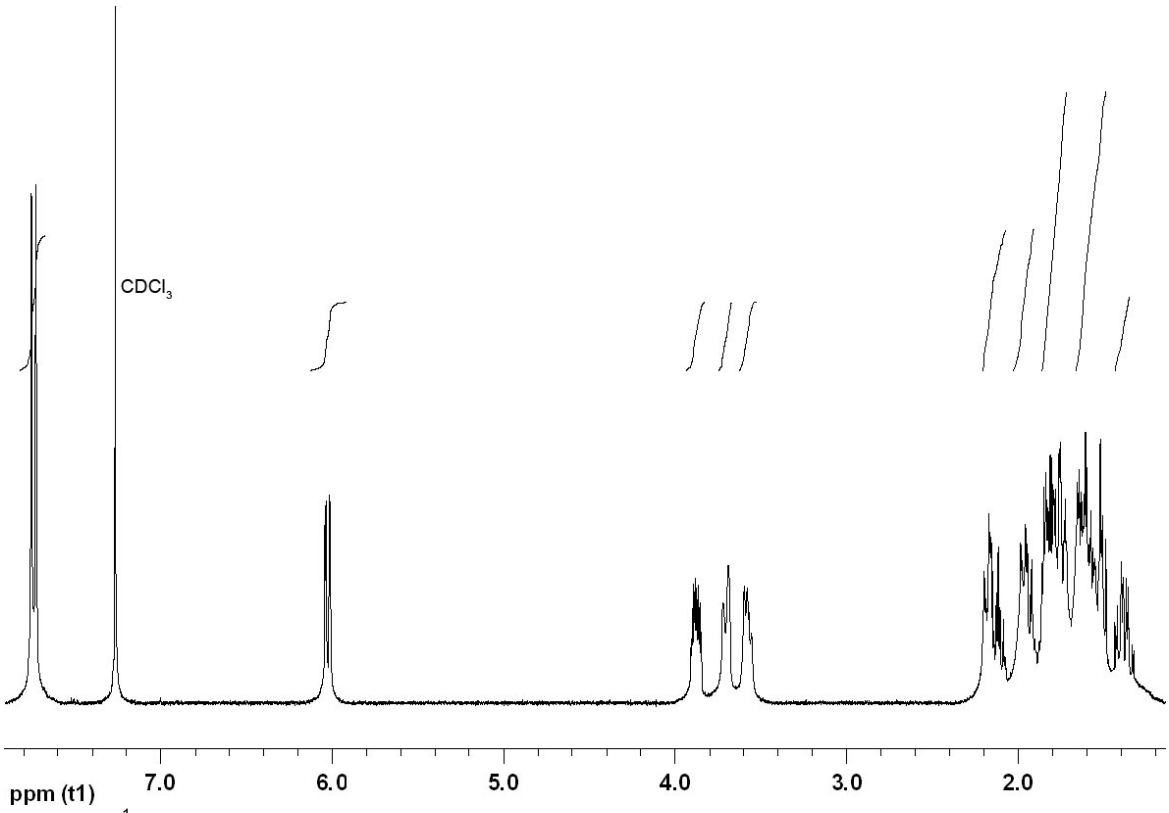

Figure 7.81: ^{1}H NMR spectrum (400 MHz; $CDCl_3$) of triazole **809g**.

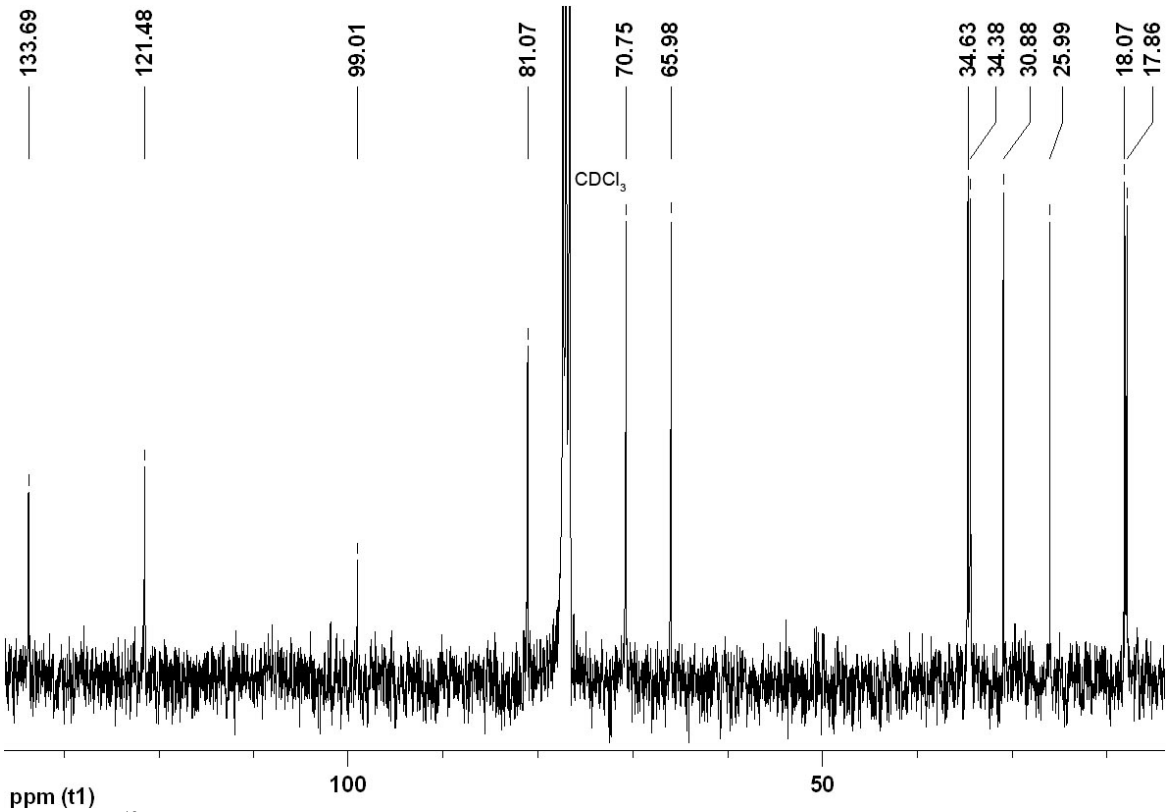

Figure 7.82: ^{13}C NMR spectrum (100 MHz; $CDCl_3$) of triazole **809g**.

Ethyl 1-{(2′*S,6′*S**,8′*S**)-8′-(Hydroxymethyl)-1′,7′-dioxaspiro[5.5]undecan-2′-yl}-1*H*-1,2,3-triazole-5-carboxylate (809h)**

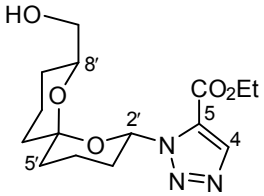

Method D: The *title compound* **809h** (2.40 mg, 93%) was prepared as a pale yellow oil from TBDPS-protected triazole **909h** (5.00 mg, 7.86 μmol), 3HF•NEt_3 (16.0 + 8.00 μL) and NEt_3 (20.0 + 10.0 μL) in anhydrous THF (700 μL) using the general procedure (method D) described above. Purification was carried out by flash chromatography using hexane–EtOAc (4:1, 3:2 to 1:4) as eluent.

HRMS (EI): found $M^{+\bullet}$, 325.1636, $C_{15}H_{23}N_3O_5$ requires 325.1638.

ν_{max} (film)/cm^{-1}: 3411br (O–H), 2925 (C–H), 2853, 1732 (C=O), 1309, 1258, 1194 (C–O), 1082 (C–O), 984.

δ_H (300 MHz; $CDCl_3$): 1.29–1.36 (1 H, m, 9′-H_A), 1.40 (3 H, t, J_{CH_3,CH_2} 7.1, OCH_2CH_3), 1.44–1.70 (4 H, m, 5′-H_A, 9′-H_B, 10′-H_A and 11′-H_A), 1.71–1.89 (4 H, m, 4′-H_A, 5′-H_B, 10′-H_B and 11′-H_B), 1.93–2.01 (1 H, m, 3′-H_A), 2.09–2.24 (2 H, m, 4′-H_B and OH), 2.53–2.68 (1 H, m, 3′-H_B), 3.59 (1 H, dd, J_{AB} 11.6 and $J_{8'\text{-}CH_2,8'}$ 6.5, 8′-CH_AH_BO), 3.75 (1 H, dd, J_{AB} 11.6 and $J_{8'\text{-}CH_2,8'}$ 3.3, 8′-CH_AH_BO), 3.95–4.14 (1 H, m, 8′-H), 4.4 (2 H, q, J_{CH_2,CH_3} 7.1, OCH_2CH_3), 6.74 (1 H, dd, $J_{2'ax,3'ax}$ 11.4 and $J_{2'ax,3'eq}$ 2.5, 2′-H_{ax}), 8.14 (1 H, s, 4-H).

δ_C (100 MHz; $CDCl_3$): 14.1 (CH_3, OCH_2CH_3), 18.2 (CH_2, C-10′), 18.3 (CH_2, C-4′), 26.3 (CH_2, C-9′), 29.6 (CH_2, C-3′), 34.6 (CH_2, C-5′ or C-11′), 34.6 (CH_2, C-5′ or C-11′), 62.1 (CH_2, OCH_2CH_3), 66.4 (CH_2, 8′-CH_2O), 70.8 (CH, C-8′), 79.8 (CH, C-2′), 99.4 (C, C-6′), 127.6 (C, C-5), 137.9 (CH, C-4), 158.6 (C, C=O).

***m/z* (EI):** 325 ($M^{+\bullet}$, 2%), 252 (M – CO_2Et, 11), 185 ($C_{10}H_{17}O_3$, 3), 184 (34), 156 (35), 153 (30), 142 (56), 128 (100), 99 (93), 97 (64), 95 (57), 71 (52), 70 (48), 67 (40), 55 (71), 41 (66).

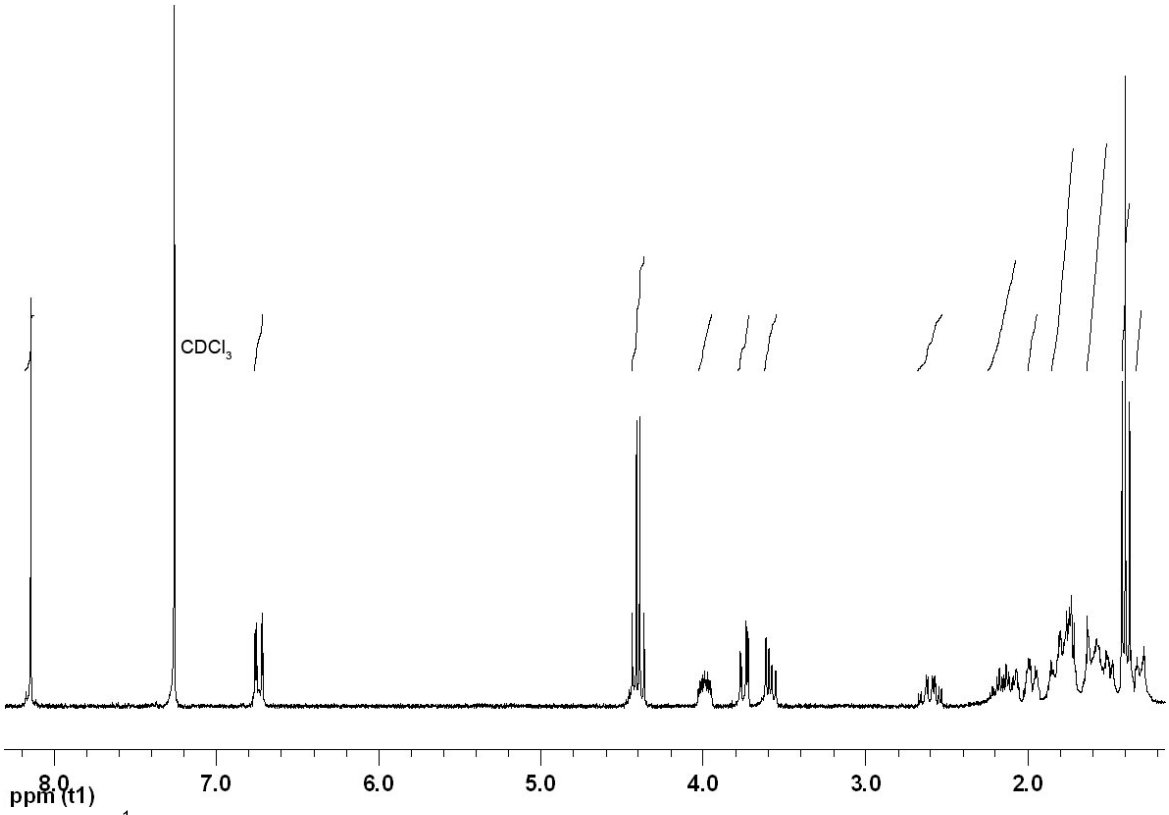

Figure 7.83: ^{1}H NMR spectrum (300 MHz; $CDCl_3$) of triazole **809h**.

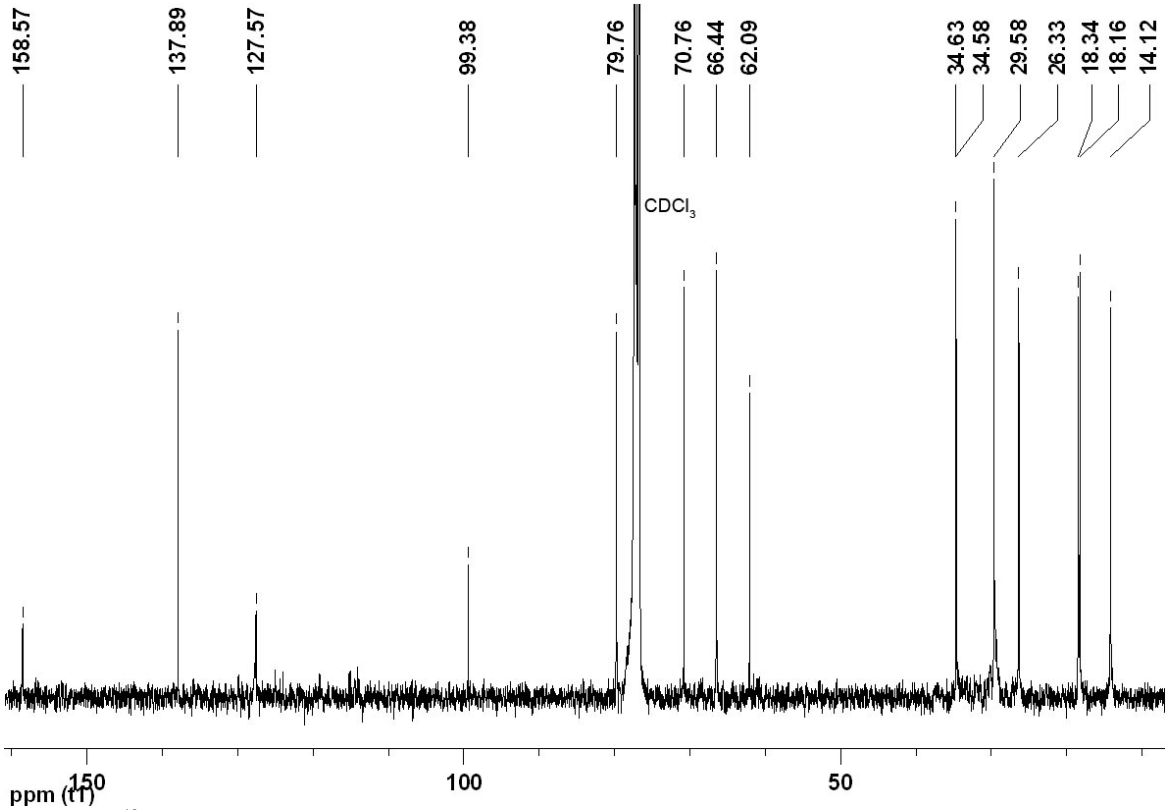

Figure 7.84: ^{13}C NMR spectrum (100 MHz; $CDCl_3$) of triazole **809h**.

7.4.2 Deprotection of Spiroacetal-Nucleosides 902

General Procedures for Deprotection of Spiroacetal Nucleosides 902

Method A: Desilylation using 3HF•NEt_3[32]

A solution of TBDPS-protected nucleoside **902** and 3HF•NEt_3 (3.0–5.4 μL per 1.0 μmol) in anhydrous THF (300 μL–1.5 mL) under an atmosphere of argon was stirred at 40 °C for 24–48 h. Saturated $NaHCO_3$ solution (2 mL) was added dropwise. The aqueous phase was extracted with EtOAc (6 x 3 mL) and the combined organic extracts were concentrated *in vacuo*. Purification by flash chromatography using the appropriate eluent yielded the hydroxylmethyl spiroacetal nucleoside.

Method B: Deacylation using NEt_3–H_2O–MeOH and Microwave[33]

To a solution of acyl-protected purine nucleosides in a mixture of NEt_3–H_2O–MeOH was irradiated in a sealed tube at 100–120 °C under microwave. After 30 min, the reaction was concentrated i*n vacuo* and saturated $NaHCO_3$ solution (0.5 mL) was added. The aqueous phase was extracted with EtOAc (5 x 3 mL) and the combined organic extracts were concentrated *in vacuo*. Purification by flash chromatography using the appropriate eluent yielded the hydroxymethyl spiroacetal nucleoside.

1-{(2′*S,6′*S**,8′*S**)-8′-(Hydroxymethyl)-1′,7′-dioxaspiro[5.5]undecan-2′-yl}-5-fluorocytidine (808a)**

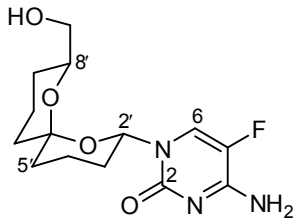

Method A: The *title compound* **808a** (2.40 mg, 77%) was prepared as a pale yellow oil from TBDPS-protected fluorocytidine **902a** (5.50 mg, 9.97 μmol) and 3HF•NEt_3 (30.0 μL) in THF (500 μL) using the general procedure (method A) described above. Purification was carried out by flash chromatography using hexane–EtOAc–MeOH (4:1:0, 0:1:0, 0:19:1 to 0:9:1) as eluent.

HRMS (FAB): found MH^+, 314.1506, $C_{14}H_{21}FN_3O_4$ requires 314.1516.

ν_{max} (film)/cm^{-1}: 3354br (O–H), 3195 (N–H), 3101 (N–H), 2927 (C–H), 1678 (C=O), 1602 (C=N), 1511, 1201 (C–O), 1133 (C–O), 979.

δ_H (300 MHz; $CDCl_3$): 1.27–1.35 (1 H, m, 9′-H_A), 1.37–1.52 (3 H, m, 3′-H_A, 5′-H_A and 11′-H_A), 1.52–1.65 (2 H, m, 9′-H_B and 10′-H_A), 1.65–1.86 (4 H, m, 4′-H_A, 5′-H_B, 10′-H_B and 11′-H_B), 1.90–1.99 (1 H, m, 3′-H_B), 2.00–2.61 (4 H, m, 4′-H_B, NH_2 and OH), 3.55 (1 H, dd, J_{AB} 11.6 and $J_{8'CH_2,8'}$ 6.3, 8′-CH_AH_BO), 3.66 (1 H, dd, J_{AB} 11.6 and $J_{8'\text{-}CH_2,8'}$ 3.4, 8′-CH_AH_BO), 3.84–3.90 (1 H, m, 8′-H), 6.03 (1 H, d, $J_{2'ax,3'ax}$ 10.8, 2′-H_{ax}), 7.51 (1 H, d, $J_{6,5F}$ 5.8, 6-H).

δ_C (100 MHz; $CDCl_3$ with a drop of CD_3OD): 18.1 (2 x CH_2, C-4′ and C-10′), 26.4 (CH_2, C-9′), 30.2 (CH_2, C-3′), 34.4 (CH_2, C-5′ or C-11′), 34.6 (CH_2, C-5′ or C-11′), 65.8 (CH_2, 8′-CH_2O), 70.9 (CH, C-8′), 77.2 (CH, C-2′), 99.2 (C, C-6′), 125.6 (CH, d, $J_{6,5F}$ 31.2, C-6), 136.6 (C, d, $J_{5,5F}$ 242.3, C-5), 153.8 (C, C-2), 157.4 (C, $J_{4,5F}$ 14.5, C-4).

δ_F (282 MHz; $CFCl_3$): -168.52 (CF, 5-F).

***m/z* (FAB):** 314 (MH^+, 21%), 185 ($C_{10}H_{17}O_3$, 64), 156 (37), 149 (28), 138 (49), 137 (90), 130 (100).

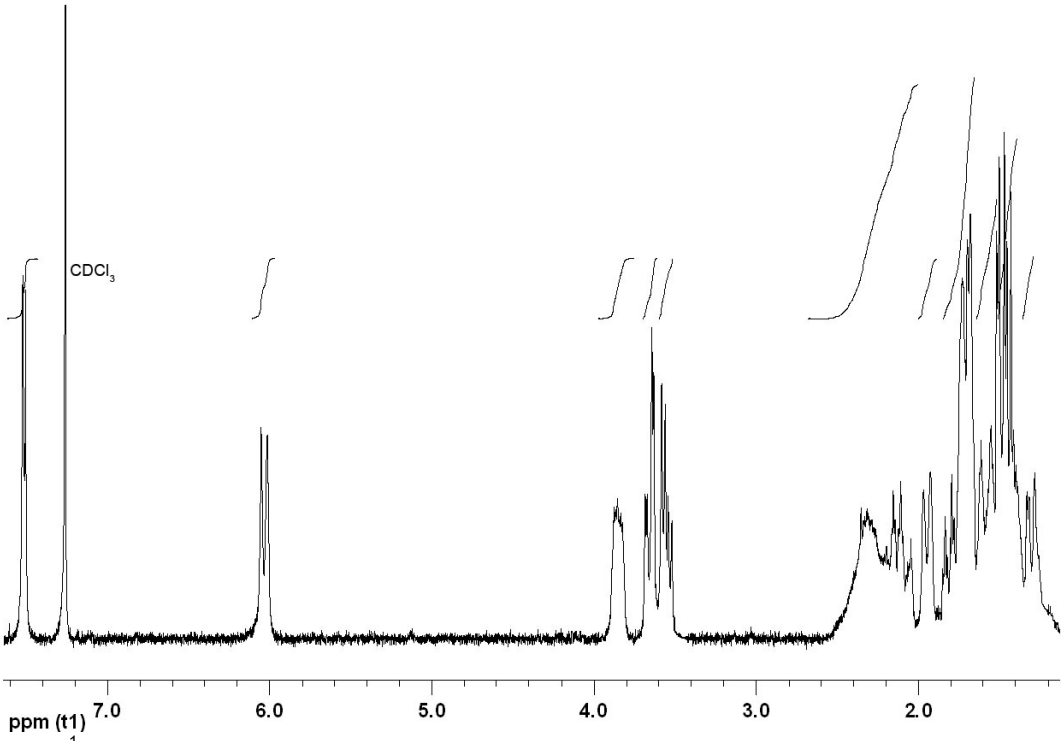

Figure 7.85: ^1H NMR spectrum (300 MHz; $CDCl_3$) of fluorocytidine **808a**.

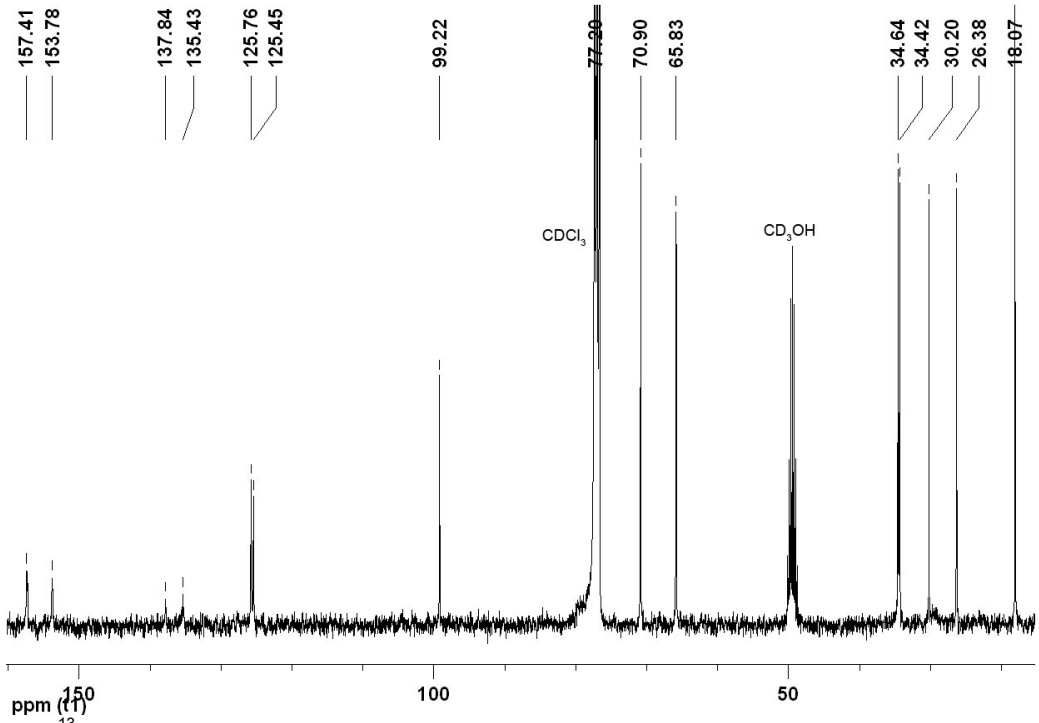

Figure 7.86: ^{13}C NMR spectrum (100 MHz; $CDCl_3$ with a drop of CD_3OD) of fluorocytidine **808a**.

1-{(2′*S,6′*S**,8′*S**)-8′-(Hydroxymethyl)-1′,7′-dioxaspiro[5.5]undecan-2′-yl}cytidine (808b)**

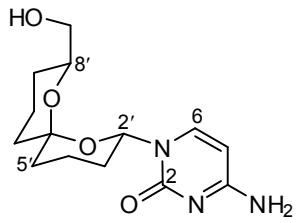

Method A: The *title compound* **808b** (3.90 mg, 69%) was prepared as a pale yellow oil from TBDPS-protected cytidine **902b** (11.0 mg, 19.1 μmol) and 3HF•NEt_3 (104 μL) in THF (700 μL) using the general procedure (method A) described above. Purification was carried out by flash chromatography using hexane–EtOAc–MeOH (4:1:0, 0:1:0 to 0:9:1) as eluent.

HRMS (FAB): found MH^+, 296.1605, $C_{14}H_{22}FN_3O_4$ requires 296.1610.

ν_{max} (film)/cm^{-1}: 3354br (O–H), 3205 (N–H), 2929 (C–H), 1646 (C=O), 1493, 1203 (C–O), 979.

δ_H (300 MHz; $CDCl_3$): 1.32–1.37 (1 H, m, 9′-H_A), 1.40–1.62 (5 H, m, 3′-H_A, 5′-H_A, 9′-H_B, 10′-H_A and 11′-H_A), 1.64–1.76 (3 H, m, 4′-H_A, 5′-H_B and 11′-H_B), 1.77–1.85 (1 H, m, 10′-H_B), 1.87–1.95 (1 H, m, 3′-H_B), 2.04–2.39 (4 H, m, 4′-H_B, NH_2 and OH), 3.55 (1 H, dd, J_{AB} 11.5 and $J_{8'CH_2,8'}$ 6.6, 8′-CH_AH_BO), 3.67 (1 H, dd, J_{AB} 11.5 and $J_{8'\text{-}CH_2,8'}$ 3.5, 8′-CH_AH_BO), 3.86–3.94 (1 H, m, 8′-H), 5.86 (1 H, d, $J_{5,6}$ 7.5, 5-H), 6.10 (1 H, dd, $J_{2'ax,3'ax}$ 11.2 and $J_{2'ax,3'eq}$ 2.0, 2′-H_{ax}), 7.50 (1 H, d, $J_{6,5}$ 7.5, 6-H).

δ_C (75 MHz; $CDCl_3$): 18.2 (CH_2, C-10′), 18.5 (CH_2, C-4′), 26.2 (CH_2, C-9′), 30.1 (CH_2, C-3′), 34.6 (CH_2, C-5′ or C-11′), 34.8 (CH_2, C-5′ or C-11′), 66.1 (CH_2, 8′-CH_2O), 70.7 (CH, C-8′), 76.7 (CH, C-2′), 94.8 (CH, C-5), 99.1 (C, C-6′), 141.5 (CH, C-6), 165.6 (C, C-2), 165.3 (C, C-4).

***m/z* (FAB):** 296 (MH^+, 10%), 185 ($C_{10}H_{17}O_3$, 12), 155 (45), 149 (32), 138 (56), 137 (100), 124 (17), 120 (20), 112 (68), 91 (37).

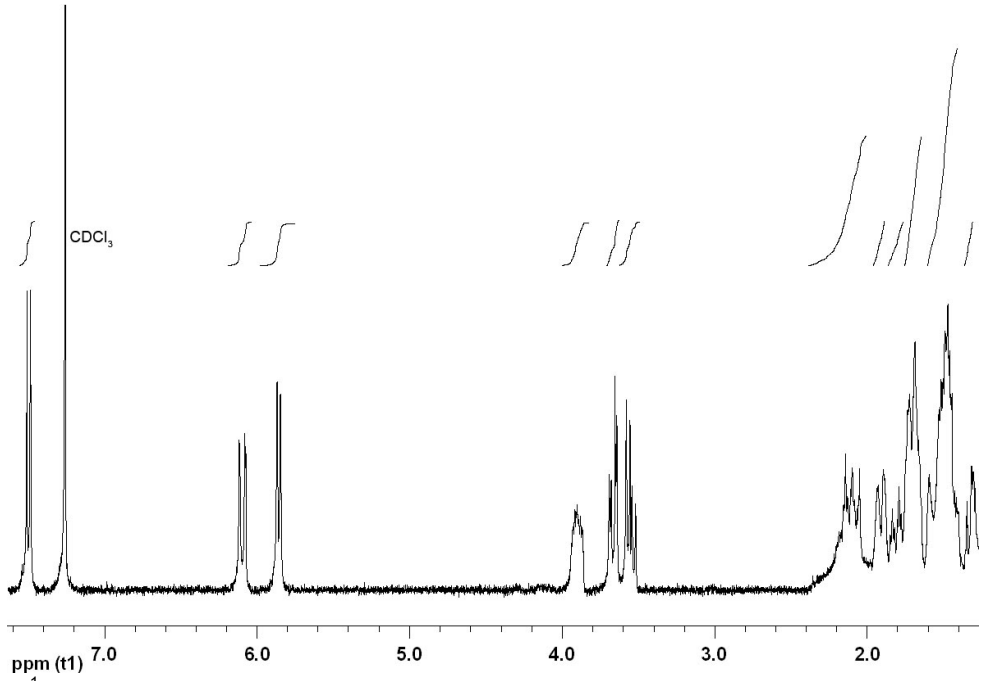

Figure 7.87: ^{1}H NMR spectrum (300 MHz; $CDCl_3$) of cytidine **808b**.

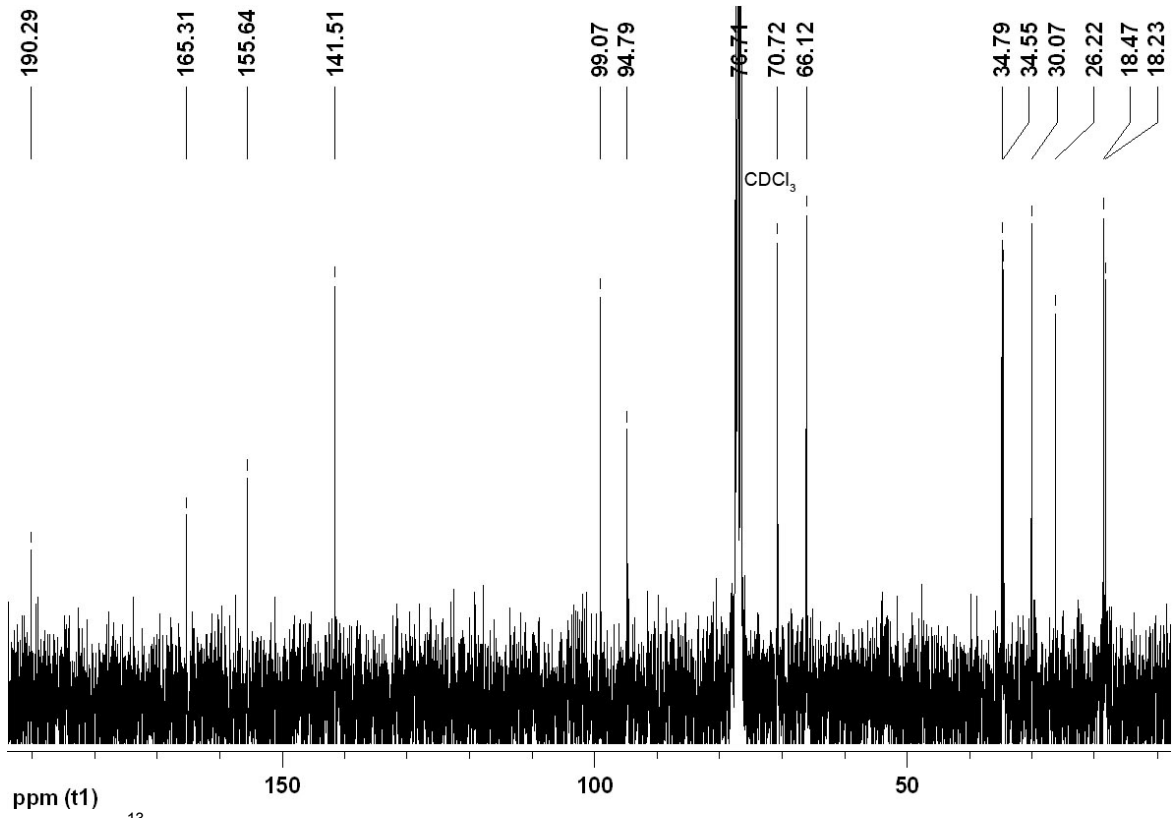

Figure 7.88: ^{13}C NMR spectrum (75 MHz; $CDCl_3$) of cytidine **808b**.

1-{(2′*S,6′*S**,8′*S**)-8′-(Hydroxymethyl)-1′,7′-dioxaspiro[5.5]undecan-2′-yl}thymidine (808c)**

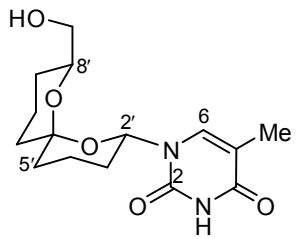

Method A: The *title compound* **808c** (3.30 mg, 79%) was prepared as a pale yellow oil from TBDPS-protected thymidine **902c** (7.40 mg, 13.5 μmol) and 3HF•NEt_3 (72.0 μL) in THF (300 μL) using the general procedure (method A) described above. Purification was carried out by flash chromatography using hexane–EtOAc (4:1 to 1:1) as eluent.

HRMS (FAB): found MH^+, 310.1525, $C_{15}H_{22}N_2O_5$ requires 310.1529.

ν_{max} (film)/cm^{-1}: 3444br (O–H), 3184 (N–H), 3044, 2945 (C–H), 1694 (C=O), 1682 (C=O), 1272 (C–O), 1092, 980.

δ_H (400 MHz; $CDCl_3$): 1.23–1.34 (1 H, m, 9′-H_A), 1.44–1.52 (2 H, m, 5′-H_A and 11′-H_A), 1.56–1.65 (3 H, m, 3′-H_A, 9′-H_B and 10′-H_A), 1.65–1.87 (5 H, m, 3′-H_B, 4′-H_A, 5′-H_B, 10′-H_B and 11′-H_B), 1.96 (3 H, d, $J_{5\text{-}CH_3,6}$ 1.1, 5-CH_3), 2.04–2.18 (1 H, m, 4′-H_B), 2.63 (1 H, t, $J_{OH,8'\text{-}CH_2}$ 5.5, OH), 3.59–3.64 (2 H, m, 8′-CH_2O), 3.82–3.89 (1 H, m, 8′-H), 6.03 (1 H, dd, $J_{2'ax,3'ax}$ 11.3, $J_{2'ax,3'eq}$ 2.2, 2′-H_{ax}), 7.22 (1 H, d, $J_{6,5\text{-}CH_3}$ 1.1, 6-H), 9.21 (1 H, br s, NH).

δ_C (100 MHz; $CDCl_3$): 12.6 (CH_3, 5-CH_3), 18.1 (CH_2, C-4′), 18.4 (CH_2, C-10′), 26.5 (CH_2, C-9′), 29.3 (CH_2, C-3′), 34.4 (CH_2, C-5′ or C-11′), 34.7 (CH_2, C-5′ or C-11′), 66.0 (CH_2, 8′-CH_2O), 70.9 (CH, C-8′), 75.8 (CH, C-2′), 99.2 (C, C-6′), 111.2 (C, C-5), 135.8 (CH, C-6), 150.9 (C, C-2), 163.6 (C, C-4).

***m/z* (FAB):** 311 (MH^+, 1%), 293 (M – OH, 7), 185 ($C_{10}H_{17}O_3$, 100), 167 (10), 127 (24), 121 (10), 99 (12), 97 (10).

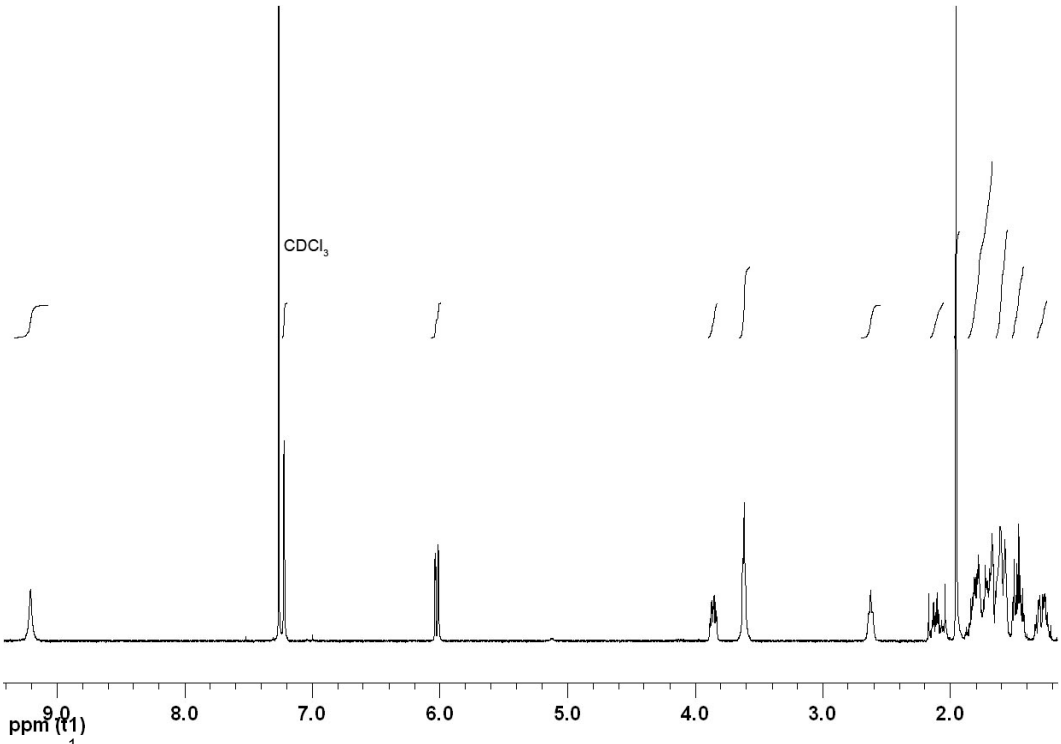

Figure 7.89: ^1H NMR spectrum (400 MHz; $CDCl_3$) of thymidine **808c**.

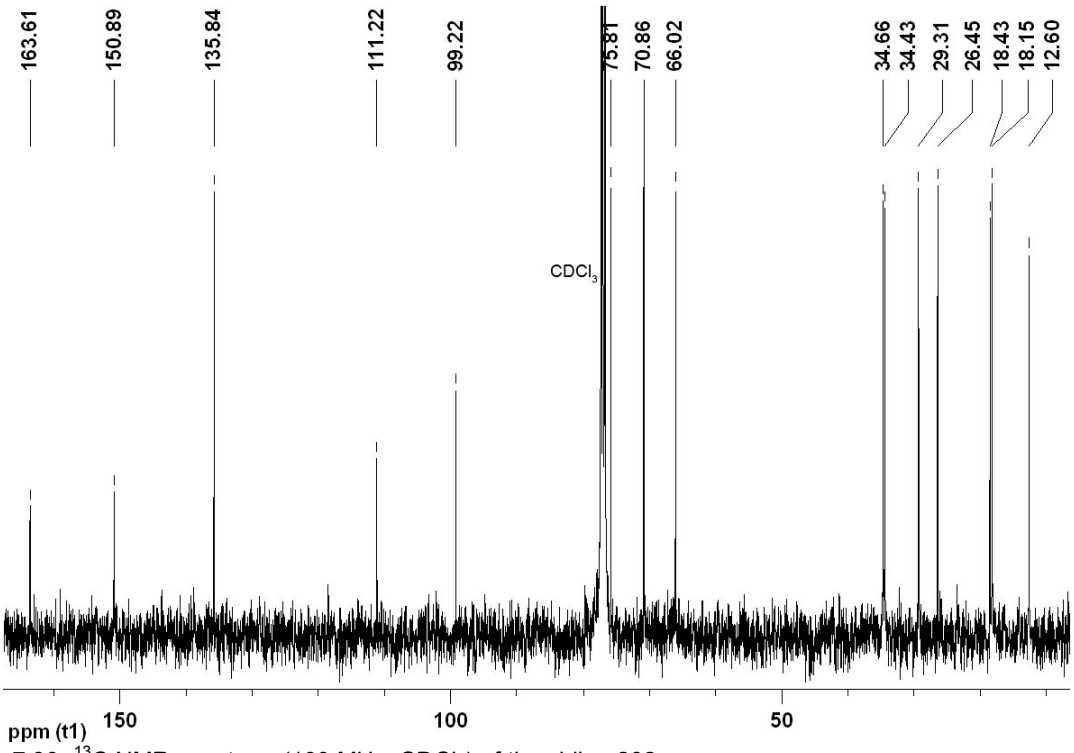

Figure 7.90: ^{13}C NMR spectrum (100 MHz; $CDCl_3$) of thymidine **808c**.

1-{(2′*S,6′*S**,8′*S**)-8′-(Hydroxymethyl)-1′,7′-dioxaspiro[5.5]undecan-2′-yl}uridine (808d)**

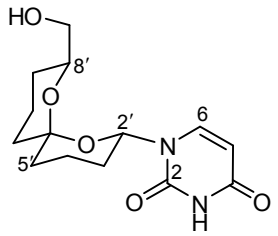

Method A: The *title compound* **808d** (2.90 mg, 73%) was prepared as a pale yellow oil from TBDPS-protected uridine **902d** (7.20 mg, 13.5 μmol) and 3HF•NEt_3 (40.5 μL) in THF (1.0 mL) using the general procedure (method A) described above. Purification was carried out by flash chromatography (twice) using hexane–EtOAc (4:1, 1:1 to 0:1) as eluent.

HRMS (FAB): found MH^+, 297.1441, $C_{14}H_{21}N_2O_5$ requires 297.1451.

ν_{max} (film)/cm^{-1}: 3439br (O–H), 3055 (N–H), 2926 (C–H), 1694 (C=O), 1682 (C=O), 1463, 1385, 1271 (C–O), 1204 (C–O), 1048, 982.

δ_H (400 MHz; $CDCl_3$): 1.29–1.37 (1 H, m, 9′-H_A), 1.45–1.52 (2 H, m, 5′-H_A and 11′-H_A), 1.53–1.64 (3 H, m, 3′-H_A, 9′-H_B and 10′-H_A), 1.66–1.82 (5 H, m, 4′-H_A, 5′-H_B, 10′-H_B, 11′-H_B and OH), 1.82–1.88 (1 H, m, 3′-H_B), 2.08–2.17 (1 H, m, 4′-H_B) 3.59 (1 H, dd, J_{AB} 11.5 and $J_{8'\text{-}CH_2,8'}$ 6.0, 8′-CH_AH_BO), 3.72 (1 H, dd, J_{AB} 11.5 and $J_{8'\text{-}CH_2,8'}$ 4.0, 8′-CH_AH_BO), 3.81–3.87 (1 H, m, 8′-H), 5.76 (1 H, d, $J_{5,6}$ 8.2, 5-H), 5.99 (1 H, dd, $J_{2'ax,3'ax}$ 11.3 and $J_{2'ax,3'eq}$ 2.3, 2′-H_{ax}), 7.43 (1 H, d, $J_{6,5}$ 8.2, 6-H), 8.86 (1 H, br s, NH).

δ_C (75 MHz; $CDCl_3$): 18.1 (CH_2, C-10′), 18.3 (CH_2, C-4′), 26.2 (CH_2, C-9′), 29.6 (CH_2, C-3′), 34.4 (CH_2, C-5′ or C-11′), 34.7 (CH_2, C-5′ or C-11′), 66.0 (CH_2, 8′-CH_2O), 70.9 (CH, C-8′), 76.2 (CH, C-2′), 99.3 (C, C-6′), 102.7 (CH, C-5), 140.1 (CH, C-6), 150.4 (C, C-2), 162.7 (C, C-4).

***m/z* (FAB):** 297 (MH^+, 6%), 185 ($C_{10}H_{17}O_3$, 34), 155 (31), 138 (41), 137 (78), 120 (17), 102 (100), 91 (19).

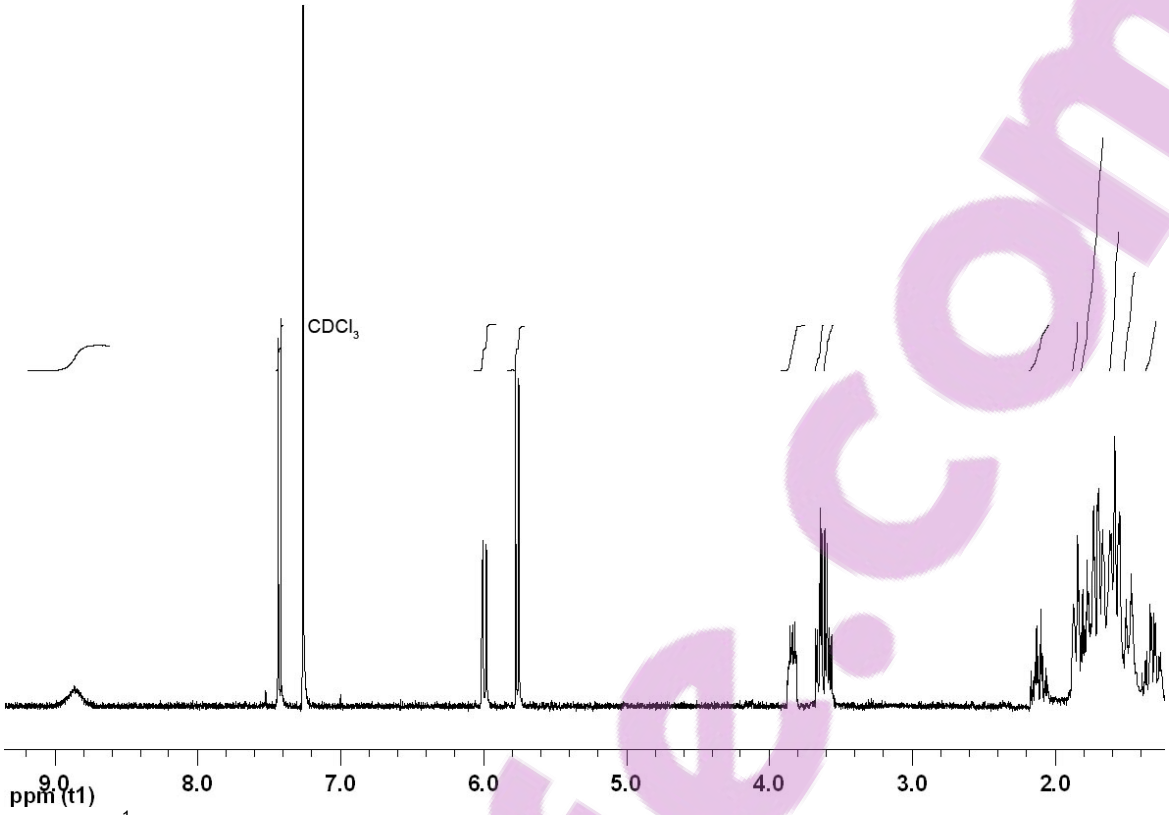

Figure 7.91: ^{1}H NMR spectrum (400 MHz; $CDCl_3$) of uridine **808d**.

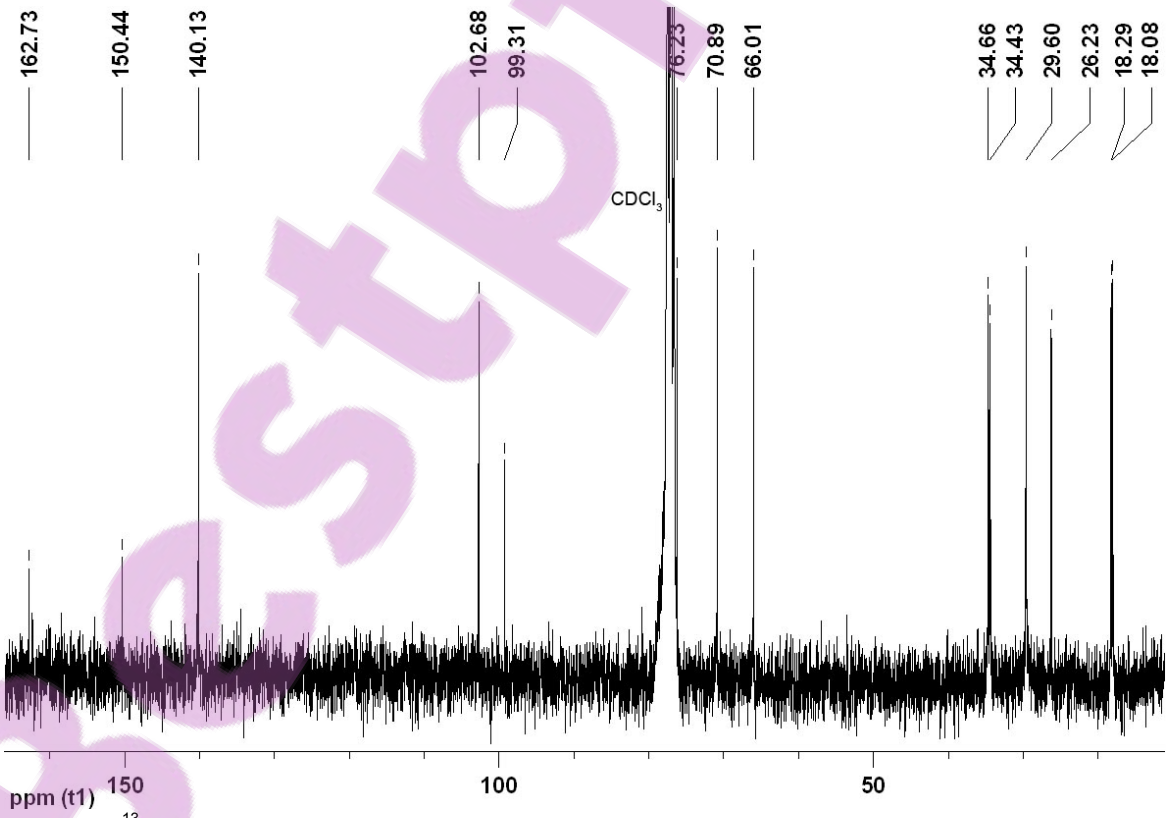

Figure 7.92: ^{13}C NMR spectrum (75 MHz; $CDCl_3$) of uridine **808d**.

1-{(2′*S,6′*S**,8′*S**)-8′-(Hydroxymethyl)-1′,7′-dioxaspiro[5.5]undecan-2′-yl}-5-fluorouridine (808e)**

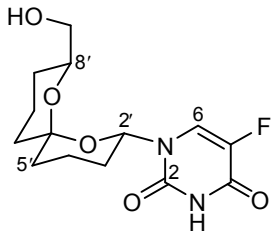

Method A: The *title compound* **808e** (1.00 mg, 65%) was prepared as a pale yellow oil from TBDPS-protected fluorouridine **902e** (2.70 mg, 4.89 μmmol) and 3HF•NEt_3 (25.0 μL) in THF (500 μL) using the general procedure (method A) described above. Purification was carried out by flash chromatography (twice) using hexane–EtOAc–MeOH (4:1:0, 0:1:0 to 0:19:1) as eluent.

HRMS (FAB): found MH^+, 315.1356, $C_{14}H_{20}FN_2O_5$ requires 315.1356.

ν_{max} (film)/cm^{-1}: 3444br (O–H), 3198 (N–H), 3064 (N–H), 2929 (C–H), 1714 (C=O), 1666 (C=O), 1373, 1265 (C–O), 1203, 1093 (C–O), 982.

δ_H (400 MHz; $CDCl_3$): 1.29–1.39 (1 H, m, 9′-H_A), 1.43–1.60 (5 H, m, 3′-H_A, 5′-H_A, 9′-H_B, 10′-H_A and 11′–H_A), 1.68–1.91 (5 H, m, 3′-H_A, 4′-H_A, 5′-H_B, 10′-H_B and 11′-H_B), 1.98–2.18 (2 H, m, 4′-H_B and OH), 3.58 (1 H, dd, J_{AB} 11.6 and $J_{8'\text{-}CH_2,8'}$ 6.1, 8′-CH_AH_BO), 3.66 (1 H, dd, J_{AB} 11.6 and $J_{8'\text{-}CH_2,8'}$ 3.7, 8′-CH_AH_BO), 3.78–3.85 (1 H, m, 8′-H), 5.96 (1 H, ddd, $J_{2'ax,3'ax}$ 11.2, $J_{2'ax,3'eq}$ = $J_{2',5F}$ 2.1, 2′-H_{ax}), 7.48 (1 H, d, $J_{6,5F}$ 6.1, 6-H), 8.88 (1 H, br s, NH).

δ_C (100 MHz; $CDCl_3$): 18.0 (CH_2, C-10′), 18.1 (CH_2, C-4′), 26.1 (CH_2, C-9′), 29.6 (CH_2, C-3′), 34.4 (CH_2, C-5′ or C-11′), 34.6 (CH_2, C-5′ or C-11′), 66.0 (CH_2, 8′-CH_2O), 71.0 (CH, C-8′), 76.7 (CH, C-2′), 99.5 (C, C-6′), 124.8 (CH, d, $J_{6,5F}$ 33.5, C-6), 141.0 (C, d, $J_{5,5F}$ 238.5, C-5), 148.8 (C, C-2), 156.3 (C, C-4).

δ_F (282 MHz; $CFCl_3$): -165.6 (CF, 5-F).

***m/z* (FAB):** 315 (MH^+, 3%), 282 (21), 185 ($C_{10}H_{17}O_3$, 24), 155 (40), 138 (50), 137 (100), 136(21), 124 (17), 120 (20), 91(24), 90 (24).

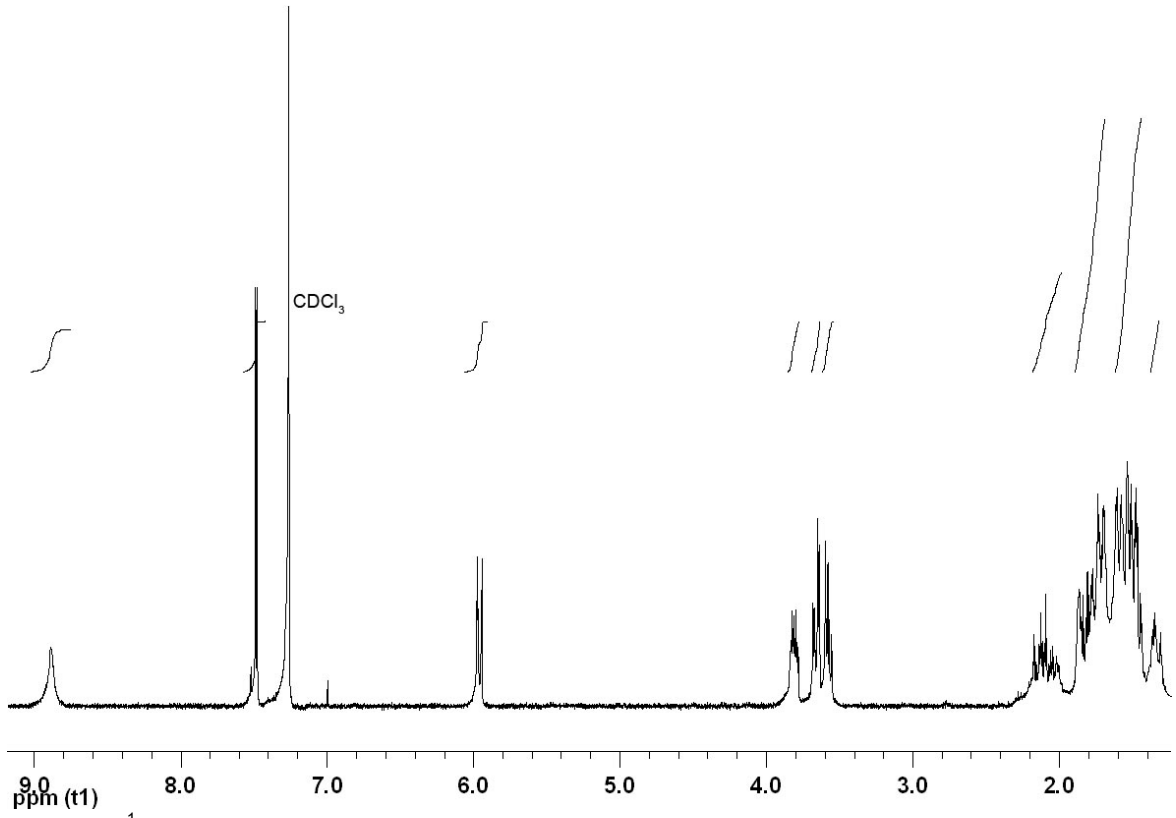

Figure 7.93: ^{1}H NMR spectrum (400 MHz; $CDCl_3$) of fluorouridine **808e**.

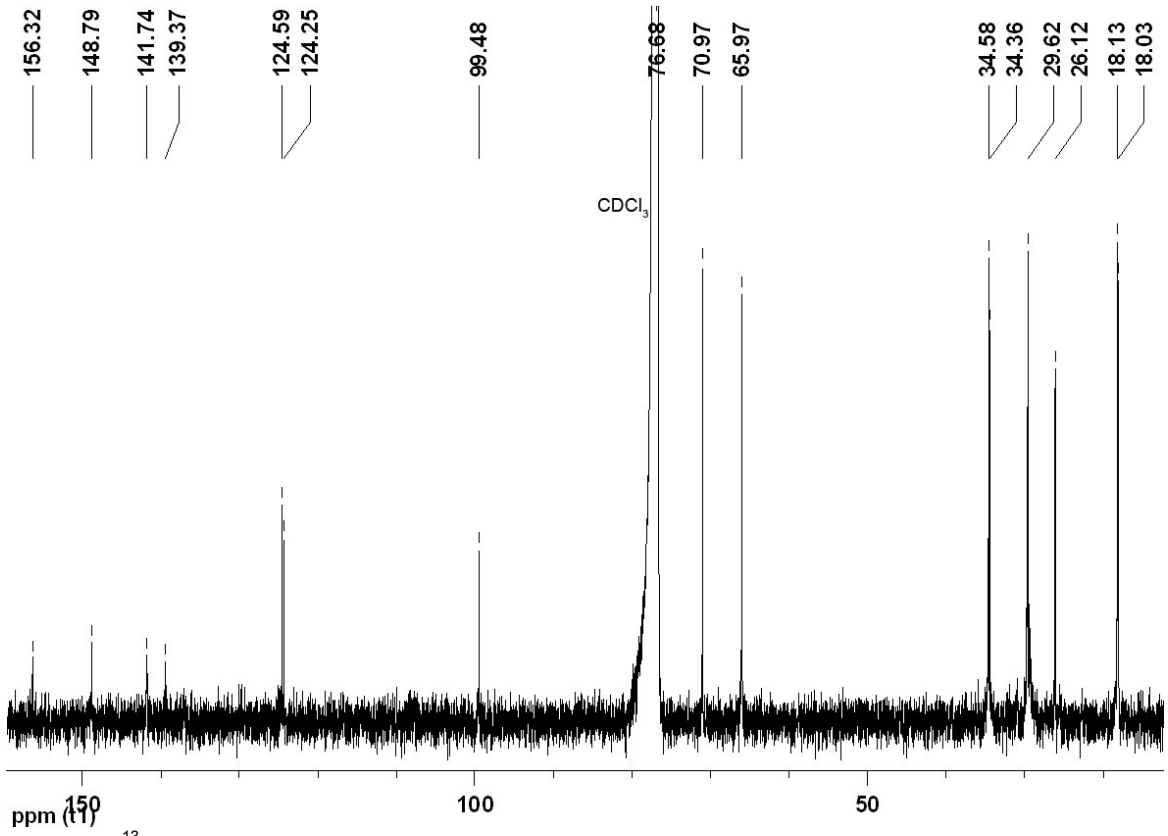

Figure 7.94: ^{13}C NMR spectrum (100 MHz; $CDCl_3$) of fluorouridine **808e**.

6-*N*-Benzoyl-9-{(2′*S,6′*S**,8′*S**)-8′-(hydroxymethyl)-1′,7′-dioxaspiro[5.5]undecan-2′-yl}adenosine (808f)**

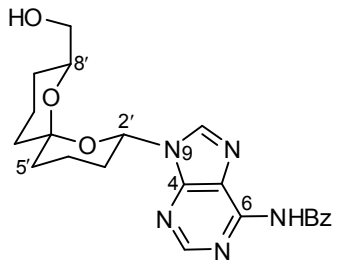

Method A: The *title compound* **808f** (6.50 mg, 85%) was prepared as a pale yellow oil from TBDPS-protected adenosine **902f** (12.0 mg, 18.1 μmol) and 3HF•NEt_3 (54.0 μL) in THF (1.5 mL) using the general procedure (method A) described above. Purification was carried out by flash chromatography (twice) using hexane–EtOAc–MeOH (4:1:0, 0:1:0 to 0:19:1) as eluent.

HRMS (FAB): found MH^+, 424.1974, $C_{22}H_{26}N_5O_4$ requires 424.1985.

ν_{max} (film)/cm^{-1}: 3395 (O–H), 3057 (N–H), 2932 (C–H), 1698 (C=O), 1614, 1582, 1455, 1258 (C–O), 1227 (C–O), 1097, 980.

δ_H (300 MHz; $CDCl_3$): 1.32–1.40 (1 H, m, 9′-H_A), 1.45–1.66 (4 H, m, 5′-H_A, 9′-H_B, 10′-H_A and 11′-H_A), 1.70–1.91 (5 H, m, 4′-H_A, 5′-H_B, 10′-H_B, 11′-H_B and OH), 2.10–2.27 (3 H, m, 3′-H_A, 3′-H_B and 4′-H_B), 3.63 (1 H, dd, J_{AB} 11.6 and $J_{8'\text{-}CH_2,8'}$ 7.0, 8′-CH_AH_BO), 3.78 (1 H, dd, J_{AB} 11.6 and $J_{8'CH_2\text{-}8'}$ 2.9, 8′-CH_AH_BO), 3.99–4.07 (1 H, m, 8′-H), 6.23 (1 H, d, $J_{2'ax,3'ax}$ 9.5, 2′-H_{ax}), 7.53 (2 H, t, *J* 7.2, Ph), 7.61 (1 H, t, *J* 7.2, Ph), 8.04 (2 H, d, *J* 7.2, Ph), 8.25 (1 H, s, 8-H), 8.80 (1 H, s, 2-H), 9.11 (1 H, br s, NH).

δ_C (100 MHz; $CDCl_3$): 18.2 (CH_2, C-10′), 18.6 (CH_2, C-4′), 26.0 (CH_2, C-9′), 30.4 (CH_2, C-3′), 34.3 (CH_2, C-5′), 34.5 (CH_2, C-11′), 66.2 (CH_2, 8′-CH_2O), 71.3 (CH, C-8′), 75.6 (CH, C-2′), 99.3 (C, C-6′), 123.0 (C, C-5), 127.9 (CH, Ph), 128.8 (CH, Ph), 132.8 (CH, Ph), 133.6 (C, Ph), 141.0 (CH, C-8), 149.6 (C, C-6), 151.6 (C, C-4), 152.7 (CH, C-2), 164.6 (C, C=O).

***m/z* (FAB):** 424 (MH^+, 8%), 185 ($C_{10}H_{17}O_3$, 3), 155 (40), 135 (51), 137 (100), 120 (20), 105 (20).

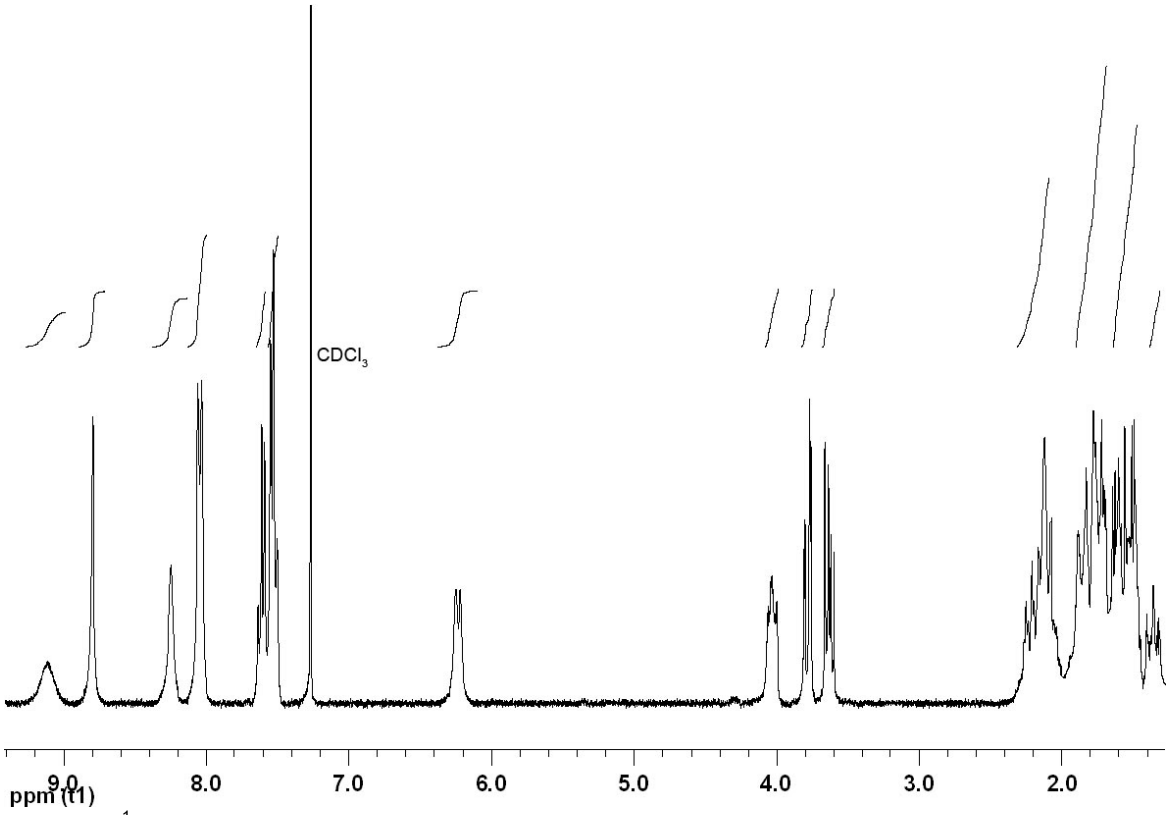

Figure 7.95: ^{1}H NMR spectrum (300 MHz; $CDCl_3$) of benzoyladenosine **808f**.

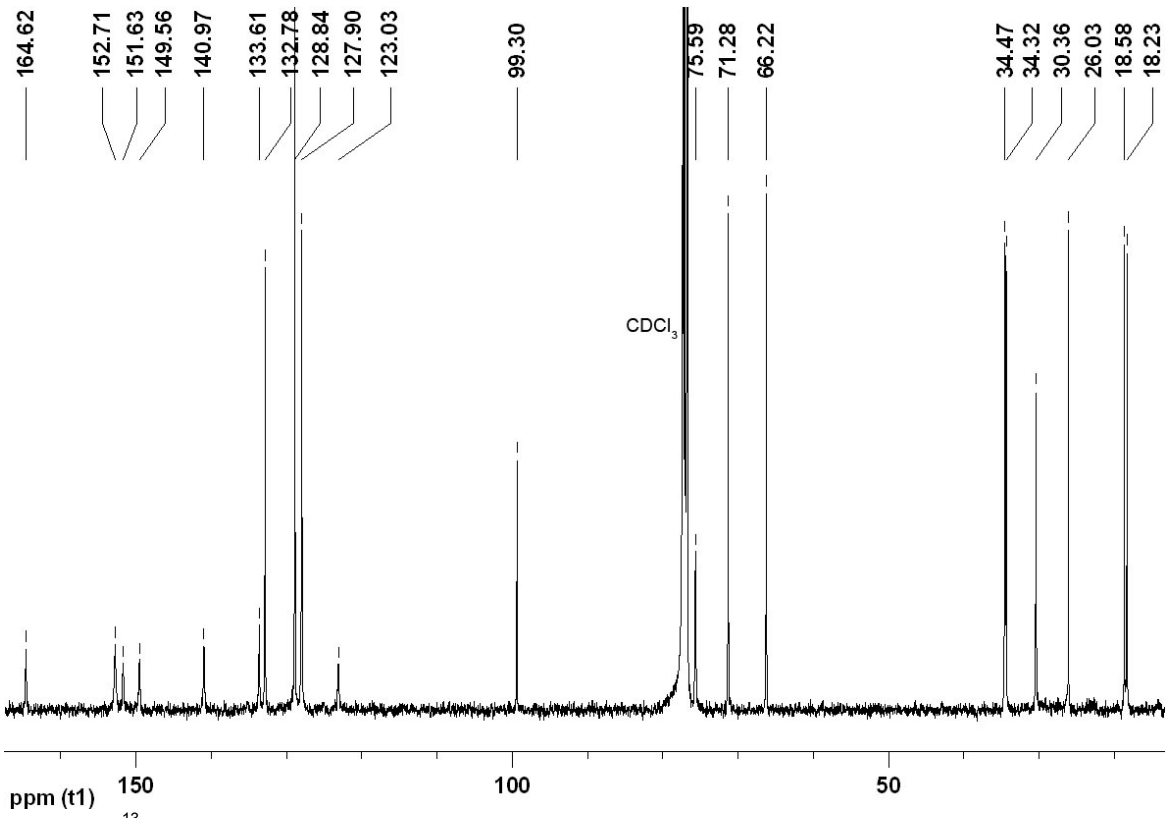

Figure 7.96: ^{13}C NMR spectrum (100 MHz; $CDCl_3$) of benzoyladenosine **808f**.

2-*N*-Acetyl-9-{(2′*S,6′*S**,8′*S**)-8′-(hydroxymethyl)-1′,7′-dioxaspiro[5.5]undecan-2′-yl}guanosine (808g)**

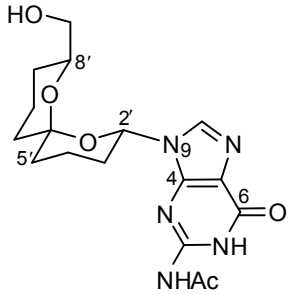

Method A: The *title compound* **808g** (2.80 mg, 91%) was prepared as a colourless oil from TBDPS-protected guanosine **902g** (5.00 mg, 8.12 μmol) and 3HF•NEt_3 (24.6 μL) in THF (750 μL) using the general procedure (method A) described above. Purification was carried out by flash chromatography hexane–EtOAc–MeOH (4:1:0, 0:1:0 to 0:9:1) as eluent followed by PLC using EtOAc–MeOH (99:1) as eluent.

HRMS (FAB): found MH^+, 378.1780, $C_{17}H_{24}N_5O_5$ requires 378.1777.

ν_{max} (film)/cm^{-1}: 3390br (O–H), 3210 (N–H), 3050 (N–H), 2941 (C–H), 1681 (C=O), 1613, 1557, 1411, 1260 (C–O), 1235 (C–O), 978.

δ_H (300 MHz; $CDCl_3$): 1.15–1.23 (1 H, m, 9′-H_A), 1.46–1.66 (4 H, m, 5′-H_A, 9′-H_B, 10′-H_A and 11′-H_A), 1.66–1.89 (4 H, m, 4′-H_A, 5′-H_B, 10′-H_B and 11′-H_B), 1.97–2.04 (2 H, m, 3′-H), 2.06–2.16 (1 H, m, 4′-H_B), 2.24 (3 H, s, $COCH_3$), 2.47 (1 H, br s, OH), 3.66 (1 H, dd, J_{AB} 11.1 and $J_{8'\text{-}CH_2,8'}$ 4.9, 8′-CH_AH_BO), 3.75 (1 H, dd, J_{AB} 11.1 and $J_{8'\text{-}CH_2,8'}$ 6.8, 8′-CH_AH_BO), 4.16–4.26 (1 H, m, 8′-H), 5.90 (1 H, dd, $J_{2'ax,3'ax}$ 9.7 and $J_{2'ax,3'eq}$ 3.5, 2′-H_{ax}), 7.87 (1 H, s, 8-H), 10.14 (1 H, br s, NH), 11.97 (1 H, br s, NH).

δ_C (75 MHz; $CDCl_3$): 18.2 (CH_2, C-10′), 18.8 (CH_2, C-4′), 24.2 (CH_3, $COCH_3$), 26.9 (CH_2, C-9′), 29.6 (CH_2, C-3′), 34.3 (CH_2, C-5′), 34.8 (CH_2, C-11′), 66.6 (CH_2, 8′-CH_2O), 70.8 (CH, C-8′), 75.0 (CH, C-2′), 99.3 (C, C-6′), 120.5 (C, C-5), 136.6 (CH, C-8), 147.8 (C, C-2), 148.2 (C, C-4), 155.5 (C, C-6), 170.9 (C, N*CO*Me).

***m/z* (FAB):** 378 (MH^+, 6%), 194 (38), 185 ($C_{10}H_{17}O_3$, 11), 155 (46), 139 (24), 138 (53), 137 (100), 120 (20), 90 (24).

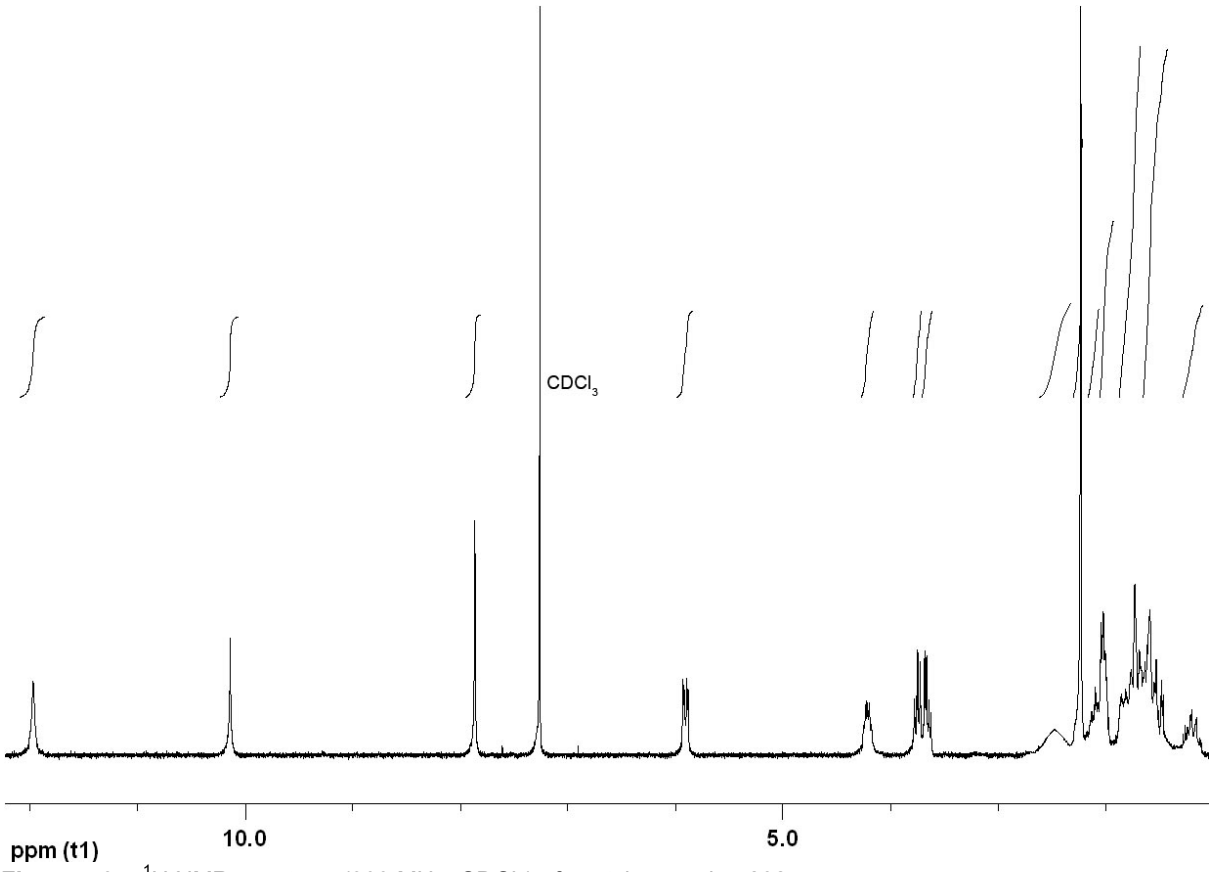

Figure 7.97: ^{1}H NMR spectrum (300 MHz; $CDCl_3$) of acetylguanosine **808g**.

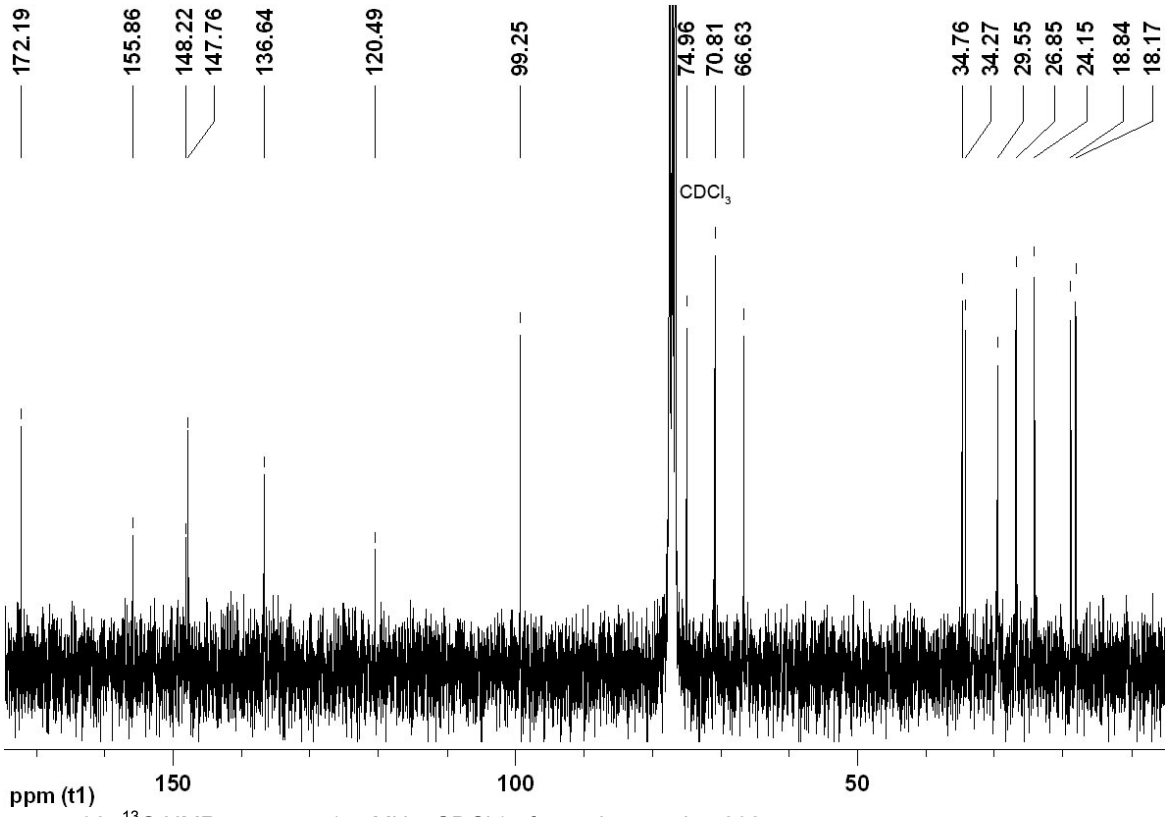

Figure 7.98: ^{13}C NMR spectrum (75 MHz; $CDCl_3$) of acetylguanosine **808g**.

2-*N*-Acetyl-7-{(2′*S,6′*S**,8′*S**)-8′-(hydroxymethyl)-1′,7′-dioxaspiro[5.5]undecan-2′-yl}guanosine (808h)**

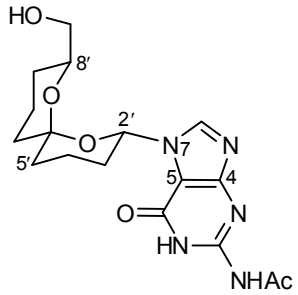

Method A: The *title compound* **808h** (2.00 mg, 82%) was prepared as a colourless oil from TBDPS-protected guanosine **902h** (4.00 mg, 6.50 μmol) and 3HF•NEt_3 (20.0 μL) in THF (750 μL) using the general procedure (method A) described above. Purification was carried out by flash chromatography using hexane–EtOAc–MeOH (1:1:0, 0:1:0 to 0:19:1) as eluent.

HRMS (FAB): found MH^+, 378.1784, $C_{17}H_{24}N_5O_5$ requires 378.1777.

ν_{max} (film)/cm^{-1}: 3429br (N–H and O–H), 2946 (C–H), 1673 (C=O), 1625, 1548, 1259, 1217 (C–O), 981, 732.

δ_H (300 MHz; $CDCl_3$): 1.27–1.34 (1 H, m, 9′-H_A), 1.46–1.70 (4 H, m, 5′-H_A, 9′-H_B, 10′-H_A and 11′-H_A), 1.70–1.85 (4 H, m, 4′-H_A, 5′-H_B, 10′-H_B and 11′-H_B), 1.89–2.00 (1 H, m, 3′-H_A), 2.10–2.18 (1 H, m, 3′-H_B), 2.18–2.25 (1 H, m, 4′-H_B), 2.40 (3 H, s, $COCH_3$), 2.79 (1 H, br s, OH), 3.54–3.64 (1 H, m, 8′-CH_AH_BO), 3.73 (1 H, dd, J_{AB} 11.5 and $J_{8'\text{-}CH_2,8'}$ 3.1, 8′-CH_AH_BO), 3.84–4.04 (1 H, m, 8′-H), 6.38 (1 H, dd, $J_{2'ax,3'ax}$ 11.1 and $J_{2'ax,3'eq}$ 2.1, 2′-H_{ax}), 8.12 (1 H, s, 8-H), 10.62 (1 H, br s, NH), 12.30 (1 H, br s, NH).

δ_C (100 MHz; $CDCl_3$): 18.3 (CH_2, C-10′), 18.5 (CH_2, C-4′), 24.6 (CH_3, COCH_3), 26.4 (CH_2, C-9′), 31.3 (CH_2, C-3′), 34.5 (CH_2, C-5′), 34.6 (CH_2, C-11′), 66.4 (CH_2, 8′-CH_2O), 71.1 (CH, C-8′), 77.9 (CH, C-2′), 99.2 (C, C-6′), 111.4 (C, C-5), 141.5 (CH, C-8), 147.6 (C, C-2), 152.9 (C, C-6), 156.7 (C, C-4), 173.0 (C, N*CO*Me).

***m/z* (FAB):** 378 (MH^+, 25%), 194 (100), 165 (28), 124 (53), 120 (75).

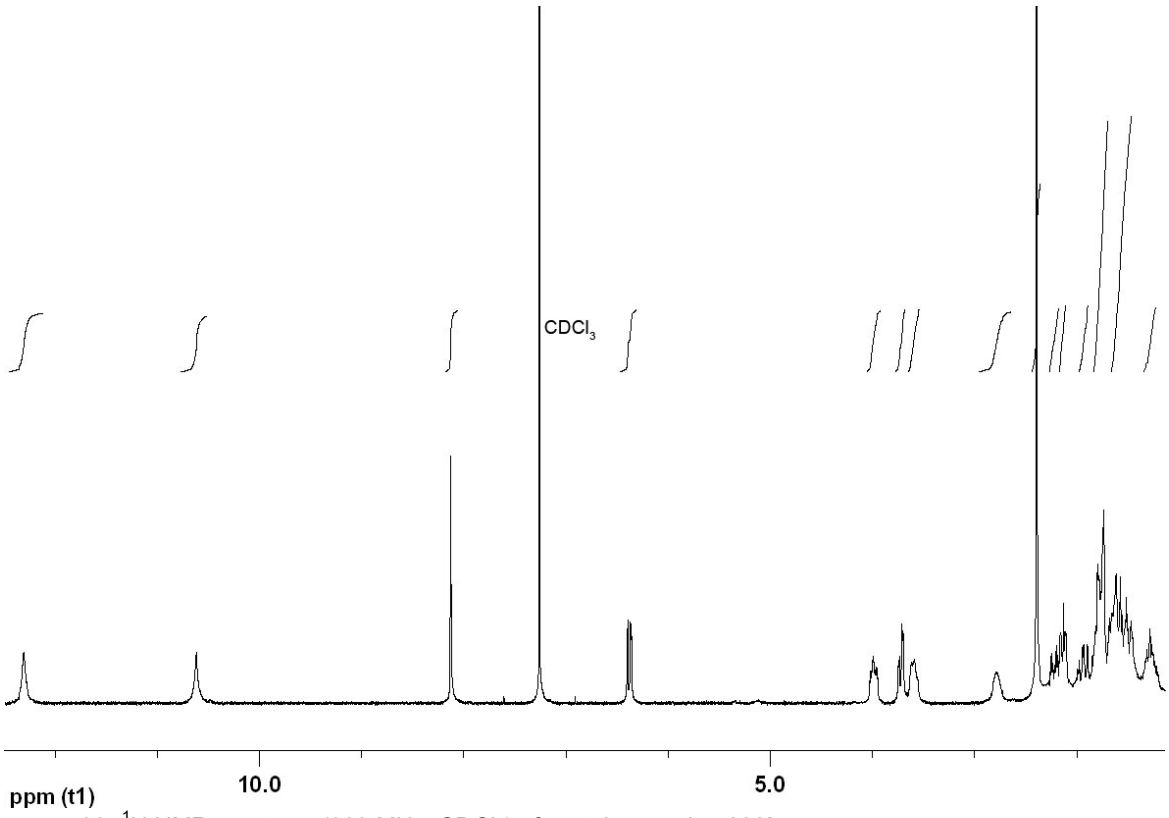

Figure 7.99: ^{1}H NMR spectrum (300 MHz; $CDCl_3$) of acetylguanosine **808h**.

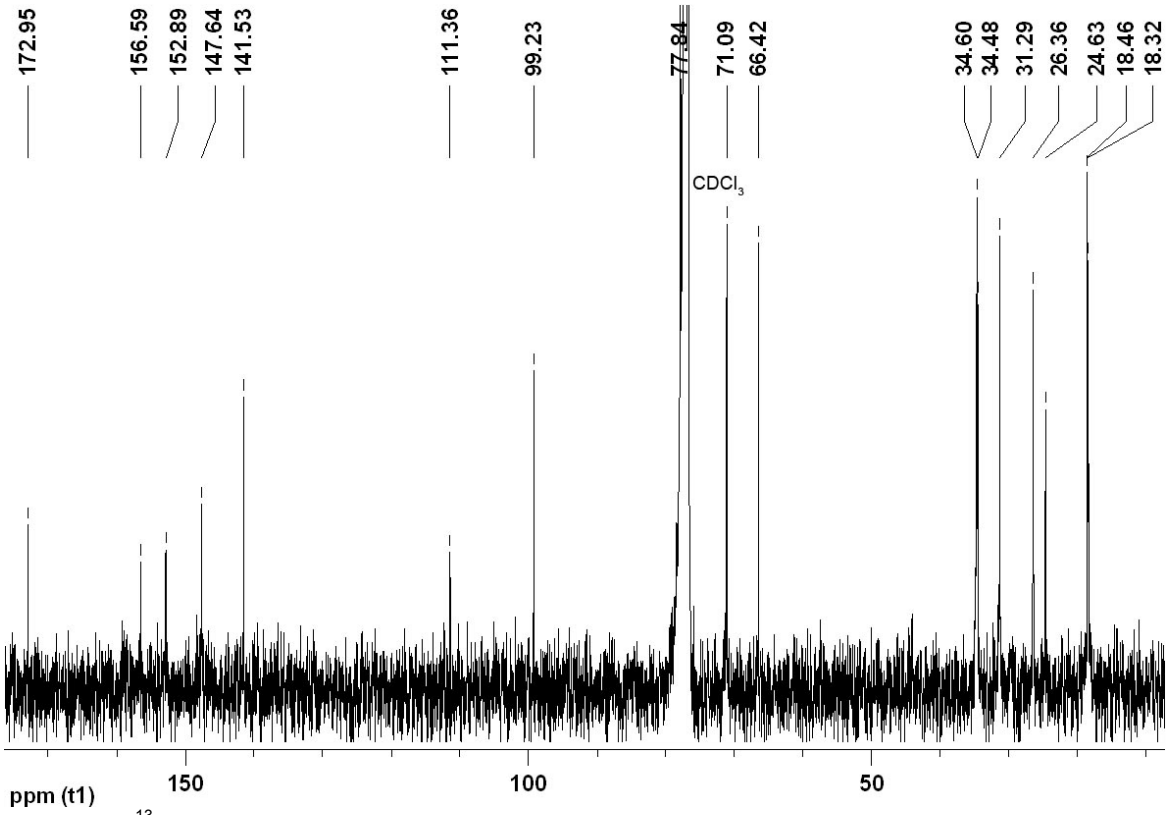

Figure 7.100: ^{13}C NMR spectrum (100 MHz; $CDCl_3$) of acetylguanosine **808h**.

9-{(2′*S,6′*S**,8′*S**)-8′-(*tert*-Butyldiphenylsilyloxymethyl)-1′,7′-dioxaspiro[5.5]undecan-2′-yl}adenosine (902i)**

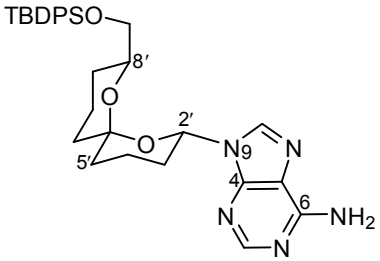

Method B: The *title compound* **902i** (8.50 mg, 90%) was prepared as a white solid from adenosine **902f** (11.2 mg, 16.9 μmol) in a 1:2:10 mixture of NEt_3–H_2O–MeOH (2.6 mL) using the general procedure (method B) described above. Purification was carried out by flash chromatography (twice) using hexane–EtOAc (4:1, 1:1 to 0:1) as eluent.

M.p.: 65.5–66.9 °C.

HRMS (FAB): found MH^+, 558.2908, $C_{31}H_{40}N_5O_3Si$ requires 558.2900.

ν_{max} (film)/cm^{-1}: 3323 (N–H), 3164 (N–H), 2931 (C–H), 2856 (C–H), 1645 (C=O), 1698, 1427, 1228, 1112 (C–O), 980, 702.

δ_H (300 MHz; $CDCl_3$): 1.08 (9 H, s, $OSiPh_2{}^tBu$), 1.31–1.39 (1 H, m, 9′-H_A), 1.42–1.53 (1 H, m, 11′-H_A), 1.53–1.67 (3 H, m, 5′-H_A, 9′-H_B and 10′-H_A), 1.71–1.86 (4 H, m, 4′-H_A, 5′-H_B, 10′-H_B and 11′-H_B), 1.95–2.06 (1 H, m, 3′-H_A), 2.06–2.16 (1 H, m, 3′-H_B), 2.16–2.26 (1 H, m, 4′-H_B), 3.67 (1 H, dd, J_{AB} 10.4 and $J_{8'\text{-}CH_2,8'}$ 4.5, 8′-CH_AH_BO), 3.77 (1 H, dd, J_{AB} 10.4 and $J_{8'\text{-}CH_2,8'}$ 5.8, 8′-CH_AH_BO), 4.01–4.10 (1 H, m, 8′-H), 5.74 (2 H, br s, NH_2), 6.09 (1 H, dd, $J_{2'ax,3'ax}$ 10.8 and $J_{2'ax,3'eq}$ 2.8, 2′-H_{ax}), 7.34–7.42 (6 H, m, Ph), 7.73–7.79 (4 H, m, Ph), 8.01 (1 H, s, 8-H), 8.33 (1 H, s, 2-H).

δ_C (75 MHz; $CDCl_3$): 18.1 (CH_2, C-10′), 18.3 (CH_2, C-4′), 19.3 (C, $OSiPh_2{}^tBu$), 26.7 (CH_2, C-9′), 26.8 (CH_3, $OSiPh_2{}^tBu$), 30.9 (CH_2, C-3′), 34.6 (CH_2, C-5′), 34.8 (CH_2, C-11′), 67.2 (CH_2, 8′-CH_2O), 70.9 (CH, C-8′), 76.4 (CH, C-2′), 98.8 (C, C-6′), 119.6 (CH, C-5), 127.6 (CH, Ph), 129.5 (CH, Ph), 129.5 (CH, Ph), 133.8 (C, Ph), 135.7 (CH, Ph), 138.8 (CH, C-8), 149.8 (C, C-4), 153.0 (CH, C-2), 155.3 (C, C-6).

***m/z* (FAB):** 558 (MH^+, 20%), 500 (M – ^{t}Bu, 15), 423 ($C_{26}H_{35}O_3Si$, 4), 199 (13), 197 (13), 137 (47), 136 (100), 135 (40).

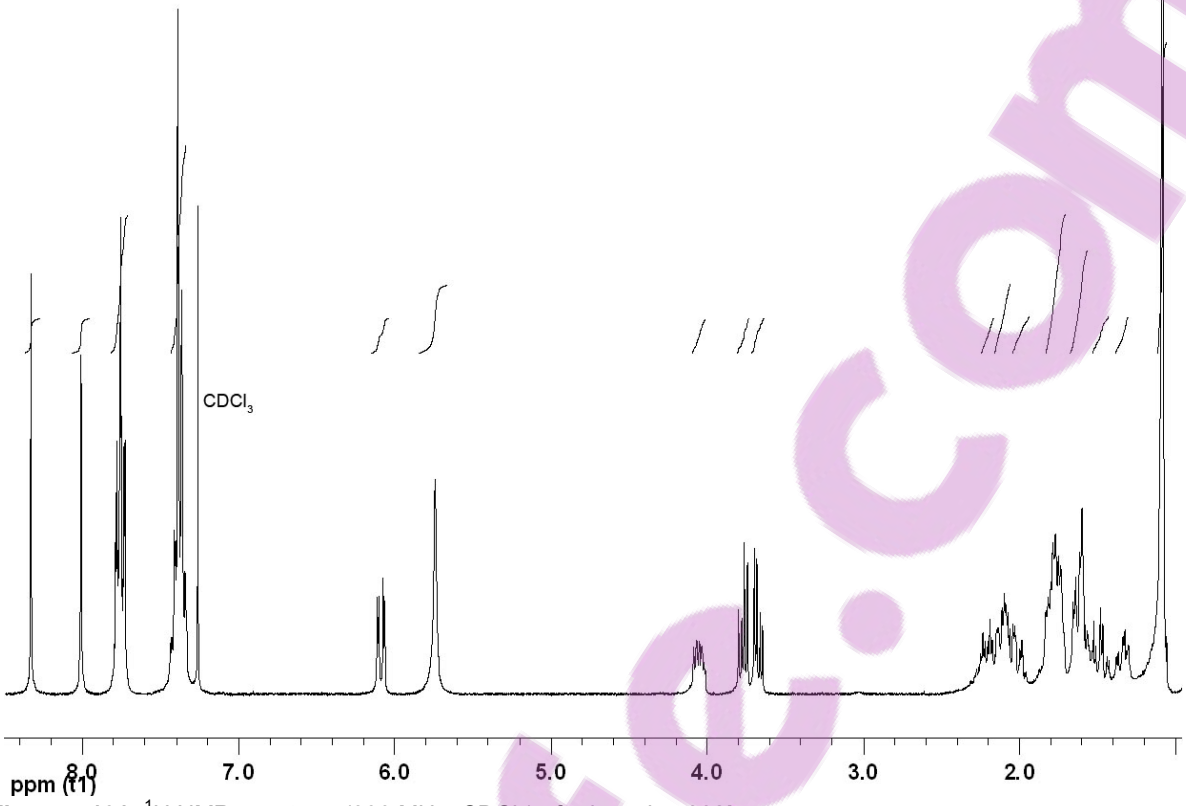

Figure 7.101: ^{1}H NMR spectrum (300 MHz; $CDCl_3$) of adenosine **902i**.

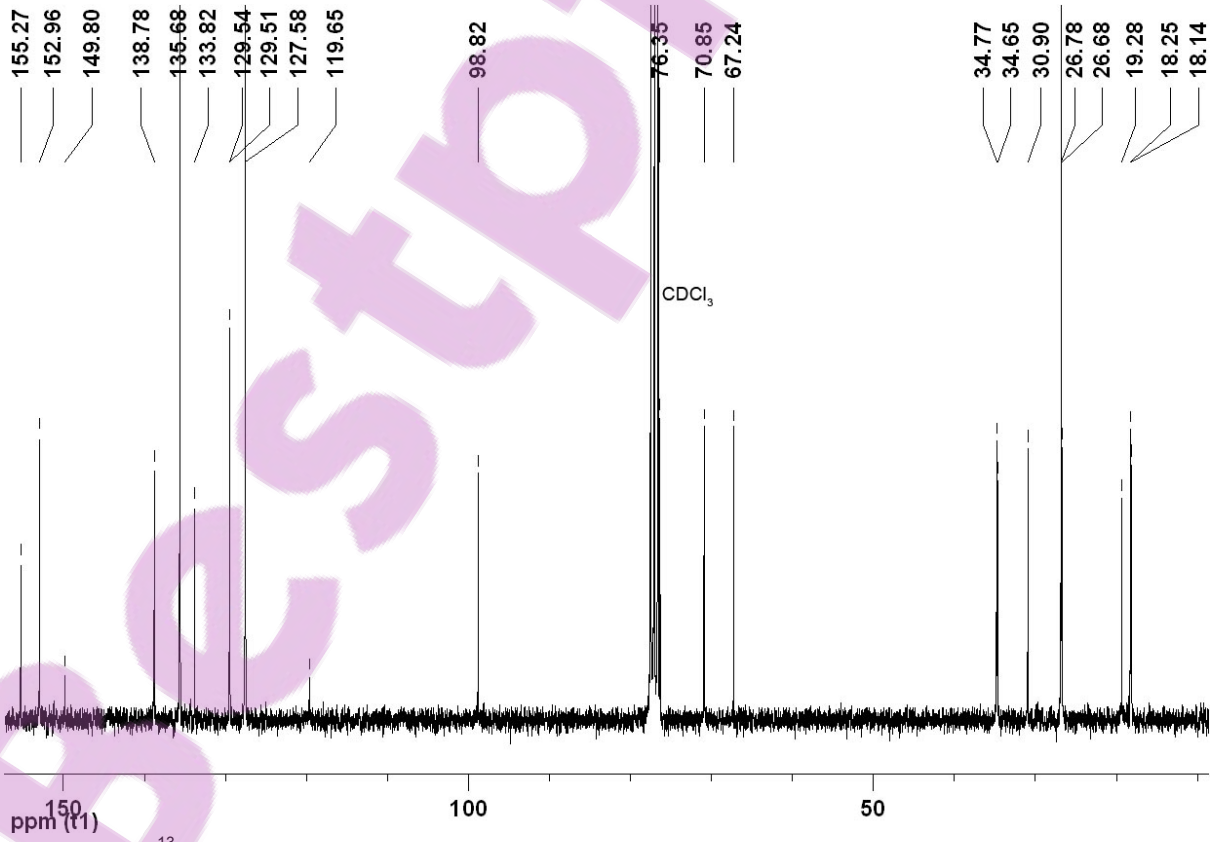

Figure 7.102: ^{13}C NMR spectrum (75 MHz; $CDCl_3$) of adenosine **902i**.

9-{(2′*S,6′*S**,8′*S**)-8′-(Hydroxymethyl)-1′,7′-dioxaspiro[5.5]undecan-2′-yl}adenosine (808i)**

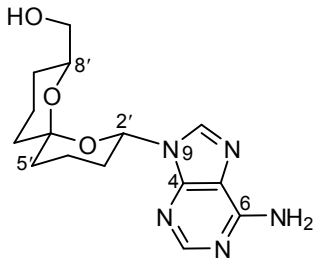

Method A: The *title compound* **808i** (4.20 mg, 92%) was prepared as a white powder from TBDPS-protected adenosine **902i** (8.00 mg, 14.3 μmol) and 3HF•NEt_3 (42.9 μL) in THF (1.5 mL) using the general procedure (method A) described above. Purification was carried out by flash chromatography using CH_2Cl_2–MeOH (99:1 to 9:1) as eluent.

M.p.: 81.2–82.7 °C.

HRMS (FAB): found MH^+, 320.1727, $C_{15}H_{22}N_5O_3$ requires 320.1723.

ν_{max} (film)/cm^{-1}: 3335br and 3194br (N–H and O–H), 2943 (C–H), 1651, 1600, 1227 (C–O), 1048, 980.

δ_H (400 MHz; CD_3OD): 1.23–1.31 (1 H, m, 9′-H_A), 1.43–1.51 (1 H, m, 11′-H_A), 1.51–1.60 (2 H, m, 9′-H_B and 10′-H_A), 1.60–1.69 (1 H, m, 5′-H_A), 1.69–1.82 (4 H, m, 4′-H_A, 5′-H_B, 10′-H_B and 11′-H_B), 2.00–2.06 (1 H, m, 3′-H_A), 2.11–2.29 (2 H, m, 3′-H_B and 4′-H_B), 3.58 (1 H, dd, J_{AB} 11.6 and $J_{8'\text{-}CH_2,8'}$ 5.9, 8′-CH_AH_BO), 3.62 (1 H, dd, J_{AB} 11.6 and $J_{8'\text{-}CH_2,8'}$ 4.3, 8′-CH_AH_BO), 3.91–3.98 (1 H, m, 8′-H), 6.06 (1 H, dd, $J_{2'ax,3'ax}$ 10.8 and $J_{2'ax,3'eq}$ 2.5, 2′-H_{ax}), 8.20 (1 H, s, 2-H), 8.31 (1 H, s, 8-H).

δ_C (100 MHz; CD_3OD): 19.3 (CH_2, C-10′), 19.4 (CH_2, C-4′), 27.7 (CH_2, C-9′), 31.5 (CH_2, C-3′), 35.6 (CH_2, C-5′), 35.8 (CH_2, C-11′), 66.7 (CH_2, 8′-CH_2O), 72.3 (CH, C-8′), 77.6 (CH, C-2′), 100.4 (C, C-6′), 120.1 (CH, C-5), 140.8 (CH, C-8), 150.3 (C, C-4), 154.0 (CH, C-2), 157.4 (C, C-6).

***m/z* (FAB):** 320 (MH^+, 100%), 275 (12), 242 (10), 185 (31), 169 (41), 120 (35).

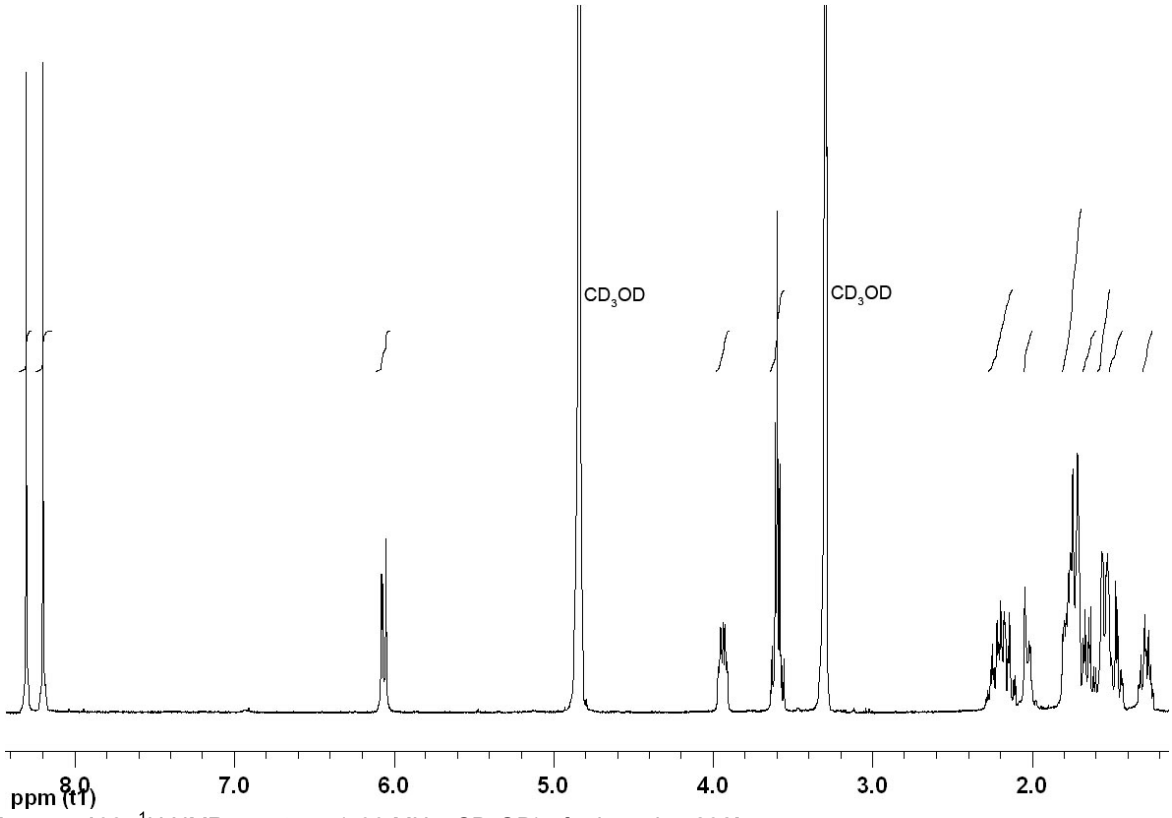

Figure 7.103: ^{1}H NMR spectrum (400 MHz; CD_3OD) of adenosine **808i**.

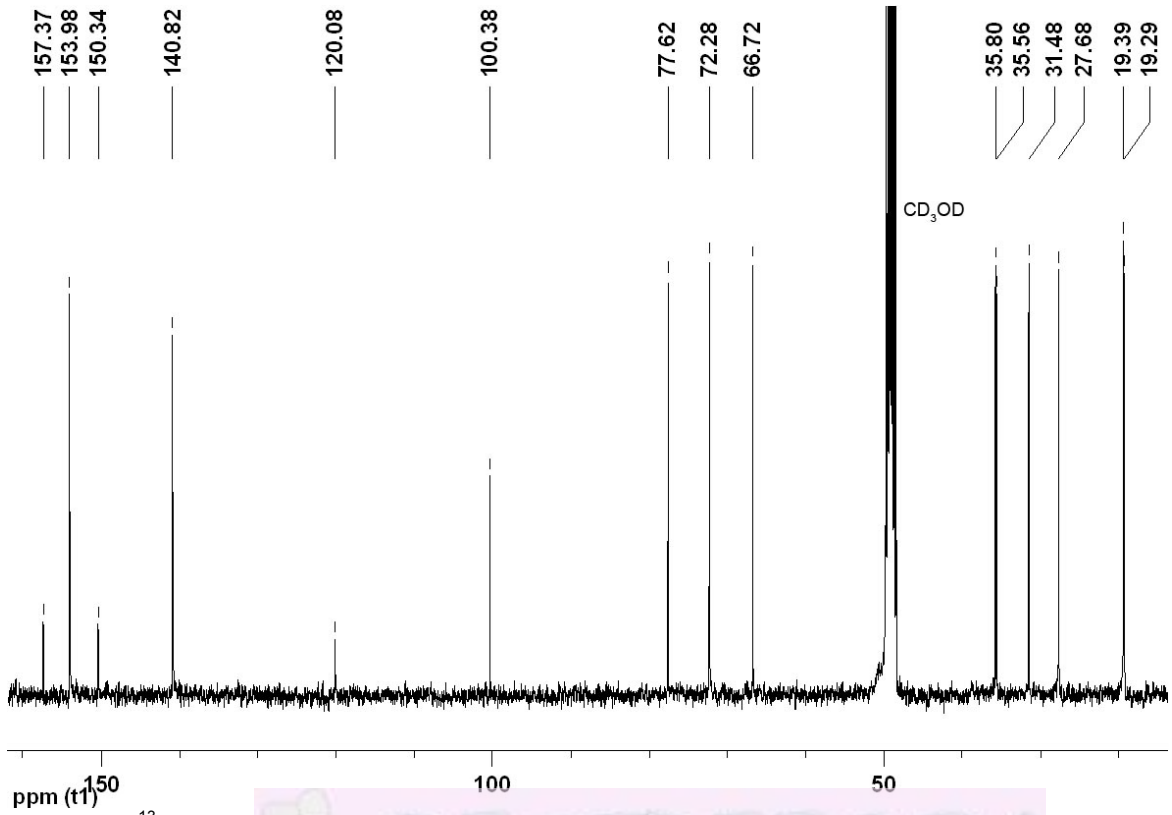

Figure 7.104: ^{13}C NMR spectrum (100 MHz; CD_3OD) of adenosine **808i**.

9-{(2′*S,6′*S**,8′*S**)-8′-(Hydroxymethyl)-1′,7′-dioxaspiro[5.5]undecan-2′-yl}guanosine (808j)**

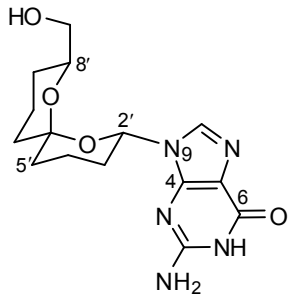

Method B: The *title compound* **808j** (2.90 mg, 93%) was prepared as a colourless oil from guanosine **808g** (3.50 mg, 9.27 μmol) in a 1:1:10 mixture NEt_3–H_2O–MeOH (3.6 mL) using the general procedure (method B) described above. Purification was carried out by flash chromatography using CH_2Cl_2–MeOH (99:1, 19:1 to 9:1) as eluent.

HRMS (FAB): found MH^+, 336.1664, $C_{15}H_{22}N_5O_4$ requires 336.1672.

ν_{max} (film)/cm^{-1}: 3412br (O–H and N–H), 2936 (C–H), 1693 (C=O), 1652, 1532, 1214 (C–O), 1182 (C–O), 978.

δ_H (300 MHz; CD_3OD): 1.19–1.30 (1 H, m, 9′-H_A), 1.42–1.53 (1 H, m, 11′-H_A), 1.54–1.68 (3 H, m, 5′-H_A, 9′-H_B and 10′-H_A), 1.68–1.89 (4 H, m, 4′-H_A, 5′-H_B, 10′-H_B and 11′-H_B), 1.96–2.05 (1 H, m, 3′-H_A), 2.05–2.16 (1 H, m, 3′-H_B), 2.16–2.30 (1 H, m, 4′-H_B), 3.58 (1 H, dd, J_{AB} 11.3 and $J_{8'\text{-}CH_2,8'}$ 4.7, 8′-CH_AH_BO), 3.64 (1 H, dd, J_{AB} 11.3 and $J_{8'\text{-}CH_2,8'}$ 5.6, 8′-CH_AH_BO), 3.99–4.07 (1 H, m, 8′-H), 5.91 (1 H, dd, $J_{2'ax,3'ax}$ 10.8 and $J_{2'ax,3'eq}$ 2.7, 2′-H_{ax}), 7.92 (1 H, s, 8-H).

δ_C (75 MHz; CD_3OD): 19.3 (CH_2, C-10′), 19.4 (CH_2, C-4′), 27.9 (CH_2, C-9′), 31.1 (CH_2, C-3′), 35.6 (CH_2, C-5′), 35.9 (CH_2, C-11′), 66.8 (CH_2, 8′-CH_2O), 72.1 (CH, C-8′), 76.8 (CH, C-2′), 100.1 (C, C-6′), 117.5 (C, C-5), 137.4 (CH, C-8), 152.9 (C, C-4), 155.5 (C, C-2), 159.5 (C, C-6).

***m/z* (FAB):** 358 (MH + Na, 24%), 336 (MH^+, 15), 273 (11), 185 ($C_{10}H_{17}O_3$, 14), 176 (21), 174 (46), 152 (100), 120 (29).

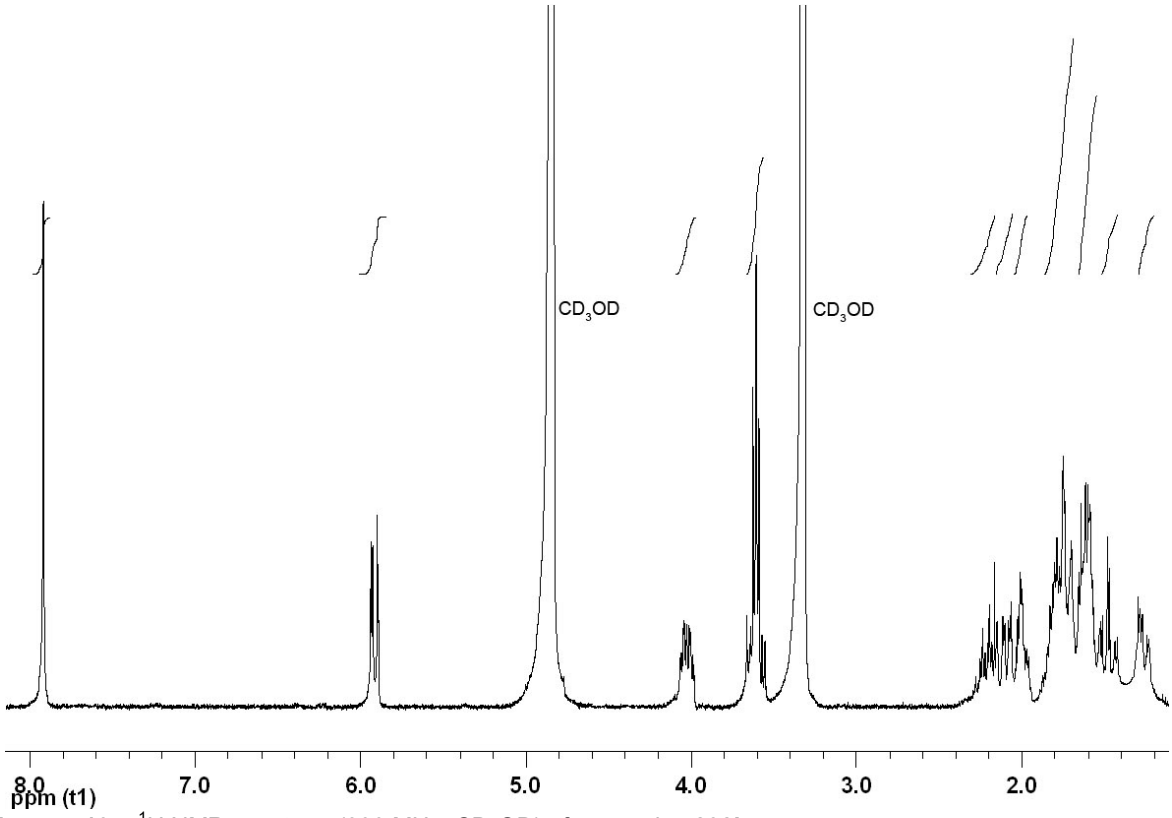

Figure 7.105: ^{1}H NMR spectrum (300 MHz; CD_3OD) of guanosine **808j**.

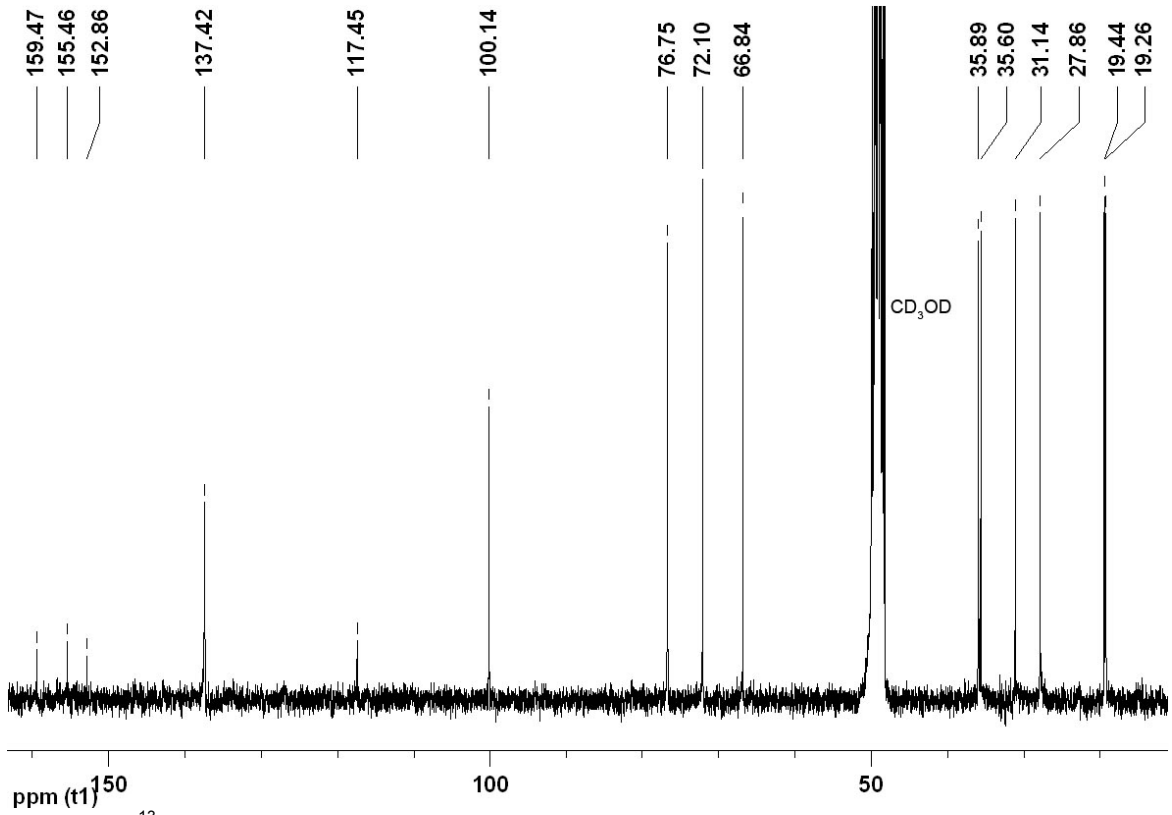

Figure 7.106: ^{13}C NMR spectrum (75 MHz; CD_3OD) of guanosine **808j**.

7-{(2′*S,6′*S**,8′*S**)-8′-(Hydroxymethyl)-1′,7′-dioxaspiro[5.5]undecan-2′-yl}guanosine (808k)**

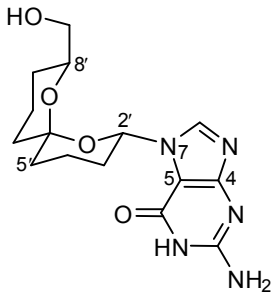

Method B: The *title compound* **808k** (1.30 mg, 86%) was prepared as a colourless oil from guanosine **808h** (1.70 mg, 4.50 μmol) in a 1:1:10 mixture NEt_3–H_2O–MeOH (3.6 mL) using the general procedure (method B) described above. Purification was carried out by flash chromatography using CH_2Cl_2–MeOH (99:1, 19:1 to 9:1) as eluent.

HRMS (FAB): found MH^+, 336.1673, $C_{15}H_{22}N_5O_4$ requires 336.1672.

ν_{max} (film)/cm^{-1}: 3308br (N–H and O–H), 2923 (C–H), 1673 (C=O), 1459, 1392, 1220 (C–O), 1090, 977.

δ_H (400 MHz; $CDCl_3$ with drops of CD_3OD): 1.12–1.19 (1 H, m, 9′-H_A), 1.38–1.57 (4 H, m, 5′-H_A, 9′-H_B, 10′-H_A and 11′-H_A), 1.64–1.79 (4 H, m, 4′-H_A, 5′-H_B, 10′-H_B and 11′-H_B), 1.79–1.88 (1 H, m, 3′-H_A), 2.01–2.09 (1 H, m, 3′-H_B), 2.09–2.20 (1 H, m, 4′-H_B), 3.49–3.58 (2 H, m, 8′-CH_2O), 3.83–3.89 (1 H, m, 8′-H), 6.18 (1 H, dd, $J_{2'ax,3'ax}$ 11.2 and $J_{2'ax,3'eq}$ 2.1, 2′-H_{ax}), 7.99 (1 H, br s, 8-H).

δ_C (100 MHz; $CDCl_3$ with drops of CD_3OD): 18.4 (CH_2, C-10′), 18.5 (CH_2, C-4′), 26.7 (CH_2, C-9′), 31.7 (CH_2, C-3′), 34.6 (CH_2, C-5′), 34.8 (CH_2, C-11′), 66.2 (CH_2, 8′-CH_2O), 71.1 (CH, C-8′), 78.2 (CH, C-2′), 99.4 (C, C-6′), 125.9 (C, C-5), 141.2 (CH, C-8), 153.4 (C, C-4), 155.4 (C, C-2), 159.5 (C, C-6).

***m/z* (FAB):** 336 (MH^+, 13%), 273 (19), 152 (100), 124 (63), 120 (81).

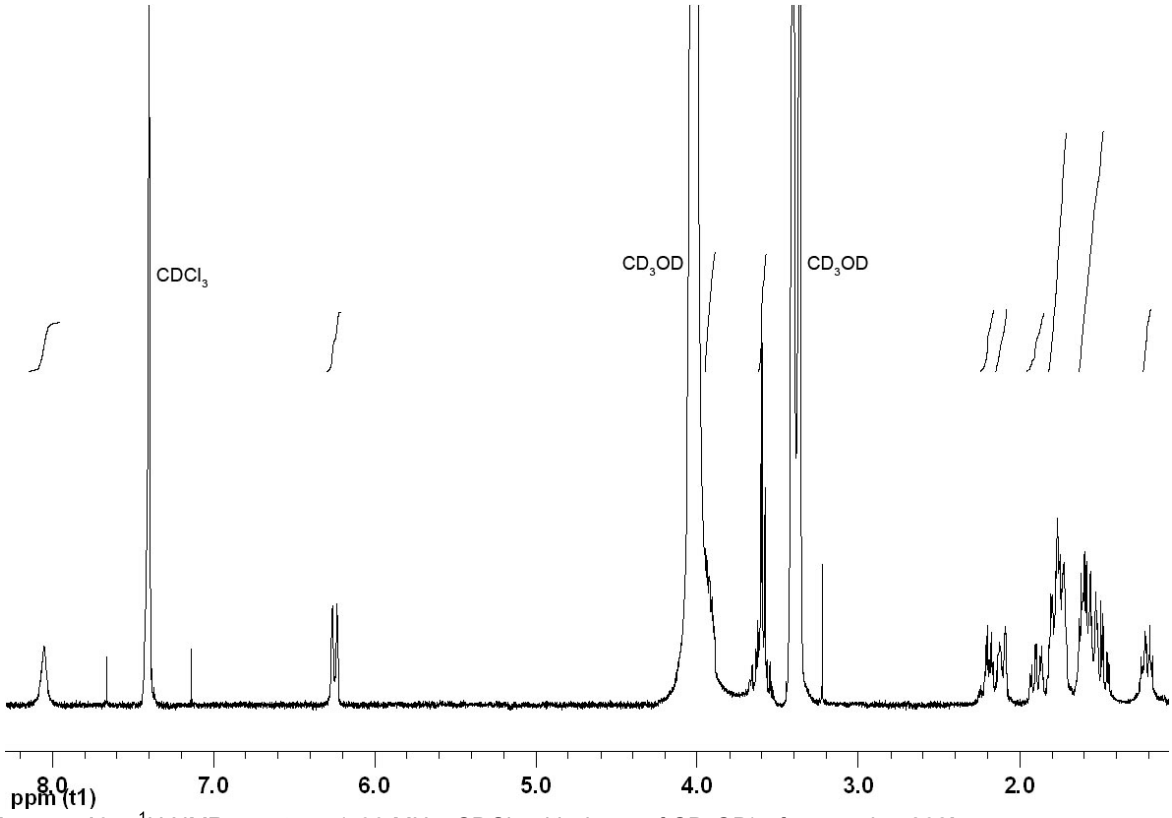

Figure 7.107: ^{1}H NMR spectrum (400 MHz; $CDCl_3$ with drops of CD_3OD) of guanosine **808k**.

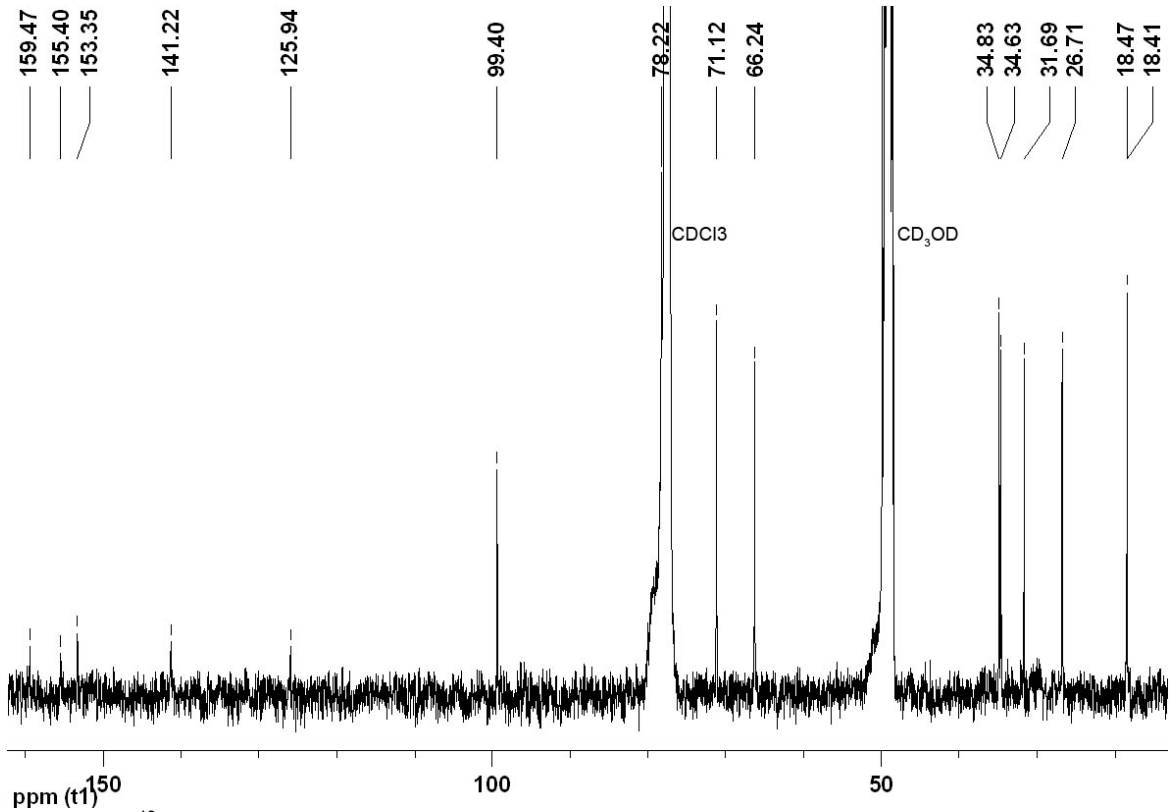

Figure 7.108: ^{13}C NMR spectrum (100 MHz; $CDCl_3$ with drops of CD_3OD) of guanosine **808k**.

7.5 References

1. W. L. F. Armarego and D. D. Perrin, *Purification of Laboratory Chemicals*, 4th edn., Pergamon, Oxford, UK, 1997.
2. C. J. Burns, M. Gill and S. Saubern, *Aust. J. Chem.*, 1997, **50**, 1067-1079.
3. R. J. Anderson, H. R. Chinn, K. Gill and C. A. Henrick, *J. Chem. Ecol.*, 1979, **5**, 919-927; M. A. Brimble, M. K. Edmonds and G. M. Williams, *Tetrahedron*, 1992, **48**, 6455-6466.
4. L. Balas, B. Jousseaume and B. Langwost, *Tetrahedron Lett.*, 1989, **30**, 4525-4526.
5. J. L. Herrmann, M. H. Berger and R. H. Schlessinger, *J. Am. Chem. Soc.*, 1979, **101**, 1544-1549.
6. C. S. Kraihanzel and M. L. Losee, *J. Org. Chem.*, 1968, **33**, 1983-1986; J. Cossy, A. Schmitt, C. Cinquin, D. Buisson and D. Belotti, *Bioorg. Med. Chem. Lett.*, 1997, **7**, 1699-1700.
7. P. J. Dunn and C. W. Rees, *J. Chem. Soc., Perkin Trans. 1*, 1987, 1579-1584.
8. J. Doubský , L. Streinz, L. Lešetický and B. Koutek, *Synlett*, 2003, 937-942.
9. W. Kitching, Personal Communication; J. E. Robinson, Bachelor of Science (Honours) Dissertation, The University of Auckland, 2001.
10. D. B. Dess and J. C. Martin, *J. Am. Chem. Soc.*, 1991, **113**, 7277-7287; D. B. Dess and J. C. Martin, *J. Org. Chem.*, 1983, **48**, 4155-4156; R. K. Boeckman, Jr., P. Shao and J. J. Mullins, *Org. Synth.*, 2000, **77**, 141-149; M. Frigerio, M. Santagostino and S. Sputore, *J. Org. Chem.*, 1999, **64**, 4537-4538.
11. A. De Mico, R. Margarita, L. Parlanti, A. Vescovi and G. Piancatelli, *J. Org. Chem.*, 1997, **62**, 6974-6977.
12. E. J. Corey and J. W. Suggs, *Tetrahedron*, 1975, **16**, 2647-2650; Y.-S. Cheng, W.-L. Liu and S.-H. Chen, *Synthesis*, 1980, 223-224.
13. K. Bowden, I. M. Heilbron, E. R. H. Jones and B. C. L. Weedon, *J. Chem. Soc.*, 1946, 39-45; A. Bowers, T. G. Halsall, E. R. H. Jones and A. J. Lemin, *J. Chem. Soc.*, 1953, 2548-2560; I. Heilbron, E. R. H. Jones and F. Sondheimer, *J. Chem. Soc.*, 1949, 604-607; L. Kürti and B. Czakó, *Strategic Applications of Named Reactions in Organic Synthesis*, 1st edn., Elsevier Academic Press, San Diego, 2005 and references cited therein.
14. J. B. Ousset, C. Mioskowski, Y.-L. Yang and J. R. Falck, *Tetrahedron Lett.*, 1984, **25**, 5903-5906.
15. H. Vorbrüggen, K. Krolikiewicz and B. Bennua, *Chem. Ber.*, 1981, **114**, 1234-1255.
16. C. W. Tornøe, C. Christensen and M. Meldal, *J. Org. Chem.*, 2002, **67**, 3057-3064.
17. J. M. Casas-Solvas, A. Vargas-Berenguel, L. F. Capitan-Vallvey and F. Santoyo-Gonzalez, *Org. Lett.*, 2004, **6**, 3687-3690.
18. R. L. Jones and N. H. Wilson, *J. Chem. Soc., Perkin Trans. 1*, 1978, 209-214.
19. H. Paulsen and U. Maaβ, *Chem. Ber.*, 1981, **114**, 346-358.
20. R. J. K. Taylor, K. Wiggins and D. H. Robinson, *Synthesis*, 1990, 589-590.
21. P. Kumar and K. Saravanan, *Tetrahedron*, 1998, **54**, 2161-2168.
22. T. Yakura, T. Kitano, M. Ikeda and J. I. Uenishi, *Tetrahedron Lett.*, 2002, **43**, 6925-6927.
23. E. Vedejs, M. J. Arnost and J. P. Hagen, *J. Org. Chem.*, 1979, **44**, 3230-3238.
24. P. C. Wälchli and C. H. Eugster, *Helv. Chim. Acta*, 1978, **61**, 885-898.
25. D. Wenkert, S. B. Ferguson, B. Porter, A. Qvarnstrom and A. T. McPhail, *J. Org. Chem.*, 1985, **50**, 4114-4119.
26. J. I. Levin, E. Turos and S. M. Weinreb, *Synth. Commun.*, 1982, **12**, 989-993.
27. K. J. Hodgetts, *ARKIVOC*, 2001, 74-79.
28. H. Vorbrüggen and C. Ruh-Pohlenz, *Org. React.*, 2000, **55**, 1-630; H. Vorbrüggen and C. Ruh-Pohlenz, *Handbook of Nucleoside Synthesis*, John Wiley & Sons, Inc., Chichester, UK, 2001.
29. R. Huisgen, *Pure Appl. Chem.*, 1989, **61**, 613-628.
30. S. J. Coats, J. S. Link, D. Gauthier and D. J. Hlasta, *Org. Lett.*, 2005, **7**, 1469-1472.
31. K. J. Doores, Y. Mimura, R. A. Dwek, P. M. Rudd, T. Elliott and B. G. Davis, *Chem. Comm.*, 2006, 1401-1403.
32. M. C. Pirrung, S. W. Shuey, D. C. Lever and L. Fallon, *Bioorg. Med. Chem. Lett.*, 1994, **4**, 1345-1346.
33. E. Söderberg, J. Westman and S. Oscarson, *J. Carbohydr. Chem.*, 2001, **20**, 397-410.

Appendices

A Crystal Structure Data for Acetate 861

Hydrogen atoms were placed in calculated positions (C–H 0.93–0.98 Å) and refined using a riding model, with U_{iso}(H) = 1.2 or 1.5 times U_{eq}(C). In the absence of significant anomalour dispersion effects, the Friedel pairs were merged before refinement.

Data collection: *SMART*[1]; cell refinement: *SAINT*[1]; data reduction: *SAINT*[1]; program used to solve structure: *SHELXS97*[2]; program used to refine structure: *SHELXL97*[2]; molecular graphics: *ORTEPIII*[3] and *Mercury*[4]; software used to prepare material for publication: *SHELXTL*[1] and *publCIF*[5].

Crystal Data	
$C_{28}H_{38}O_5Si$	D_x = 1.216 Mg m^{-3}
M_r 482.67	Mo–K$_\alpha$ radiation
Monoclinic, $P2_1/c$	λ = 0.71073 Å
a = 15.8559 (3) Å	Cell parameters from 5363 reflections
b = 9.7240 (2) Å	θ = 2.27–26.42°
c = 18.42670 (10) Å	μ = 0.124 mm^{-1}
β = 111.8760 (10)°	T = 293(2) K
V = 2636.50 (8) Å^3	Prism, white
Z = 4, F_{000} = 1040	0.28 x 0.18 x 0.12 mm

Table A.1: Crystal data of acetate **861**.

Data Collection	
Bruker SMART CCD diffractometer	14917 measured reflections
Radiation source: fine-focus sealed tube	5363 independent reflections
Monochromator: graphite	3081 reflections with $I > 2\sigma(I)$
Area detector ω scans	R_{int} = 0.1392
Absorption correction: multi-scan (SADABS[6])	θ_{max} = 26.42°
T_{min} = 0.9661	h = -14→19
T_{max} = 0.9853	k = -12→9
	l = -22→23

Table A.2: Data collection of crystal of acetate **861**.

Refinement	
Refinement on F^2, Least-square matrix: full	Secondary atom site location: difference Fourier map
$R[F^2 > 2\sigma(F^2)]$ = 0.0790	Hydrogen site location: inferred from neighbouring sites
$wR(F^2)$ = 0.244	H-atom parameters constrained
5363 reflections 307 parameters	$w=1/[\sigma^2(F_o^2)+(0.1346P)^2+0.0000P]$ where $P=(F_o^2+2F_c^2)/3$
S = 0.98	$\Delta\rho_{max}$ = 0.692 e Å^{-3}, $\Delta\rho_{min}$ = -0.969 e Å^{-3}
Primary atom site location: structure-invariant direct methods	Extinction correction: none

Table A.3: Refinement of crystal of acetate **861**.

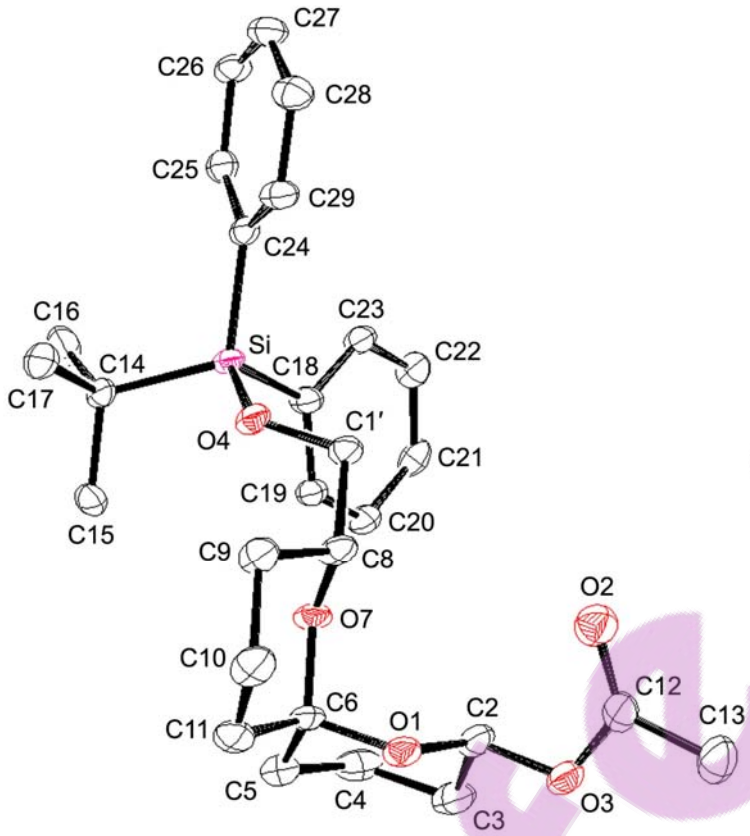

Figure A.1: The molecular structure and atom numbering scheme of acetate **861** with displacement ellipsoids drawn at the 50% probability level.

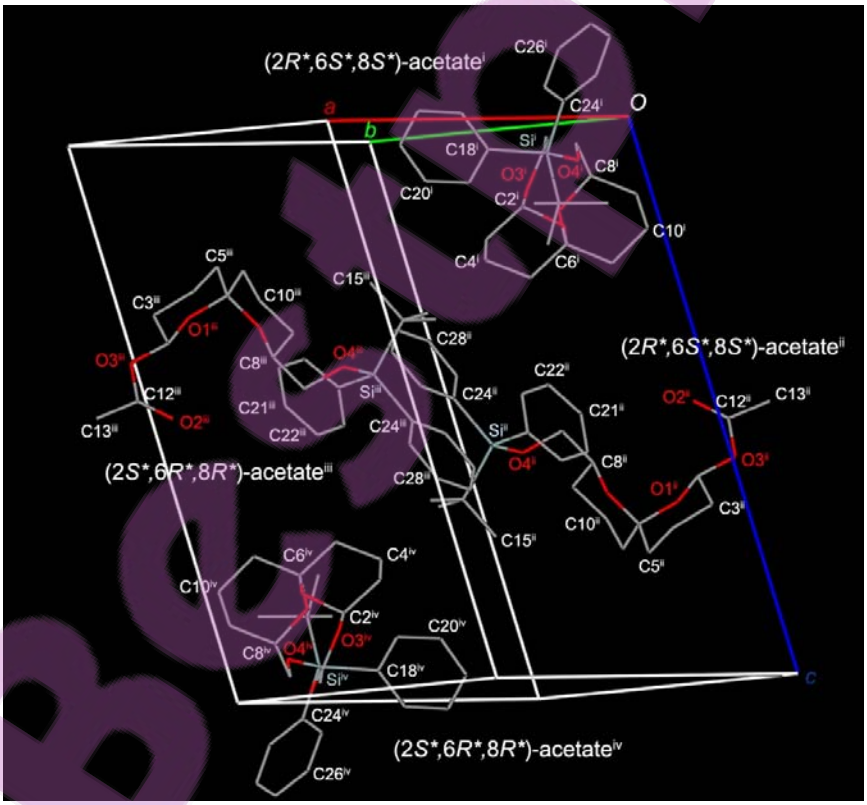

Figure A.2: Molecular packing of racemic acetate units. Hydrogen atoms are omitted for clarity. The origin of the unit cell is labelled as *O* while cell axes are labelled as *a* (red), *b* (green) and *c* (blue), respectively.

[Symmetry code: (i) *x*, -1+*y*, *z*; (ii) *x*, 1.5-*y*, 0.5+*z*; (iii) 1-*x*, -0.5+*y*, 0.5-*z*; (iv) 1-*x*, 2-*y*, 1-*z*.]

Atom	*x*	*y*	*z*	$U_{(eq)}$	*Atom*	*x*	*y*	*z*	$U_{(eq)}$
Si	3226 (1)	9814 (1)	640 (1)	18 (1)	C(13)	-1656 (4)	15181 (5)	127 (3)	39 (1)
O(1)	529 (2)	13063 (2)	1818 (2)	25 (1)	C(14)	4039 (3)	9012 (3)	1573 (2)	21 (1)
O(2)	-592 (2)	13512 (3)	39 (2)	35 (1)	C(15)	4081 (3)	9866 (4)	2284 (2)	25 (1)
O(3)	-210 (2)	14889 (3)	1102 (2)	29 (1)	C(16)	5004 (3)	8864 (5)	1575 (2)	33 (1)
O(4)	2272 (2)	9782 (2)	782 (2)	22 (1)	C(17)	3667 (3)	7578 (4)	1636 (2)	30 (1)
O(7)	1664 (2)	11797 (2)	1596 (1)	23 (1)	C(18)	3535 (3)	11625 (4)	486 (2)	23 (1)
C(1′)	1476 (3)	10593 (4)	432 (2)	22 (1)	C(19)	3599 (3)	12645 (4)	1039 (2)	23 (1)
C(2)	655 (3)	14247 (4)	1416 (2)	26 (1)	C(20)	3838 (3)	13987 (4)	952 (2)	27 (1)
C(3)	1325 (3)	15233 (4)	1959 (3)	33 (1)	C(21)	3993 (3)	14359 (4)	280 (2)	27 (1)
C(4)	2231 (3)	14478 (4)	2355 (3)	34 (1)	C(22)	3913 (3)	13386 (4)	-286 (2)	27 (1)
C(5)	2081 (3)	13151 (4)	2735 (2)	32 (1)	C(23)	3695 (3)	12034 (4)	-184 (2)	23 (1)
C(6)	1339 (3)	12267 (4)	2179 (2)	25 (1)	C(24)	3099 (3)	8747 (3)	-244 (2)	20 (1)
C(8)	1039 (3)	10906 (4)	1015 (2)	23 (1)	C(25)	3824 (3)	8476 (4)	-485 (2)	23 (1)
C(9)	837 (3)	9636 (4)	1397 (2)	27 (1)	C(26)	3706 (3)	7650 (4)	-1135 (2)	26 (1)
C(10)	427 (3)	10070 (4)	1995 (3)	33 (1)	C(27)	2867 (3)	7099 (4)	-1555 (2)	29 (1)
C(11)	1065 (4)	11073 (4)	2576 (2)	33 (1)	C(28)	2135 (3)	7359 (4)	-1337 (2)	28 (1)
C(12)	-778 (3)	14426 (4)	398 (2)	28 (1)	C(29)	2265 (3)	8168 (4)	-677 (2)	24 (1)

Table A.4: Atomic coordinates (x 10^4) and equivalent isotropic displacement parameters ($Å^2$ x 10^3). $U_{(eq)}$ is defined as one third of the trace of the orthogonalised U_{ij} tensor.

Bond	*Length (Å)*	*Bond*	*Length (Å)*	*Bond*	*Length (Å)*
Si–O(4)	1.630 (3)	C(5)–C(6)	1.508 (6)	C(17)–H(17_A)	0.9600
Si–C(14)	1.890 (4)	C(6)–C(11)	1.519 (5)	C(17)–H(17_B)	0.9600
Si–C(18)	1.877 (4)	C(8)–H(8_A)	0.9800	C(17)–H(17_C)	0.9600
Si–C(24)	1.877 (4)	C(8)–C(9)	1.513 (5)	C(18)–C(19)	1.399 (5)
O(1)–C(2)	1.424 (4)	C(9)–H(9_A)	0.9700	C(18)–C(23)	1.407 (5)
O(1)–C(6)	1.434 (5)	C(9)–H(9_B)	0.9700	C(19)–H(19_A)	0.9300
O(2)–C(12)	1.208 (5)	C(9)–C(10)	1.533 (5)	C(19)–C(20)	1.385 (5)
O(3)–C(2)	1.420 (5)	C(10)–H(10_A)	0.9700	C(20)–H(20_A)	0.9300
O(3)–C(12)	1.352 (5)	C(10)–H(10_B)	0.9700	C(20)–C(21)	1.396 (5)
O(4)–C(1′)	1.423 (5)	C(10)–C(11)	1.521 (6)	C(21)–H(21_A)	0.9300
O(7)–C(6)	1.430 (4)	C(11)–H(11_A)	0.9700	C(21)–C(22)	1.379 (5)
O(7)–C(8)	1.446 (5)	C(11)–H(11_B)	0.9700	C(22)–H(22_A)	0.9300
C(1′)–H($1'_A$)	0.9700	C(12)–C(13)	1.486 (6)	C(22)–C(23)	1.390 (5)
C(1′)–H($1'_B$)	0.9700	C(13)–H(13_A)	0.9600	C(23)–H(23_A)	0.9300
C(1′)–C(8)	1.510 (5)	C(13)–H(13_B)	0.9600	C(24)–C(25)	1.402 (5)
C(2)–H(2_A)	0.9800	C(13)–H(13_C)	0.9600	C(24)–C(29)	1.385 (6)
C(2)–C(3)	1.502 (6)	C(14)–C(15)	1.532 (5)	C(25)–H(25_A)	0.9300
C(3)–H(3_A)	0.9700	C(14)–C(16)	1.535 (6)	C(25)–C(26)	1.396 (5)
C(3)–H(3_B)	0.9700	C(14)–C(17)	1.536 (5)	C(26)–H(26_A)	0.9300
C(3)–C(4)	1.534 (7)	C(15)–H(15_A)	0.9600	C(26)–C(27)	1.374 (6)
C(4)–H(4_A)	0.9700	C(15)–H(15_B)	0.9600	C(27)–H(27_A)	0.9300
C(4)–H(4_B)	0.9700	C(15)–H(15_C)	0.9600	C(27)–C(28)	1.386 (6)
C(4)–C(5)	1.529 (6)	C(16)–H(16_A)	0.9600	C(28)–H(28_A)	0.9300
C(5)–H(5_A)	0.9700	C(16)–H(16_B)	0.9600	C(28)–C(29)	1.397 (5)
C(5)–H(5_B)	0.9700	C(16)–H(16_C)	0.9600	C(29)–H(29_A)	0.9300

Table A.5: Bond length of acetate **861**.

Bonds	*Angle(°)*	*Bonds*	*Angle(°)*	*Bonds*	*Angle(°)*
O(4)–Si–C(24)	108.85 (17)	O(7)–C(8)–C(9)	110.5 (3)	H(16_A)–C(16)–H(16_B)	109.5
O(4)–Si–C(18)	110.63 (16)	O(7)–C(8)–H(8_A)	108.9	H(16_A)–C(16)–H(16_C)	109.5
O(4)–Si–C(14)	101.83 (16)	C(1′)–C(8)–C(9)	113.5 (3)	H(16_B)–C(16)–H(16_C)	109.5
C(24)–Si–C(18)	109.69 (15)	C(1′)–C(8)–H(8_A)	108.9	C(14)–C(17)–H(17_A)	109.5
C(24)–Si–C(14)	112.18 (16)	C(9)–C(8)–H(8_A)	108.9	C(14)–C(17)–H(17_B)	109.5
C(18)–Si–C(14)	113.36 (18)	C(8)–C(9)–C(10)	109.2 (3)	C(14)–C(17)–H(17_C)	109.5
C(2)–O(1)–C(6)	113.7 (3)	C(8)–C(9)–H(9_A)	109.8	H(17_A)–C(17)–H(17_B)	109.5
C(12)–O(3)–C(2)	116.2 (3)	C(8)–C(9)–H(9_B)	109.8	H(17_A)–C(17)–H(17_C)	109.5
C(1′)–O(4)–Si	129.5 (2)	C(10)–C(9)–H(9_A)	109.8	H(17_B)–C(17)–H(17_C)	109.5
C(6)–O(7)–C(8)	114.1 (3)	C(10)–C(9)–H(9_B)	109.8	C(19)–C(18)–C(23)	116.8 (3)
O(4)–C(1′)–C(8)	110.7 (3)	H(9_A)–C(9)–H(9_B)	108.3	C(19)–C(18)–Si	120.5 (3)
O(4)–C(1′)–H($1'_A$)	109.5	C(11)–C(10)–C(9)	109.5 (4)	C(23)–C(18)–Si	122.7 (3)
O(4)–C(1′)–H($1'_B$)	109.5	C(11)–C(10)–H(10_A)	109.8	C(20)–C(19)–C(18)	122.1 (3)
C(8)–C(1′)–H($1'_A$)	109.5	C(11)–C(10)–H(10_B)	109.8	C(20)–C(19)–H(19_A)	118.9
C(8)–C(1′)–H($1'_B$)	109.5	C(9)–C(10)–H(10_A)	109.8	C(18)–C(19)–H(19_A)	118.9
H($1'_A$)–C(1′)–H($1'_B$)	108.1	C(9)–C(10)–H(10_B)	109.8	C(19)–C(20)–C(21)	119.6 (3)
O(3)–C(2)–O(1)	105.4 (3)	H(10_A)–C(10)–H(10_B)	108.2	C(19)–C(20)–H(20_A)	120.2
O(3)–C(2)–C(3)	109.1 (3)	C(6)–C(11)–C(10)	112.7 (3)	C(21)–C(20)–H(20_A)	120.2
O(3)–C(2)–H(2_A)	110.2	C(6)–C(11)–H(11_A)	109.1	C(22)–C(21)–C(20)	119.7 (3)
O(1)–C(2)–C(3)	111.7 (3)	C(6)–C(11)–H(11_B)	109.1	C(22)–C(21)–H(21_A)	120.1
O(1)–C(2)–H(2_A)	110.2	C(10)–C(11)–H(11_A)	109.1	C(20)–C(21)–H(21_A)	120.1
C(3)–C(2)–H(2_A)	110.2	C(10)–C(11)–H(11_B)	109.1	C(21)–C(22)–C(23)	120.3 (3)
C(2)–C(3)–C(4)	108.4 (3)	H(11_A)–C(11)–H(11_B)	107.8	C(21)–C(22)–H(22_A)	119.9
C(2)–C(3)–H(3_A)	110.0	O(2)–C(12)–O(3)	124.0 (4)	C(23)–C(22)–H(22_A)	119.9
C(2)–C(3)–H(3_B)	110.0	O(2)–C(12)–C(13)	124.7 (4)	C(22)–C(23)–C(18)	121.4 (3)
C(4)–C(3)–H(3_A)	110.0	O(3)–C(12)–C(13)	111.3 (4)	C(22)–C(23)–H(23_A)	119.3
C(4)–C(3)–H(3_B)	110.0	C(12)–C(13)–H(13_A)	109.5	C(18)–C(23)–H(23_A)	119.3
H(3_A)–C(3)–H(3_B)	108.4	C(12)–C(13)–H(13_B)	109.5	C(29)–C(24)–C(25)	117.4 (3)
C(5)–C(4)–C(3)	110.1 (4)	C(12)–C(13)–H(13_C)	109.5	C(29)–C(24)–Si	119.7 (3)
C(5)–C(4)–H(4_A)	109.6	H(13_A)–C(13)–H(13_B)	109.5	C(25)–C(24)–Si	122.9 (3)
C(5)–C(4)–H(4_B)	109.6	H(13_A)–C(13)–H(13_C)	109.5	C(26)–C(25)–C(24)	121.1 (4)
C(3)–C(4)–H(4_A)	109.6	H(13_B)–C(13)–H(13_C)	109.5	C(26)–C(25)–H(25_A)	119.4
C(3)–C(4)–H(4_B)	109.6	C(15)–C(14)–C(16)	108.8 (4)	C(24)–C(25)–H(25_A)	119.4
H(4_A)–C(4)–H(4_B)	108.2	C(15)–C(14)–C(17)	108.8 (3)	C(27)–C(26)–C(25)	119.9 (4)
C(6)–C(5)–C(4)	112.6 (3)	C(16)–C(14)–C(17)	109.0 (3)	C(27)–C(26)–H(26_A)	120.0
C(6)–C(5)–H(5_A)	109.1	C(15)–C(14)–Si	110.6 (3)	C(25)–C(26)–H(26_A)	120.0
C(6)–C(5)–H(5_B)	109.1	C(16)–C(14)–Si	112.5 (3)	C(26)–C(27)–C(28)	120.4 (3)
C(4)–C(5)–H(5_A)	109.1	C(17)–C(14)–Si	107.0 (3)	C(26)–C(27)–H(27_A)	119.8
C(4)–C(5)–H(5_B)	109.1	C(14)–C(15)–H(15_A)	109.5	C(28)–C(27)–H(27_A)	119.8
H(5_A)–C(5)–H(5_B)	107.8	C(14)–C(15)–H(15_B)	109.5	C(27)–C(28)–C(29)	119.1 (4)
O(7)–C(6)–O(1)	109.6 (3)	C(14)–C(15)–H(15_C)	109.5	C(27)–C(28)–H(28_A)	120.4
O(7)–C(6)–C(5)	106.5 (3)	H(15_A)–C(15)–H(15_B)	109.5	C(29)–C(28)–H(28_A)	120.4
O(7)–C(6)–C(11)	111.5 (3)	H(15_A)–C(15)–H(15_C)	109.5	C(24)–C(29)–C(28)	122.0 (4)
O(1)–C(6)–C(5)	110.1 (3)	H(15_B)–C(15)–H(15_C)	109.5	C(24)–C(29)–H(29_A)	119.0
O(1)–C(6)–C(11)	105.6 (3)	C(14)–C(16)–H(16_A)	109.5	C(28)–C(29)–H(29_A)	119.0
C(5)–C(6)–C(11)	113.5 (3)	C(14)–C(16)–H(16_B)	109.5		
O(7)–C(8)–C(1′)	106.1 (3)	C(14)–C(16)–H(16_C)	109.5		

Table A.6: Bond angle of acetate **861**.

Atom	U_{11}	U_{22}	U_{33}	U_{12}	U_{13}	U_{23}
Si	26 (6)	14 (5)	21 (5)	0 (4)	15 (5)	−1 (4)
O(1)	35 (18)	22 (13)	28 (14)	4 (12)	23 (14)	3 (11)
O(2)	38 (2)	34 (16)	36 (16)	4 (14)	19 (16)	3 (13)
O(3)	36 (19)	26 (14)	32 (16)	11 (13)	22 (15)	6 (12)
O(4)	29 (17)	16 (12)	27 (14)	3 (12)	19 (14)	1 (11)
O(7)	33 (18)	21 (13)	25 (14)	1 (12)	22 (14)	−2 (11)
C(1′)	31 (2)	19 (17)	23 (19)	2 (17)	18 (19)	2 (15)
C(2)	32 (3)	22 (18)	32 (2)	7 (18)	21 (2)	4 (17)
C(3)	43 (3)	26 (2)	38 (2)	2 (2)	23 (2)	−5 (19)
C(4)	34 (3)	34 (2)	36 (2)	−5 (2)	16 (2)	−16 (19)
C(5)	38 (3)	33 (2)	28 (2)	9 (2)	15 (2)	−4 (18)
C(6)	36 (3)	25 (19)	23 (19)	9 (18)	20 (2)	1 (16)
C(8)	29 (2)	19 (18)	31 (2)	2 (17)	22 (2)	1 (16)
C(9)	35 (3)	21 (19)	34 (2)	1 (18)	23 (2)	4 (17)
C(10)	41 (3)	30 (2)	44 (3)	5 (2)	34 (2)	9 (19)
C(11)	49 (3)	33 (2)	31 (2)	10 (2)	31 (2)	8 (19)
C(12)	31 (3)	28 (2)	30 (2)	6 (19)	19 (2)	11 (18)
C(13)	42 (3)	40 (2)	43 (3)	15 (2)	25 (3)	18 (2)
C(14)	28 (2)	16 (17)	23 (19)	3 (16)	16 (19)	4 (15)
C(15)	35 (3)	22 (18)	19 (19)	0 (18)	12 (19)	2 (15)
C(16)	30 (3)	46 (2)	25 (2)	9 (2)	11 (2)	9 (19)
C(17)	45 (3)	18 (18)	30 (2)	2 (18)	18 (2)	3 (16)
C(18)	33 (3)	17 (17)	23 (19)	−1 (17)	15 (19)	−2 (15)
C(19)	31 (3)	18 (17)	22 (19)	2 (17)	13 (19)	−2 (15)
C(20)	37 (3)	18 (18)	28 (2)	2 (18)	14 (2)	−3 (16)
C(21)	27 (2)	16 (17)	41 (2)	0 (17)	15 (2)	3 (17)
C(22)	32 (3)	22 (19)	34 (2)	0 (18)	20 (2)	6 (17)
C(23)	32 (3)	17 (17)	26 (2)	3 (17)	17 (2)	1 (15)
C(24)	28 (2)	14 (16)	21 (18)	2 (16)	13 (18)	2 (15)
C(25)	30 (2)	19 (18)	24 (19)	1 (17)	13 (2)	3 (15)
C(26)	38 (3)	24 (19)	27 (2)	5 (19)	23 (2)	0 (17)
C(27)	46 (3)	22 (19)	24 (2)	−2 (2)	20 (2)	−4 (16)
C(28)	39 (3)	20 (18)	27 (2)	−7 (19)	15 (2)	−4 (16)
C(29)	35 (3)	19 (18)	25 (2)	−2 (18)	17 (2)	−4 (16)

Table A.7: Anisotropic displacement parameters of acetate **861** ($Å^2$ x 10^3).

Atom	*x*	*y*	*z*	$U_{(eq)}$
$H(1'_A)$	1047	10103	-10	27
$H(1'_B)$	1633	11447	242	27
$H(2_A)$	855	13975	993	31
$H(3_A)$	1101	15561	2351	40
$H(3_B)$	1409	16018	1669	40
$H(4_A)$	2493	14263	1969	40
$H(4_B)$	2653	15067	2749	40

Atom	*x*	*y*	*z*	$U_{(eq)}$
$H(15_A)$	4496	9444	2752	37
$H(15_B)$	3488	9911	2308	37
$H(15_C)$	4287	10779	2238	37
$H(16_A)$	5391	8452	2058	50
$H(16_B)$	5236	9755	1523	50
$H(16_C)$	4989	8292	1146	50
$H(17_A)$	4064	7136	2105	45

H(5_A)	2643	12631	2925	39	H(17_B)	3633	7037	1190	45
H(5_B)	1924	13382	3182	39	H(17_C)	3071	7664	1653	45
H(8_A)	470	11405	748	28	H(19_A)	3476	12415	1480	27
H(9_A)	1393	9122	1656	33	H(20_A)	3895	14636	1338	32
H(9_B)	414	9049	1003	33	H(21_A)	4149	15260	215	33
H(10_A)	-159	10503	1729	40	H(22_A)	4005	13635	-738	32
H(10_B)	336	9267	2270	40	H(23_A)	3654	11386	-567	28
H(11_A)	770	11430	2913	40	H(25_A)	4392	8853	-207	28
H(11_B)	1607	10585	2903	40	H(26_A)	4196	7472	-1283	32
H(13_A)	-2043	14835	-374	59	H(27_A)	2790	6549	-1988	35
H(13_B)	-1546	16143	85	59	H(28_A)	1565	6999	-1626	34
H(13_C)	-1945	15052	497	59	H(29_A)	1776	8322	-525	29

Table A.8: Hydrogen coordinates (x 10^4) and equivalent isotropic displacement parameters of acetate **861** ($Å^2$ x 10^3).

B Crystal Structure Data for Uridine 902d

The following crystal structure data has been published by the author.[7]

Hydrogen atoms were placed in calculated positions (C–H 0.93–0.98 Å) and refined using a riding model, with U_{iso}(H) = 1.2 or 1.5 times U_{eq}(C). In the absence of significant anomalour dispersion effects, the Friedel pairs were merged before refinement.

Data collection: *SMART*[1]; cell refinement: *SAINT*[1]; data reduction: *SAINT*[1]; program used to solve structure: *SHELXS97*[2]; program used to refine structure: *SHELXL97*[2]; molecular graphics: *ORTEPIII*[3] and *Mercury*[4]; software used to prepare material for publication: *SHELXTL*[1] and *publCIF*[5].

Crystal Data	
$C_{30}H_{38}N_2O_5Si$	D_x = 1.289 Mg m^{-3}
M_r 534.71	Mo–K_α radiation
Monoclinic, $P2_1/n$	λ = 0.71073 Å
a = 14.7960 (2) Å	Cell parameters from 5612 reflections
b = 12.5092 (2) Å	θ = 1.79–26.38°
c = 15.09350 (10) Å	μ = 0.128 mm^{-1}
β = 99.4200 (10)°	T = 293(2) K
V = 2755.93 (6) $Å^3$	Needle, pale yellow
Z = 4, F_{000} = 1144	0.32 x 0.26 x 0.12 mm

Table B.1: Crystal data of uridine **902d**.

Data Collection	
Bruker SMART CCD diffractometer	15898 measured reflections
Radiation source: fine-focus sealed tube	5612 independent reflections
Monochromator: graphite	4327 reflections with $I > 2\sigma(I)$
Area detector ω scans	R_{int} = 0.0436
Absorption correction: multi-scan (SADABS)[6]	θ_{max} = 26.38°
T_{min} = 0.9603	h = -14→18
T_{max} = 0.9848	k = -15→12
	l = -18→18

Table B.2: Data collection of crystal of uridine **902d**.

Refinement	
Refinement on F^2, Least-square matrix: full	Secondary atom site location: difference Fourier map
$R[F^2 > 2\sigma(F^2)]$ = 0.0520	Hydrogen site location: inferred from neighbouring sites
$wR(F^2)$ = 0.111	H-atom parameters constrained
S = 1.09	$w=1/[\sigma^2(F_o^2)+(0.0251P)^2+2.8069P]$
5612 reflections	where $P=(F_o^2+2F_c^2)/3$
343 parameters	$\Delta\rho_{max}$ = 0.297 e Å^{-3}
Primary atom site location: structure-invariant direct methods	$\Delta\rho_{min}$ = -0.338 e Å^{-3}

Table B.3: Refinement of crystal of uridine **902d**.

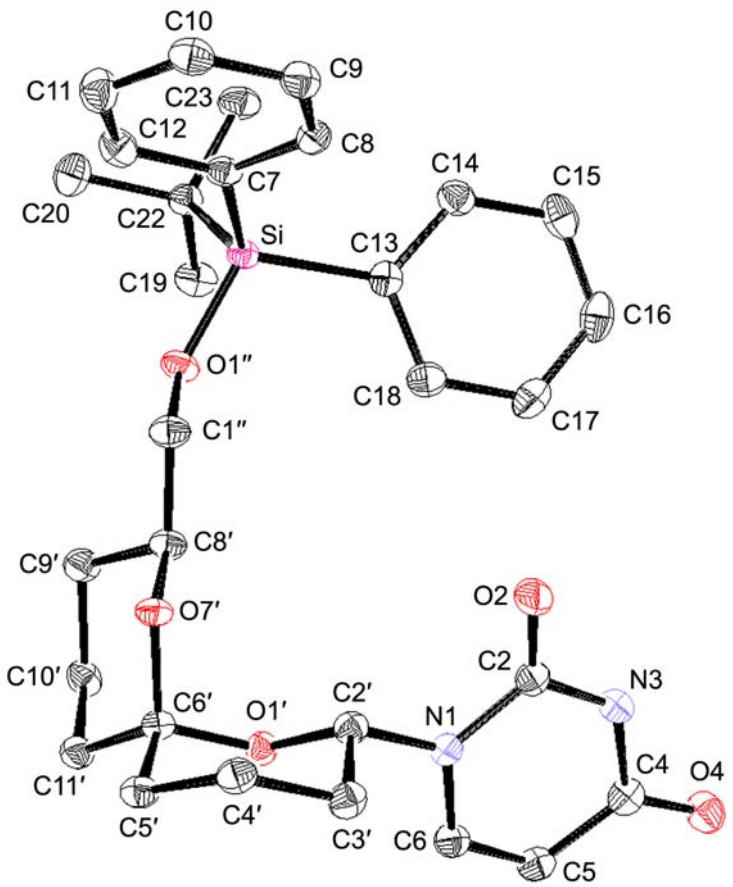

Figure B.1: The molecular structure and atom numbering scheme of uridine **902d** with displacement ellipsoids drawn at the 50% probability level.

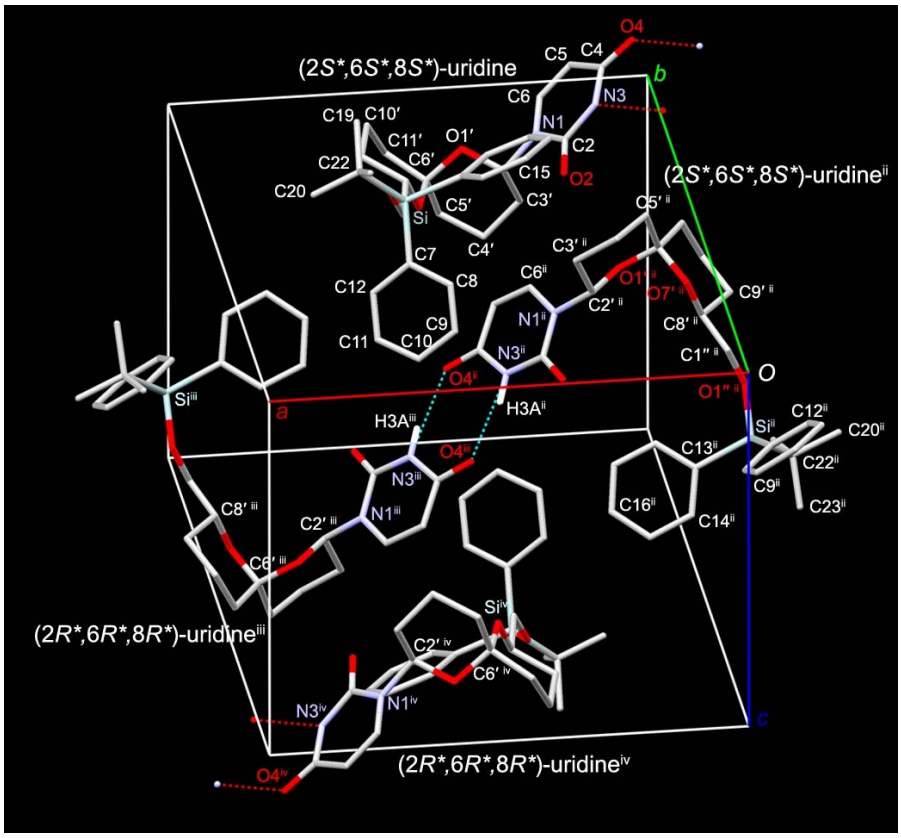

Figure B.2: Molecular packing of racemic uridine units. (*2'R**,*6R*'*,8'*R**)- and (2'*S**,6'*S**,8'*S**)-uridines are connected to each other by intermolecular hydrogen bonds. Dashed lines represent hydrogen bonds. Most hydrogen atoms that are not involved in hydrogen bonding, have been omitted for clarity. The origin of the unit cell is labelled as *O* while cell axes are labelled as *a* (red), *b* (green) and *c* (blue), respectively.

[Symmetry code: (ii) 0.5-*x*, -0.5+*y*, 0.5-*z*; (iii) 0.5+*x*, 1.5-*y*, 0.5+*z*; (iv) -*x*+1, -*y*+1, -*z*+1.]

Atom	*x*	*y*	*z*	$U_{(eq)}$
Si	5579 (1)	7510 (1)	1001 (1)	16 (1)
O(1')	3605 (1)	11240 (1)	2826 (1)	17 (1)
O(1'')	5679 (1)	8603 (1)	1621 (1)	20 (1)
O(7')	4764 (1)	10015 (1)	3362 (1)	18 (1)
O(2)	1956 (1)	8965 (1)	1733 (1)	25 (1)
O(4)	33 (1)	11378 (1)	155 (1)	27 (1)
N(1)	2169 (1)	10739 (1)	2103 (1)	18 (1)
N(3)	1047 (1)	10209 (1)	914 (1)	21 (1)
C(1'')	5353 (2)	8756 (2)	2452 (1)	21 (1)
C(2)	1743 (2)	9899 (2)	1591 (1)	19 (1)
C(2')	2899 (2)	10472 (2)	2855 (1)	18 (1)
C(3')	2559 (2)	10493 (2)	3750 (1)	20 (1)
C(4')	3360 (2)	10254 (2)	4499 (1)	20 (1)
C(4)	694 (2)	11231 (2)	750 (1)	21 (1)
C(5)	1174 (2)	12046 (2)	1321 (1)	20 (1)
C(5')	4136 (2)	11040 (2)	4438 (1)	20 (1)
C(6')	4397 (2)	11050 (2)	3501 (1)	17 (1)
C(6)	1874 (2)	11782 (2)	1965 (1)	20 (1)
C(7)	5740 (2)	6317 (2)	1766 (1)	17 (1)

Atom	*x*	*y*	*z*	$U_{(eq)}$
C(8)	5048 (2)	5550 (2)	1766 (1)	19 (1)
C(8')	5064 (2)	9910 (2)	2499 (1)	19 (1)
C(9')	5817 (2)	10710 (2)	2415 (2)	22 (1)
C(9)	5126 (2)	4730 (2)	2393 (1)	21 (1)
C(10)	5895 (2)	4652 (2)	3043 (2)	23 (1)
C(10')	5465 (2)	11840 (2)	2518 (1)	21 (1)
C(11')	5074 (2)	11935 (2)	3394 (1)	19 (1)
C(11)	6603 (2)	5389 (2)	3057 (2)	25 (1)
C(12)	6522 (2)	6211 (2)	2430 (2)	23 (1)
C(13)	4403 (2)	7426 (2)	319 (1)	19 (1)
C(14)	4147 (2)	6600 (2)	-307 (1)	23 (1)
C(15)	3273 (2)	6542 (2)	-811 (2)	26 (1)
C(16)	2627 (2)	7308 (2)	-681 (2)	29 (1)
C(17)	2848 (2)	8121 (2)	-62 (2)	28 (1)
C(18)	3731 (2)	8183 (2)	422 (2)	23 (1)
C(19)	6314 (2)	8794 (2)	-205 (2)	26 (1)
C(20)	7444 (2)	7706 (2)	838 (2)	27 (1)
C(22)	6486 (2)	7704 (2)	267 (1)	19 (1)
C(23)	6452 (2)	6814 (2)	-439 (2)	26 (1)

Table B.4: Atomic coordinates (x 10^4) and equivalent isotropic displacement parameters ($Å^2$ x 10^3). $U_{(eq)}$ is defined as one third of the trace of the orthogonalised U_{ij} tensor.

Bond	*Length (Å)*	*Bond*	*Length (Å)*	*Bond*	*Length (Å)*
Si–O(1″)	1.6491 (15)	C(4′)–C(5′)	1.526 (3)	C(11)–H(11_A)	0.9300
Si–C(7)	1.878 (2)	C(4)–C(5)	1.445 (3)	C(11)–C(12)	1.389 (3)
Si–C(13)	1.875 (2)	C(5)–H(5_A)	0.9300	C(12)–H(12_A)	0.9300
Si–C(22)	1.891 (2)	C(5)–C(6)	1.341 (3)	C(13)–C(14)	1.409 (3)
O(1′)–C(2′)	1.425 (2)	C(5′)–H($5'_A$)	0.9700	C(13)–C(18)	1.400 (3)
O(1′)–C(6′)	1.442 (3)	C(5′)–H($5'_B$)	0.9700	C(14)–H(14_A)	0.9300
O(1″)–C(1″)	1.428 (2)	C(5′)–C(6′)	1.525 (3)	C(14)–C(15)	1.391 (3)
O(7′)–C(6′)	1.433 (2)	C(6′)–C(11′)	1.519 (3)	C(15)–H(15_A)	0.9300
O(7′)–C(8′)	1.449 (2)	C(6)–H(6_A)	0.9300	C(15)–C(16)	1.390 (3)
O(2)–C(2)	1.220 (3)	C(7)–C(8)	1.403 (3)	C(16)–H(16_A)	0.9300
O(4)–C(4)	1.229 (3)	C(7)–C(12)	1.408 (3)	C(16)–C(17)	1.384 (3)
N(1)–C(2)	1.393 (3)	C(8)–H(8_A)	0.9300	C(17)–H(17_A)	0.9300
N(1)–C(2′)	1.472 (3)	C(8)–C(9)	1.387 (3)	C(17)–C(18)	1.391 (3)
N(1)–C(6)	1.380 (3)	C(8′)–H($8'_A$)	0.9800	C(18)–H(18_A)	0.9300
N(3)–H(3_A)	0.8600	C(8′)–C(9′)	1.518 (3)	C(19)–H(19_A)	0.9600
N(3)–C(2)	1.381 (3)	C(9′)–H($9'_A$)	0.9700	C(19)–H(19_B)	0.9600
N(3)–C(4)	1.388 (3)	C(9′)–H($9'_B$)	0.9700	C(19)–H(19_C)	0.9600
C(1″)–H($1''_A$)	0.9700	C(9′)–C(10′)	1.523 (3)	C(19)–C(22)	1.540 (3)
C(1″)–H($1''_B$)	0.9700	C(9)–H(9_A)	0.9300	C(20)–H(20_A)	0.9600
C(1″)–C(8′)	1.512 (3)	C(9)–C(10)	1.379 (3)	C(20)–H(20_B)	0.9600
C(2′)–H($2'_A$)	0.9800	C(10)–H(10_A)	0.9300	C(20)–H(20_C)	0.9600
C(2′)–C(3′)	1.516 (3)	C(10)–C(11)	1.393 (3)	C(20)–C(22)	1.534 (3)
C(3′)–H($3'_A$)	0.9700	C(10′)–H($10'_A$)	0.9700	C(22)–C(23)	1.536 (3)
C(3′)–H($3'_B$)	0.9700	C(10′)–H($10'_B$)	0.9700	C(23)–H(23_A)	0.9600
C(3′)–C(4′)	1.528 (3)	C(10′)–C(11′)	1.533 (3)	C(23)–H(23_B)	0.9600
C(4′)–H($4'_A$)	0.9700	C(11′)–H($11'_A$)	0.9700	C(23)–H(23_C)	0.9600
C(4′)–H($4'_B$)	0.9700	C(11′)–H($11'_B$)	0.9700		

Table B.5: Bond length of uridine **902d**.

D–H· · ·*A*	*D*–H	H· · ·*A*	*D*· · ·*A*	*D*–H· · ·*A*
N(3)–H(3_A) · · ·O(4)^i	0.86 Å	2.03 Å	2.873 (2) Å	166°

Table B.6: Hydrogen-bond geometry. Symmetry code: (i) -*x*, -*y*+2, -*z*.

Bonds	*Angle(°)*	*Bonds*	*Angle(°)*	*Bonds*	*Angle(°)*
O(1″)–Si–C(13)	110.29 (9)	C(6′)–C(5′)–H(5′$_A$)	109.3	H(11′$_A$)–C(11′)–H(11′$_B$)	107.8
O(1″)–Si–C(7)	108.65 (8)	C(6′)–C(5′)–H(5′$_B$)	109.3	C(12)–C(11)–C(10)	119.9 (2)
O(1″)–Si–C(22)	102.72 (9)	C(4′)–C(5′)–H(5′$_A$)	109.3	C(12)–C(11)–H(11$_A$)	120.0
C(13)–Si–C(7)	107.79 (10)	C(4′)–C(5′)–H(5′$_B$)	109.3	C(10)–C(11)–H(11$_A$)	120.0
C(13)–Si–C(22)	111.66 (9)	H(5′$_A$)–C(5′)–H(5′$_B$)	107.9	C(11)–C(12)–C(7)	121.6 (2)
C(7)–Si–C(22)	115.59 (10)	O(7)–C(6′)–O(1′)	109.20 (16)	C(11)–C(12)–H(12$_A$)	119.2
C(2′)–O(1′)–C(6′)	112.48 (15)	O(7)–C(6′)–C(11′)	111.75 (17)	C(7)–C(12)–H(12$_A$)	119.2
C(1″)–O(1″)–Si	126.65 (13)	O(7)–C(6′)–C(5′)	106.73 (16)	C(18)–C(13)–C(14)	116.9 (2)
C(6′)–O(7)–C(8′)	113.14 (15)	O(1′)–C(6′)–C(11′)	106.17 (16)	C(18)–C(13)–Si	120.88 (17)
C(6)–N(1)–C(2)	121.73 (18)	O(1′)–C(6′)–C(5′)	110.88 (17)	C(14)–C(13)–Si	122.19 (17)
C(6)–N(1)–C(2′)	120.30 (17)	C(11′)–C(6′)–C(5′)	112.14 (17)	C(15)–C(14)–C(13)	121.9 (2)
C(2)–N(1)–C(2′)	117.74 (17)	C(5)–C(6)–N(1)	122.0 (2)	C(15)–C(14)–H(14$_A$)	119.0
C(2)–N(3)–C(4)	127.16 (19)	C(5)–C(6)–H(6$_A$)	119.0	C(13)–C(14)–H(14$_A$)	119.0
C(2)–N(3)–H(3$_A$)	116.4	N(1)–C(6)–H(6$_A$)	119.0	C(16)–C(15)–C(14)	119.1 (2)
C(2)–N(3)–H(3$_B$)	116.4	C(8)–C(7)–C(12)	116.7 (2)	C(16)–C(15)–H(15$_A$)	120.5
O(1″)–C(1″)–C(8′)	107.92 (17)	C(8)–C(7)–Si	121.68 (17)	C(14)–C(15)–H(15$_A$)	120.5
O(1″)–C(1″)–H(1″$_A$)	110.1	C(12)–C(7)–Si	121.27 (16)	C(17)–C(16)–C(15)	120.7 (2)
O(1″)–C(1″)–H(1″$_B$)	110.1	C(9)–C(8)–C(7)	121.8 (2)	C(17)–C(16)–H(16$_A$)	119.7
C(8′)–C(1″)–H(1″$_A$)	110.1	C(9)–C(8)–H(8$_A$)	119.1	C(15)–C(16)–H(16$_A$)	119.7
C(8′)–C(1″)–H(1″$_B$)	110.1	C(7)–C(8)–H(8$_A$)	119.1	C(16)–C(17)–C(18)	119.6 (2)
H(1″$_A$)–C(1″)–H(1″$_B$)	108.4	O(7)–C(8′)–C(1″)	105.03 (16)	C(16)–C(17)–H(17$_A$)	120.2
O(2)–C(2)–N(1)	123.0 (2)	O(7)–C(8′)–C(9′)	110.61 (17)	C(18)–C(17)–H(17$_A$)	120.2
O(2)–C(2)–N(3)	122.6 (2)	O(7)–C(8′)–H(8′$_A$)	109.0	C(17)–C(18)–C(13)	121.8 (2)
N(3)–C(2)–N(1)	114.42 (19)	C(1″)–C(8′)–C(9′)	114.08 (19)	C(17)–C(18)–H(18$_A$)	119.1
O(1′)–C(2′)–N(1)	105.77 (16)	C(1″)–C(8′)–H(8′$_A$)	109.0	C(13)–C(18)–H(18$_A$)	119.1
O(1′)–C(2′)–C(3′)	111.57 (17)	C(9′)–C(8′)–H(8′$_A$)	109.0	C(22)–C(19)–H(19$_A$)	109.5
O(1′)–C(2′)–H(2′$_A$)	109.1	C(8′)–C(9′)–C(10′)	109.60 (18)	C(22)–C(19)–H(19$_B$)	109.5
N(1)–C(2′)–C(3′)	112.05 (17)	C(8′)–C(9′)–H(9′$_A$)	109.8	C(22)–C(19)–H(19$_C$)	109.5
N(1)–C(2′)–H(2′$_A$)	109.1	C(8′)–C(9′)–H(9′$_B$)	109.8	H(19$_A$)–C(19)–H(19$_B$)	109.5
C(3′)–C(2′)–H(2′$_A$)	109.1	C(10′)–C(9′)–H(9′$_A$)	109.8	H(19$_A$)–C(19)–H(19$_C$)	109.5
C(2′)–C(3′)–C(4′)	109.02 (18)	C(8′)–C(9′)–H(9′$_B$)	109.8	H(19$_B$)–C(19)–H(19$_C$)	109.5
C(2′)–C(3′)–H(3′$_A$)	109.9	H(9′$_A$)–C(9′)–H(9′$_B$)	108.2	C(22)–C(20)–H(20$_A$)	109.5
C(2′)–C(3′)–H(3′$_B$)	109.9	C(10)–C(9)–C(8)	120.3 (2)	C(22)–C(20)–H(20$_B$)	109.5
C(4′)–C(3′)–H(3′$_A$)	109.9	C(10)–C(9)–H(9$_A$)	119.9	C(22)–C(20)–H(20$_C$)	109.5
C(4′)–C(3′)–H(3′$_B$)	109.9	C(8)–C(9)–H(9$_A$)	119.9	H(20$_A$)–C(20)–H(20$_B$)	109.5
H(3′$_A$)–C(3′)–H(3′$_B$)	108.3	C(9)–C(10)–C(11)	119.7 (2)	H(20$_A$)–C(20)–H(20$_C$)	109.5
C(5′)–C(4′)–C(3′)	109.21 (17)	C(9)–C(10)–H(10$_A$)	120.2	H(20$_B$)–C(20)–H(20$_C$)	109.5
C(5′)–C(4′)–H(4′$_A$)	109.8	C(11)–C(10)–H(10$_A$)	120.2	C(20)–C(22)–C(23)	108.30 (19)
C(5′)–C(4′)–H(4′$_B$)	109.8	C(9′)–C(10′)–C(11′)	110.13 (18)	C(20)–C(22)–C(19)	108.97 (19)
C(3′)–C(4′)–H(4′$_A$)	109.8	C(9′)–C(10′)–H(10′$_A$)	109.6	C(23)–C(22)–C(19)	109.75 (18)
C(3′)–C(4′)–H(4′$_B$)	109.8	C(9′)–C(10′)–H(10′$_B$)	109.6	C(20)–C(22)–Si	110.46 (14)
H(4′$_A$)–C(4′)–H(4′$_B$)	108.3	C(11′)–C(10′)–H(10′$_A$)	109.6	C(23)–C(22)–Si	111.55 (15)
O(4)–C(4)–N(3)	120.0 (2)	C(11′)–C(10′)–H(10′$_B$)	109.6	C(19)–C(22)–Si	107.78 (15)
O(4)–C(4)–C(5)	125.8 (2)	H(10′$_A$)–C(10′)–H(10′$_B$)	108.1	C(22)–C(23)–H(23$_A$)	109.5
N(3)–C(4)–C(5)	114.18 (19)	C(6′)–C(11′)–C(10′)	112.58 (17)	C(22)–C(23)–H(23$_B$)	109.5
C(6)–C(5)–C(4)	120.3 (2)	C(6′)–C(11′)–H(11′$_A$)	109.1	C(22)–C(23)–H(23$_C$)	109.5
C(6)–C(5)–H(5$_A$)	119.9	C(6′)–C(11′)–H(11′$_B$)	109.1	H(23$_A$)–C(23)–H(23$_B$)	109.5
C(4)–C(5)–H(5$_A$)	119.9	C(10′)–C(11′)–H(11′$_A$)	109.1	H(23$_A$)–C(23)–H(23$_C$)	109.5
C(6′)–C(5′)–C(4′)	111.68 (17)	C(10′)–C(11′)–H(11′$_B$)	109.1	H(23$_B$)–C(23)–H(23$_C$)	109.5

Table B.7: Bond angle of uridine **902d**.

Atom	U_{11}	U_{22}	U_{33}	U_{12}	U_{13}	U_{23}
Si	17 (3)	14 (3)	18 (3)	0 (2)	6 (2)	−1 (2)
O(1′)	15 (8)	18 (8)	19 (7)	−1 (6)	3 (6)	0 (6)
O(1″)	24 (9)	18 (8)	20 (7)	−2 (6)	10 (7)	−5 (6)
O(7)	21 (8)	16 (7)	18 (7)	2 (6)	8 (6)	−2 (6)
O(2)	26 (9)	18 (8)	31 (9)	1 (7)	0 (7)	−1 (7)
O(4)	29 (9)	25 (9)	24 (8)	0 (7)	−3 (7)	3 (7)
N(1)	16 (9)	18 (9)	19 (9)	1 (7)	3 (7)	0 (7)
N(3)	23 (10)	19 (9)	19 (9)	−1 (8)	3 (8)	−2 (8)
C(1″)	26 (12)	20 (11)	18 (10)	3 (9)	8 (9)	0 (9)
C(2)	18 (11)	22 (11)	19 (10)	−1 (9)	7 (9)	0 (9)
C(2′)	19 (11)	16 (10)	20 (10)	1 (9)	4 (9)	1 (8)
C(3′)	19 (11)	20 (11)	24 (11)	−1 (9)	8 (9)	2 (9)
C(4′)	21 (12)	22 (11)	18 (10)	2 (9)	7 (9)	0 (9)
C(4)	22 (12)	23 (12)	19 (11)	0 (9)	6 (9)	5 (9)
C(5)	22 (12)	17 (11)	23 (11)	2 (9)	7 (9)	4 (9)
C(5′)	22 (12)	19 (11)	19 (10)	2 (9)	6 (9)	−2 (9)
C(6′)	17 (11)	16 (10)	19 (10)	2 (9)	3 (9)	−2 (8)
C(6)	21 (12)	17 (11)	23 (11)	−2 (9)	7 (9)	1 (9)
C(7)	20 (11)	17 (10)	17 (10)	1 (9)	7 (9)	−3 (8)
C(8)	16 (11)	20 (11)	21 (11)	1 (9)	5 (9)	−1 (9)
C(8′)	22 (12)	18 (11)	16 (10)	2 (9)	6 (9)	−2 (8)
C(9′)	21 (12)	22 (11)	24 (11)	−2 (9)	8 (10)	−3 (9)
C(9)	21 (12)	19 (11)	26 (11)	−3 (9)	9 (10)	−1 (9)
C(10)	30 (13)	17 (11)	21 (11)	1 (10)	7 (10)	2 (9)
C(10′)	22 (12)	19 (11)	23 (11)	−6 (9)	6 (9)	−1 (9)
C(11′)	19 (11)	18 (11)	22 (11)	−2 (9)	5 (9)	−2 (9)
C(11)	25 (13)	27 (12)	23 (11)	−1 (10)	−1 (10)	2 (10)
C(12)	25 (13)	21 (11)	24 (11)	−4 (10)	5 (10)	−1 (9)
C(13)	20 (11)	19 (11)	18 (10)	−2 (9)	5 (9)	3 (9)
C(14)	24 (13)	23 (12)	24 (11)	−2 (10)	7 (10)	−2 (9)
C(15)	30 (14)	30 (13)	19 (11)	−11 (11)	3 (10)	0 (10)
C(16)	21 (12)	39 (15)	24 (11)	−4 (11)	−2 (10)	11 (11)
C(17)	22 (13)	30 (13)	31 (13)	5 (10)	3 (10)	4 (11)
C(18)	26 (13)	21 (11)	24 (11)	2 (10)	5 (10)	2 (9)
C(19)	32 (14)	23 (12)	25 (12)	−1 (10)	12 (10)	1 (10)
C(20)	21 (12)	33 (14)	28 (12)	−2 (10)	8 (10)	3 (10)
C(22)	19 (11)	19 (11)	20 (10)	0 (9)	7 (9)	0 (9)
C(23)	29 (14)	23 (12)	28 (12)	1 (10)	14 (11)	−3 (10)

Table B.8: Anisotropic displacement parameters of uridine **902d** ($Å^2$ x 10^3).

Atom	x	y	z	$U_{(eq)}$
H(3_A)	807	9715	555	25
H($1''_A$)	5834	8591	2951	25
H($1''_B$)	4837	8287	2484	25
H($2'_A$)	3136	9758	2758	22
H($3'_A$)	2081	9962	3752	25
H($3'_B$)	2304	11190	3844	25
H($4'_A$)	3162	10321	5079	24
H($4'_B$)	3572	9528	4440	24
H(5_A)	996	12758	1242	25
H($5'_A$)	3947	11752	4585	23
H($5'_B$)	4667	10844	4873	23
H(6_A)	2169	12317	2331	24
H(8_A)	4524	5591	1334	23
H($8'_A$)	4542	10045	2021	22
H($9'_A$)	6008	10634	1833	26
H($9'_B$)	6343	10573	2875	26
H(9_A)	4657	4231	2374	25
H($10'_A$)	4993	12008	2012	25
H($10'_B$)	5963	12346	2523	25
H(10_A)	5940	4110	3470	27
H($11'_A$)	5573	11913	3898	23
H($11'_B$)	4770	12621	3406	23
H(11_A)	7128	5331	3486	30
H(12_A)	6997	6702	2449	28
H(14_A)	4575	6079	-386	28
H(15_A)	3123	5998	-1229	32
H(16_A)	2040	7274	-1014	34
H(17_A)	2409	8623	30	33
H(18_A)	3880	8742	826	28
H(19_A)	6769	8915	-580	39
H(19_B)	6350	9350	238	39
H(19_C)	5717	8798	-566	39
H(20_A)	7896	7806	456	40
H(20_B)	7549	7037	1149	40
H(20_C)	7486	8278	1267	40
H(23_A)	6922	6932	-797	39
H(23_B)	5863	6818	-818	39
H(23_C)	6548	6134	-142	39

Table B.9: Hydrogen coordinates (x 10^4) and equivalent isotropic displacement parameters of uridine **902d** ($Å^2$ x 10^3).

C References

1. Seimens Analytical X-ray Instruments Inc, *Seimens SHELXTL, SMART and SAINT*, Maidison, Wisconsin, USA, 1995.
2. G. M. Sheldrick, *Acta Crystallogr., Sect. A: Found. Crystallogr.*, 2008, **A64**, 112-122.
3. M. N. Burnett and C. K. Johnson, *ORTEPIII.*, Report ORNL-6895. Oak Ridge National Laboratory, Tennessee, USA, 1996.
4. C. F. Macrae, P. R. Edgington, P. MaCabe, E. Pidcock, G. P. Shields, P. Taylor, M. Towler and J. van de Streek, *J. Appl. Crystallogr.*, 2006, **39**, 453-457.
5. S. P. Westrip, *publCIP*, (2008) In preparation.
6. G. M. Sheldrick, *SADABS*, University of Göttingen, Germany, 1996.
7. K. W. Choi, M. A. Brimble and T. Groutso, *Acta Crystallogr. Sect. E: Struct. Rep. Online*, 2008, **E64**, O715-U1424.